

**A BIOMECHANICAL CHARACTERIZATION OF INTRAMEDULLARY REAMING IN  
THE HUMAN TIBIA**

By

Kari L. Puma

April 17<sup>th</sup>, 2015

A thesis submitted to the Faculty of the Graduate School of the University at Buffalo,  
State University of New York in partial fulfillment of the requirements for the degree of

Master of Science

Department of Mechanical & Aerospace Engineering

UMI Number: 1594769

All rights reserved

INFORMATION TO ALL USERS

The quality of this reproduction is dependent upon the quality of the copy submitted.

In the unlikely event that the author did not send a complete manuscript and there are missing pages, these will be noted. Also, if material had to be removed, a note will indicate the deletion.



UMI 1594769

Published by ProQuest LLC (2015). Copyright in the Dissertation held by the Author.

Microform Edition © ProQuest LLC.

All rights reserved. This work is protected against unauthorized copying under Title 17, United States Code



ProQuest LLC.  
789 East Eisenhower Parkway  
P.O. Box 1346  
Ann Arbor, MI 48106 - 1346

**Copyright by  
Kari L. Puma  
2015**

## **ACKNOWLEDGMENTS**

I would like to express my gratitude to Dr. Mark Ehrensberger, Dr. Paul Phillips, Mr. Craig Howard, Mr. Gary Victor, and my thesis committee members, Dr. Robert Baier and Dr. Venkat Krovi for their contributions and guidance to this work.



# TABLE OF CONTENTS

ABSTRACT	VI
1. TIBIAL ANATOMY	1
1.1 STRUCTURE	1
1.2 VASCULATURE	2
2. TIBIAL SHAFT FRACTURES AND INTERNAL FIXATION	3
3. INTRAMEDULLARY REAMING	4
3.1 REAMING SYSTEM AND PROCEDURE	5
4. POTENTIAL COMPLICATIONS OF INTRAMEDULLARY REAMING	7
4.1 INTRAMEDULLARY PRESSURE INCREASE	7
4.2 INTRAMEDULLARY TEMPERATURE INCREASE	8
4.3 VASCULAR DAMAGE	9
5. PREVIOUS INVESTIGATIONS OF REAMER CUTTING MECHANICS	9
6. SPECIFIC AIMS	12
6.1 AIM 1	12
6.2 AIM 2	13
6.3 AIM 3	13
7. MATERIALS AND METHODS	14
7.1 HANDHELD REAMER EVALUATION SYSTEM	14
7.2 MOTION CAPTURE SYSTEM	15
7.3 REAMERS	16
7.4 SPECIMEN COLLECTION AND PREPARATION	16
7.5 REAMING PROCEDURE	17
7.6 DATA ANALYSIS	18
7.7 STATISTICAL ANALYSIS	24
8. RESULTS	25
8.1 GENERAL CHARACTERIZATION OF REAMING MECHANICS	25
8.2 OPERATOR DIFFERENCES AND CHANGES IN MECHANICS FROM THE REAMER ASSOCIATED WITH INITIAL CHATTER ACKNOWLEDGMENT TO THE LARGEST REAMER USED	26
9. DISCUSSION	27
10. LIMITATIONS	29
11. CONCLUSION	30
12. FUTURE WORK	30
13. APPENDIX	32

13.1	SAMPLE 1 RESULTS	32
	LEFT: ATTENDING	32
	RIGHT: RESIDENT	42
13.2	SAMPLE 2 RESULTS	52
	LEFT: ATTENDING	52
	RIGHT: RESIDENT	62
13.3	SAMPLE 3 RESULTS	74
	LEFT: RESIDENT	74
	RIGHT: ATTENDING	96
13.4	SAMPLE 4 RESULTS	116
	LEFT: RESIDENT	116
	RIGHT: ATTENDING	138
13.5	SAMPLE 5 RESULTS	156
	LEFT: RESIDENT	156
	RIGHT: ATTENDING	178
13.6	SAMPLE 6 RESULTS	200
	LEFT: ATTENDING	200
	RIGHT: RESIDENT	220
13.7	SAMPLE 7 RESULTS	240
	LEFT: RESIDENT	240
	RIGHT: ATTENDING	254
14.	REFERENCES	268

## **ABSTRACT**

Intramedullary reaming is a technique used in orthopaedic trauma surgical procedures in which the intramedullary canal of a long bone is enlarged and prepared for the implantation of a nail to repair a fracture. Several complications of intramedullary reaming have been described in literature, including elevations in intramedullary pressure and temperature and damage to the blood vessels in the bone. However, the mechanics of intramedullary reaming in the human when performed by a surgeon have not been widely investigated. The purpose of this investigation was to characterize the mechanics of intramedullary reaming, using a novel reamer evaluation tool, performed by two operators of different experience levels. A surgical reaming system was modified with a wireless, custom sensor to measure axial force, torque and RPM of the reamer during use.

Ten cadaveric matched tibial pairs were harvested under IRB approval, and one bone of each pair was reamed by the attending orthopaedic trauma surgeon, the other by the orthopaedic surgery resident (PGY-2). Reaming began with a 9mm diameter reamer and proceeded in 0.5mm increments until the declaration of audible chatter, after which reaming proceeded to a maximum of 1.5mm beyond this point. Axial force, torque and reamer displacement were recorded, from which the time to reach the distal end and the mechanical work to reach the distal end were determined. These parameters were compared between operators at the reamer associated with chatter and the maximum reamer size beyond chatter, and also within individual operators to determine how the mechanics changed from initial chatter acknowledgement to the last, largest reamer used. Three matched pairs were excluded from analysis due to unforeseen difficulties during data collection or with the experimental procedure.

Analysis revealed that operator mechanics were not statistically different, with the exception of the application of axial load at the maximum reamer size beyond the declaration of chatter. The resident applied more axial force on the reamer than the attending surgeon for the

maximum reamer size. For each operator, force, work and time increased from reaming at chatter to the last reamer used. The results of this study suggest that although the reaming procedure is not strongly operator dependent, there is likely to be a mechanical component of clinical concern associated with continued reaming after noticeable initial chatter. Additional studies with larger sample sizes and operator populations are necessary in order to draw further conclusions.

# 1. TIBIAL ANATOMY

## 1.1 STRUCTURE

The tibia (Figure 1) is the second largest bone in the human skeleton and is the larger of the two bones located below the knee in the lower limb. It is classified as a long bone and serves to support the weight of the body and to connect and transmit forces between the knee and the ankle joints. The proximal epiphysis consists of relatively flat medial and lateral condyles that form the tibial plateau. The tibial plateau articulates with the condyles of the distal femur to form the primary articulation of the knee joint. The distal epiphysis of the tibia is laterally rotated and the medial malleolus projects inferiorly on the medial side to articulate with the talus to form a portion of the ankle joint. The tibia also articulates with the fibula at the proximal and distal tibiofibular joints [1].

Both the proximal and distal epiphyses of the tibia are mainly comprised of cancellous bone deep to a thin layer of dense, cortical bone. Cancellous bone consists of struts of interconnected trabeculae that form a porous structure with a high surface to mass ratio. This structure provides the epiphyses of the bone with their superior damping ability, as load is transmitted from both the ankle and

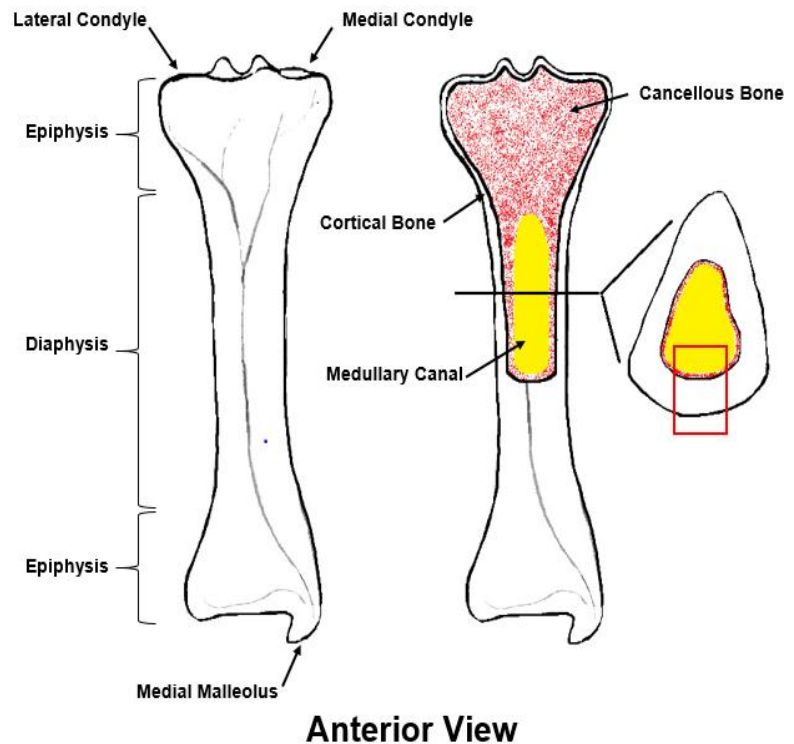


Figure 1: Basic Anatomy of the Right Tibia

the torso to the knee joint [2]. The diaphysis is triangular and hollow, consisting of a thick layer of cortical bone superficial to a very thin shell of cancellous bone. Cortical bone comprises osteon units, each consisting of several concentric layers of lamella. The collagen fibers within the lamella are arranged along the longitudinal axis, providing the bone with its excellent axial strength. The cortical bone surrounding the hollow canal is therefore responsible for bearing the majority of any unidirectional force applied to the tibia [2].

The hollow center of the tibial body is the medullary cavity that houses bone marrow. Red marrow that is rich in hemopoietic stem cells is present at birth, but over time transitions to yellow marrow consisting mostly of fat cells. The thin shell of cancellous bone surrounding the medullary cavity is lined by the endosteum. The endosteum is an incomplete, single-cell layer of tissue consisting of epithelial cells, osteoblasts, osteoprogenitors, osteoclasts and an extracellular matrix that aids in protecting the inner surface of the bone [2]. The superficial surface of the tibia is also covered by a layer of connective tissue known as the periosteum. The periosteum is a dense, irregular layer of connective tissue with an outer fibrous layer and an inner cellular layer that serves to isolate the bone, provide a location for blood and nerve routing as well as muscle and tendon attachment, and aids in bone growth and repair [2].

## **1.2 VASCULATURE**

The major source of blood to the diaphysis of the tibia is supplied by the nutrient artery, arising from a branch of the posterior tibial artery that enters the tibia through the nutrient foramen near the soleal line [1]. The nutrient artery divides into ascending and descending branches within the medullary cavity, which further branch into arterioles that transverse the endosteum [3]. Together, the nutrient artery and the corresponding endosteal branches constitute two-thirds of the blood supply within the tibial shaft [3, 4]. Additional blood is supplied to the tibial shaft via small periosteal arteries that surround the superficial surface of the bone within the periosteum and from arterial branches that feed the surrounding muscles. The

periosteal supply mainly arises from branches of the anterior tibial artery [1]. Once inside the bone, these vessels form anastomoses with the extended branches of the nutrient artery. The proximal epiphysis of the tibia is supplied via branches of the genicular artery and the distal epiphysis is supplied via arterial branches near the ankle joint [1, 4].

## 2. TIBIAL SHAFT FRACTURES AND INTERNAL FIXATION

Diaphyseal tibia fractures are one of the most common fractures of long bones and can arise from a variety of injury mechanisms [5]. Low-energy fractures of the tibial shaft can result from low-impact falls from standing or from sporting injuries [5]. Such fractures tend to be simple and non-displaced, and therefore typically respond well to treatment [6]. High-energy fractures of the diaphysis can occur as a result of high-impact trauma, including falls from heights, automobile-pedestrian accidents, motorcycle crashes or motor vehicle accidents [5]. Such

accidents often result in severely displaced or open fractures of the tibia that cause surrounding soft tissue injury and bony comminution. Due to the subcutaneous nature of the bone and the damage to surrounding soft tissues and blood supply, high-energy fractures generally have more complications when healing [6]. In both cases, the type and

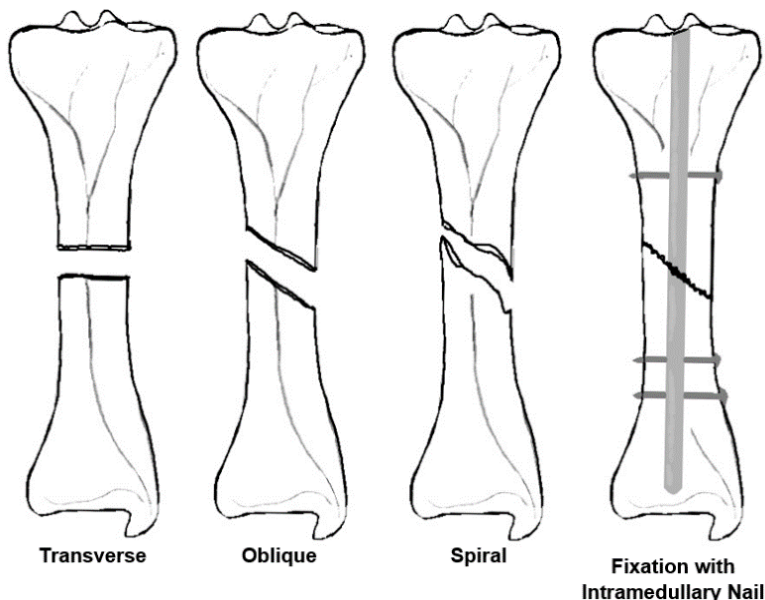


Figure 2: Examples of Tibial Shaft Fractures and Intramedullary Fixation

severity of a fracture is dependent on the strength of the bone and is directly related to the rate and magnitude of the impact [7].

Proper treatment of a tibial shaft fracture is crucial to achieve union and avoid infection, deformity and permanent disability. Diaphyseal fractures of the tibia are often treated via reduction and internal fixation involving the implantation of plates, nails and screws [5]. Due to the hollow nature of the diaphysis, intramedullary (IM) nailing is an optimal treatment option for such fractures (Figure 2). An intramedullary nail is a symmetric, cylindrical stainless steel or titanium rod that is inserted into the medullary canal of a long bone following fracture reduction to maintain the alignment as the fracture heals. The nail has high axial compressive strength and resistance to bending moments, allowing it to withstand normal loading patterns experienced by the tibia [7]. Thus, shortly following implantation, the patient is able to bear weight on the limb while the fracture is healing [5]. Prior to internal fixation options, long bone fractures were treated using traction, plaster and external fixation methods that resulted in long periods of healing and patient inactivity [8].

### **3. INTRAMEDULLARY REAMING**

Intramedullary nailing was revolutionized in 1939 by Gerhard Küntscher, an orthopaedic surgeon in Hamburg, Germany who introduced a reaming technique to treat long bone fractures in soldiers during the Second World War. Reaming is a technique used during an intramedullary nailing procedure to enlarge the diameter of the medullary canal by cutting away layers of the inner bone wall via a series of sharp, rotating cutting tools. In comparison to boring tools, reamers are multi-point cutting devices that accurately remove small amounts of material to provide superior surface finish. The IM reaming process shapes the canal and prepares the interface for a larger diameter nail with improved bending and torsional stiffness [7]. Prior to the practice of reaming, the size and geometry of the implant was limited by the native geometry of the bone and intramedullary cavity [9].



The introduction of reamed IM nailing with interlocking bolts was initially well accepted in the European medical community. However, not long after Küntscher introduced the technique, a group dedicated to the study of bone fracture healing (AO) studied and presented the potential injurious effects of IM nailing with reaming and introduced a well-researched, unreamed nailing system [9]. This largely divided the European medical community between the teachings of AO and Küntscher, and IM reaming became a somewhat controversial practice. Since that time, research has demonstrated that in comparison to non-reamed nailing techniques, reaming of closed fractures does not negatively impact fracture healing and does not cause significant differences in operative times, transfusion requirements or prolonged hypoxia [10, 11]. It has also been shown that reaming debris can collect at the fracture site and autograft the fracture, which may contribute to faster union [12].

### 3.1 REAMING SYSTEM AND PROCEDURE

The reamer system is an assembly of components including a reamer head, shaft and guidewire operated with a surgical power tool (Figure 3). During an IM nailing operation for a closed tibial shaft fracture, an incision is generally made through the lateral or medial patellar tendon and the point of entry on the anterior edge of the tibial plateau is exposed [5]. The medullary cavity is then opened with an awl. A guidewire (Figure 3a) is passed down the cavity, and after fracture reduction, is passed through the fracture line and into the distal fragment of the bone. The guidewire is a few millimeters in diameter, which allows the cannulated reamer



**Figure 3: Intramedullary Reamer Assembly**

head to slide over it. The blunt tip of the guidewire should be securely pressed into the distal fragment under x-ray visualization [13].

The reamer shaft (Figure 3b) is a lightweight and flexible rod to which the reamer head attaches. These shafts are generally made of Nitinol for superior torsional strength and flexibility, and are designed to elastically deform to match the natural curvature of long bone as the reamer travels down the IM canal [14]. High torsional strength allows the shaft to withstand the force experienced when reaming with large reamer heads [15]. Once attached to the power unit, a front cutting reamer head is passed over the guidewire and reaming begins to enlarge the medullary canal.

The reamer head (Figure 3c) is the main component of the reamer system that executes the enlarging of the medullary canal. The design of the reamer head is imperative to its performance; the device should be hollow and have deep, spiral cutting flutes that help to drive debris backwards behind the reamer to avoid clogging at the cutting edge [15]. The reamer head is typically passed once through the canal before being removed and replaced with a reamer of a larger diameter, typically in 0.5 mm increments. Reaming proceeds until the surgeon perceives the phenomenon known as chatter. The acknowledgment of cortical chatter is a subjective event when the operator perceives the reamer vibrating and can hear the reamer cut the cortical bone within the bone shaft. Chatter is used as an indicator as to how large the canal should be reamed; it is assumed that at this point the intramedullary nail will substantially contact the inner canal walls [16]. Following the onset of chatter during surgery, the canal would typically be reamed 1 to 1.5mm beyond where chatter was heard in order to accommodate a larger, more stable implant [17]. It is suggested that the canal be reamed to be 1mm larger than the diameter of the IM nail that is to be implanted [5, 17].

## **4. POTENTIAL COMPLICATIONS OF INTRAMEDULLARY REAMING**

### **4.1 INTRAMEDULLARY PRESSURE INCREASE**

It has been well documented in literature that intramedullary reaming can cause an increase in intramedullary pressure. When an object (such as an awl, guidewire, reamer or nail) is inserted into the medullary canal, bone marrow volume is displaced as described by Pascal's Law of transmission of fluid pressure, and the pressure within the canal is elevated [18]. To overcome this, medullary contents decompress through the fracture line, insertion site or outward into systemic circulation [19]. The correlation between elevated intramedullary pressure and fat embolism has been demonstrated via intraoperative transoesophageal echocardiography and histological analysis in animal studies; such analysis determined that emboli tend to increase in size and number with increasing medullary pressure [20]. Medullary content that is forced into systemic circulation has the potential to cause mechanical occlusion of the pulmonary vessels, disrupt blood flow and increase pulmonary vascular resistance which can lead to pulmonary embolism [18].

Acknowledging the correlation between intramedullary pressure and embolism, there is clinical concern regarding the magnitude of pressure increase during intramedullary reaming. The magnitude of the intramedullary pressure elevation is dependent on patient specific factors and surgical technique. The native geometry of the bone, the fracture type and location, and the patient's overall pulmonary and circulatory health influence the IM pressure increase and subsequent systemic risks [18]. Technique specific factors include compressive loading on the reamer, quality of the cutting edge and speed of reamer rotation. Increased compressive loading and dull, worn reamer teeth both can significantly contribute to increased intramedullary pressure [18, 21-23], while increasing rotational speed during advancement may help prevent IM pressure elevation [15, 24].

## 4.2 INTRAMEDULLARY TEMPERATURE INCREASE

Another potentially harmful effect of intramedullary reaming is the generation of heat within the bone cavity that can result in irreversible bone cell death known as thermal necrosis. The destruction of viable bone cells and tissue hinders the proper healing of the fracture. Previous literature has discussed that the threshold for irreversible thermal damage to bone is dependent on both the temperature and the amount of time the tissue is exposed to heat, but thermal necrosis has been microscopically visible after tissue exposure to 47 degrees C for one minute [25, 26]. Heat generation during reaming of the medullary canal has been theoretically estimated using heat conduction equations and simplified models of the bone reamer system [27]. These models demonstrated the correlation between surgical technique and heat generation. Similar to intramedullary pressure increases, poor reamer quality and increased compressive force theoretically result in elevated intramedullary temperatures. This was mathematically demonstrated by Baumgart et al.; the frictional energy generated due to translational advancement of the reamer,  $w$ , increases with increasing axial compression through the relationship described in Equation 1 [27].

Subsequent animal studies in canine and porcine models have also demonstrated the importance of the appropriate sized reamers specific to the bone geometry, as well as the importance of reamer quality in minimizing the generation of heat during reaming [28, 29]. Although multiple studies have reported the magnitude of temperature elevation under normal reaming conditions via the insertion of thermocouples, there have been several limitations identified with such protocols due to their invasive nature and limited positioning options of the measurement devices [30]. As of late, a reliable, validated and non-invasive testing method for accurately measuring intracortical temperature does not exist [17].

$$\text{Frictional energy, } w = \tau v = \mu \sigma v = \mu v \frac{F}{A}, \text{ where:} \quad [\text{Eq. 1}]$$

$\mu$  = coefficient of friction

$v$  = relative velocity of reamer advancement

$\tau$  = shear stress

$\sigma$  = compressive stress

$F$  = axial force

$A$  = contact area

### 4.3 VASCULAR DAMAGE

The endosteal blood supply of the inner bone cortex is severely damaged if not entirely destroyed during an IM reaming procedure due to contact with the reamer [31, 32]. As a result, there are concerns regarding change and impairment in cortical blood flow and the subsequent effects on fracture healing and the prevention of bone necrosis. A 70% reduction in cortical blood supply has been reported following intramedullary reaming, compared to a 30% reduction when reaming was not used [31]. The magnitude of vessel damage is proportional to the extent of intramedullary reaming [32]. Although initially destroyed, the blood supply increases six weeks following the reaming procedure and regenerates almost entirely within twelve weeks [33, 34].

## 5. PREVIOUS INVESTIGATIONS OF REAMER CUTTING MECHANICS

Much of the scientific and technological research regarding intramedullary reaming has been focused on the main concerns regarding the procedure, including intramedullary pressure and temperature elevations [15, 18-24, 27-40]. There is also abundant literature regarding the investigation of the autografting effect and clinical outcomes following intramedullary nailing with reaming [8, 11, 12, 17, 41-43]. However, the study of IM reamer cutting mechanics and the

development of improved technology to analyze these mechanics have been completed by only a few [21, 44, 45].

The compressive force exerted by the surgeon during intramedullary reaming was first reported in 1993 by Müller et al. [21]. The purpose of the study was to investigate the relationship between the axial compression applied by the surgeon and resulting changes in intramedullary pressure. Polyurethane femora were used to determine typical compressive forces applied during reaming when performed by five surgeons. Human cadaveric femora that had been hydrogenated for 24 hours in a saline solution were also reamed to determine if the polyurethane femora were appropriate analogs for analyzing axial reaming mechanics, as well as measuring intramedullary pressure. Reaming proceeded with the specimen housed in a 37°C water bath.

Axial compression was measured by affixing strain gauges to a clamp which secured the femur. Pressure was measured in the human femora through the insertion of water-filled tubes through the cortex in the mid-diaphysis and the metaphysis. A piezoresistive pressure transducer was attached to the tube to determine changes in intramedullary pressure. The results of this study demonstrated an increase in intramedullary pressure with increasing axial compression, which was significantly pronounced for the smaller reamer heads (9mm to 11mm). Specifically, it was reported that an increase in axial compression of 1.8 times results in a 4.7 and 3.1 magnitude increase in the mid-diaphyseal and metaphyseal pressures, respectively. Therefore, delicate reaming can lead to a 79% reduction in intramedullary pressure in the diaphysis and a 68% reduction in the metaphysis [21]. This study did not measure torsional forces and did not remark on the rotational speed used during reaming.

Acknowledging the lack of reported data regarding cutting forces and torques that occur during the intramedullary reaming procedure, Peindl et al. designed a biomechanical study that

assessed these parameters for several typical IM reaming systems [44]. Reamer heads (9mm – 14mm) from Howmedica, Smith & Nephew, Synthes and Zimmer were acquired and a vertical milling machine was instrumented with a stepper motor, a linear variable displacement transducer (LVDT) and a load transducer to control the feed rate of the reamer and measure the outcomes. This study specifically analyzed the relationship between the reamer head design and the cutting mechanics; therefore each reamer head was attached to an identical, solid reamer shaft to eliminate differences due to shaft variability. Each reamer set was tested in three hard oak blocks that were pre-reamed with an 8.5mm diameter canal to simulate the intramedullary cavity. The canal was not lubricated in order maintain consistency between samples. Advancement rates of 1.0 and 7.6 cm/sec and rotational speeds of 250 and 750 RPM were utilized to study the effect of feed rate and drilling speed on the cutting mechanics.

The authors reported significantly higher axial and torsional loads when advancing at 7.6 cm/sec compared to advancing at 1.0 cm/sec. Increasing the rotational speed of the reamer did not result in significant differences in the maximum axial load, but the mean axial and torsional loads were significantly reduced for the smaller reamer heads at this speed. The maximum axial load generally decreased with increasing reamer head size, while the maximum torque remained relatively stable or slightly increased with increasing reamer head size. With regard to reamer head design, the results of this study suggest that a front-cutting, long-tapered head that is capable of self-centering is optimal for dynamic stability of the intramedullary reamer.

Research has also contributed to the development of specialized tools that can be used to measure the mechanics of reaming in various ways. For example, Ho et al. developed a specialized guidewire containing MEMS sensors capable of measuring and wirelessly transmitting temperature, force and pressure information during reaming [45]. This design eliminates the need to mount the bone to transducers or create holes for the insertion of sensors. The initial design of the guidewire was capable of measuring pressure, but was

designed to later incorporate additional sensors for measuring temperature and force simultaneously.

A miniature piezoresistive pressure transducer was encased in the tip of a guidewire and a specialized bearing signal transmission system was created to supply power to the instrument and transmit the information. In a subsequent experiment by the same group, polyvinylidene fluoride (PVDF) piezoelectric rate-of-force sensors were created to eventually be integrated into the guidewire system. An x-y positioning table (intended to eventually to be replaced by a computer controlled reaming system) was controlled by a force-reflection joystick via the internet to cause contact between the PVDF sensor and a vibrating beam. The force on the sensor as a result of contact was then transmitted over the internet from Hong Kong to Michigan, where the force was played back by the force-reflection joystick. These specialized sensors have applications in reaming research and robotic, telemetric surgery and haptics, although reaming research has yet to be completed using this tool. Developing medical tools that are capable of sensing the local environment and providing feedback to the surgeon throughout the procedure will help to reduce adverse events and help control certain aspects of the operation.

## **6. SPECIFIC AIMS**

### **6.1 AIM 1**

*Characterize the cutting mechanics of intramedullary reaming in cadaveric tibial specimens using a novel handheld reamer evaluation system and provide a range of loading conditions for several reamer sizes to support product development initiatives.*

Assessing the axial and torsional loads experienced during reaming in long bone is imperative for the development of product specifications for new, future intramedullary reamer systems. Such information can provide insight to design requirements including compressive



strength, compressive modulus, torsional strength and torsional rigidity for new reamer head and reamer shaft designs. This information can also help determine safe loading thresholds for reaming and could be used in the future to provide real-time, visual feedback of loading conditions in the operating room to help surgeons remain within safe conditions.

## **6.2 AIM 2**

*Assess reaming mechanics when performed by two operators of different experience levels, and determine if there is a mechanical difference in the execution of the reaming procedure.*

It is of interest to examine the human factors affecting the reaming procedure and how such factors vary between operators. In this experiment, the reaming procedure was performed by an experienced trauma surgeon and a second year orthopaedic resident. It was hypothesized that differences in experience level would not affect reaming mechanics.

## **6.3 AIM 3**

*Assess how reaming mechanics change between the reamer sizes associated with chatter and the largest reamer size used after the declaration of chatter. Additionally, analyze the outcomes to determine if there is mechanical rationale to support the surgeons' acknowledgment of reamer chatter.*

It is of interest to analyze and compare reaming mechanics at two critical events, representing the initial cutting of cortical bone (chatter) and the largest reamer used. Such information also may contribute to determining if there is a quantitative mechanical component, such as an axial force requirement, to accompany the perception of reamer chatter.

## 7. MATERIALS AND METHODS

### 7.1 HANDHELD REAMER EVALUATION SYSTEM

Our lab has modified a handheld electronic surgical power unit (Universal Power System, Zimmer Inc., Warsaw, IN USA) with a 350 RPM Zimmer coupling to include a rotating telemetric load and torque sensor between the power unit and reamer shaft (Figure 4). The intention of the device modification is to quantify the mechanical forces exerted on the reamer

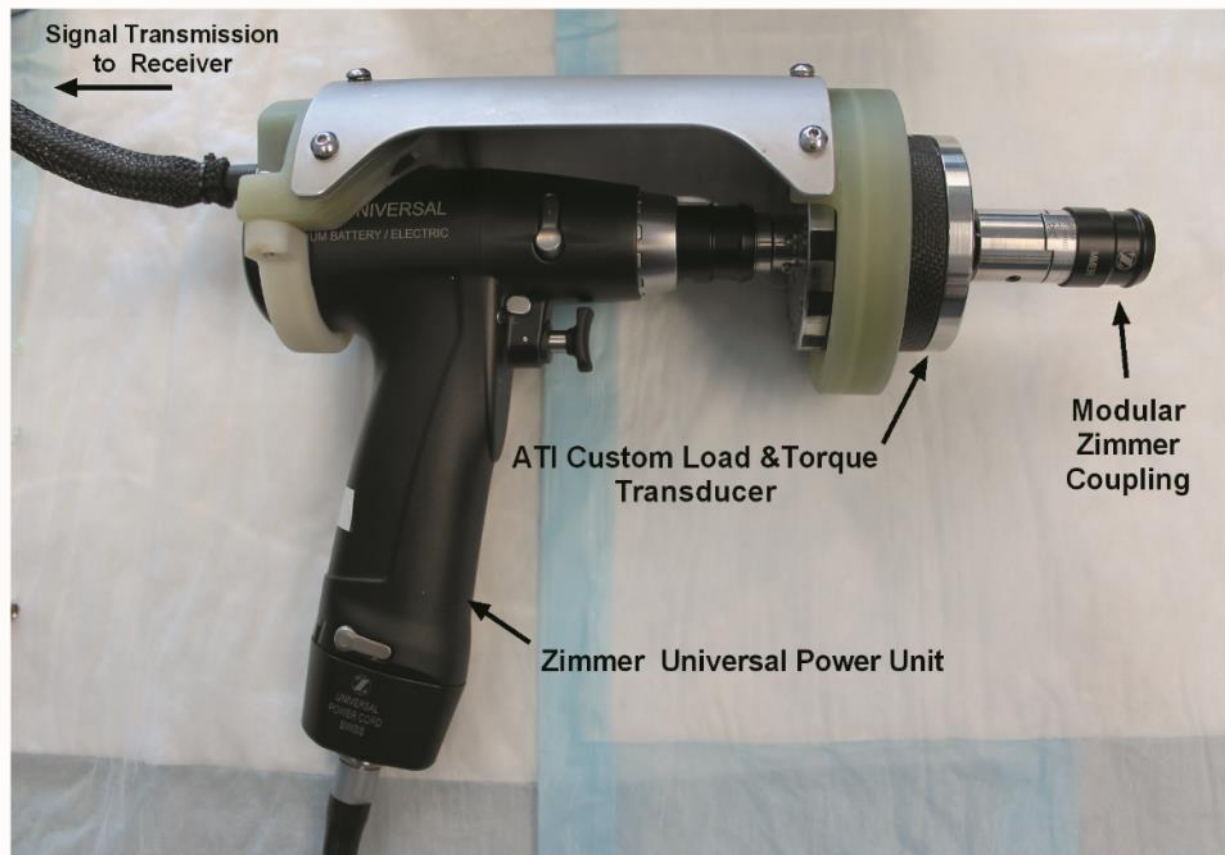


**Figure 4: Handheld Reamer Evaluation System**

and the rotational speed used by the surgeon during a reaming procedure. The custom, dual axis wireless sensor (Advanced Telemetrics International [ATI], Spring Valley, OH USA) contains two strain gauge devices housed within the sensor body that measure rotary torque and axial force. The sensor body also encompasses an optical tachometer to measure rotational speed of the reamer. The sensor unit is inductively powered through the compact

outer housing attached to the surgical power unit, which allows it to rotate freely with the reamer. The sensor unit and corresponding couplings are hollow to allow the passage of the guidewire through the device for intramedullary reaming procedures. The signals are telemetrically transmitted from the sensor to the receiver (Model 3125iR-2, ATI), and the analog outputs are fed into a data acquisition unit (ODAU, Northern Digital, Inc., Waterloo, Ontario CA) and into a motion capture system (Optotrak 3020 Northern Digital, Inc., Waterloo, Ontario CA). The receiver internally filters the signal based on user input; for this study all signals were filtered at 10Hz.

## 7.2 MOTION CAPTURE SYSTEM

The Optotrak 3020 system is capable of capturing the three-dimensional position of infrared emitting markers in real-time using a three lens position sensor. The system displays the marker coordinates and can calculate the relative change in position with respect to the

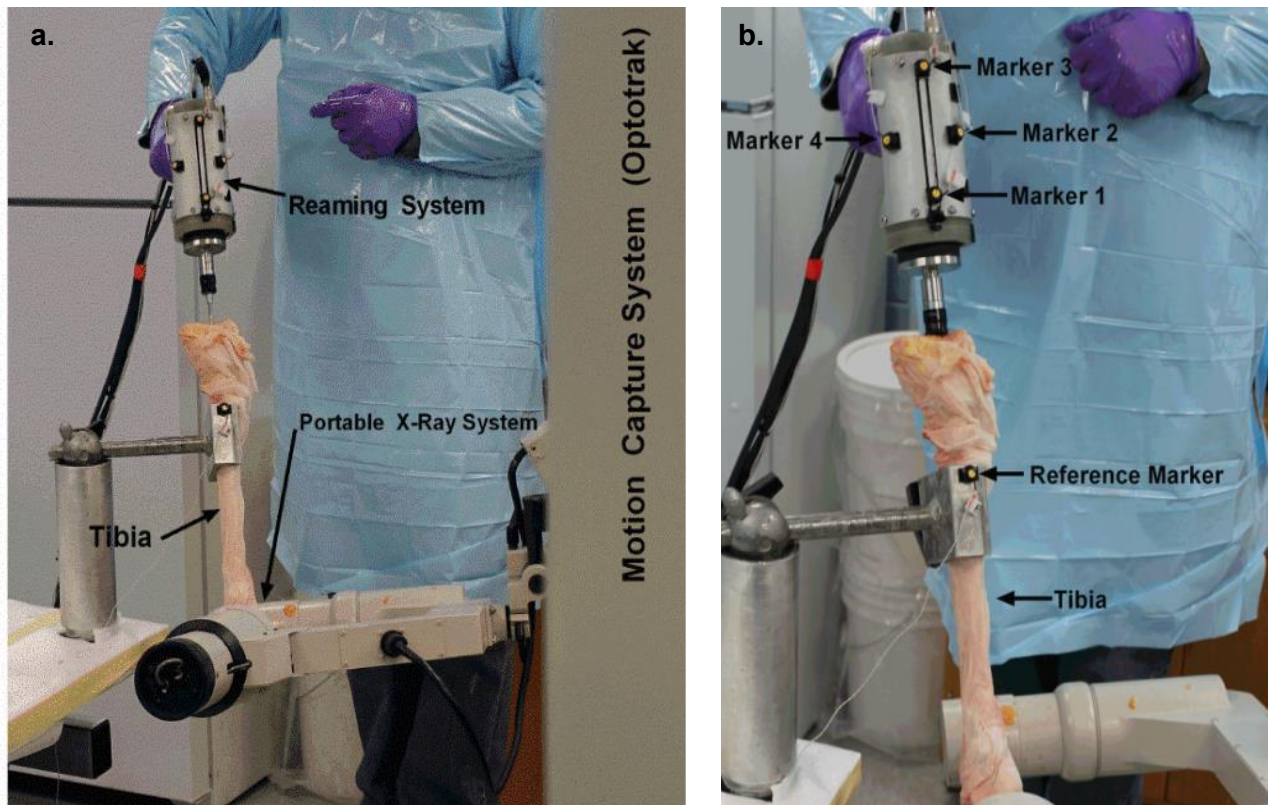


Figure 5: (a) Experimental Set Up (b) Optotrak Reference Markers

sensor or with respect to a fixed marker. For this study, the Optotrak was configured to capture marker positions at a frame rate of 100 Hz and synchronously acquire the mechanical data fed into the data acquisition unit. Four Optotrak markers were affixed to the top of the reaming unit and one marker was attached to the jig in which the bone was held (Figure 5). The system was configured to calculate the shortest distance between the markers on the reaming unit and the fixed marker on the jig.

### 7.3 REAMERS

A set of side-cutting, modular intramedullary reamer heads sizes 9.5mm through 14mm in half millimeter increments, a front cutting 9mm reamer and a modular Nitinol reamer shaft were acquired (Figure 6, Intramedullary Flexible Reamer, MPS Precimed, Corgémont Switzerland). The reamer heads are made of 420 Stainless Steel with a Titanium-Nitride coating. The teeth are reverse cutting to help retract the reamer from the canal.

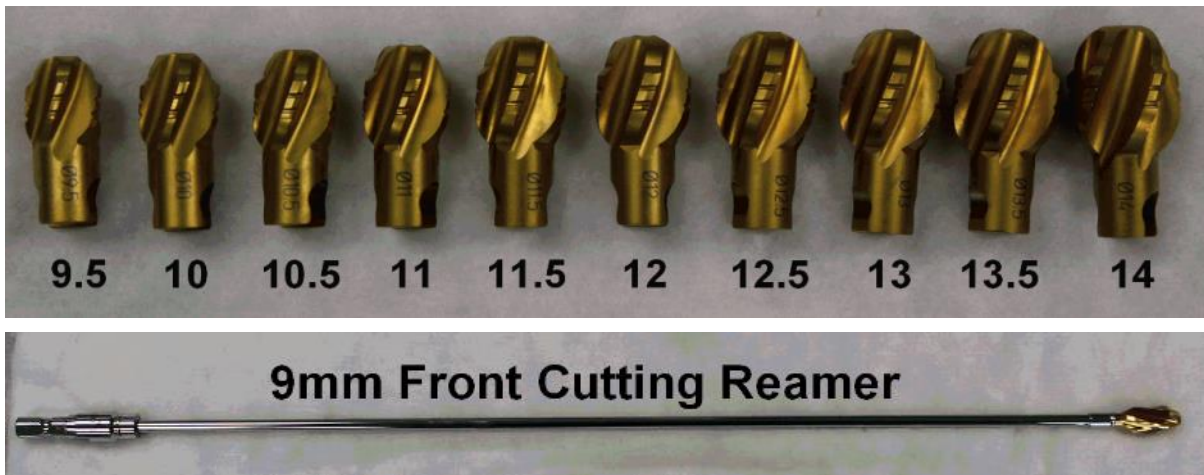


Figure 6: MPS Precimed Intramedullary Reamer Set

### 7.4 SPECIMEN COLLECTION AND PREPARATION

Five male and five female tibial pairs (mean age at death =  $81.7 \pm 5.56$  years) were harvested from fresh cadavers under IRB approval at the University at Buffalo. Cadavers were placed in the supine position and the patella and vastus medialis were identified. A deep

incision was made from the medial border of the patella to the center of the ankle along the anterior border of the tibia. The ligamentous structures of the knee and the soft tissue surrounding the tibia were sharply dissected away from the bone. The proximal and distal tibiofibular joints as well as the interosseous membrane and the capsular structures of the ankle were divided and the tibia was removed. Cotton mesh cloth soaked in a saline solution was wrapped around the entirety of the bone and the specimen was sealed in plastic and stored in a freezer until use. Prior to reaming, anterior-posterior and lateral x-ray images of the bones were obtained for reference.

## 7.5 REAMING PROCEDURE

All specimens were removed from the freezer and thawed at room temperature for approximately 18 hours prior to beginning the experiment. The tibia was secured in a jig at an orientation approximately 60 degrees with respect to the horizontal, as shown in Figure 7. A standard industrial electric drill was used to create an 11/32 inch diameter hole in the anterior tibial plateau between the lateral and medial tibial spines to gain access to the intramedullary canal. The 2mm diameter guidewire was inserted into the canal and secured into the distal epiphysis of the bone, after which its placement was confirmed via radiograph.

Reaming began with a 9mm front-cutting reamer, after which reaming proceeded with side-cutting reamers with increasing diameters in 0.5mm increments. Prior to advancement down the



**Figure 7: Tibia Orientation in Jig**



canal, each reamer head was submerged just below the surface of the tibial plateau, and the operator spun the reamer at maximum speed for approximately two seconds without applying compressive force in order to record residual load and torque due to weight and orientation of the device. Reaming proceeded 1.5mm beyond the acknowledgment of audible chatter, which was declared aloud by the operator and recorded, or until the 14mm diameter reamer was used. During each pass of the reamer, axial force, torque, rotational speed and position of the Optotrak markers were collected for the entirety of the procedure. Following use, the reamers and shaft were rinsed and brush-cleaned with a soap solution and dried. Each operator reamed one bone of each matched pair and specimen order for each operator was selected via random number generation using Excel. Operators were blind to specimen information for the duration of data collection.

## 7.6 DATA ANALYSIS

The axial force, rotary torque and rotational speed data was collected at 100 Hz in Optotrak and saved to a text file for each reamer. Microsoft Excel was used to convert the data from the raw signal (V) to the correct units based on calibration data provided by the sensor manufacturer as described in Equations 2 through 4.

$$\text{Axial Force: } 0.00 - 50.00 \text{ kg} = 0.00 - 10.00 \text{ V}, 37.186 \text{ kg} = 7.437 \text{ V} \quad [\text{Eq. 2}]$$

$$\text{Rotary Torque: } 0.00 - 20.00 \text{ Nm} = 0.00 - 10.00 \text{ V}, 9.539 \text{ Nm} = 4.770 \text{ V} \quad [\text{Eq. 3}]$$

$$\text{RPM: } 0 - 500 \text{ RPM} = 0.00 - 10.00 \text{ V} \quad [\text{Eq. 4}]$$

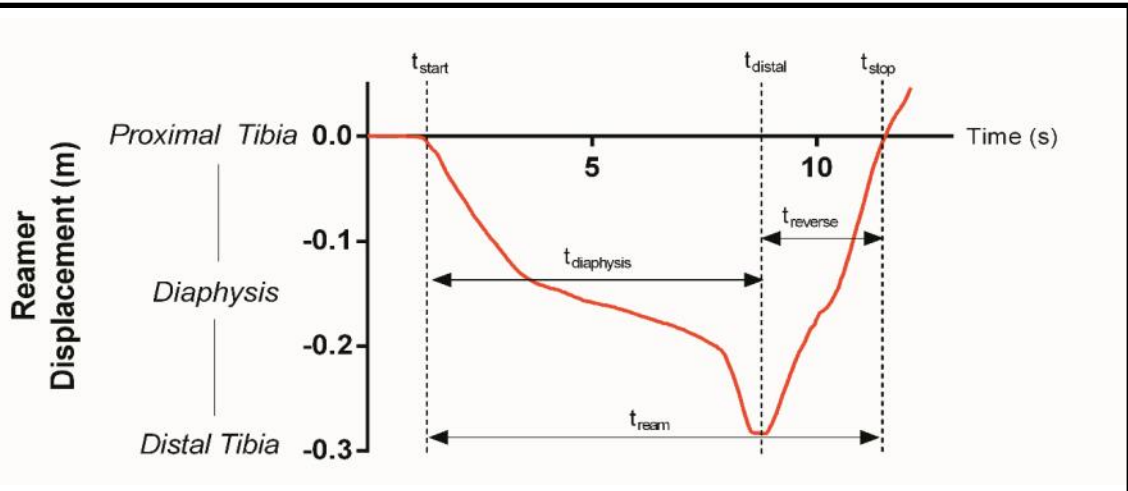
The mechanical data acquired in Optotrak required normalization to account for the inherent weight and the orientation of the sensor in space once in the operators' hands. The first 100 data points (1 second) of the load, torque and rotational speed data were separately averaged and the signals were adjusted by each amount, respectively. The calculated distance between Marker 1 and the reference marker was used to determine the displacement of the reamer over time (Figure 8).

From the displacement versus time curve for each reamer, the time in which the reamer began moving in the proximal tibia was identified as  $t_{start}$ . The minimum point of this curve, indicating maximum reamer displacement, was identified as  $t_{distal}$  as at this point the reamer had reached the distal tibia. The time frame between  $t_{start}$  and  $t_{distal}$  was termed  $t_{diaphysis}$ , as during this time frame the reamer was traveling from the proximal tibia to the distal tibia through the intramedullary canal in the diaphysis. Near the location of maximum displacement, the reamer tended to remain stagnant for a short period, indicated by the flat portion at the minimum point of the displacement versus time curve.

When a drastic change in slope was demonstrated in the displacement versus time curve immediately prior to the location of maximum displacement, it was assumed that at this point the reamer exited the diaphysis and entered the distal epiphysis of the bone. The intramedullary canal tapers outward at this portion of the bone, and therefore less resistance was felt by the reamer and the operator, allowing it to displace faster. The time at which the reamer returned to the starting position, or proximal tibia, was identified and termed  $t_{stop}$ . The time frame in which the reamer traveled back through the diaphysis was termed  $t_{reverse}$ . Lastly, the time from the initial movement of the reamer at the proximal tibia to the return of the reamer to the proximal tibia was termed the reaming window,  $t_{ream}$ . Further data analysis proceeded only within the identified reaming window,  $t_{ream}$ , or only within the diaphysis,  $t_{diaphysis}$ .

Measured outcomes for each reamer included maximum axial force in the diaphysis and in the reaming window, maximum torque in the diaphysis, work to travel through the diaphysis and time to travel through the diaphysis. Maximum axial force in the diaphysis and maximum torque in the diaphysis were identified prior to the stationary position of the reamer on the displacement versus time curve, as at this location the reamer was no longer in the intramedullary canal. Axial force and torque were graphed as a function of time and as a function of reamer displacement (Figures 9-12). Work to travel through the diaphysis was calculated using Equation 5 and was graphed as a function of displacement (Figure 13). This analysis was repeated for all reamer sizes used in each bone. Three of the ten tibial pairs were excluded from data analysis due to unforeseen difficulties during data collection and problems encountered during the reaming procedure.





Time / Location	Description	Equivalent Equation
<i>Proximal Tibia</i>	Starting location of reamer	
$t_{start}$	Time at which reamer began moving	
<i>Distal Tibia</i>	Location of max. reamer displacement	
$t_{distal}$	Time at which reamer reached the distal tibia	
<i>Diaphysis</i>	Segment between proximal and distal tibia	
$t_{diaphysis}$	Time for reamer to travel through diaphysis	$t_{distal} - t_{start}$
$t_{stop}$	Time at which reamer returned to starting position	
$t_{reverse}$	Time for reamer to withdraw from diaphysis	$t_{stop} - t_{distal}$
$t_{ream}$	Time for complete pass of reamer from start to finish	$t_{stop} - t_{start}$

**Figure 8: Example of Reamer Displacement vs. Time Curve**

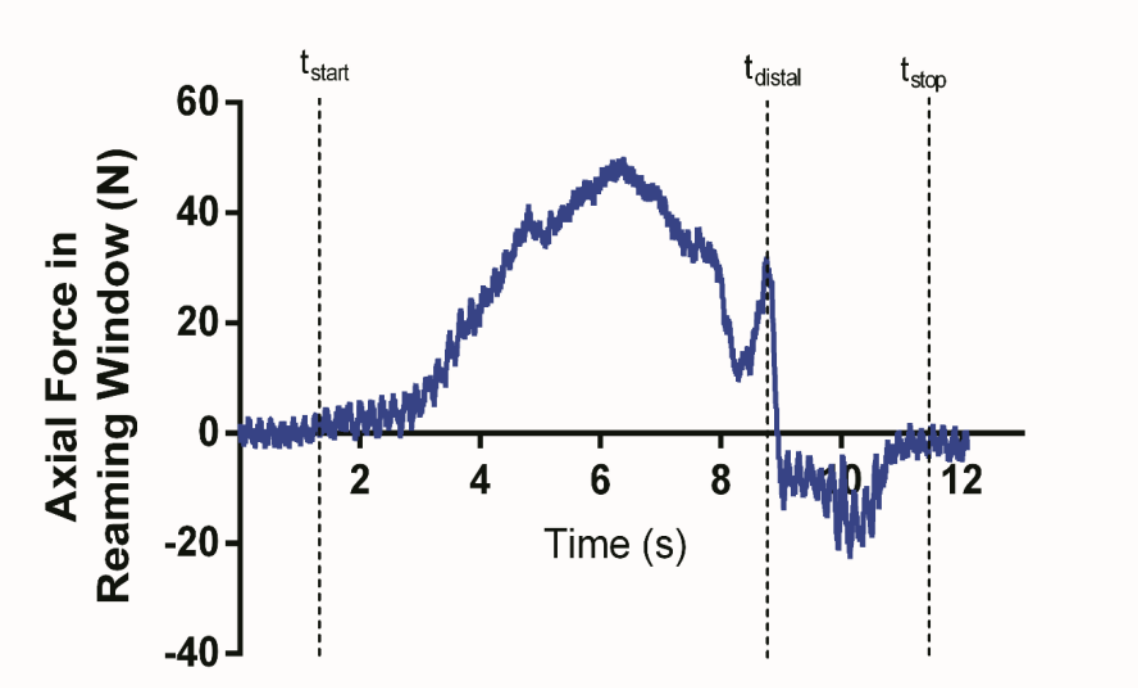


Figure 9: Example of Axial Force vs. Time in Reaming Window

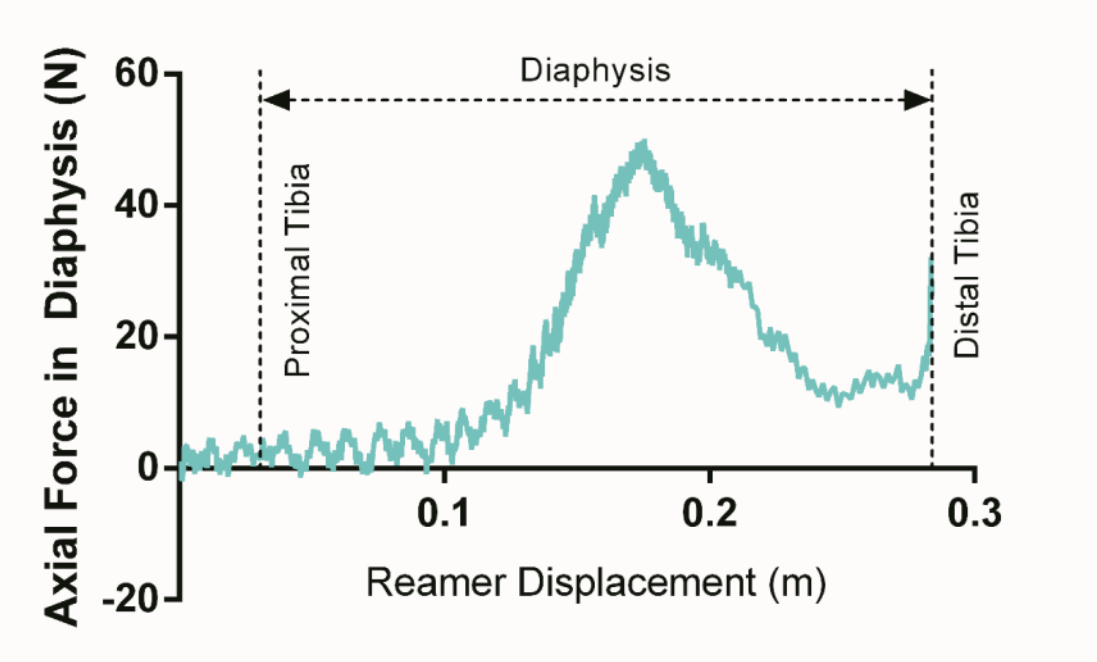


Figure 10: Example of Axial Force vs. Displacement in Diaphysis

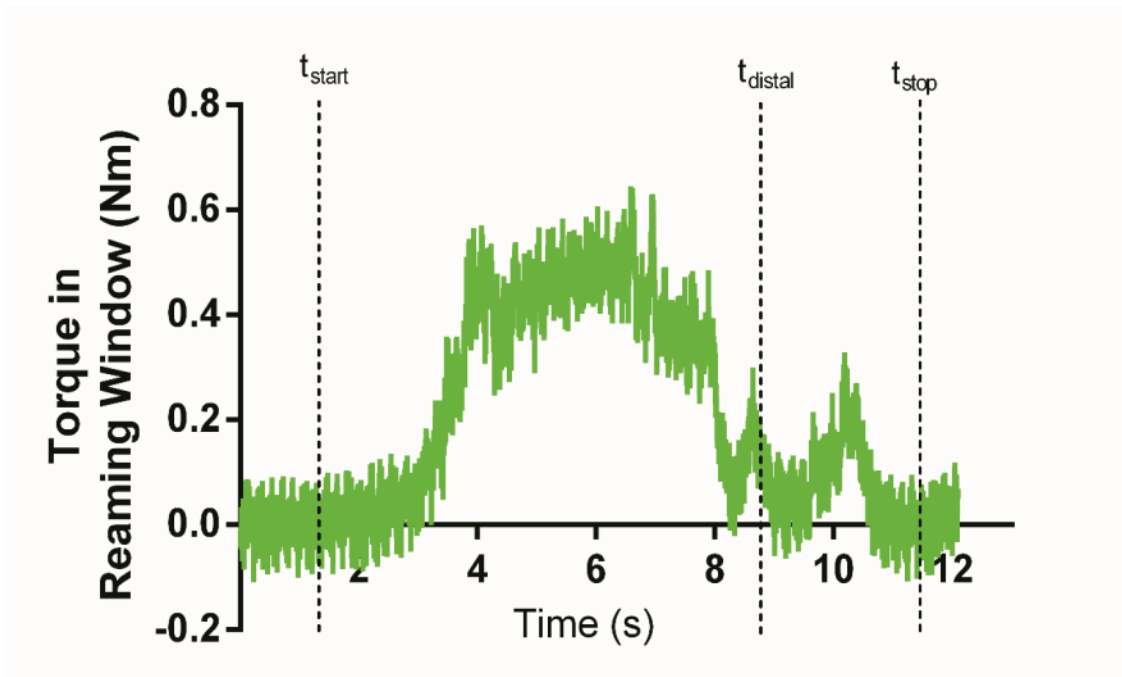


Figure 11: Example of Torque vs. Time in Reaming Window

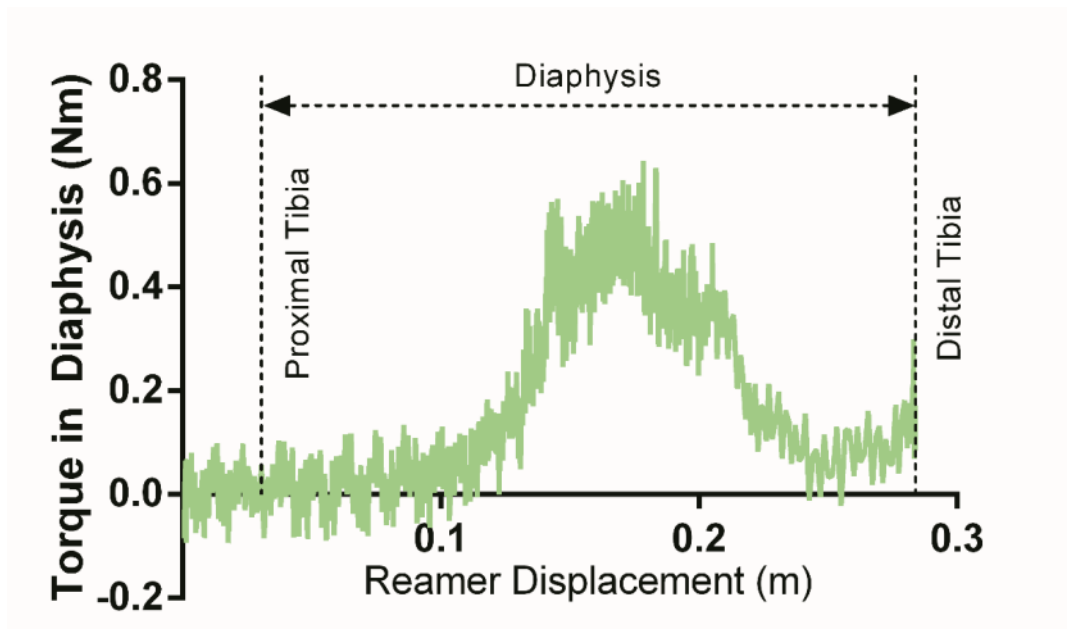


Figure 12: Example of Torque vs. Displacement in Diaphysis

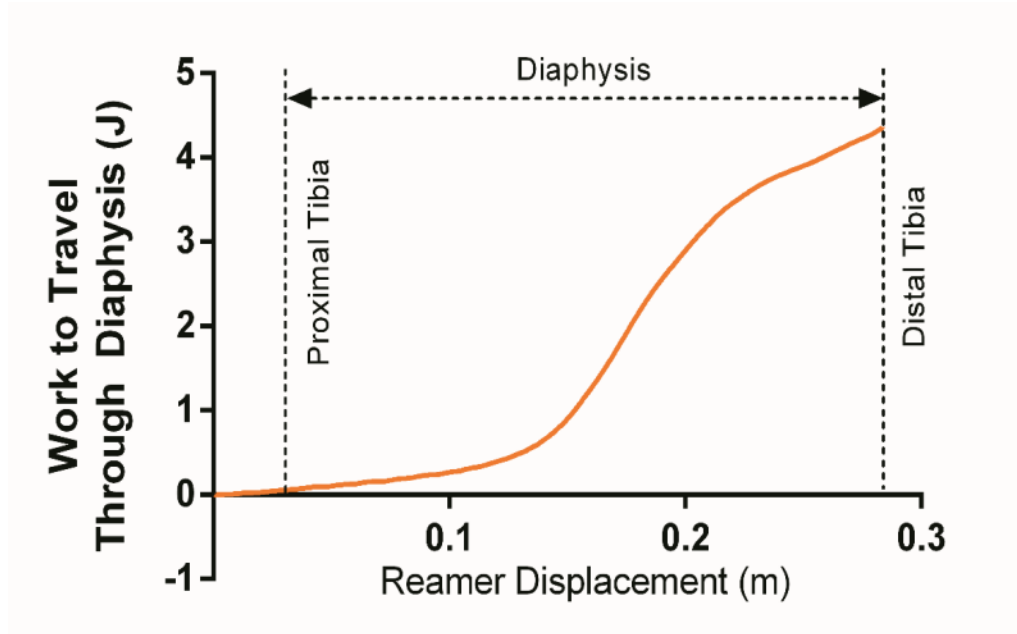


Figure 13: Example of Work to Travel through Diaphysis vs. Displacement

$$Work = \int_a^b F(x)dx \approx \lim \sum_{k=1}^n F(t_k) \Delta x_k \quad [\text{Eq. 5}]$$

where  $t_k = (x_{k-1}, x_k)$

## 7.7 STATISTICAL ANALYSIS

Reaming mechanics were compared at two distinct events: at the reamer size associated with chatter and at the maximum reamer size above chatter, i.e. the last reamer used. Two-tailed, paired T-tests were performed in Microsoft Excel to compare the mechanics between operators at both events and to compare events within individual operators. Mechanics analyzed at these events included maximum axial force and maximum torque in the diaphysis prior to reaching the distal end, work to travel through the diaphysis and time to travel through the diaphysis. Statistically significant differences were defined as  $p < 0.05$ .

## 8. RESULTS

### 8.1 GENERAL CHARACTERIZATION OF REAMING MECHANICS

Reamer Size (mm)	Overall Maximum Axial Force (N)	Maximum Axial Force in Diaphysis (N)	Maximum Torque in Diaphysis (Nm)	Overall Maximum Tensile Force (N)	Time to Travel through Diaphysis (s)	N
9	21.46 – 80.11	9.88 – 43.24	0.123 – 0.811	6.06 – 23.93	3.79 – 9.22	14
9.5	32.13 – 98.36	7.18 – 52.56	0.211 – 0.670	7.80 – 29.11	4.38 – 7.88	14
10	17.60 – 78.34	7.69 – 66.13	0.137 – 0.786	7.80 – 30.68	3.67 – 8.35	14
10.5	19.78 – 82.67	6.99 – 82.67	0.141 – 1.139	7.15 – 31.60	4.32 – 11.56	14
11	22.47 – 77.14	7.28 – 71.45	0.157 – 0.960	9.29 – 49.26	3.27 – 12.95	14
11.5	23.60 – 87.99	8.78 – 87.99	0.192 – 1.048	7.70 – 31.88	3.83 – 15.13	11
12	23.91 – 59.85	11.26 – 59.85	0.225 – 0.827	9.98 – 24.07	4.48 – 11.48	10
12.5	30.32 – 86.77	13.04 – 35.45	0.223 – 0.601	10.67 – 21.40	4.84 – 8.31	8
13	22.86 – 72.84	16.42 – 58.26	0.294 – 0.742	11.87 – 24.64	5.19 – 7.76	8
13.5	26.41 – 92.47	23.04 – 67.12	0.353 – 1.314	13.89 – 26.77	4.85 – 12.78	7
14	36.90 – 88.79	36.90 – 88.79	0.489 – 0.982	14.27 – 22.83	6.23 – 10.57	4

**Table 1: Ranges of maximum axial force, torque, tensile force and time to ream through diaphysis for each reamer size tested.**

Table 1 reports the range of maximum compressive and tensile forces, torques and times to ream through the diaphysis for each reamer size. The reported ranges are operator independent; therefore the reported values were determined using both Operator A and Operator B data, combined.

## 8.2 OPERATOR DIFFERENCES AND CHANGES IN MECHANICS FROM THE REAMER ASSOCIATED WITH INITIAL CHATTER ACKNOWLEDGMENT TO THE LARGEST REAMER USED

	Operator A (Resident)	Operator B (Attending)	P-value
<b>Axial Force in Diaphysis (N)</b>			
At Chatter	30.23 ± 8.62	22.49 ± 14.28	0.068
Last Reamer Post Chatter	63.95 ± 18.15	45.56 ± 18.16	0.035
P-value	0.002	0.002	
<b>Torque in Diaphysis (Nm)</b>			
At Chatter	0.61 ± 0.27	0.36 ± 0.15	0.062
Last Reamer Post Chatter	0.87 ± 0.18	0.72 ± 0.18	0.109
P-value	0.056	<0.001	
<b>Work to Travel Through Diaphysis (J)</b>			
At Chatter	2.63 ± 1.01	2.43 ± 1.39	0.578
Last Reamer Post Chatter	5.60 ± 1.64	4.52 ± 2.11	0.127
P-value	0.002	0.003	
<b>Time to Travel Through Diaphysis (s)</b>			
At Chatter	5.89 ± 0.70	5.47 ± 1.10	0.086
Last Reamer Post Chatter	10.73 ± 2.84	10.20 ± 2.61	0.506
P-value	0.005	0.002	

**Table 2: Mechanics for each operator at chatter acknowledge and at the last reamer used.**

Table 2 reports the mean maximum axial force, maximum torque, work to travel through the diaphysis and time to travel through the diaphysis for each operator when they declared chatter and at the maximum reamer size after which chatter was declared (last reamer). P-values are included to report the results from the paired t-tests used to compare mechanics

between operators at chatter acknowledgement and at last reamer used, and to compare the mechanics for each operator individually at chatter and at the last reamer used.

## **9. DISCUSSION**

The purpose of this investigation was to characterize the mechanics of intramedullary reaming in long bone when performed by two operators of different experience levels, both using the same novel reamer evaluation tool. This study aimed to support product development initiatives of new reamer systems by providing a range of loading conditions for several reamer sizes. Additionally, this experiment served to determine if there was a mechanical difference in the execution of the reaming procedure when performed by two operators of different experience levels and assess how reaming mechanics changed between chatter acknowledgment and the last reamer used. Previously, similar experiments analyzed reaming mechanics on the bench or by affixing the bone or substitute material to external sensors to measure such outcomes [21, 44]. This study allowed for the combination of displacement information with in-line mechanics, permitting the additional calculation of work and time to complete the reaming.

Regarding the ranges of reaming mechanics, maximum compressive and tensile forces and torques encountered when reaming have not previously been reported. This information is important for new product development, as it can support the development of design criteria such as compressive strength and modulus, torsional strength, modulus and rigidity for new intramedullary reamer systems. When testing potential new materials or constructs for reamer systems, this information may be beneficial to include in specification requirements for failure mechanics. These data are also valuable for the development of life cycle experiments to analyze the wear of reamers over time under simulated loading conditions, similar to what they would be subject to in the operating room.

This experiment also aimed to determine if the mechanics of reaming were operator dependent. Statistical analysis revealed no significant differences between operators with respect to maximum axial force in the diaphysis, maximum torque in the diaphysis, work to travel through the diaphysis and time to ream through the diaphysis between operators at the reamer sizes in which they declared chatter. This suggests that there may be a mechanical component associated with the declaration of chatter rather than just the audible signals, as both operators applied similar compressive forces ( $30.23 \pm 8.62$  N,  $22.49 \pm 14.28$  N) when they acknowledged chatter. However, this requires additional analysis and a larger sample size to further investigate. At the maximum reamer size beyond chatter, analysis revealed no significant differences between operators with respect to maximum torque, work and time to travel through the diaphysis. However, there was a significant difference between the operators axial force applied at the maximum reamer size. The orthopaedic resident (Operator A), demonstrated a larger mean maximum axial force ( $63.95 \pm 18.15$  N) than the attending surgeon (Operator B,  $45.56 \pm 18.16$  N) after chatter. This difference could possibly be attributed to differences in experience level and extent of training, but again additional experiments with larger sample sizes and operator populations would be required to draw this conclusion.

Lastly, this investigation also intended to determine if and how reaming mechanics vary with increasing reamer sizes. However, it was not possible to directly compare reamer sizes due to variability in sample geometry and quality that hindered the ability to consistently ream up to the same diameter in each sample. Therefore, the data were compared at the reamer size corresponding to the declaration of chatter and at the maximum reamer size above chatter (the last reamer used) with the assumption that, at the point of chatter acknowledgment, the operators felt that it was the first instance in which the reamer was contacting and cutting cortical bone. For each individual operator, there was a significant increase in maximum axial force, work to travel through the diaphysis and time to travel through the diaphysis from the



declaration of chatter to the last reamer used. Operator B demonstrated a significant increase in torque from chatter to completion. Operator A did not exhibit a significant increase. Although not statistically significant ( $p$ -value = 0.056), Operator A's mean maximum torque increased from  $0.61 \pm 0.27$  Nm to  $0.87 \pm 0.18$  Nm.

According to literature [18, 21, 22, 24, 27], an increase in axial compression can result in increased cortical temperature and intramedullary pressure. This study demonstrated increased axial compression and work from the point of chatter to the last reamer used. Although reaming 1mm to 1.5mm beyond the declaration of chatter is a typical practice and allows for the implantation of a larger diameter intramedullary nail, this increase in compression and work could be dangerous to the patient as it could potentially lead to elevated intramedullary pressure and temperature. In this study, the mean maximum axial compression doubled from the point of chatter to the last reamer used for both operators (Operator A:  $30.23 \pm 8.62$  N to  $63.95 \pm 18.15$  N, Operator B:  $22.49 \pm 14.28$  N to  $45.56 \pm 18.16$  N) and based on previous literature, this theoretically should result in a 5.2 magnitude increase in mid-diaphyseal intramedullary pressure [21]. Further experimentation is warranted to analyze how this magnitude of increase in axial compression and work truly affects both intramedullary pressure and cortical temperature by measuring both outcomes in human bone.

## **10. LIMITATIONS**

Various limitations exist in this study, as this is a preliminary evaluation. An IM reaming procedure generally is performed as part of a trauma operation which does not have a typical patient population. This study only assessed the IM reaming procedure in bones harvested from elderly cadavers due to limited specimen availability. In addition, an accurate assessment of bone quality was not performed and therefore variability in bone quality between pairs was not accounted for. However, all bones were harvested from elderly cadavers and therefore were

likely osteoporotic. As the bones were harvested from the cadavers and prepared in the lab, reaming was not performed at physiologic temperature and pressure which may ultimately affect marrow viscosity and marrow movement. Suction and irrigation were not used in order reduce variability between procedures.

Data were compared with respect to the point of audible chatter and last reamer used after the first acknowledgment of chatter. However, as the declaration of chatter is a subjective event, it was assumed that at this point the operator was certain that this was the first instance in which the reamer was contacting the cortical wall of the bone. This subjectivity could be avoided in the future by accurately measuring the dimensions of the bone and intramedullary canal prior to reaming using high-resolution computed tomography in order to estimate which reamer size will be the first to contact the cortical wall.

## **11. CONCLUSION**

In brief, the results of this study suggest that the reaming procedure is generally not operator dependent, although the sample size and number of operators included were likely not large enough to firmly draw this conclusion. It was evident, however, that axial compression, work and time to travel through the diaphysis of the bone increased between initial chatter and the maximum reamer size used, which may be of concern with regard to possible subsequent adverse events including rises in intramedullary pressure and cortical temperature. Further research is required to analyze exactly how intramedullary pressure and temperature will change with various parameters studied using the novel handheld reamer evaluation system.

## **12. FUTURE WORK**

Acknowledging the limitations of this study, there is a multitude of further experiments that can be derived from this current work. It is of interest to understand how the cutting mechanics of reaming influence the well-known complications associated with the procedure.

This study could be replicated with the introduction of additional transducers to record other outcomes including changes in intramedullary pressure and cortical temperature. As previously mentioned, investigations of these relationships have already been performed; however this was not with the variability of manual, human operation and the monitoring of in-line axial and torsional forces.

In vivo animal studies may also be of interest in order to maintain physiologic conditions during the procedure and provide the ability to more accurately measure the quality of bone being reamed. Clinical studies, in which the reaming procedure is performed in the operating room using the novel handheld reamer evaluation system are also possible once particular challenges are overcome. Such challenges include device sterilization, in which the sensors need to be protected from internal damage during traditional sterilization techniques or need to be contained within a sterile drape in the operating room.

Further investigation of the development of other reaming systems and the reaming of other bones can also be performed. This system has the capability to adapt to other systems including acetabular, humeral and glenoid reamers, as well as tunnel reamers for knee ligament reconstruction operations. In addition, new intramedullary reaming systems can be tested to evaluate the effect of design or procedure characteristics, including aspiration and suction of the marrow content of the intramedullary cavity. The handheld reamer evaluation system can be adapted to couple to various power units, including drivers required for the use of the reamer-irrigator-aspirator system.

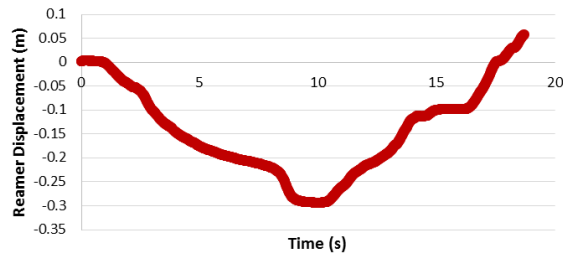
# 13. APPENDIX

## 13.1 SAMPLE 1 RESULTS

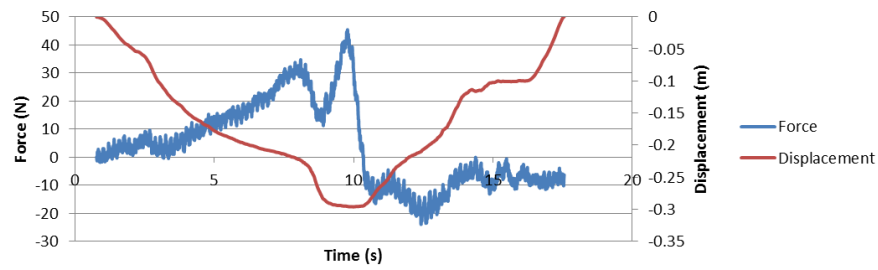
LEFT: ATTENDING

9MM

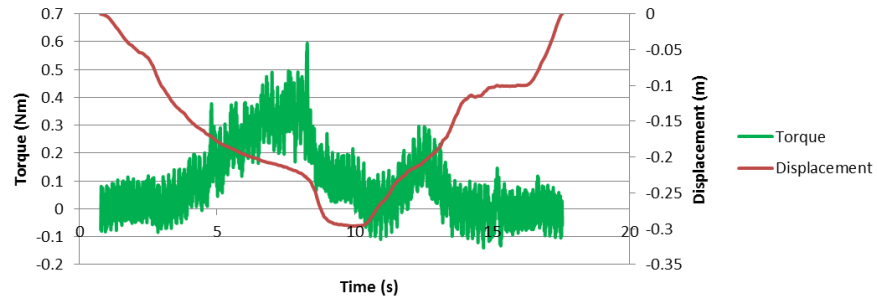
**SAMPLE NO. 1 - Left - Attending:  
9mm**



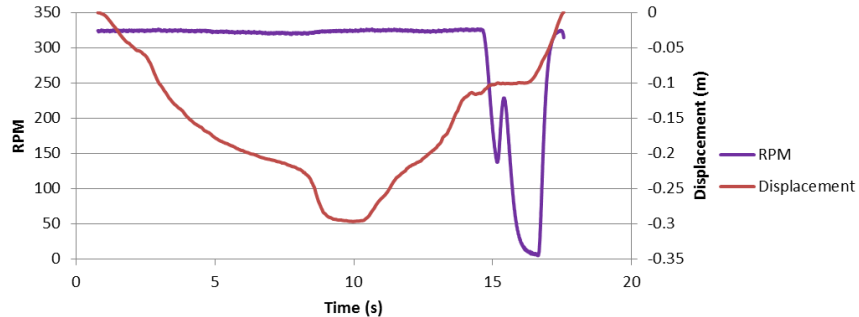
**SAMPLE NO. 1 - Left - Attending: 9mm**



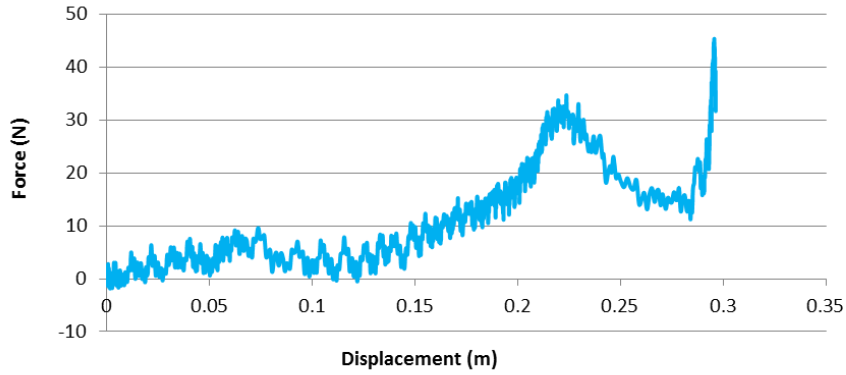
**SAMPLE NO. 1 - Left - Attending: 9mm**



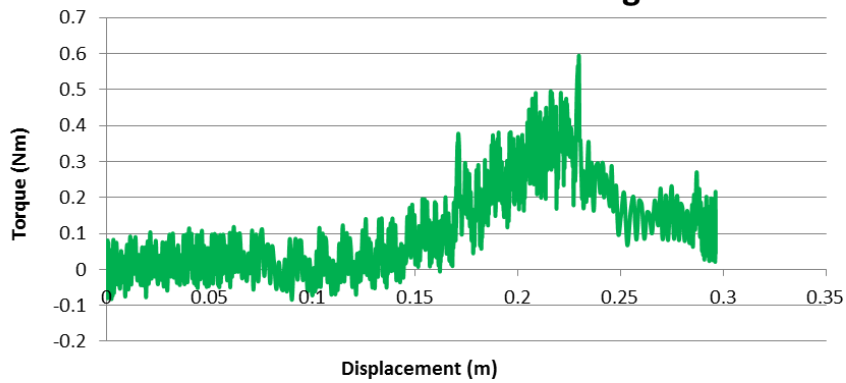
**SAMPLE NO. 1 - Left - Attending: 9mm**



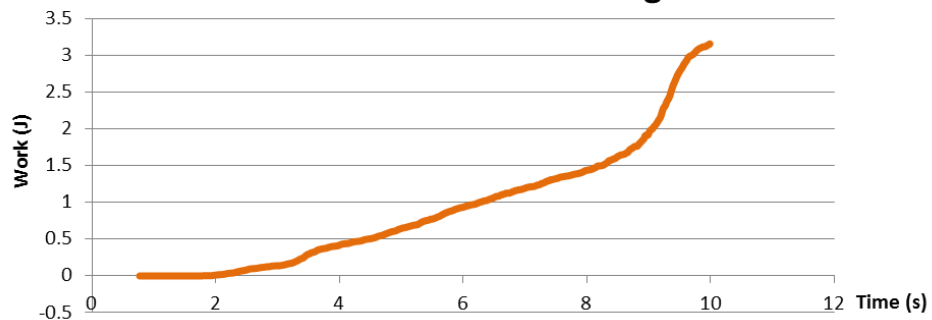
**SAMPLE NO. 1 - Left - Attending: 9mm**



**SAMPLE NO. 1 - Left - Attending: 9mm**

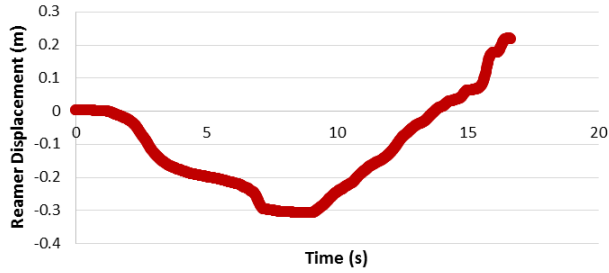


**SAMPLE NO. 1 - Left - Attending: 9mm**

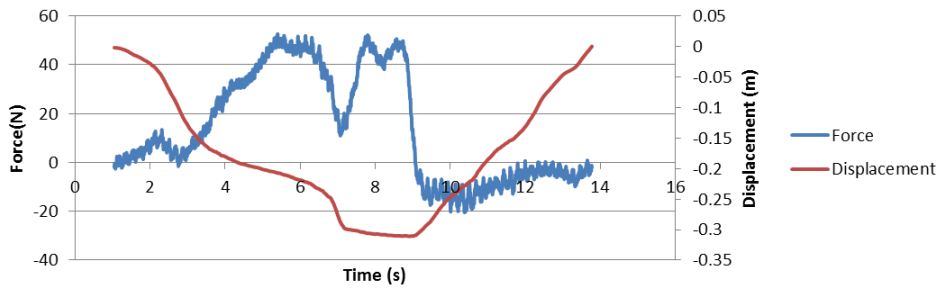


9.5MM

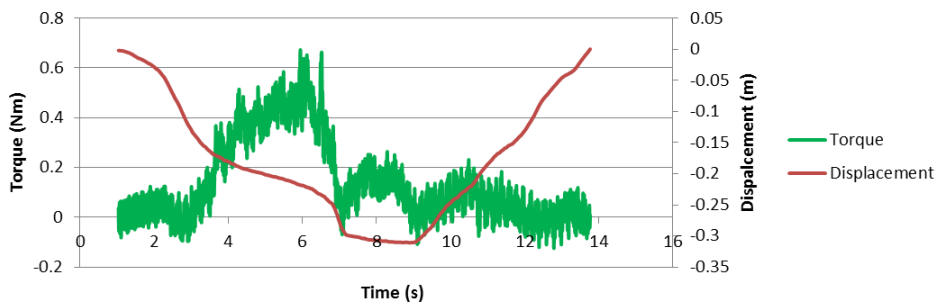
**SAMPLE NO. 1 - Left - Attending:  
9.5mm CHATTER**



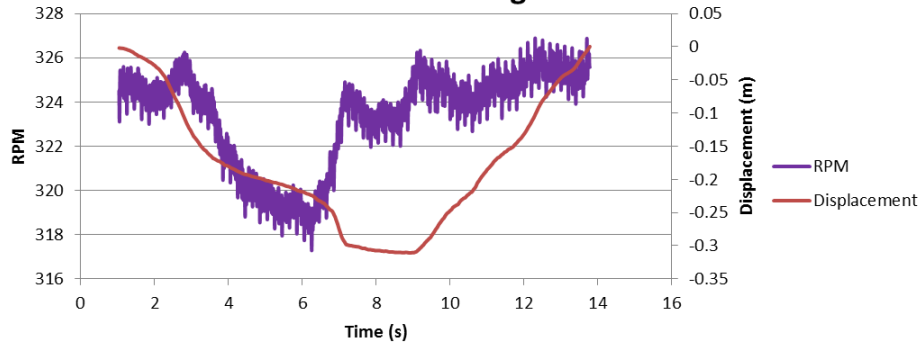
**SAMPLE NO. 1 - Left - Attending: 9.5mm CHATTER**



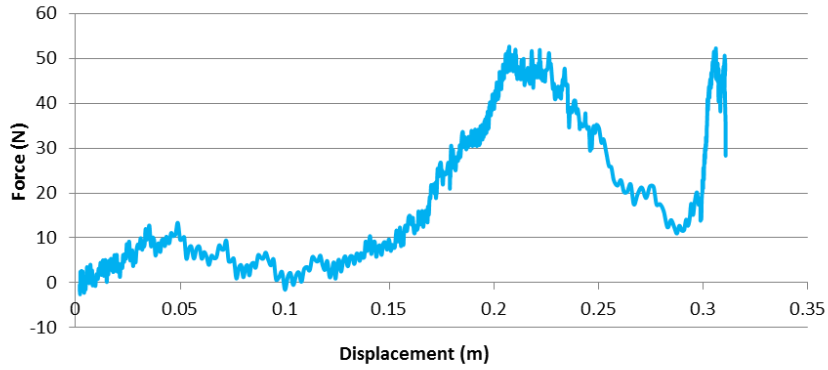
**SAMPLE NO. 1 - Left - Attending: 9.5mm CHATTER**



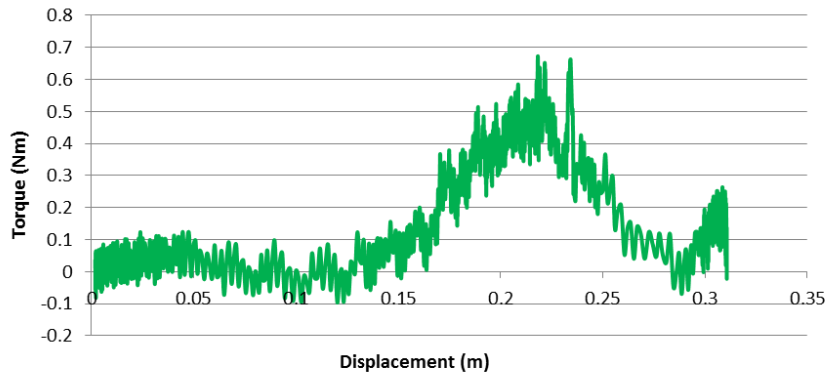
**SAMPLE NO. 1 - Left - Attending: 9.5mm CHATTER**



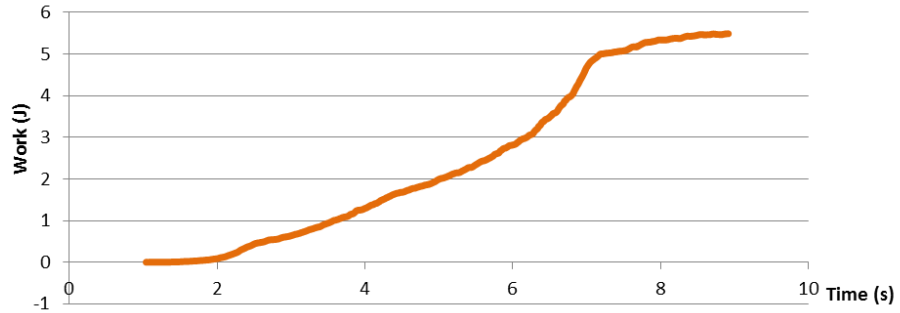
**SAMPLE NO. 1 - Left - Attending: 9.5mm CHATTER**



**SAMPLE NO. 1 - Left - Attending: 9.5mm CHATTER**

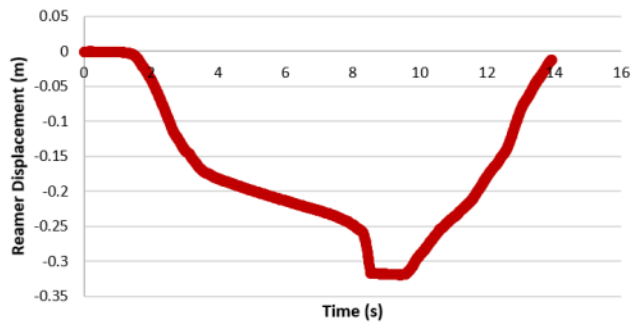


**SAMPLE NO. 1 - Left - Attending: 9.5mm CHATTER**

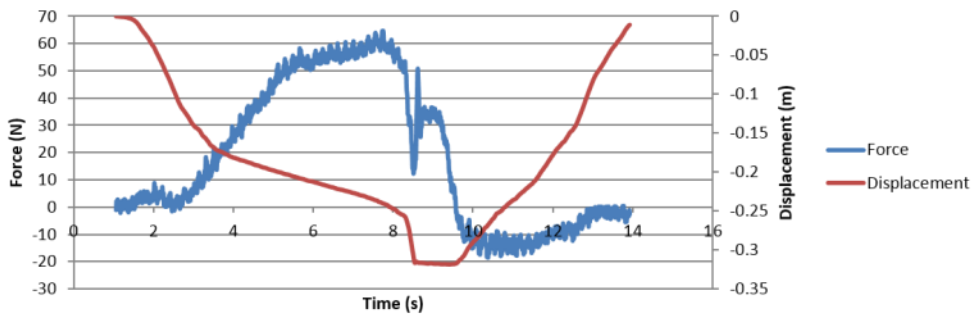


10MM

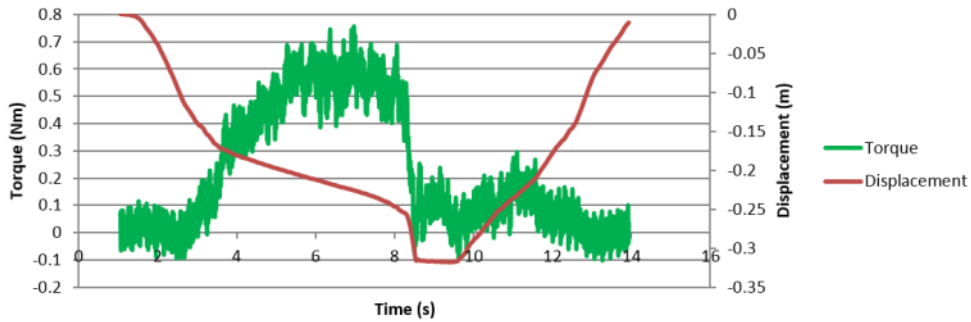
SAMPLE NO. 1 - Left - Attending: 10mm



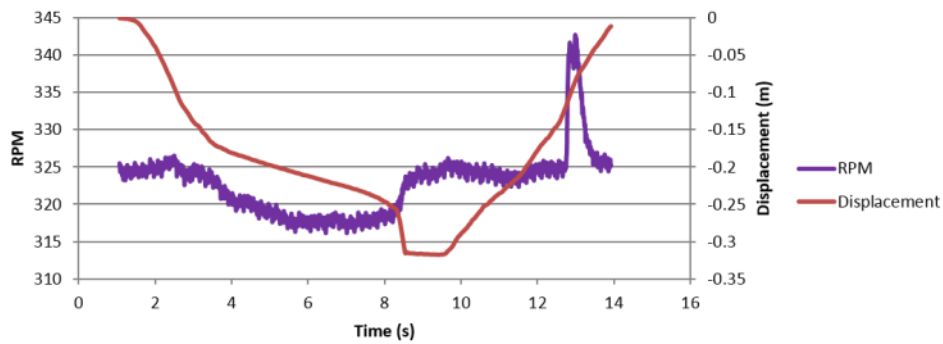
SAMPLE NO. 1 - Left - Attending: 10mm



SAMPLE NO. 1 - Left - Attending: 10mm

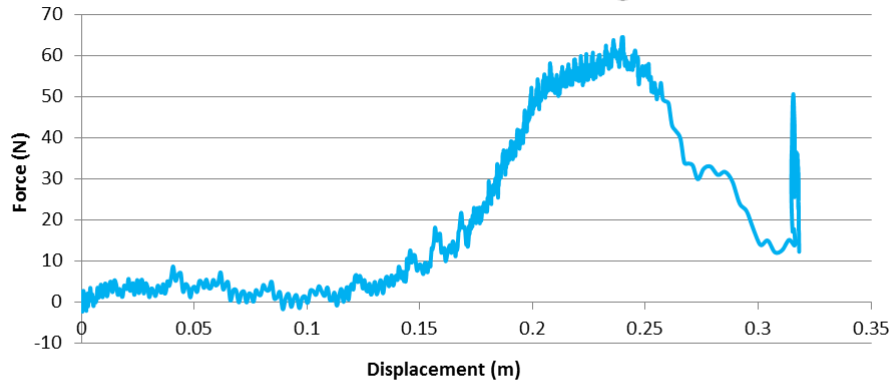


SAMPLE NO. 1 - Left - Attending: 10mm

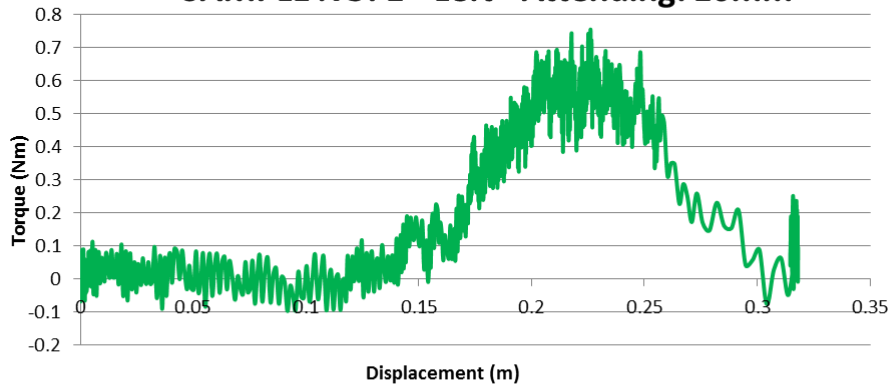




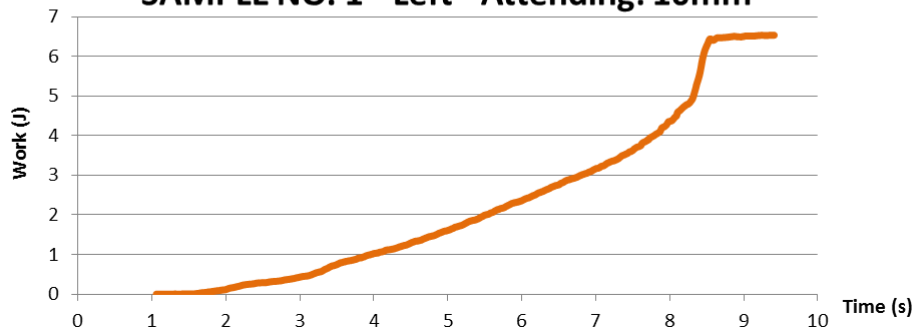
**SAMPLE NO. 1 - Left - Attending: 10mm**



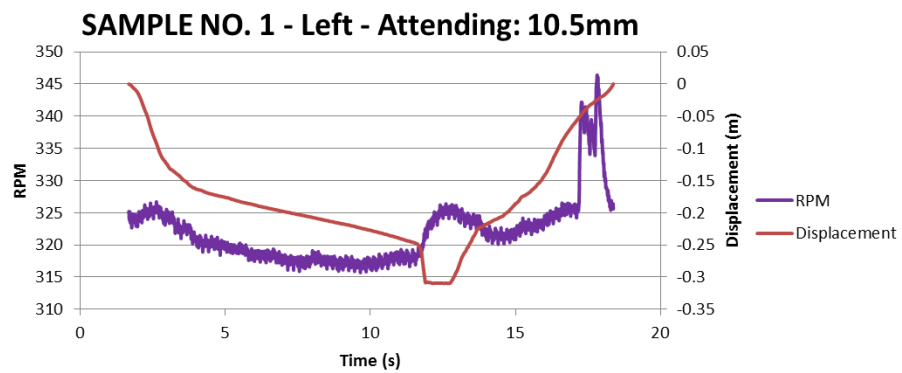
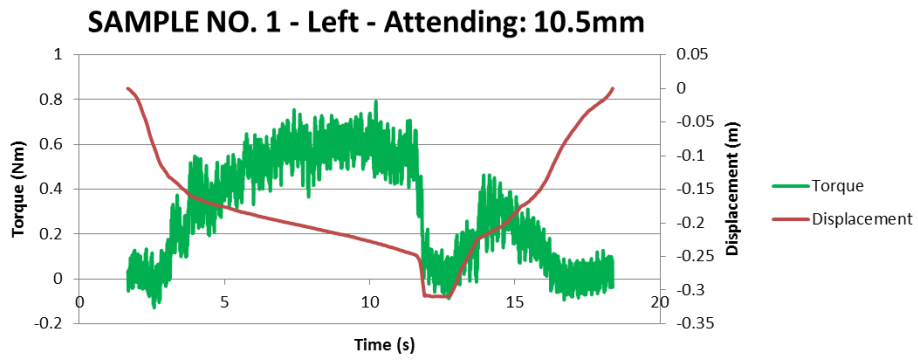
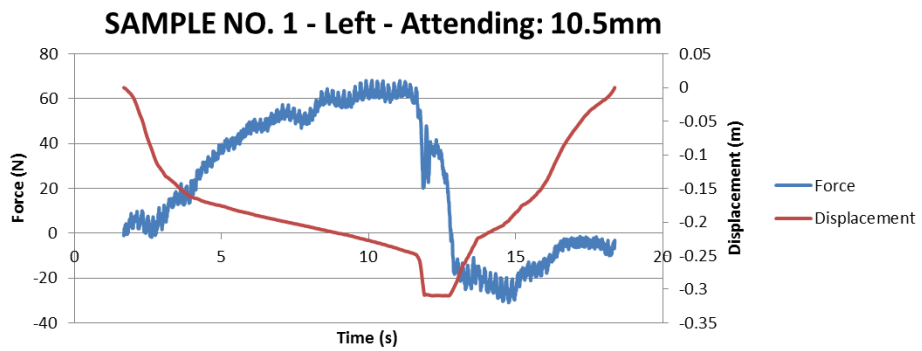
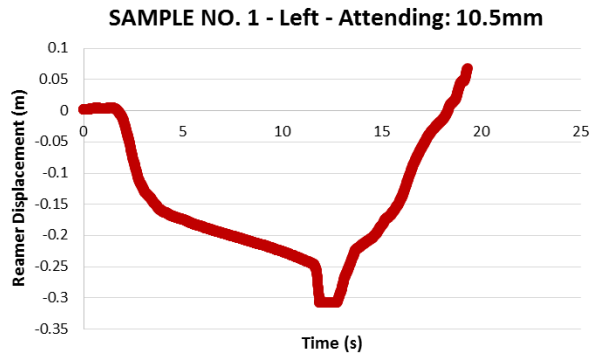
**SAMPLE NO. 1 - Left - Attending: 10mm**



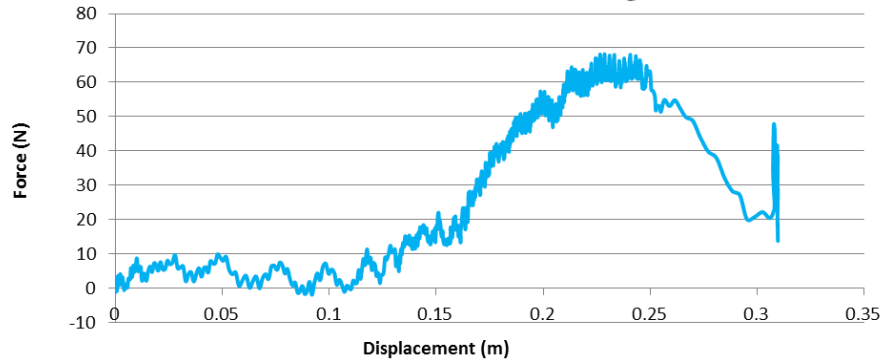
**SAMPLE NO. 1 - Left - Attending: 10mm**



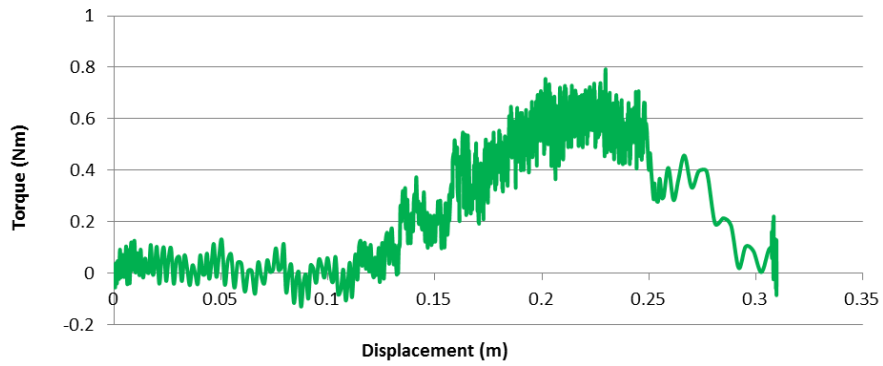
10.5MM



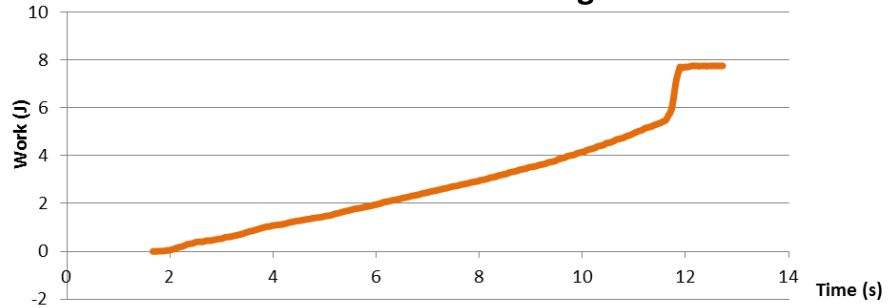
**SAMPLE NO. 1 - Left - Attending: 10.5mm**



**SAMPLE NO. 1 - Left - Attending: 10.5mm**

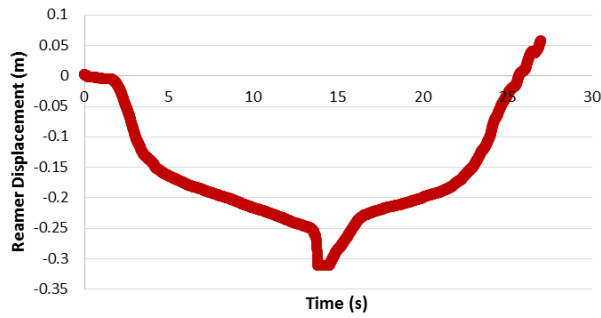


**SAMPLE NO. 1 - Left - Attending: 10.5mm**

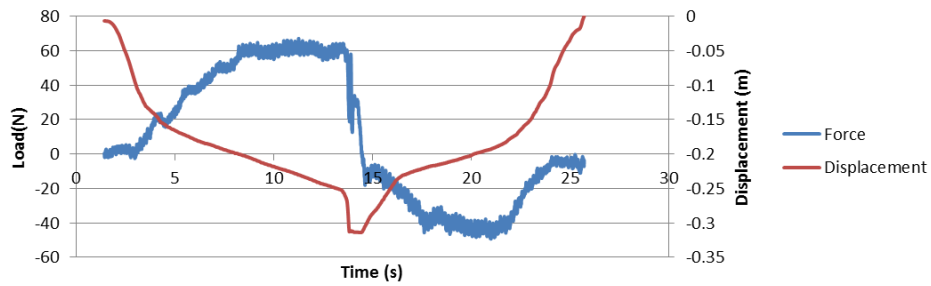


11MM

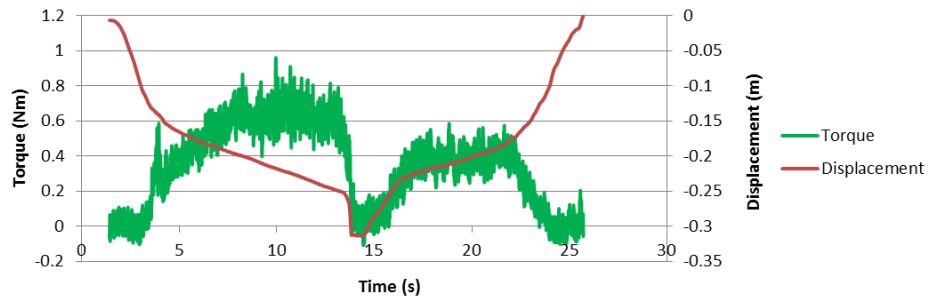
SAMPLE NO. 1 - Left - Attending: 11mm



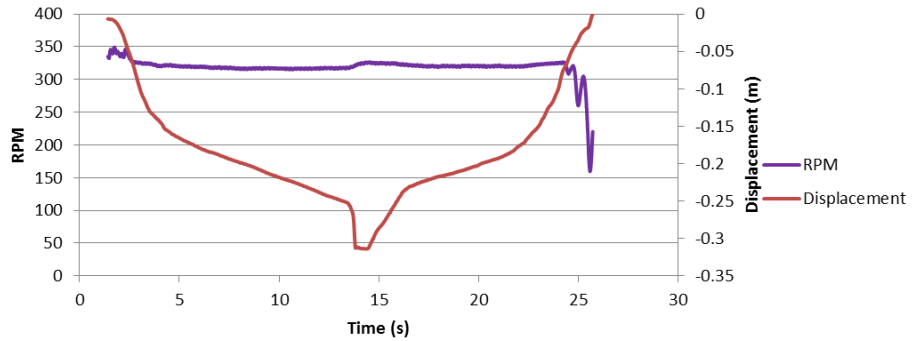
SAMPLE NO. 1 - Left - Attending: 11mm



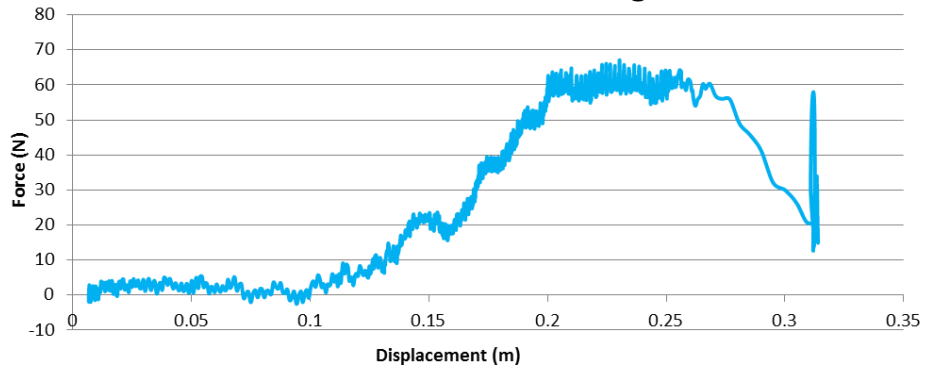
SAMPLE NO. 1 - Left - Attending: 11mm



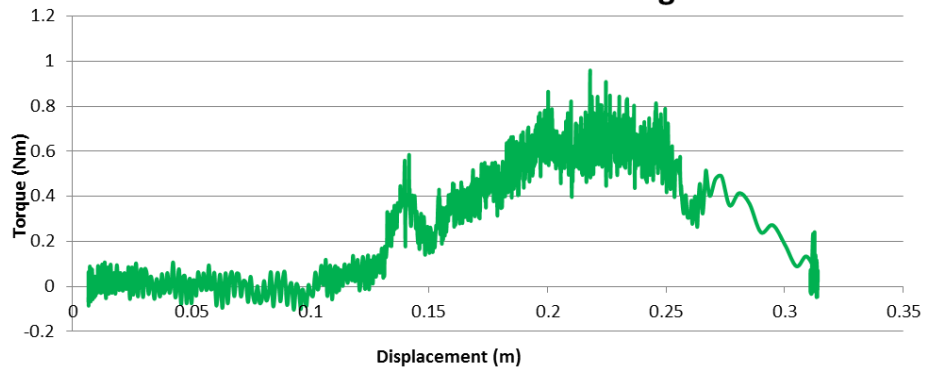
SAMPLE NO. 1 - Left - Attending: 11mm



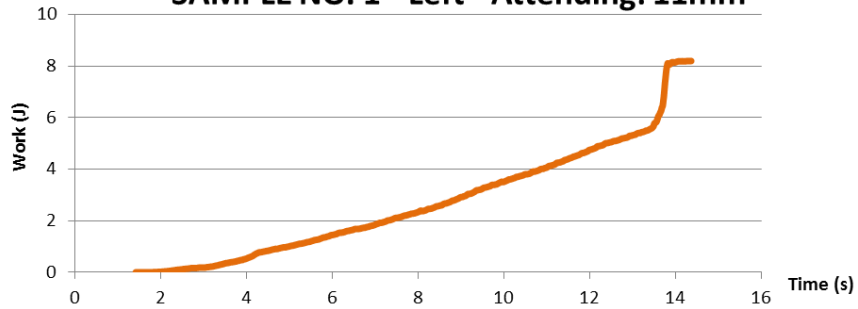
**SAMPLE NO. 1 - Left - Attending: 11mm**



**SAMPLE NO. 1 - Left - Attending: 11mm**



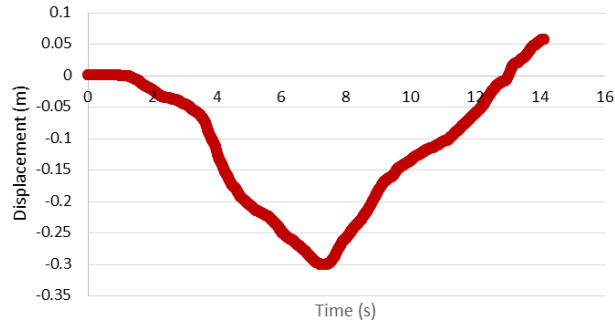
**SAMPLE NO. 1 - Left - Attending: 11mm**



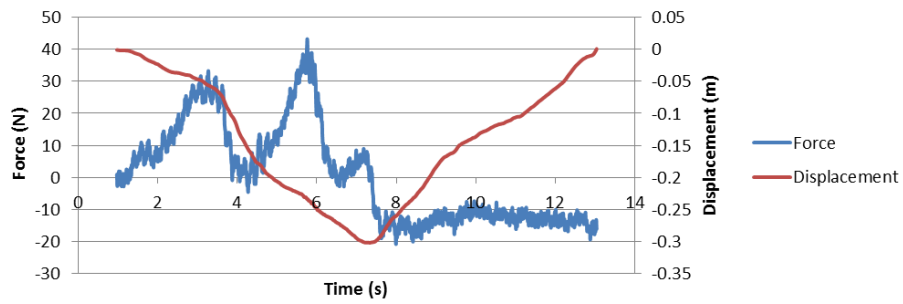
RIGHT: RESIDENT

9MM

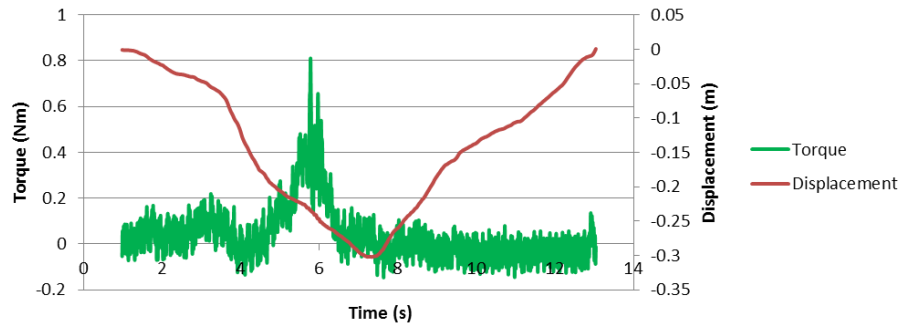
**SAMPLE NO. 1 - Right - Resident: 9mm**



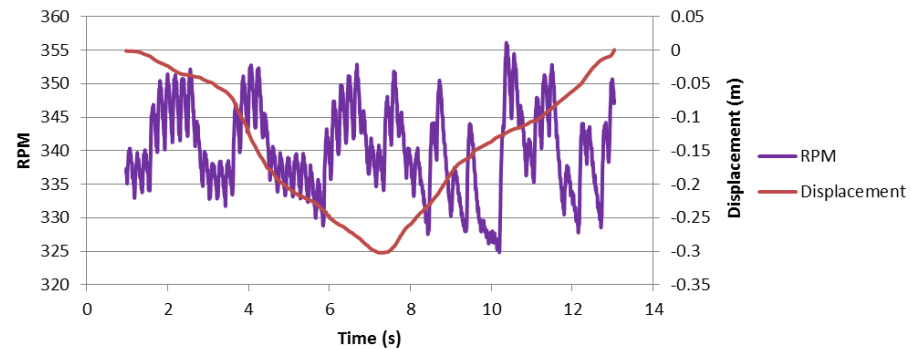
**SAMPLE NO. 1 - Right - Resident: 9mm**

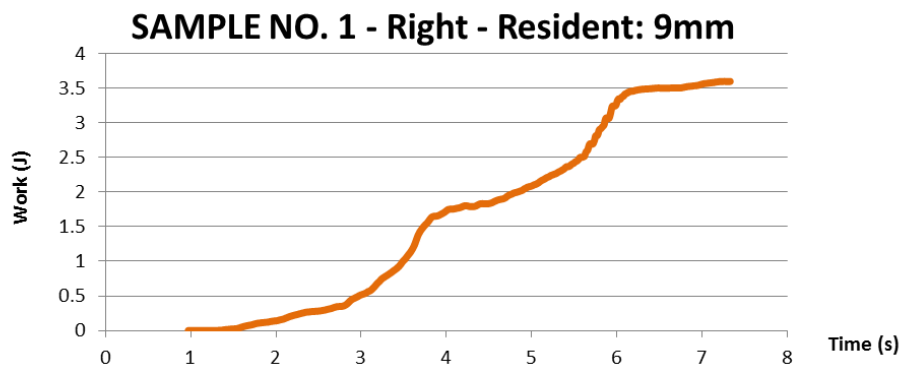
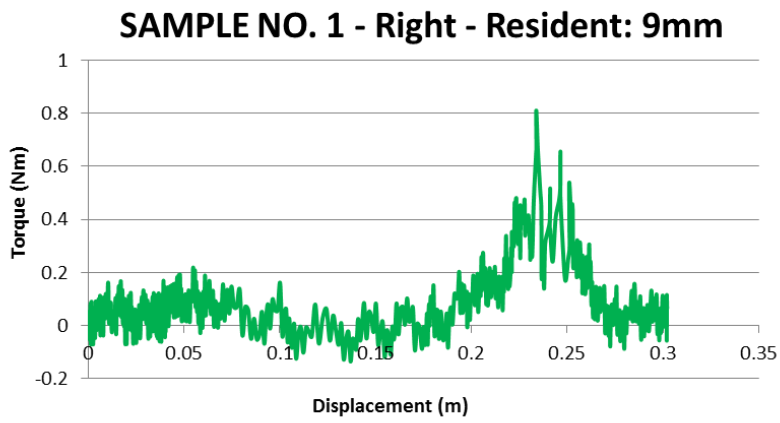
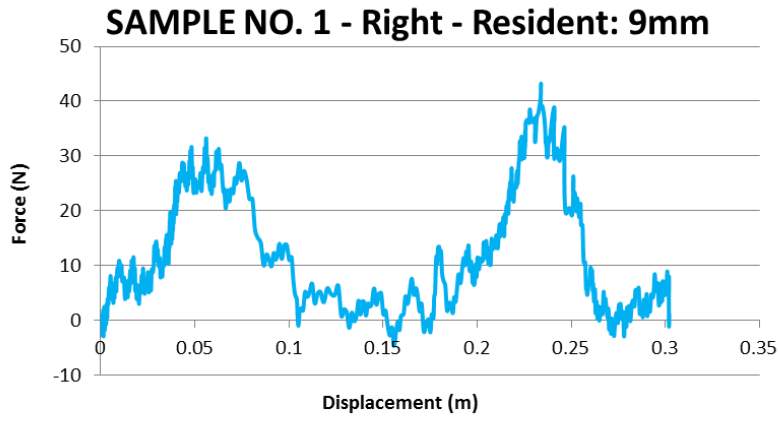


**SAMPLE NO. 1 - Right - Resident: 9mm**



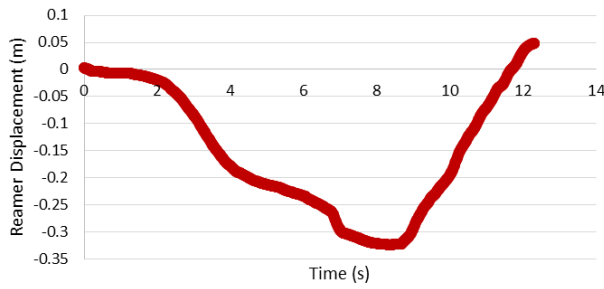
**SAMPLE NO. 1 - Right - Resident: 9mm**



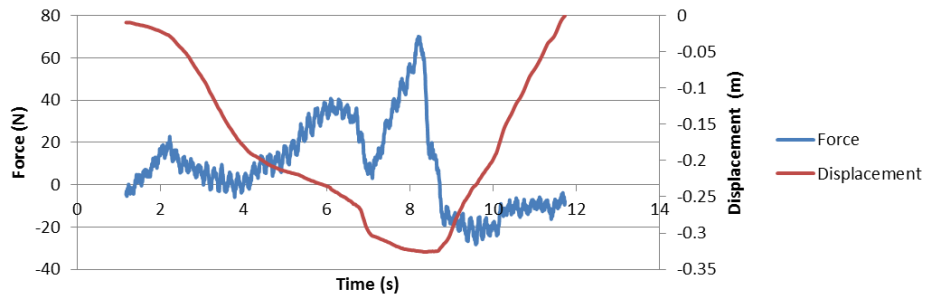


9.5MM

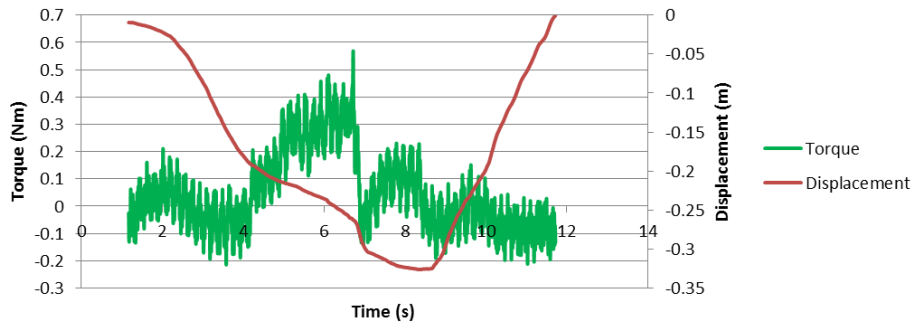
**SAMPLE NO. 1 - Right - Resident: 9.5mm  
CHATTER**



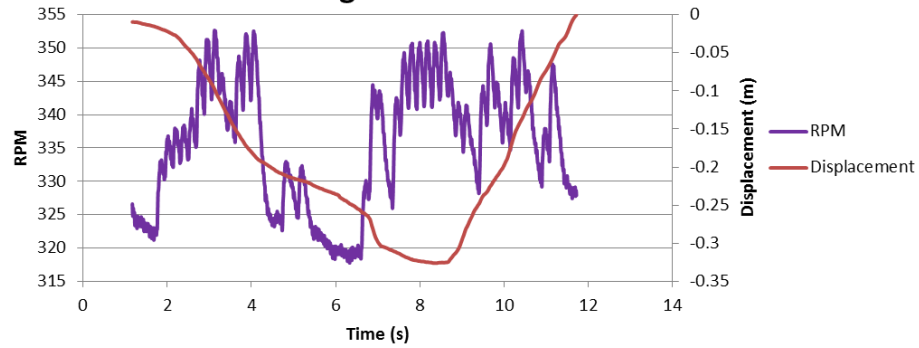
**SAMPLE NO. 1 - Right - Resident: 9.5mm CHATTER**



**SAMPLE NO. 1 - Right - Resident: 9.5mm CHATTER**

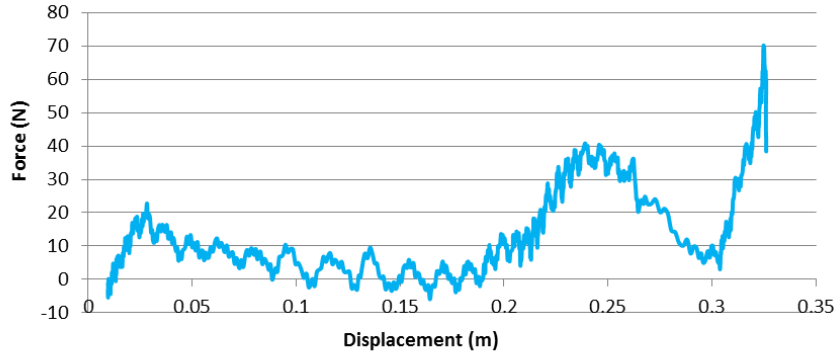


**SAMPLE NO. 1 - Right - Resident: 9.5mm CHATTER**

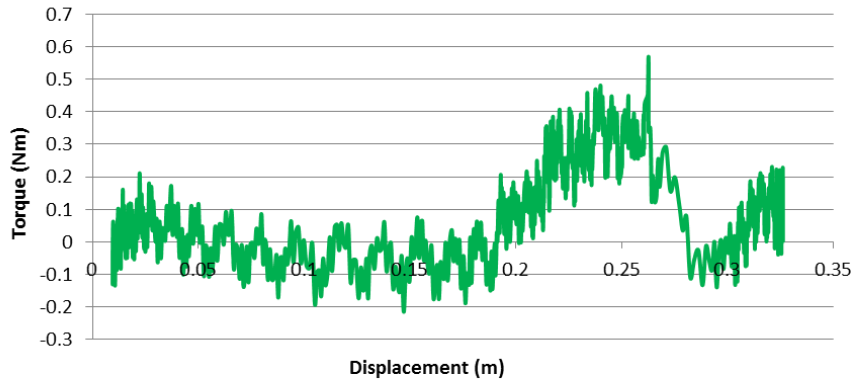




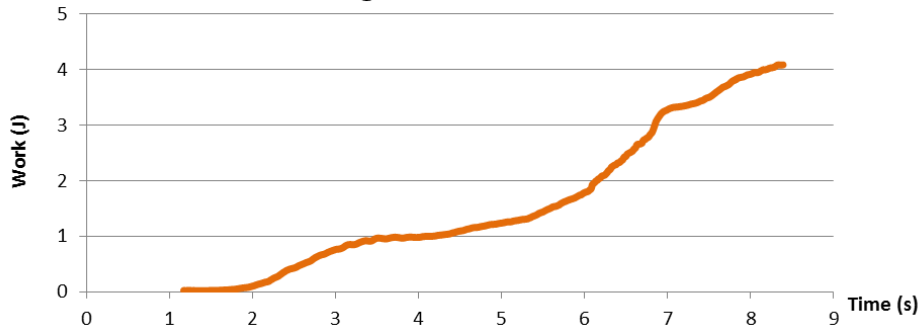
**SAMPLE NO. 1 - Right - Resident: 9.5mm  
CHATTER**



**SAMPLE NO. 1 - Right - Resident: 9.5mm CHATTER**

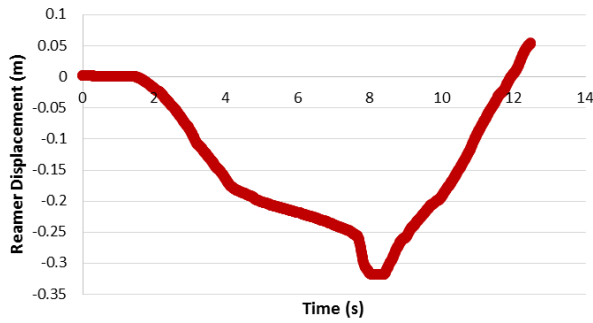


**SAMPLE NO. 1 - Right - Resident: 9.5mm CHATTER**

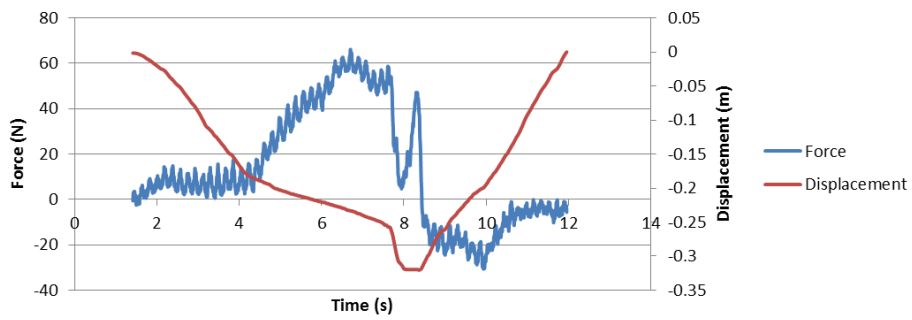


10MM

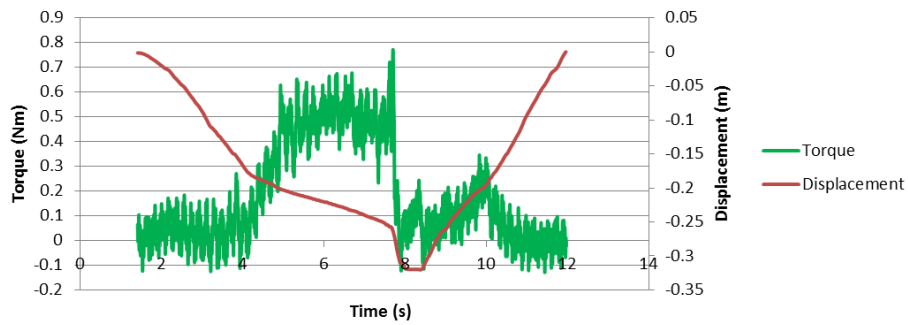
SAMPLE NO. 1 - Right - Resident: 10mm



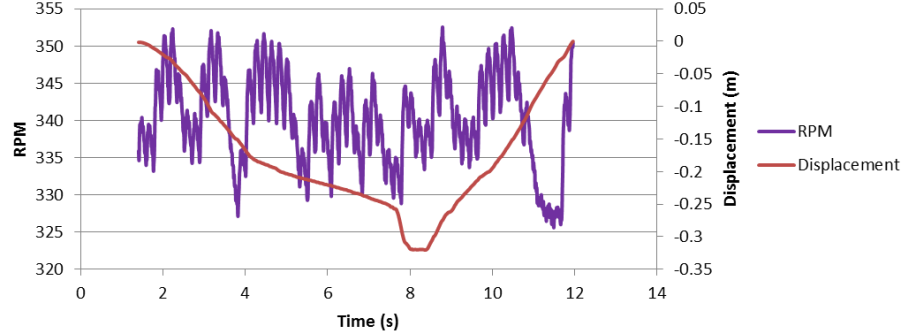
SAMPLE NO. 1 - Right - Resident: 10mm

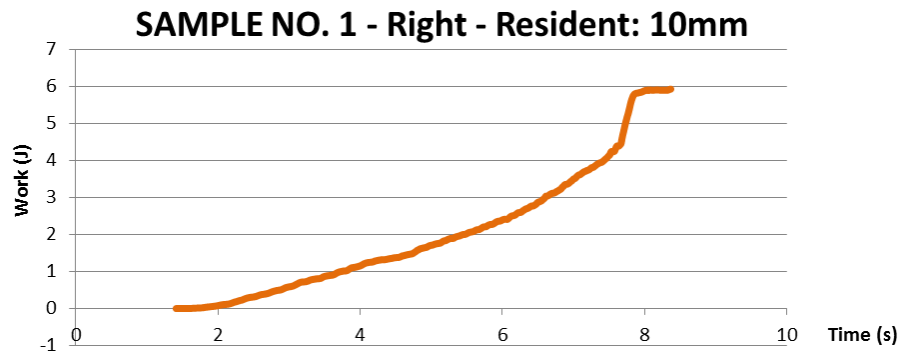
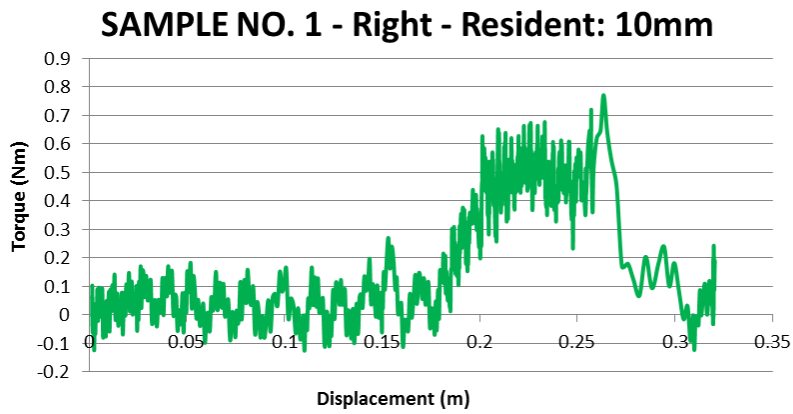
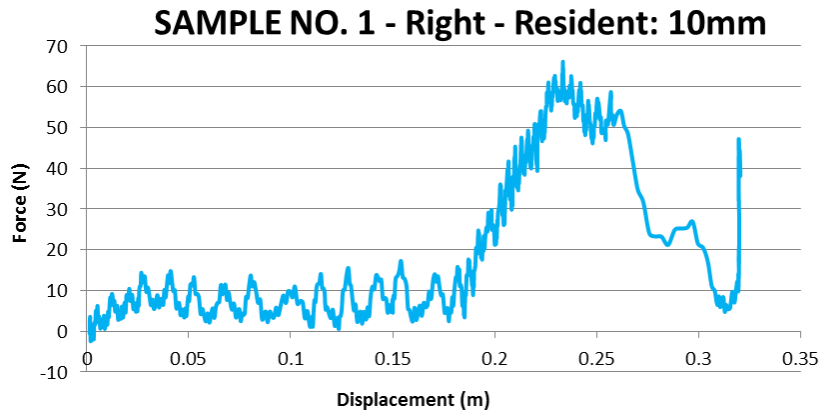


SAMPLE NO. 1 - Right - Resident: 10mm

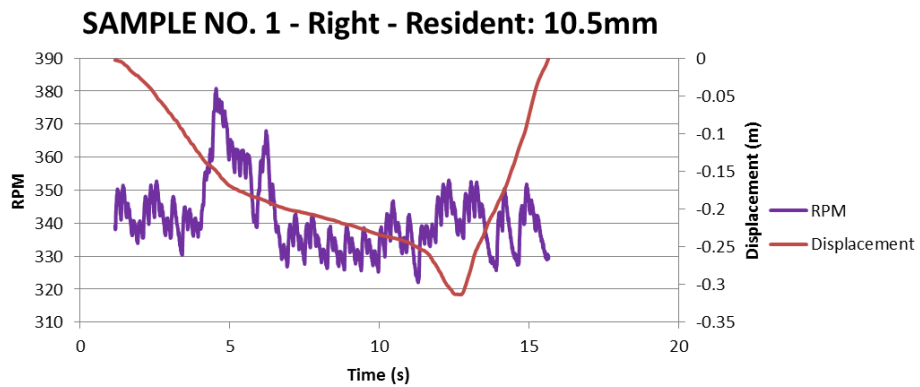
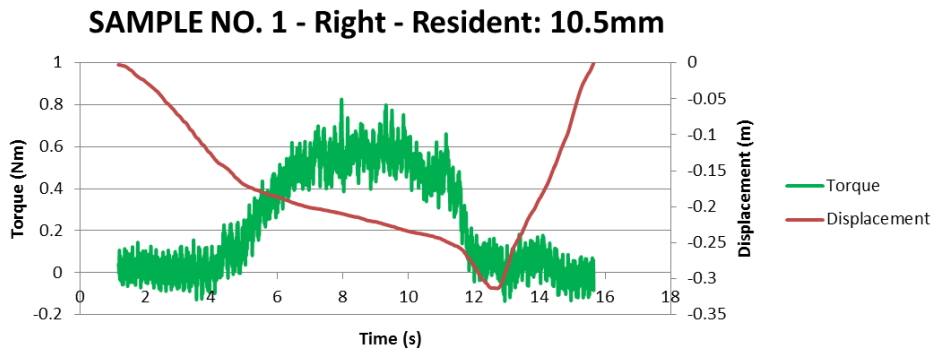
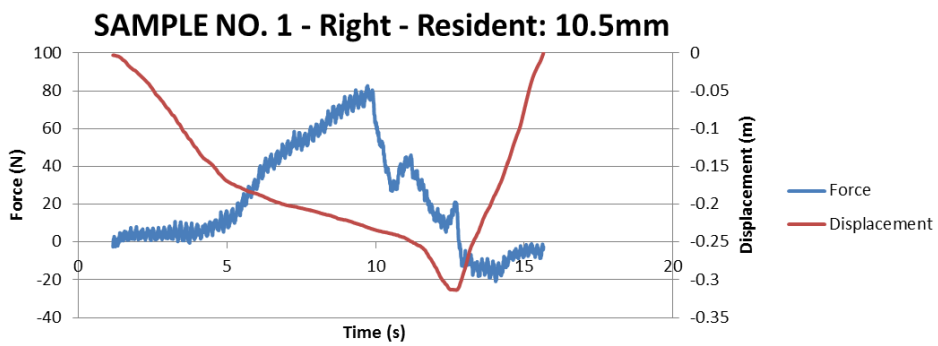
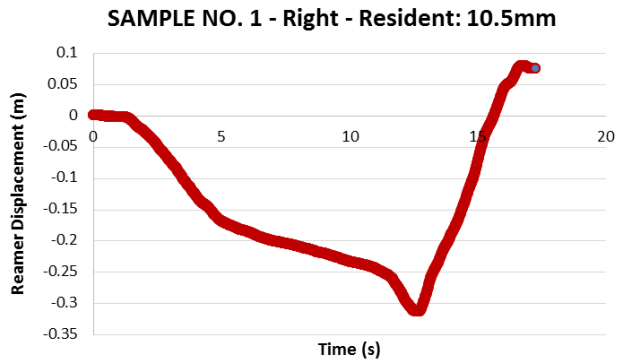


SAMPLE NO. 1 - Right - Resident: 10mm

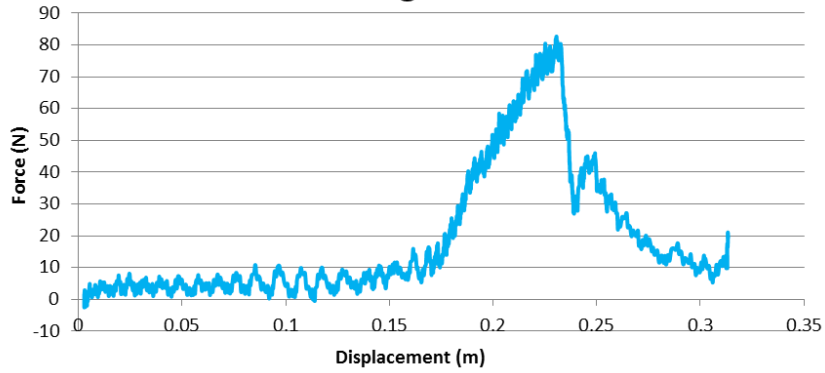




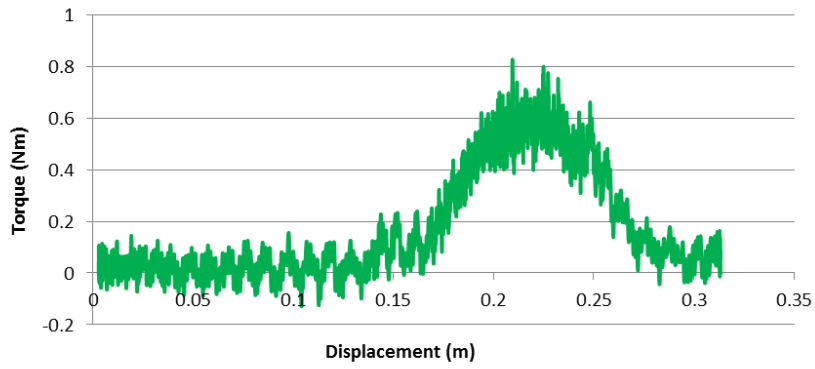
10.5MM



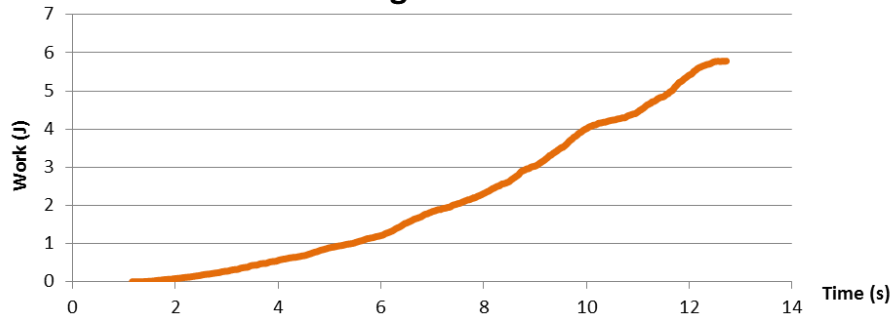
**SAMPLE NO. 1 - Right - Resident: 10.5mm**



**SAMPLE NO. 1 - Right - Resident: 10.5mm**

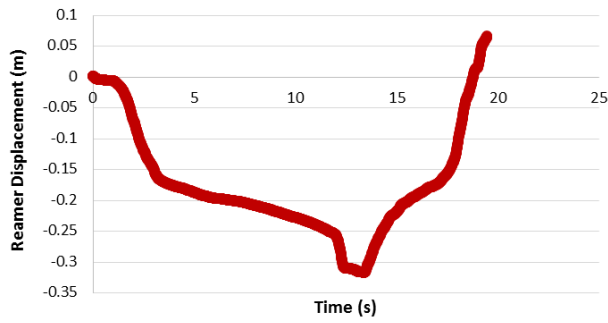


**SAMPLE NO. 1 - Right - Resident: 10.5mm**

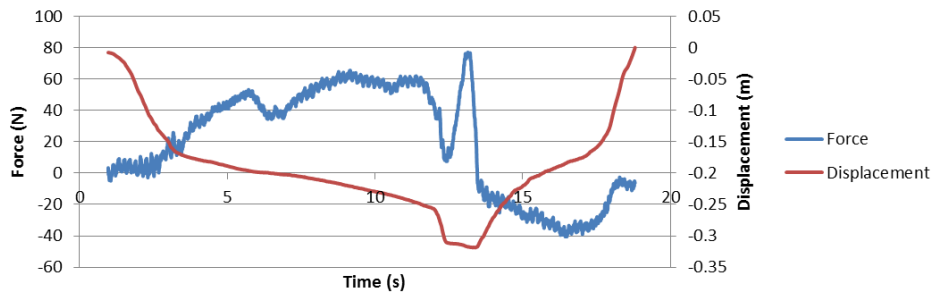


11MM

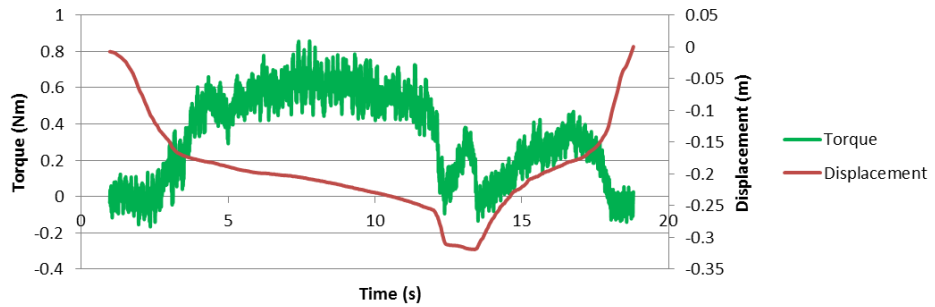
**SAMPLE NO. 1 - Right - Resident: 11mm**



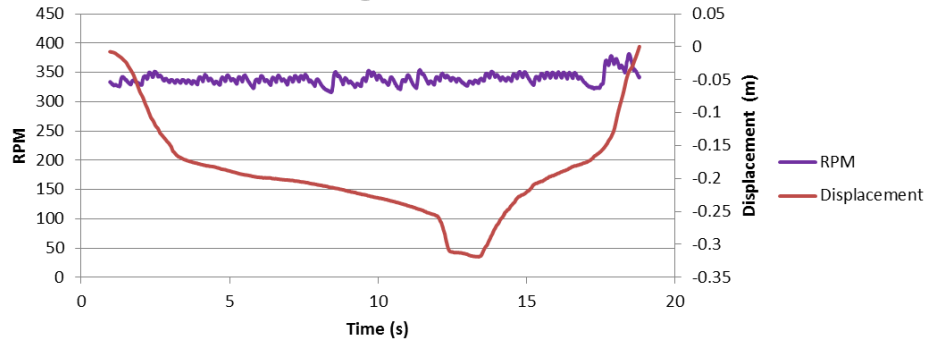
**SAMPLE NO. 1 - Right - Resident: 11mm**



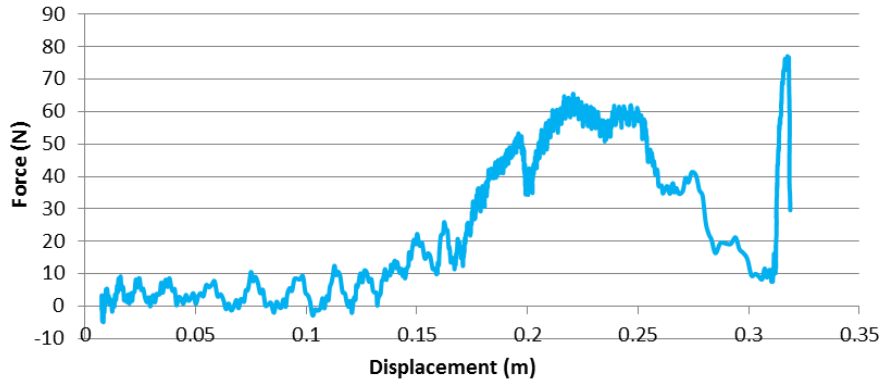
**SAMPLE NO. 1 - Right - Resident: 11mm**



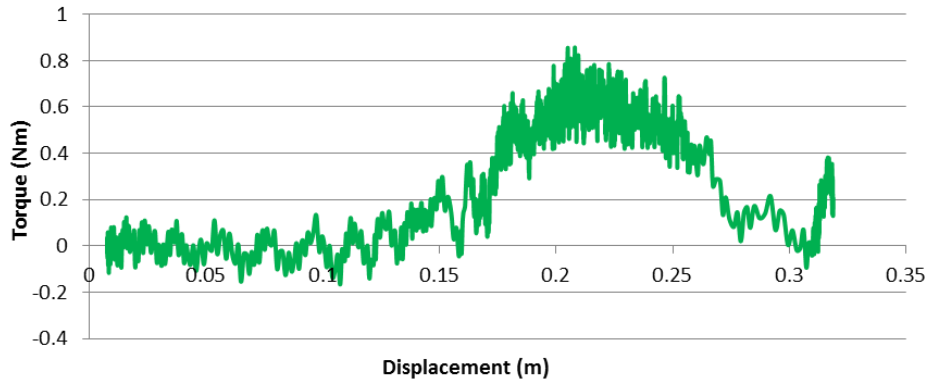
**SAMPLE NO. 1 - Right - Resident: 11mm**



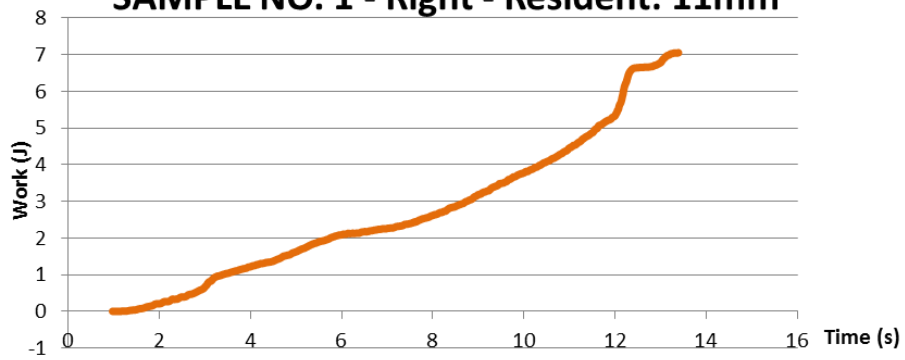
**SAMPLE NO. 1 - Right - Resident: 11mm**



**SAMPLE NO. 1 - Right - Resident: 11mm**



**SAMPLE NO. 1 - Right - Resident: 11mm**

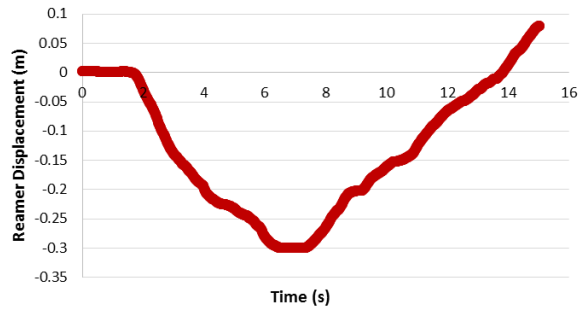


## 13.2 SAMPLE 2 RESULTS

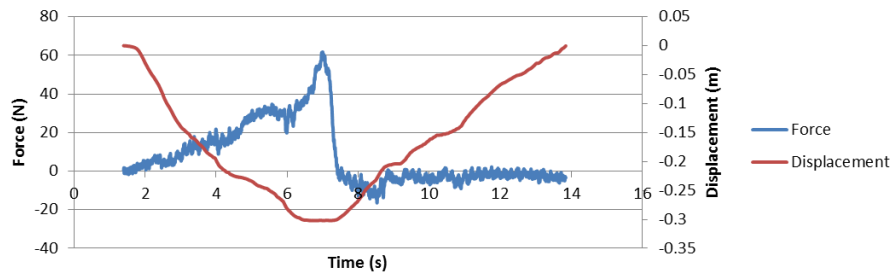
LEFT: ATTENDING

9MM

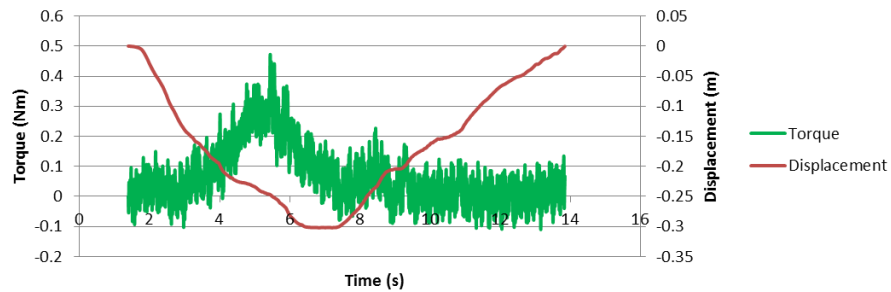
SAMPLE NO. 2 - Left - Attending: 9mm



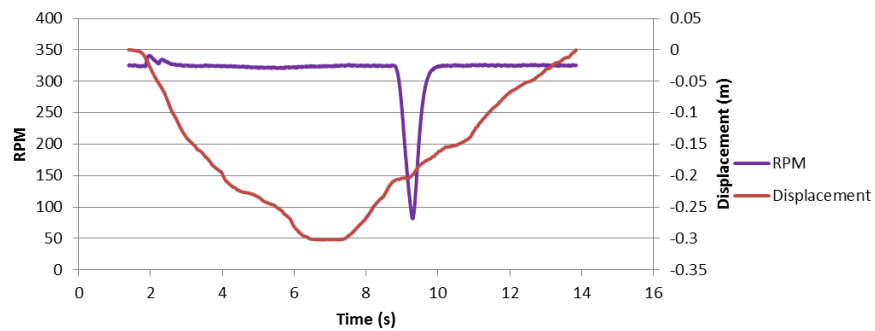
SAMPLE NO. 2 - Left - Attending: 9mm



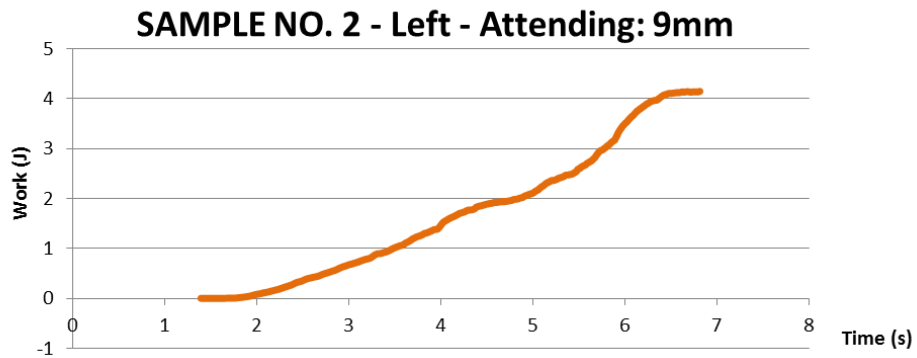
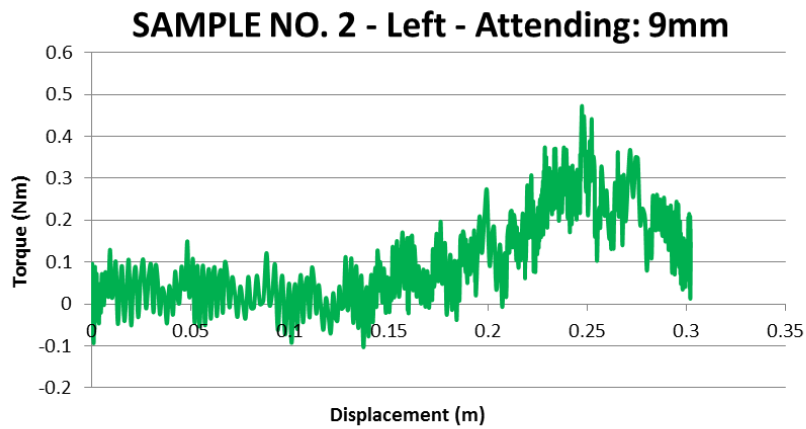
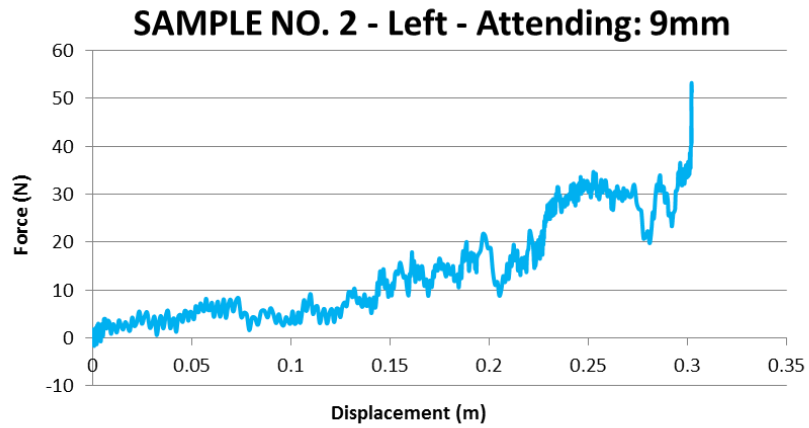
SAMPLE NO. 2 - Left - Attending: 9mm



SAMPLE NO. 2 - Left - Attending: 9mm

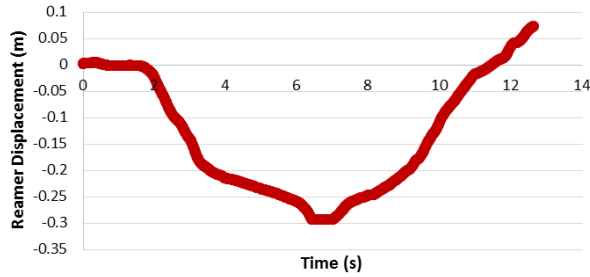




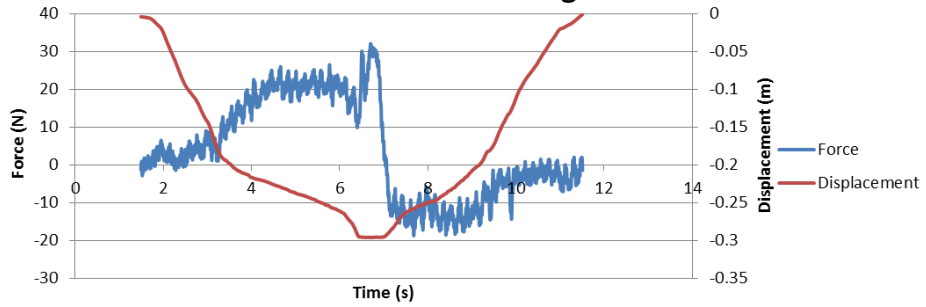


9.5MM

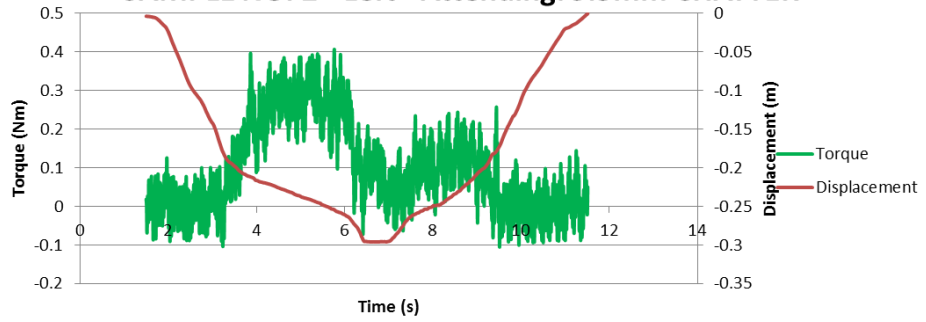
**SAMPLE NO. 2 - Left - Attending: 9.5mm  
CHATTER**



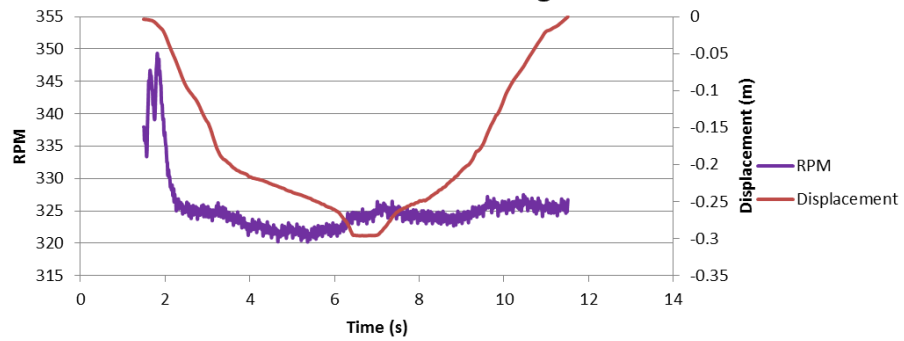
**SAMPLE NO. 2 - Left - Attending: 9.5mm CHATTER**



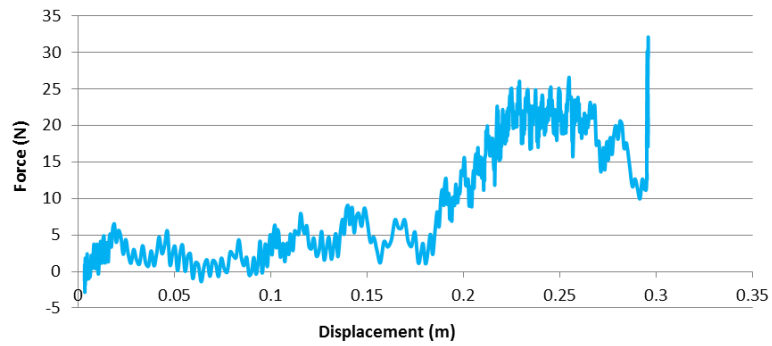
**SAMPLE NO. 2 - Left - Attending: 9.5mm CHATTER**



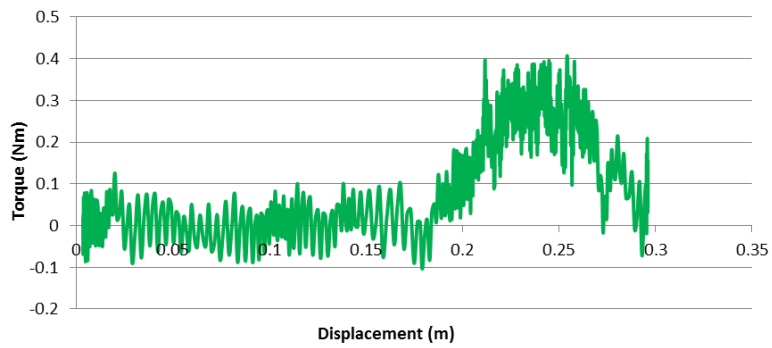
**SAMPLE NO. 2 - Left - Attending: 9.5mm CHATTER**



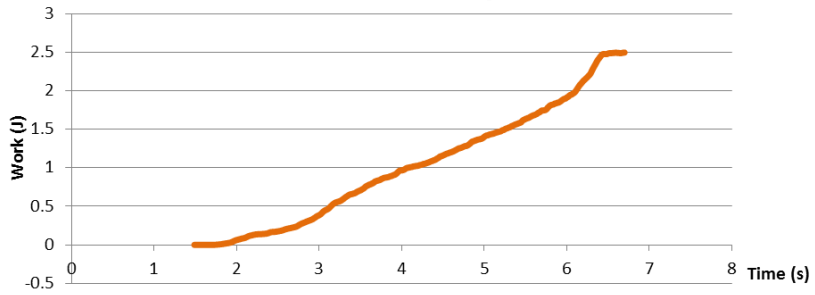
**SAMPLE NO. 2 - Left - Attending: 9.5mm CHATTER**



**SAMPLE NO. 2 - Left - Attending: 9.5mm CHATTER**

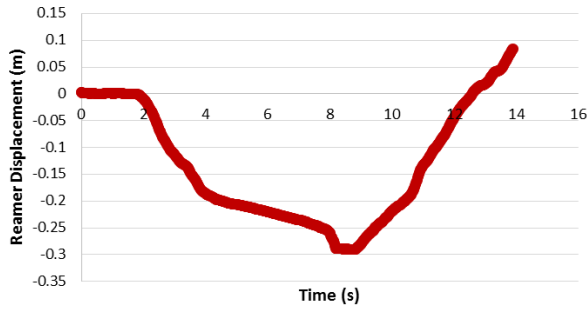


**SAMPLE NO. 2 - Left - Attending: 9.5mm CHATTER**

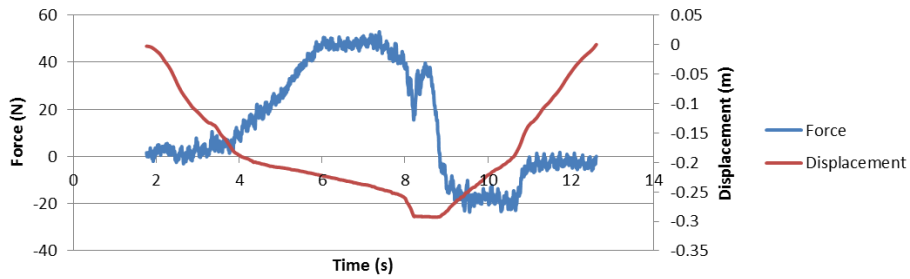


10MM

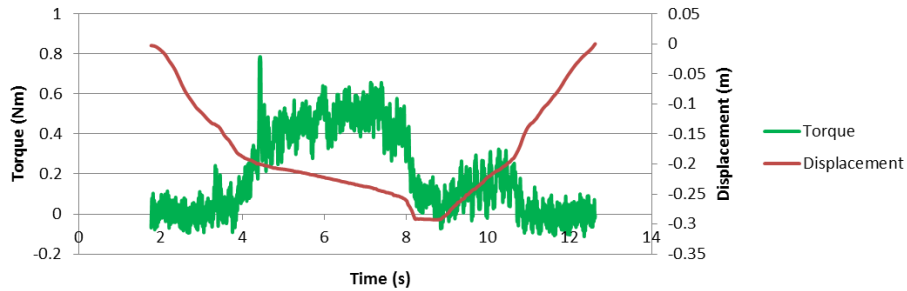
SAMPLE NO. 2 - Left - Attending: 10mm



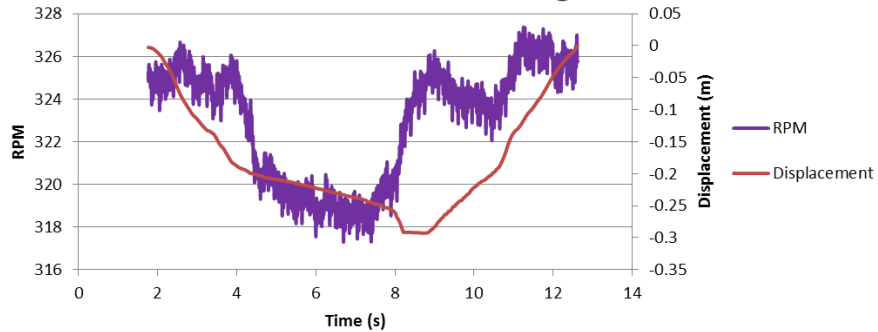
SAMPLE NO. 2 - Left - Attending: 10mm



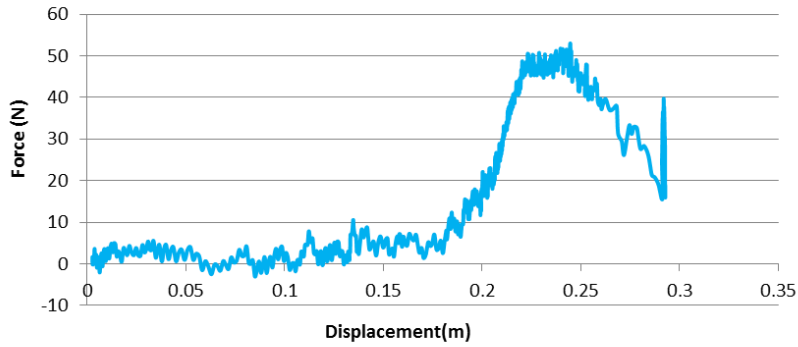
SAMPLE NO. 2 - Left - Attending: 10mm



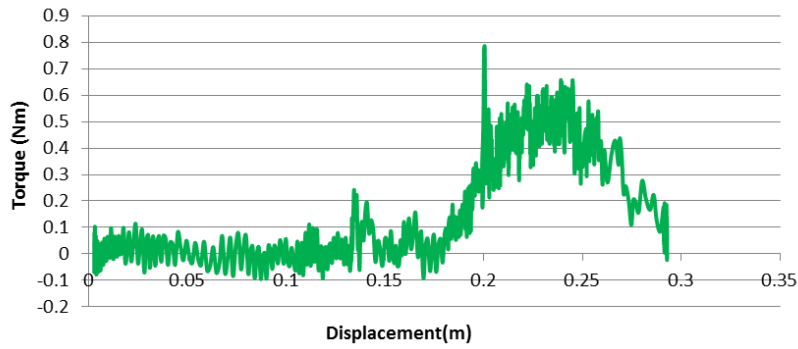
SAMPLE NO. 2 - Left - Attending: 10mm



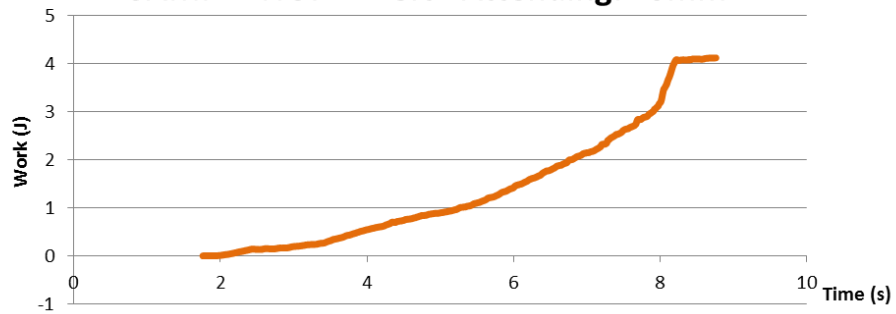
**SAMPLE NO. 2 - Left - Attending: 10mm**



**SAMPLE NO. 2 - Left - Attending: 10mm**

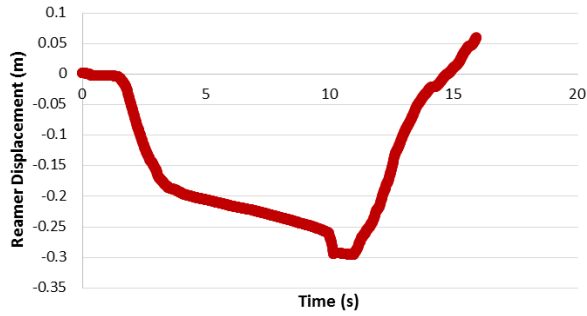


**SAMPLE NO. 2 - Left - Attending: 10mm**

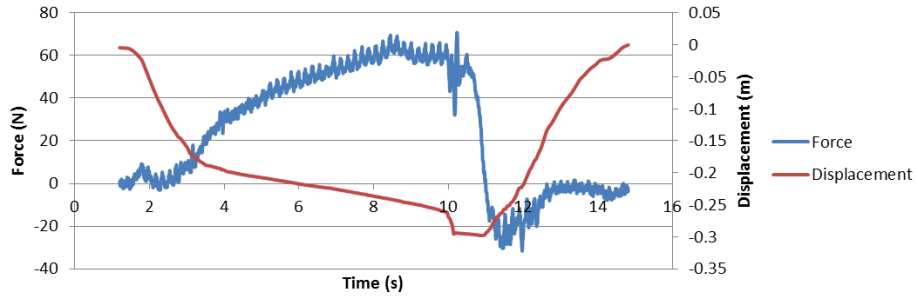


10.5MM

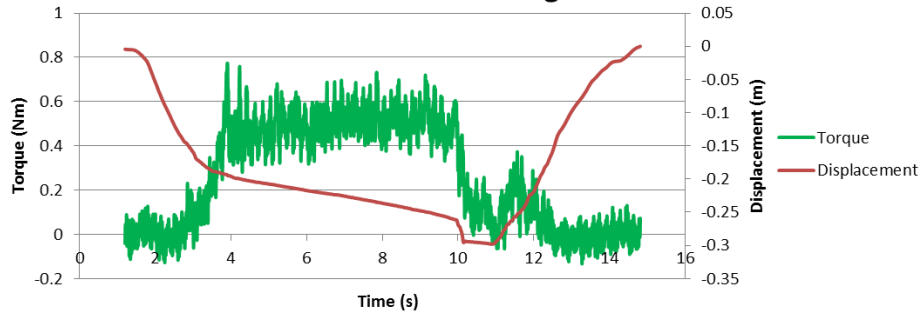
SAMPLE NO. 2 - Left - Attending: 10.5mm



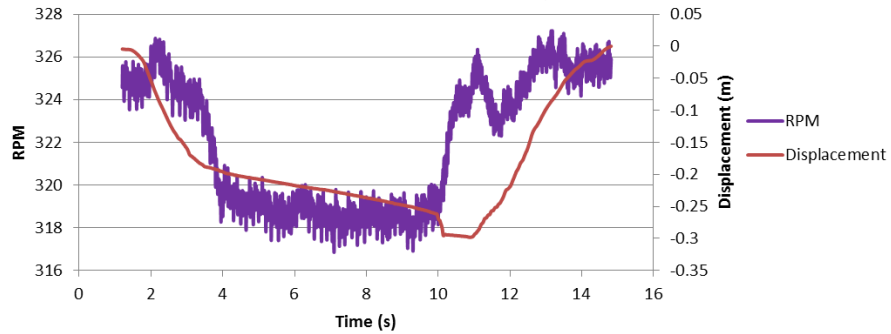
SAMPLE NO. 2 - Left - Attending: 10.5mm



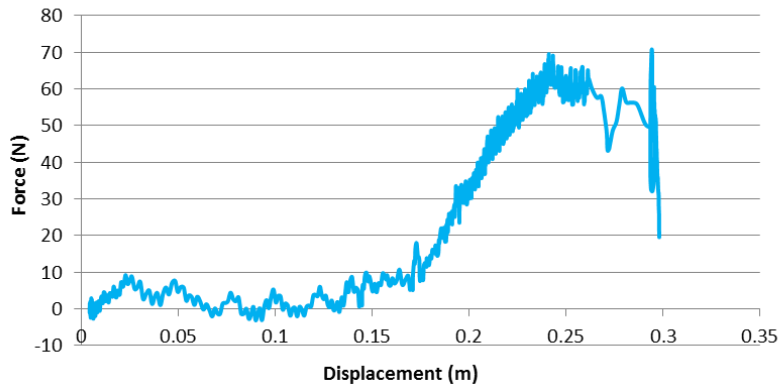
SAMPLE NO. 2 - Left - Attending: 10.5mm



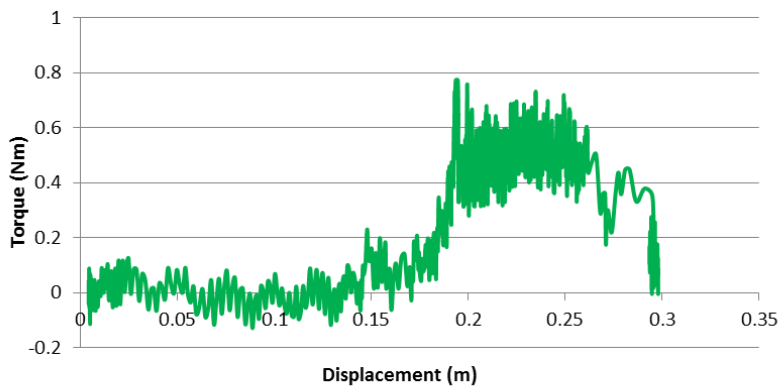
SAMPLE NO. 2 - Left - Attending: 10.5mm



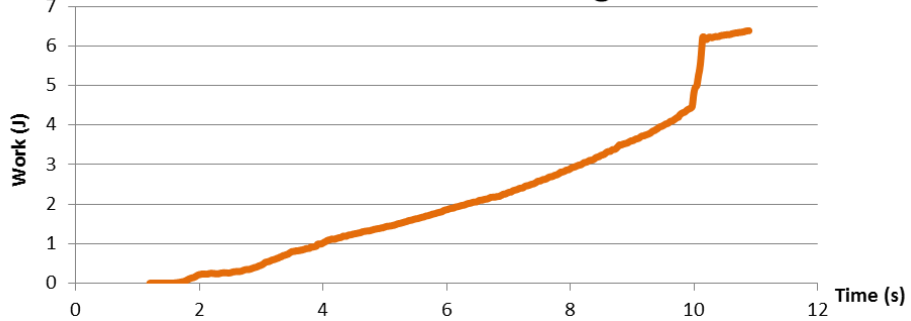
**SAMPLE NO. 2 - Left - Attending: 10.5mm**



**SAMPLE NO. 2 - Left - Attending: 10.5mm**

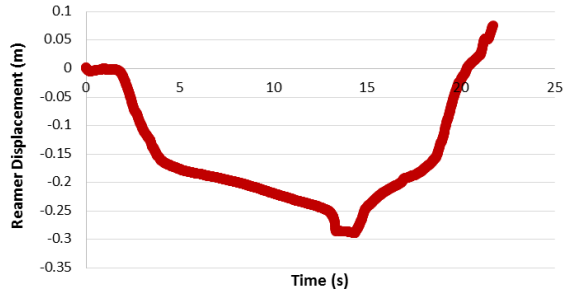


**SAMPLE NO. 2 - Left - Attending: 10.5mm**

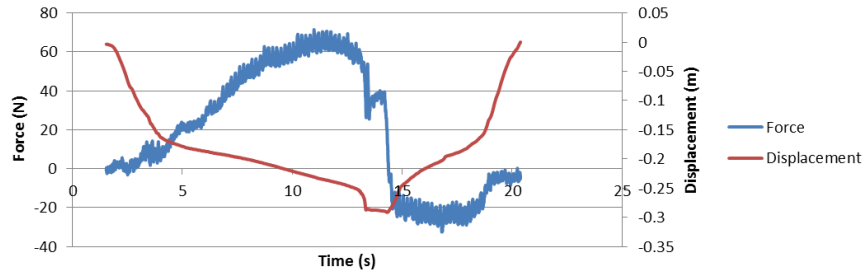


11MM

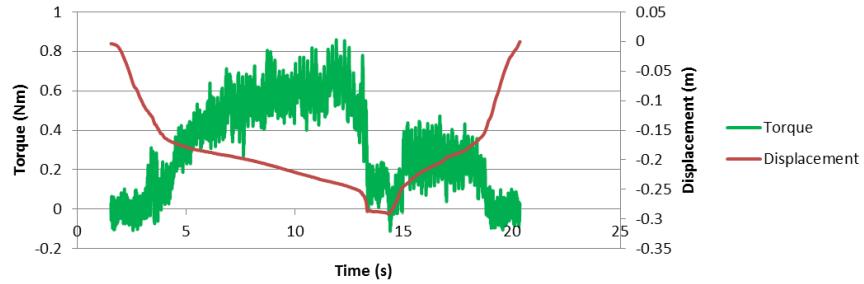
SAMPLE NO. 2 - Left - Attending: 11mm



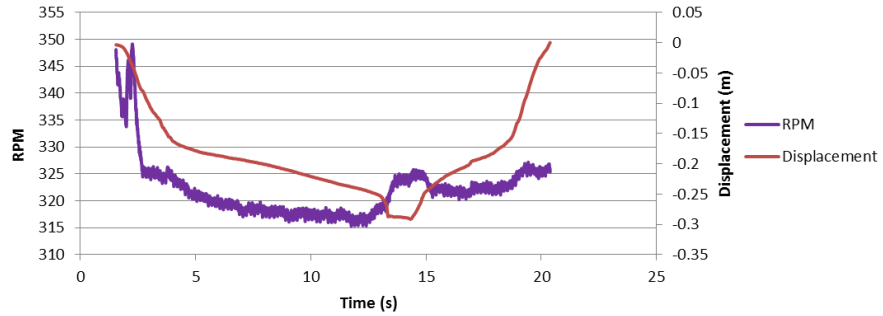
SAMPLE NO. 2 - Left - Attending: 11mm



SAMPLE NO. 2 - Left - Attending: 11mm

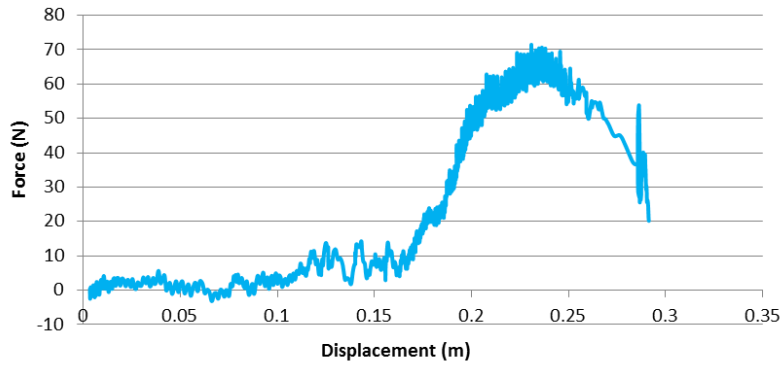


SAMPLE NO. 2 - Left - Attending: 11mm

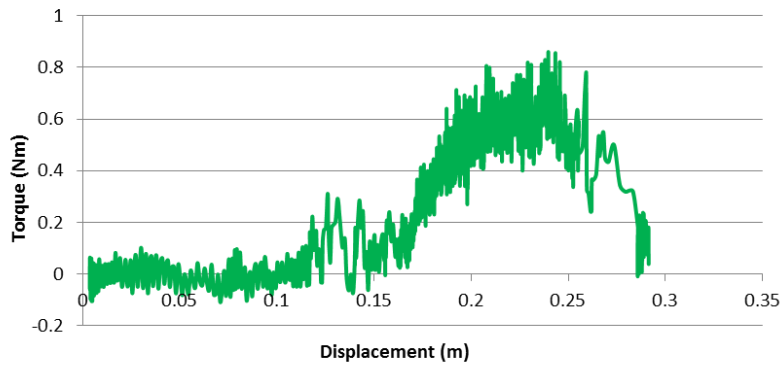




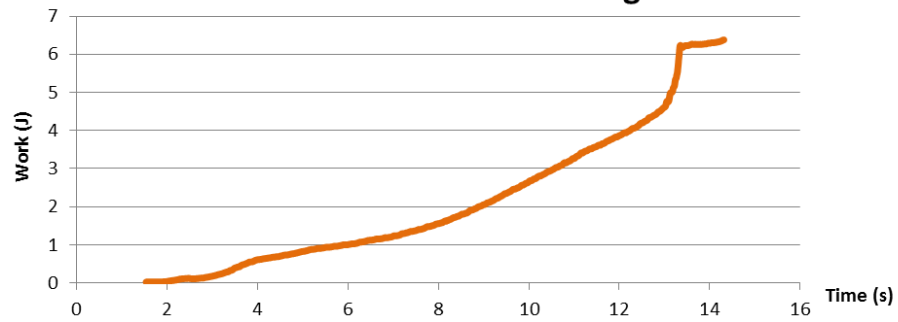
**SAMPLE NO. 2 - Left - Attending: 11mm**



**SAMPLE NO. 2 - Left - Attending: 11mm**



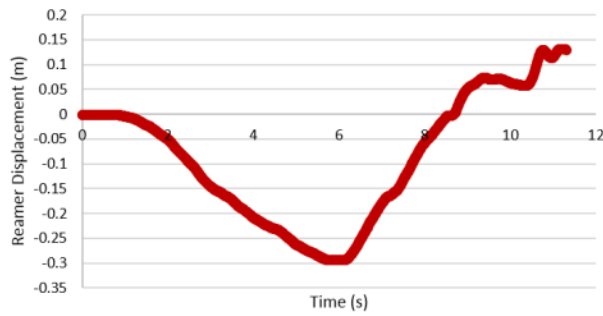
**SAMPLE NO. 2 - Left - Attending: 11mm**



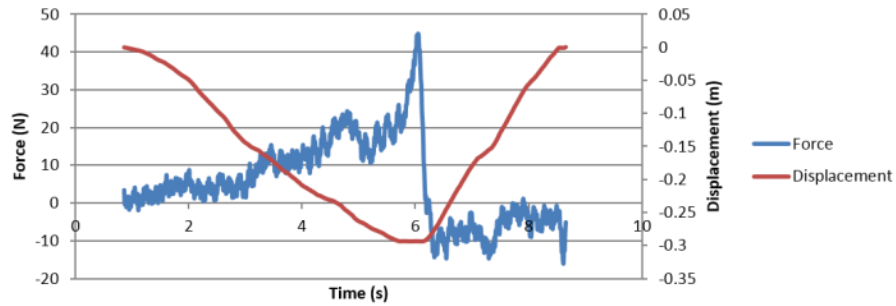
RIGHT: RESIDENT

9MM

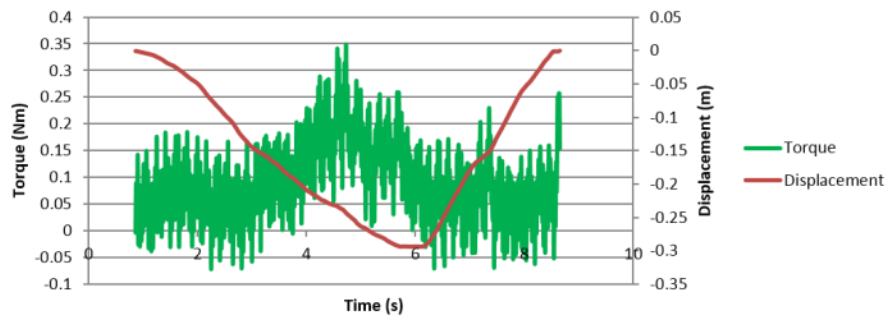
**SAMPLE NO. 2 - Right - Resident: 9mm**



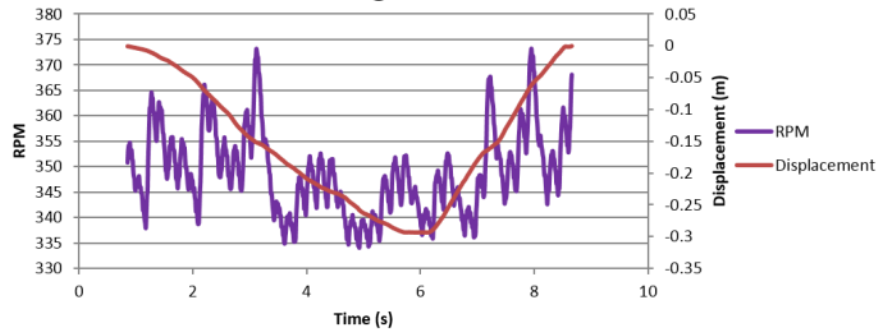
**SAMPLE NO. 2 - Right - Resident: 9mm**



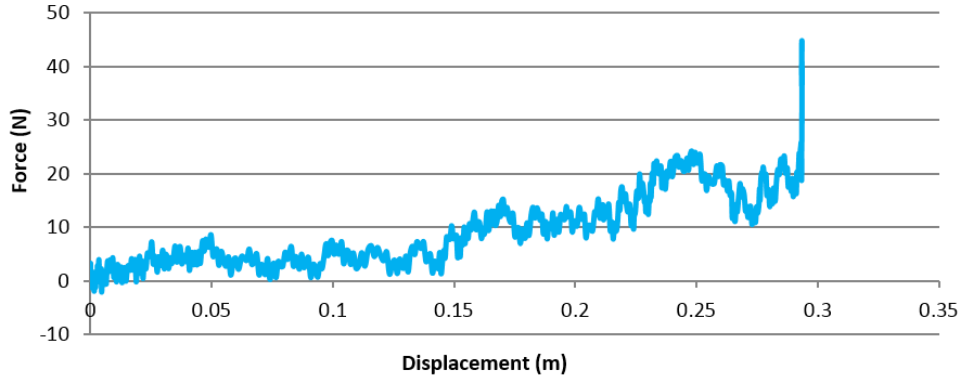
**SAMPLE NO. 2 - Right - Resident: 9mm**



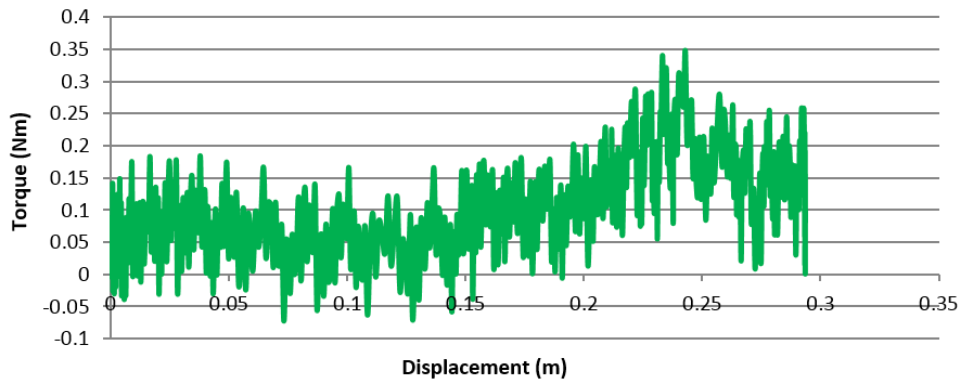
**SAMPLE NO. 2 - Right - Resident: 9mm**



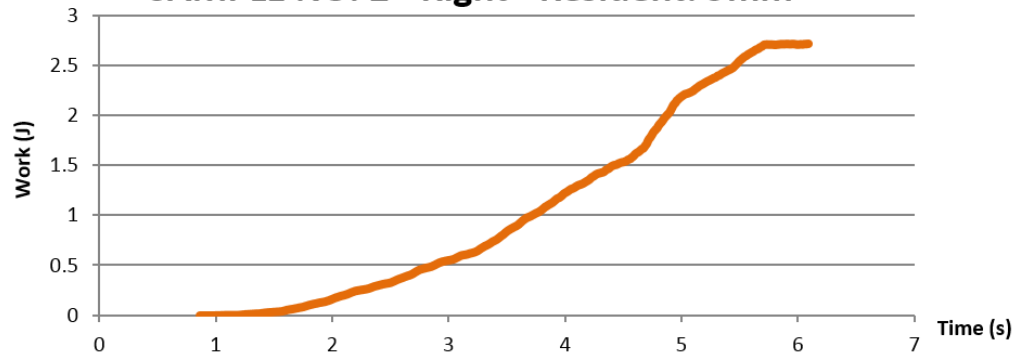
### SAMPLE NO. 2 - Right - Resident: 9mm



### SAMPLE NO. 2 - Right - Resident: 9mm

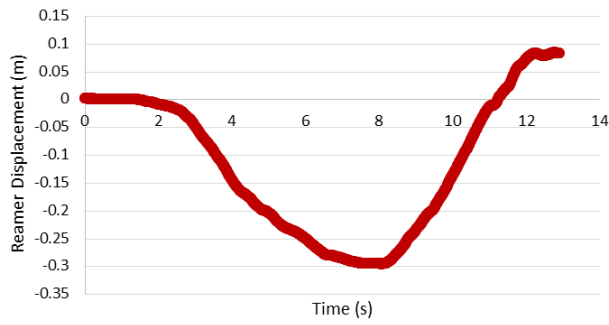


### SAMPLE NO. 2 - Right - Resident: 9mm

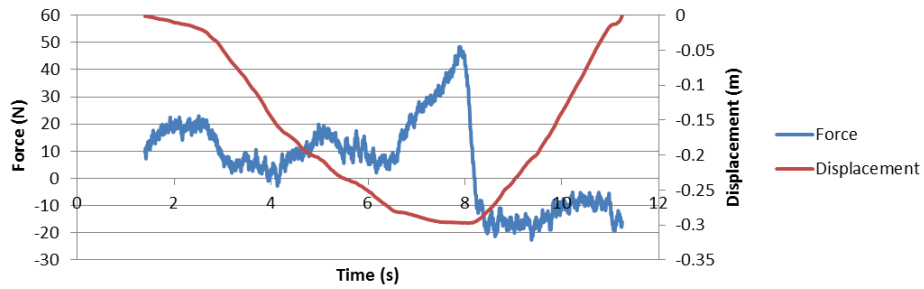


9.5MM

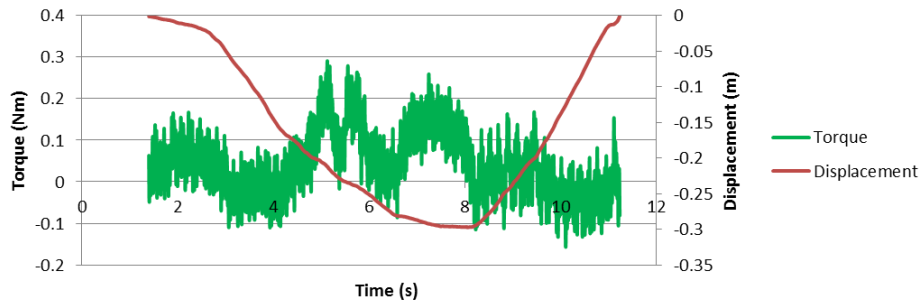
**SAMPLE NO. 2 - Right - Resident: 9.5mm**



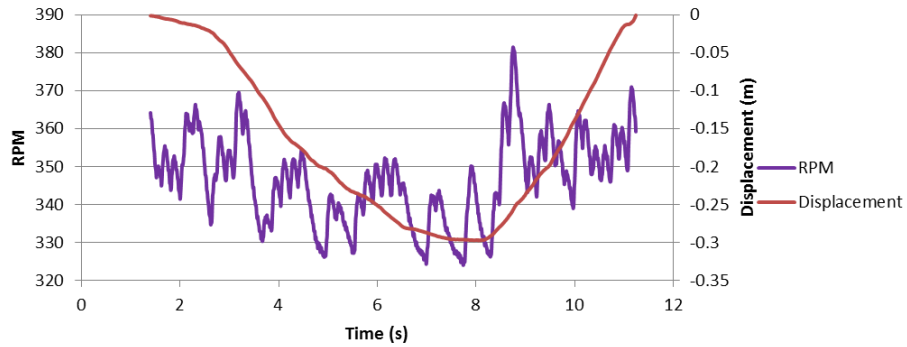
**SAMPLE NO. 2 - Right - Resident: 9.5mm**



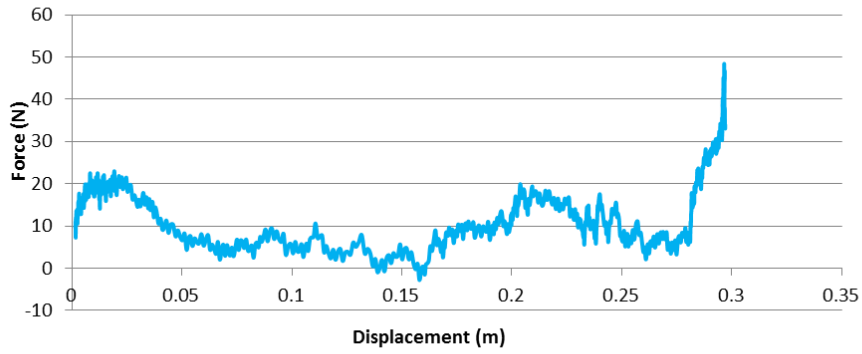
**SAMPLE NO. 2 - Right - Resident: 9.5mm**



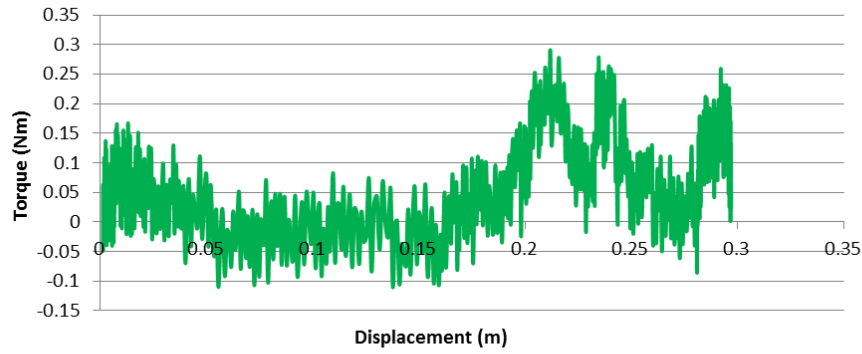
**SAMPLE NO. 2 - Right - Resident: 9.5mm**



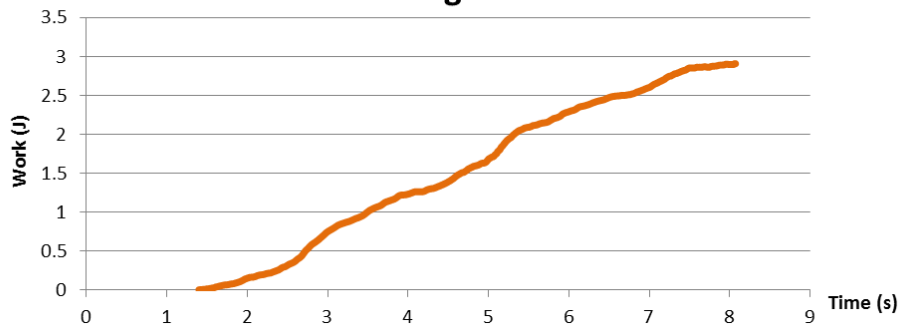
### SAMPLE NO. 2 - Right - Resident: 9.5mm



### SAMPLE NO. 2 - Right - Resident: 9.5mm

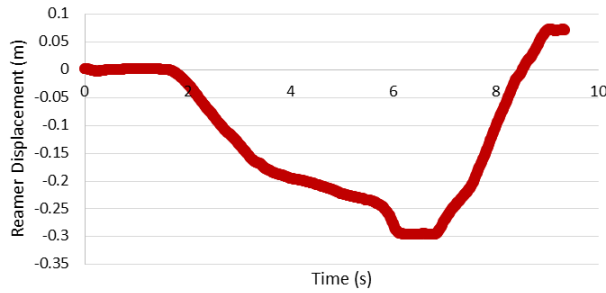


### SAMPLE NO. 2 - Right - Resident: 9.5mm

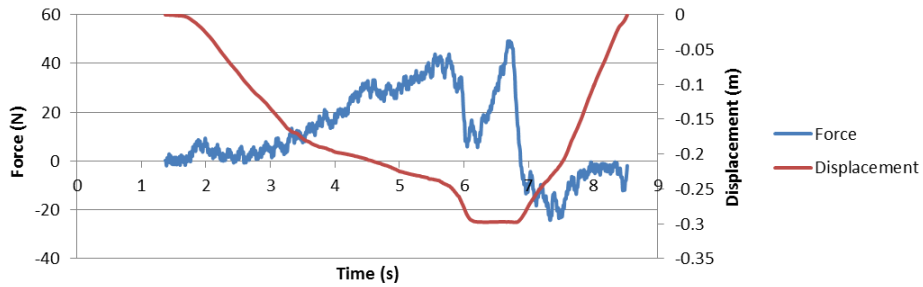


10MM

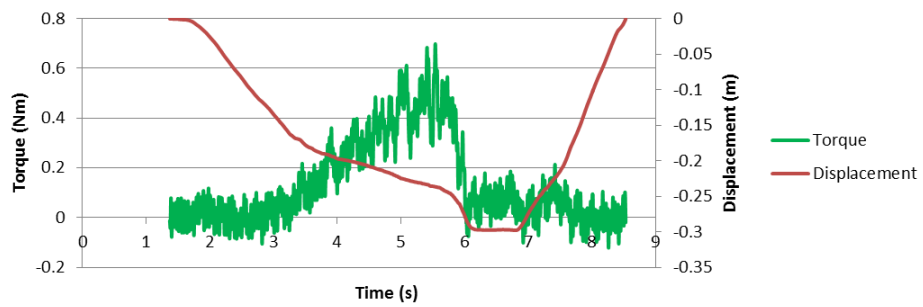
**SAMPLE NO. 2 - Right - Resident: 10mm  
CHATTER**



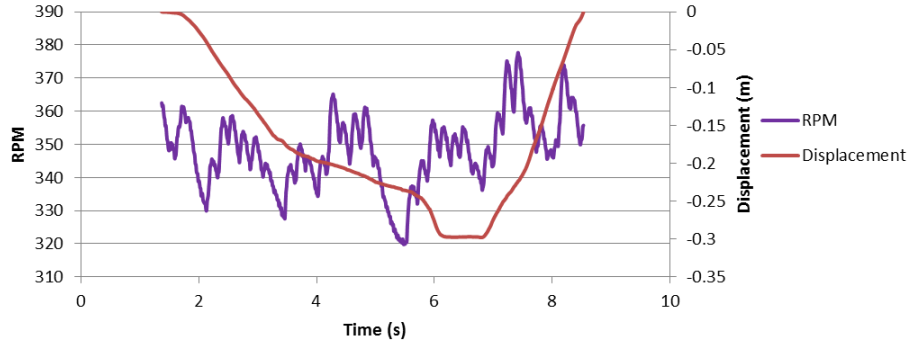
**SAMPLE NO. 2 - Right - Resident: 10mm CHATTER**



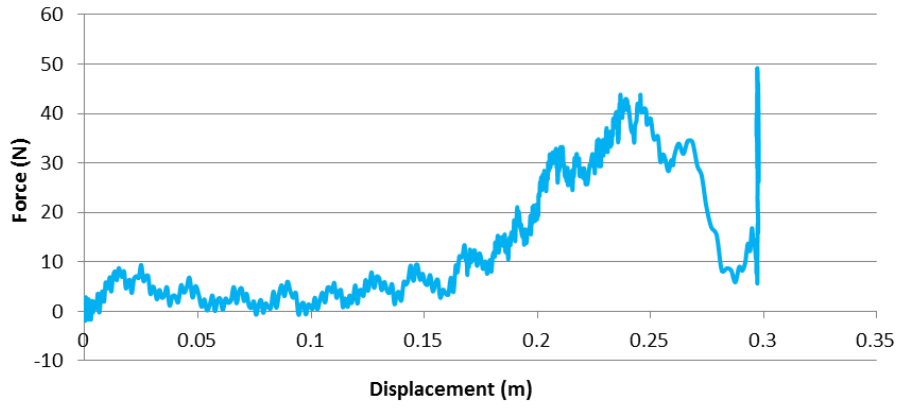
**SAMPLE NO. 2 - Right - Resident: 10mm CHATTER**



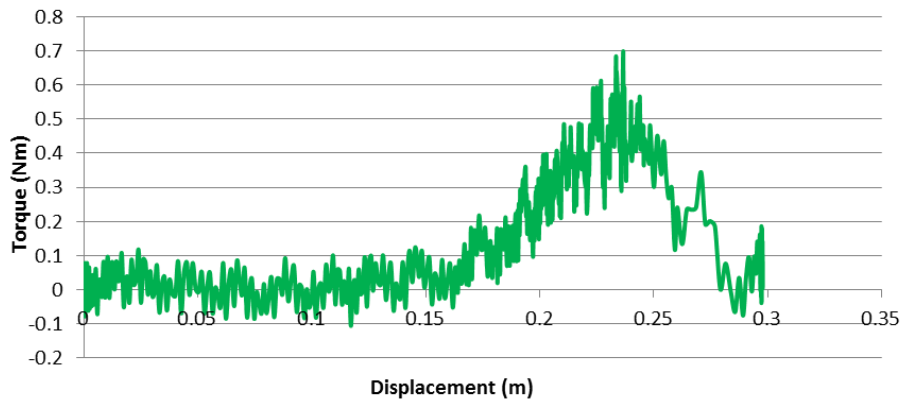
**SAMPLE NO. 2 - Right - Resident: 10mm CHATTER**



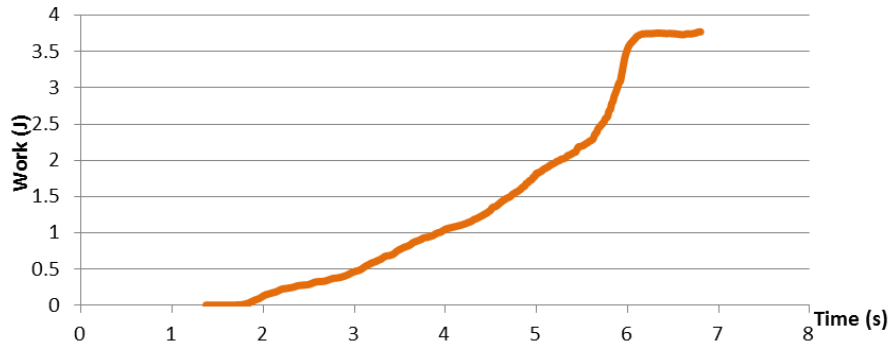
**SAMPLE NO. 2 - Right - Resident: 10mm CHATTER**



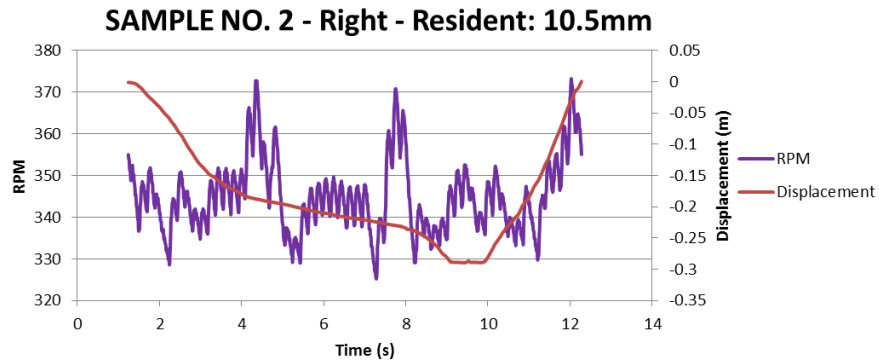
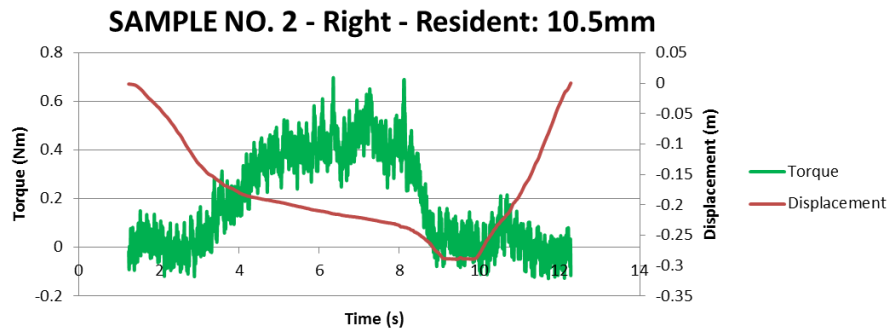
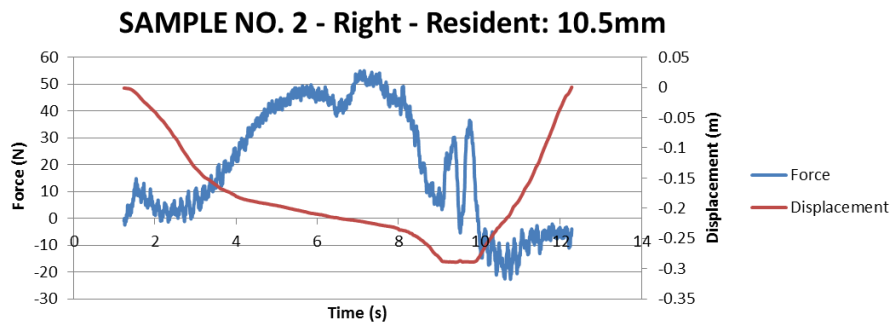
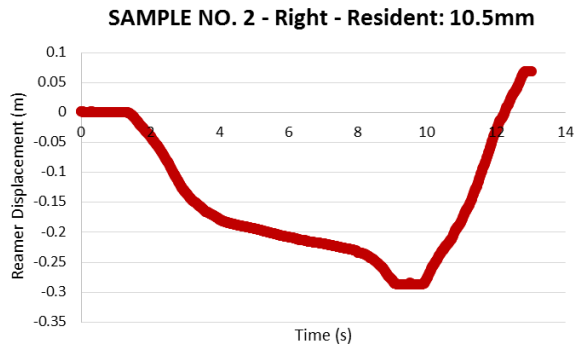
**SAMPLE NO. 2 - Right - Resident: 10mm CHATTER**



**SAMPLE NO. 2 - Right - Resident: 10mm CHATTER**

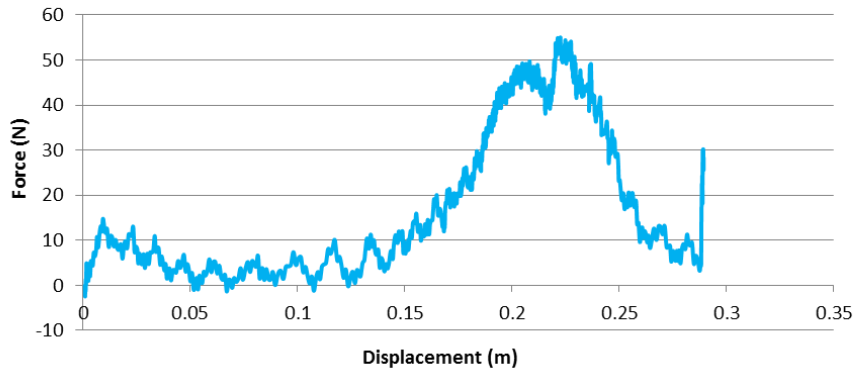


10.5MM

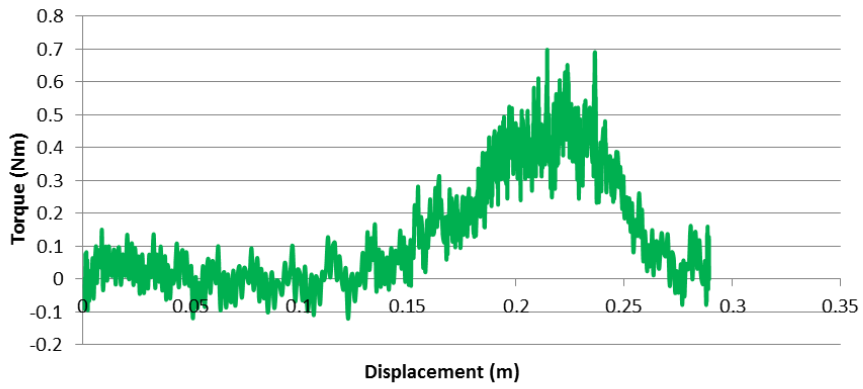




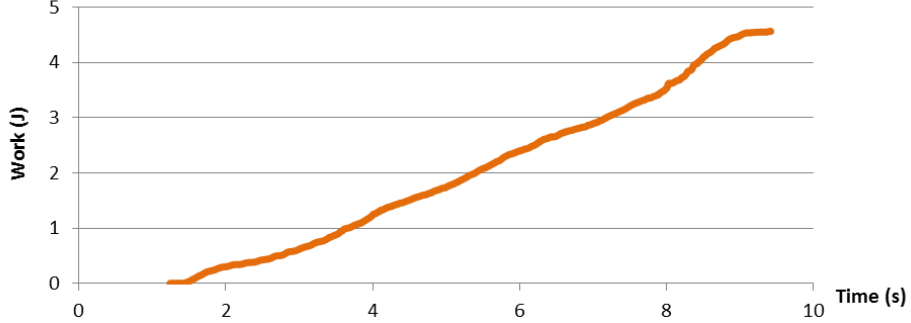
**SAMPLE NO. 2 - Right - Resident: 10.5mm**



**SAMPLE NO. 2 - Right - Resident: 10.5mm**

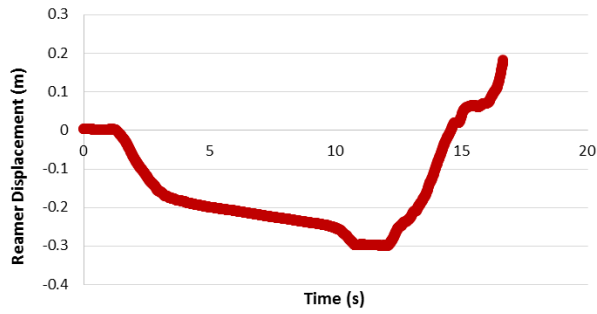


**SAMPLE NO. 2 - Right - Resident: 10.5mm**

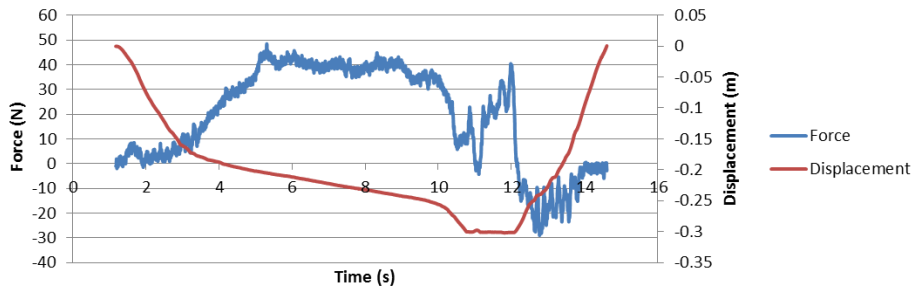


11MM

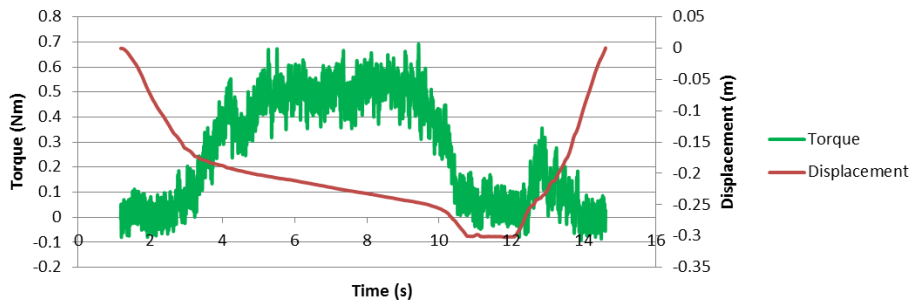
SAMPLE NO. 2 - Right - Resident: 11mm



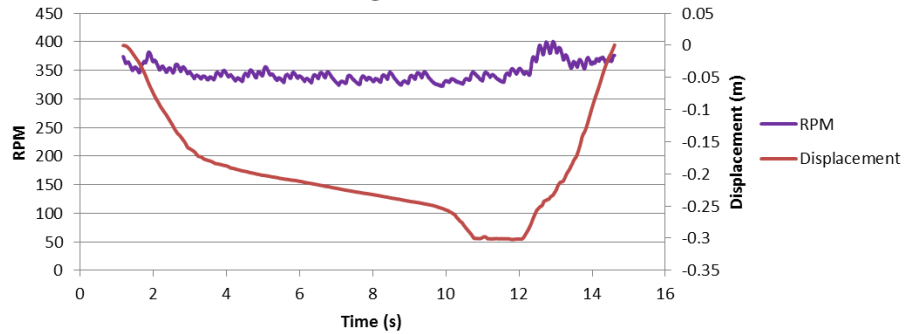
SAMPLE NO. 2 - Right - Resident: 11mm



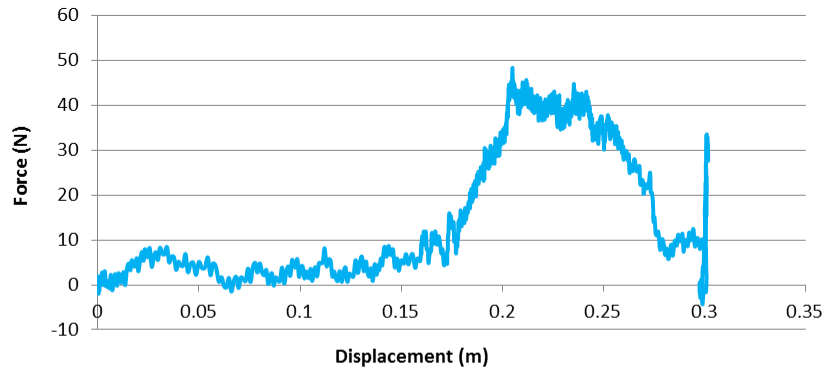
SAMPLE NO. 2 - Right - Resident: 11mm



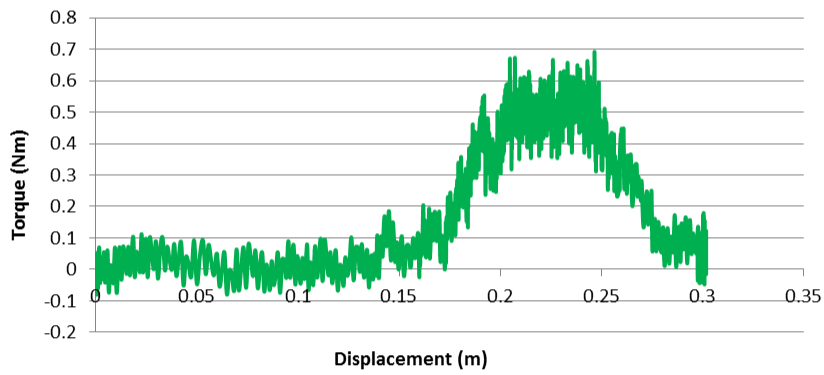
SAMPLE NO. 2 - Right - Resident: 11mm



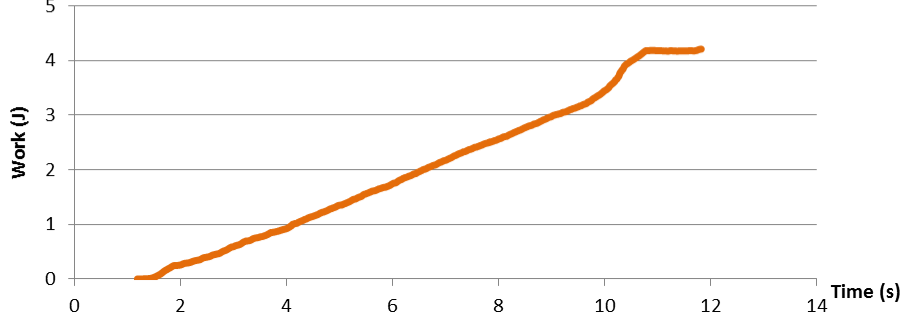
**SAMPLE NO. 2 - Right - Resident: 11mm**



**SAMPLE NO. 2 - Right - Resident: 11mm**

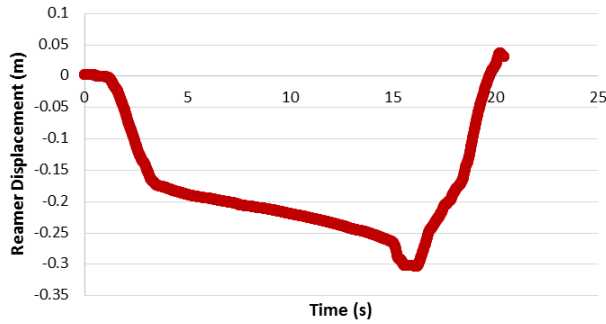


**SAMPLE NO. 2 - Right - Resident: 11mm**

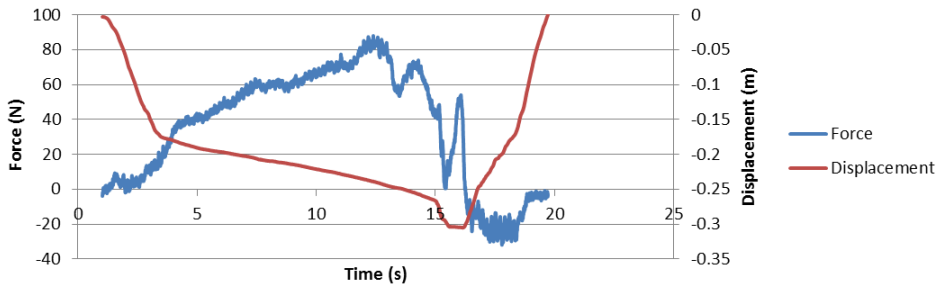


11.5MM

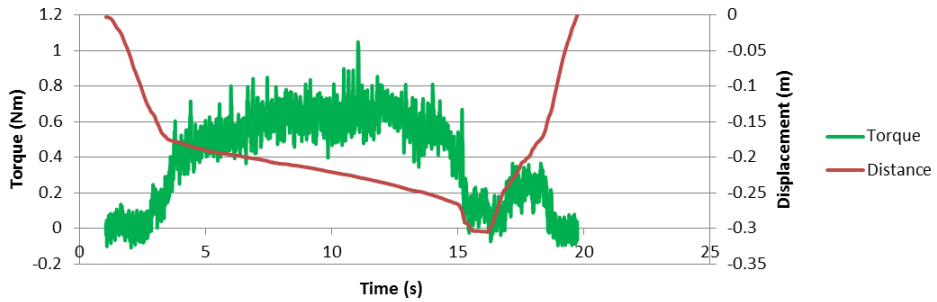
SAMPLE NO. 2 - Right - Resident: 11.5mm



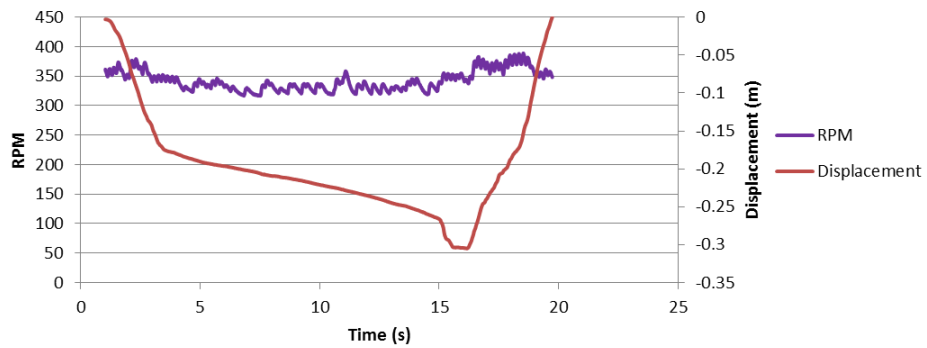
SAMPLE NO. 2 - Right - Resident: 11.5mm



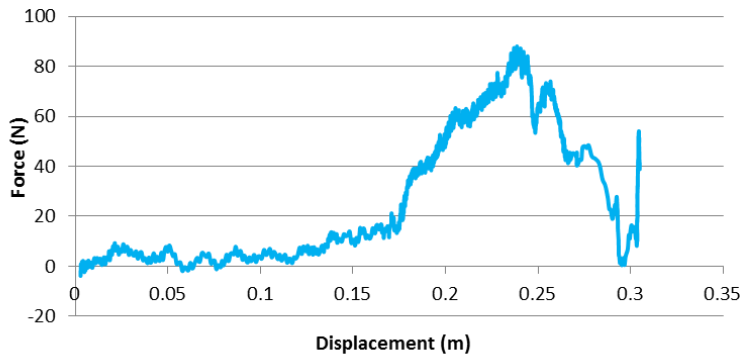
SAMPLE NO. 2 - Right - Resident: 11.5mm



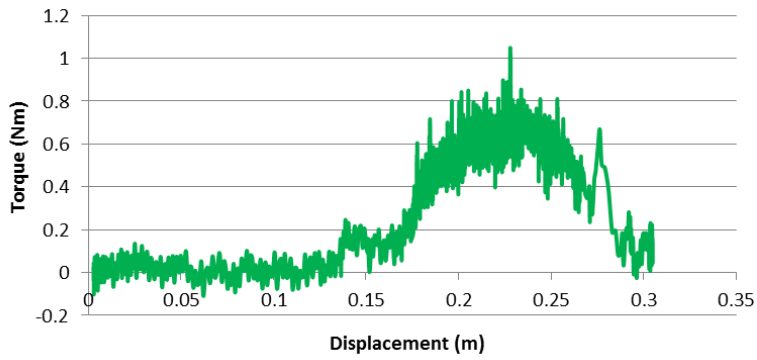
SAMPLE NO. 2 - Right - Resident: 11.5mm



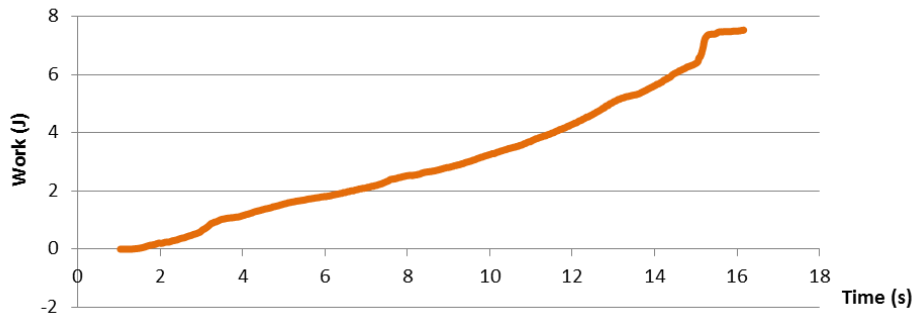
**SAMPLE NO. 2 - Right - Resident: 11.5mm**



**SAMPLE NO. 2 - Right - Resident: 11.5mm**



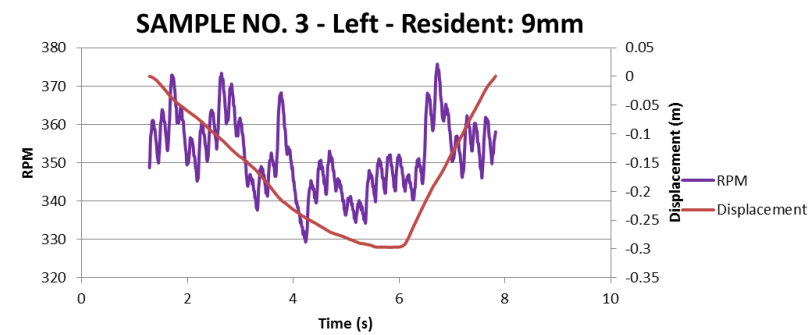
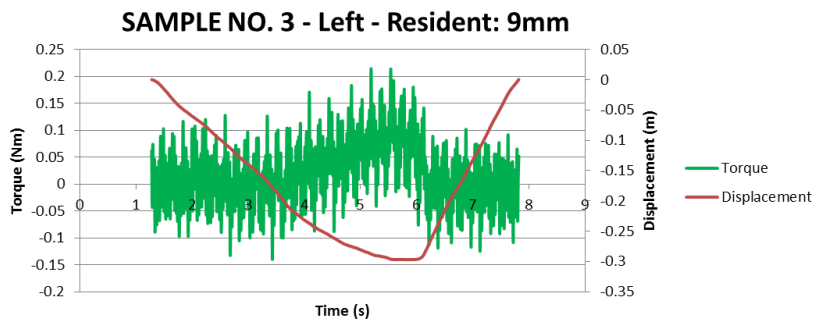
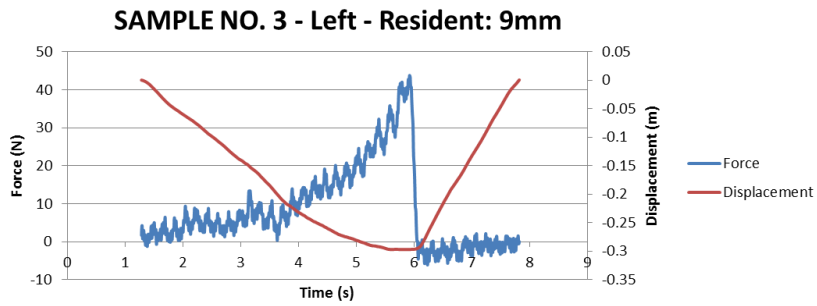
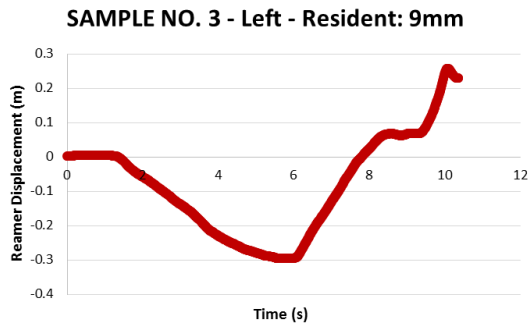
**SAMPLE NO. 2 - Right - Resident: 11.5mm**



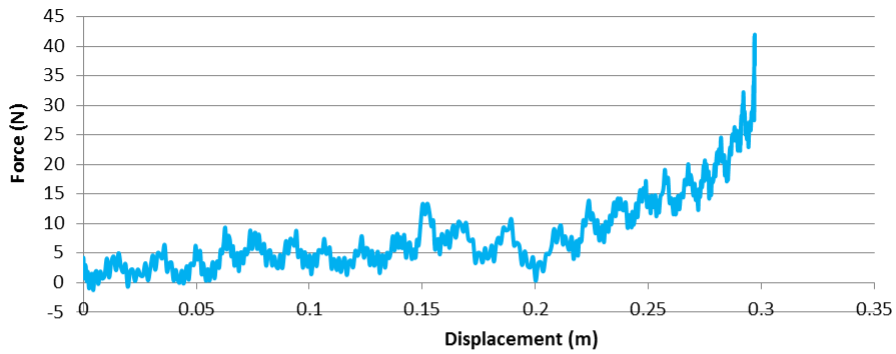
### 13.3 SAMPLE 3 RESULTS

LEFT: RESIDENT

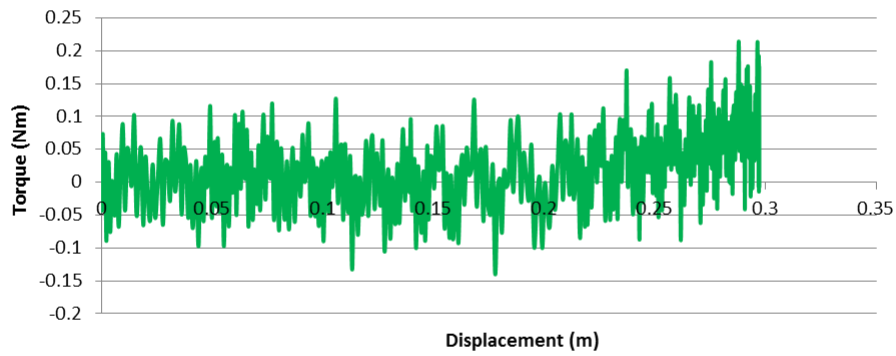
9MM



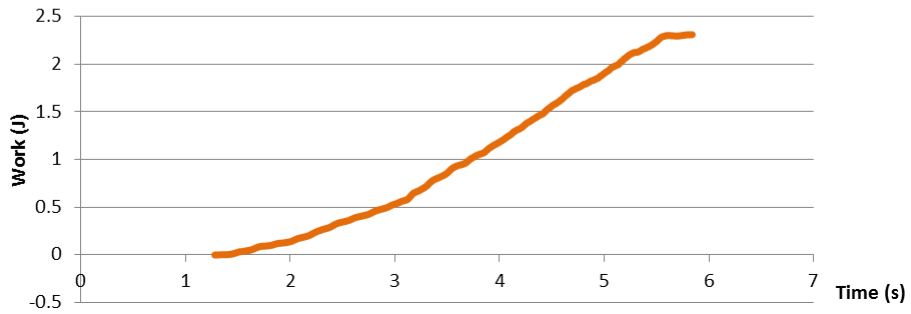
**SAMPLE NO. 3 - Left - Resident: 9mm**



**SAMPLE NO. 3 - Left - Resident: 9mm**

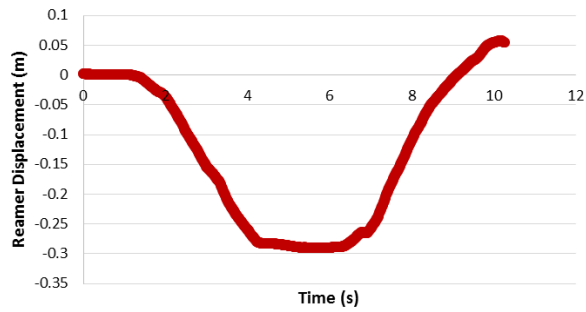


**SAMPLE NO. 3 - Left - Resident: 9mm**

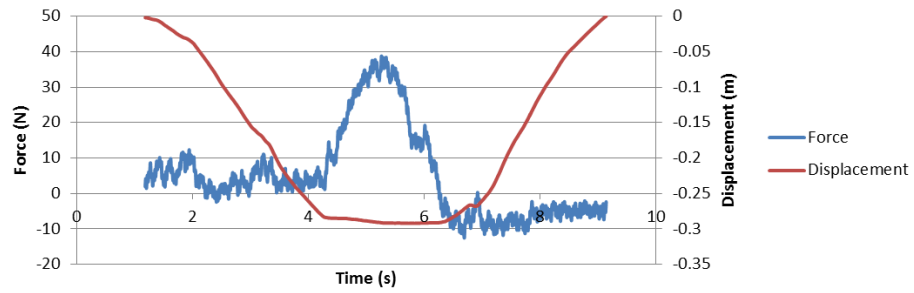


9.5MM

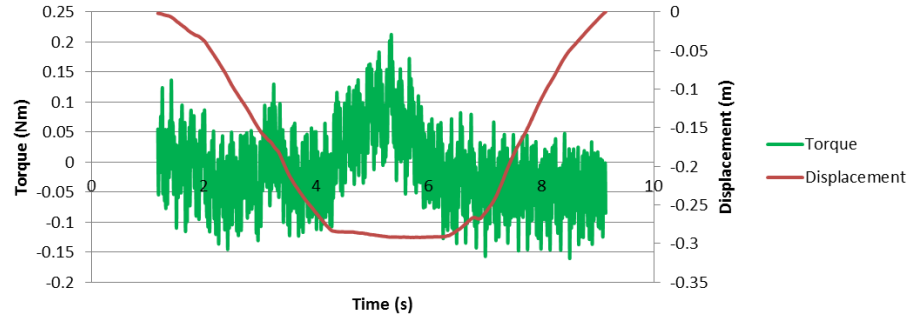
**SAMPLE NO. 3 - Left - Resident: 9.5mm**



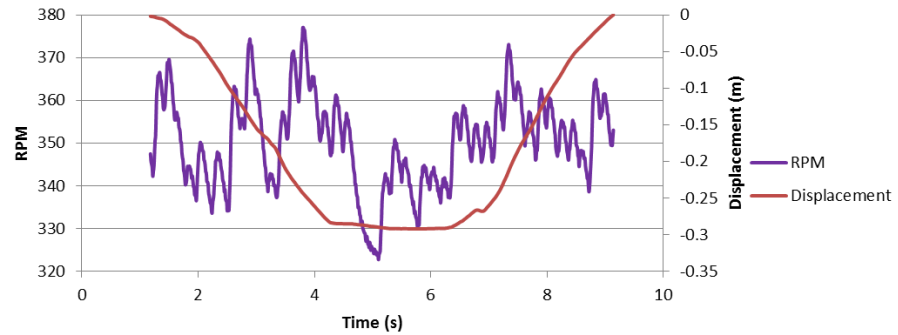
**SAMPLE NO. 3 - Left - Resident: 9.5mm**



**SAMPLE NO. 3 - Left - Resident: 9.5mm**

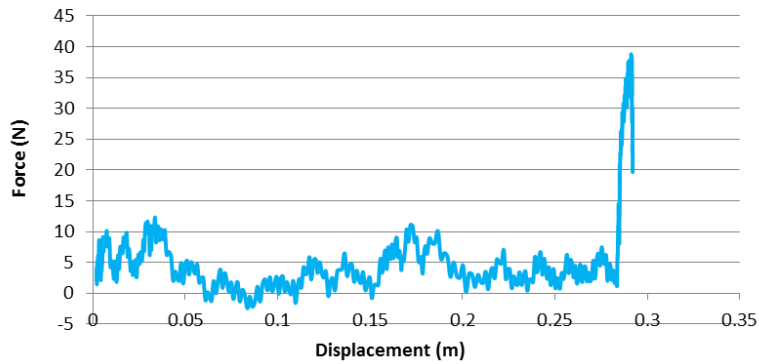


**SAMPLE NO. 3 - Left - Resident: 9.5mm**

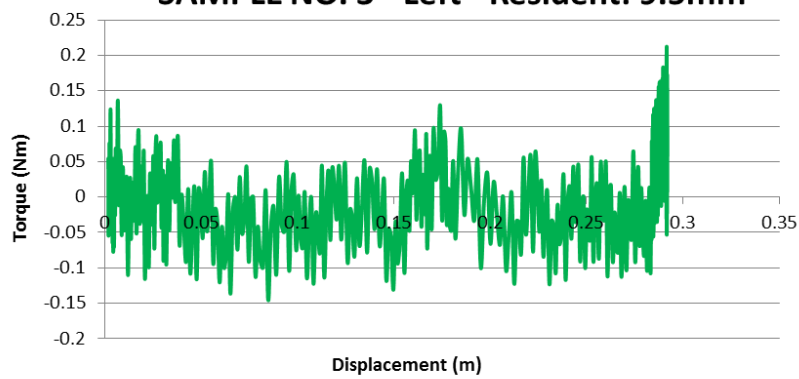




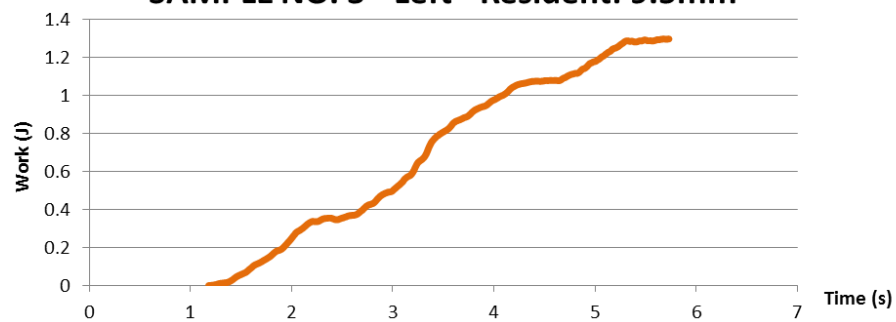
**SAMPLE NO. 3 - Left - Resident: 9.5mm**



**SAMPLE NO. 3 - Left - Resident: 9.5mm**

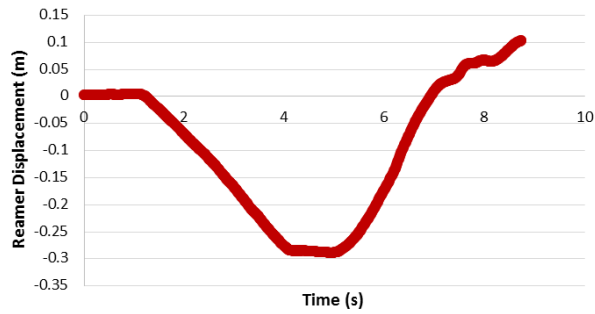


**SAMPLE NO. 3 - Left - Resident: 9.5mm**

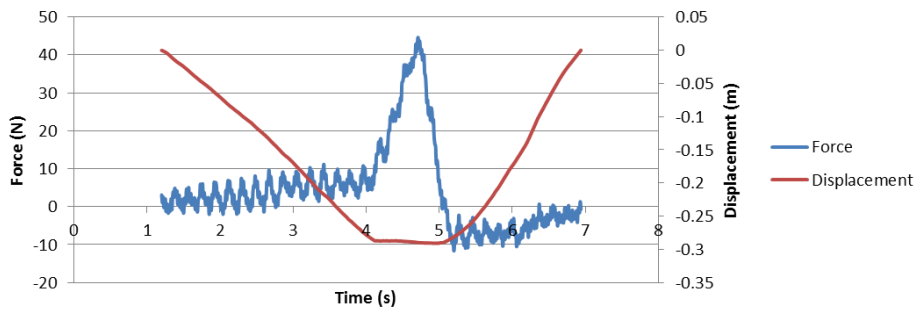


10MM

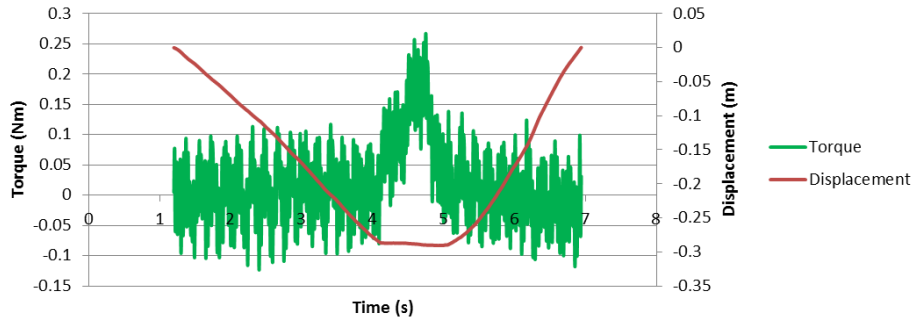
SAMPLE NO. 3 - Left - Resident: 10mm



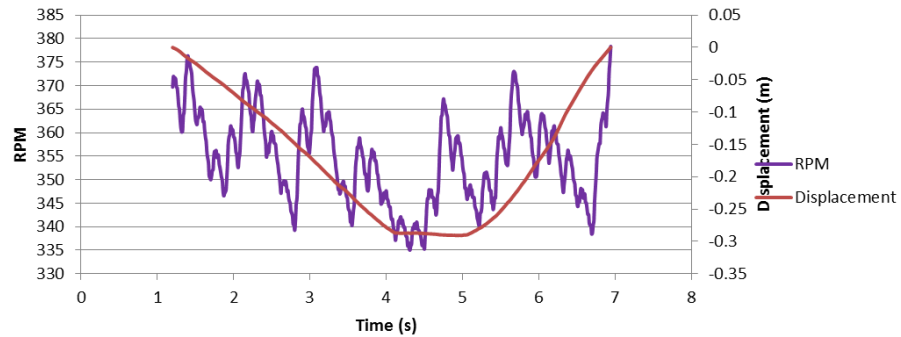
SAMPLE NO. 3 - Left - Resident: 10mm



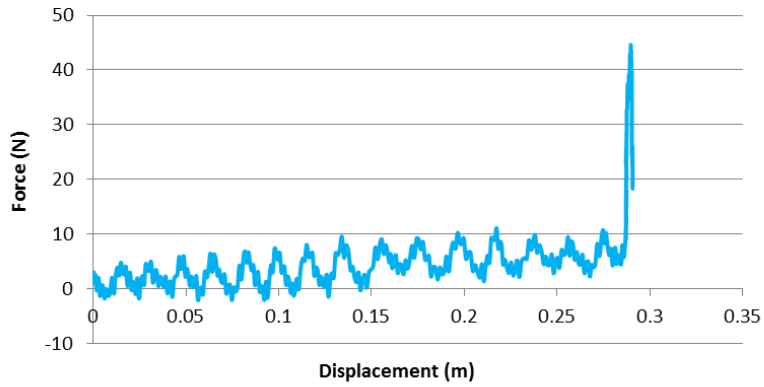
SAMPLE NO. 3 - Left - Resident: 10mm



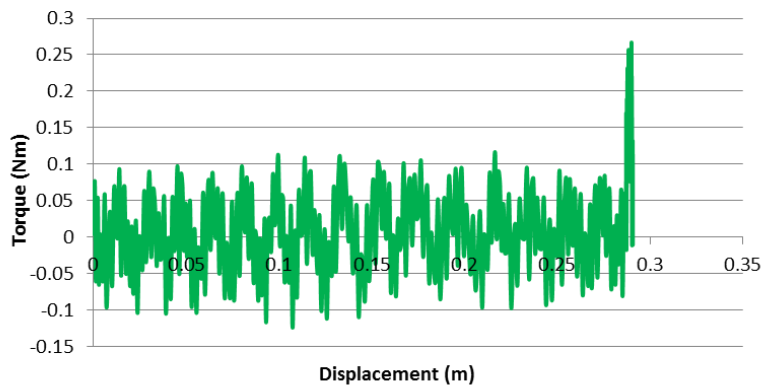
SAMPLE NO. 3 - Left - Resident: 10mm



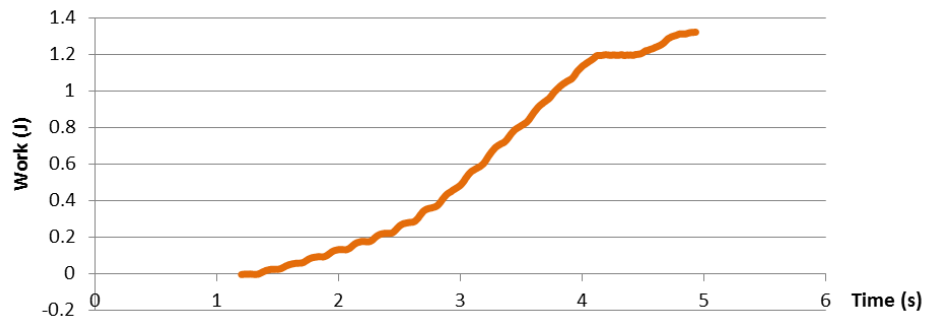
**SAMPLE NO. 3 - Left - Resident: 10mm**



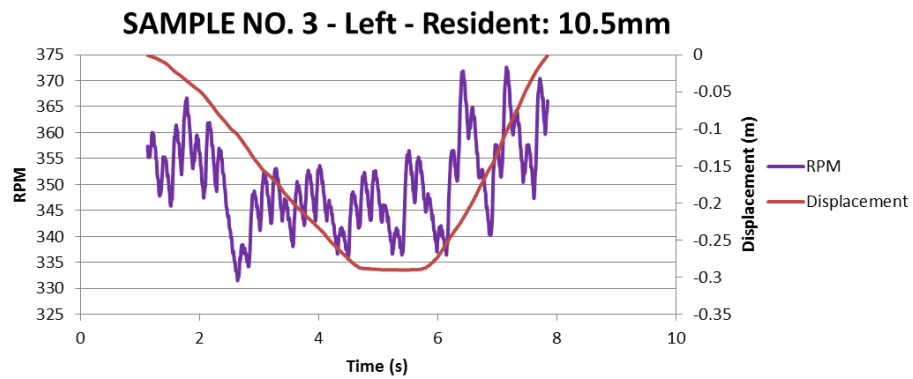
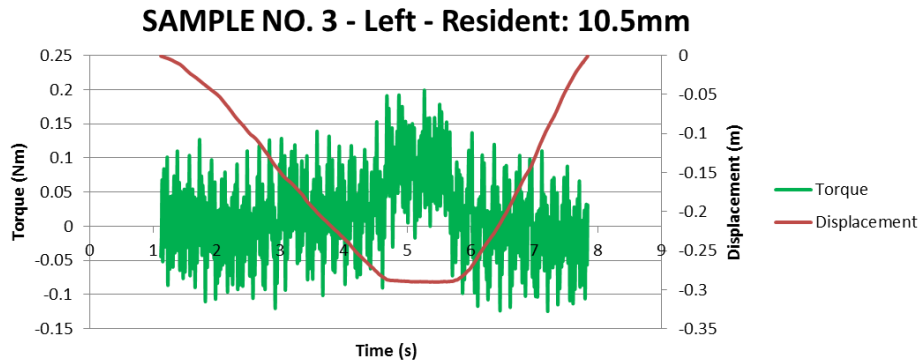
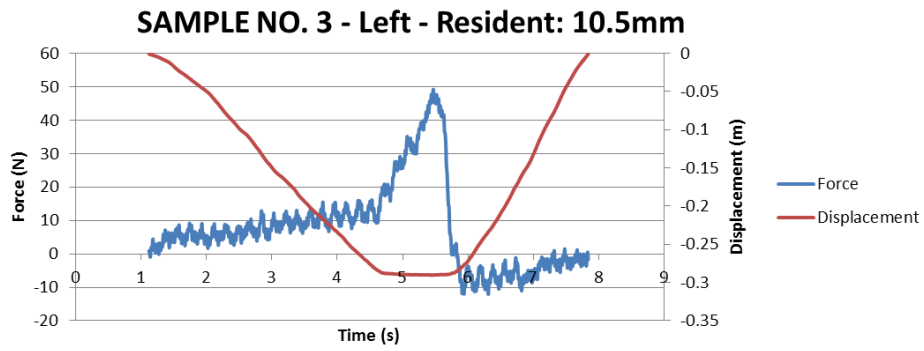
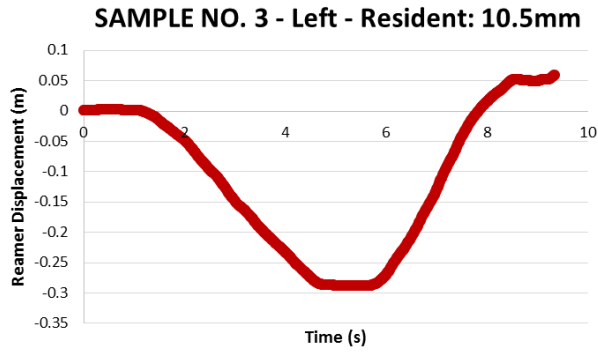
**SAMPLE NO. 3 - Left - Resident: 10mm**



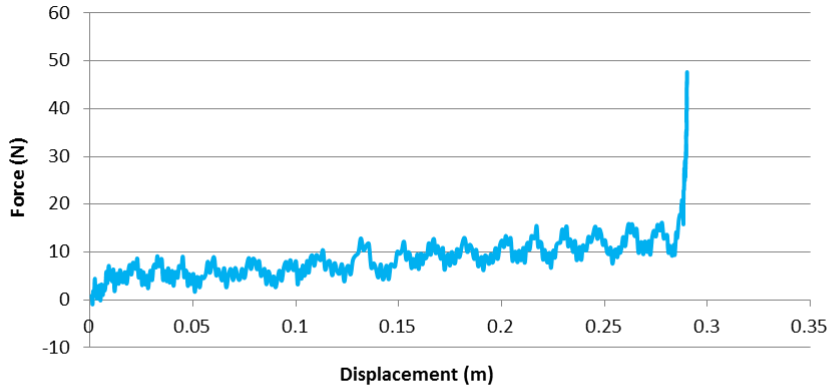
**SAMPLE NO. 3 - Left - Resident: 10mm**



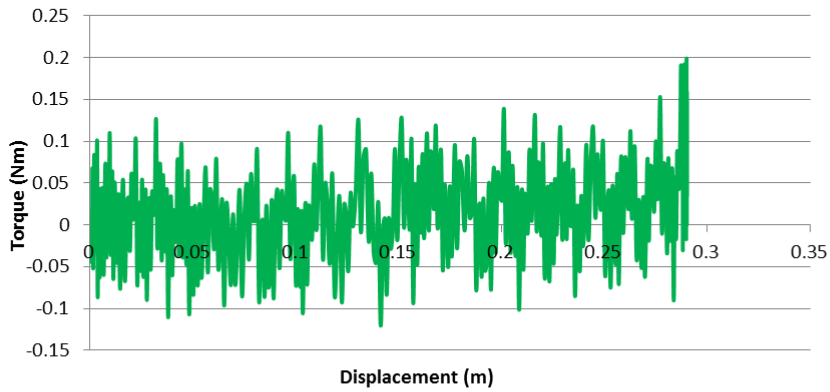
10.5MM



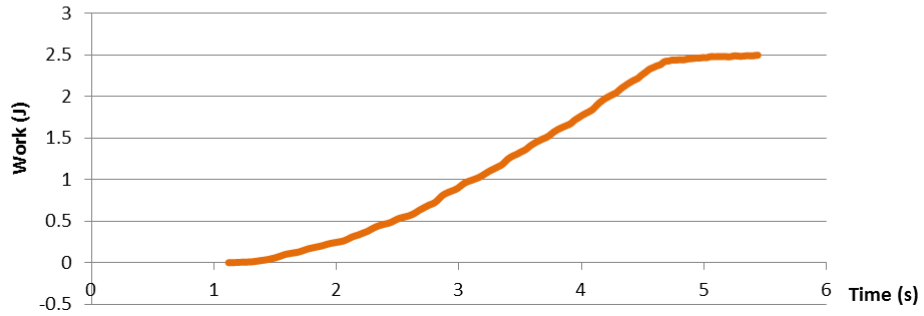
**SAMPLE NO. 3 - Left - Resident: 10.5mm**



**SAMPLE NO. 3 - Left - Resident: 10.5mm**

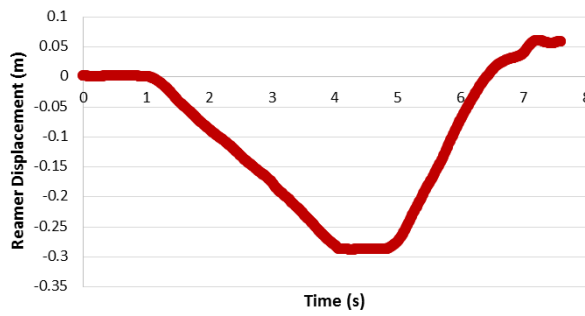


**SAMPLE NO. 3 - Left - Resident: 10.5mm**

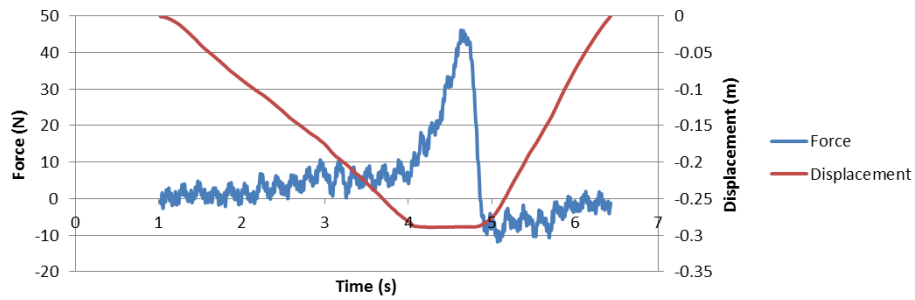


11MM

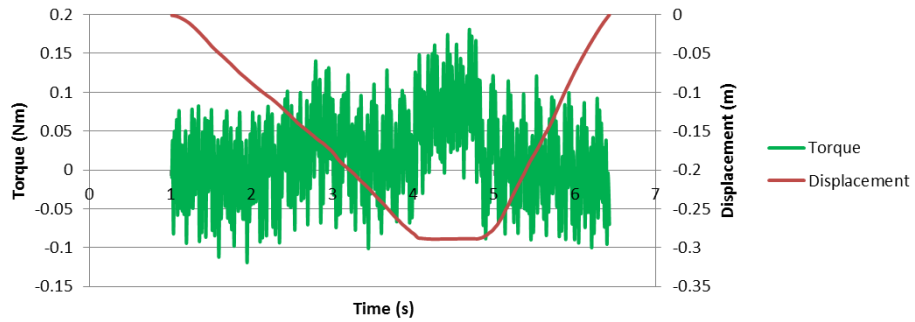
SAMPLE NO. 3 - Left - Resident: 11mm



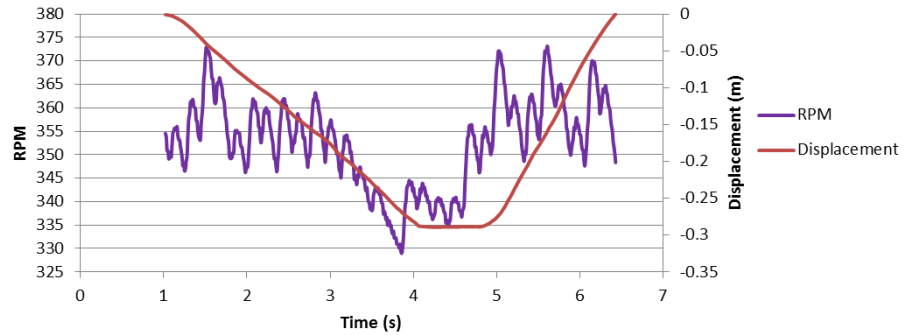
SAMPLE NO. 3 - Left - Resident: 11mm



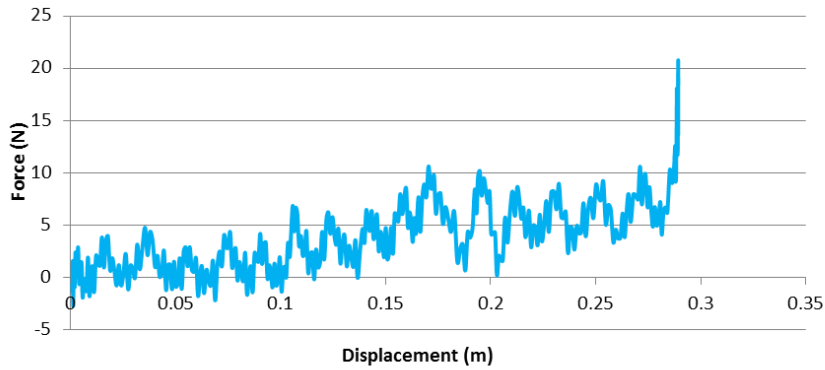
SAMPLE NO. 3 - Left - Resident: 11mm



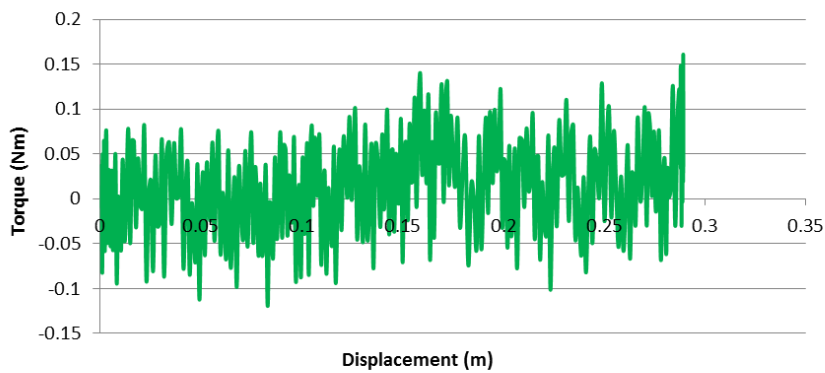
SAMPLE NO. 3 - Left - Resident: 11mm



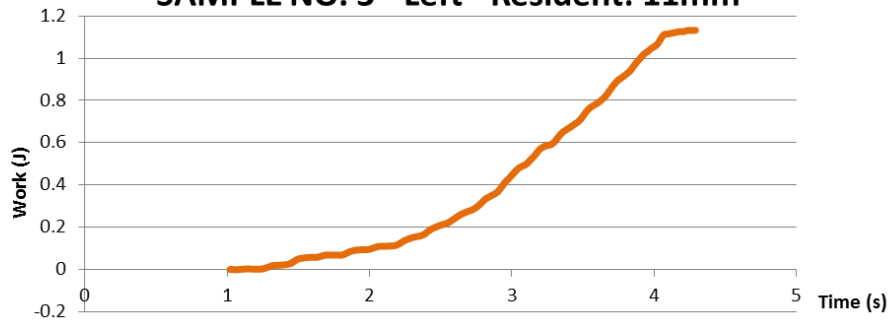
**SAMPLE NO. 3 - Left - Resident: 11mm**



**SAMPLE NO. 3 - Left - Resident: 11mm**

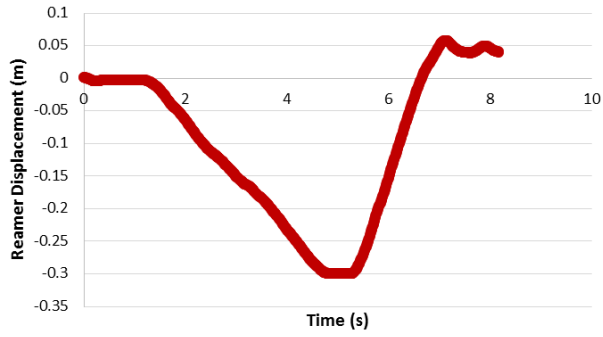


**SAMPLE NO. 3 - Left - Resident: 11mm**

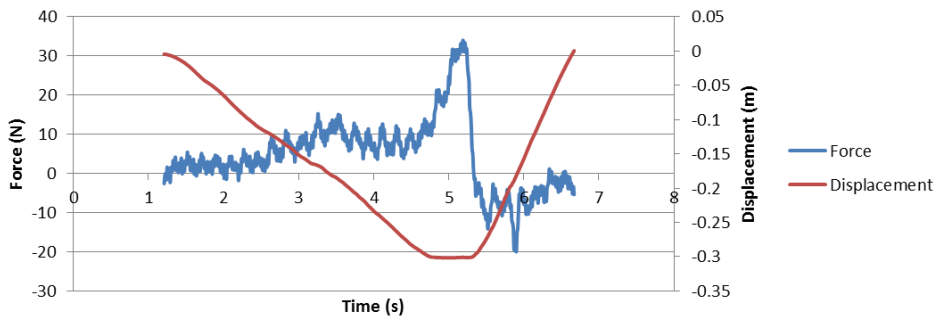


11.5

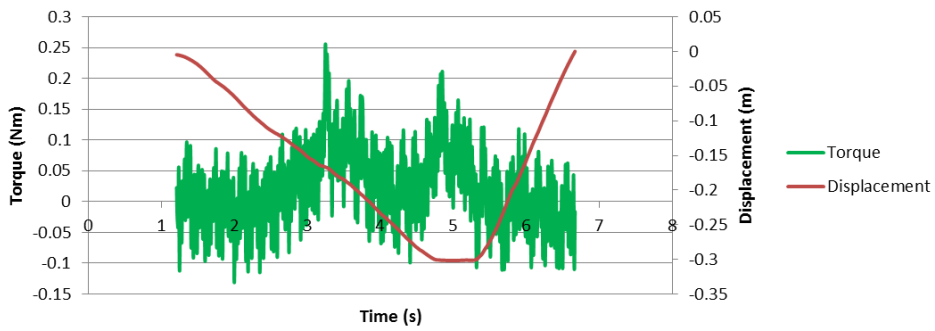
**SAMPLE NO. 3 - Left - Resident: 11.5mm**



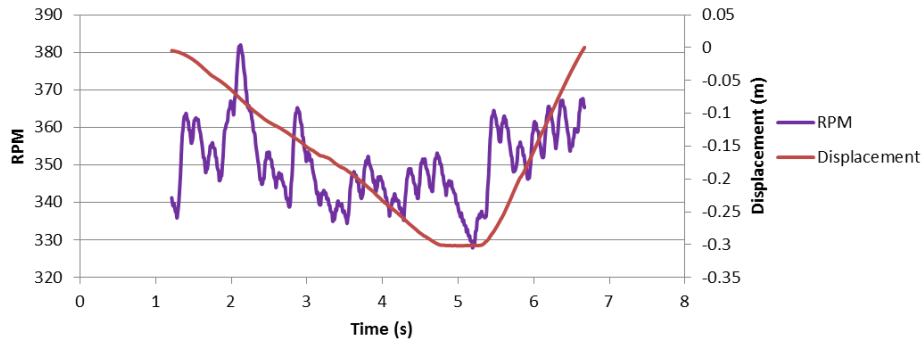
**SAMPLE NO. 3 - Left - Resident: 11.5mm**



**SAMPLE NO. 3 - Left - Resident: 11.5mm**

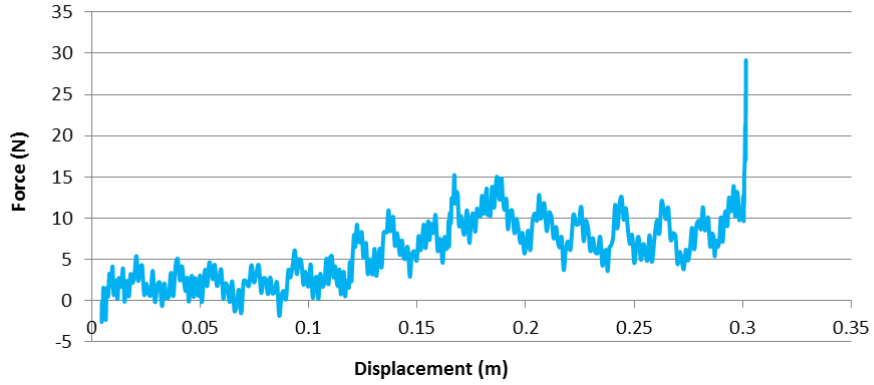


**SAMPLE NO. 3 - Left - Resident: 11.5mm**

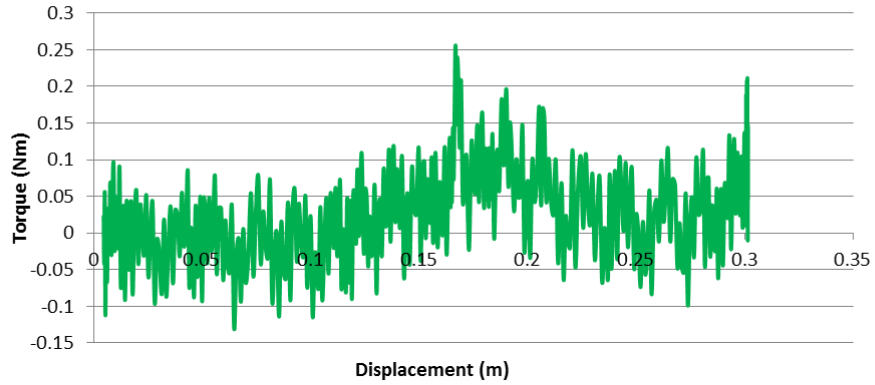




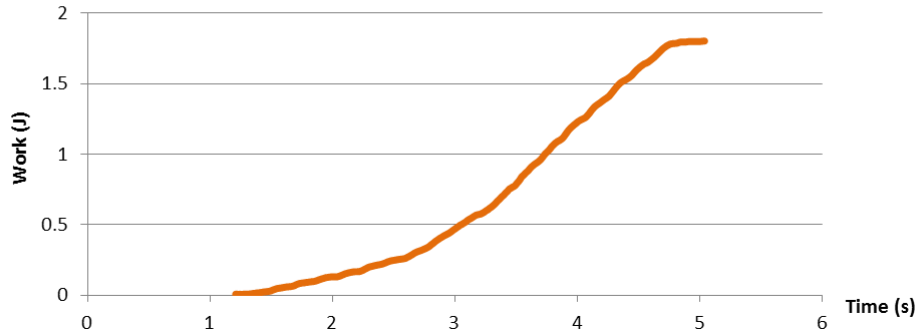
**SAMPLE NO. 3 - Left - Resident: 11.5mm**



**SAMPLE NO. 3 - Left - Resident: 11.5mm**

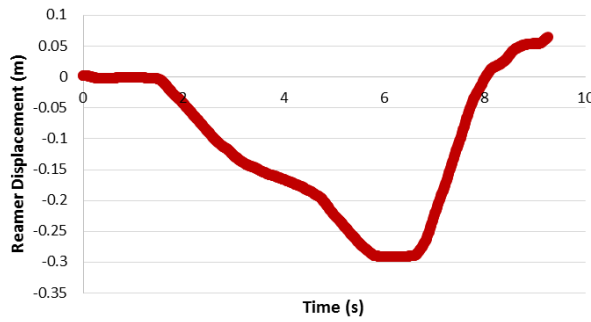


**SAMPLE NO. 3 - Left - Resident: 11.5mm**

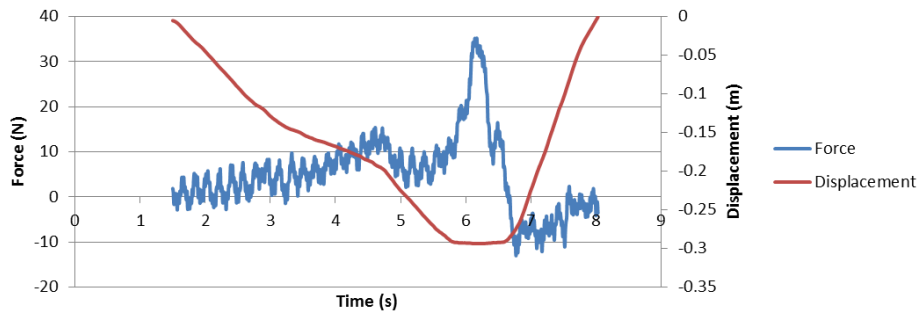


12MM

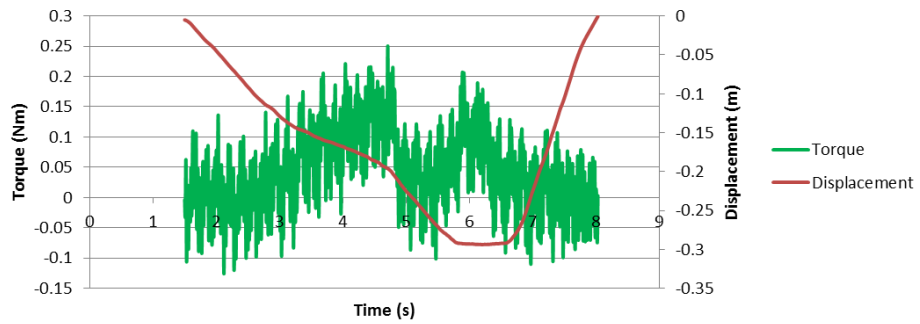
SAMPLE NO. 3 - Left - Resident: 12mm



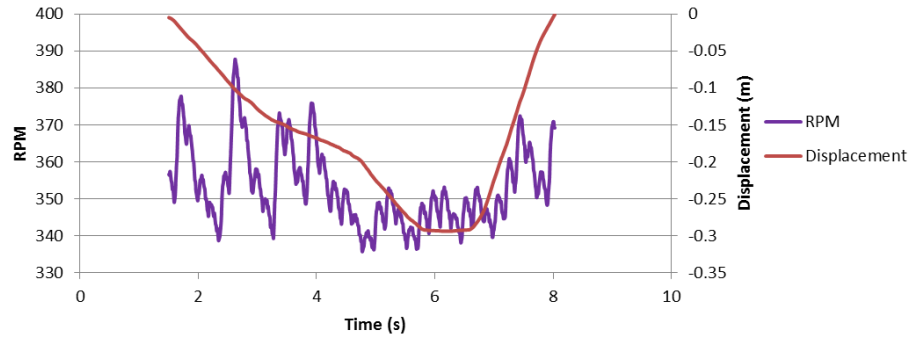
SAMPLE NO. 3 - Left - Resident: 12mm

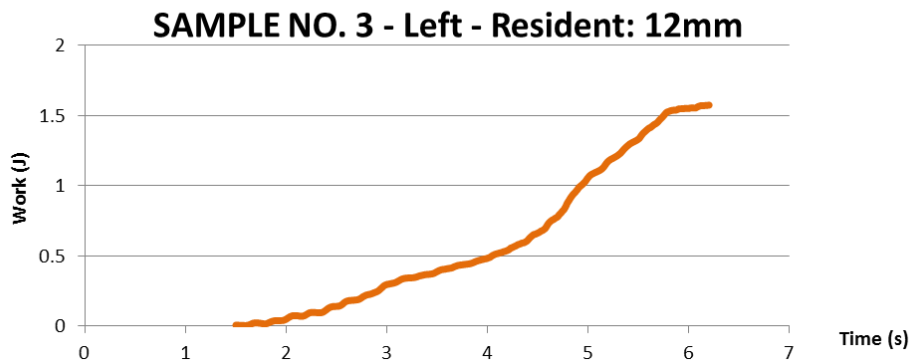
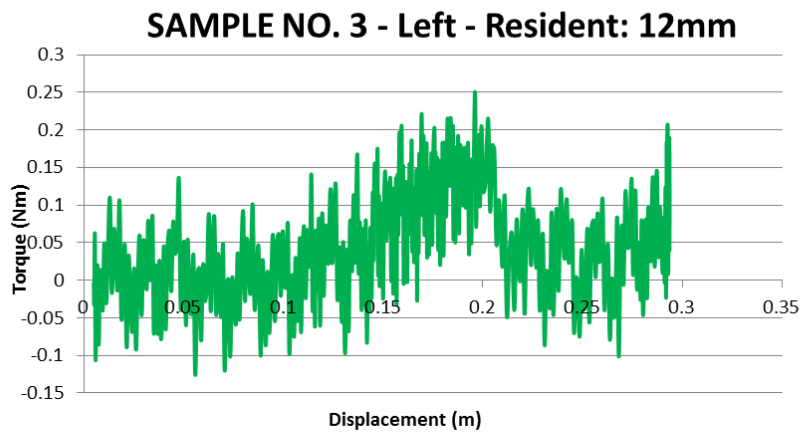
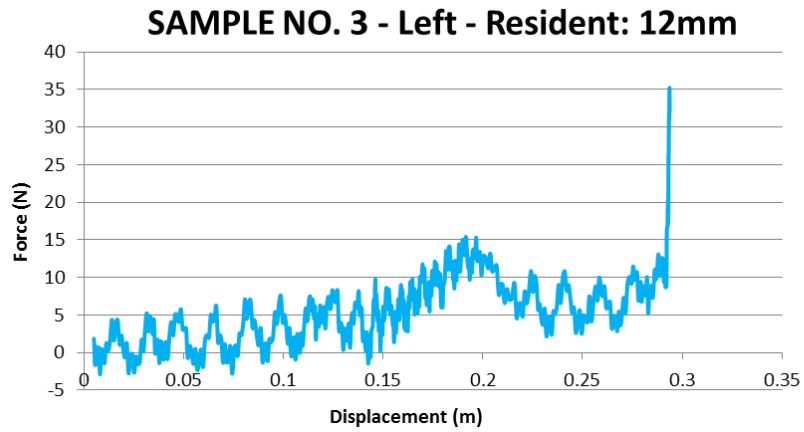


SAMPLE NO. 3 - Left - Resident: 12mm



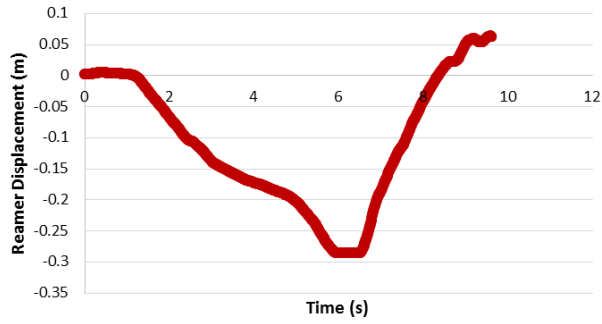
SAMPLE NO. 3 - Left - Resident: 12mm



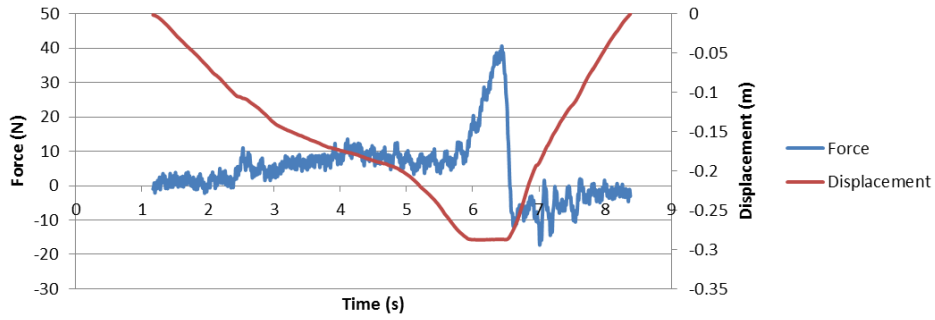


12.5MM

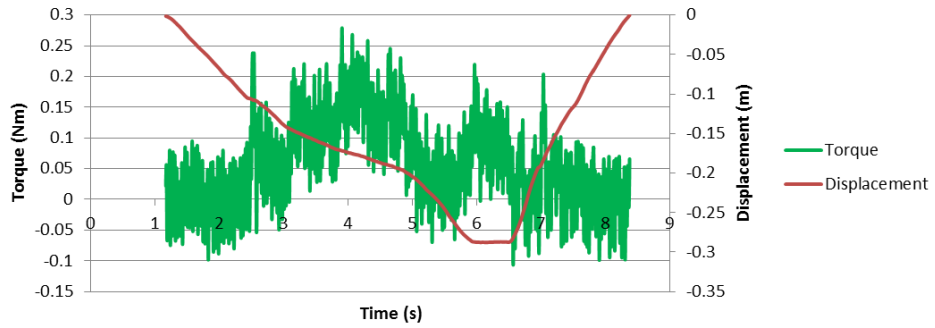
**SAMPLE NO. 3 - Left - Resident: 12.5mm**



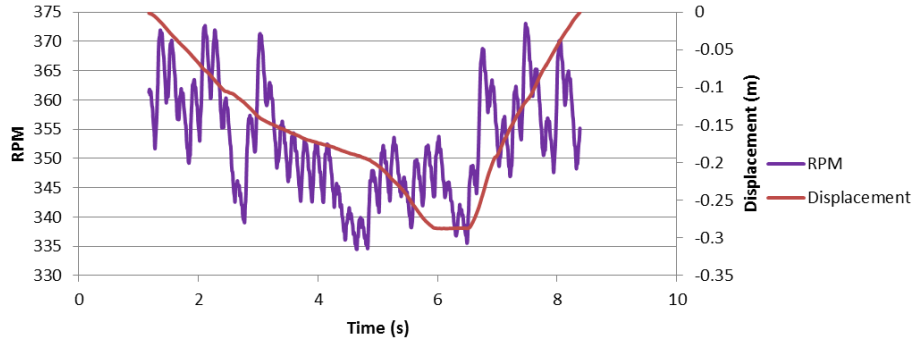
**SAMPLE NO. 3 - Left - Resident: 12.5mm**



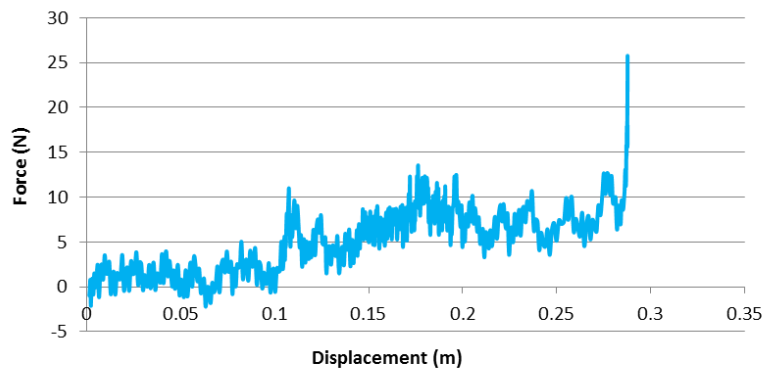
**SAMPLE NO. 3 - Left - Resident: 12.5mm**



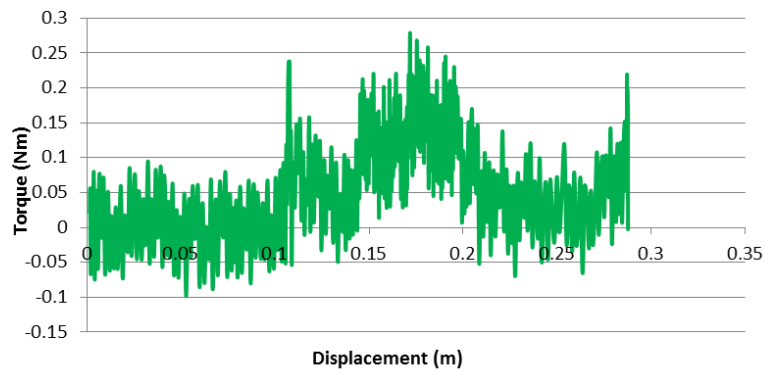
**SAMPLE NO. 3 - Left - Resident: 12.5mm**



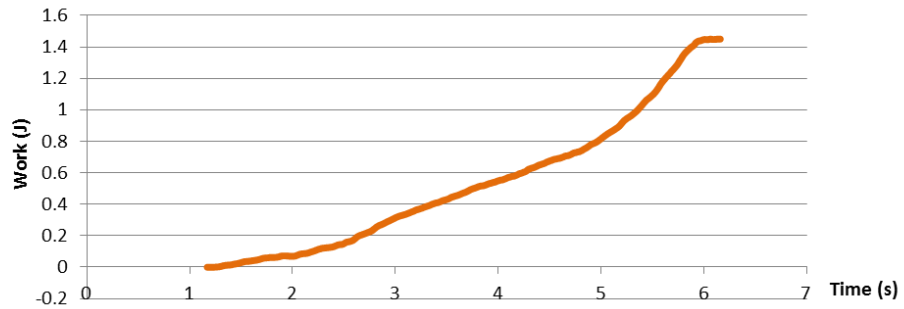
**SAMPLE NO. 3 - Left - Resident: 12.5mm**



**SAMPLE NO. 3 - Left - Resident: 12.5mm**

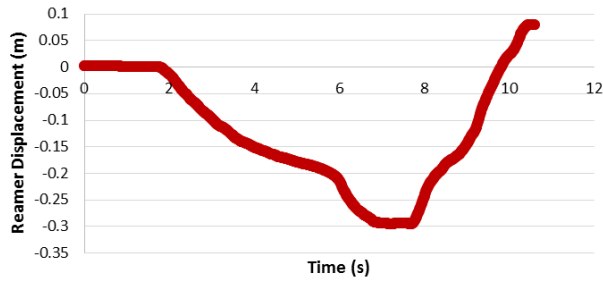


**SAMPLE NO. 3 - Left - Resident: 12.5mm**

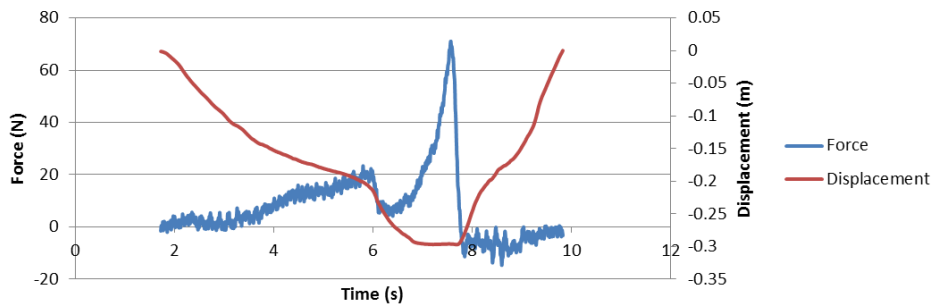


13MM

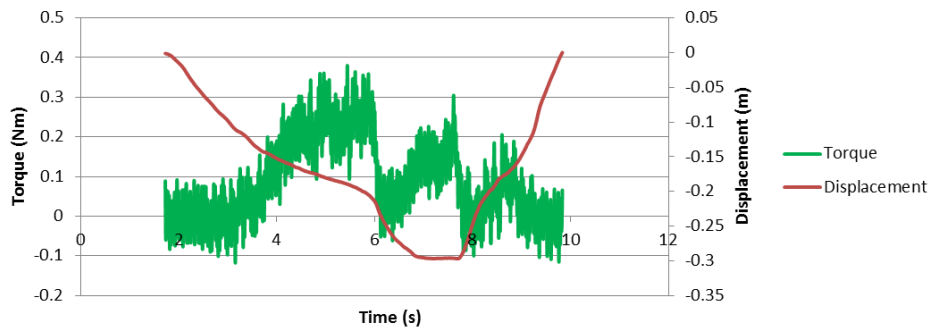
**SAMPLE NO. 3 - Left - Resident: 13mm CHATTER**



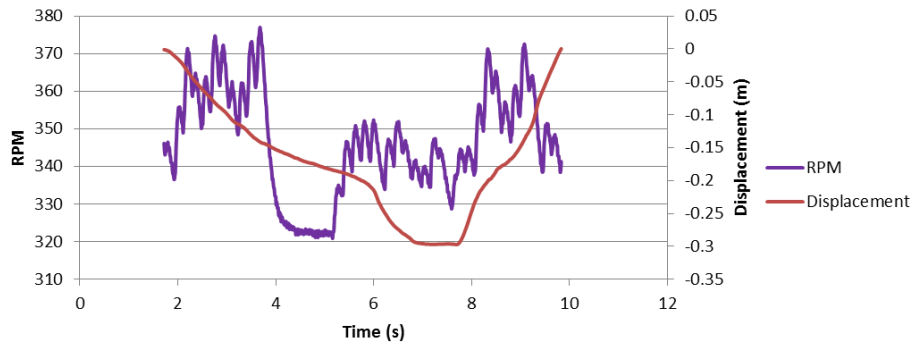
**SAMPLE NO. 3 - Left - Resident: 13mm CHATTER**



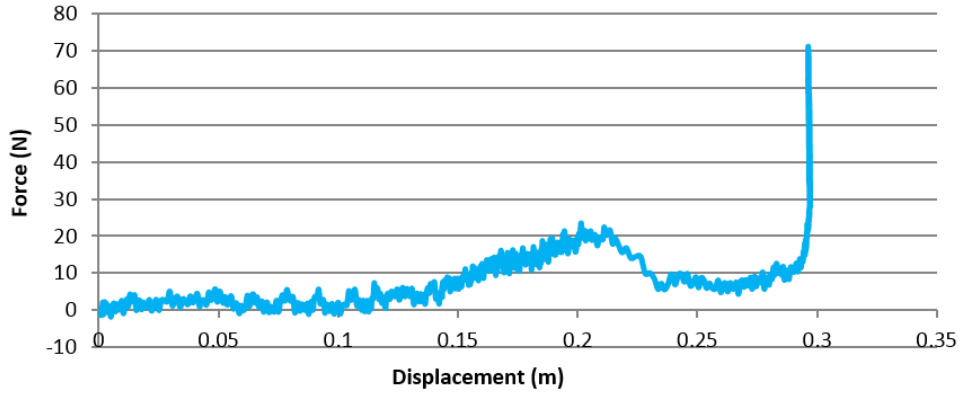
**SAMPLE NO. 3 - Left - Resident: 13mm CHATTER**



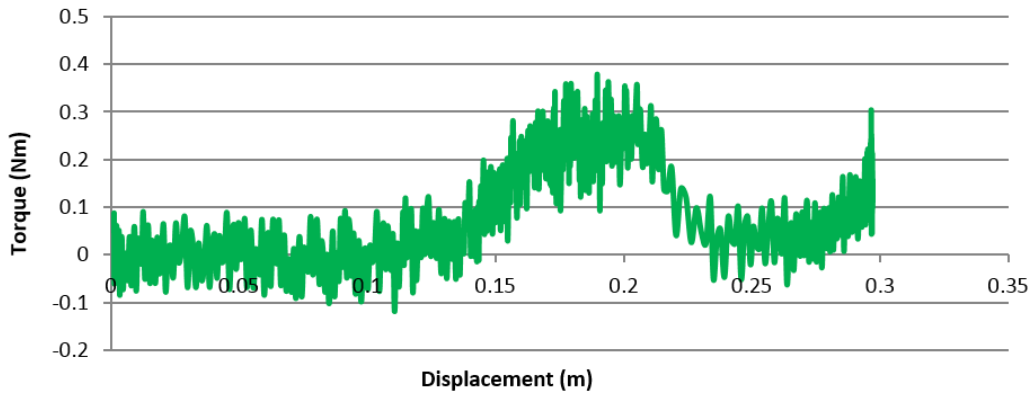
**SAMPLE NO. 3 - Left - Resident: 13mm CHATTER**



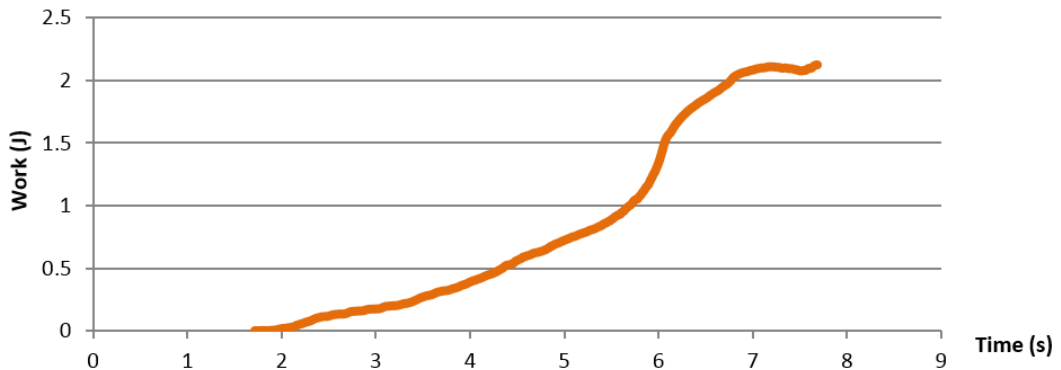
**SAMPLE NO. 3 - Left - Resident: 13mm CHATTER**



**SAMPLE NO. 3 - Left - Resident: 13mm CHATTER**

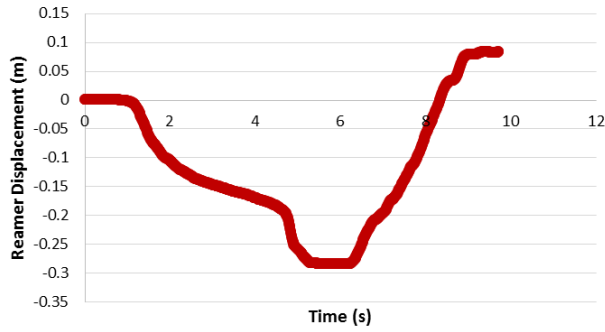


**SAMPLE NO. 3 - Left - Resident: 13mm CHATTER**

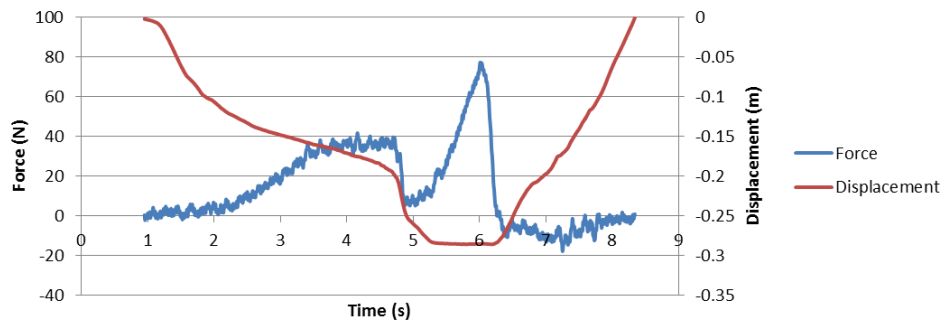


13.5MM

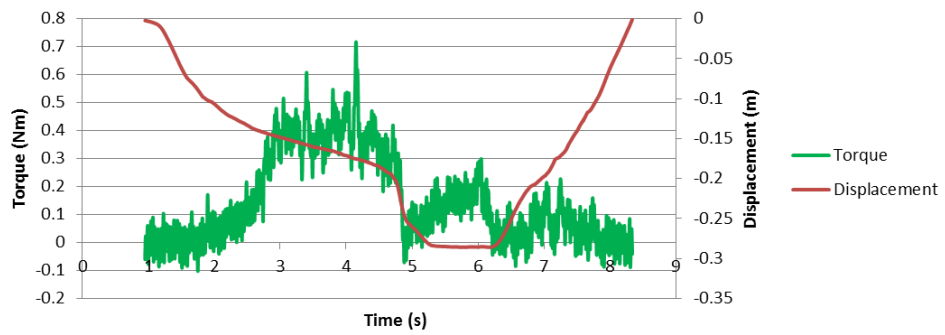
SAMPLE NO. 3 - Left - Resident: 13.5mm



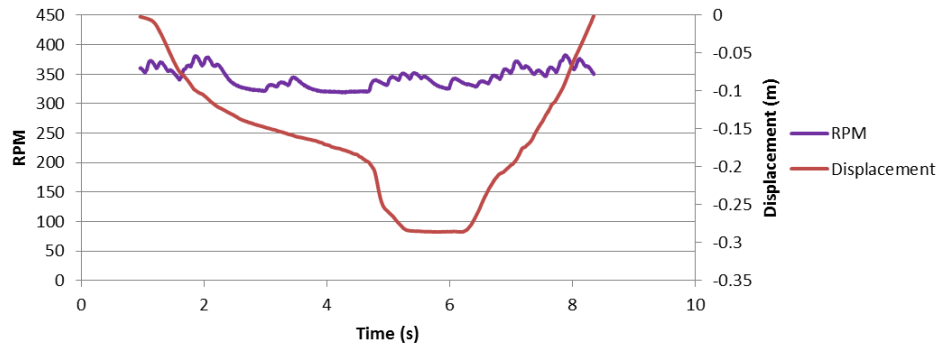
SAMPLE NO. 3 - Left - Resident: 13.5mm



SAMPLE NO. 3 - Left - Resident: 13.5mm

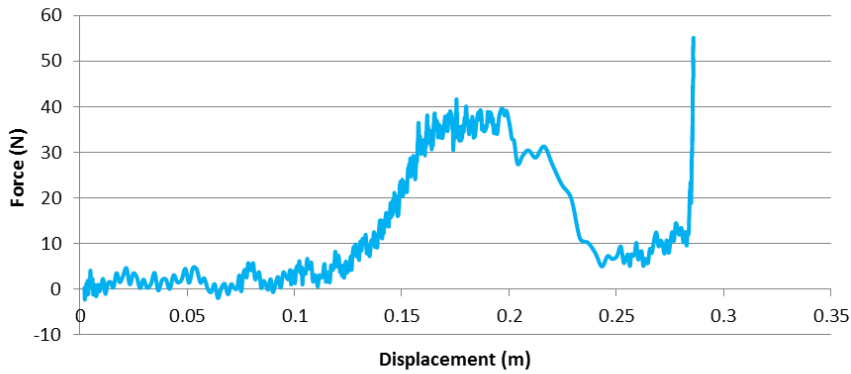


SAMPLE NO. 3 - Left - Resident: 13.5mm

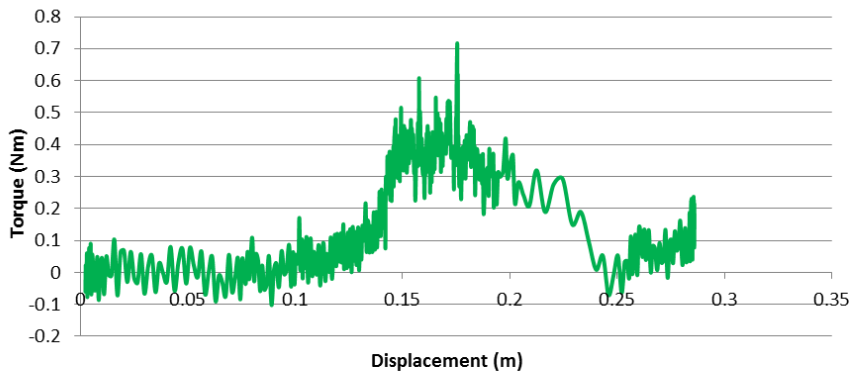




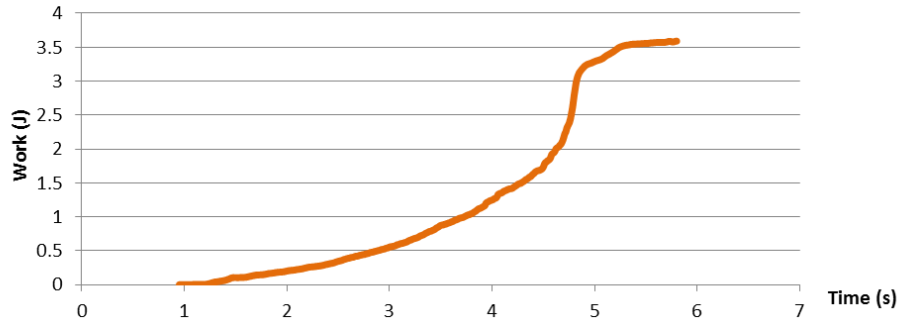
**SAMPLE NO. 3 - Left - Resident: 13.5mm**



**SAMPLE NO. 3 - Left - Resident: 13.5mm**

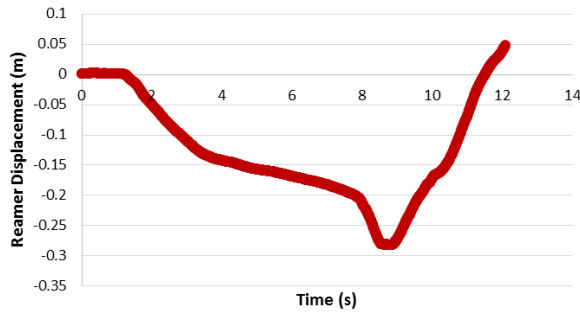


**SAMPLE NO. 3 - Left - Resident: 13.5mm**

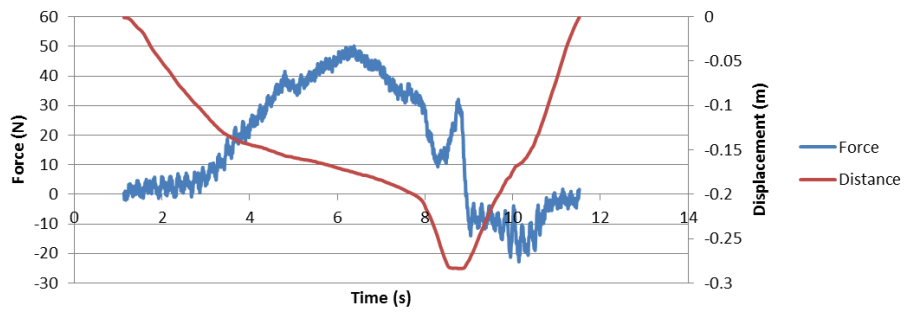


14MM

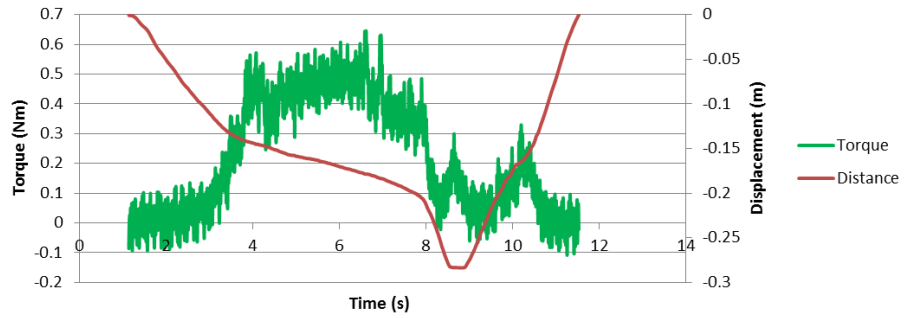
SAMPLE NO. 3 - Left - Resident: 14mm



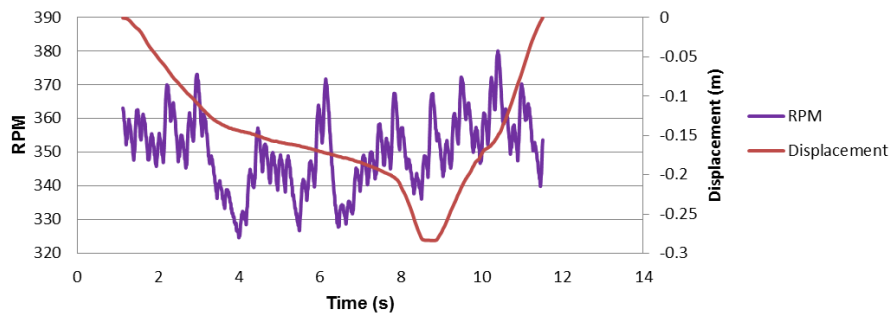
SAMPLE NO. 3 - Left - Resident: 14mm



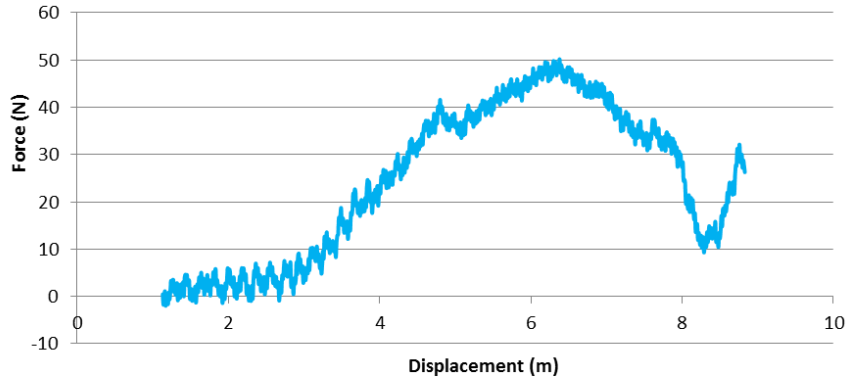
SAMPLE NO. 3 - Left - Resident: 14mm



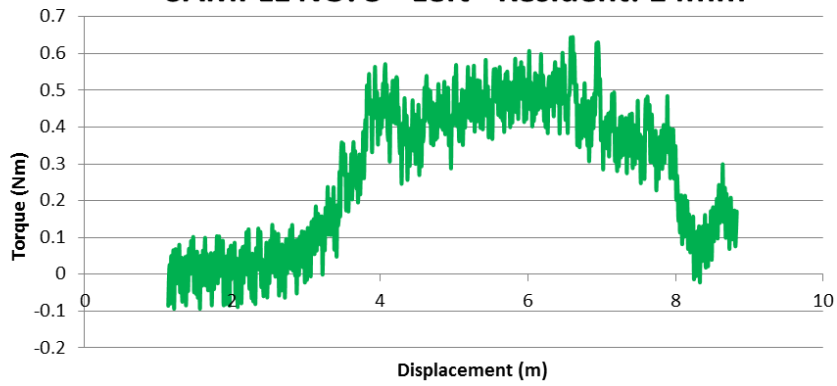
SAMPLE NO. 3 - Left - Resident: 14mm



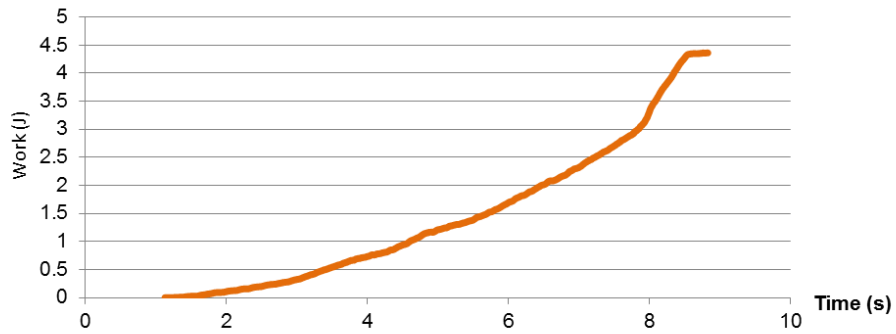
**SAMPLE NO. 3 - Left - Resident: 14mm**



**SAMPLE NO. 3 - Left - Resident: 14mm**

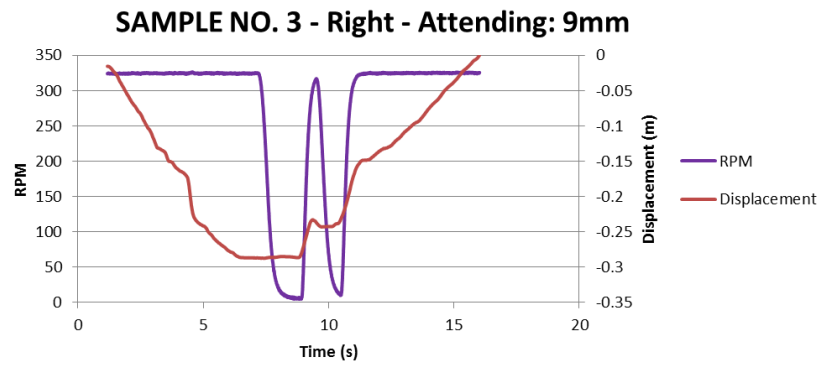
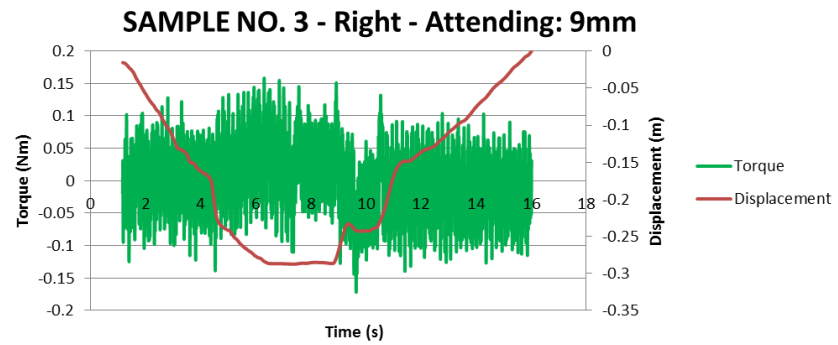
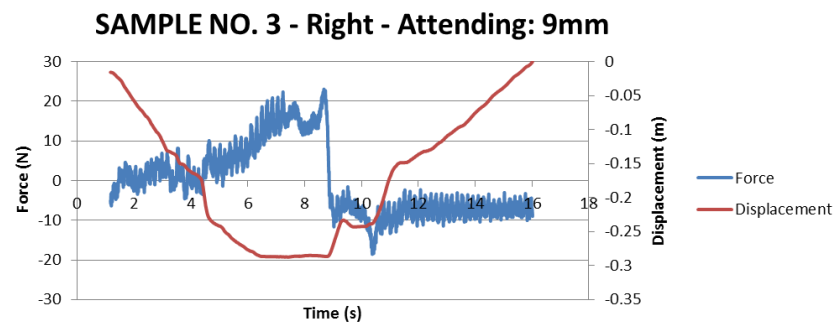
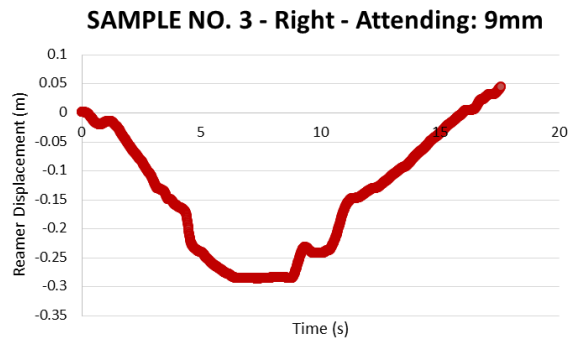


**SAMPLE NO. 3 - Left - Resident: 14mm**

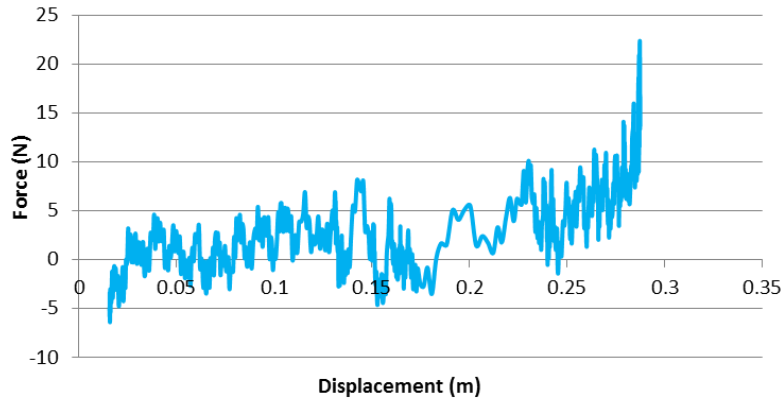


RIGHT: ATTENDING

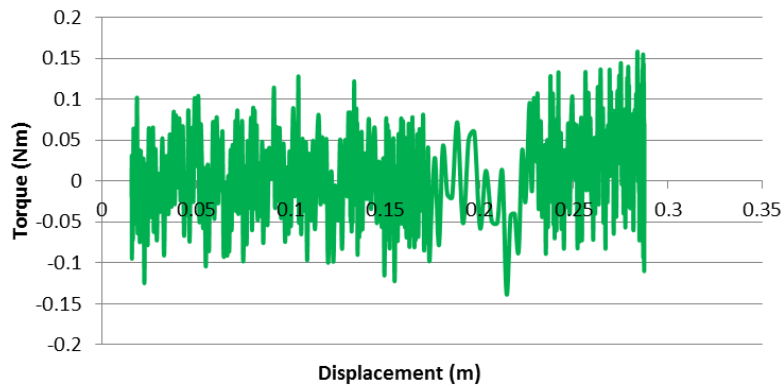
9MM



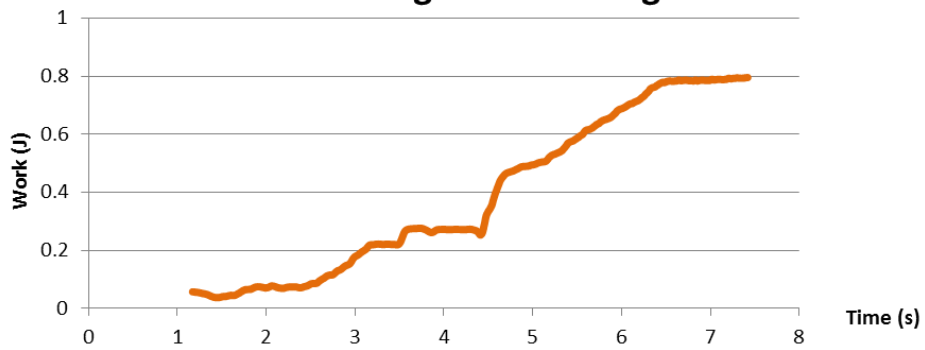
**SAMPLE NO. 3 - Right - Attending: 9mm**



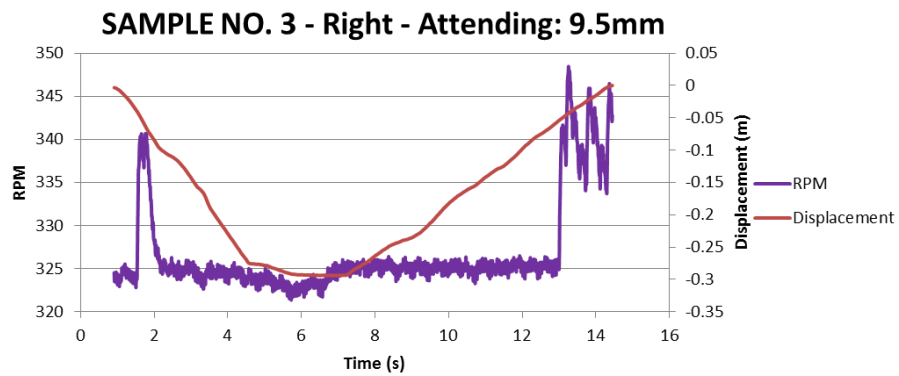
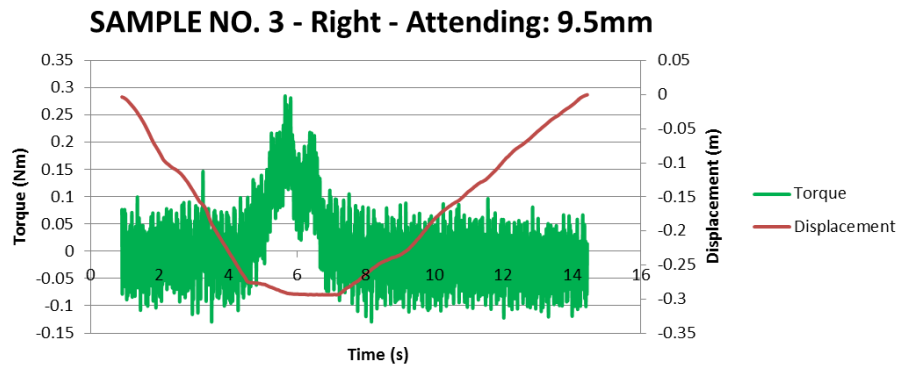
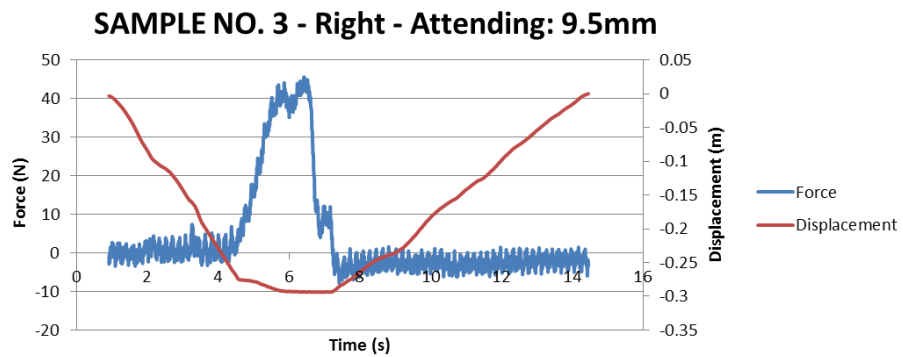
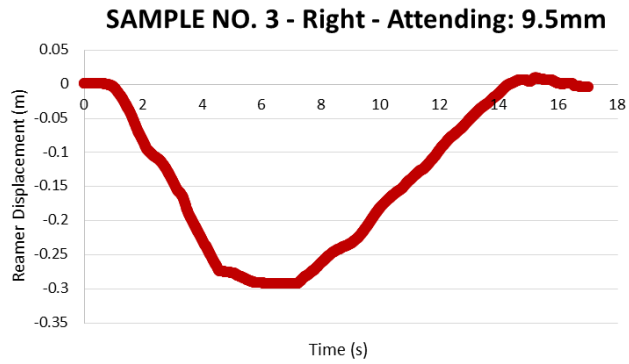
**SAMPLE NO. 3 - Right - Attending: 9mm**



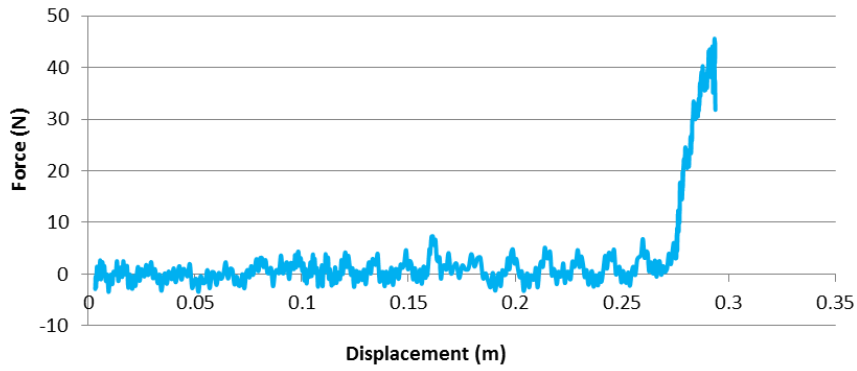
**SAMPLE NO. 3 - Right - Attending: 9mm**



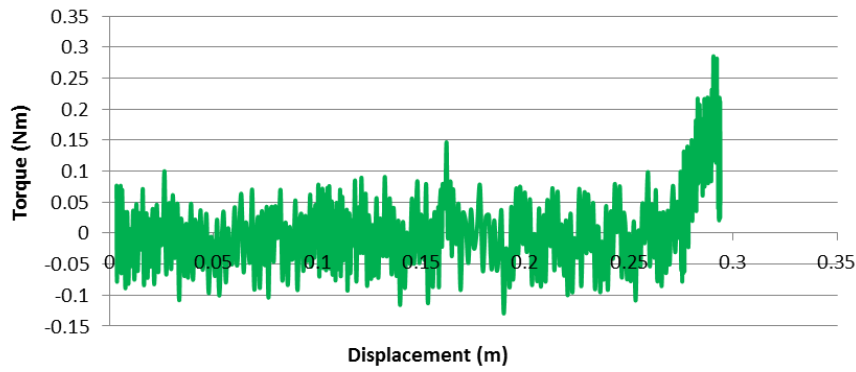
9.5MM



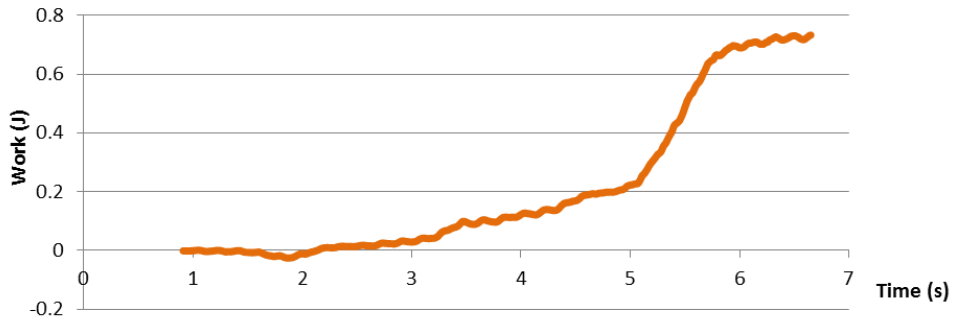
**SAMPLE NO. 3 - Right - Attending: 9.5mm**



**SAMPLE NO. 3 - Right - Attending: 9.5mm**

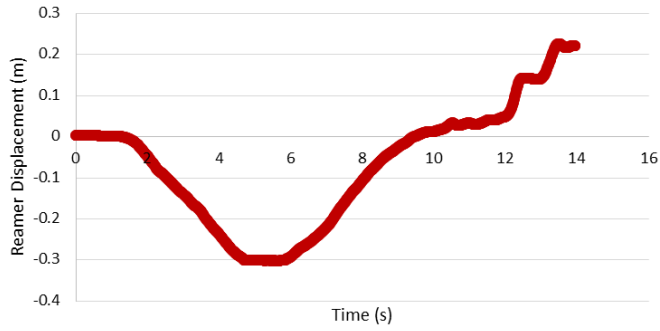


**SAMPLE NO. 3 - Right - Attending: 9.5mm**

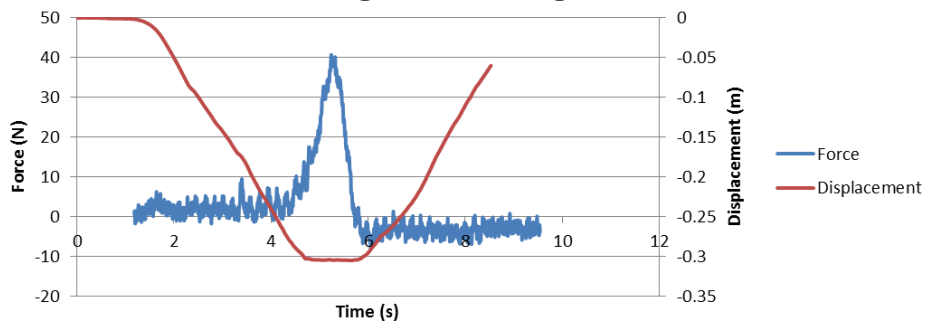


10MM

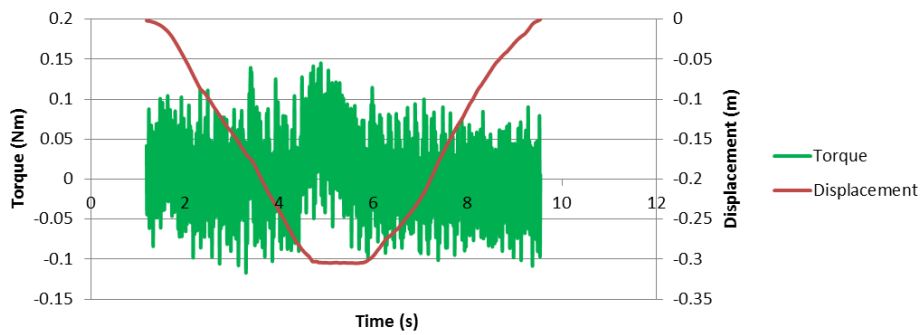
**SAMPLE NO. 3 - Right - Attending: 10mm**



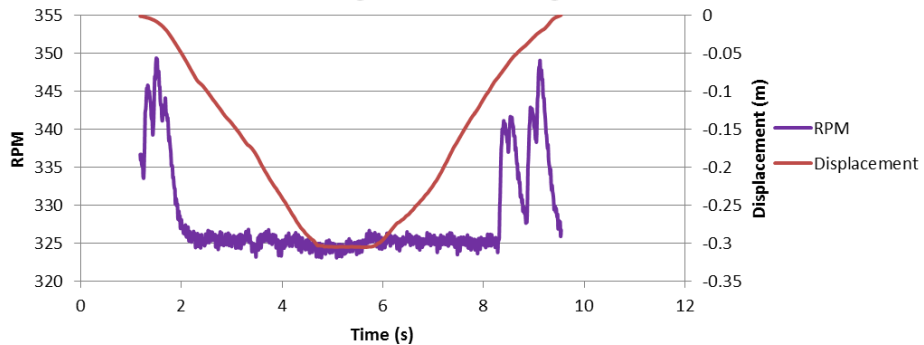
**SAMPLE NO. 3 - Right - Attending: 10mm**



**SAMPLE NO. 3 - Right - Attending: 10mm**

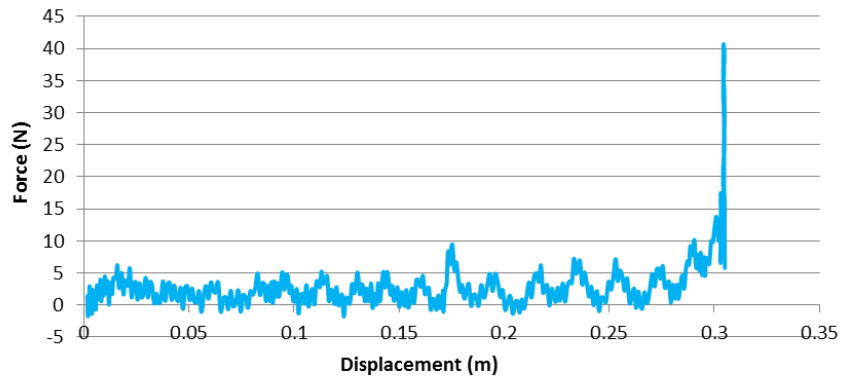


**SAMPLE NO. 3 - Right - Attending: 10mm**

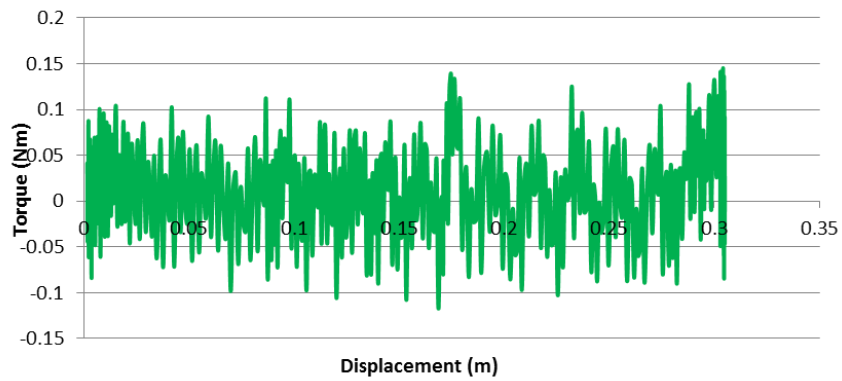




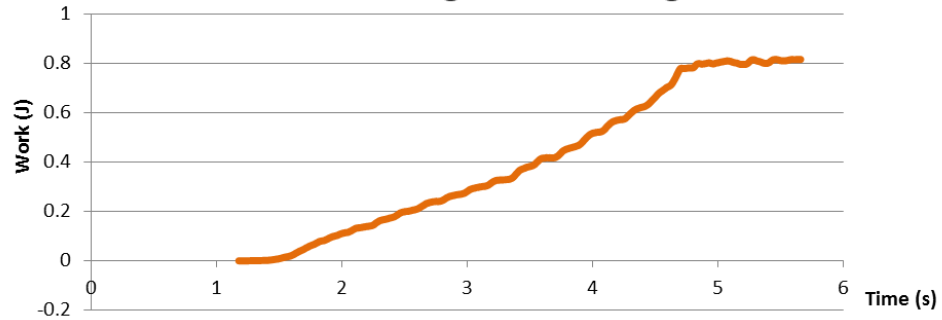
**SAMPLE NO. 3 - Right - Attending: 10mm**



**SAMPLE NO. 3 - Right - Attending: 10mm**

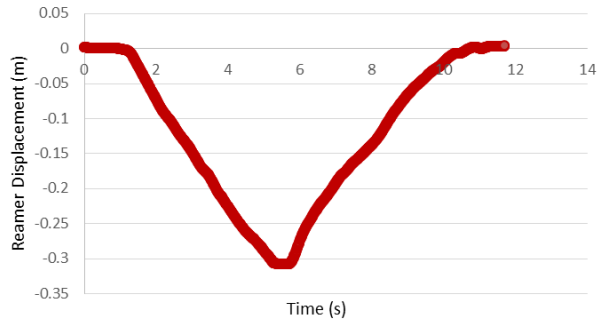


**SAMPLE NO. 3 - Right - Attending: 10mm**

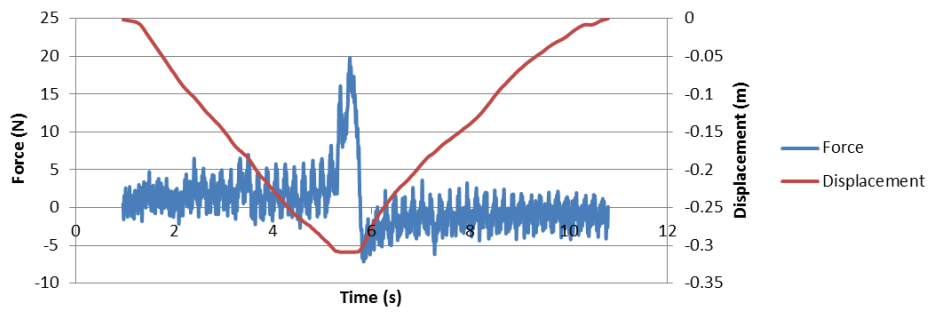


10.5MM

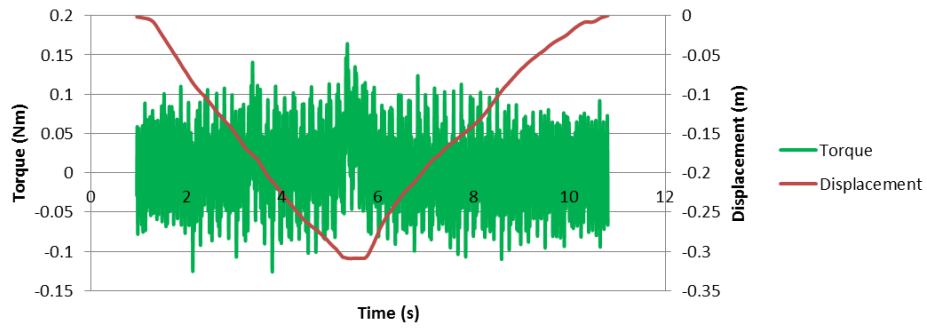
**SAMPLE NO. 3 - Right - Attending: 10.5mm**



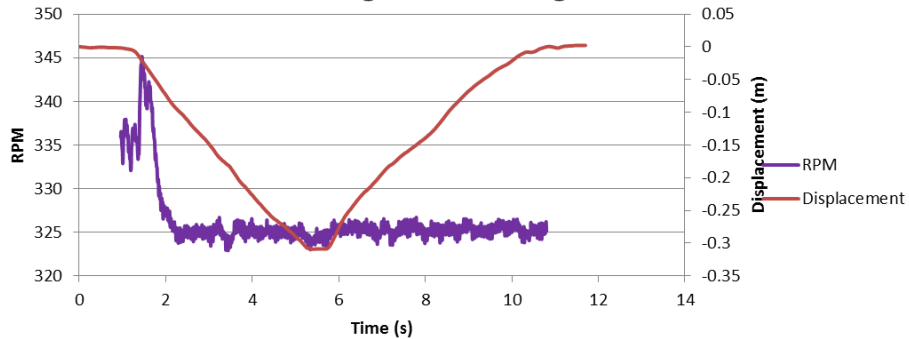
**SAMPLE NO. 3 - Right - Attending: 10.5mm**



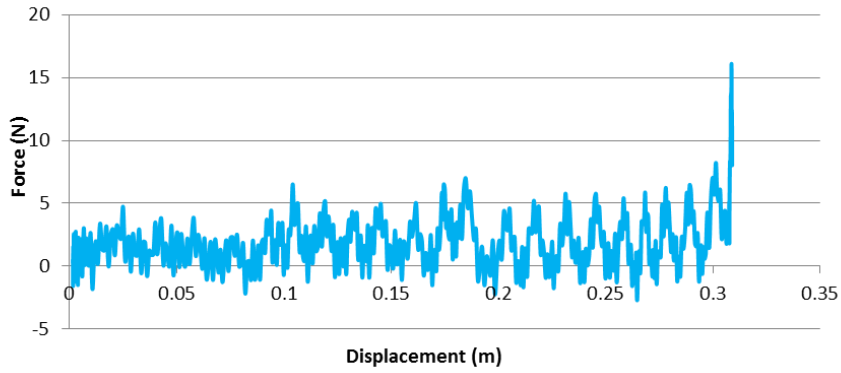
**SAMPLE NO. 3 - Right - Attending: 10.5mm**



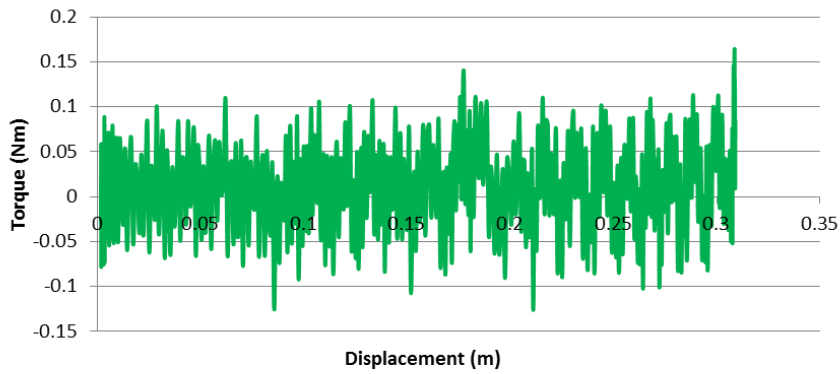
**SAMPLE NO. 3 - Right - Attending: 10.5mm**



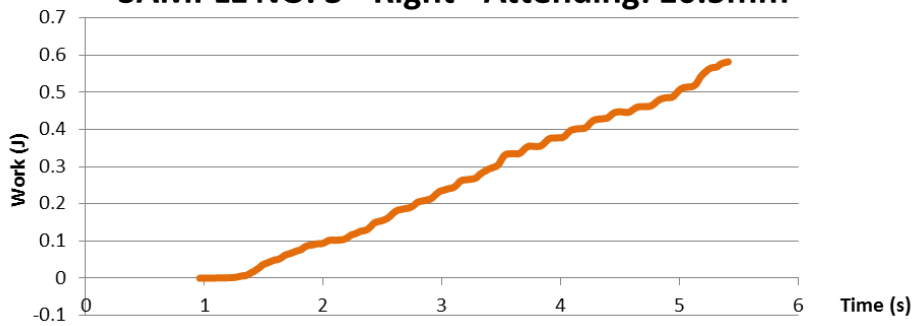
**SAMPLE NO. 3 - Right - Attending: 10.5mm**



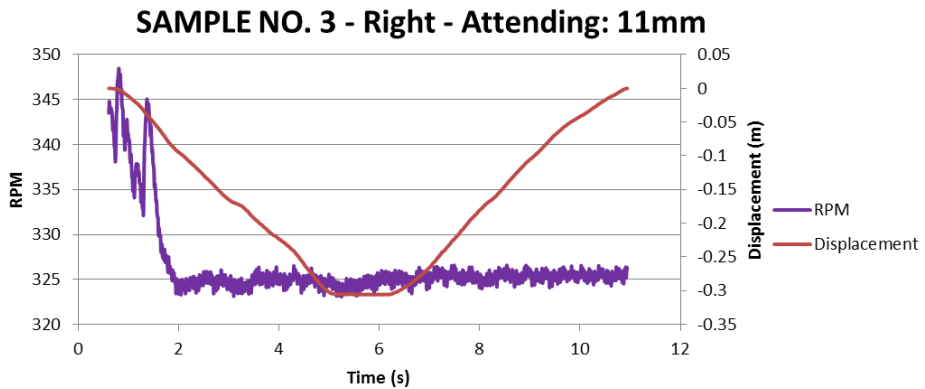
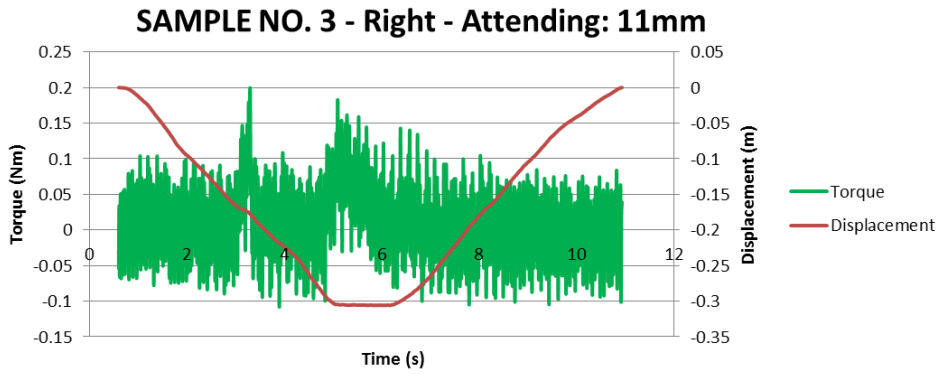
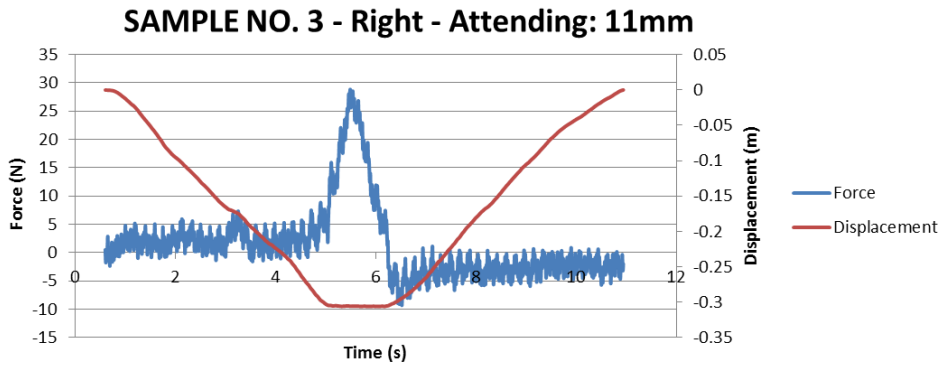
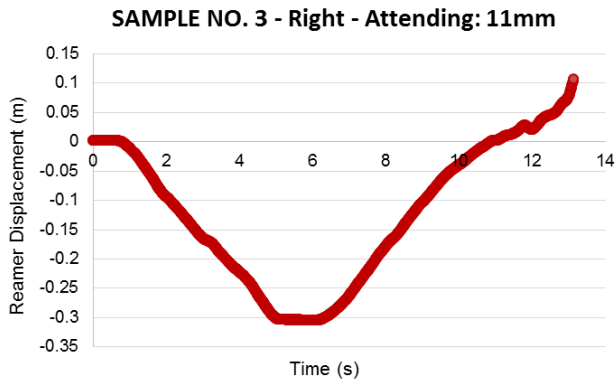
**SAMPLE NO. 3 - Right - Attending: 10.5mm**



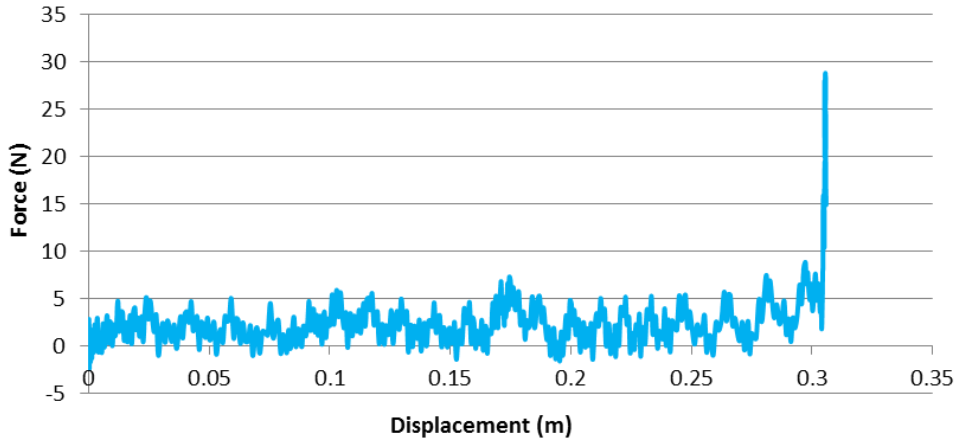
**SAMPLE NO. 3 - Right - Attending: 10.5mm**



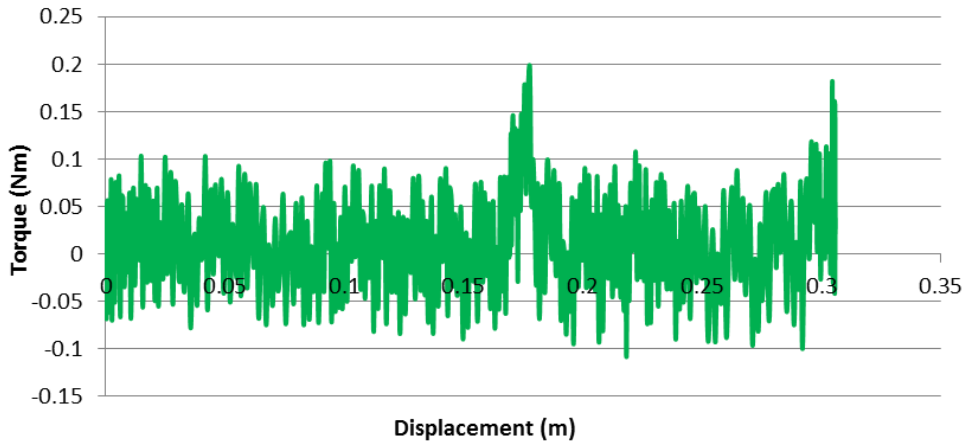
11MM



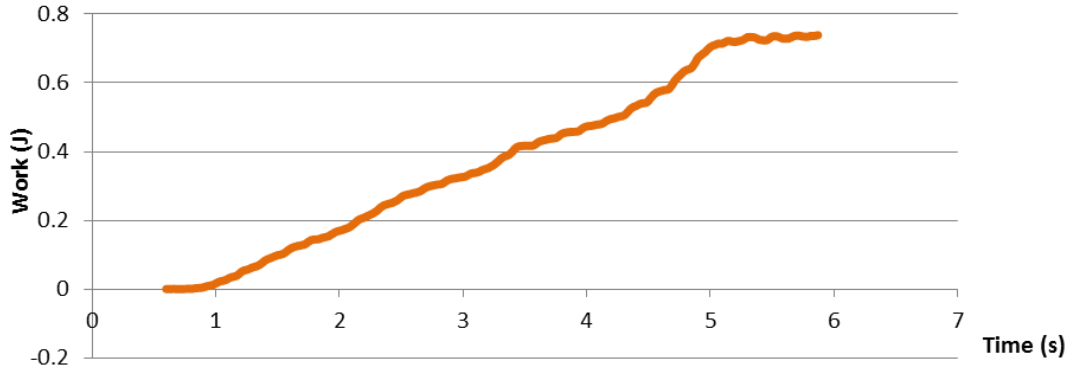
### SAMPLE NO. 3 - Right - Attending: 11mm



### SAMPLE NO. 3 - Right - Attending: 11mm

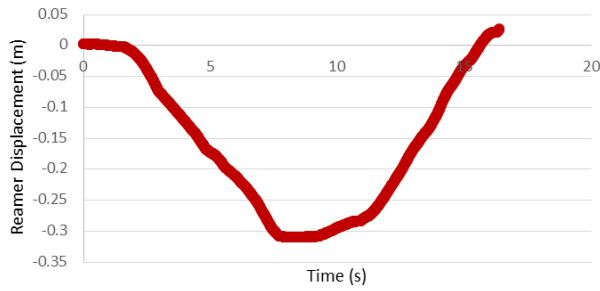


### SAMPLE NO. 3 - Right - Attending: 11mm

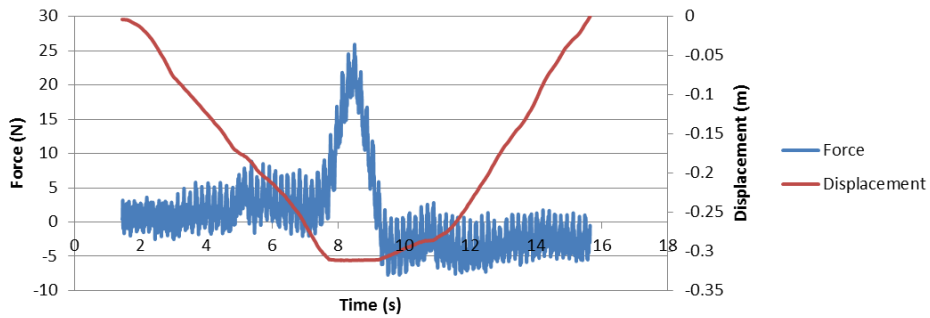


11.5MM

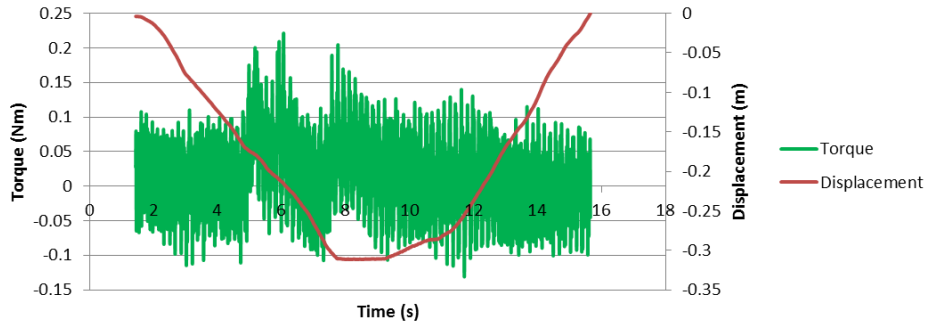
**SAMPLE NO. 3 - Right - Attending:  
11.5mm**



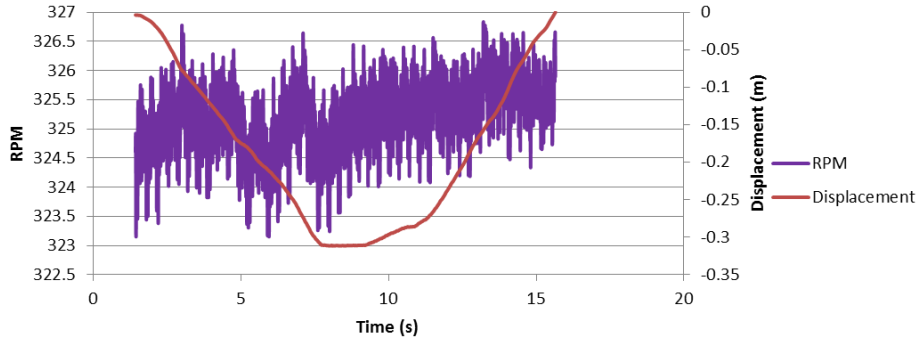
**SAMPLE NO. 3 - Right - Attending: 11.5mm**



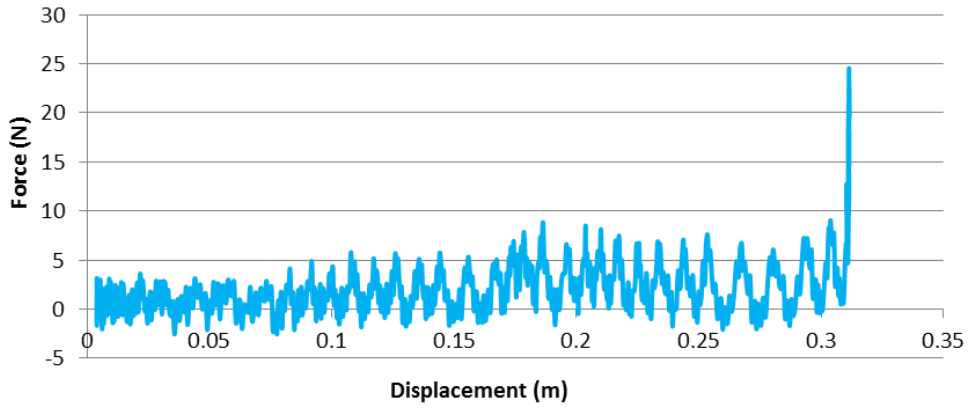
**SAMPLE NO. 3 - Right - Attending: 11.5mm**



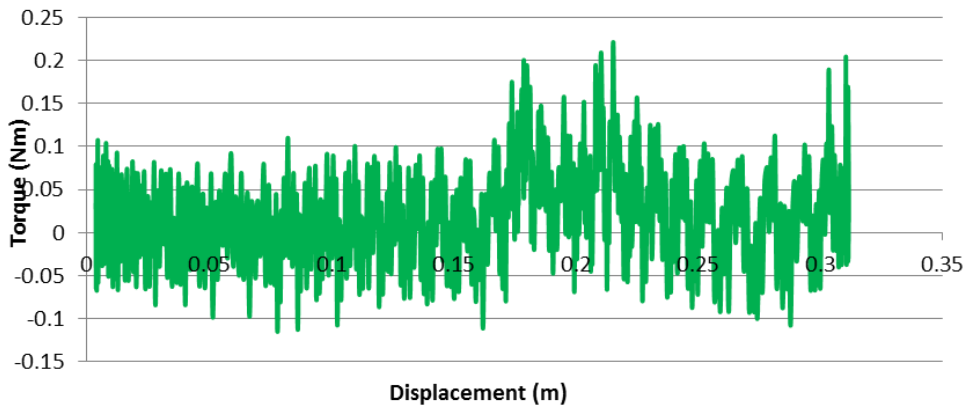
**SAMPLE NO. 3 - Right - Attending: 11.5mm**



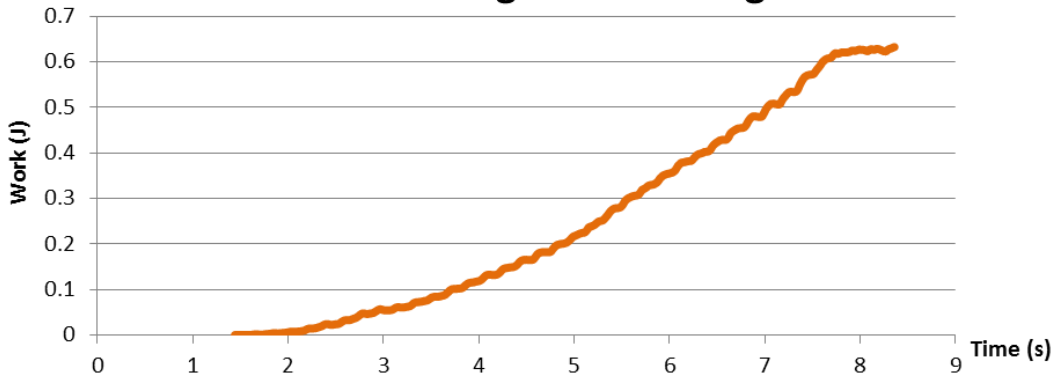
### SAMPLE NO. 3 - Right - Attending: 11.5mm



### SAMPLE NO. 3 - Right - Attending: 11.5mm

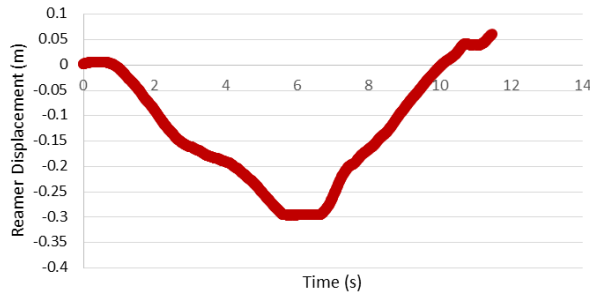


### SAMPLE NO. 3 - Right - Attending: 11.5mm

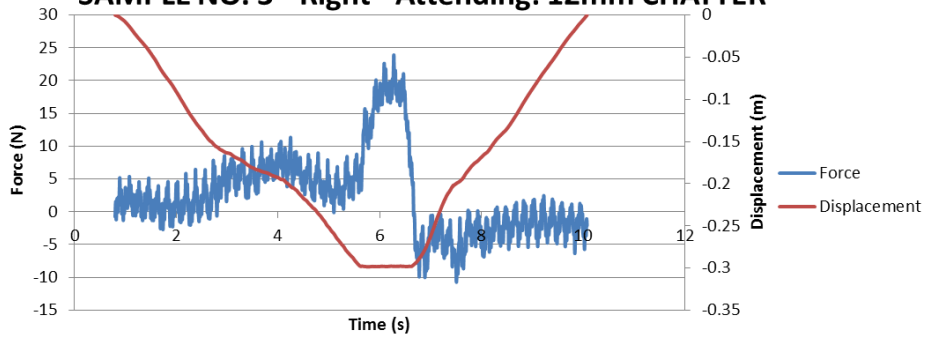


12MM

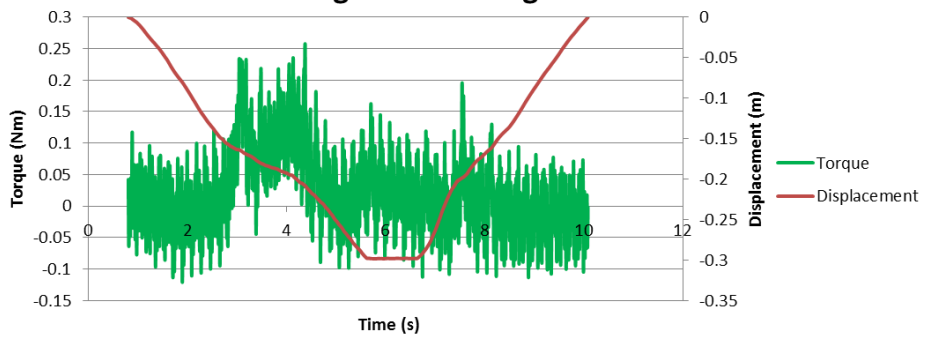
**SAMPLE NO. 3 - Right - Attending: 12mm CHATTER**



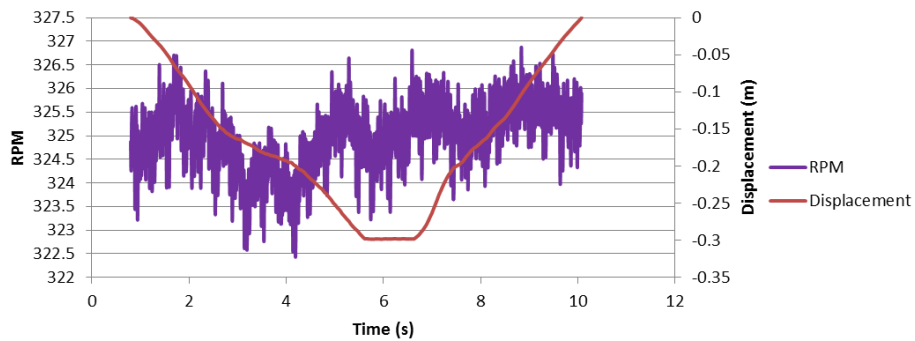
**SAMPLE NO. 3 - Right - Attending: 12mm CHATTER**



**SAMPLE NO. 3 - Right - Attending: 12mm CHATTER**

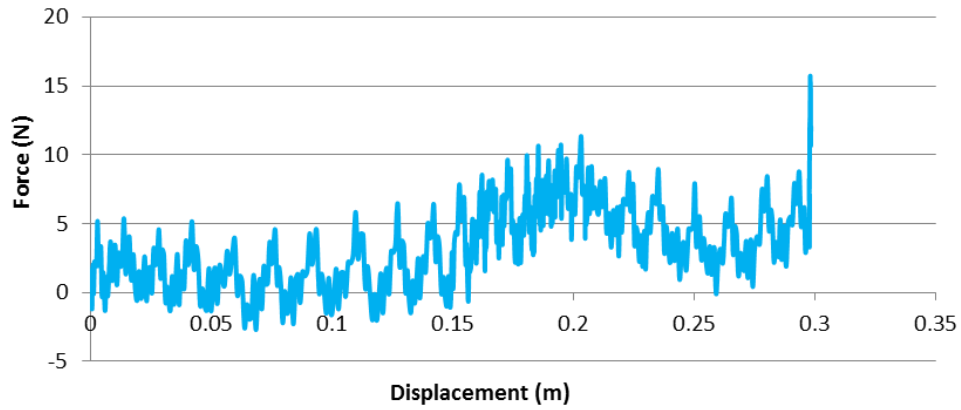


**SAMPLE NO. 3 - Right - Attending: 12mm CHATTER**

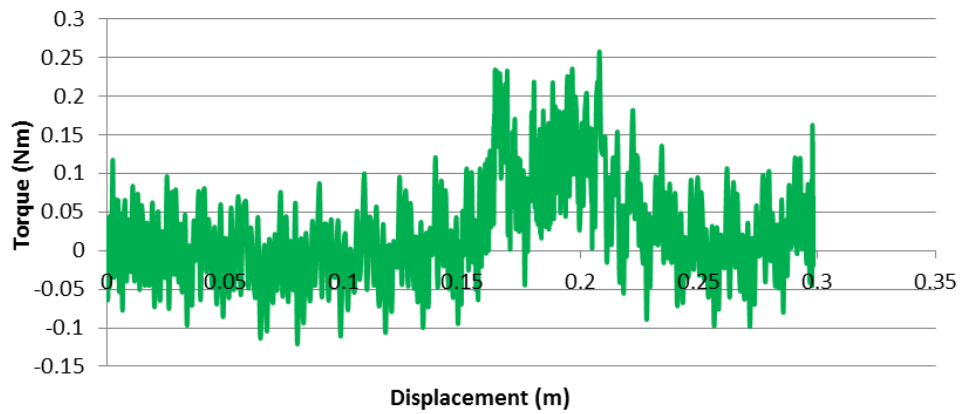




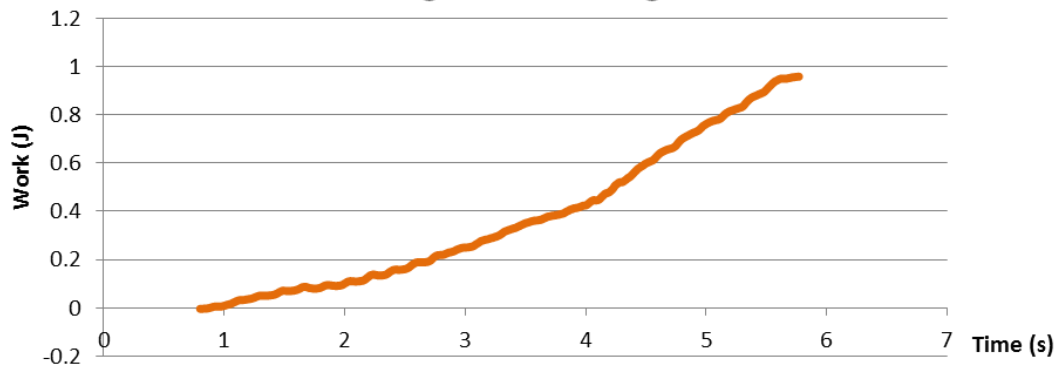
**SAMPLE NO. 3 - Right - Attending: 12mm  
CHATTER**



**SAMPLE NO. 3 - Right - Attending: 12mm  
CHATTER**

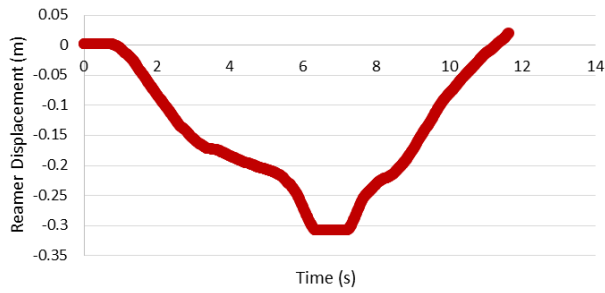


**SAMPLE NO. 3 - Right - Attending: 12mm CHATTER**

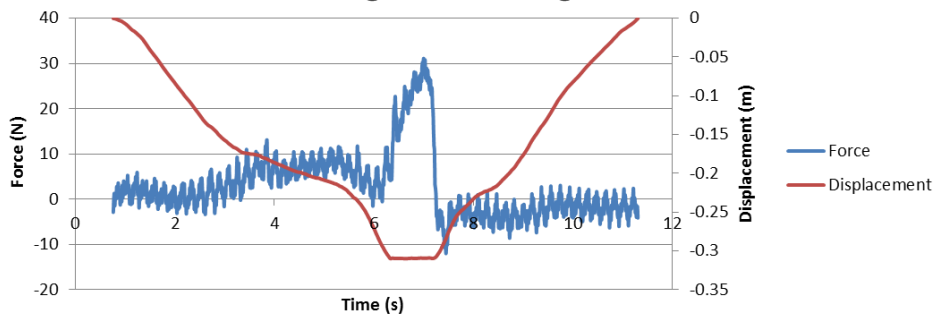


12.5MM

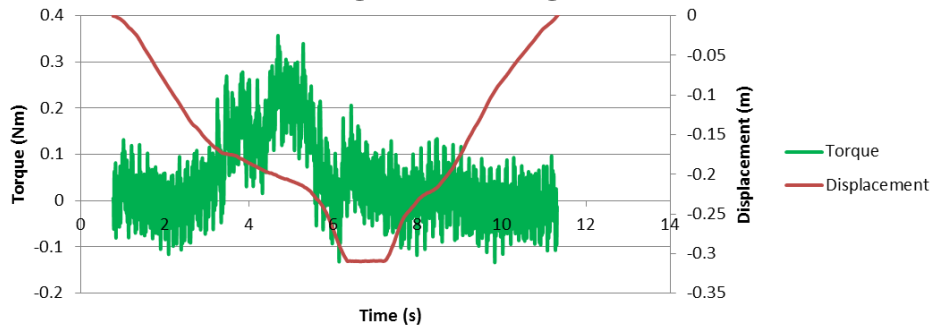
**SAMPLE NO. 3 - Right - Attending:  
12.5mm**



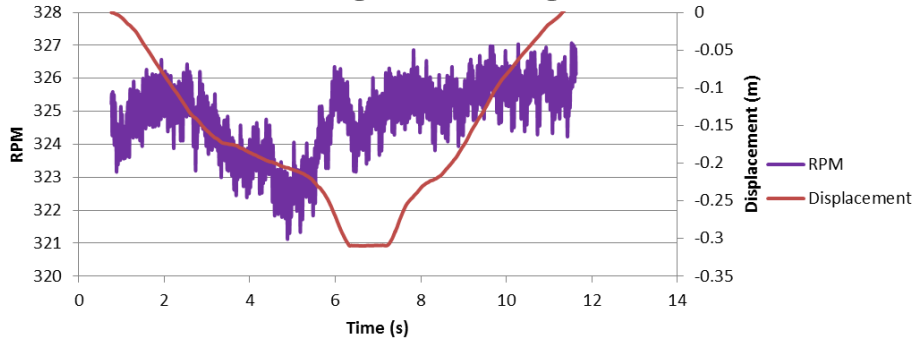
**SAMPLE NO. 3 - Right - Attending: 12.5mm**



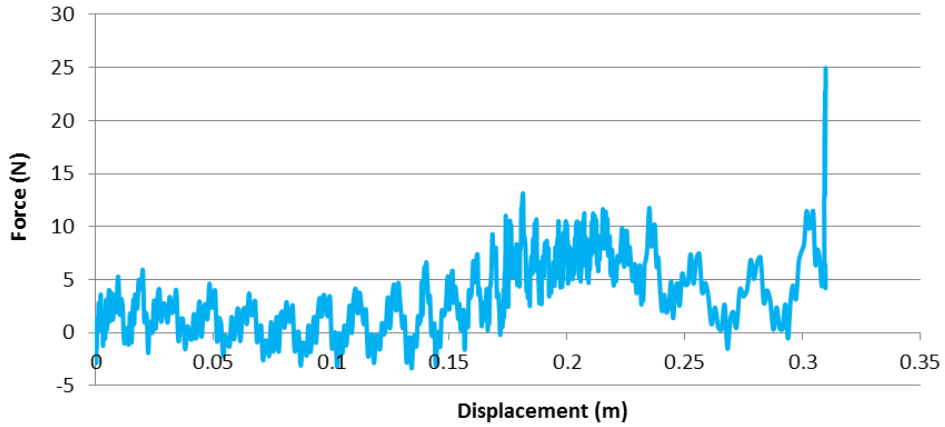
**SAMPLE NO. 3 - Right - Attending: 12.5mm**



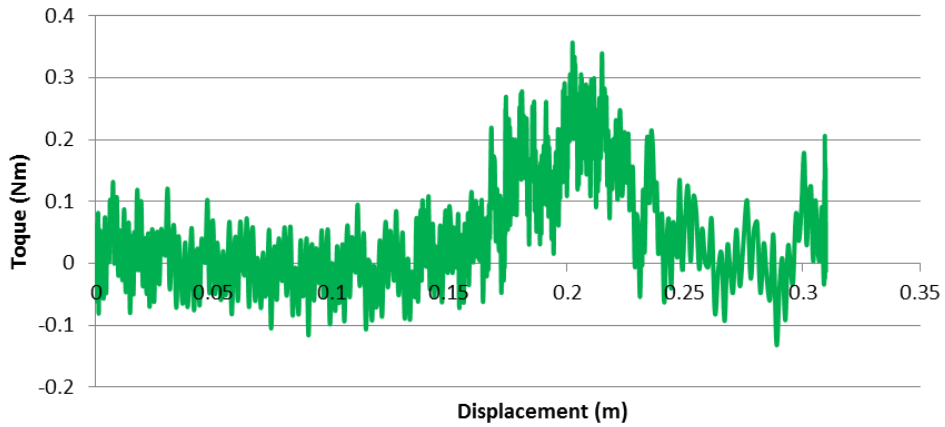
**SAMPLE NO. 3 - Right - Attending: 12.5mm**



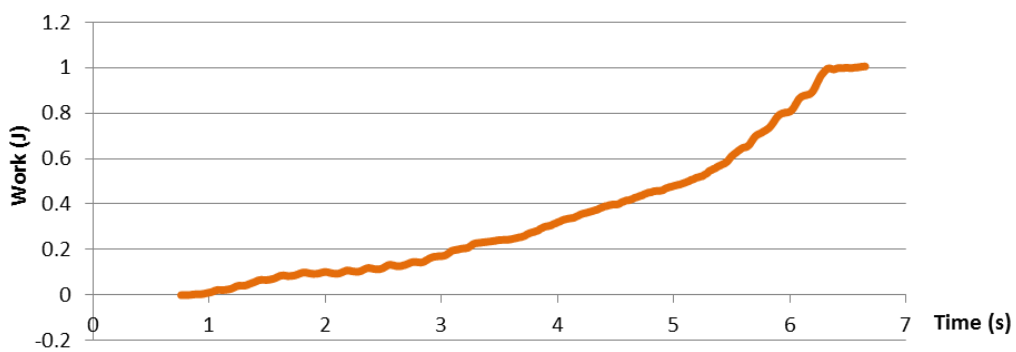
**SAMPLE NO. 3 - Right - Attending: 12.5mm**



**SAMPLE NO. 3 - Right - Attending: 12.5mm**

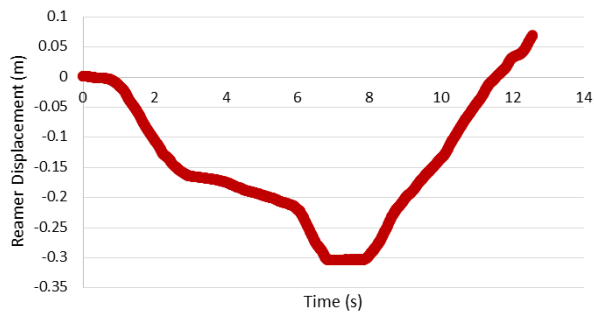


**SAMPLE NO. 3 - Right - Attending: 12.5mm**

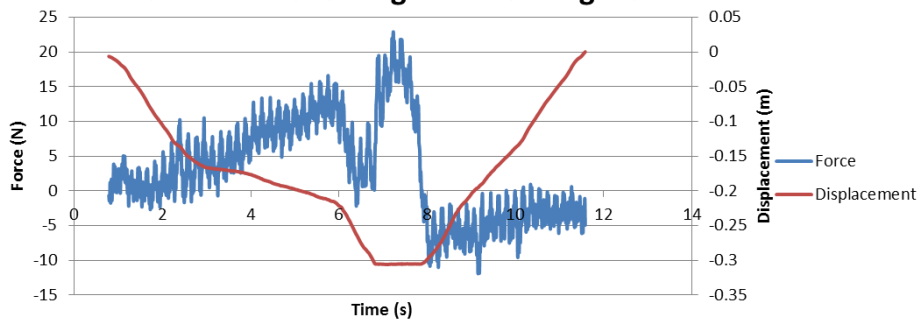


13MM

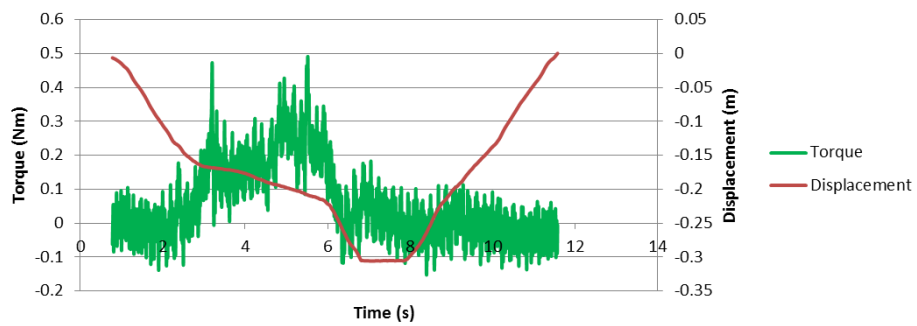
SAMPLE NO. 3 - Right - Attending: 13mm



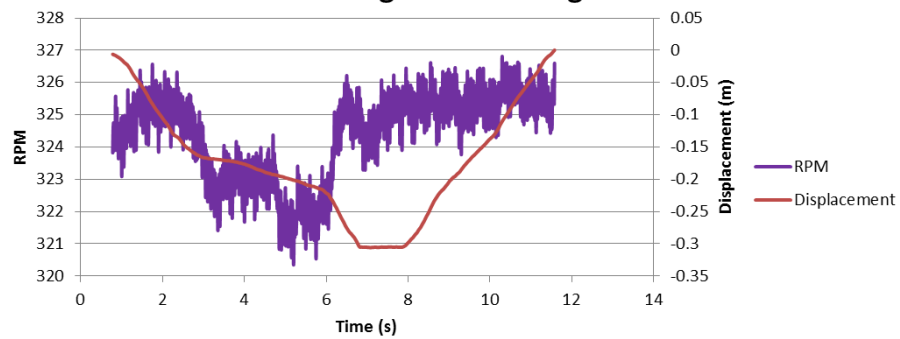
SAMPLE NO. 3 - Right - Attending: 13mm



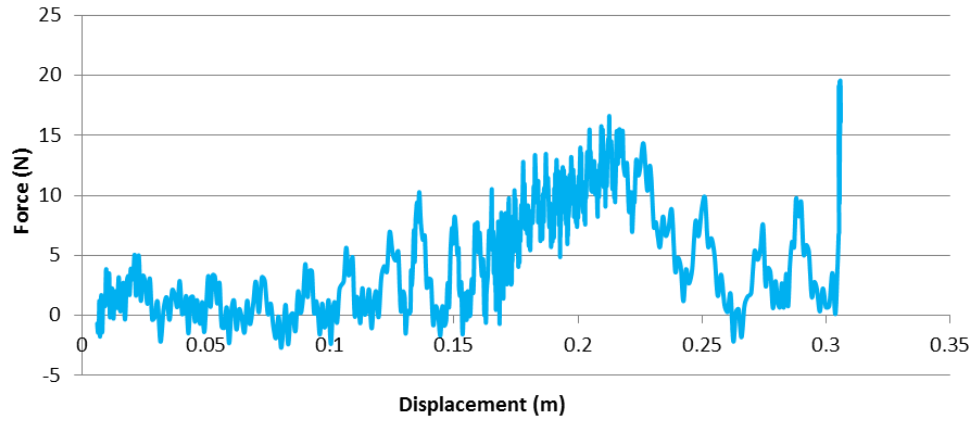
SAMPLE NO. 3 - Right - Attending: 13mm



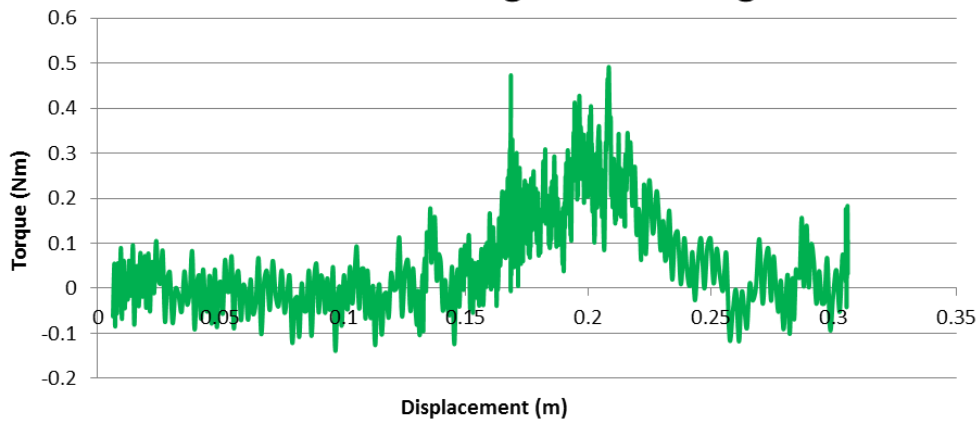
SAMPLE NO. 3 - Right - Attending: 13mm



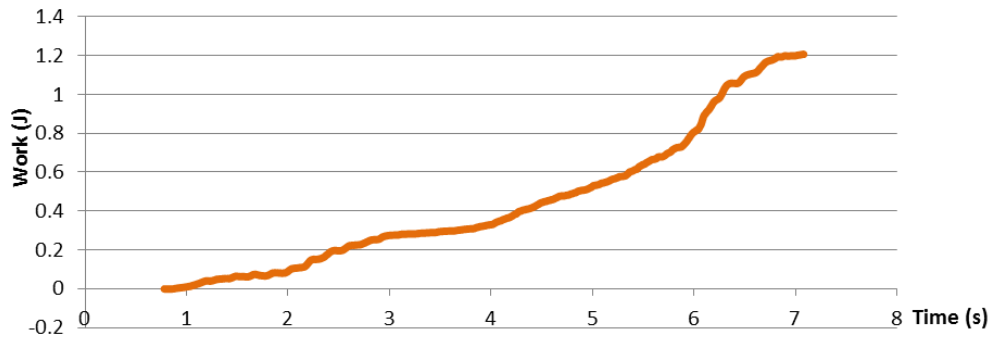
**SAMPLE NO. 3 - Right - Attending: 13mm**



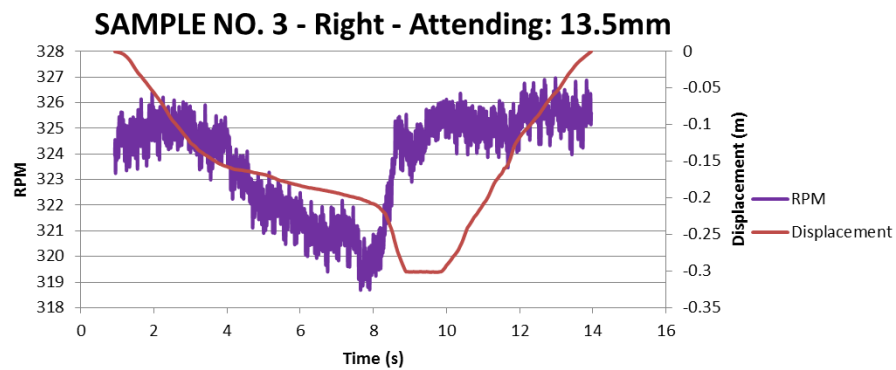
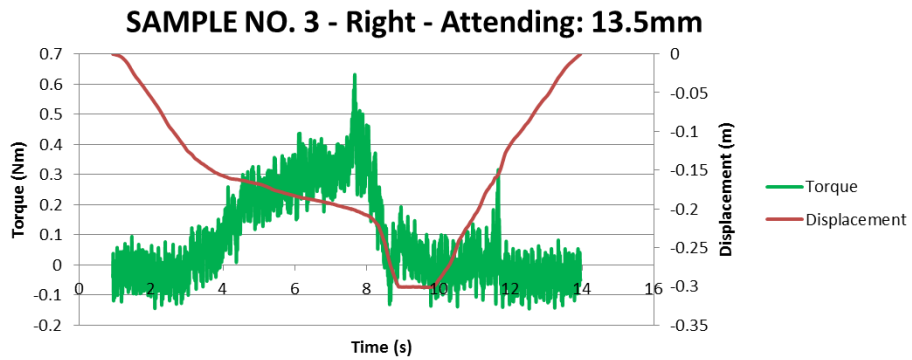
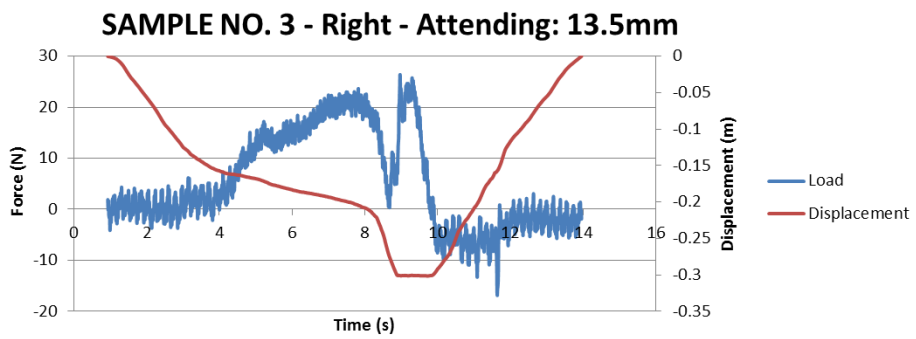
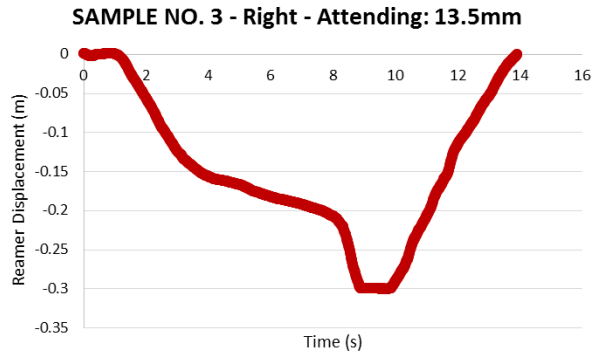
**SAMPLE NO. 3 - Right - Attending: 13mm**



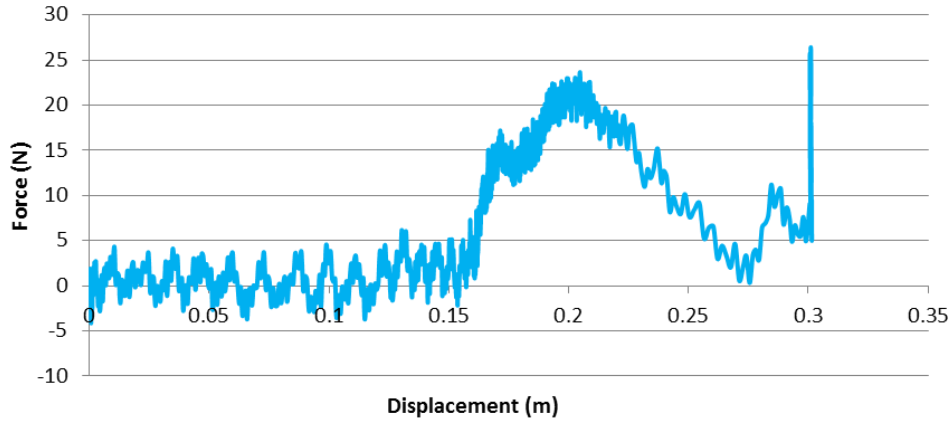
**SAMPLE NO. 3 - Right - Attending: 13mm**



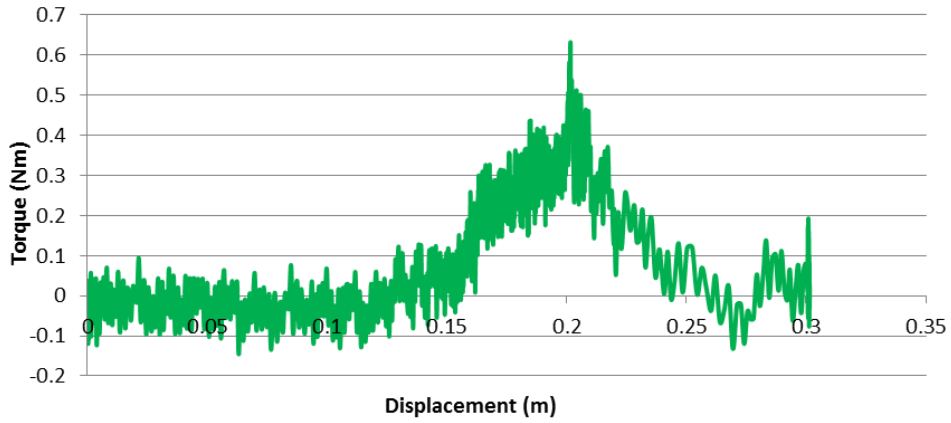
13.5MM



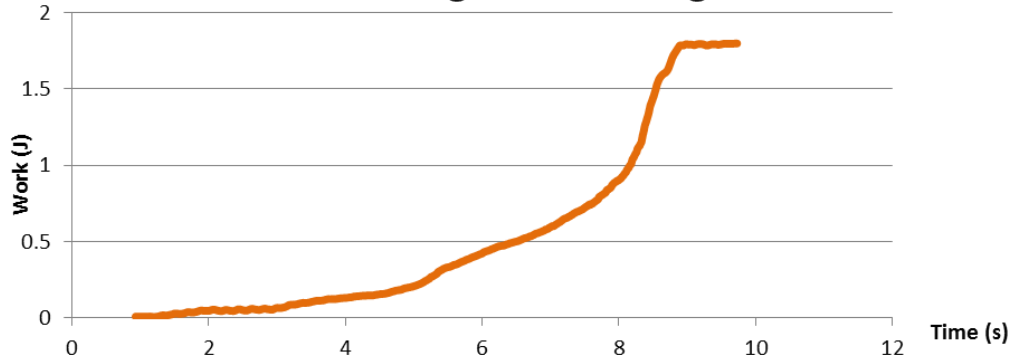
**SAMPLE NO. 3 - Right - Attending: 13.5mm**



**SAMPLE NO. 3 - Right - Attending: 13.5mm**



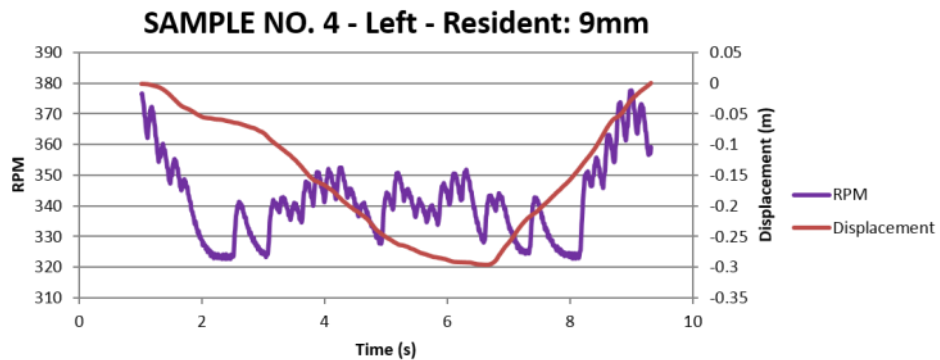
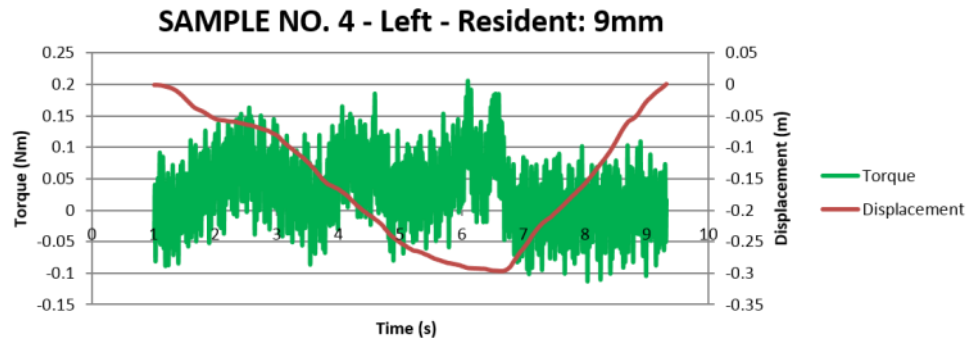
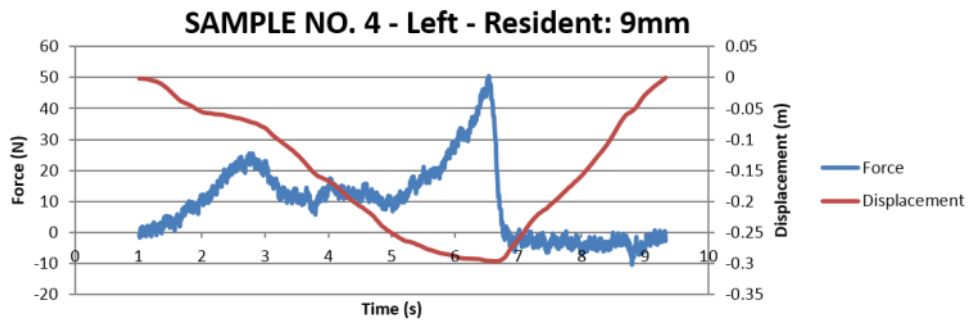
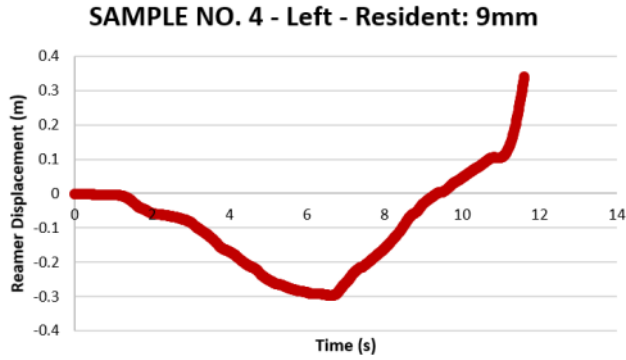
**SAMPLE NO. 3 - Right - Attending: 13.5mm**



## 13.4 SAMPLE 4 RESULTS

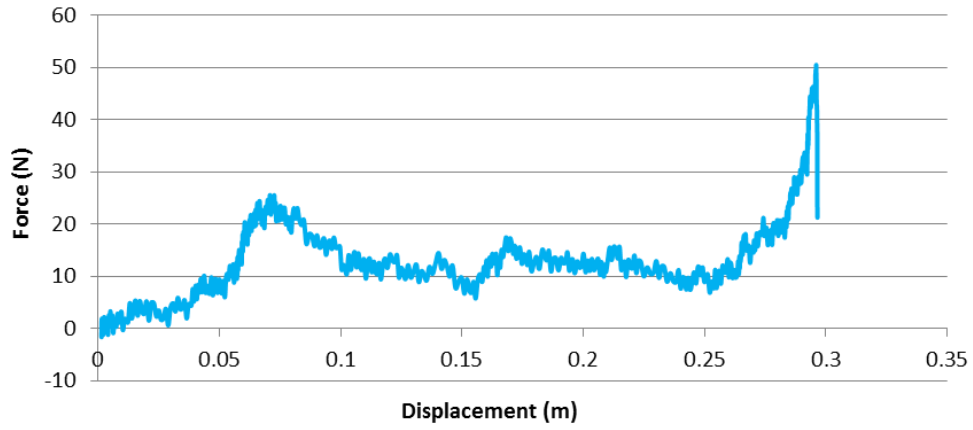
LEFT: RESIDENT

9MM

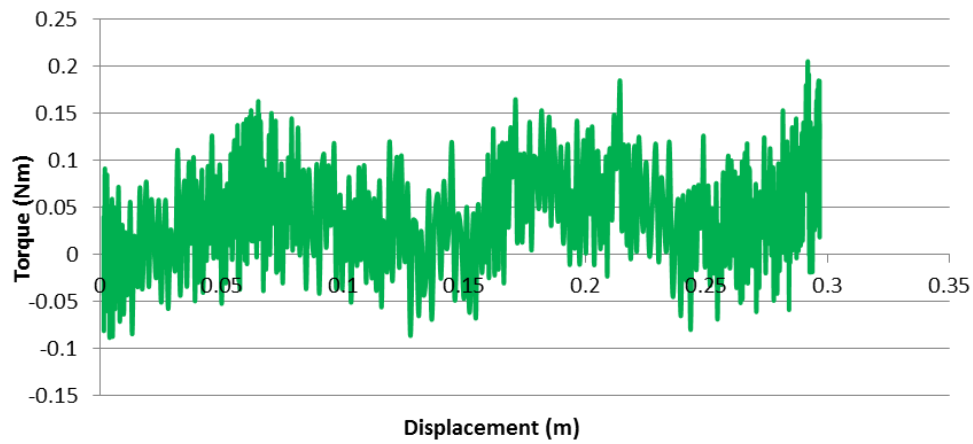




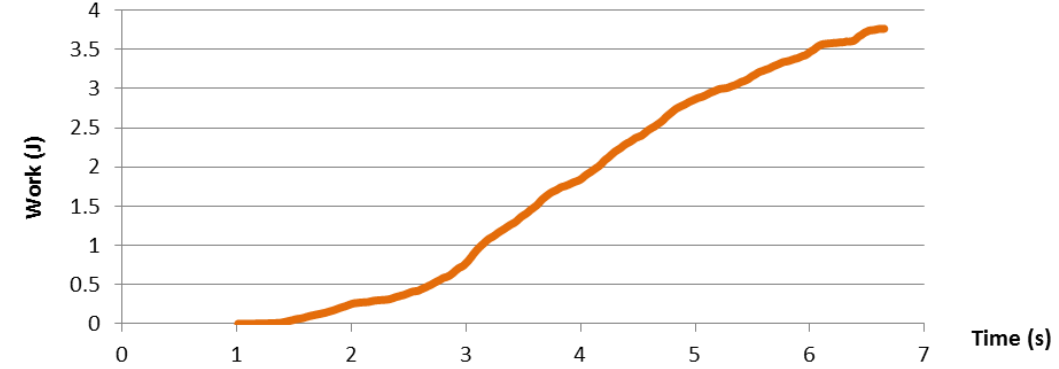
**SAMPLE NO. 4 - Left - Resident: 9mm**



**SAMPLE NO. 4 - Left - Resident: 9mm**

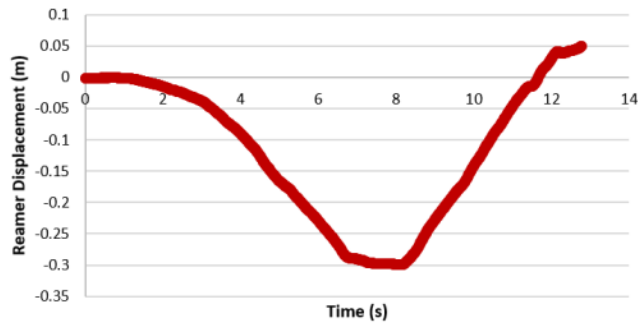


**SAMPLE NO. 4 - Left - Resident: 9mm**

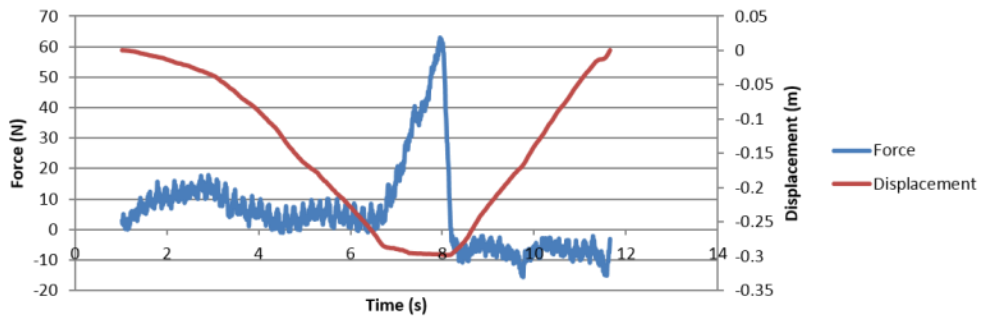


9.5MM

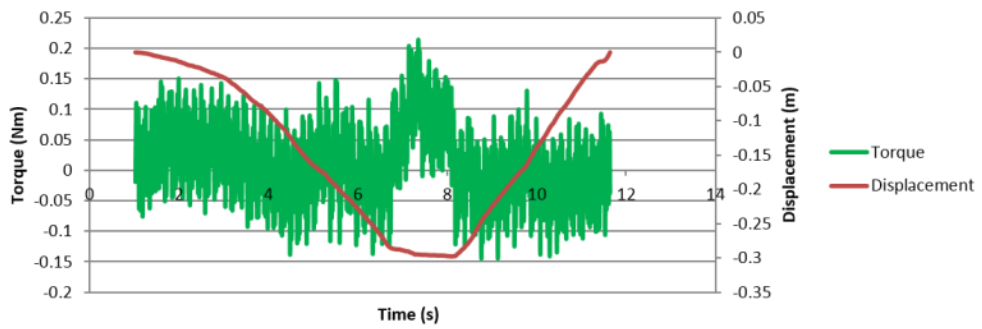
SAMPLE NO. 4 - Left - Resident: 9.5mm



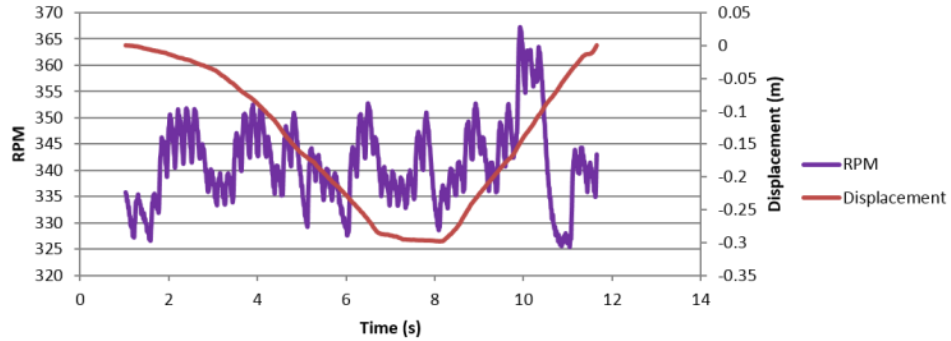
SAMPLE NO. 4 - Left - Resident: 9.5mm



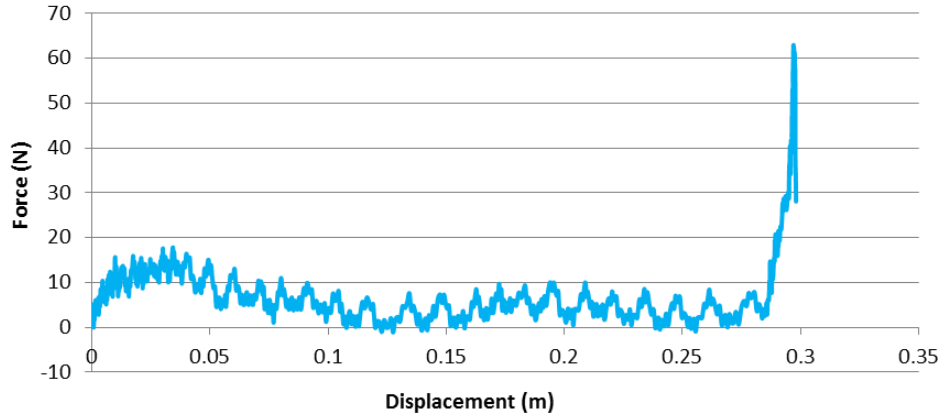
SAMPLE NO. 4 - Left - Resident: 9.5mm



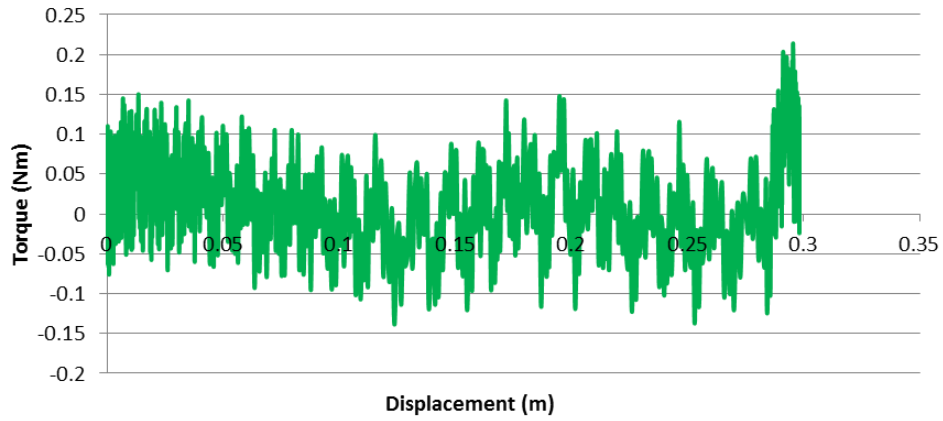
SAMPLE NO. 4 - Left - Resident: 9.5mm



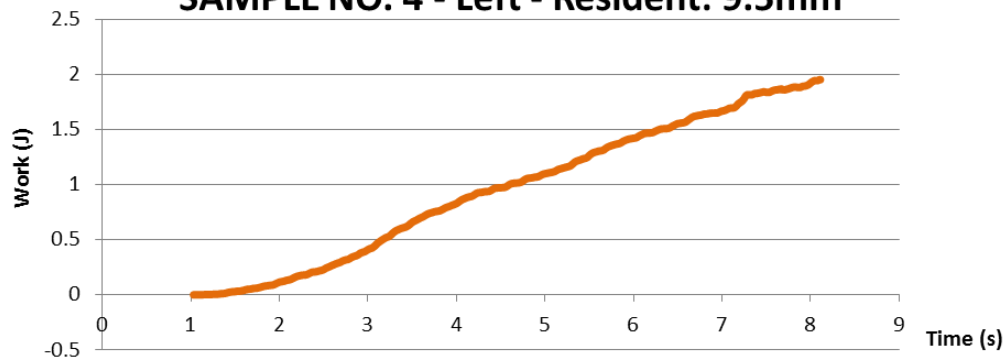
**SAMPLE NO. 4 - Left - Resident: 9.5mm**



**SAMPLE NO. 4 - Left - Resident: 9.5mm**

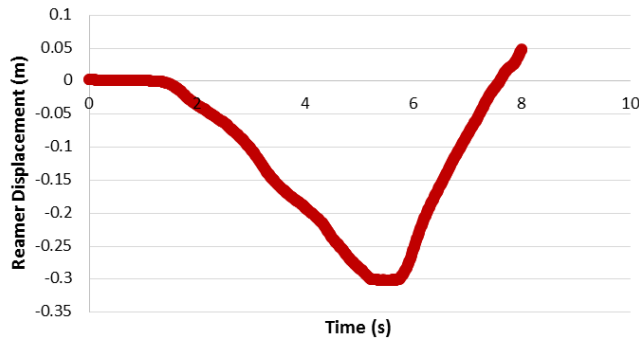


**SAMPLE NO. 4 - Left - Resident: 9.5mm**

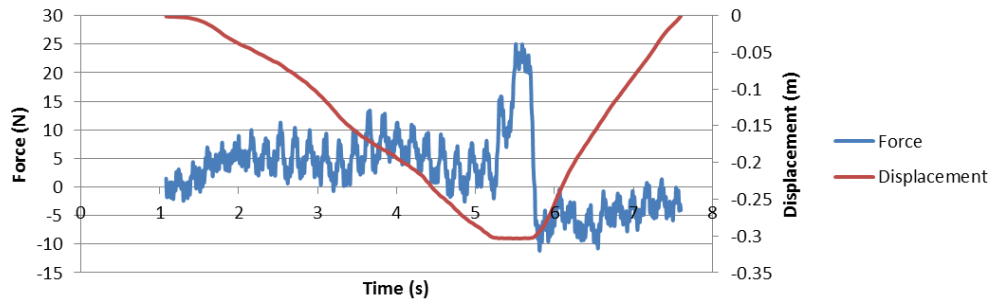


10MM

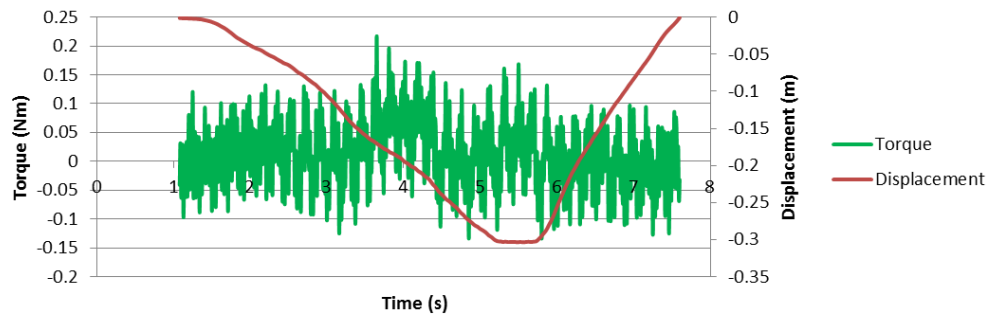
SAMPLE NO. 4 - Left - Resident: 10mm



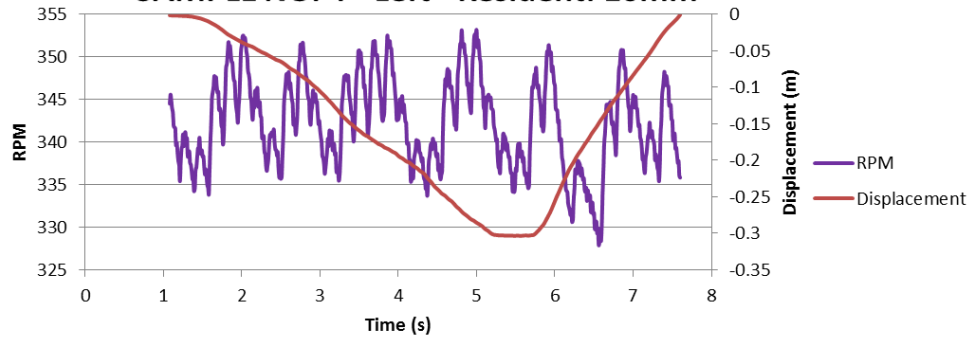
SAMPLE NO. 4 - Left - Resident: 10mm



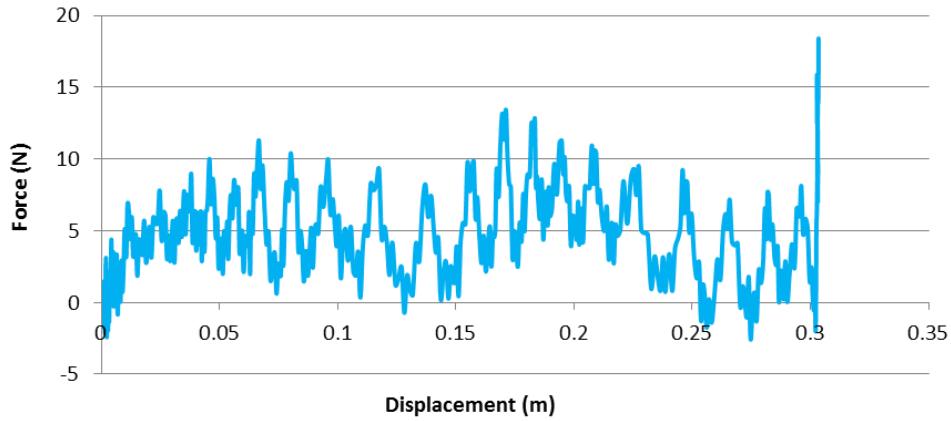
SAMPLE NO. 4 - Left - Resident: 10mm



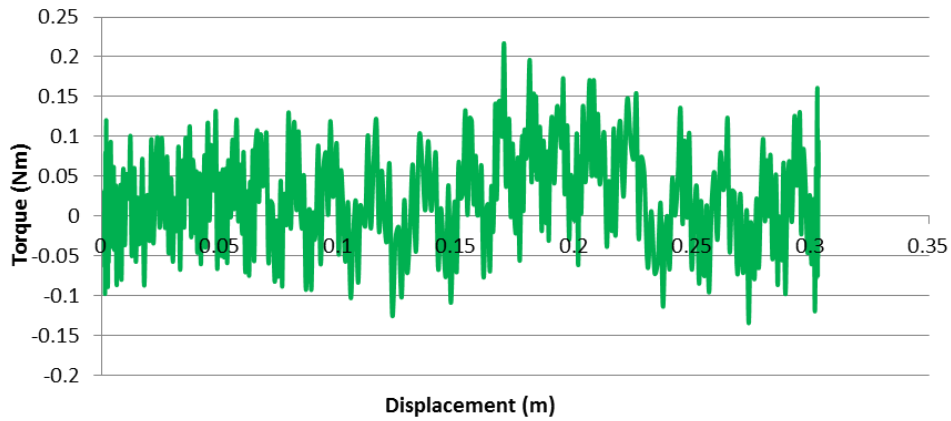
SAMPLE NO. 4 - Left - Resident: 10mm



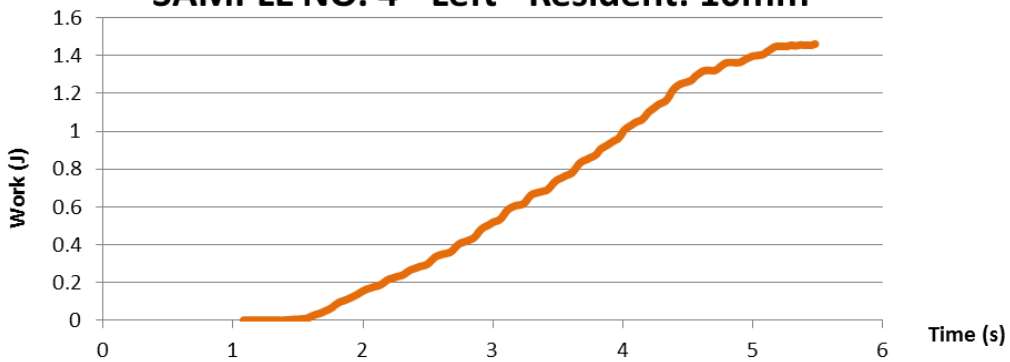
**SAMPLE NO. 4 - Left - Resident: 10mm**



**SAMPLE NO. 4 - Left - Resident: 10mm**

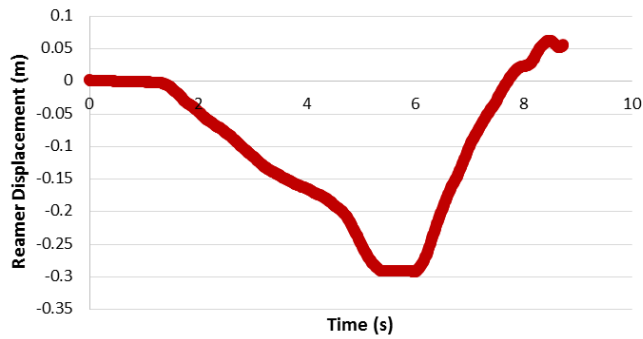


**SAMPLE NO. 4 - Left - Resident: 10mm**

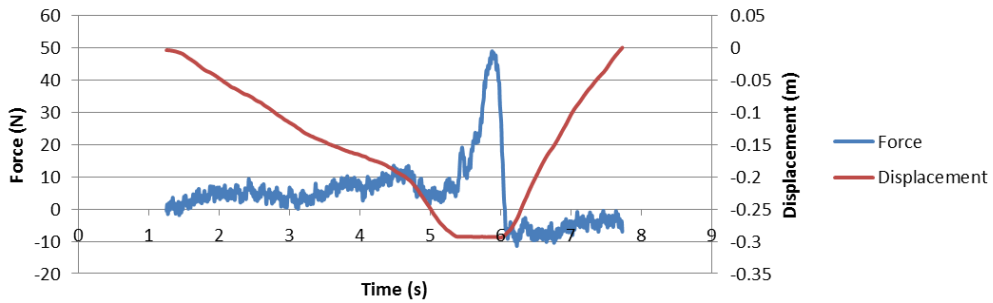


10.5MM

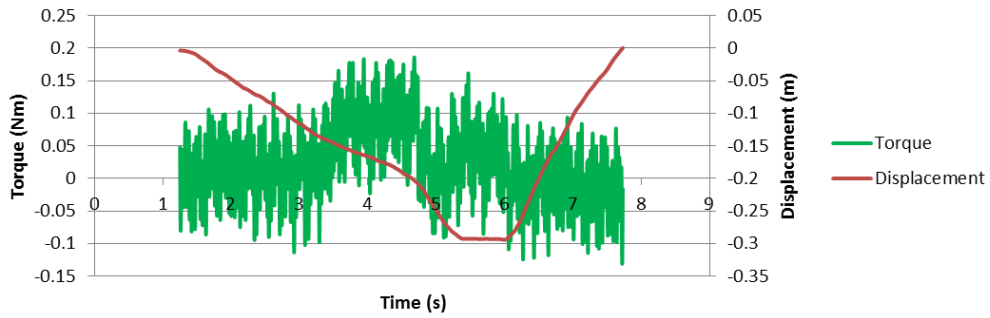
SAMPLE NO. 4 - Left - Resident: 10.5mm



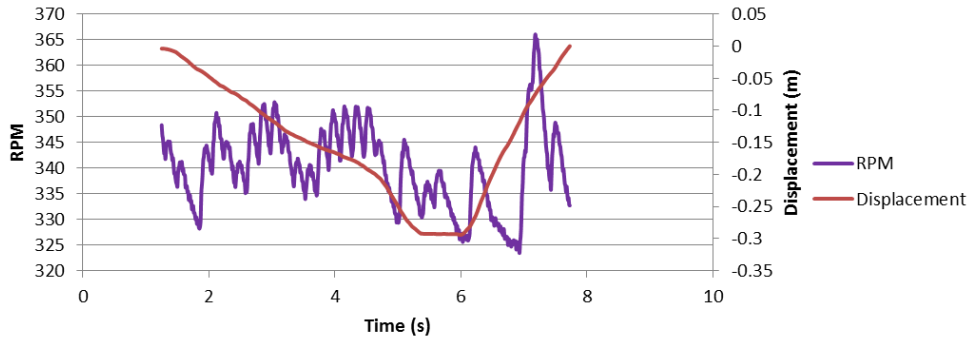
SAMPLE NO. 4 - Left - Resident: 10.5mm



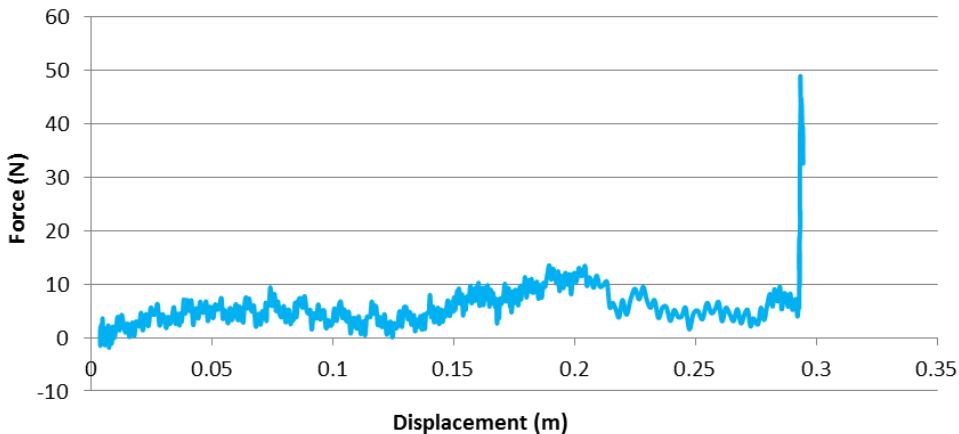
SAMPLE NO. 4 - Left - Resident: 10.5mm



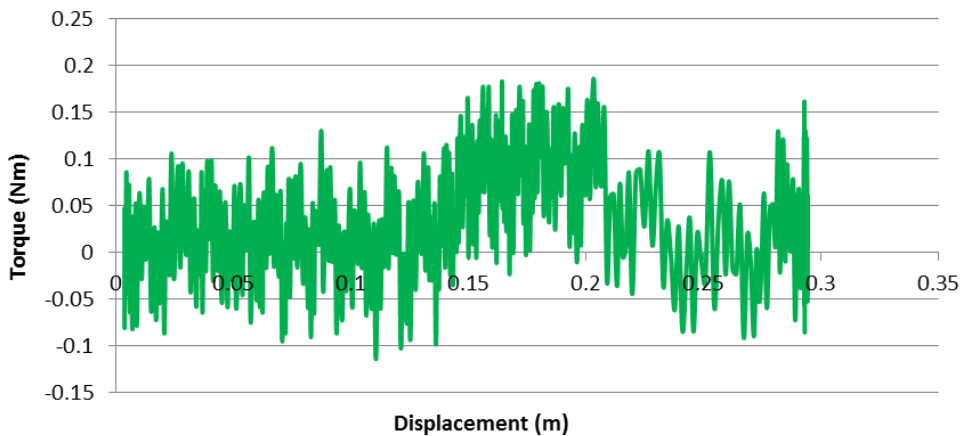
SAMPLE NO. 4 - Left - Resident: 10.5mm



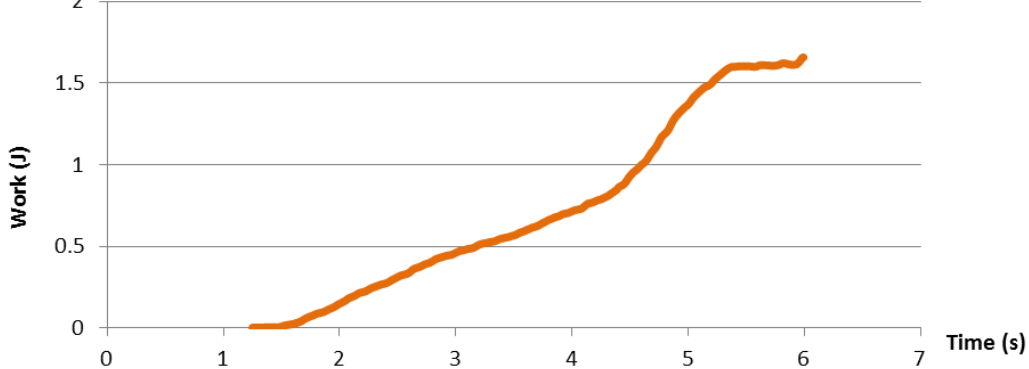
**SAMPLE NO. 4 - Left - Resident: 10.5mm**



**SAMPLE NO. 4 - Left - Resident: 10.5mm**

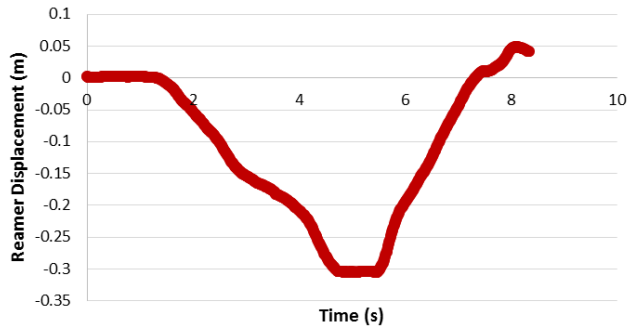


**SAMPLE NO. 4 - Left - Resident: 10.5mm**

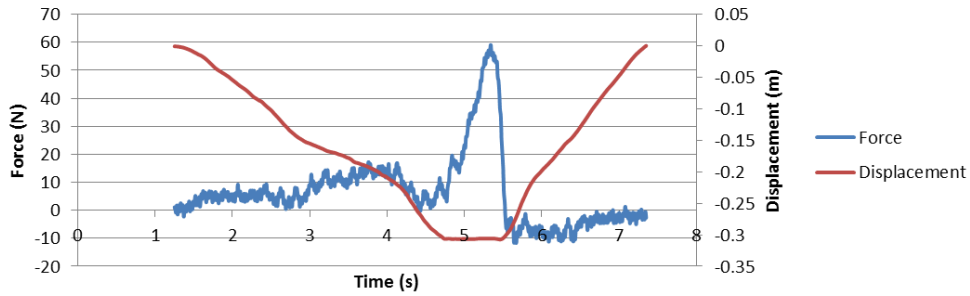


11MM

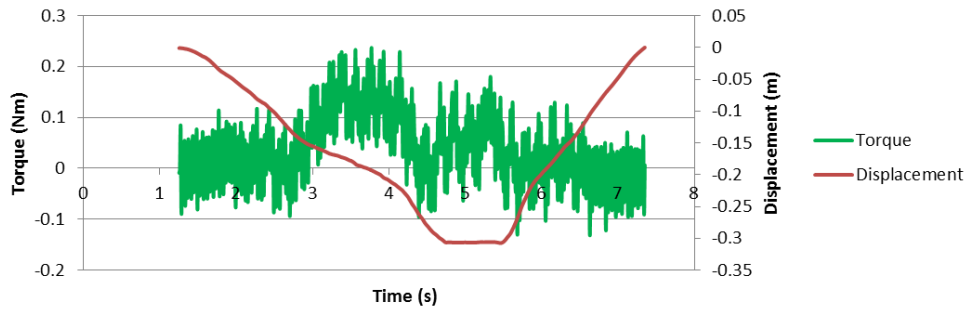
SAMPLE NO. 4 - Left - Resident: 11mm



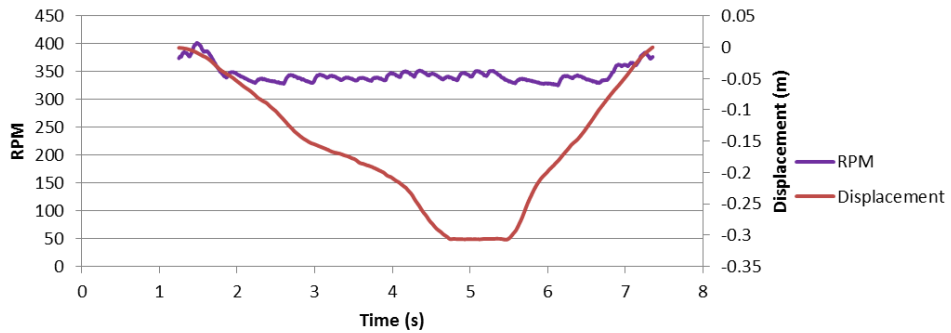
SAMPLE NO. 4 - Left - Resident: 11mm



SAMPLE NO. 4 - Left - Resident: 11mm

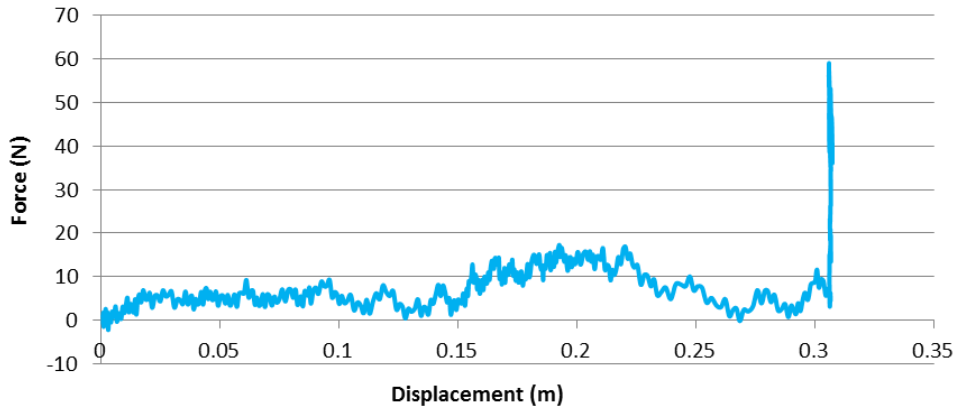


SAMPLE NO. 4 - Left - Resident: 11mm

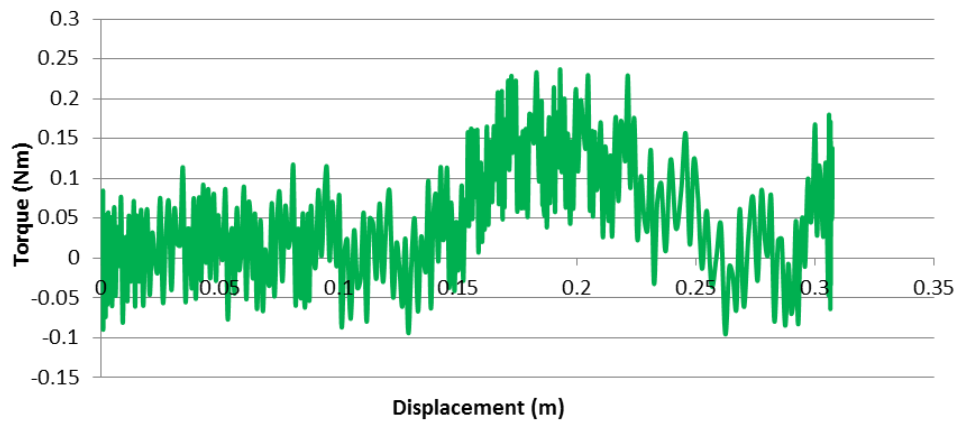




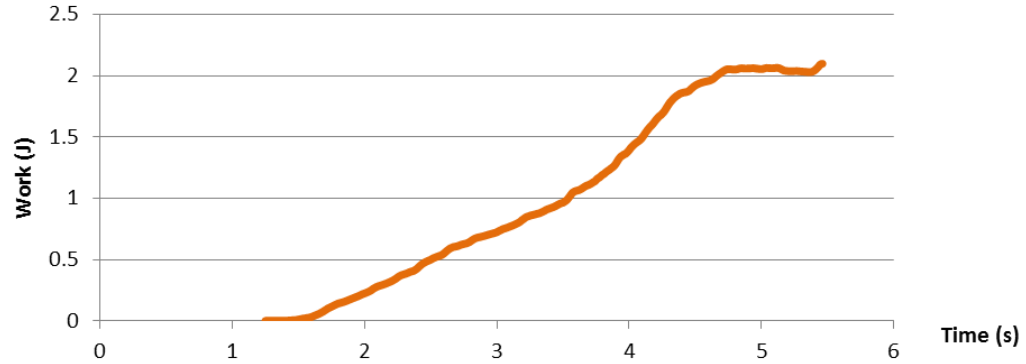
**SAMPLE NO. 4 - Left - Resident: 11mm**



**SAMPLE NO. 4 - Left - Resident: 11mm**

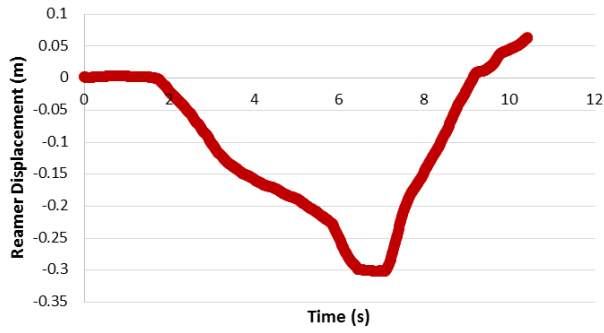


**SAMPLE NO. 4 - Left - Resident: 11mm**

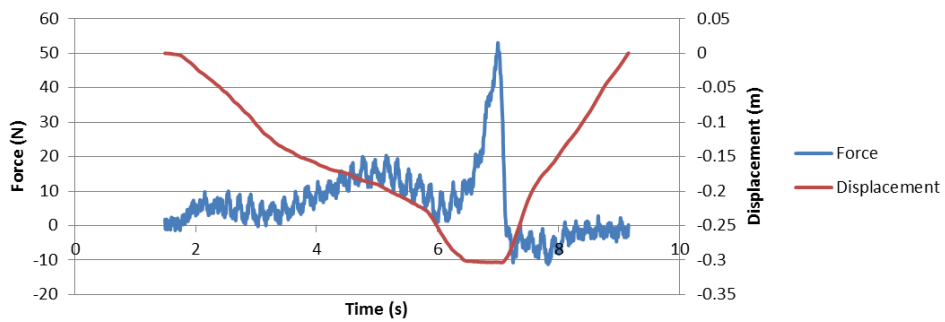


11.5MM

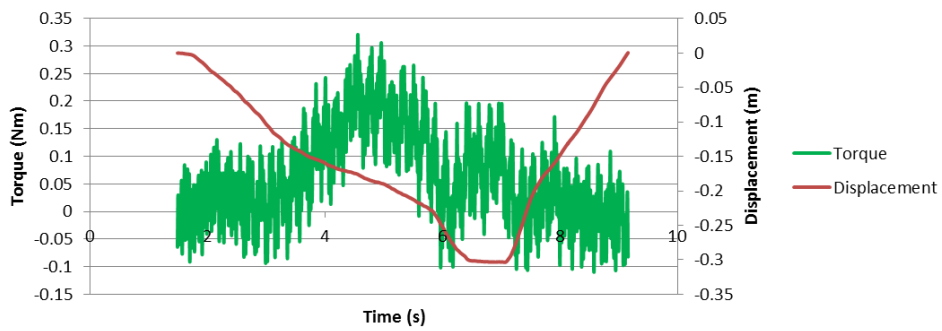
SAMPLE NO. 4 - Left - Resident: 11.5mm



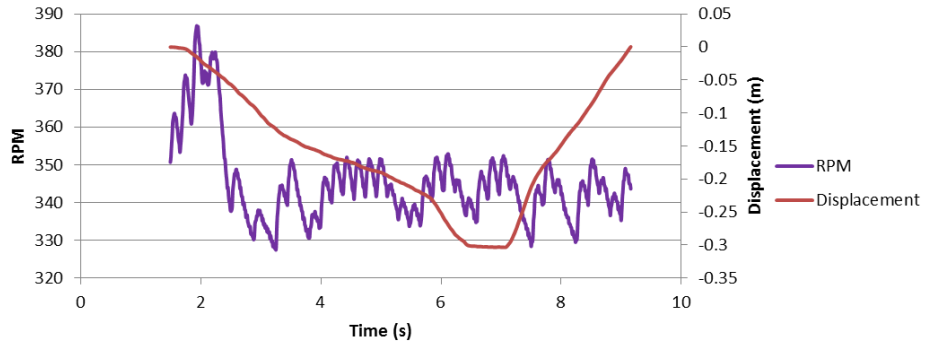
SAMPLE NO. 4 - Left - Resident: 11.5mm



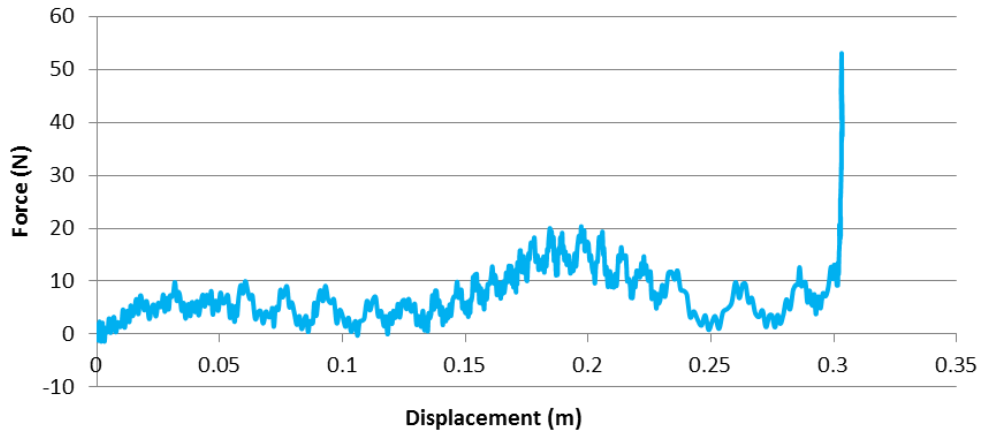
SAMPLE NO. 4 - Left - Resident: 11.5mm



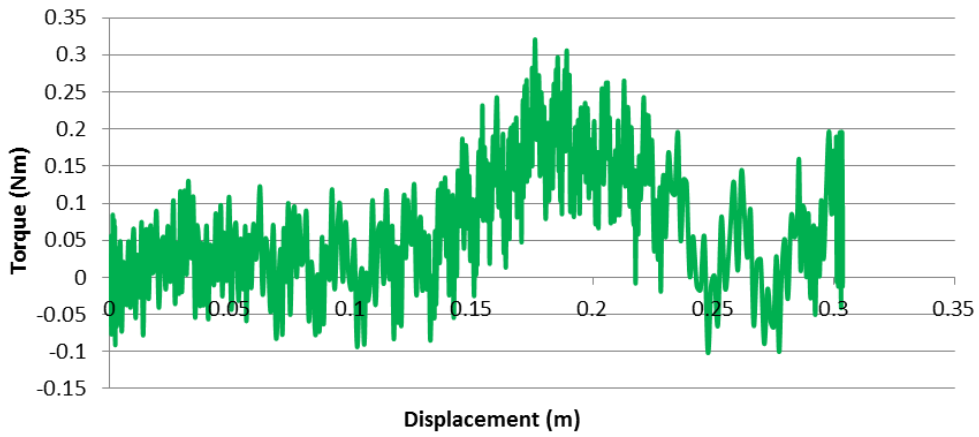
SAMPLE NO. 4 - Left - Resident: 11.5mm



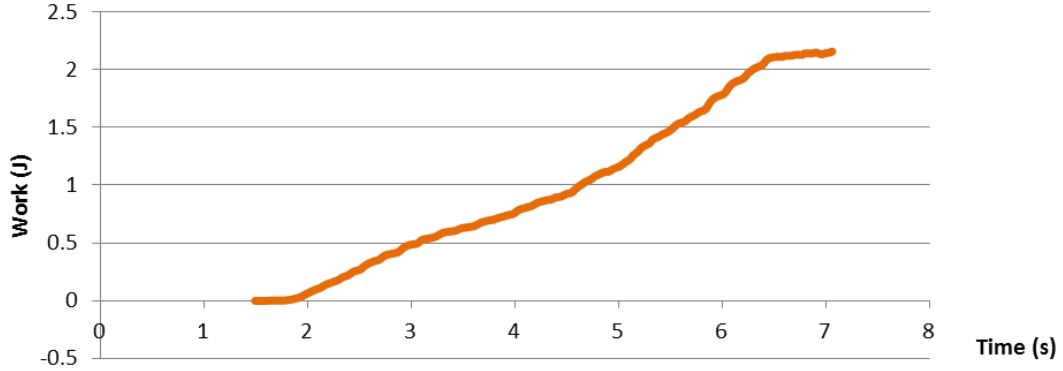
**SAMPLE NO. 4 - Left - Resident: 11.5mm**



**SAMPLE NO. 4 - Left - Resident: 11.5mm**

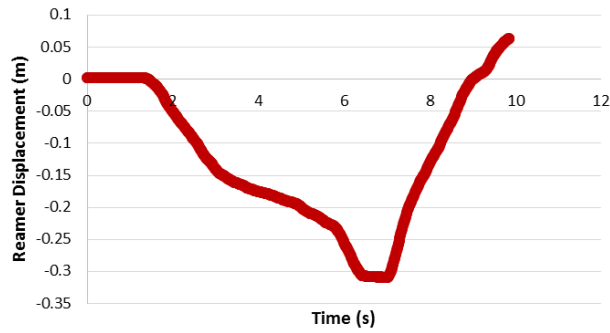


**SAMPLE NO. 4 - Left - Resident: 11.5mm**

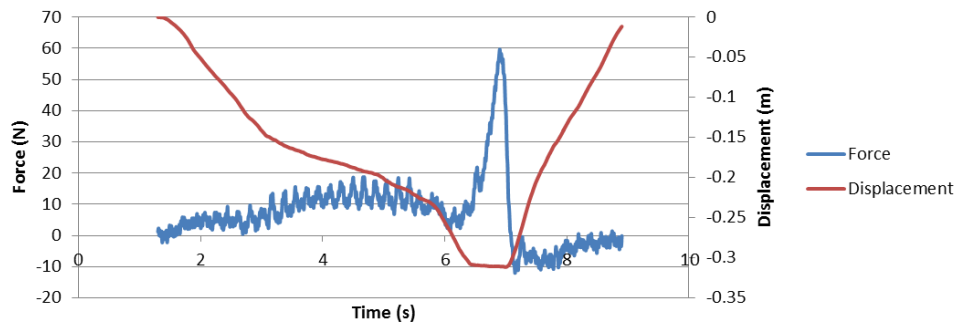


12MM

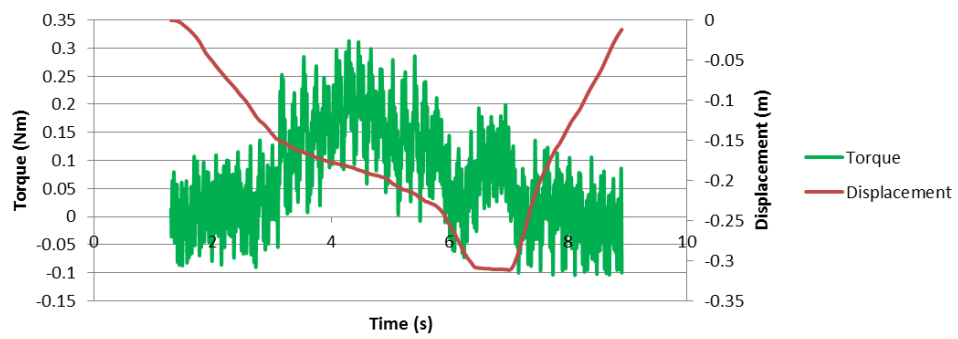
**SAMPLE NO. 4 - Left - Resident: 12mm**



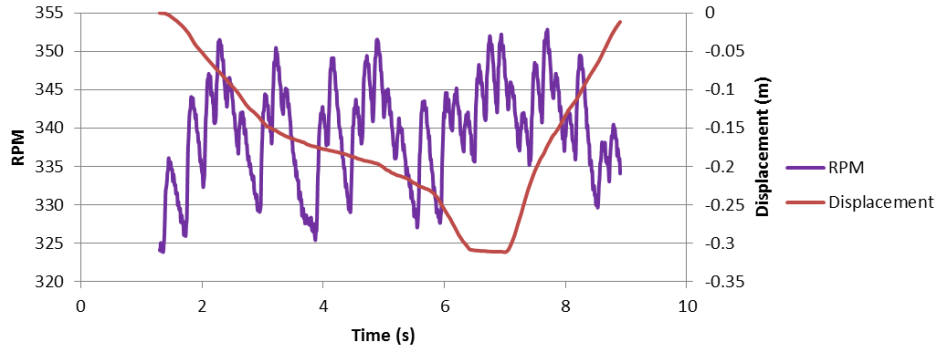
**SAMPLE NO. 4 - Left - Resident: 12mm**



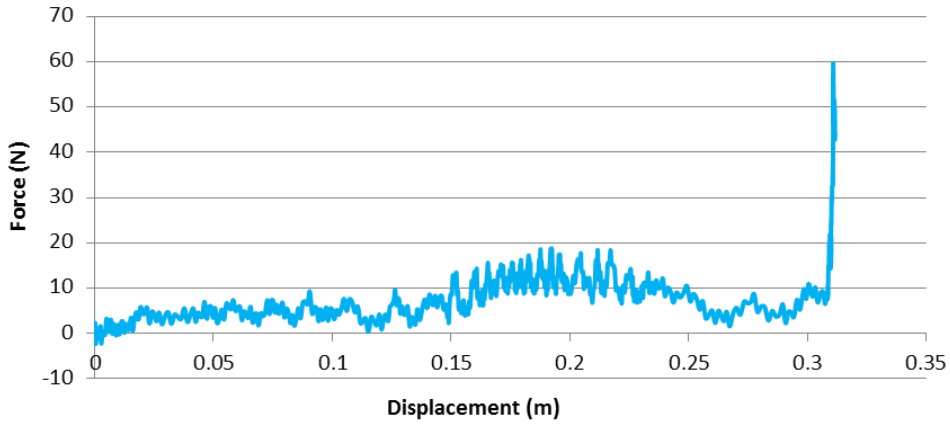
**SAMPLE NO. 4 - Left - Resident: 12mm**



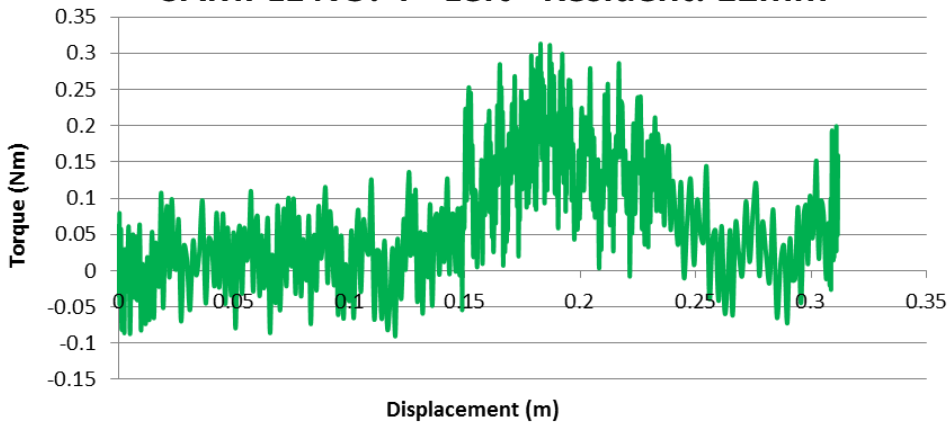
**SAMPLE NO. 4 - Left - Resident: 12mm**



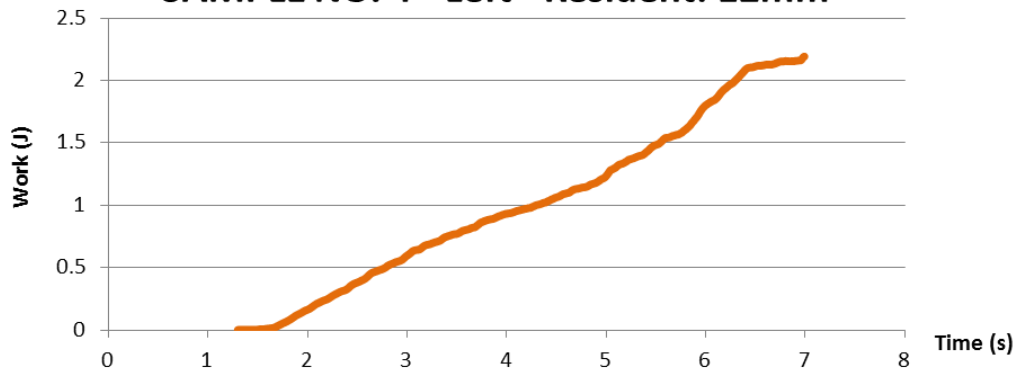
**SAMPLE NO. 4 - Left - Resident: 12mm**



**SAMPLE NO. 4 - Left - Resident: 12mm**

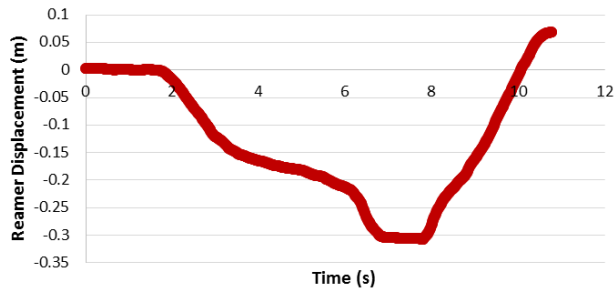


**SAMPLE NO. 4 - Left - Resident: 12mm**

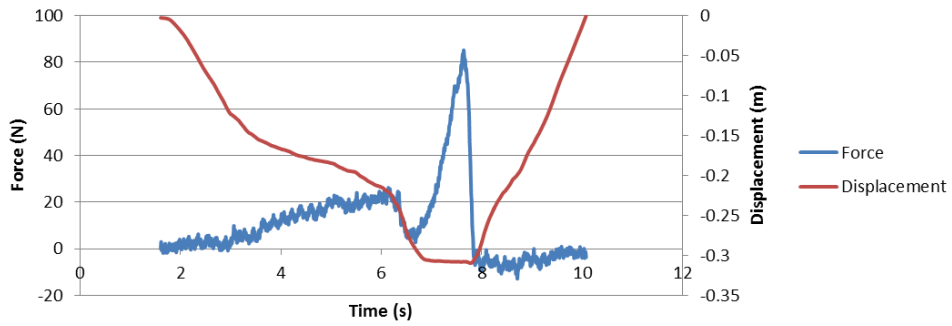


12.5MM

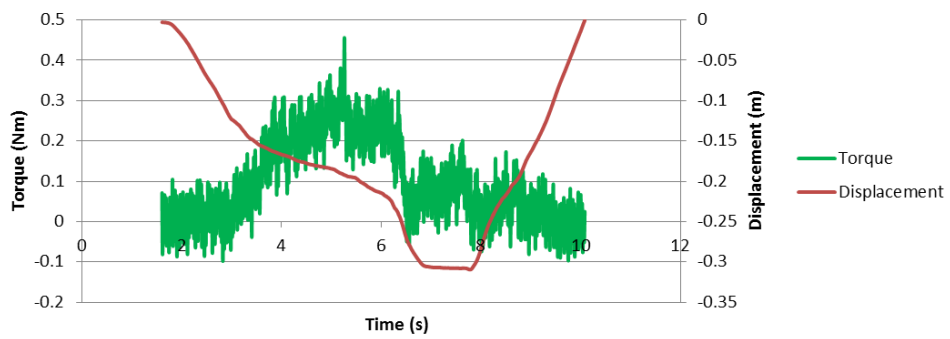
**SAMPLE NO. 4 - Left - Resident: 12.5mm  
CHATTER**



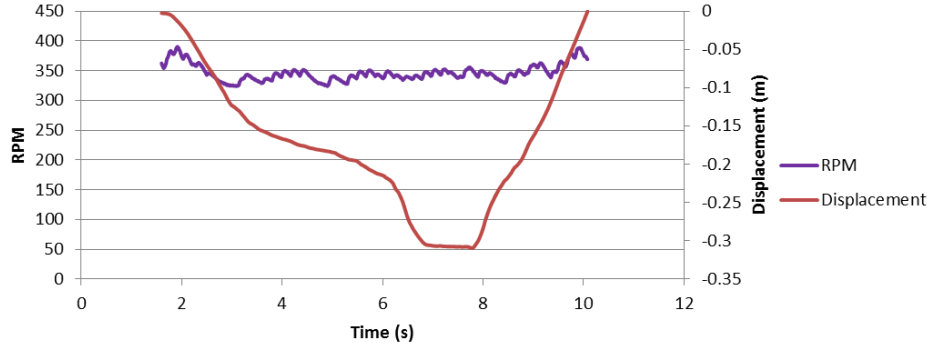
**SAMPLE NO. 4 - Left - Resident: 12.5mm CHATTER**



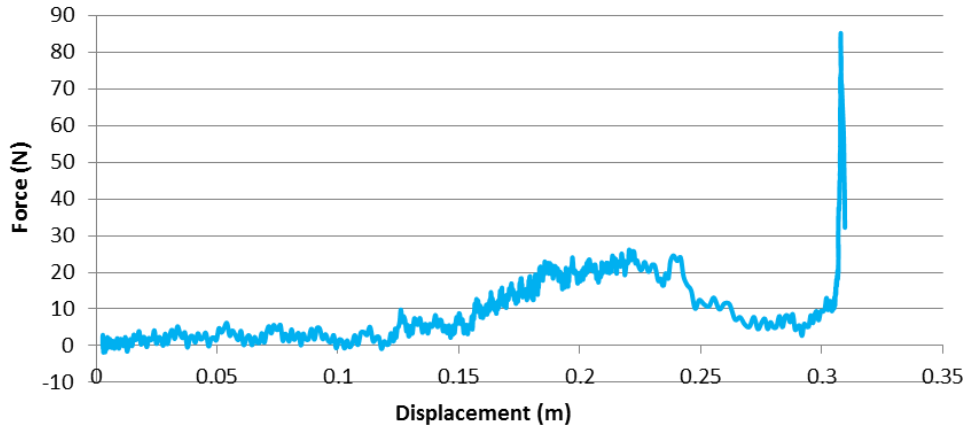
**SAMPLE NO. 4 - Left - Resident: 12.5mm CHATTER**



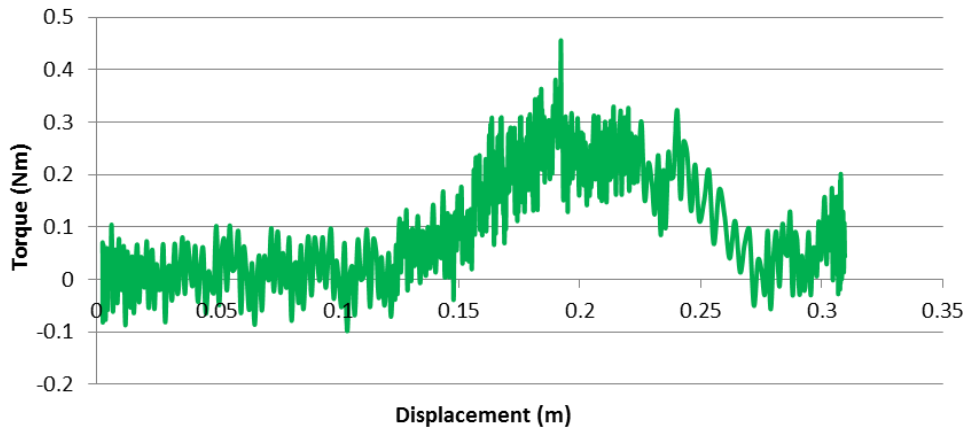
**SAMPLE NO. 4 - Left - Resident: 12.5mm CHATTER**



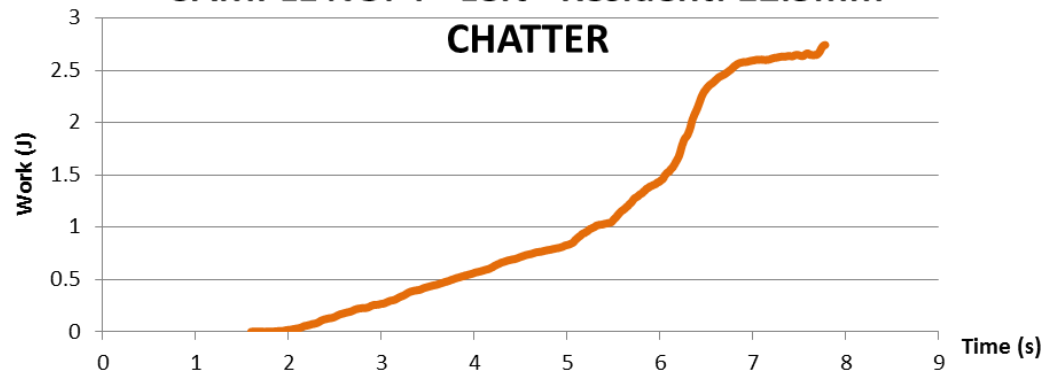
**SAMPLE NO. 4 - Left - Resident: 12.5mm CHATTER**



**SAMPLE NO. 4 - Left - Resident: 12.5mm CHATTER**

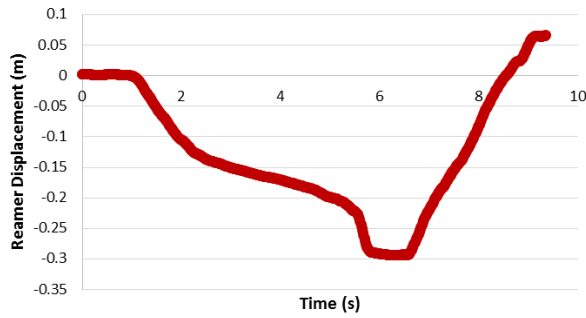


**SAMPLE NO. 4 - Left - Resident: 12.5mm CHATTER**

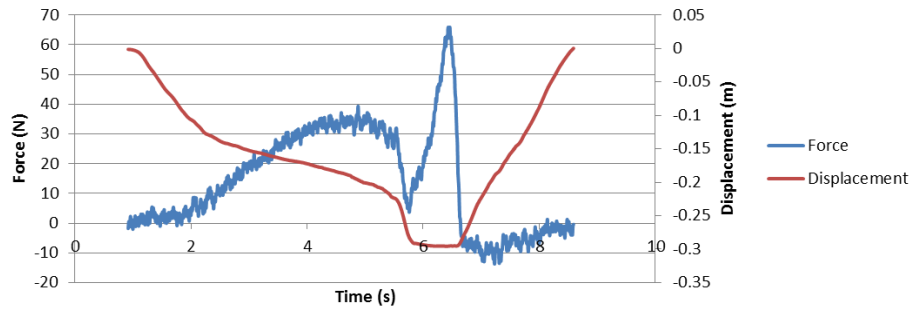


13MM

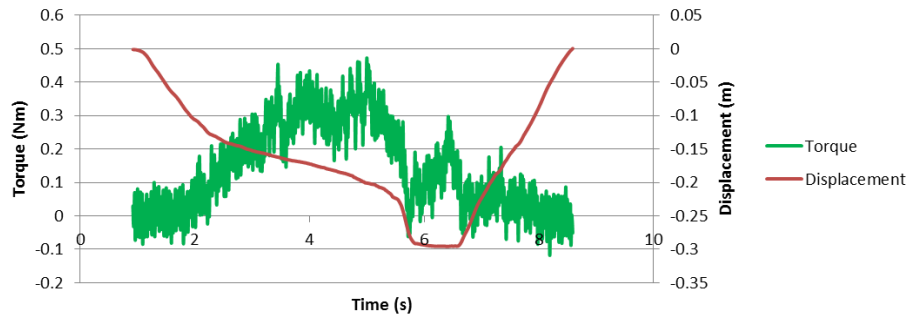
SAMPLE NO. 4 - Left - Resident: 13mm



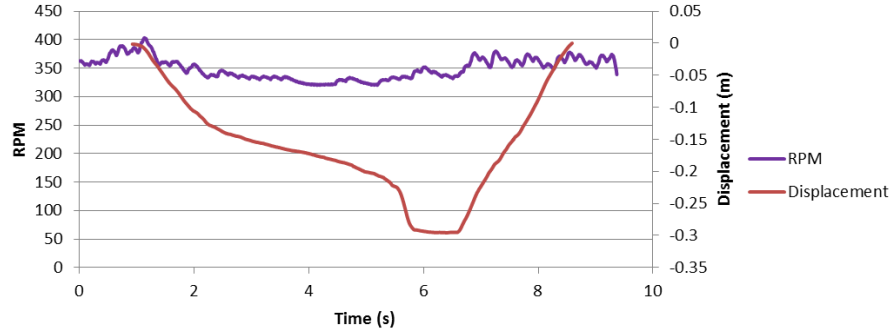
SAMPLE NO. 4 - Left - Resident: 13mm



SAMPLE NO. 4 - Left - Resident: 13mm

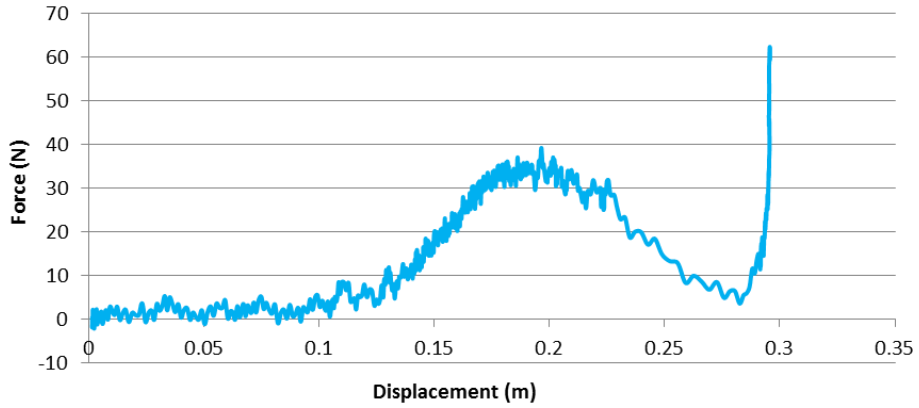


SAMPLE NO. 4 - Left - Resident: 13mm

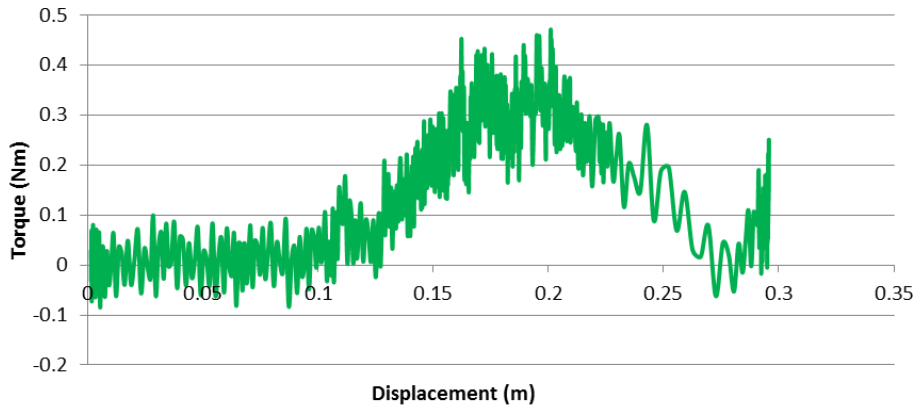




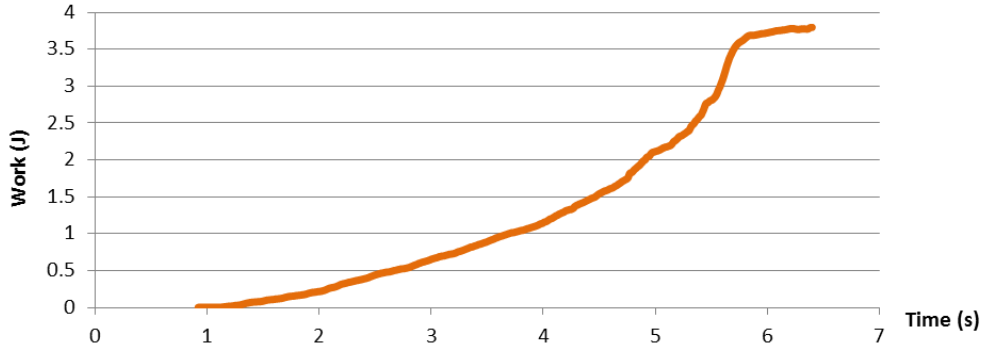
**SAMPLE NO. 4 - Left - Resident: 13mm**



**SAMPLE NO. 4 - Left - Resident: 13mm**

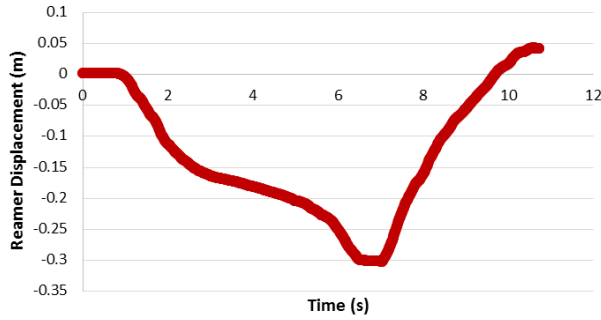


**SAMPLE NO. 4 - Left - Resident: 13mm**

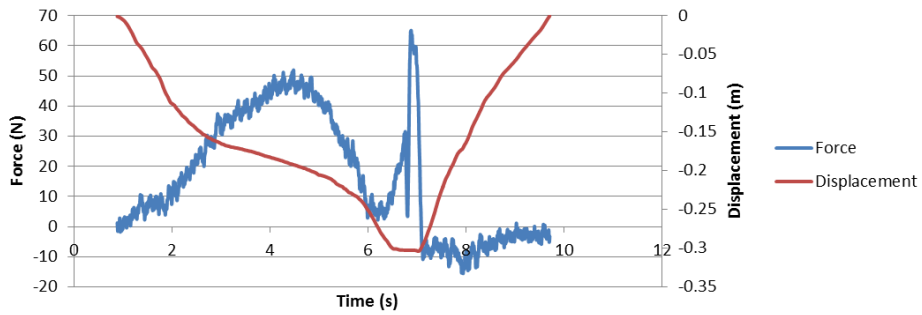


13.5MM

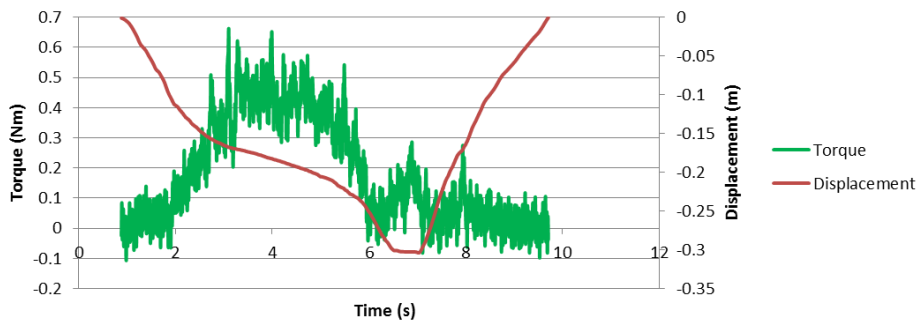
**SAMPLE NO. 4 - Left - Resident: 13.5mm**



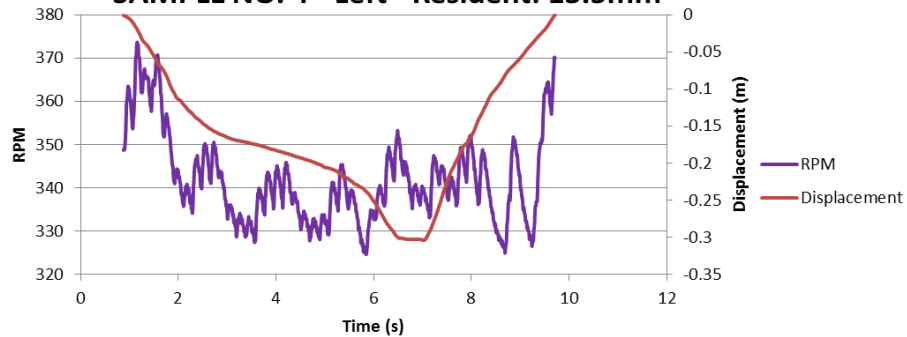
**SAMPLE NO. 4 - Left - Resident: 13.5mm**



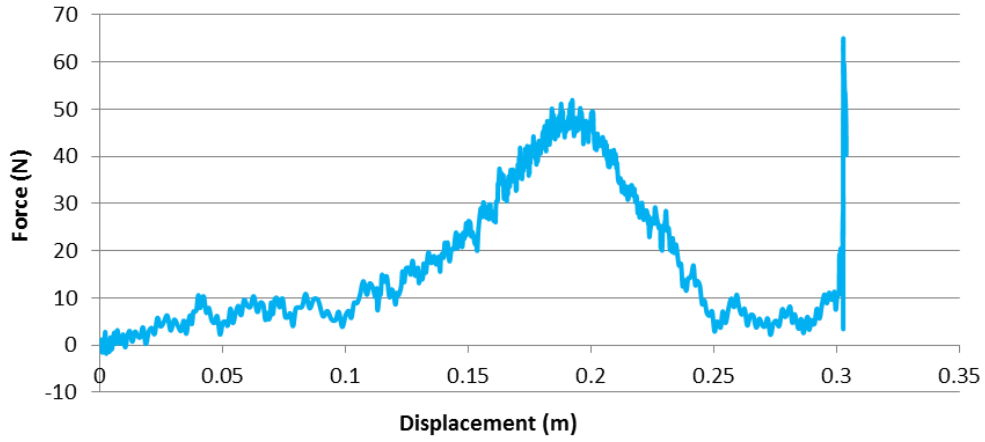
**SAMPLE NO. 4 - Left - Resident: 13.5mm**



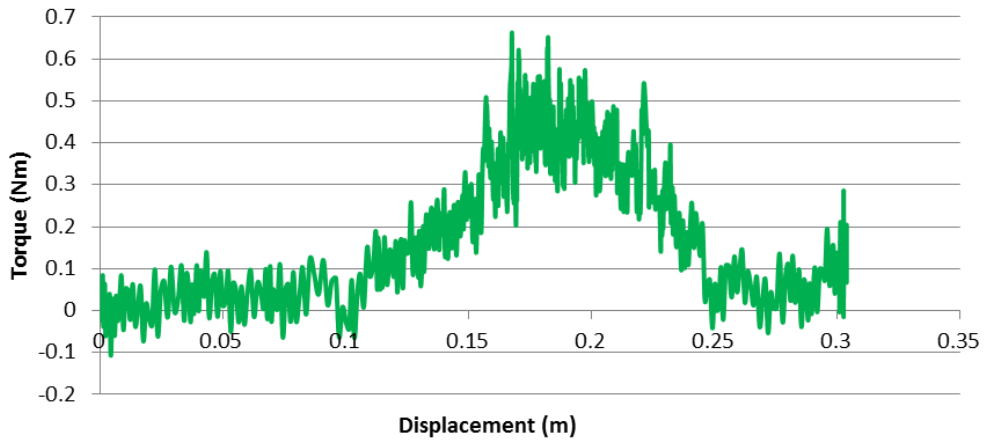
**SAMPLE NO. 4 - Left - Resident: 13.5mm**



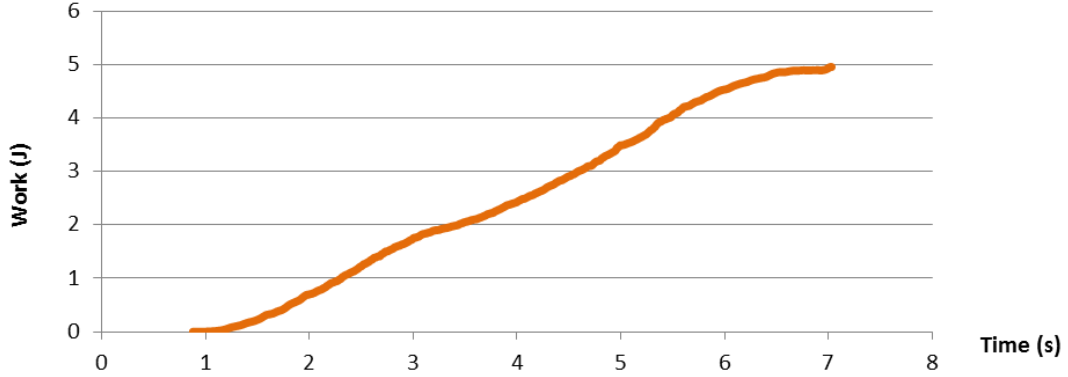
### SAMPLE NO. 4 - Left - Resident: 13.5mm



### SAMPLE NO. 4 - Left - Resident: 13.5mm

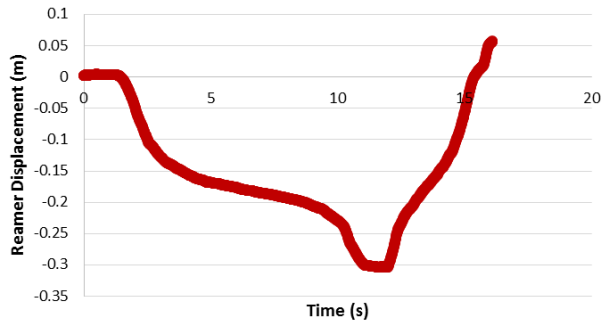


### SAMPLE NO. 4 - Left - Resident: 13.5mm

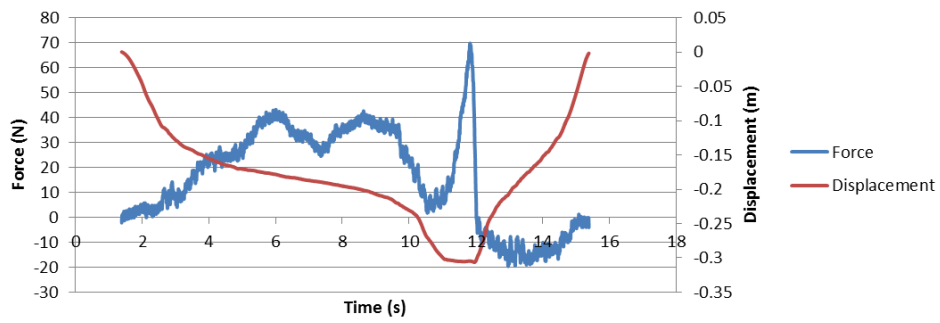


14MM

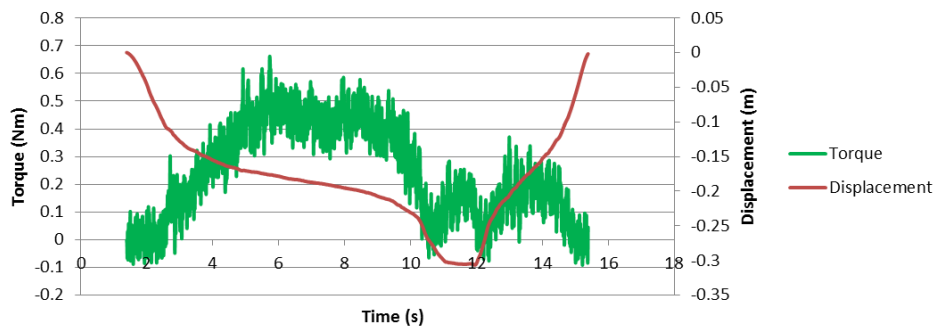
SAMPLE NO. 4 - Left - Resident: 14mm



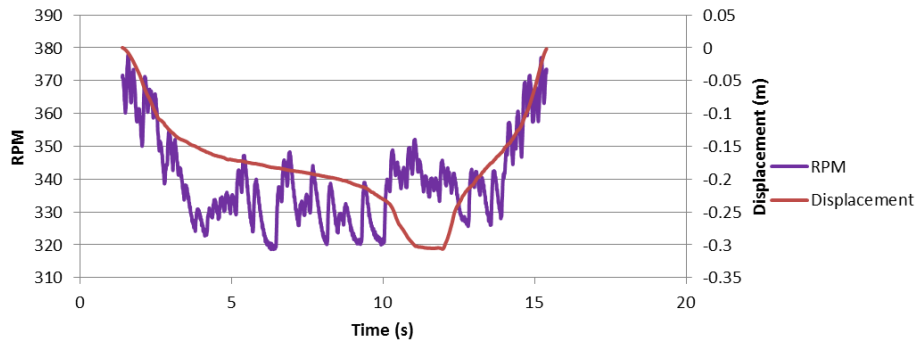
SAMPLE NO. 4 - Left - Resident: 14mm



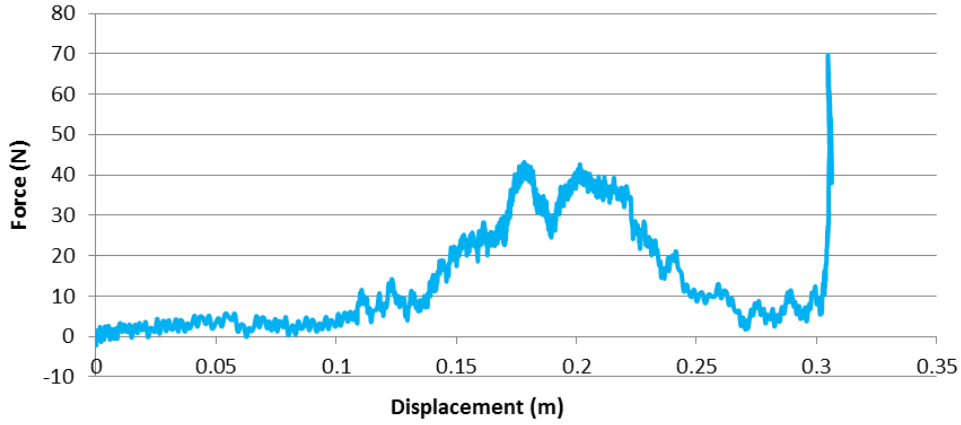
SAMPLE NO. 4 - Left - Resident: 14mm



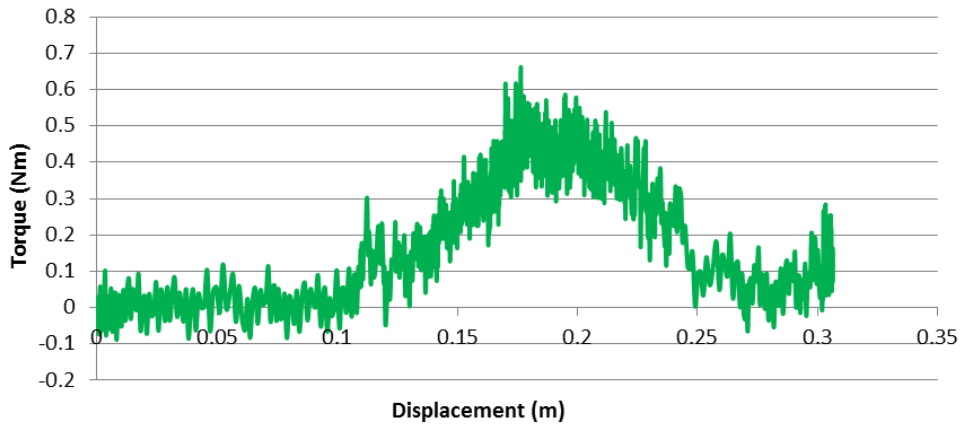
SAMPLE NO. 4 - Left - Resident: 14mm



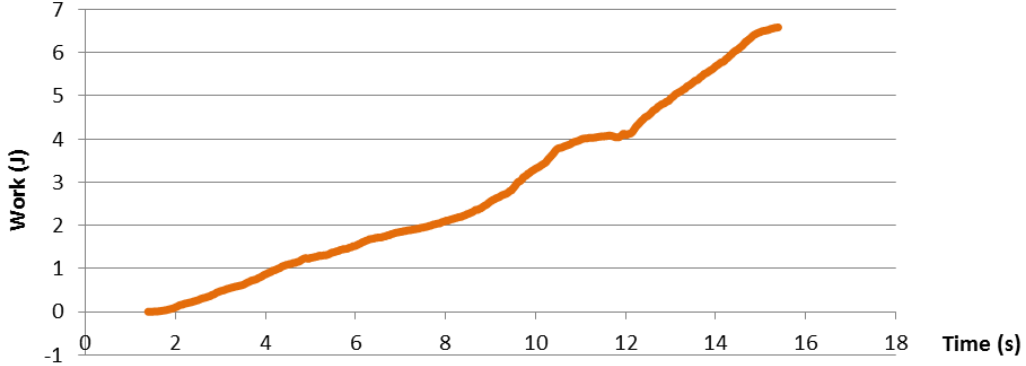
**SAMPLE NO. 4 - Left - Resident: 14mm**



**SAMPLE NO. 4 - Left - Resident: 14mm**



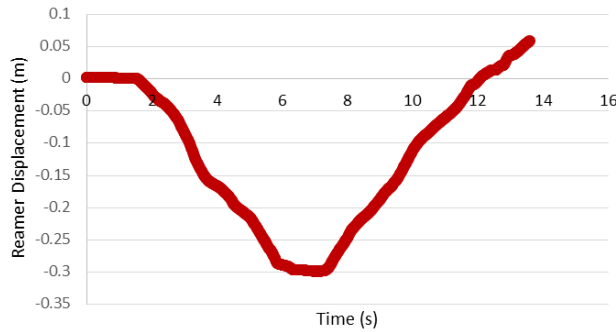
**SAMPLE NO. 4 - Left - Resident: 14mm**



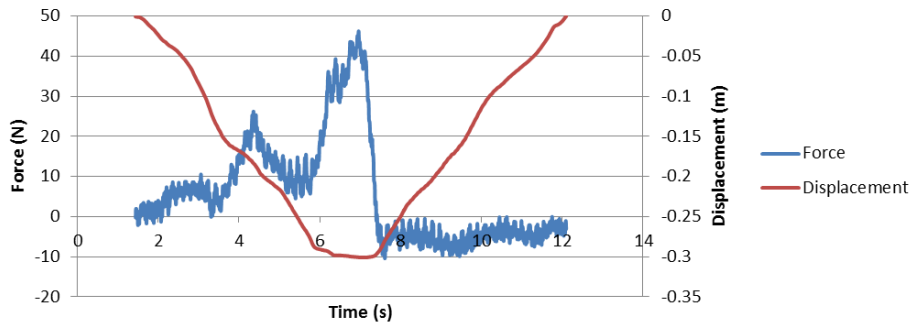
RIGHT: ATTENDING

9MM

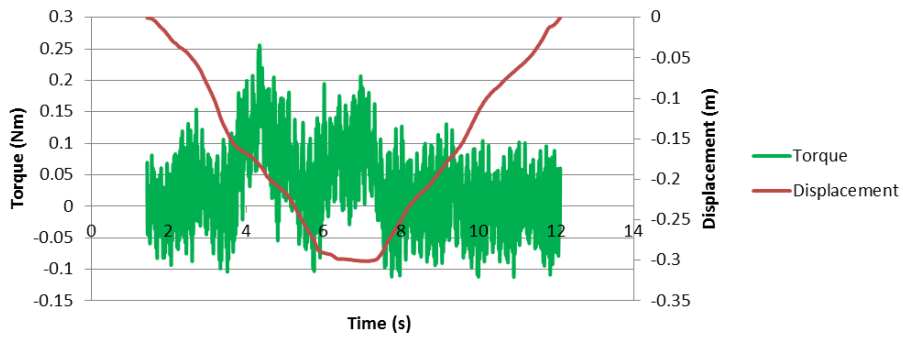
**SAMPLE NO. 4 - Right - Attending: 9mm**



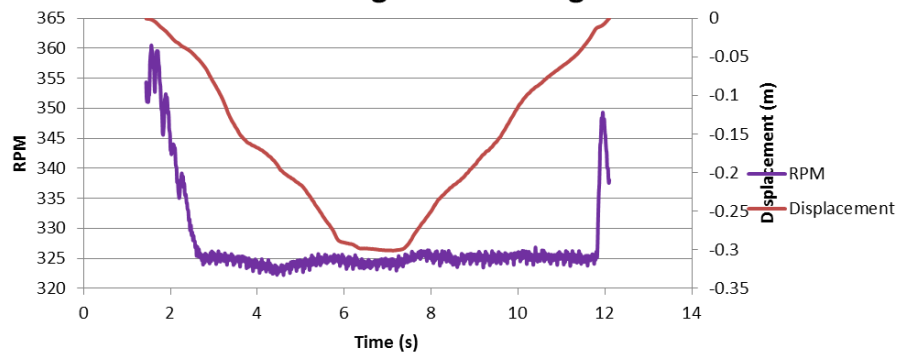
**SAMPLE NO. 4 - Right - Attending: 9mm**



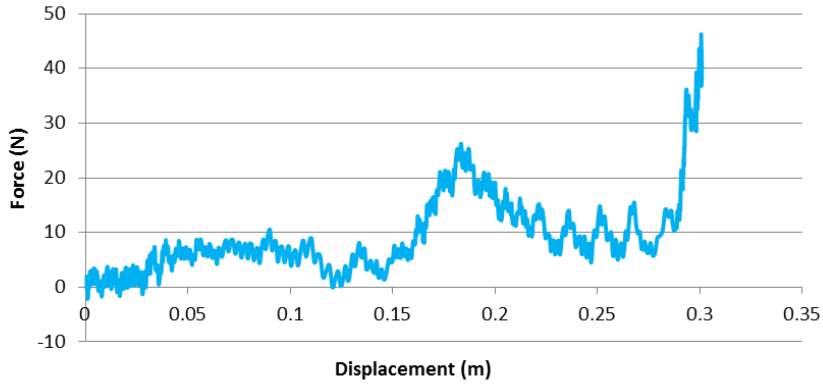
**SAMPLE NO. 4 - Right - Attending: 9mm**



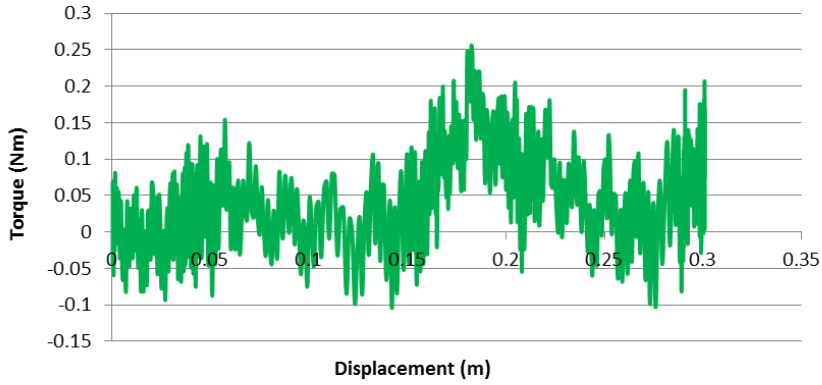
**SAMPLE NO. 4 - Right - Attending: 9mm**



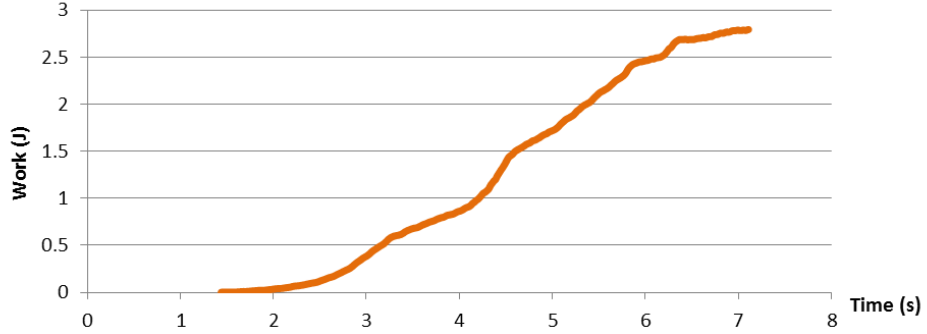
**SAMPLE NO. 4 - Right - Attending: 9mm**



**SAMPLE NO. 4 - Right - Attending: 9mm**

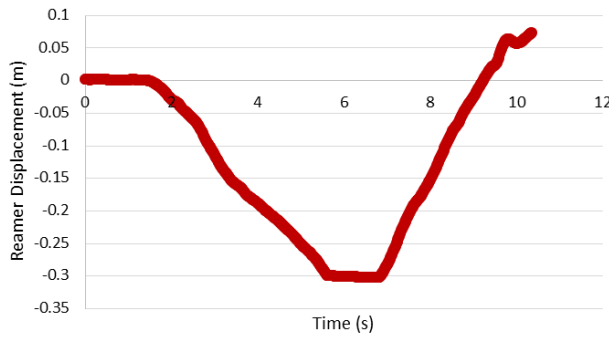


**SAMPLE NO. 4 - Right - Attending: 9mm**

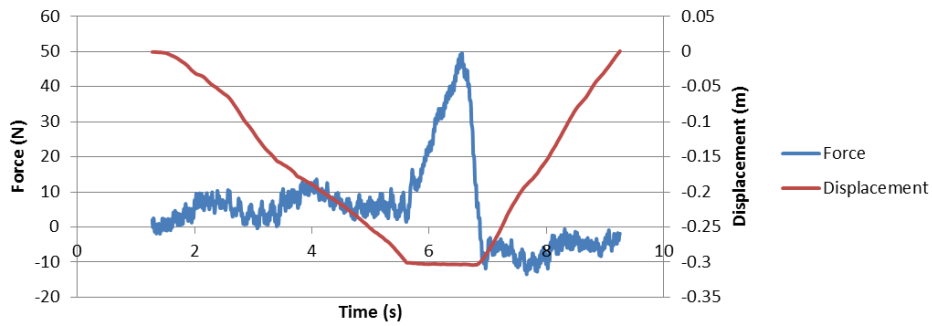


9.5MM

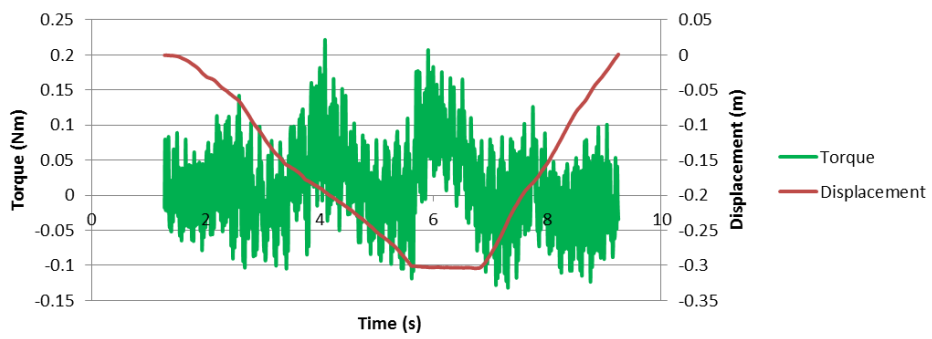
SAMPLE NO. 4 - Right - Attending: 9.5mm



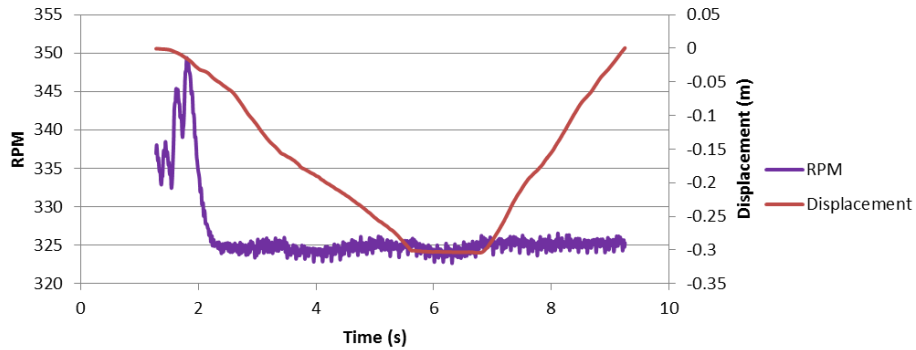
SAMPLE NO. 4 - Right - Attending: 9.5mm



SAMPLE NO. 4 - Right - Attending: 9.5mm

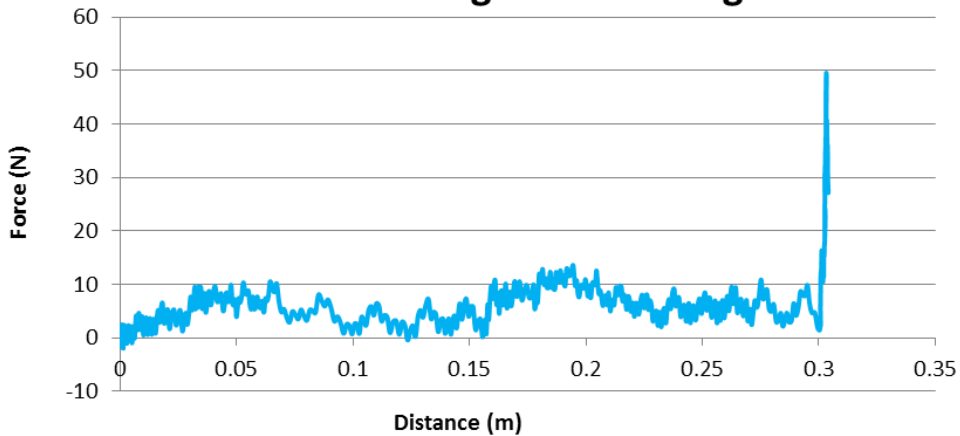


SAMPLE NO. 4 - Right - Attending: 9.5mm

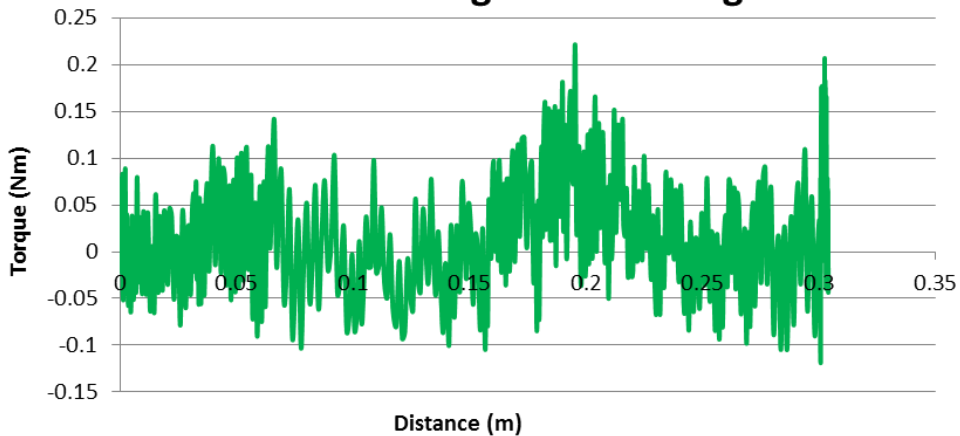




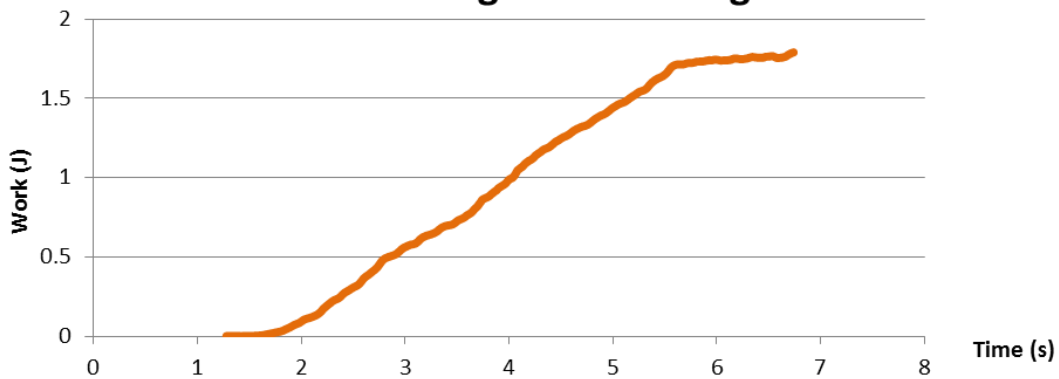
**SAMPLE NO. 4 - Right - Attending: 9.5mm**



**SAMPLE NO. 4 - Right - Attending: 9.5mm**

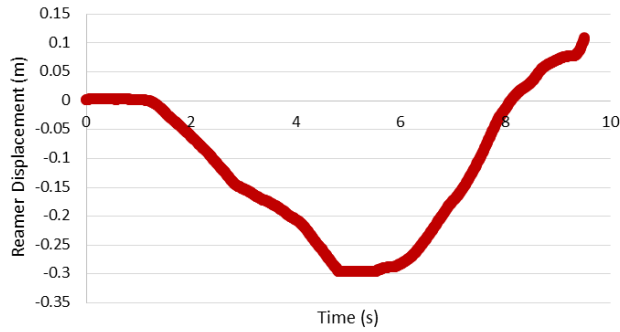


**SAMPLE NO. 4 - Right - Attending: 9.5mm**

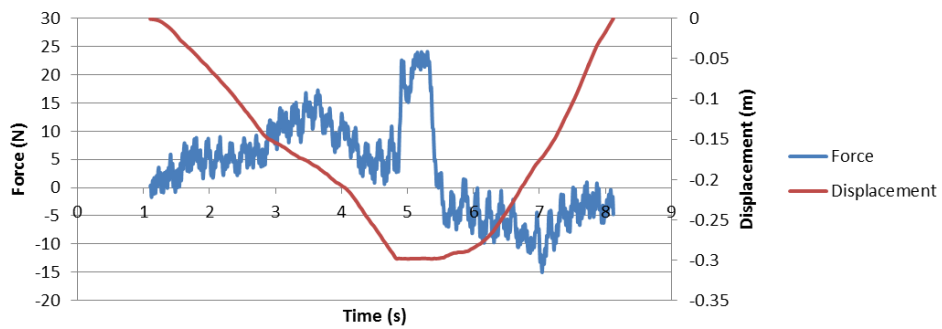


10MM

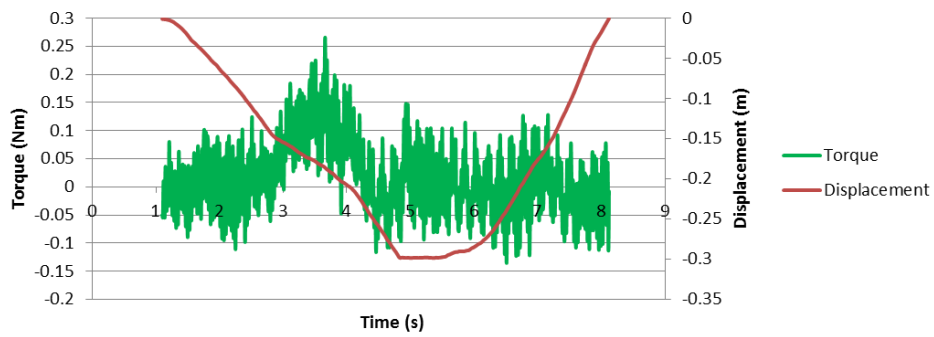
**SAMPLE NO. 4 - Right - Attending: 10mm**



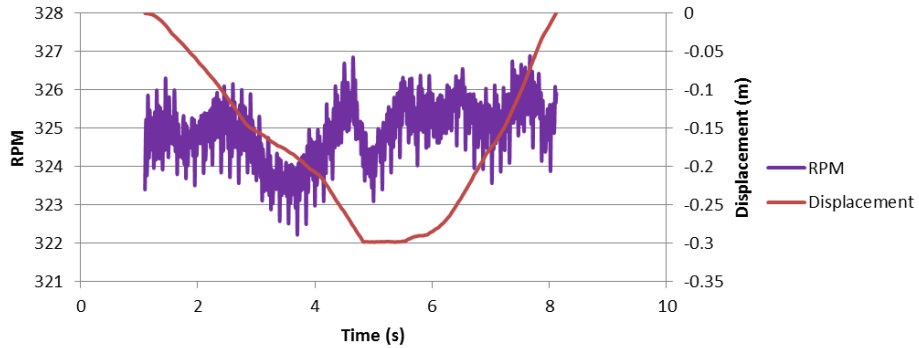
**SAMPLE NO. 4 - Right - Attending: 10mm**



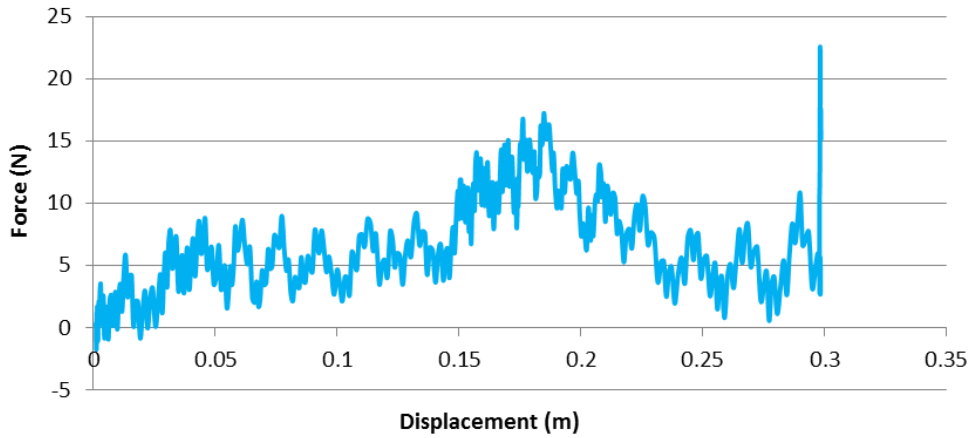
**SAMPLE NO. 4 - Right - Attending: 10mm**



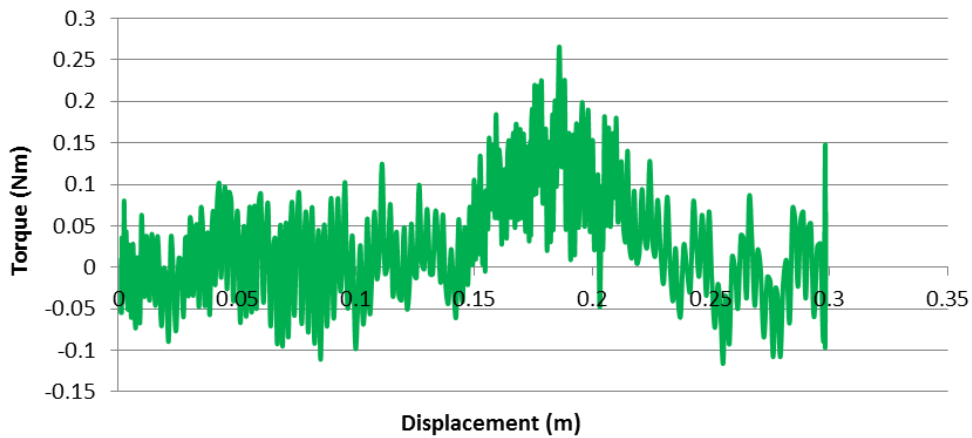
**SAMPLE NO. 4 - Right - Attending: 10mm**



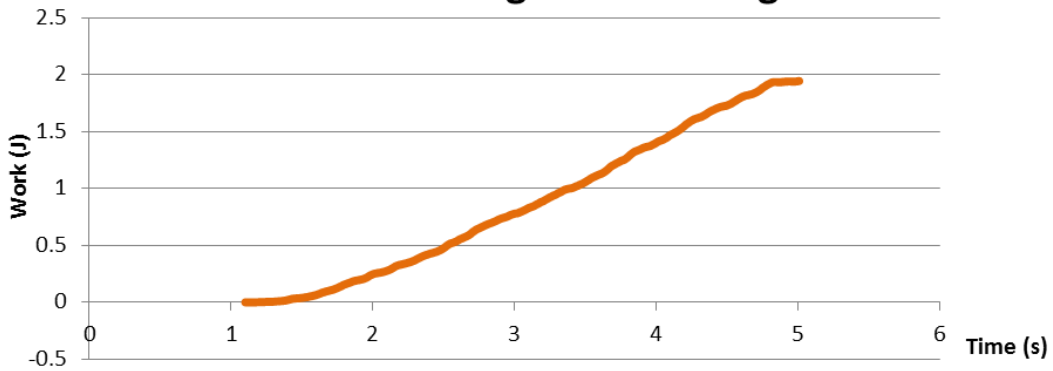
### SAMPLE NO. 4 - Right - Attending: 10mm



### SAMPLE NO. 4 - Right - Attending: 10mm

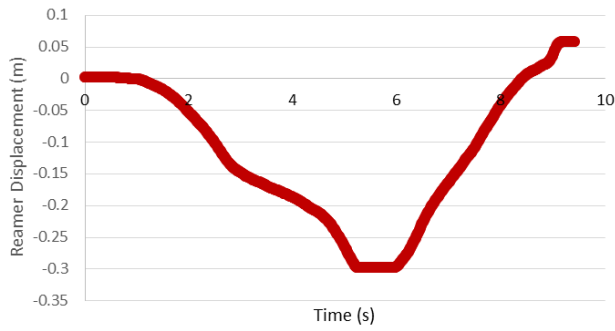


### SAMPLE NO. 4 - Right - Attending: 10mm

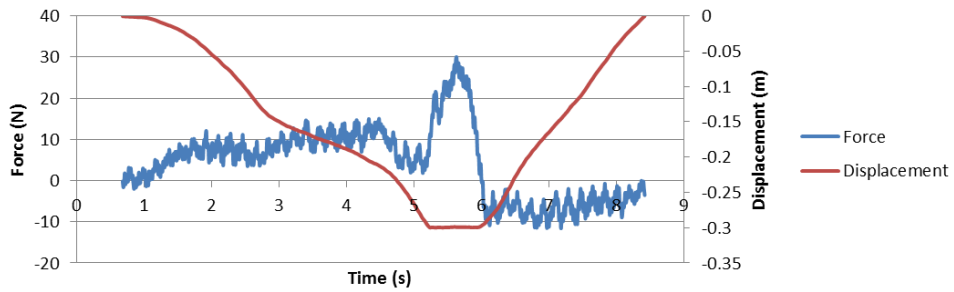


10.5MM

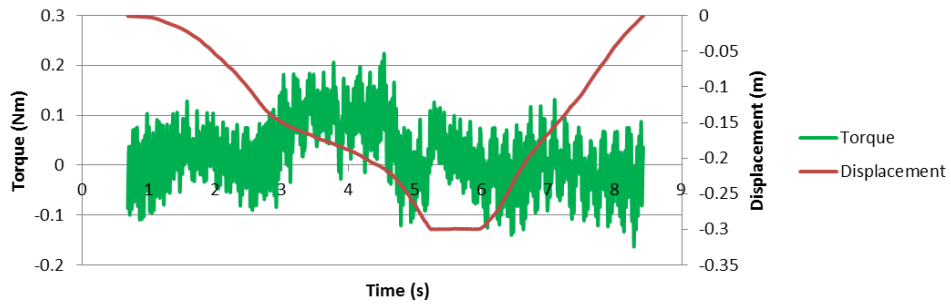
SAMPLE NO. 4 - Right - Attending: 10.5mm



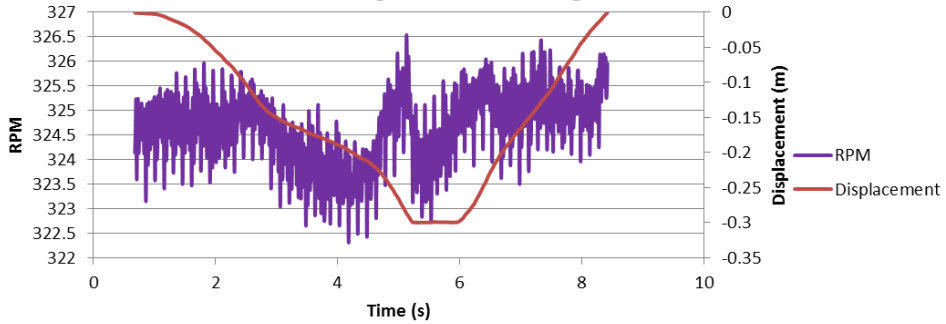
SAMPLE NO. 4 - Right - Attending: 10.5mm



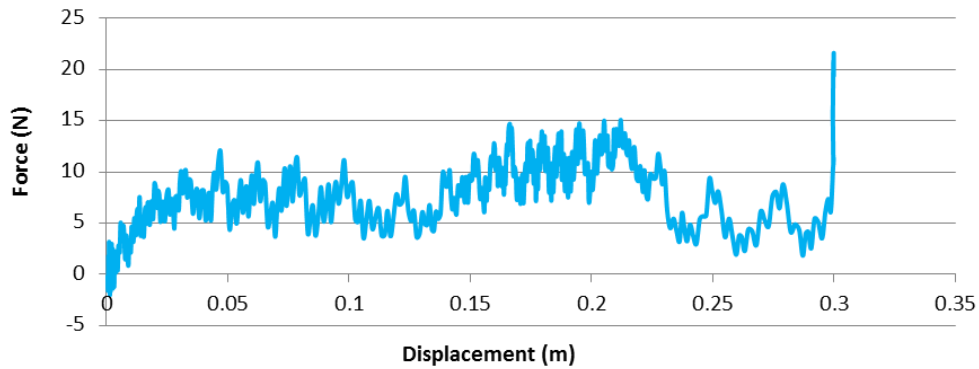
SAMPLE NO. 4 - Right - Attending: 10.5mm



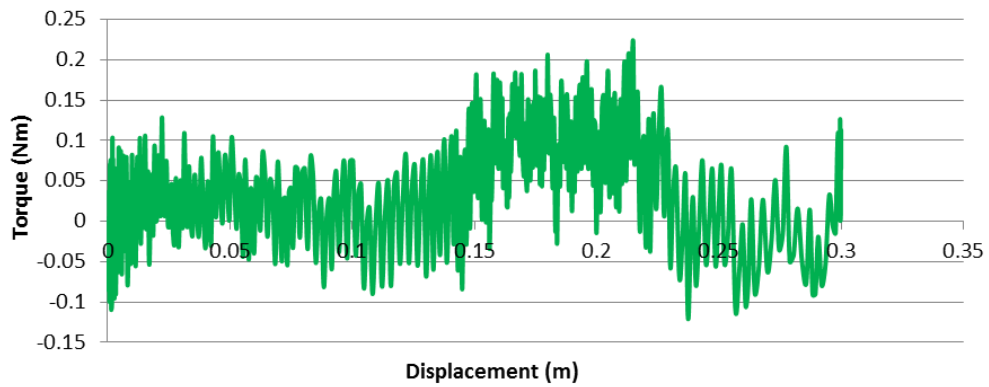
SAMPLE NO. 4 - Right - Attending: 10.5mm



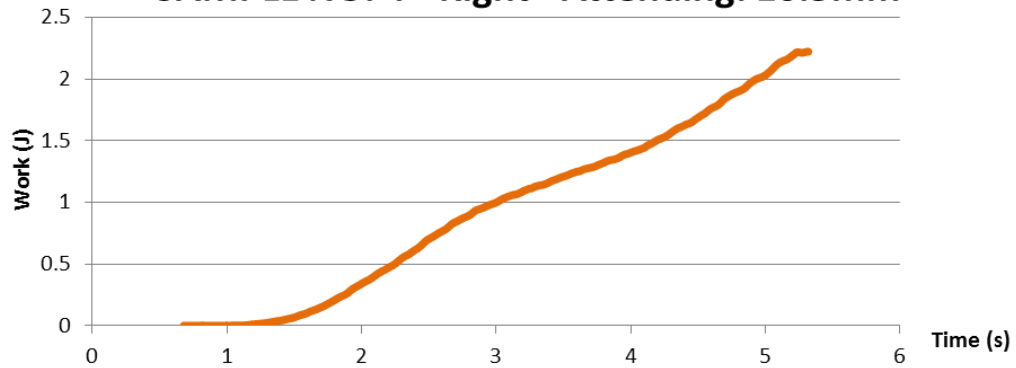
**SAMPLE NO. 4 - Right - Attending: 10.5mm**



**SAMPLE NO. 4 - Right - Attending: 10.5mm**

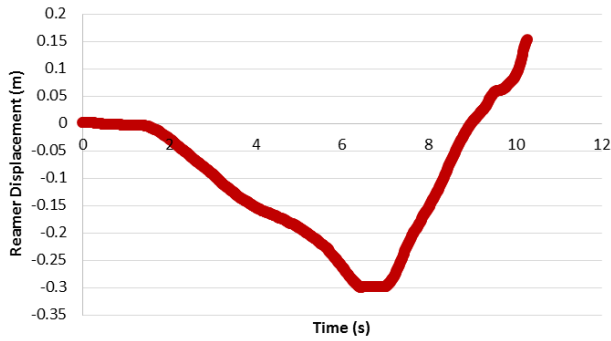


**SAMPLE NO. 4 - Right - Attending: 10.5mm**

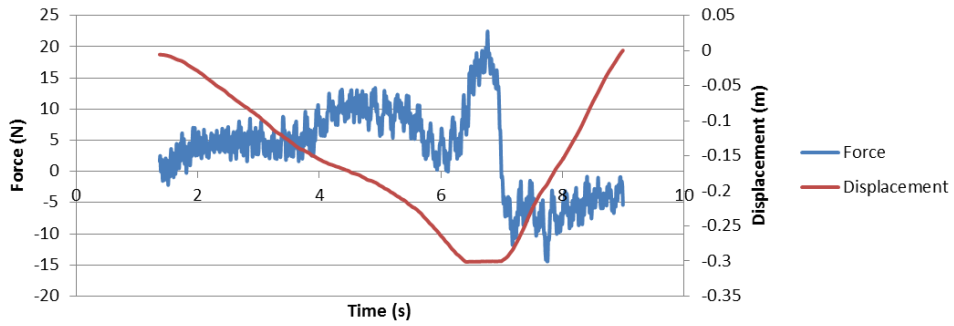


11MM

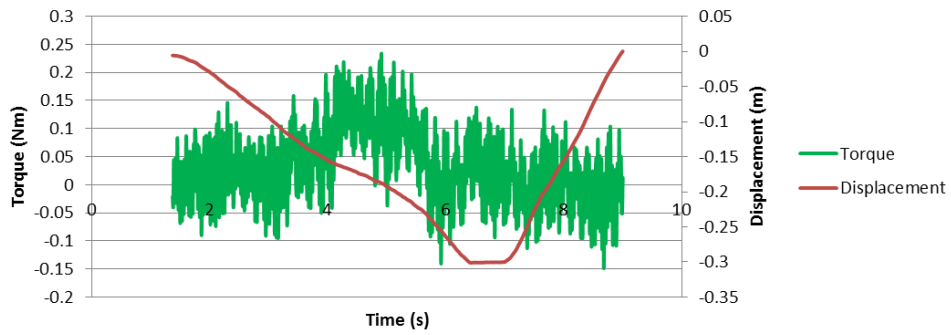
SAMPLE NO. 4 - Right - Attending: 11mm



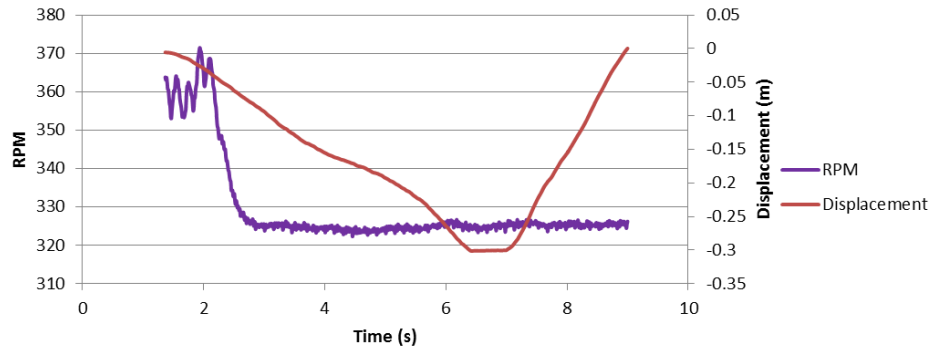
SAMPLE NO. 4 - Right - Attending: 11mm



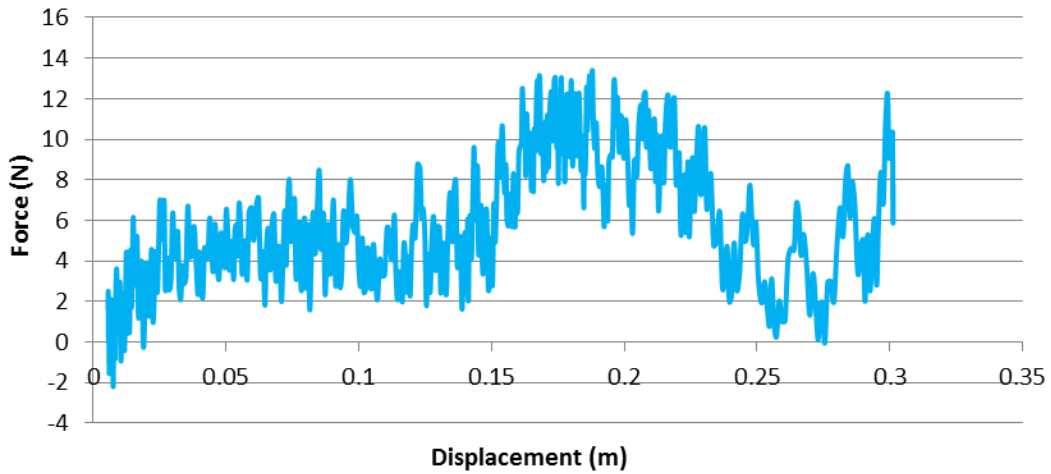
SAMPLE NO. 4 - Right - Attending: 11mm



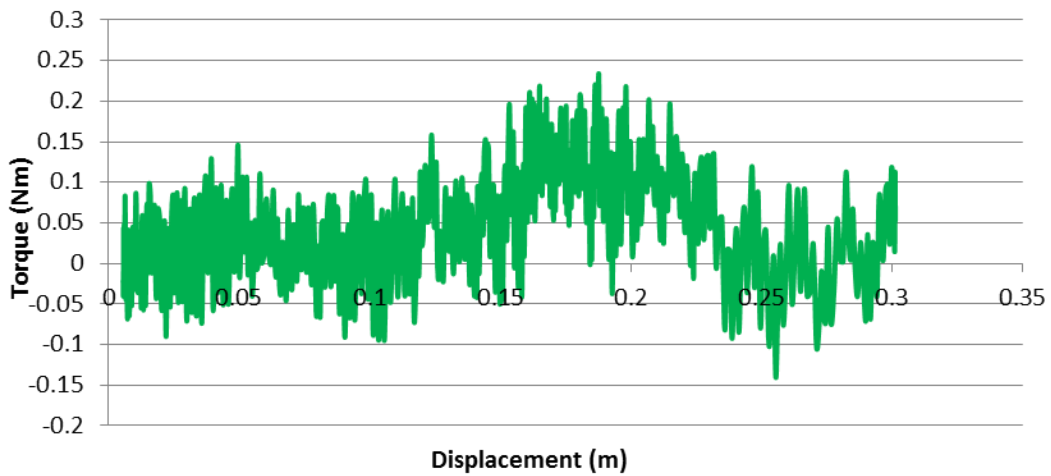
SAMPLE NO. 4 - Right - Attending: 11mm



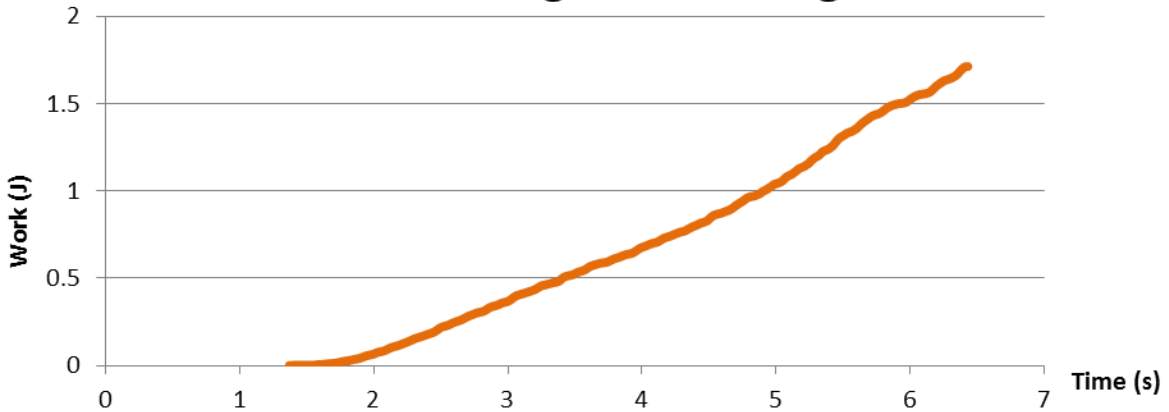
### SAMPLE NO. 4 - Right - Attending: 11mm



### SAMPLE NO. 4 - Right - Attending: 11mm

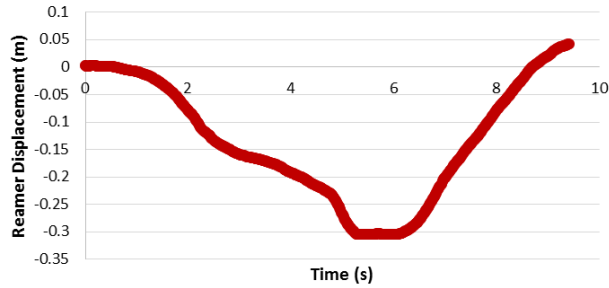


### SAMPLE NO. 4 - Right - Attending: 11mm

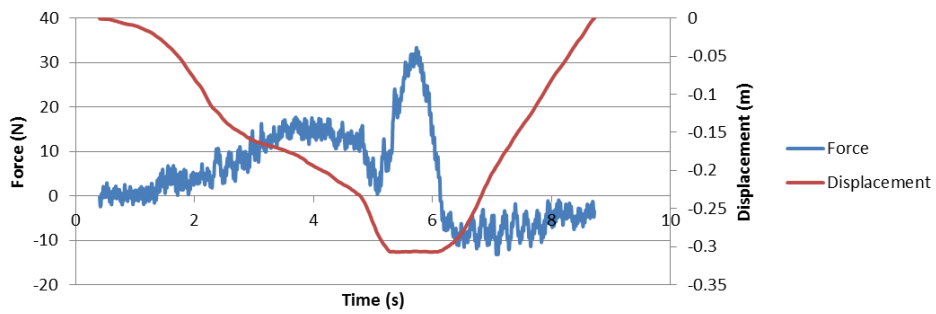


11.5MM

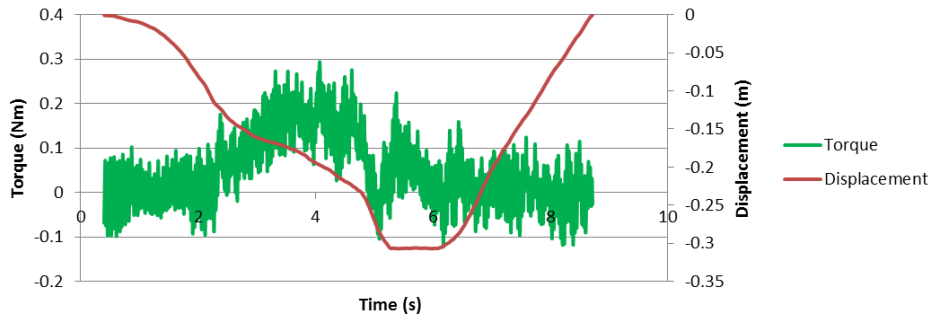
**SAMPLE NO. 4 - Right - Attending: 11.5mm CHATTER**



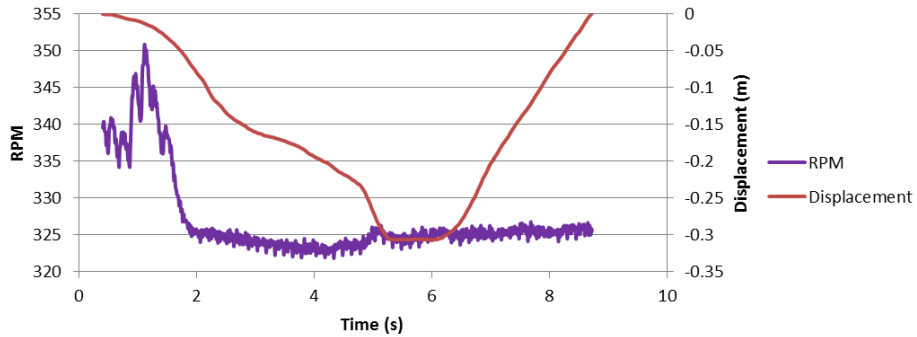
**SAMPLE NO. 4 - Right - Attending: 11.5mm CHATTER**



**SAMPLE NO. 4 - Right - Attending: 11.5mm CHATTER**

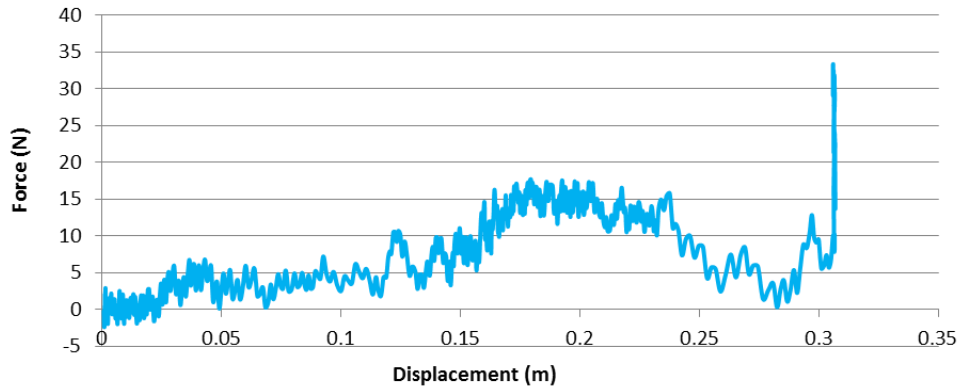


**SAMPLE NO. 4 - Right - Attending: 11.5mm CHATTER**

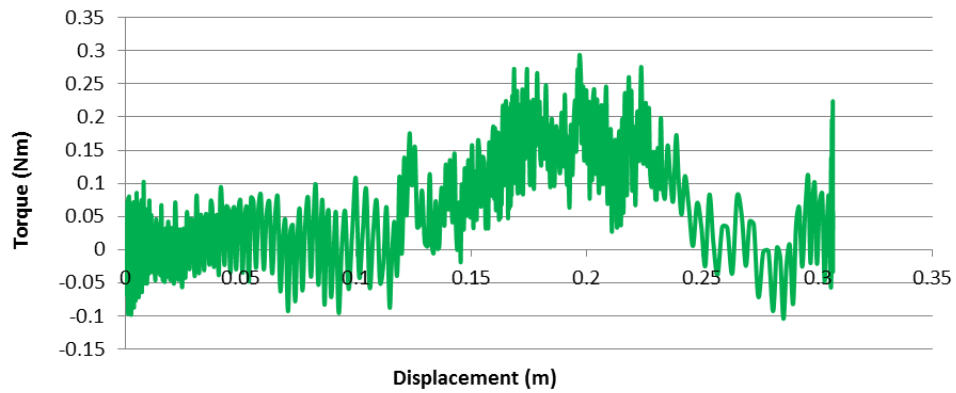




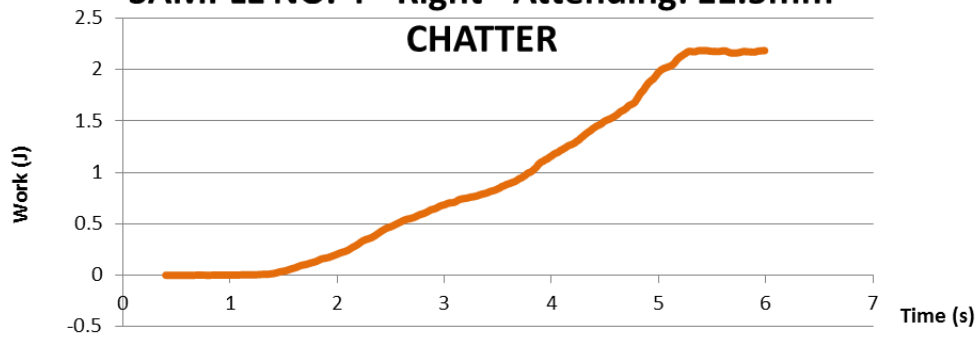
**SAMPLE NO. 4 - Right - Attending: 11.5mm CHATTER**



**SAMPLE NO. 4 - Right - Attending: 11.5mm CHATTER**

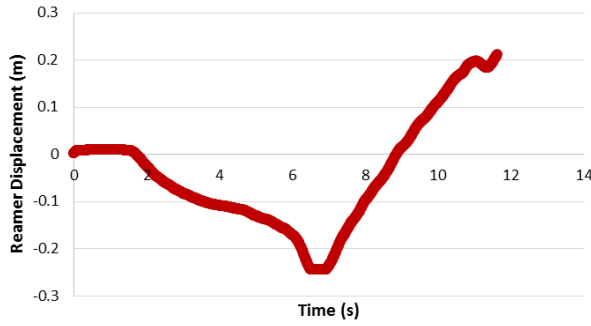


**SAMPLE NO. 4 - Right - Attending: 11.5mm CHATTER**

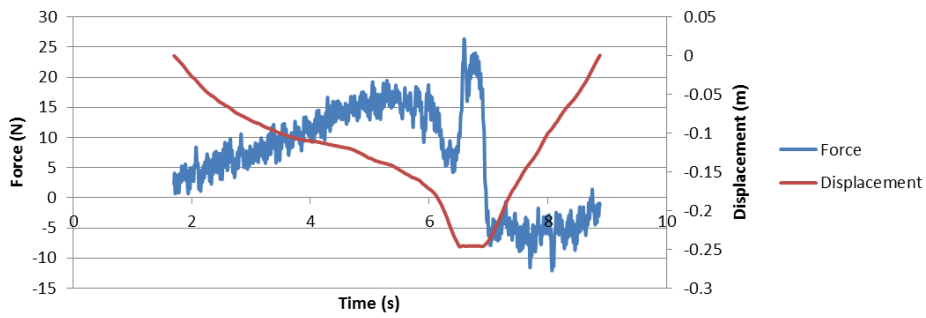


12MM

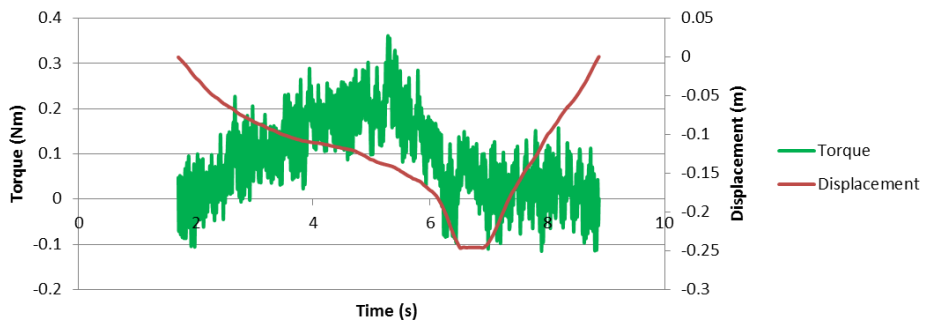
SAMPLE NO. 4 - Right - Attending: 12mm



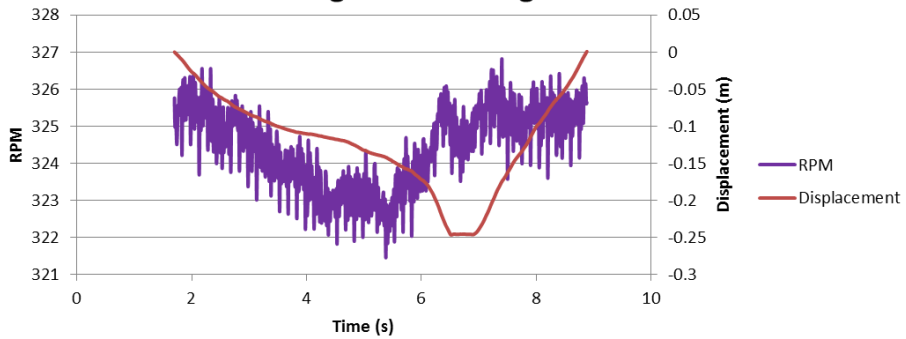
SAMPLE NO. 4 - Right - Attending: 12mm



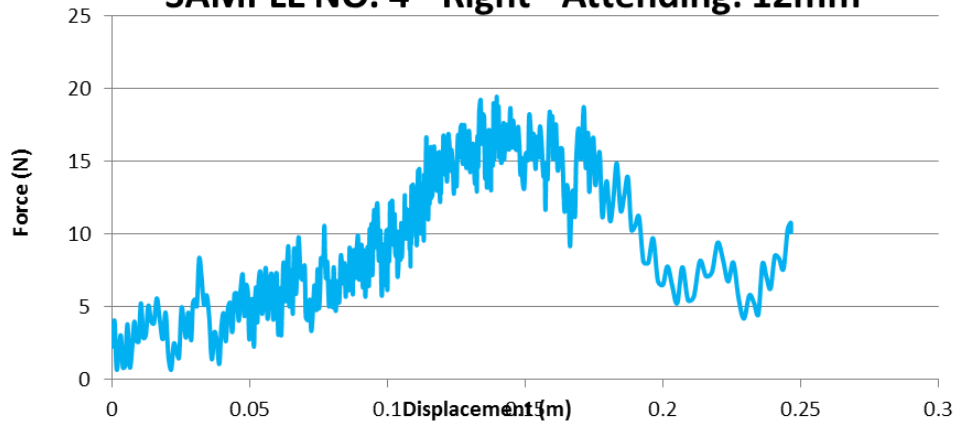
SAMPLE NO. 4 - Right - Attending: 12mm



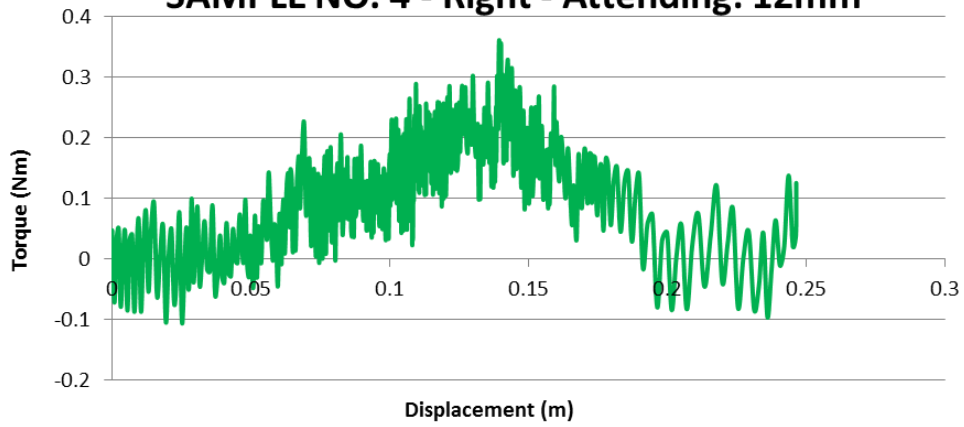
SAMPLE NO. 4 - Right - Attending: 12mm



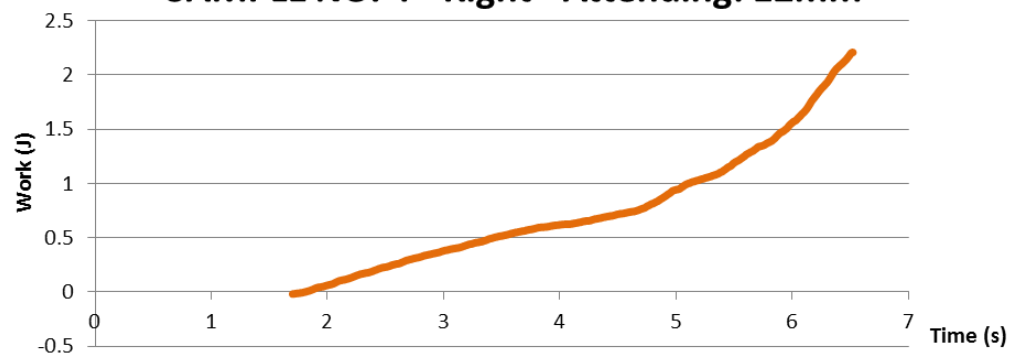
**SAMPLE NO. 4 - Right - Attending: 12mm**



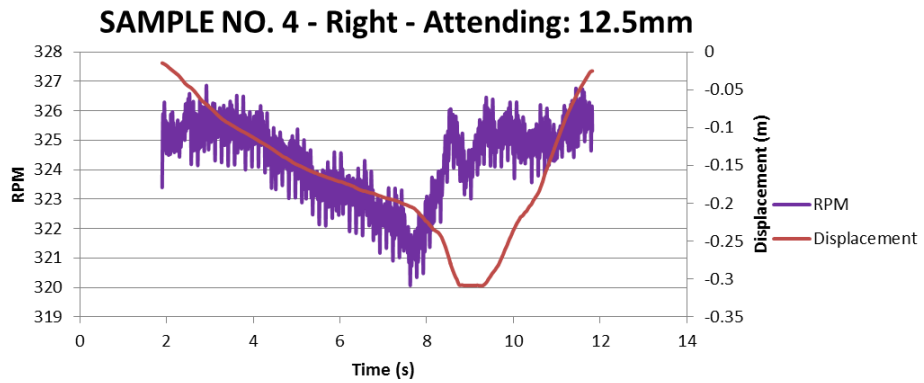
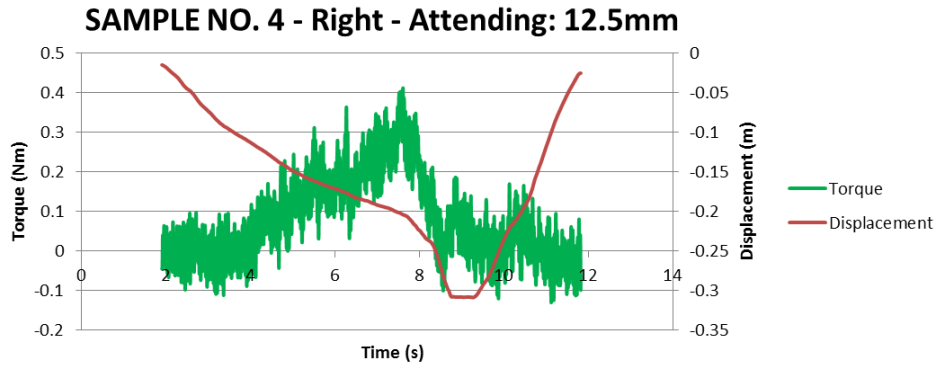
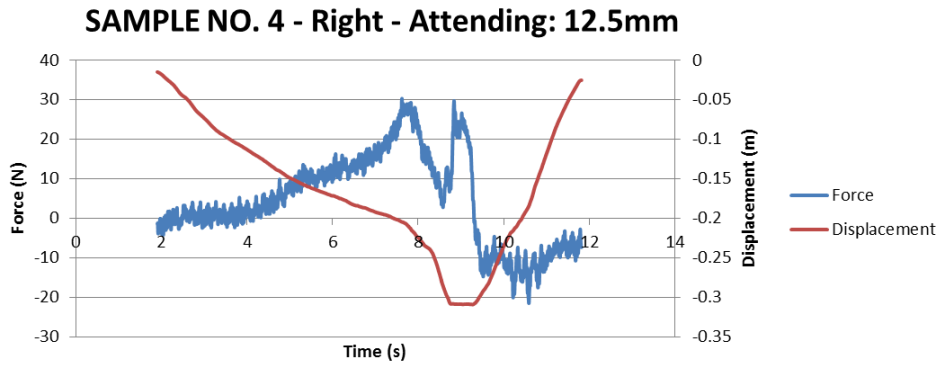
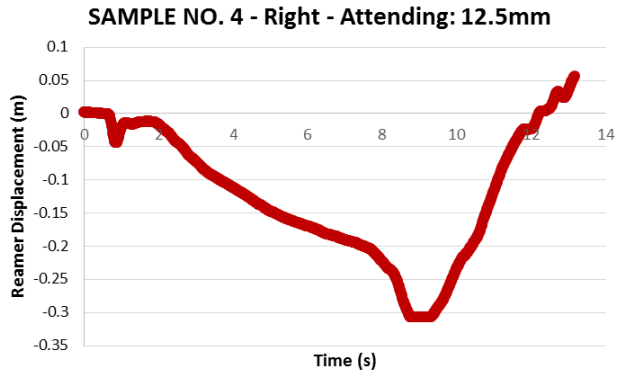
**SAMPLE NO. 4 - Right - Attending: 12mm**



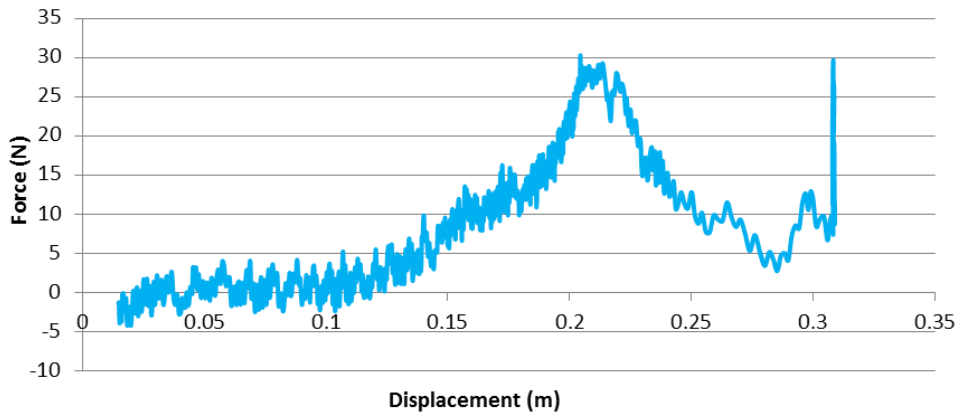
**SAMPLE NO. 4 - Right - Attending: 12mm**



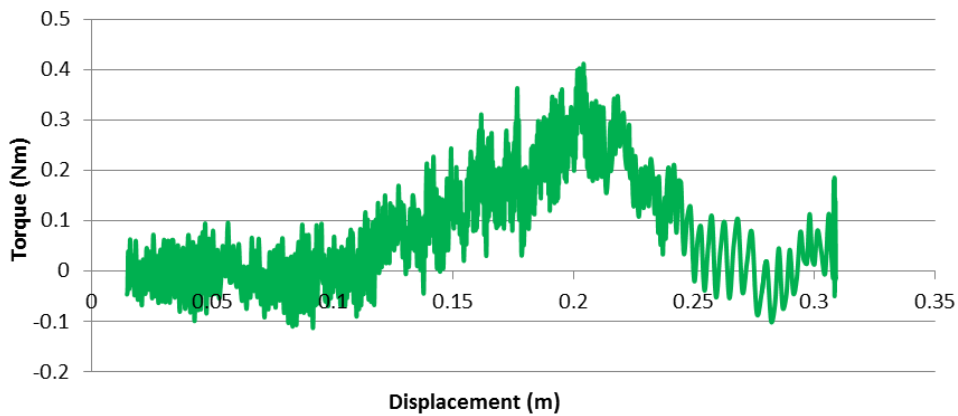
12.5MM



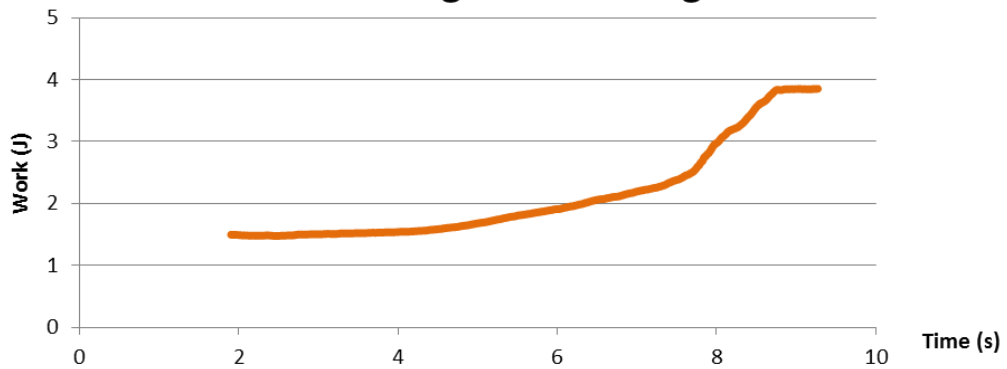
### SAMPLE NO. 4 - Right - Attending: 12.5mm



### SAMPLE NO. 4 - Right - Attending: 12.5mm

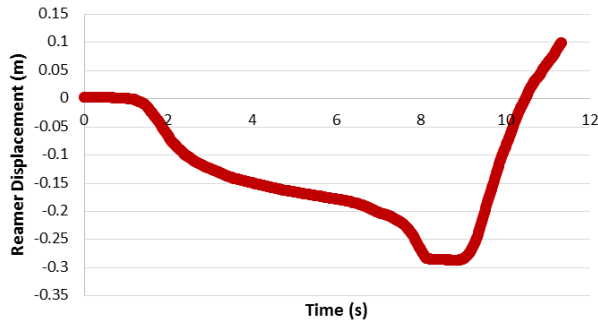


### SAMPLE NO. 4 - Right - Attending: 12.5mm

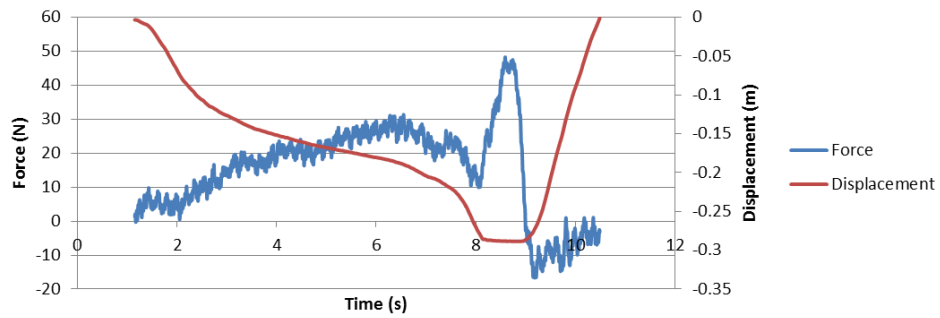


13MM

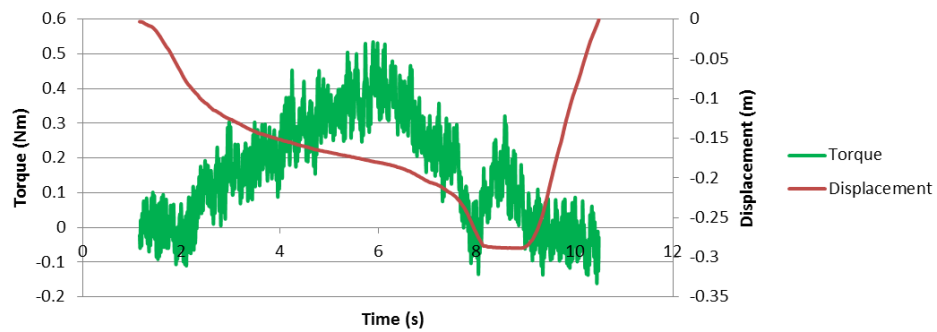
SAMPLE NO. 4 - Right - Attending: 13mm



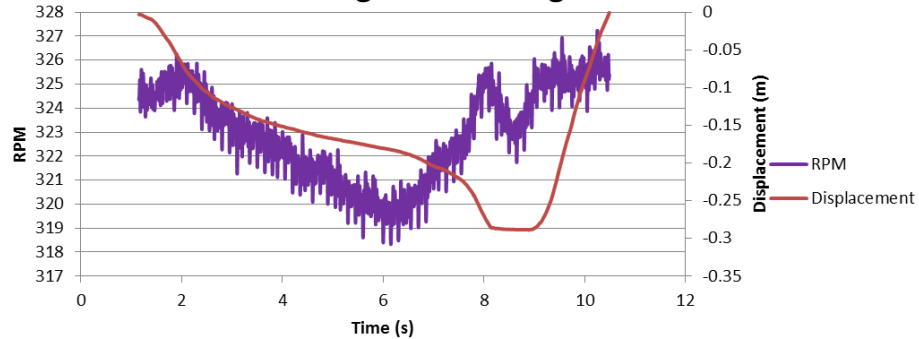
SAMPLE NO. 4 - Right - Attending: 13mm



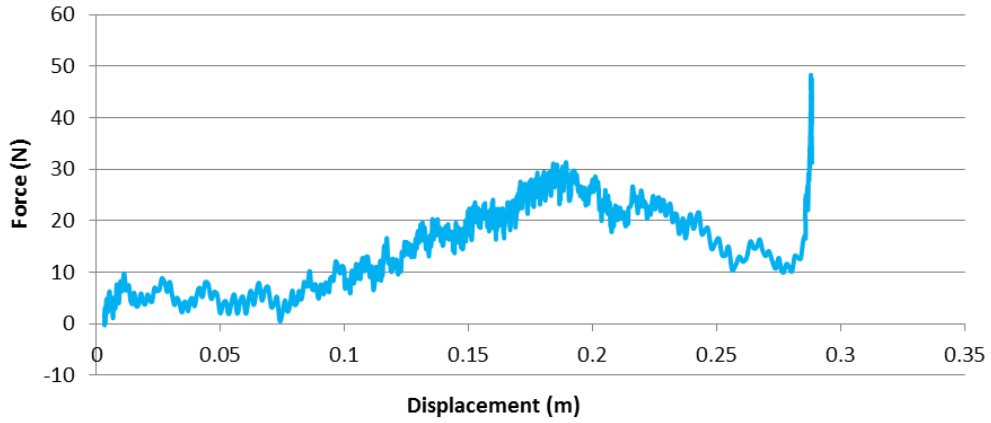
SAMPLE NO. 4 - Right - Attending: 13mm



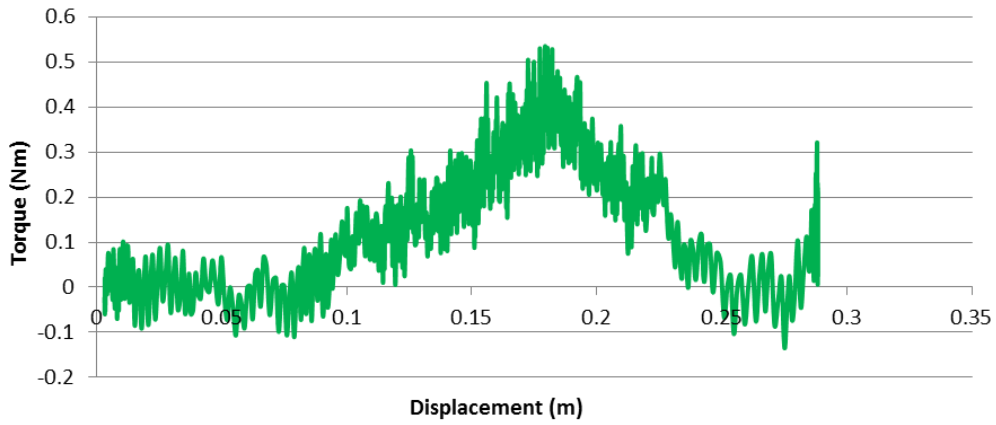
SAMPLE NO. 4 - Right - Attending: 13mm



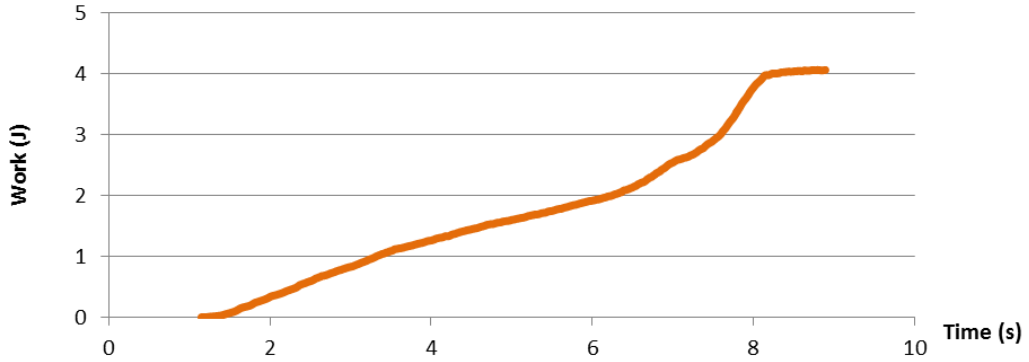
**SAMPLE NO. 4 - Right - Attending: 13mm**



**SAMPLE NO. 4 - Right - Attending: 13mm**



**SAMPLE NO. 4 - Right - Attending: 13mm**

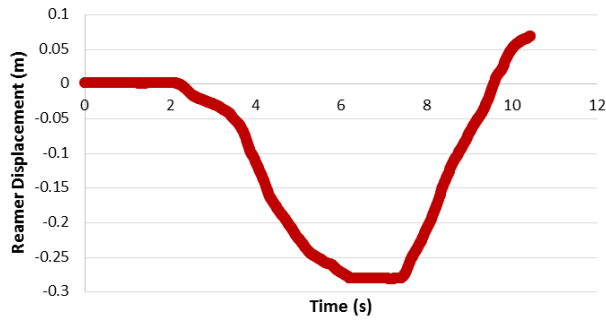


# 13.5 SAMPLE 5 RESULTS

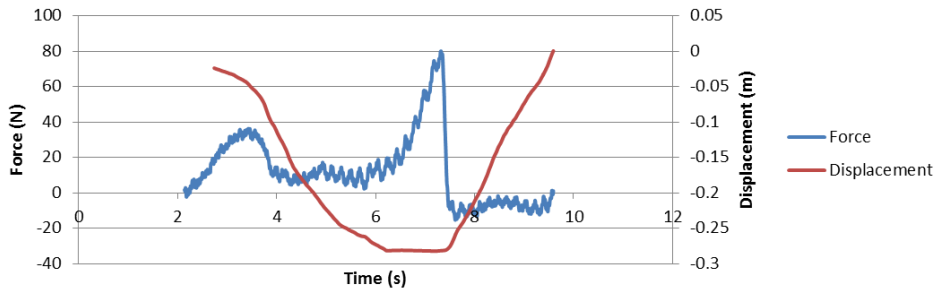
LEFT: RESIDENT

9MM

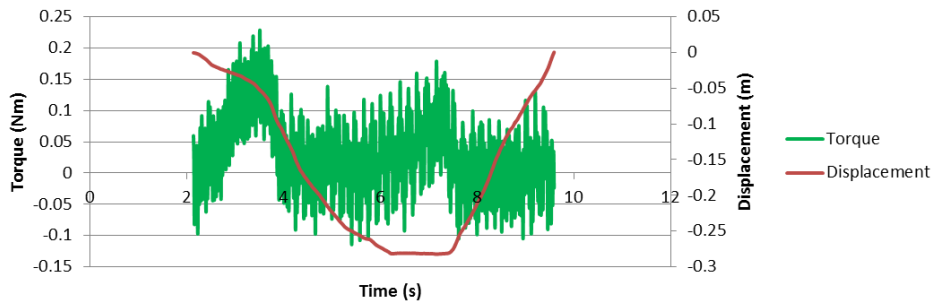
### SAMPLE NO. 5 - Left - Resident: 9mm



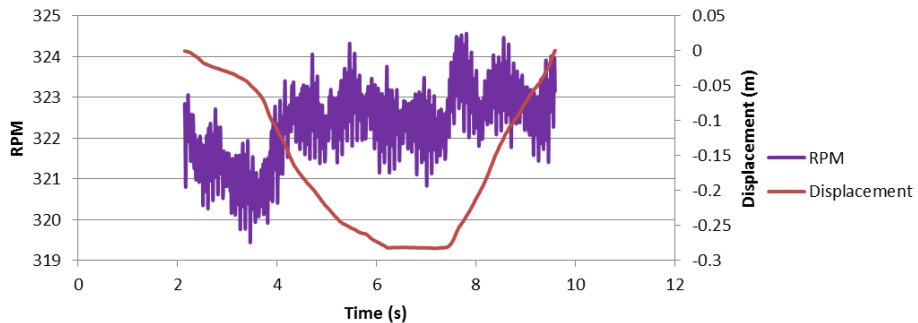
### SAMPLE NO. 5 - Left - Resident: 9mm



### SAMPLE NO. 5 - Left - Resident: 9mm

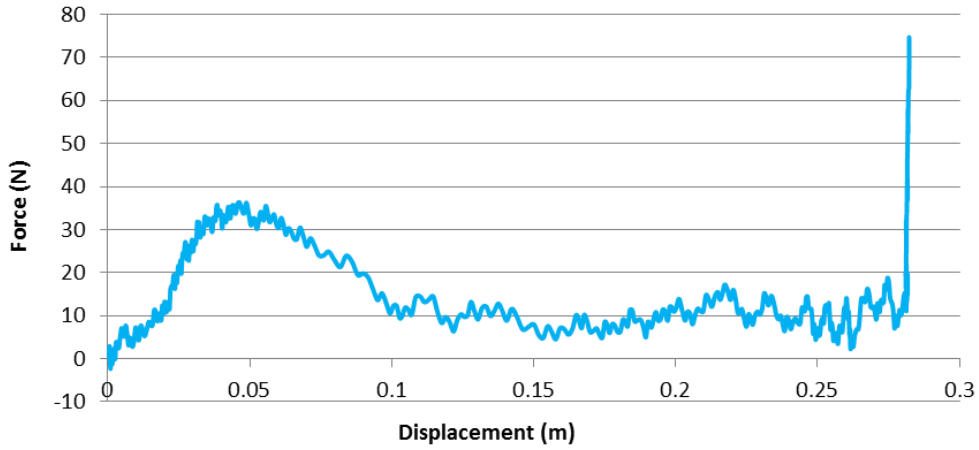


### SAMPLE NO. 5 - Left - Resident: 9mm

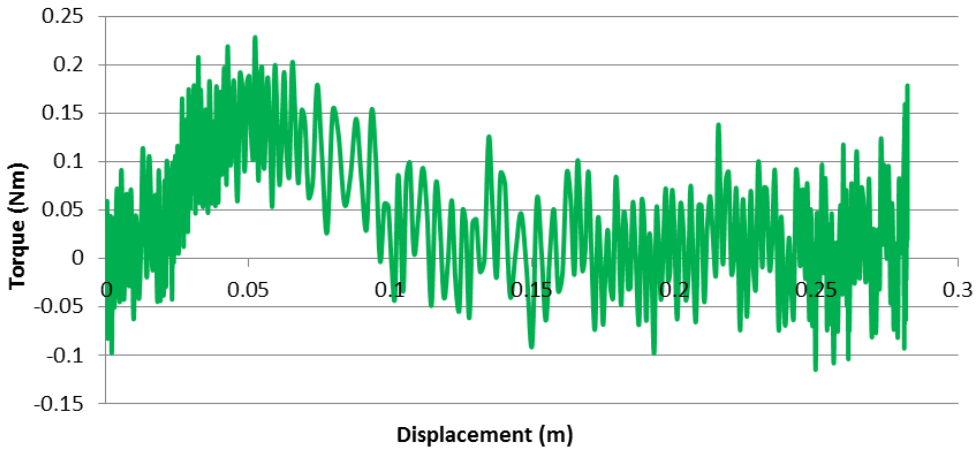




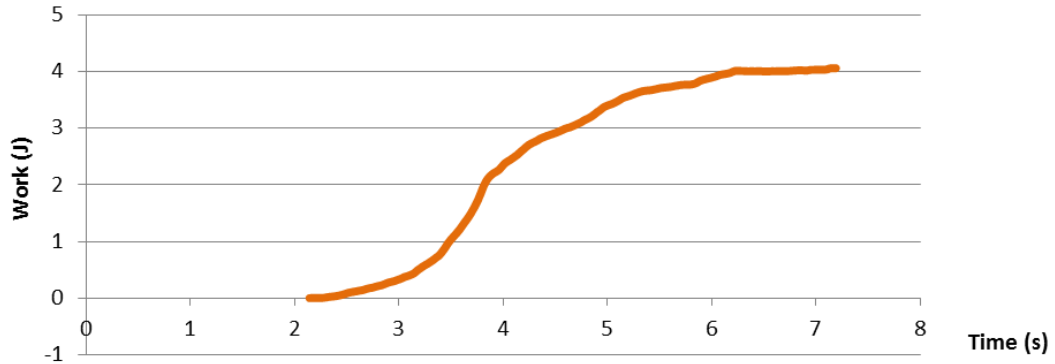
**SAMPLE NO. 5 - Left - Resident: 9mm**



**SAMPLE NO. 5 - Left - Resident: 9mm**

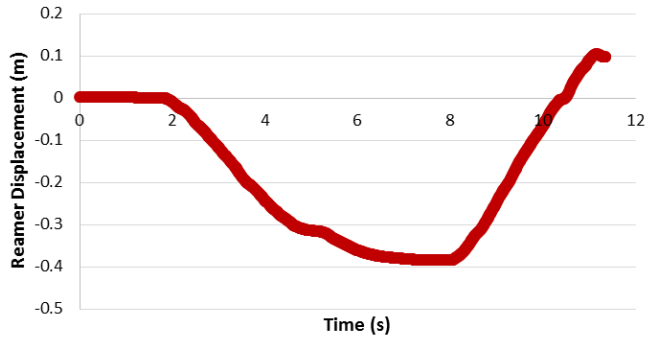


**SAMPLE NO. 5 - Left - Resident: 9mm**

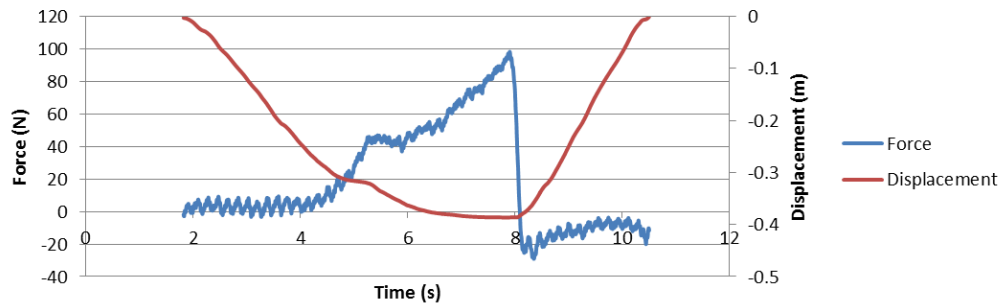


9.5MM

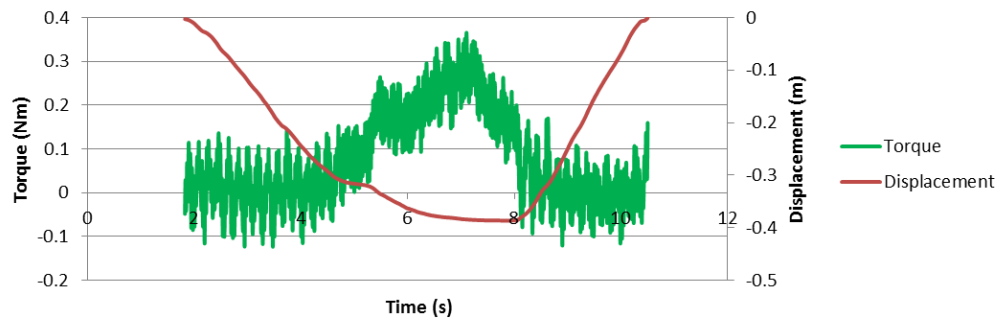
**SAMPLE NO. 5 - Left - Resident: 9.5mm**



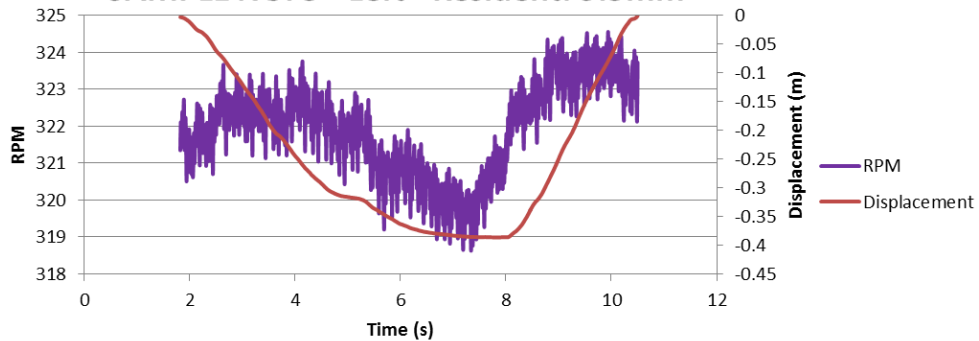
**SAMPLE NO. 5 - Left - Resident: 9.5mm**



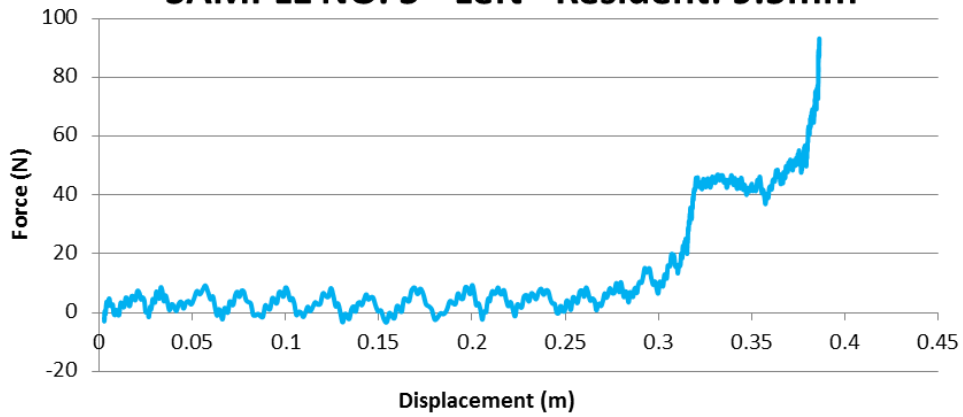
**SAMPLE NO. 5 - Left - Resident: 9.5mm**



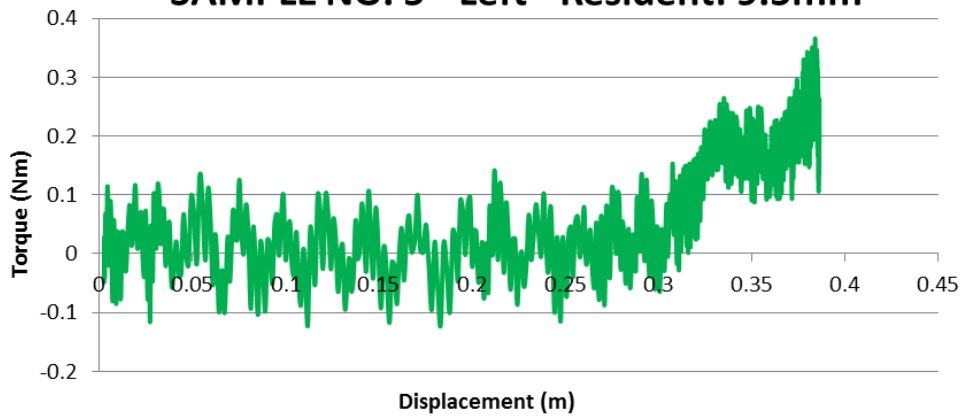
**SAMPLE NO. 5 - Left - Resident: 9.5mm**



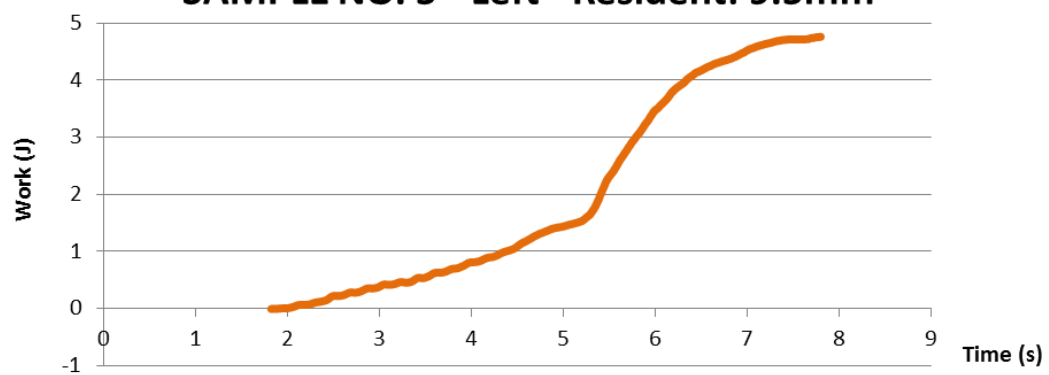
**SAMPLE NO. 5 - Left - Resident: 9.5mm**



**SAMPLE NO. 5 - Left - Resident: 9.5mm**

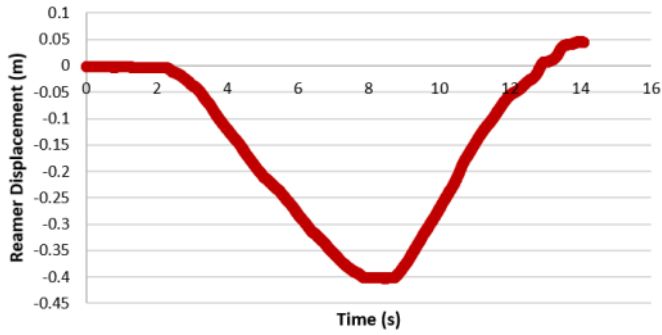


**SAMPLE NO. 5 - Left - Resident: 9.5mm**

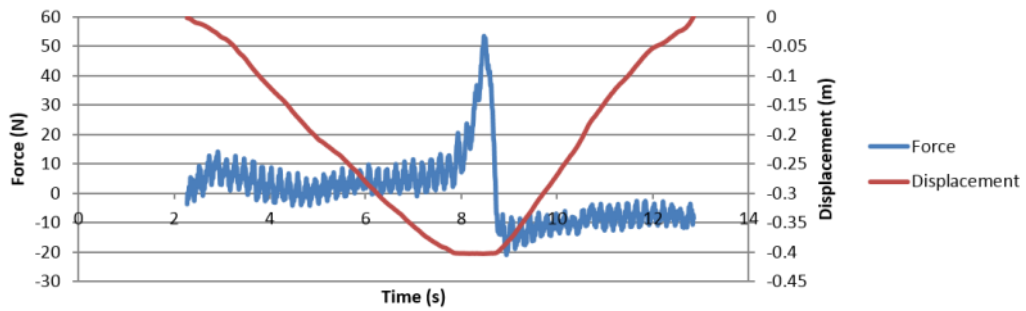


10MM

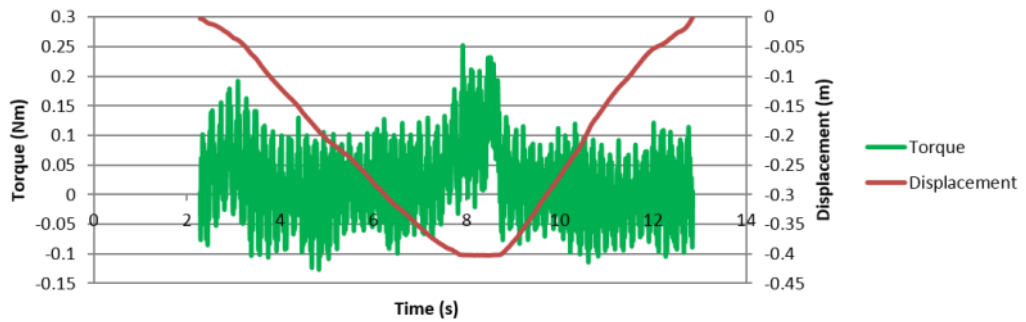
SAMPLE NO. 5 - Left - Resident: 10mm



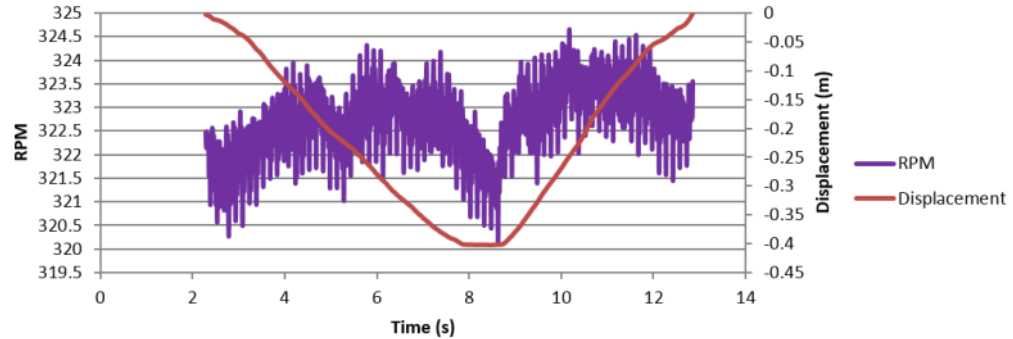
SAMPLE NO. 5 - Left - Resident: 10mm



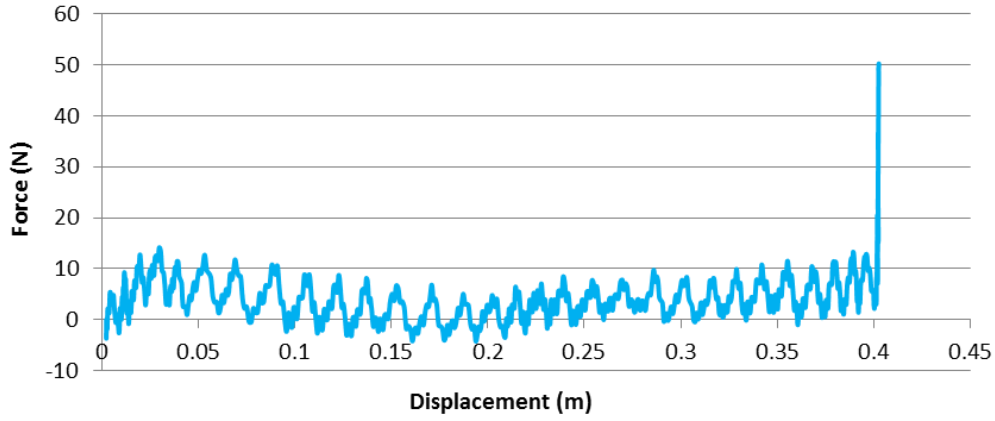
SAMPLE NO. 5 - Left - Resident: 10mm



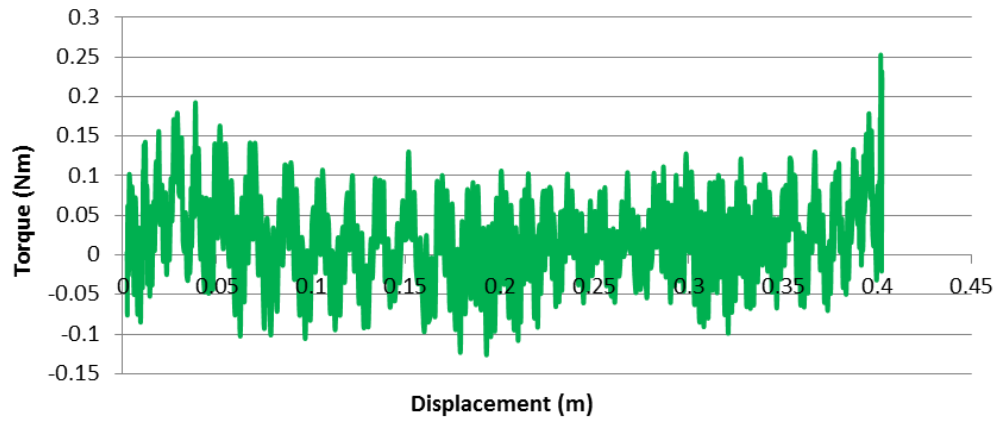
SAMPLE NO. 5 - Left - Resident: 10mm



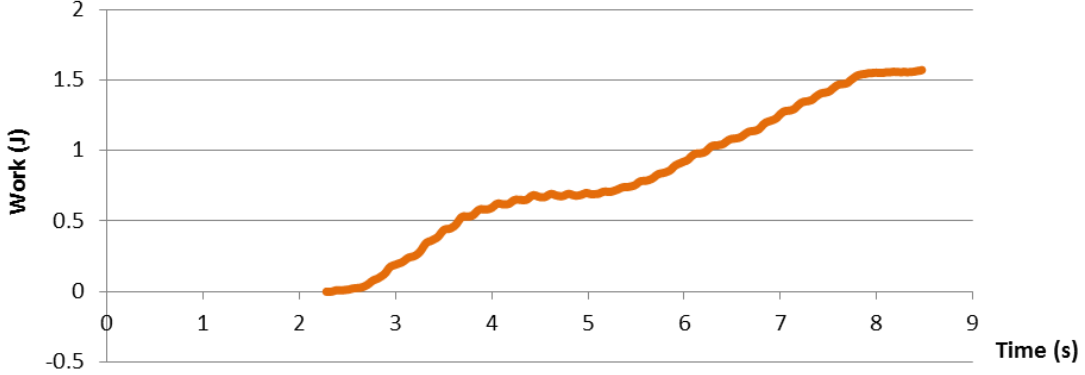
**SAMPLE NO. 5 - Left - Resident: 10mm**



**SAMPLE NO. 5 - Left - Resident: 10mm**

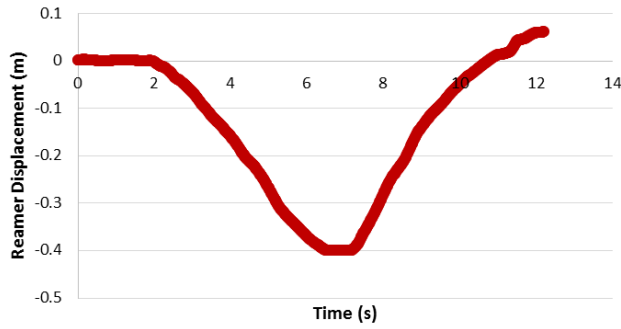


**SAMPLE NO. 5 - Left - Resident: 10mm**

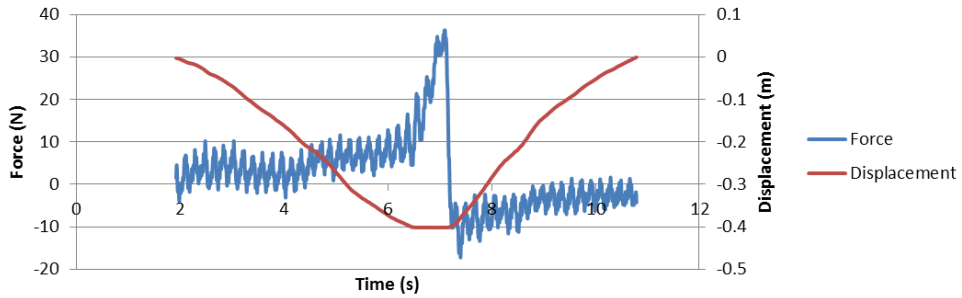


10.5MM

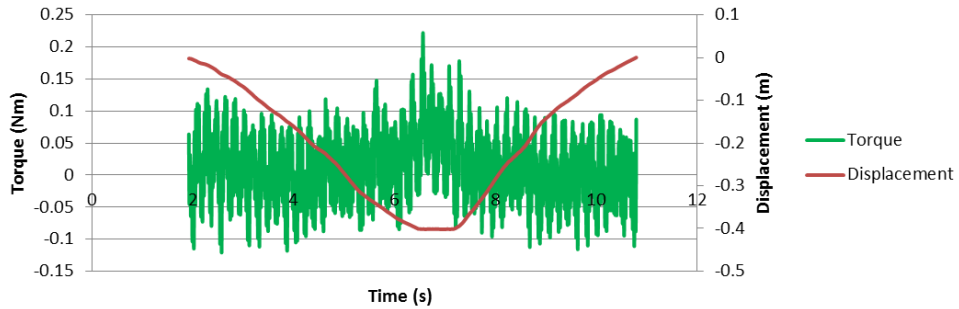
**SAMPLE NO. 5 - Left - Resident: 10.5mm**



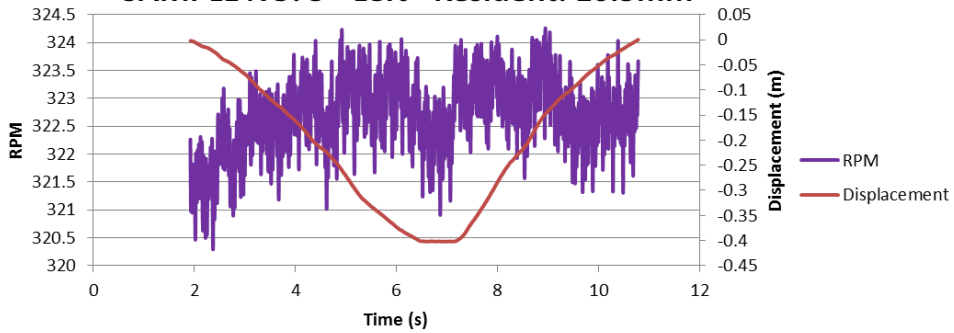
**SAMPLE NO. 5 - Left - Resident: 10.5mm**



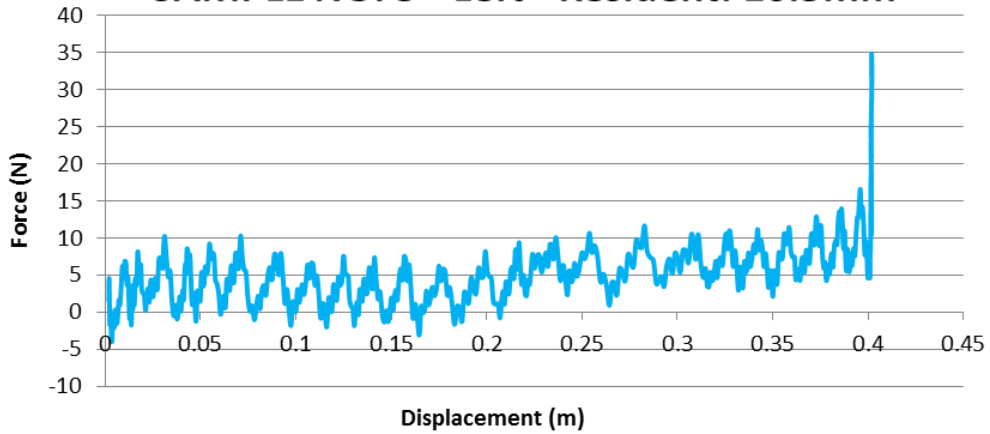
**SAMPLE NO. 5 - Left - Resident: 10.5mm**



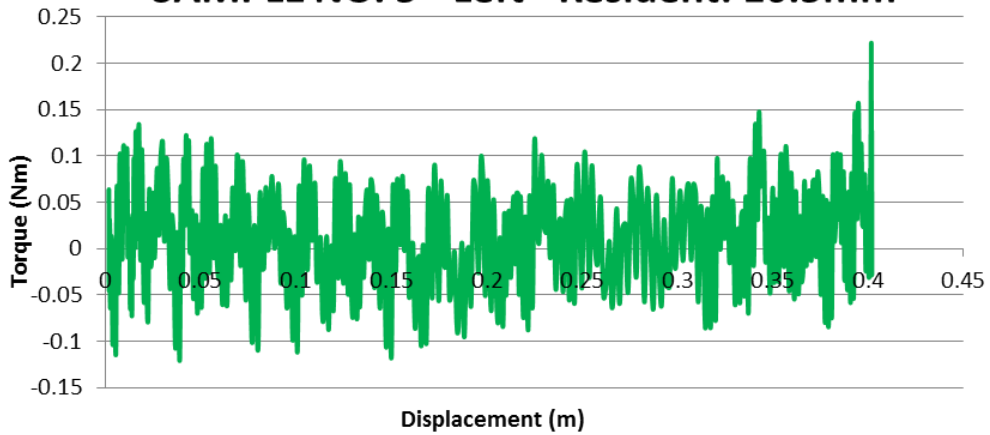
**SAMPLE NO. 5 - Left - Resident: 10.5mm**



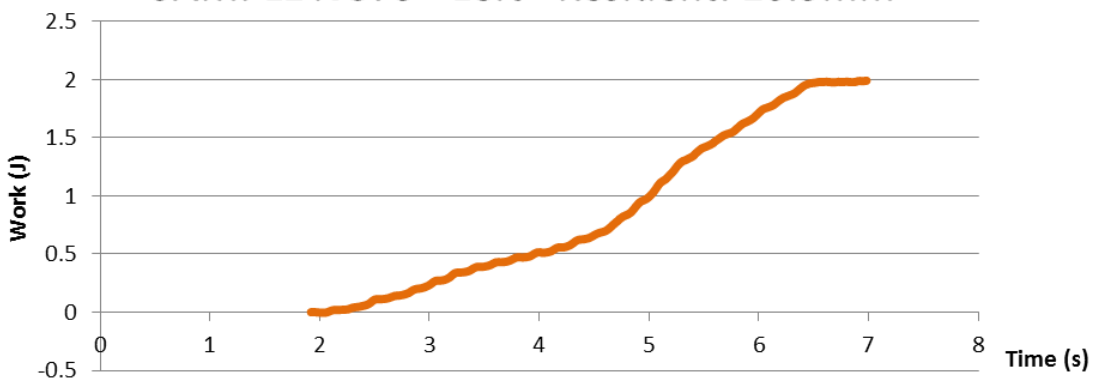
**SAMPLE NO. 5 - Left - Resident: 10.5mm**



**SAMPLE NO. 5 - Left - Resident: 10.5mm**

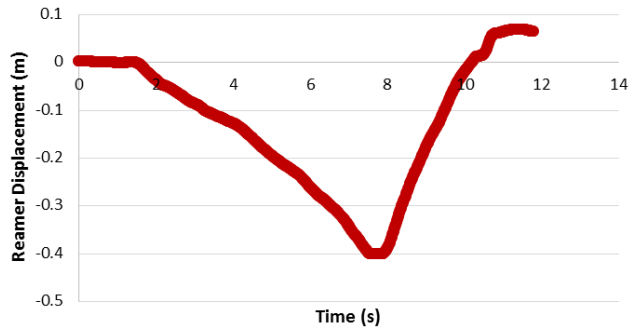


**SAMPLE NO. 5 - Left - Resident: 10.5mm**

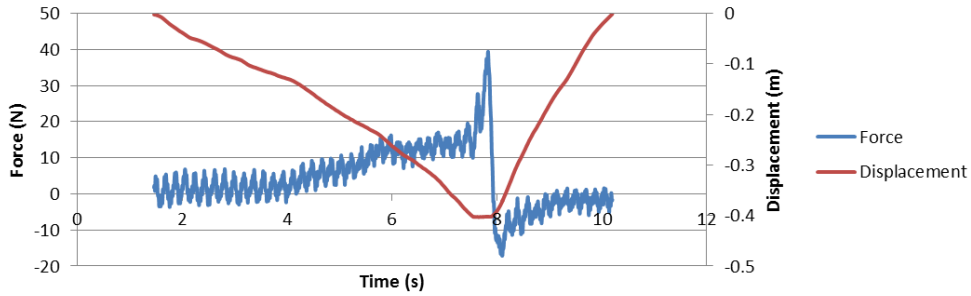


11MM

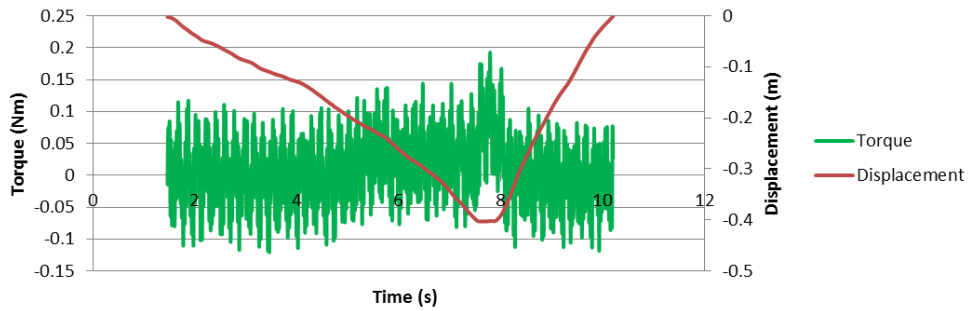
**SAMPLE NO. 5 - Left - Resident: 11mm**



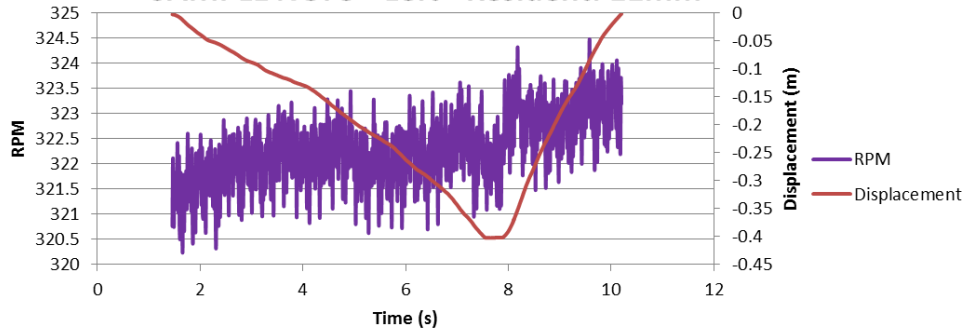
**SAMPLE NO. 5 - Left - Resident: 11mm**



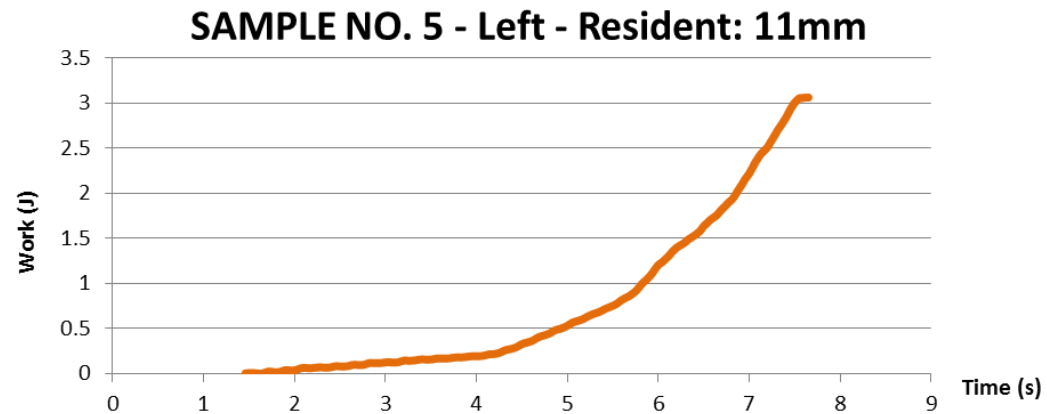
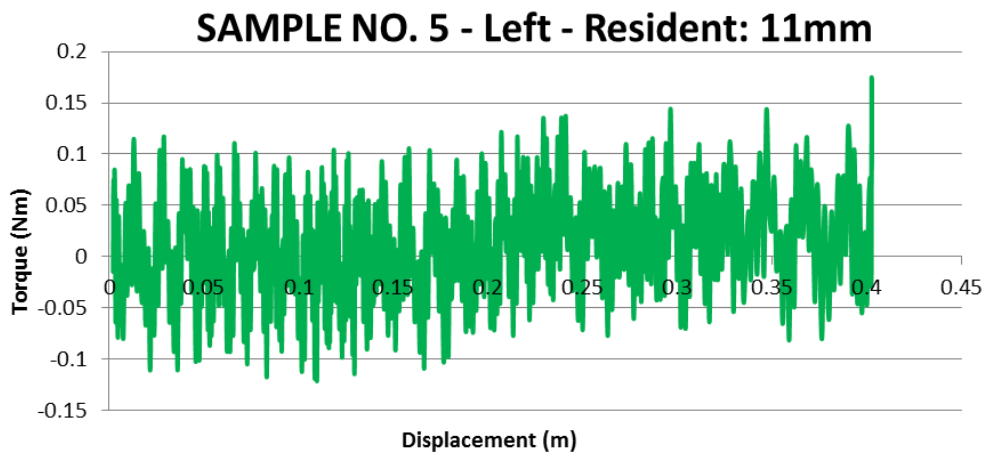
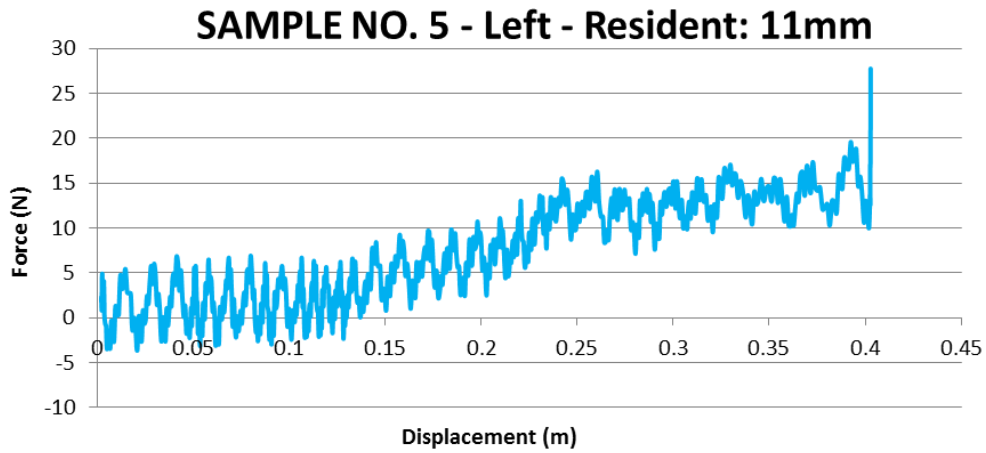
**SAMPLE NO. 5 - Left - Resident: 11mm**



**SAMPLE NO. 5 - Left - Resident: 11mm**

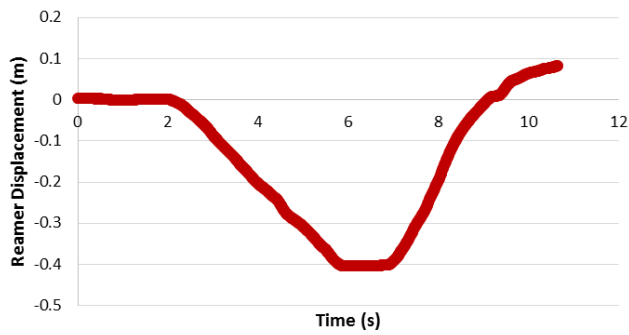




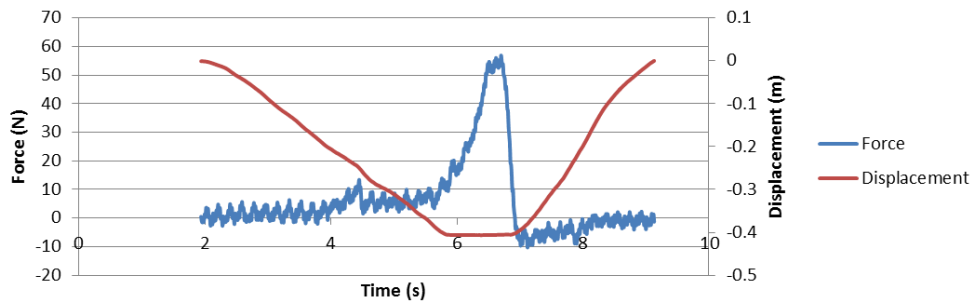


11.5MM

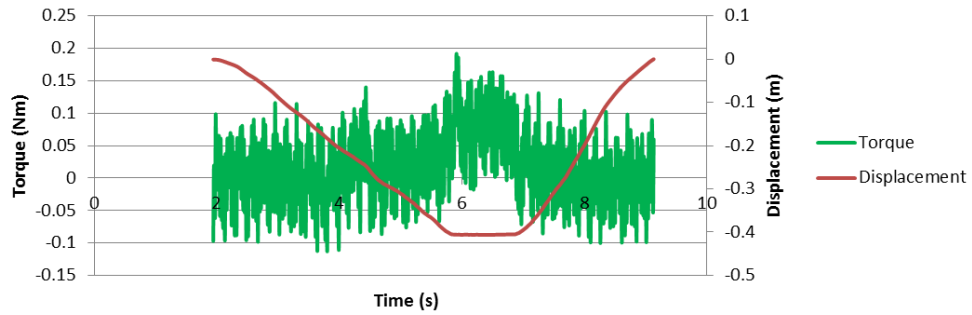
SAMPLE NO. 5 - Left - Resident: 11.5mm



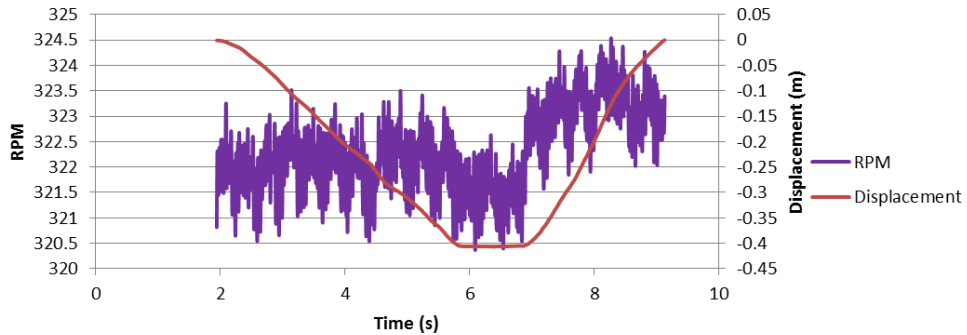
SAMPLE NO. 5 - Left - Resident: 11.5mm



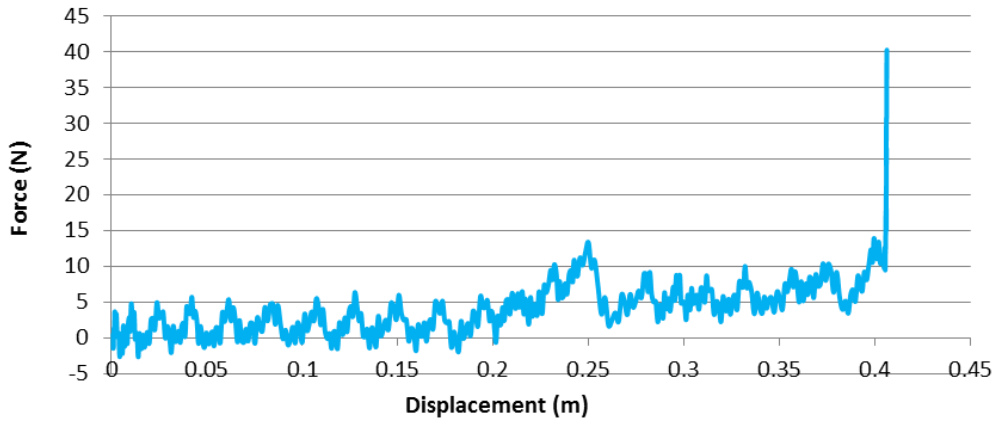
SAMPLE NO. 5 - Left - Resident: 11.5mm



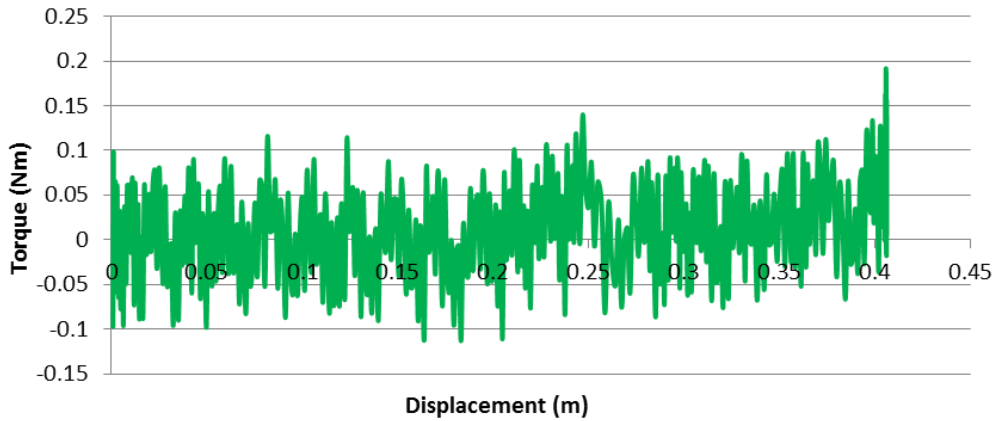
SAMPLE NO. 5 - Left - Resident: 11.5mm



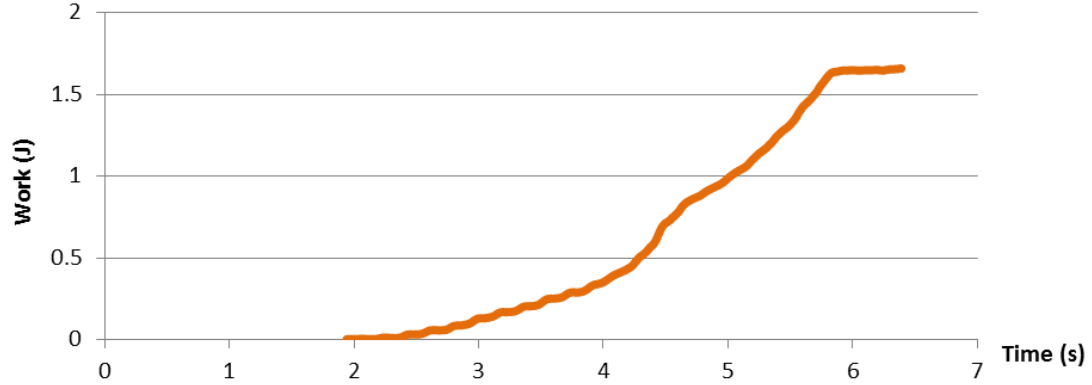
**SAMPLE NO. 5 - Left - Resident: 11.5mm**



**SAMPLE NO. 5 - Left - Resident: 11.5mm**

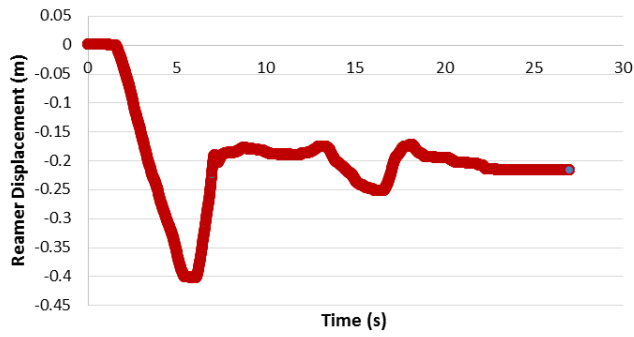


**SAMPLE NO. 5 - Left - Resident: 11.5mm**

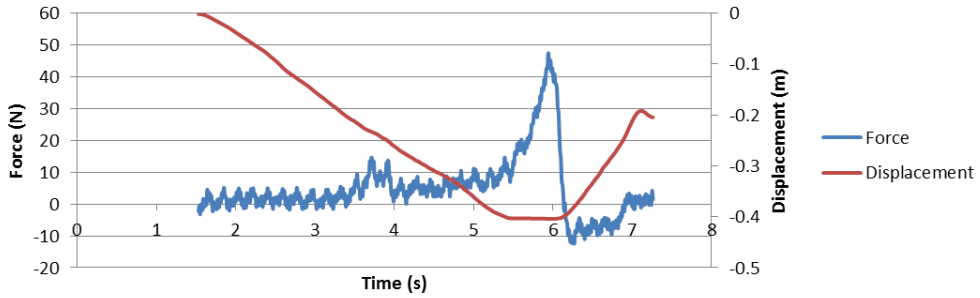


12MM

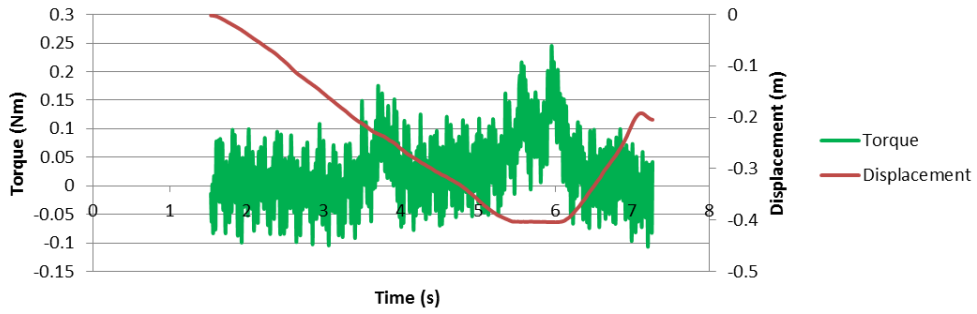
SAMPLE NO. 5 - Left - Resident: 12mm



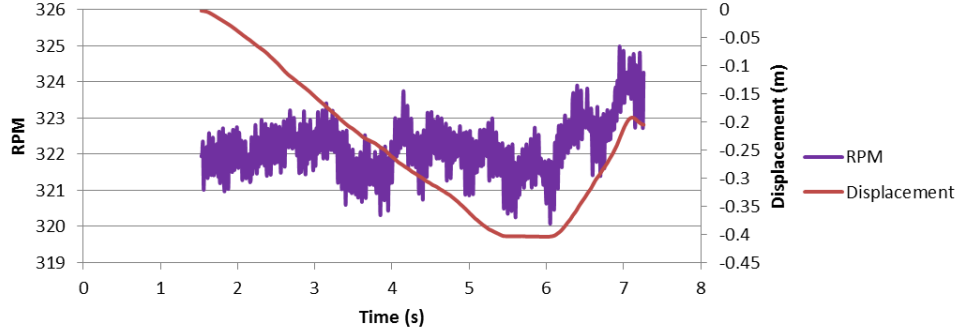
SAMPLE NO. 5 - Left - Resident: 12mm



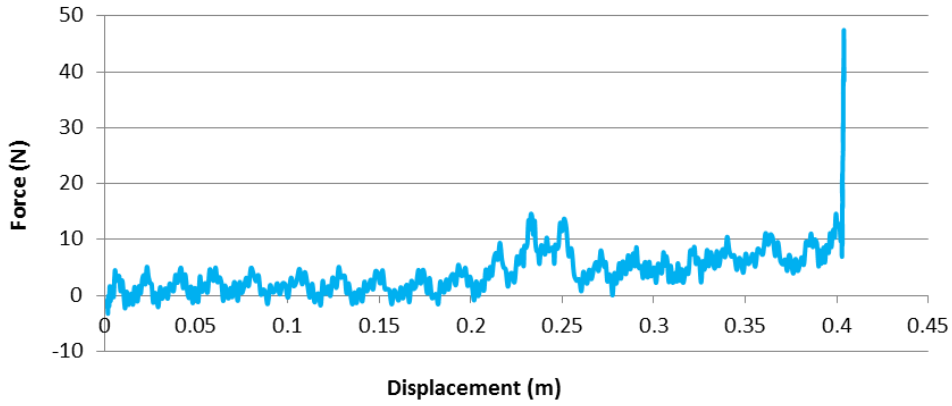
SAMPLE NO. 5 - Left - Resident: 12mm



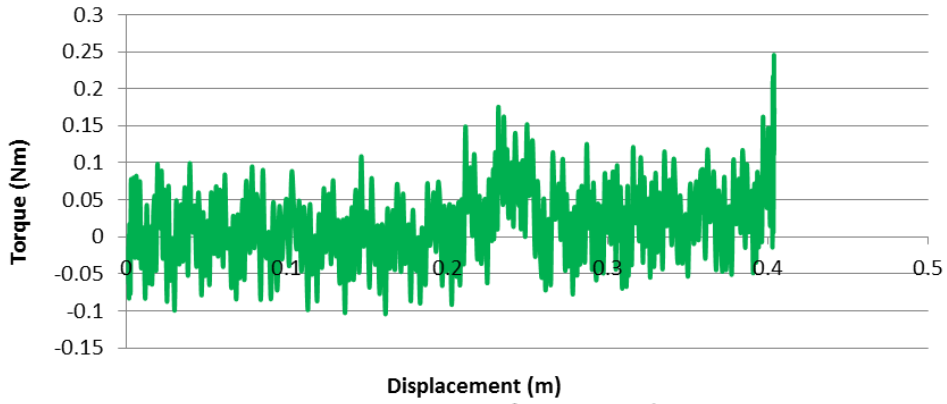
SAMPLE NO. 5 - Left - Resident: 12mm



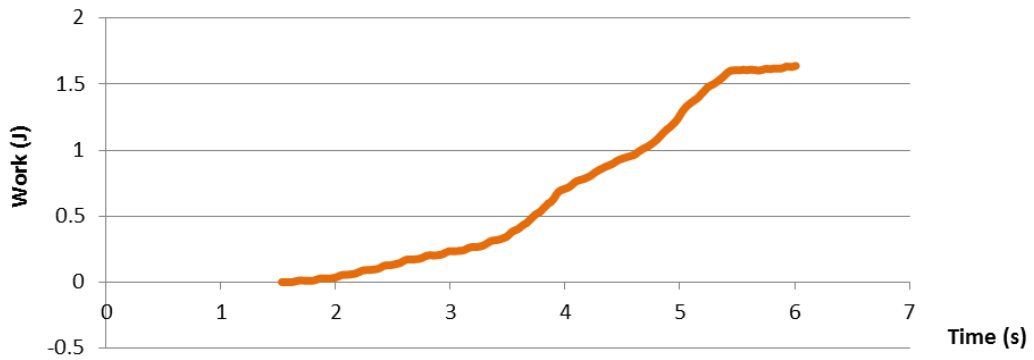
**SAMPLE NO. 5 - Left - Resident: 12mm**



**SAMPLE NO. 5 - Left - Resident: 12mm**

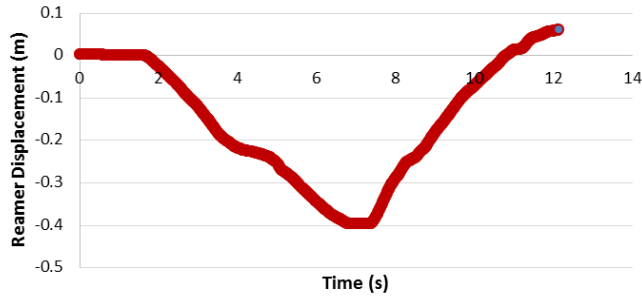


**SAMPLE NO. 5 - Left - Resident: 12mm**

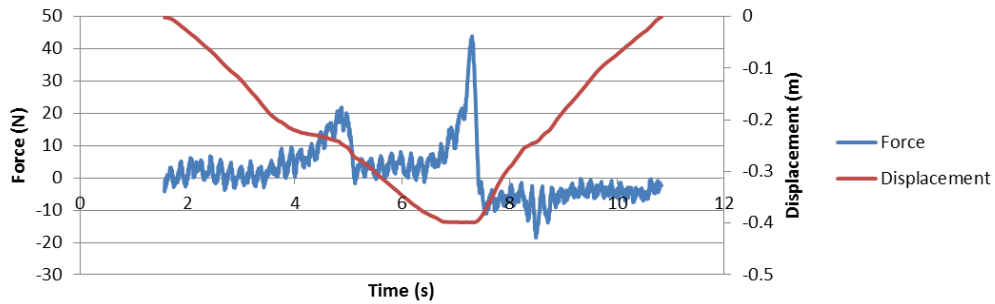


12.5MM

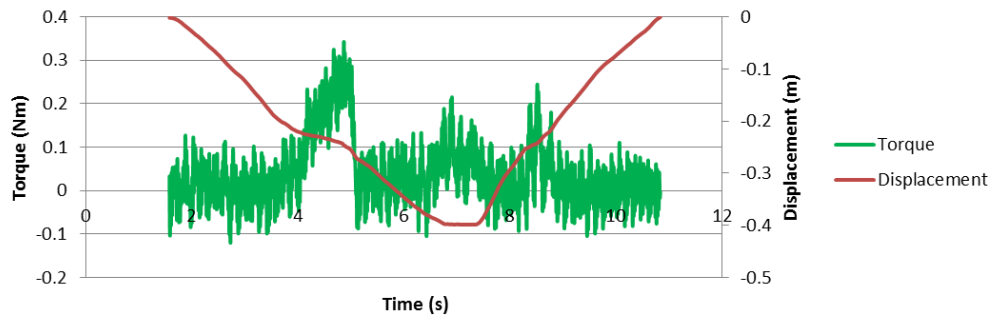
**SAMPLE NO. 5 - Left - Resident: 12.5mm  
CHATTER**



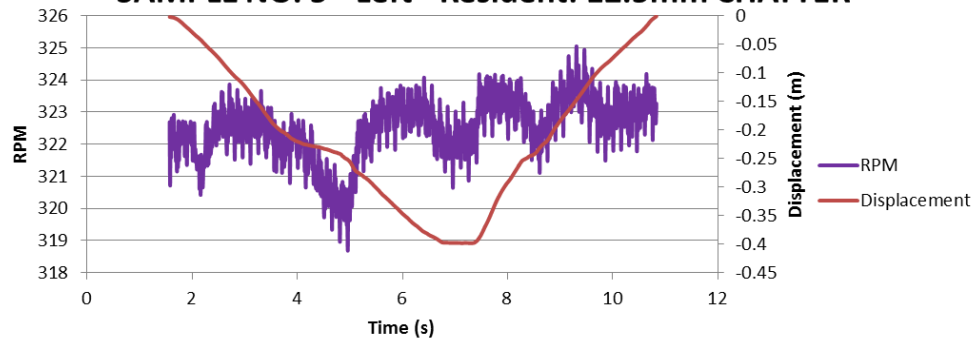
**SAMPLE NO. 5 - Left - Resident: 12.5mm CHATTER**



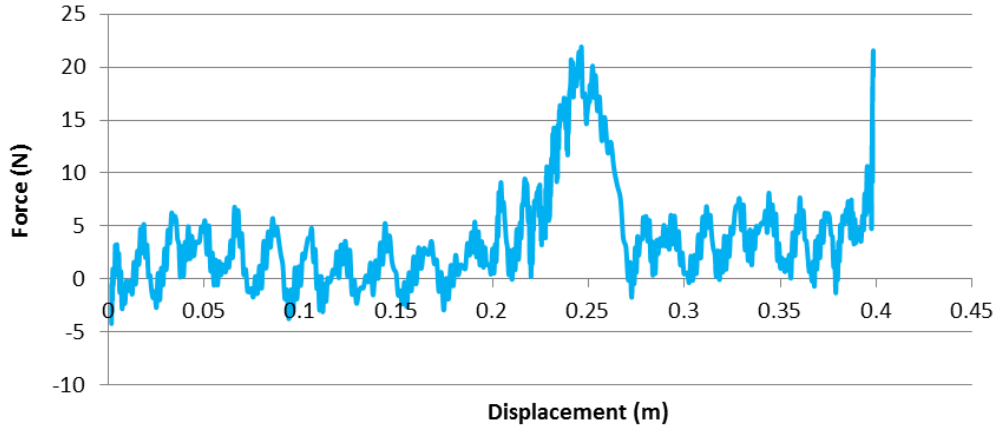
**SAMPLE NO. 5 - Left - Resident: 12.5mm CHATTER**



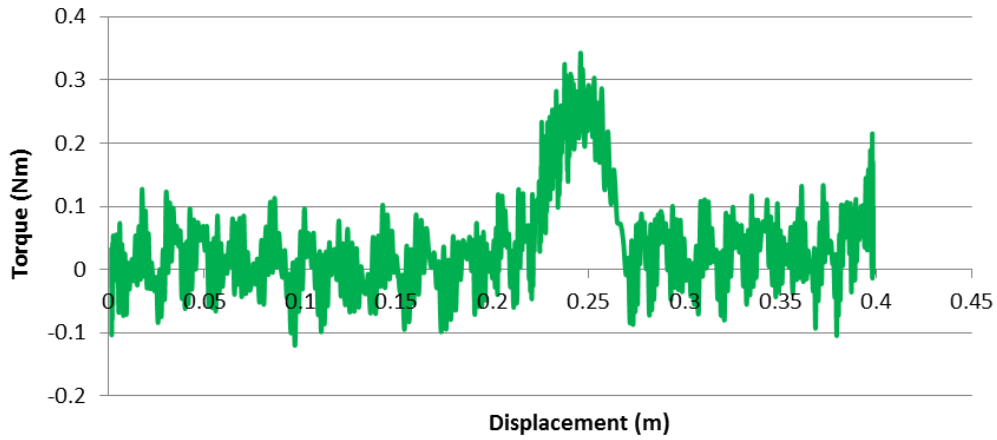
**SAMPLE NO. 5 - Left - Resident: 12.5mm CHATTER**



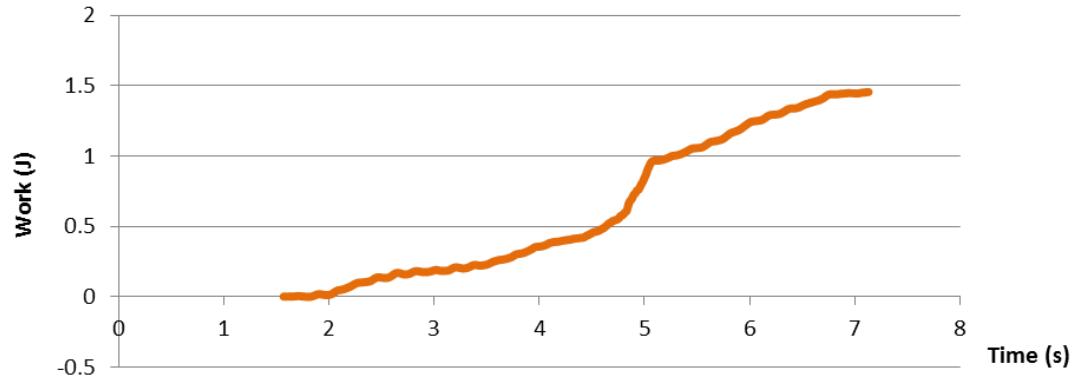
**SAMPLE NO. 5 - Left - Resident: 12.5mm CHATTER**



**SAMPLE NO. 5 - Left - Resident: 12.5mm CHATTER**

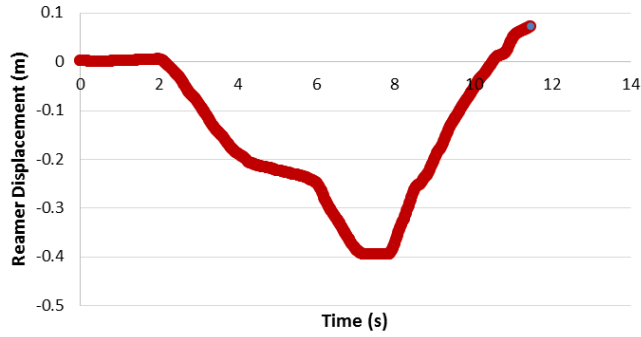


**SAMPLE NO. 5 - Left - Resident: 12.5mm CHATTER**

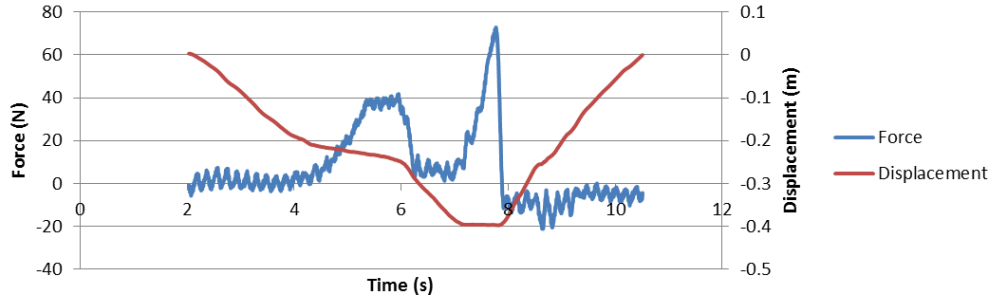


13MM

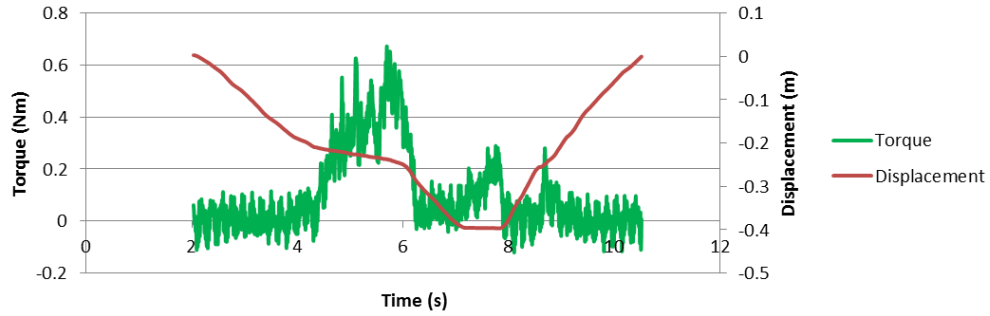
**SAMPLE NO. 5 - Left - Resident: 13mm**



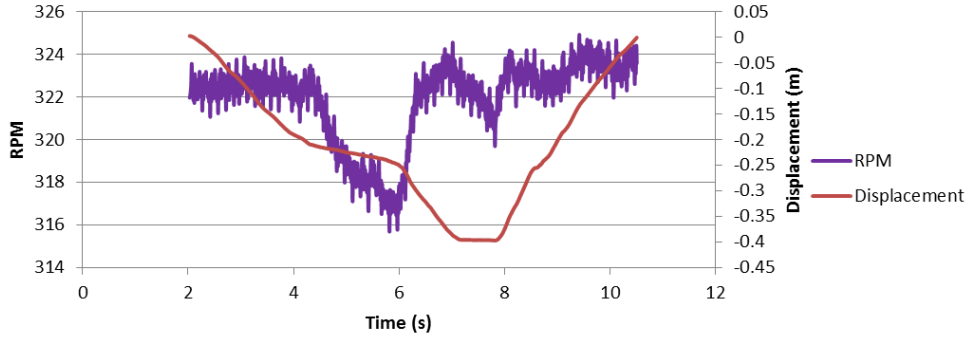
**SAMPLE NO. 5 - Left - Resident: 13mm**



**SAMPLE NO. 5 - Left - Resident: 13mm**

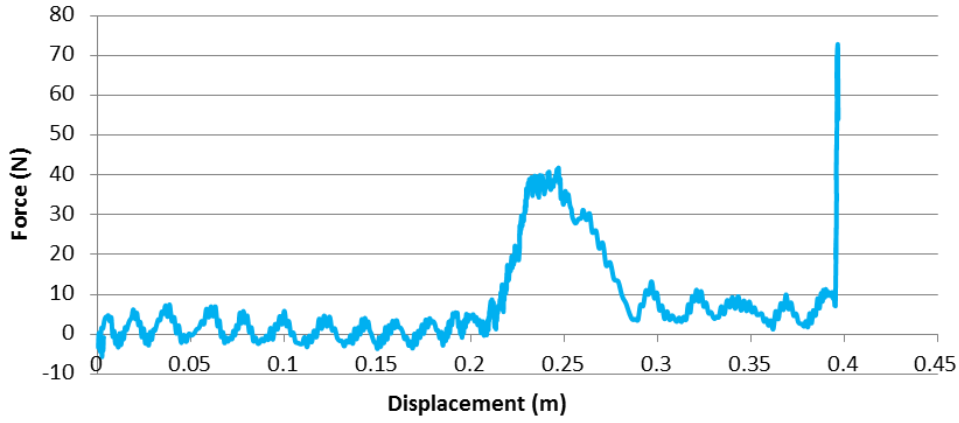


**SAMPLE NO. 5 - Left - Resident: 13mm**

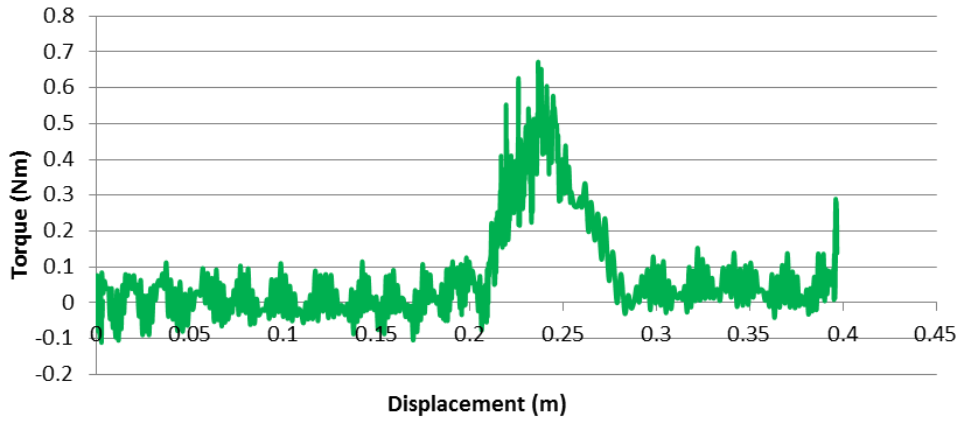




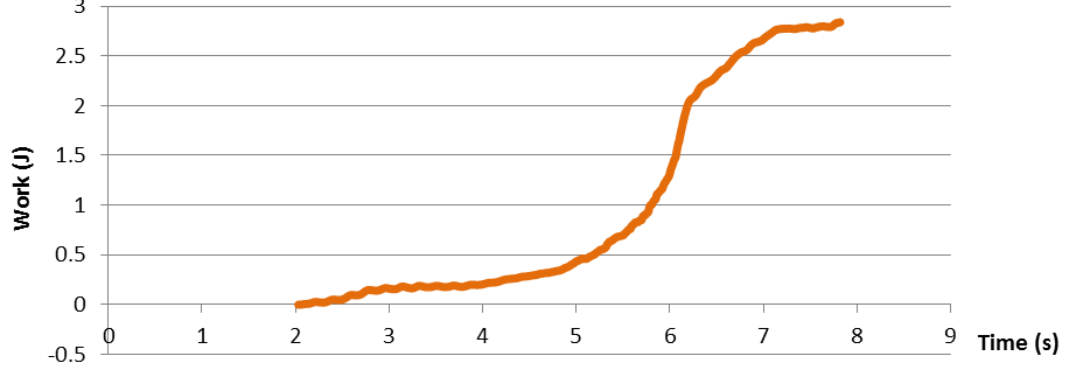
**SAMPLE NO. 5 - Left - Resident: 13mm**



**SAMPLE NO. 5 - Left - Resident: 13mm**

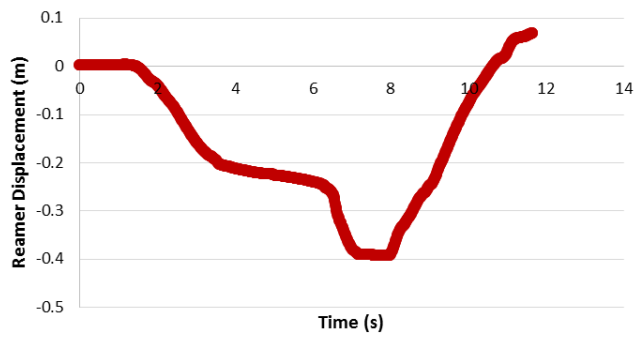


**SAMPLE NO. 5 - Left - Resident: 13mm**

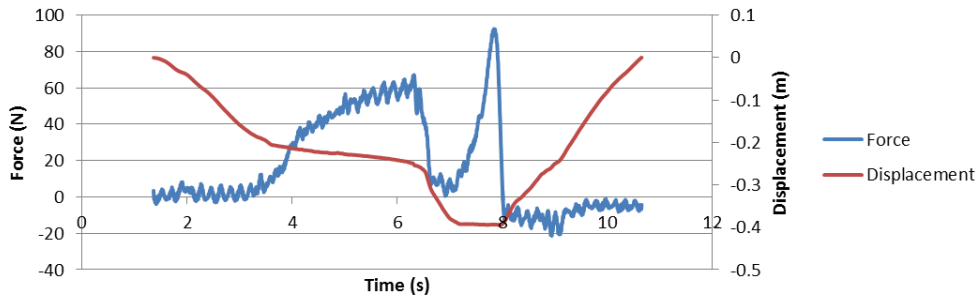


13.5MM

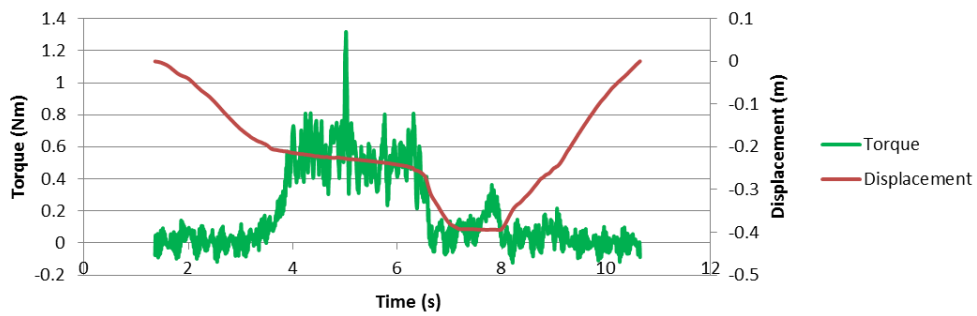
SAMPLE NO. 5 - Left - Resident: 13.5mm



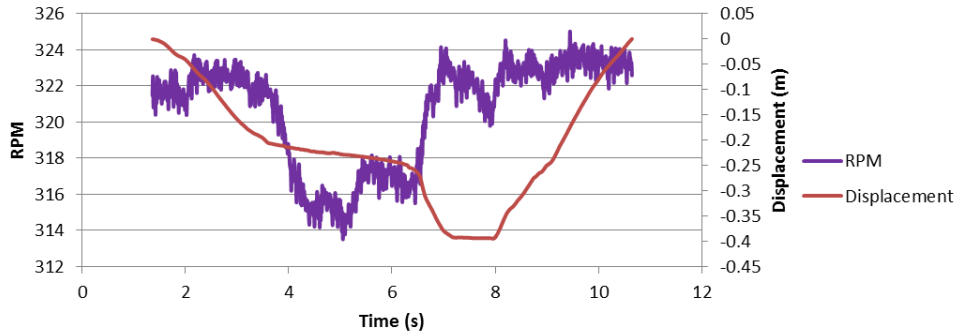
SAMPLE NO. 5 - Left - Resident: 13.5mm



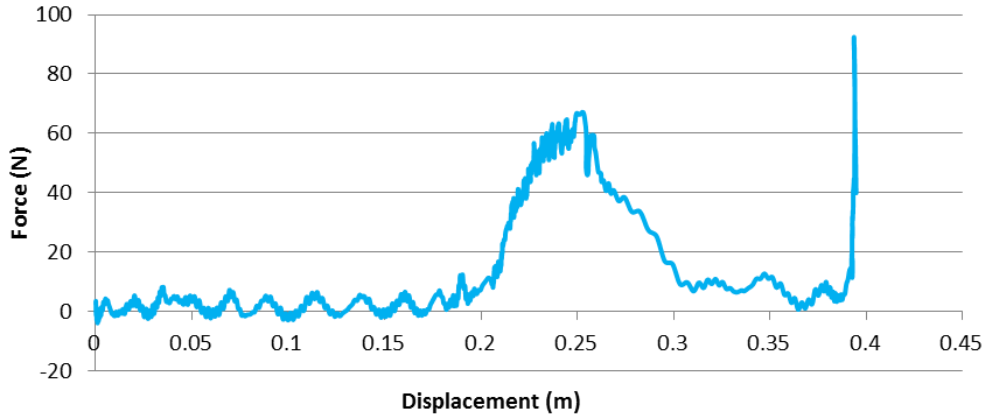
SAMPLE NO. 5 - Left - Resident: 13.5mm



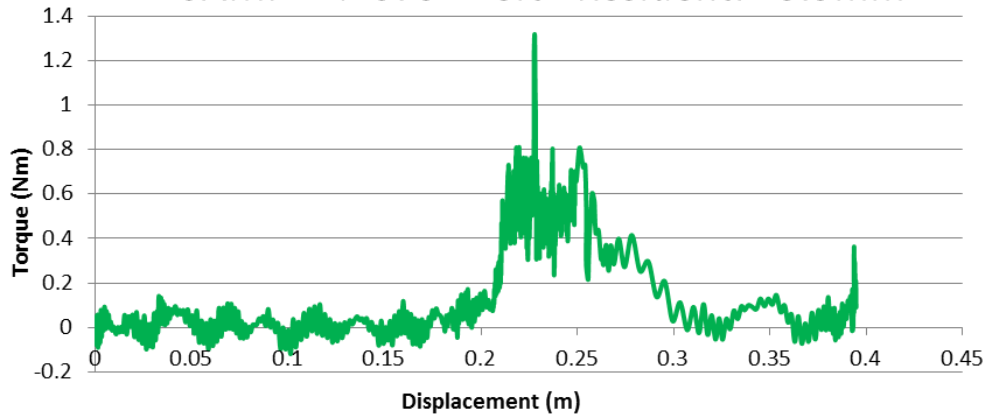
SAMPLE NO. 5 - Left - Resident: 13.5mm



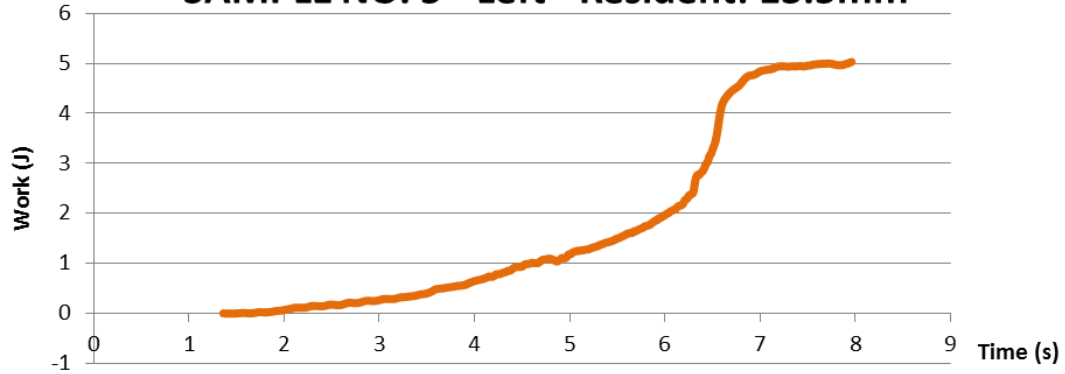
**SAMPLE NO. 5 - Left - Resident: 13.5mm**



**SAMPLE NO. 5 - Left - Resident: 13.5mm**

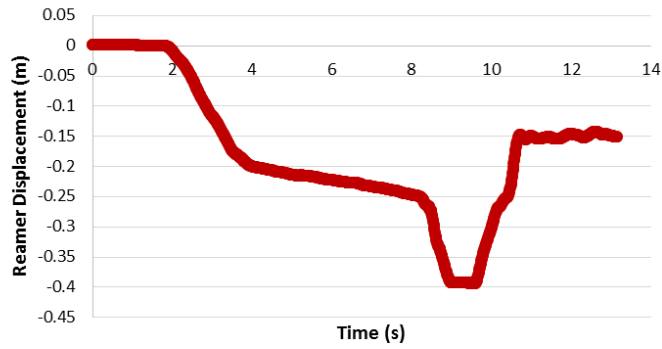


**SAMPLE NO. 5 - Left - Resident: 13.5mm**

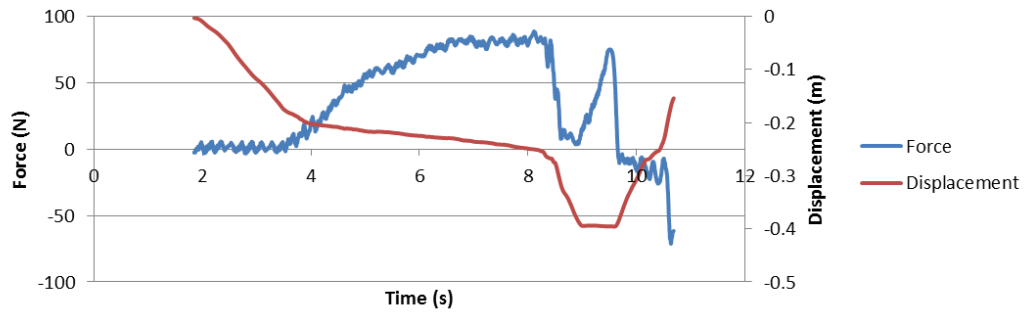


14MM

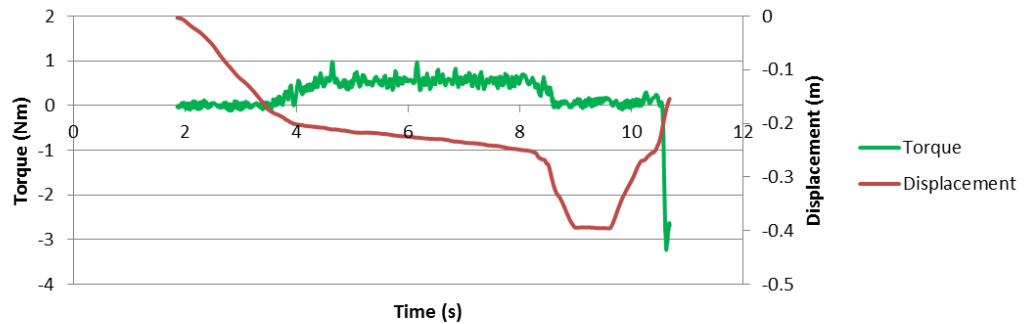
**SAMPLE NO. 5 - Left - Resident: 14mm**



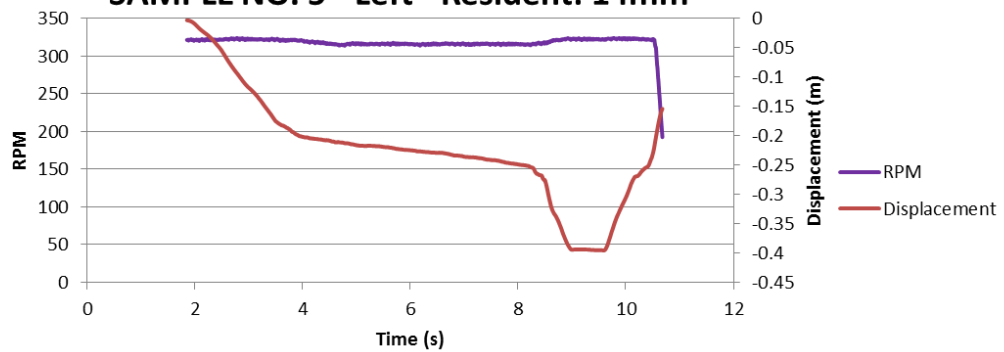
**SAMPLE NO. 5 - Left - Resident: 14mm**



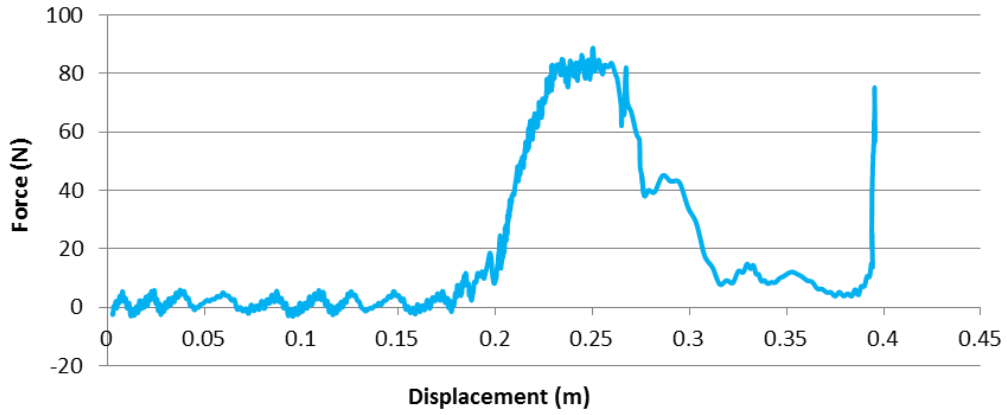
**SAMPLE NO. 5 - Left - Resident: 14mm**



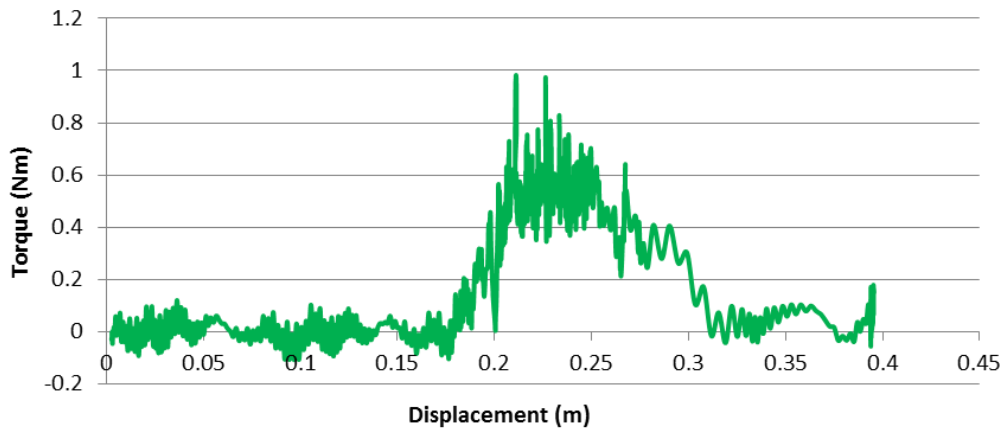
**SAMPLE NO. 5 - Left - Resident: 14mm**



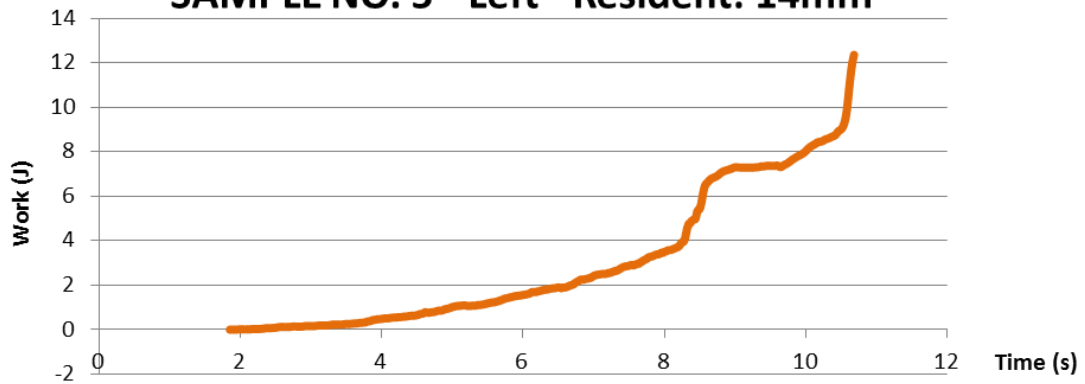
**SAMPLE NO. 5 - Left - Resident: 14mm**



**SAMPLE NO. 5 - Left - Resident: 14mm**



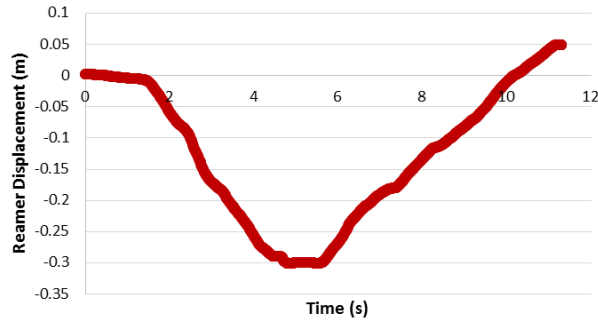
**SAMPLE NO. 5 - Left - Resident: 14mm**



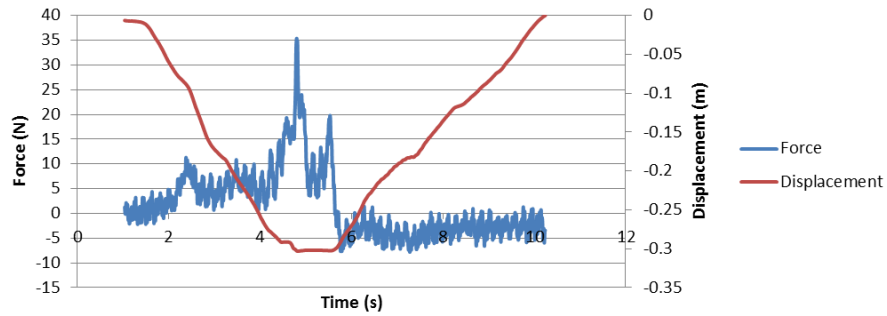
RIGHT: ATTENDING

9MM

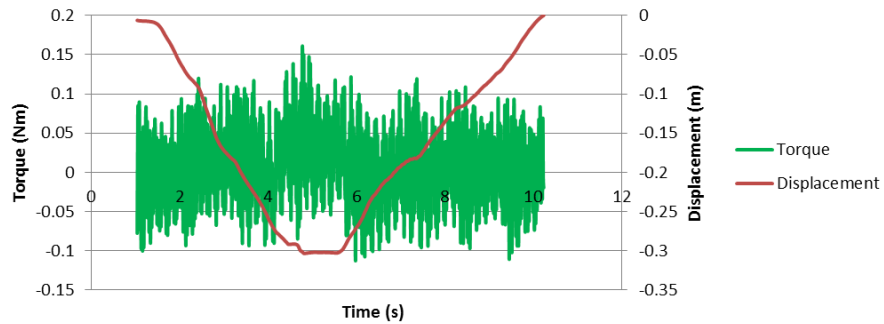
**SAMPLE NO. 5 - Right - Attending: 9mm**



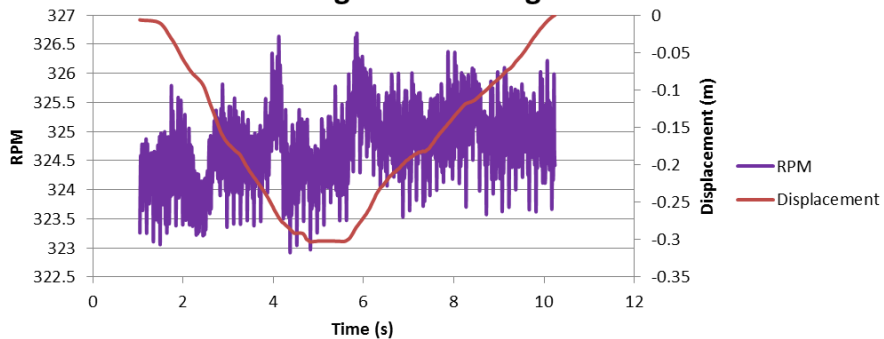
**SAMPLE NO. 5 - Right - Attending: 9mm**



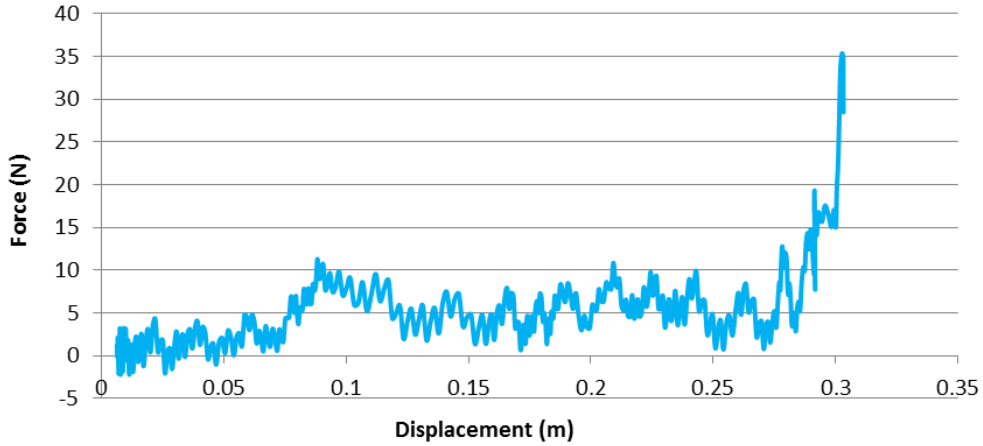
**SAMPLE NO. 5 - Right - Attending: 9mm**



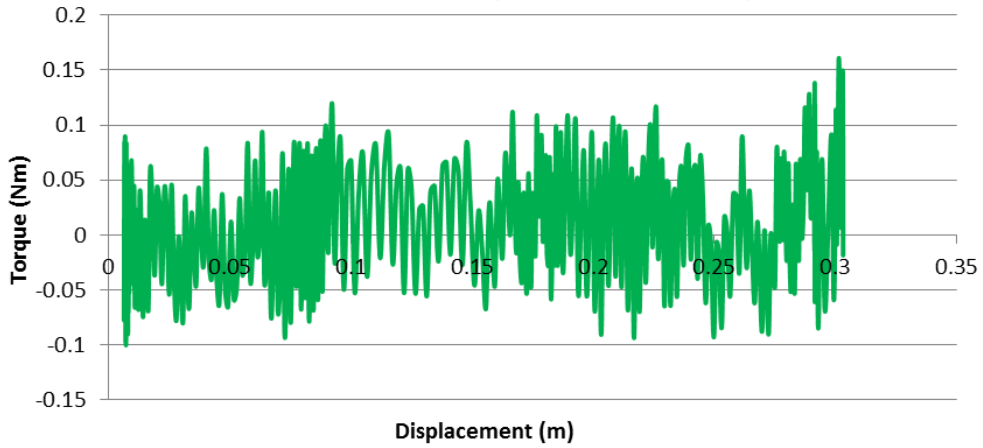
**SAMPLE NO. 5 - Right - Attending: 9mm**



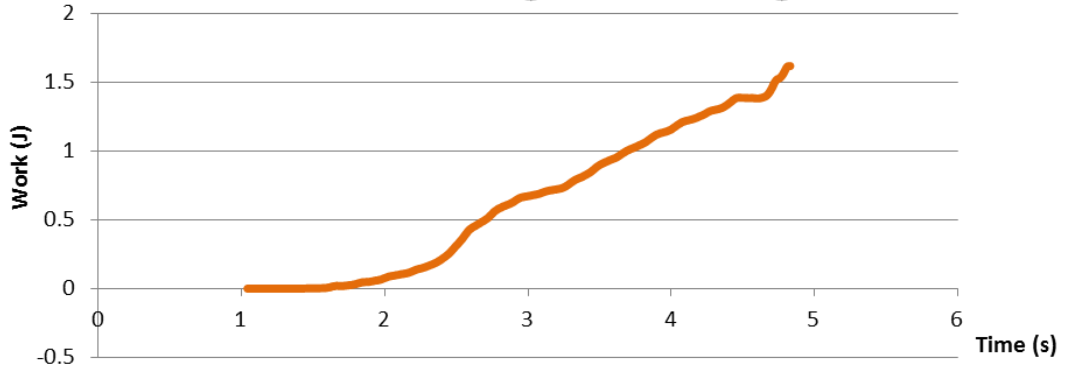
### SAMPLE NO. 5 - Right - Attending: 9mm



### SAMPLE NO. 5 - Right - Attending: 9mm

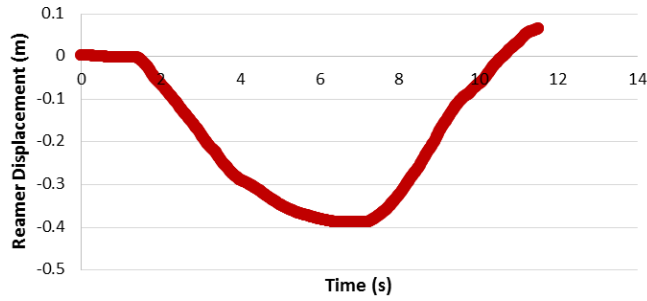


### SAMPLE NO. 5 - Right - Attending: 9mm

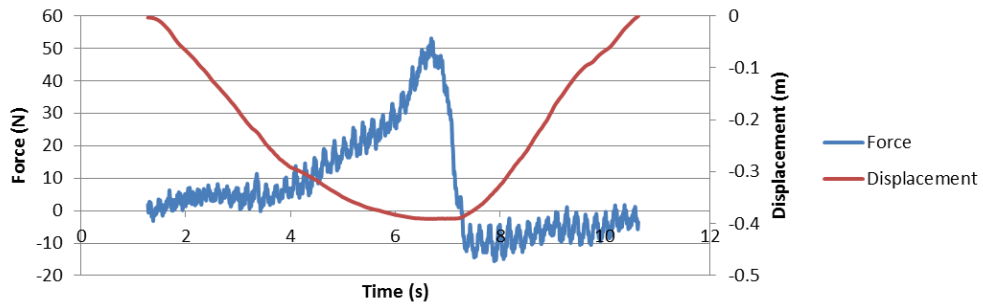


9.5MM

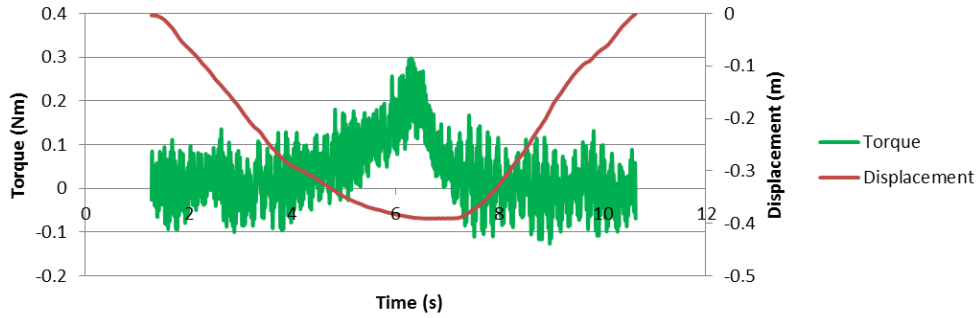
**SAMPLE NO. 5 - Right - Attending:  
9.5mm**



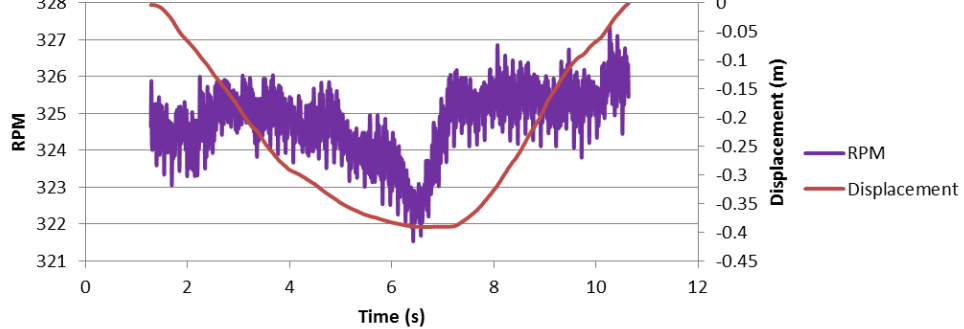
**SAMPLE NO. 5 - Right - Attending: 9.5mm**



**SAMPLE NO. 5 - Right - Attending: 9.5mm**

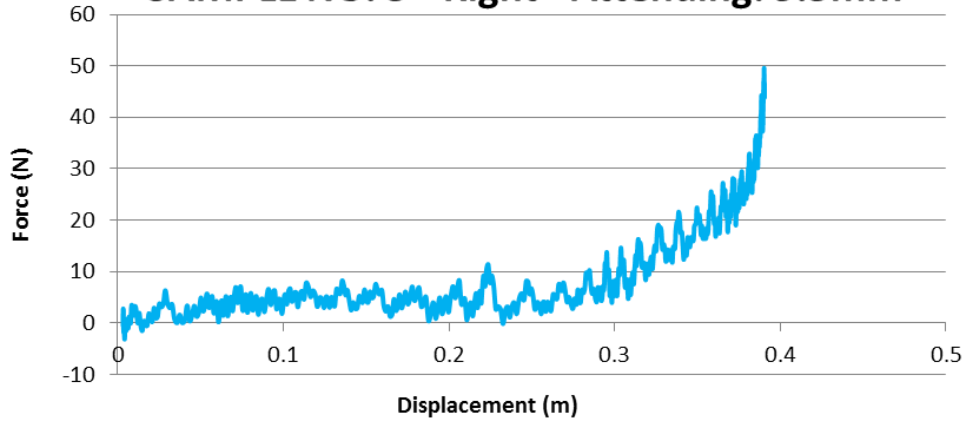


**SAMPLE NO. 5 - Right - Attending: 9.5mm**

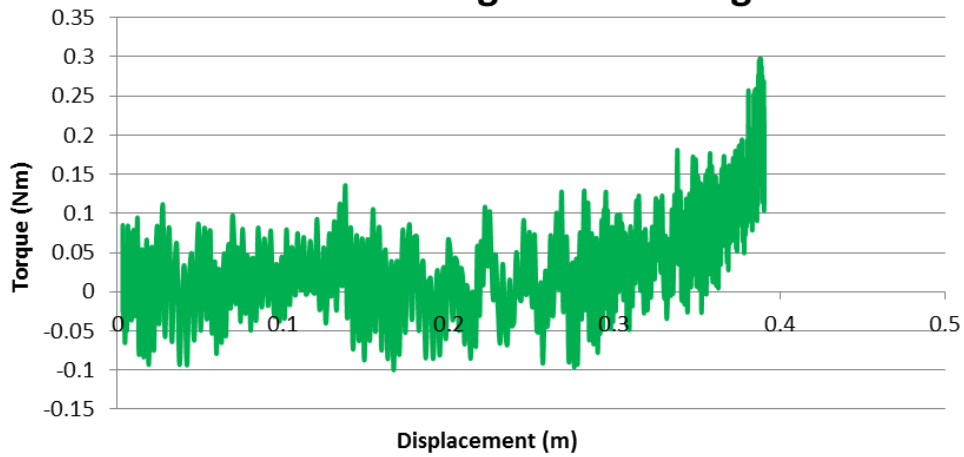




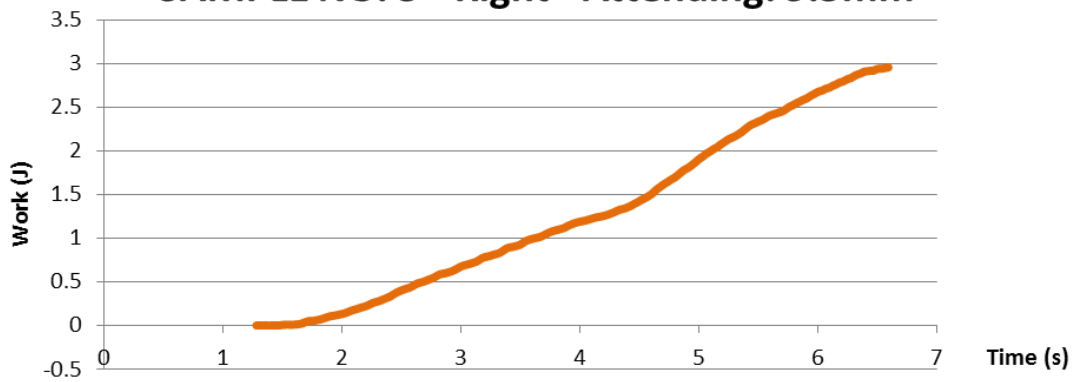
**SAMPLE NO. 5 - Right - Attending: 9.5mm**



**SAMPLE NO. 5 - Right - Attending: 9.5mm**

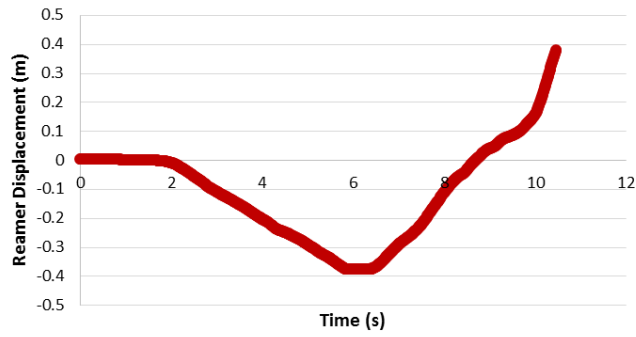


**SAMPLE NO. 5 - Right - Attending: 9.5mm**

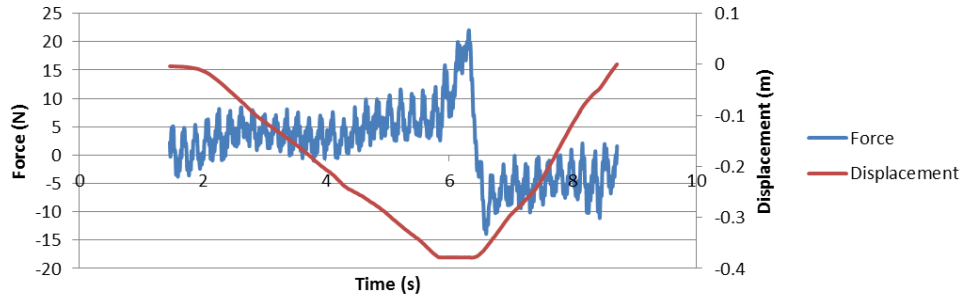


10MM

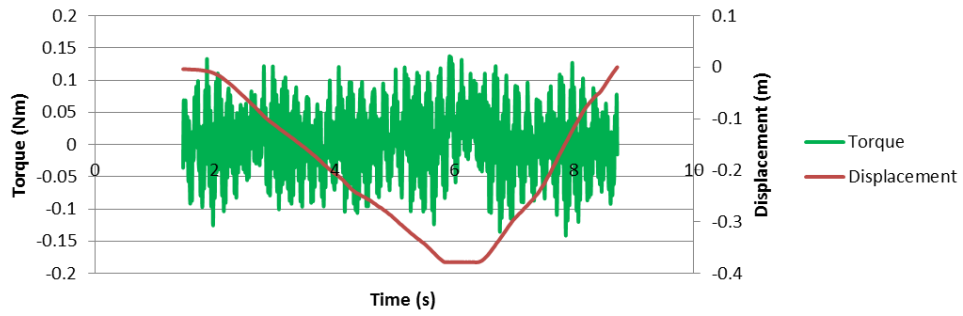
**SAMPLE NO. 5 - Right - Attending: 10mm**



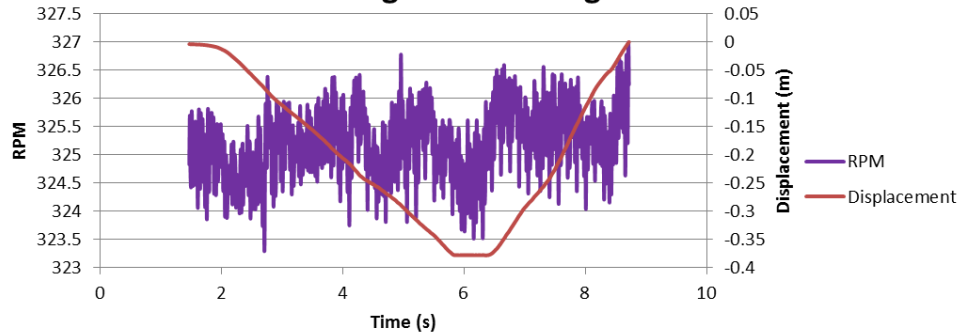
**SAMPLE NO. 5 - Right - Attending: 10mm**



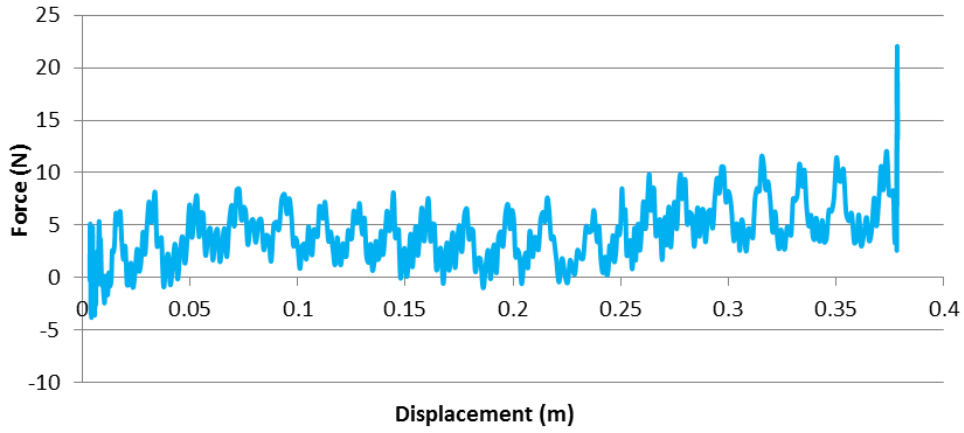
**SAMPLE NO. 5 - Right - Attending: 10mm**



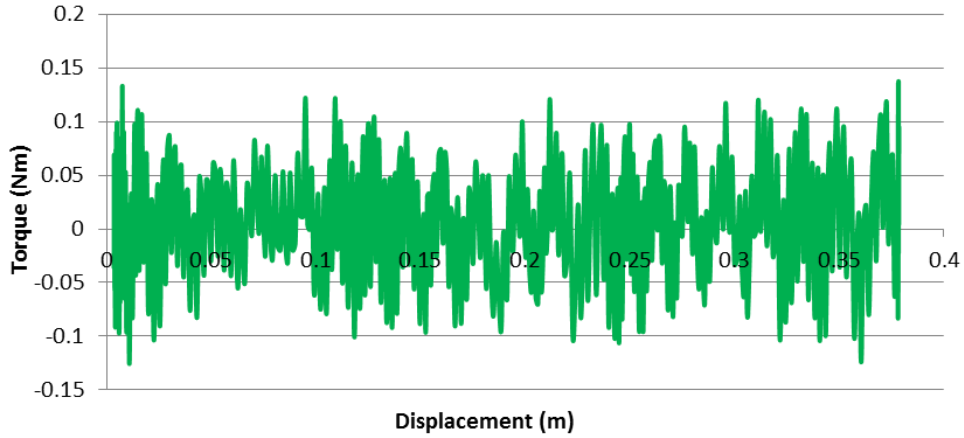
**SAMPLE NO. 5 - Right - Attending: 10mm**



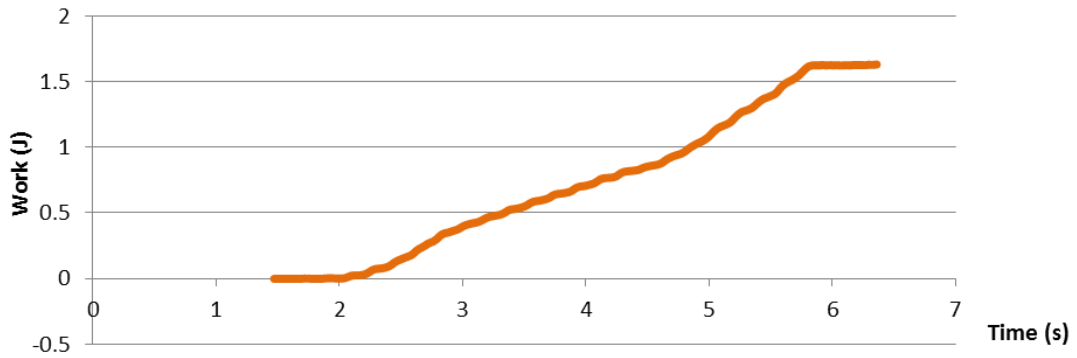
**SAMPLE NO. 5 - Right - Attending: 10mm**



**SAMPLE NO. 5 - Right - Attending: 10mm**

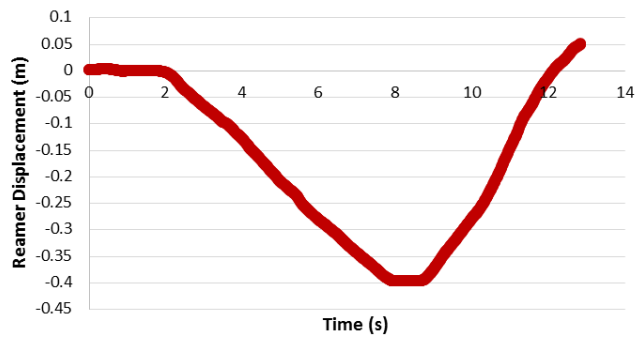


**SAMPLE NO. 5 - Right - Attending: 10mm**

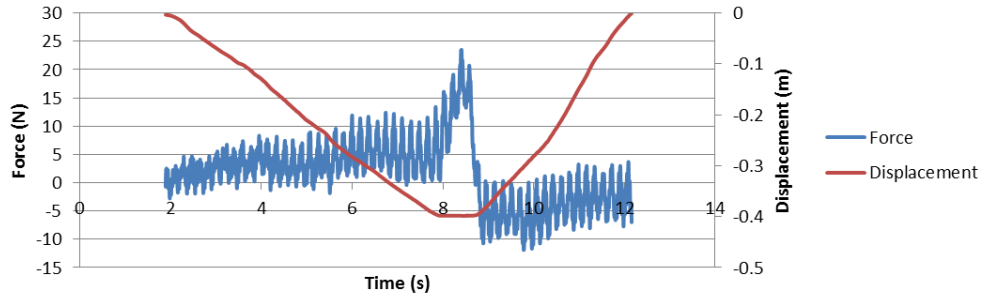


10.5MM

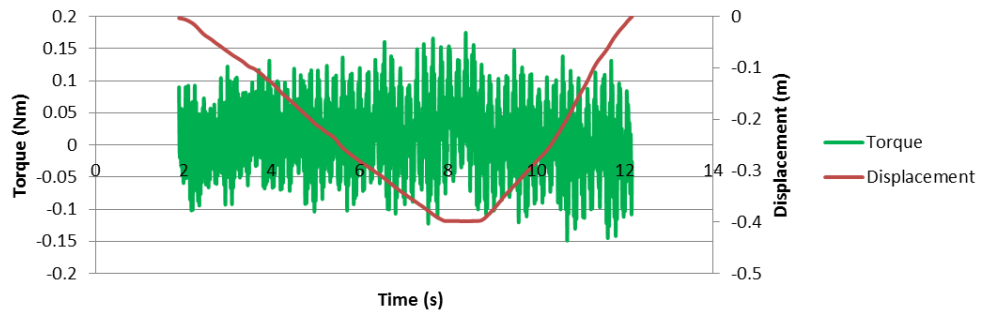
SAMPLE NO. 5 - Right - Attending: 10.5mm



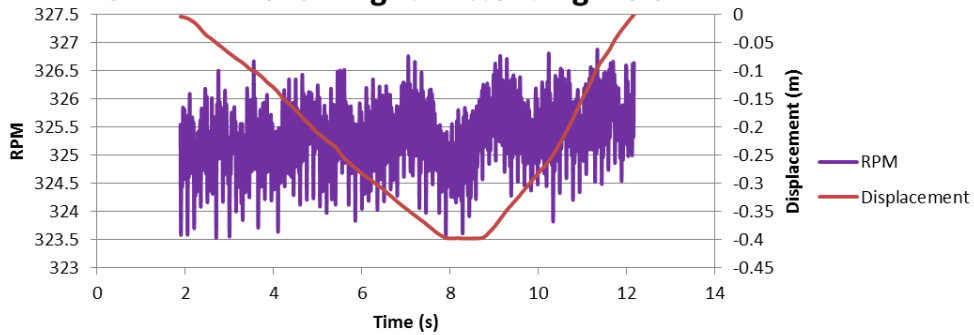
SAMPLE NO. 5 - Right - Attending: 10.5mm



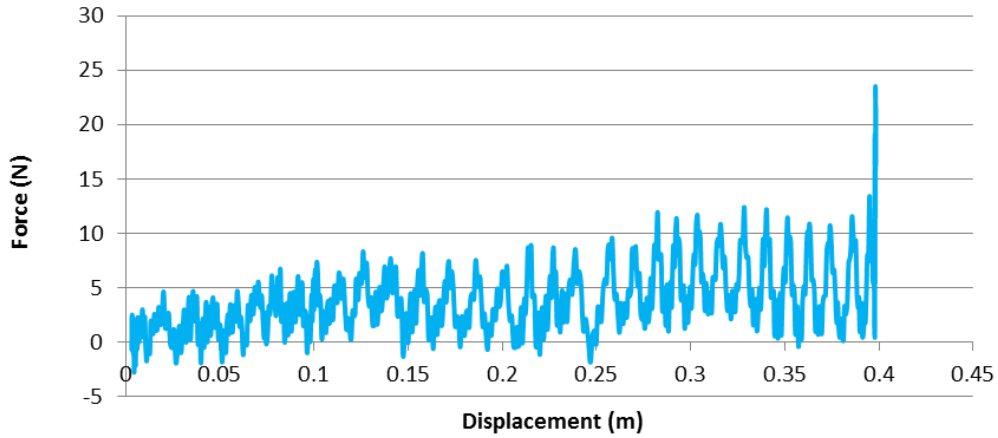
SAMPLE NO. 5 - Right - Attending: 10.5mm



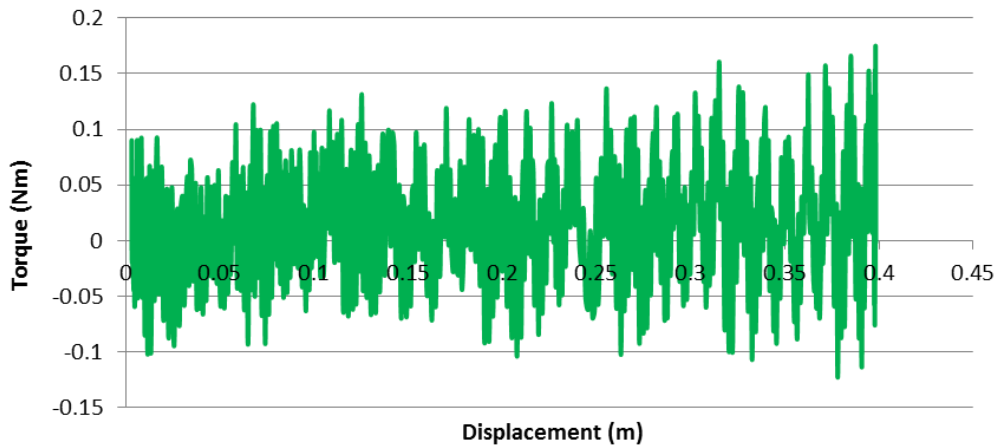
SAMPLE NO. 5 - Right - Attending: 10.5mm



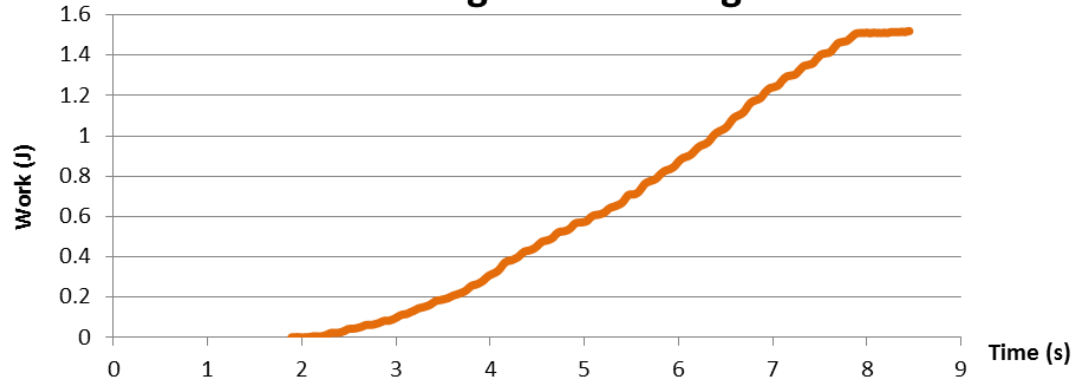
**SAMPLE NO. 5 - Right - Attending: 10.5mm**



**SAMPLE NO. 5 - Right - Attending: 10.5mm**

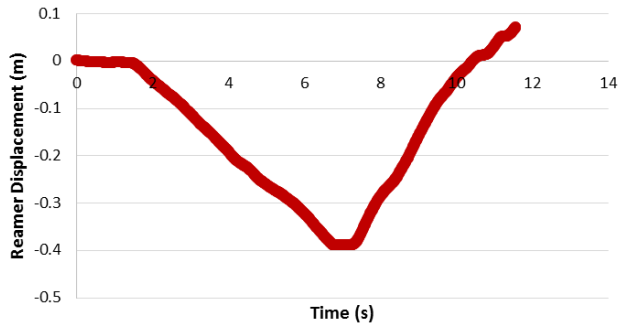


**SAMPLE NO. 5 - Right - Attending: 10.5mm**

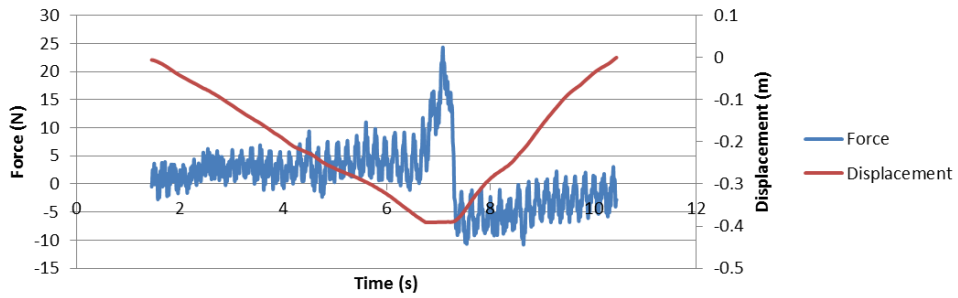


11MM

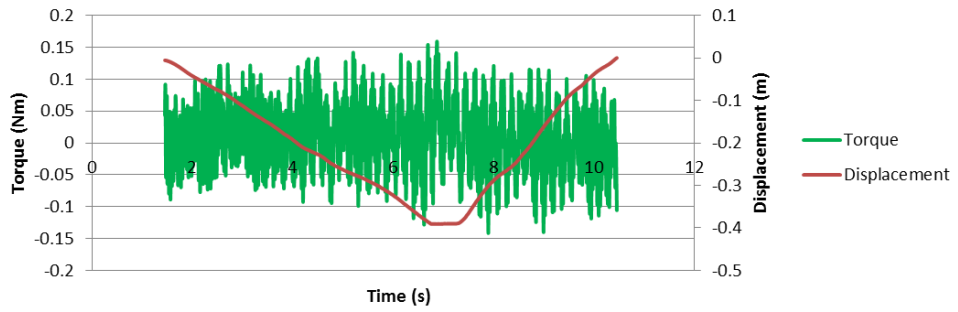
SAMPLE NO. 5 - Right - Attending: 11mm



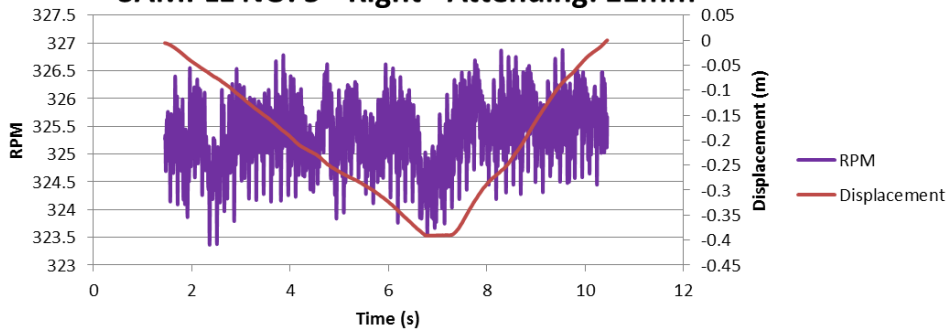
SAMPLE NO. 5 - Right - Attending: 11mm



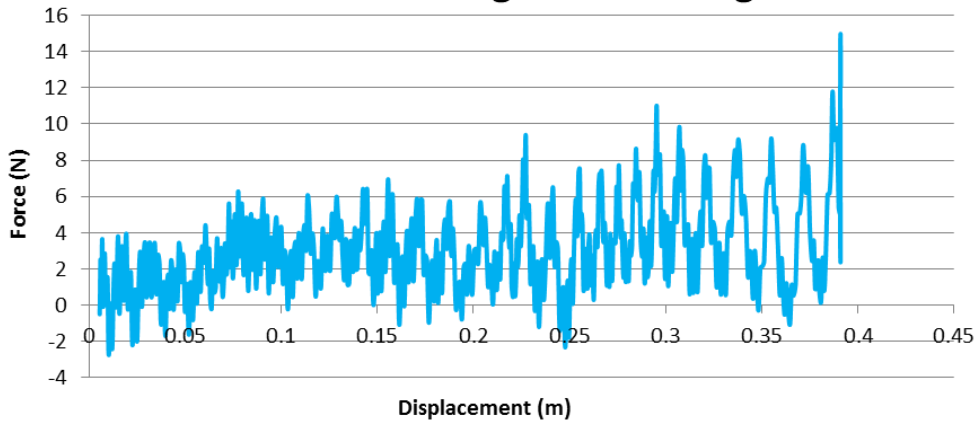
SAMPLE NO. 5 - Right - Attending: 11mm



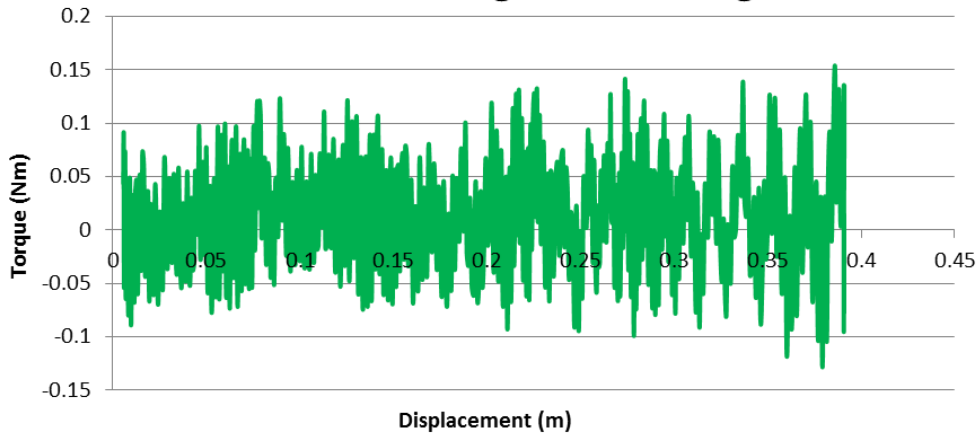
SAMPLE NO. 5 - Right - Attending: 11mm



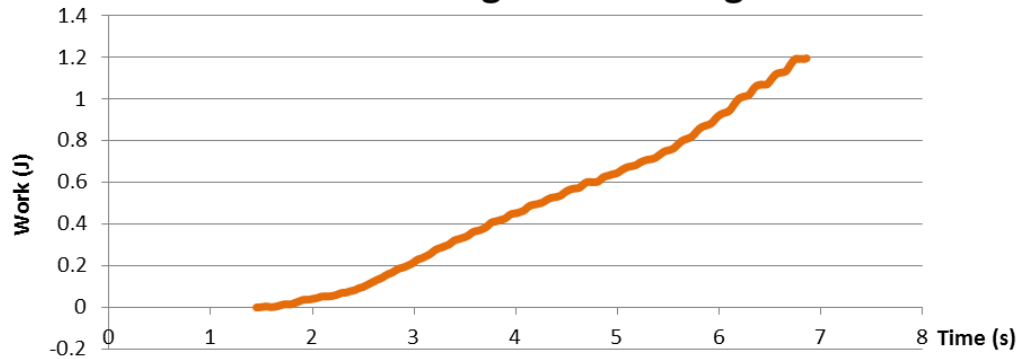
**SAMPLE NO. 5 - Right - Attending: 11mm**



**SAMPLE NO. 5 - Right - Attending: 11mm**

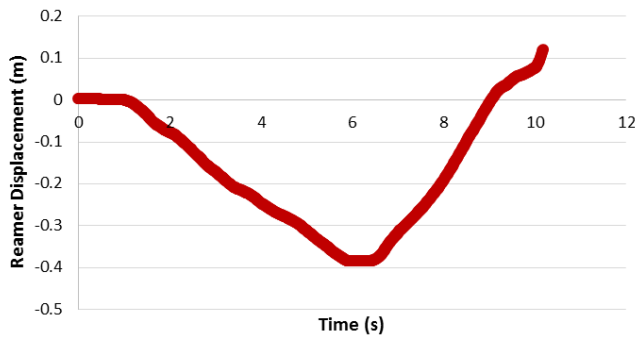


**SAMPLE NO. 5 - Right - Attending: 11mm**

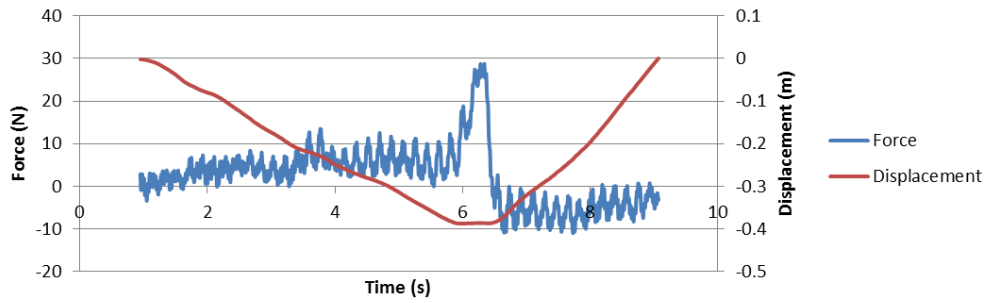


11.5MM

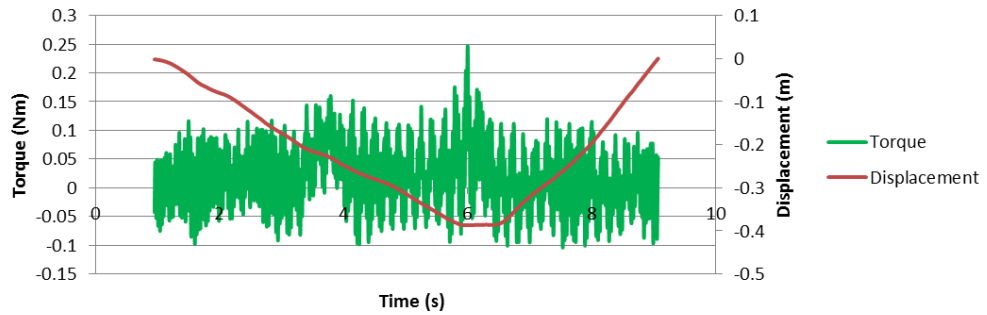
SAMPLE NO. 5 - Right - Attending: 11.5mm



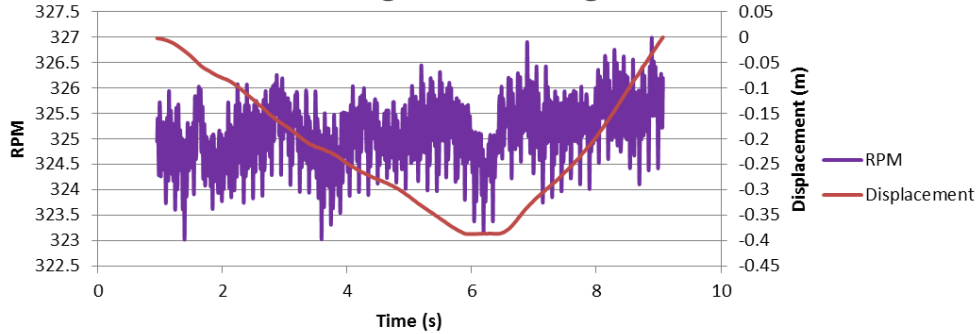
SAMPLE NO. 5 - Right - Attending: 11.5mm



SAMPLE NO. 5 - Right - Attending: 11.5mm

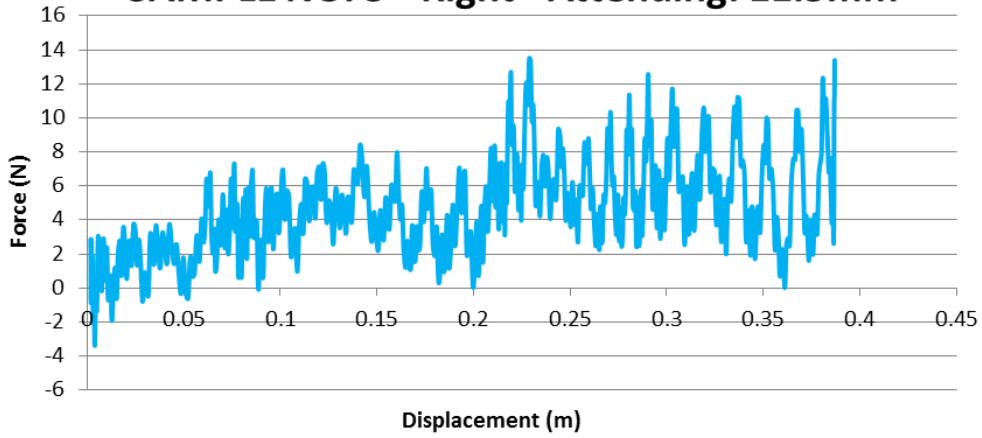


SAMPLE NO. 5 - Right - Attending: 11.5mm

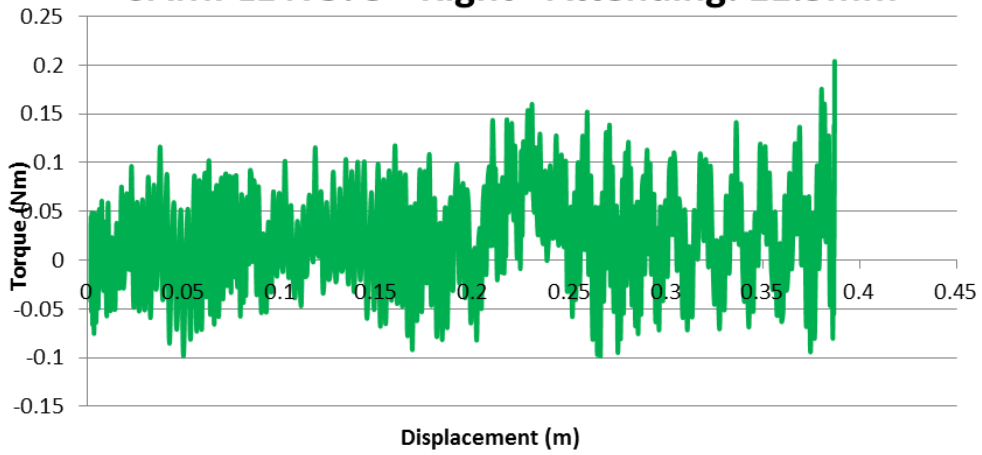




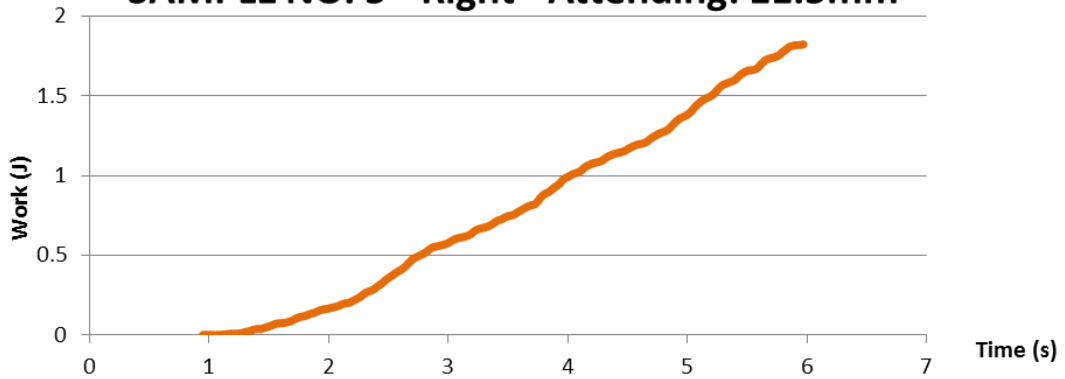
**SAMPLE NO. 5 - Right - Attending: 11.5mm**



**SAMPLE NO. 5 - Right - Attending: 11.5mm**

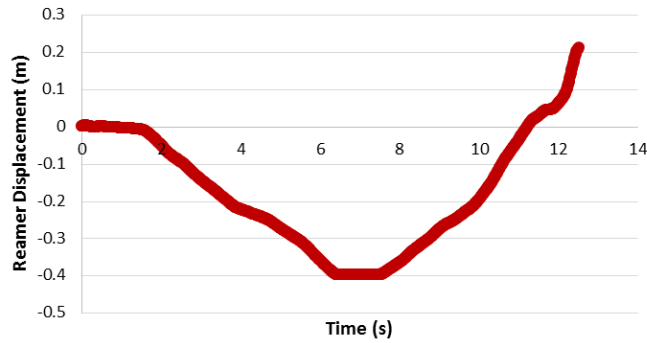


**SAMPLE NO. 5 - Right - Attending: 11.5mm**

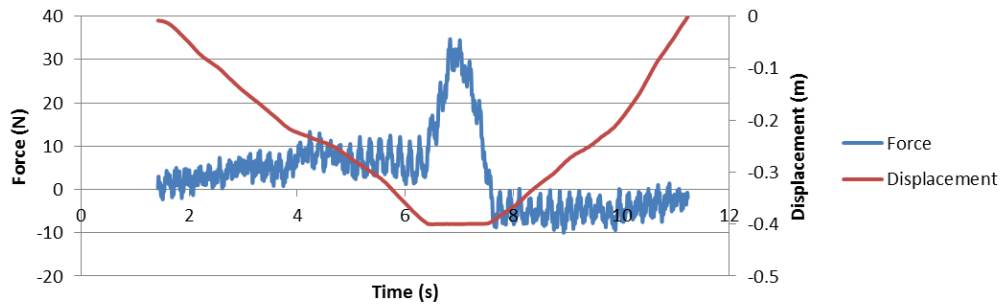


12MM

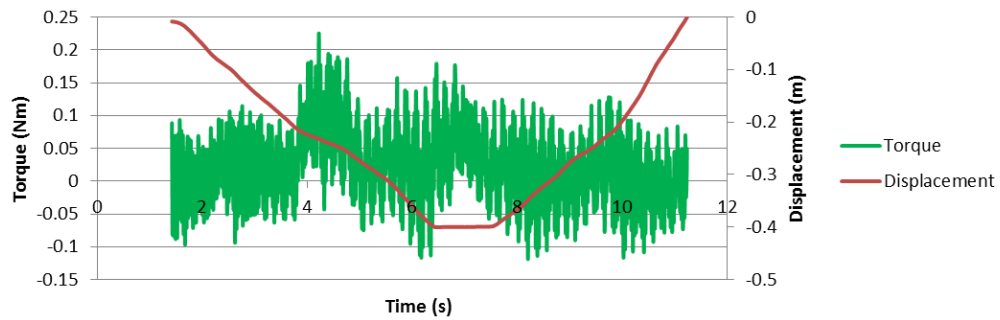
**SAMPLE NO. 5 - Right - Attending: 12mm**



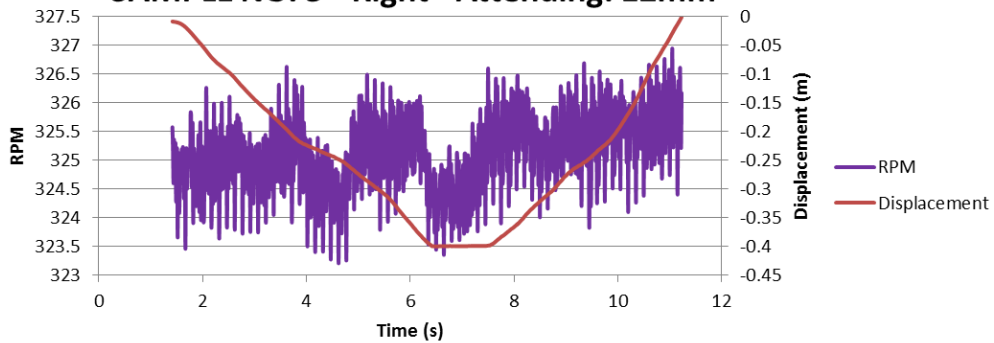
**SAMPLE NO. 5 - Right - Attending: 12mm**



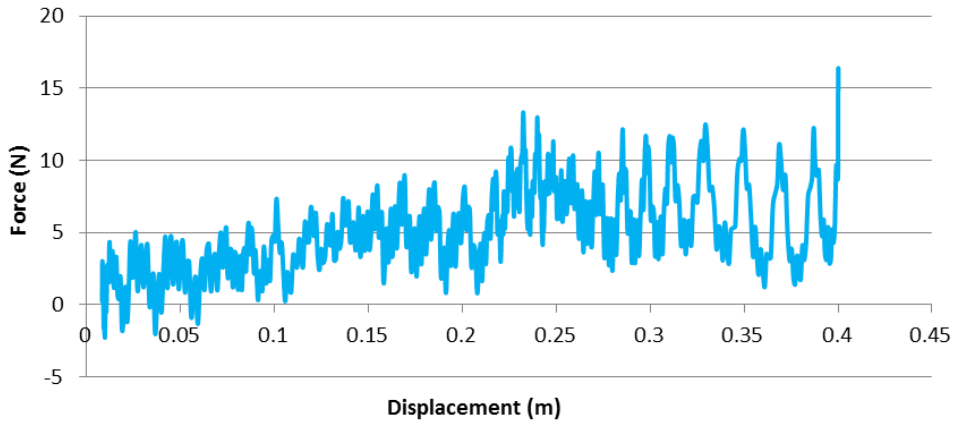
**SAMPLE NO. 5 - Right - Attending: 12mm**



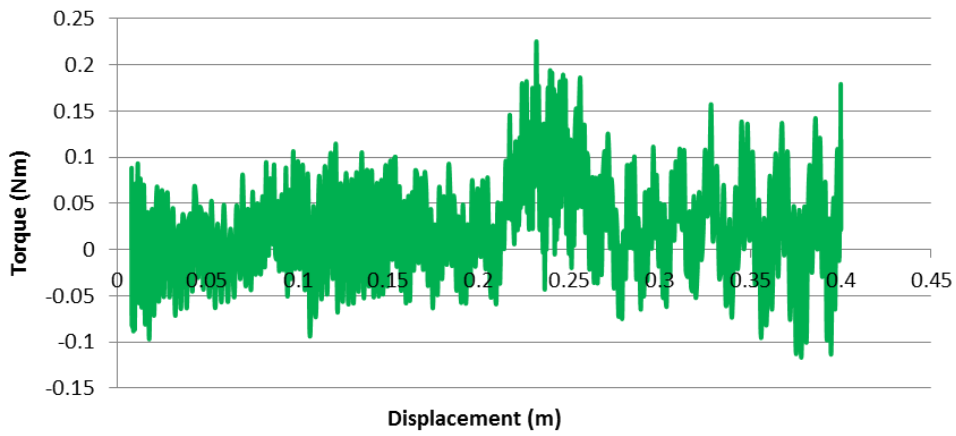
**SAMPLE NO. 5 - Right - Attending: 12mm**



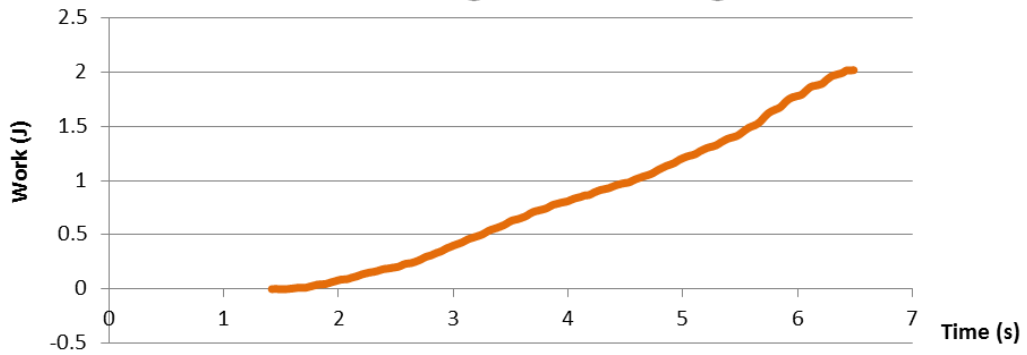
**SAMPLE NO. 5 - Right - Attending: 12mm**



**SAMPLE NO. 5 - Right - Attending: 12mm**

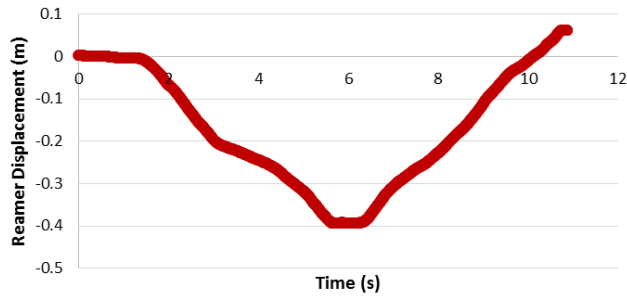


**SAMPLE NO. 5 - Right - Attending: 12mm**

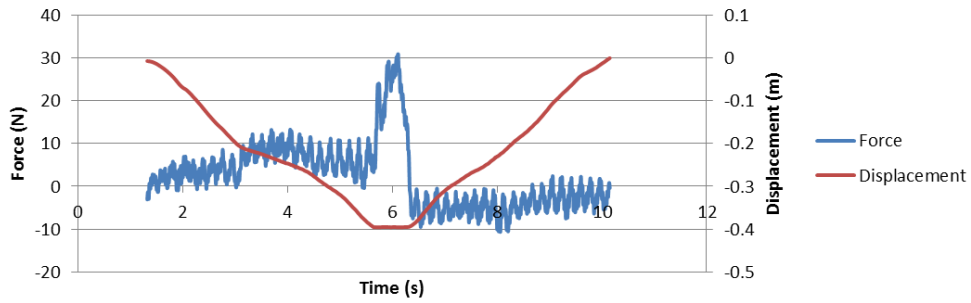


12.5MM

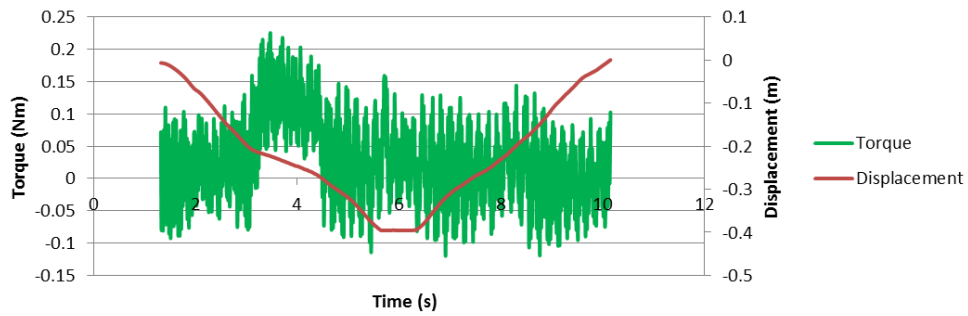
**SAMPLE NO. 5 - Right - Attending: 12.5mm  
CHATTER**



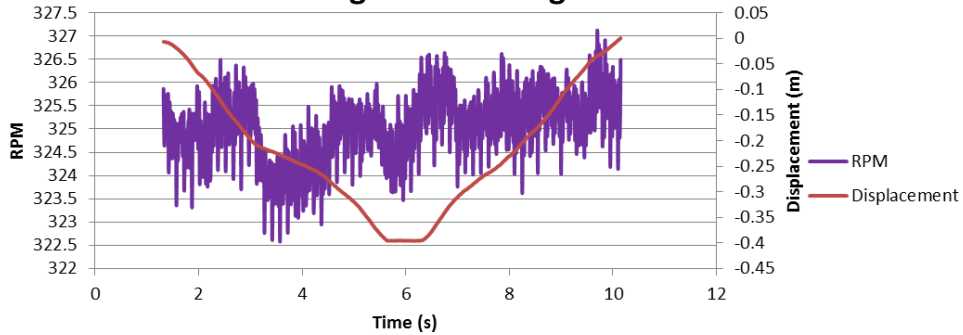
**SAMPLE NO. 5 - Right - Attending: 12.5mm CHATTER**



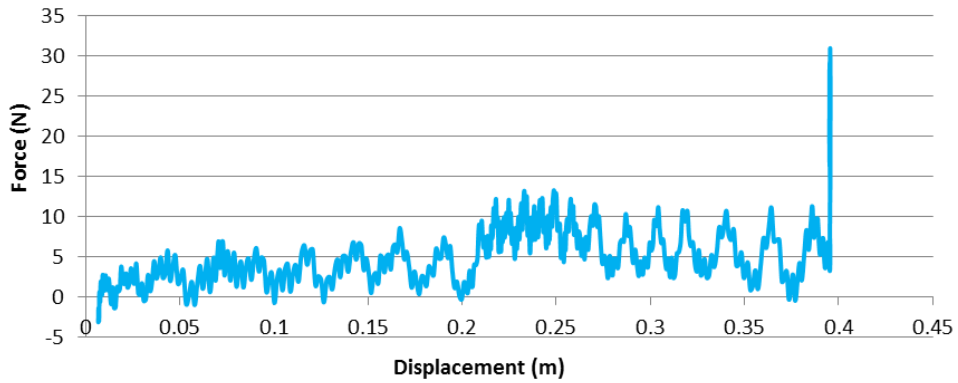
**SAMPLE NO. 5 - Right - Attending: 12.5mm CHATTER**



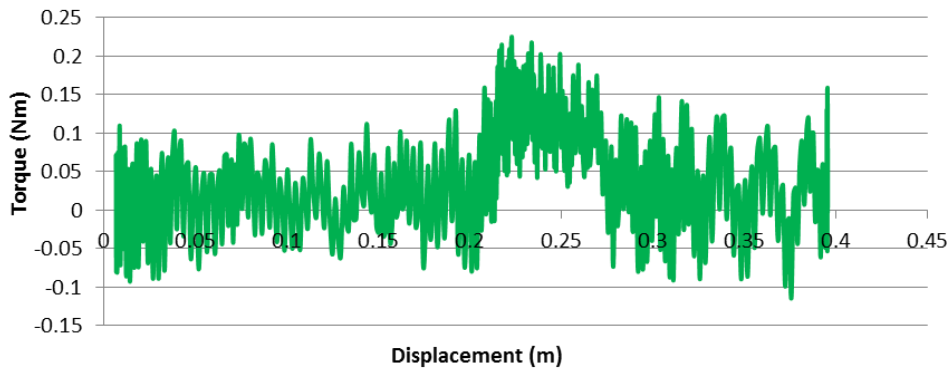
**SAMPLE NO. 5 - Right - Attending: 12.5mm CHATTER**



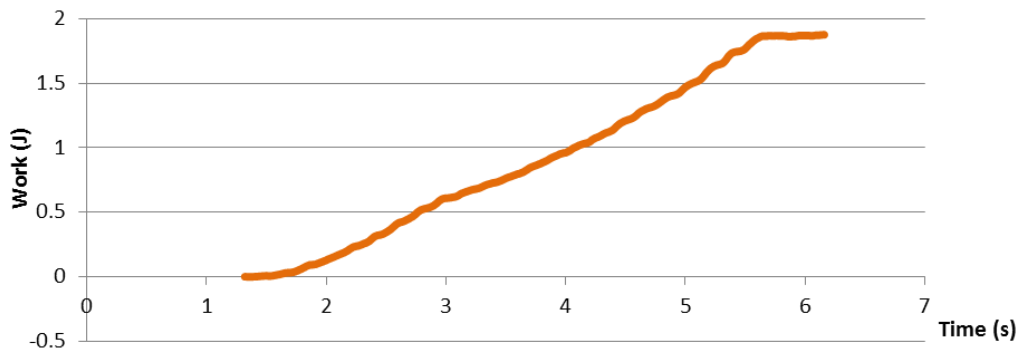
### SAMPLE NO. 5 - Right - Attending: 12.5mm CHATTER



### SAMPLE NO. 5 - Right - Attending: 12.5mm CHATTER

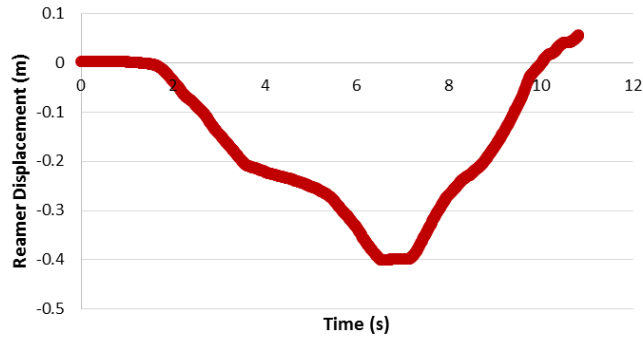


### SAMPLE NO. 5 - Right - Attending: 12.5mm CHATTER

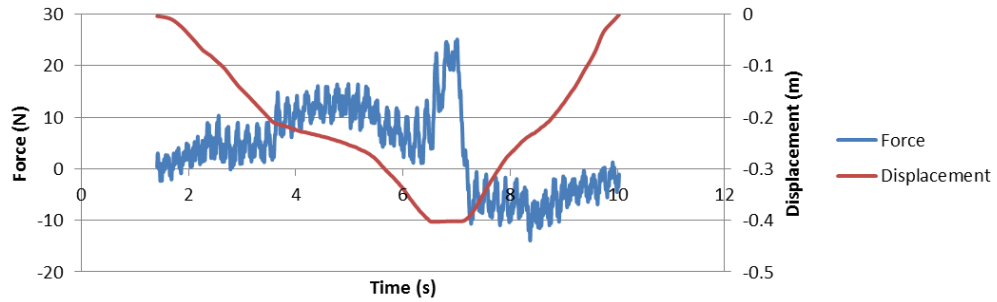


13MM

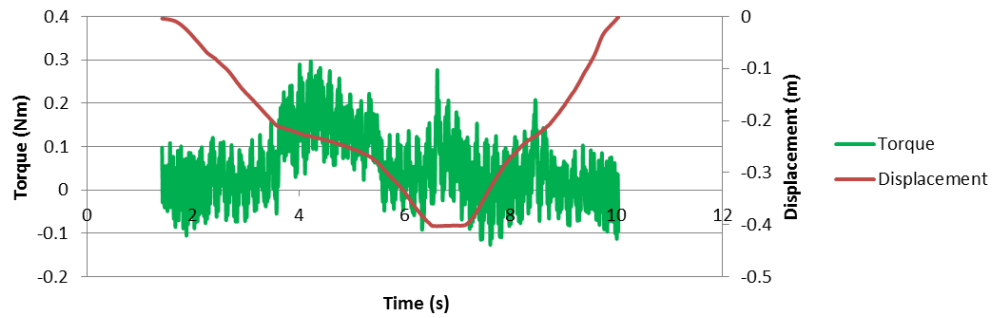
**SAMPLE NO. 5 - Right - Attending: 13mm**



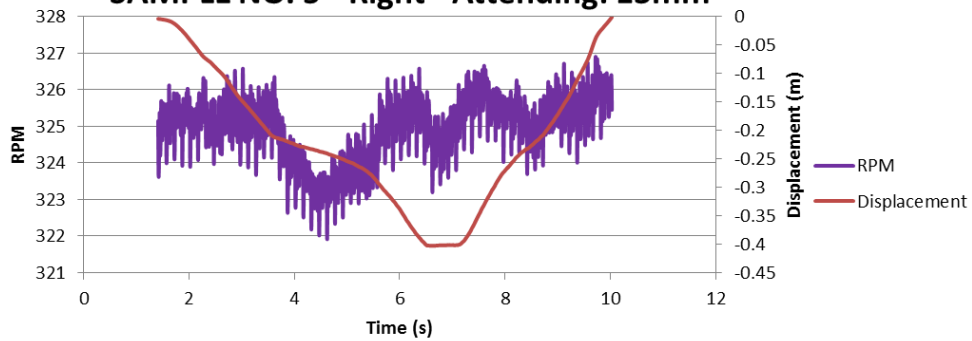
**SAMPLE NO. 5 - Right - Attending: 13mm**



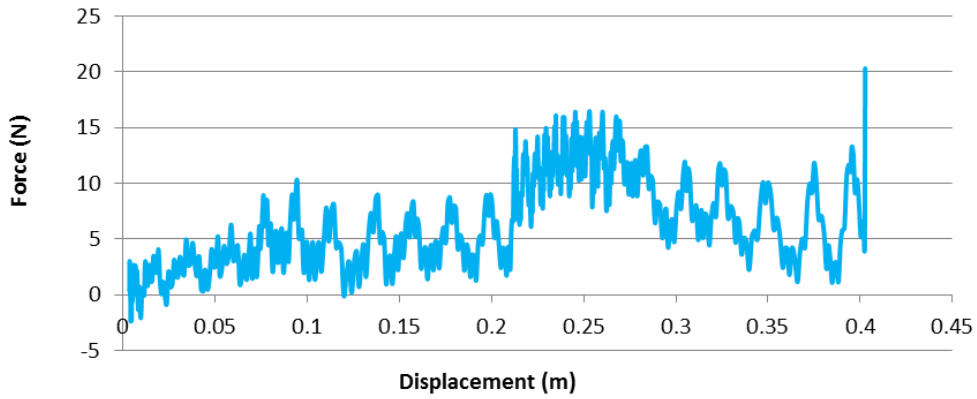
**SAMPLE NO. 5 - Right - Attending: 13mm**



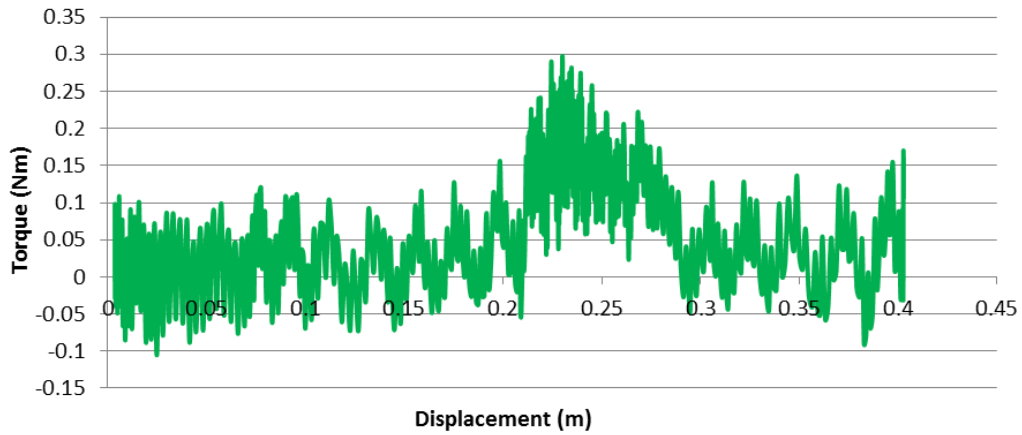
**SAMPLE NO. 5 - Right - Attending: 13mm**



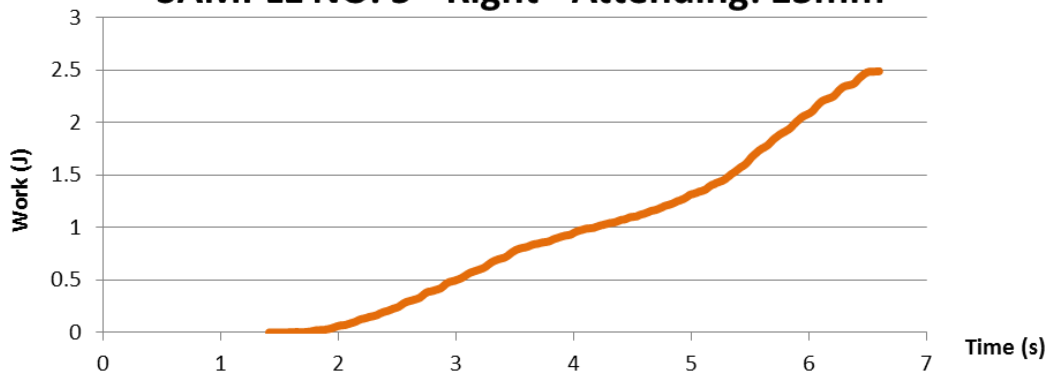
### SAMPLE NO. 5 - Right - Attending: 13mm



### SAMPLE NO. 5 - Right - Attending: 13mm

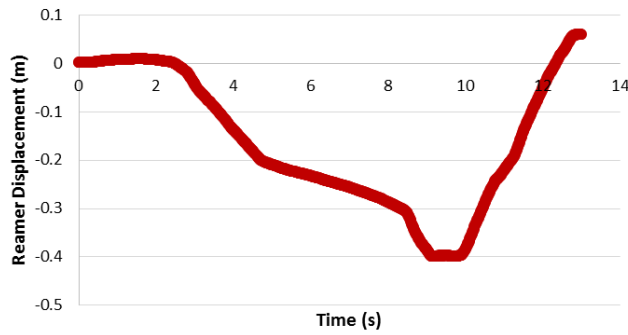


### SAMPLE NO. 5 - Right - Attending: 13mm

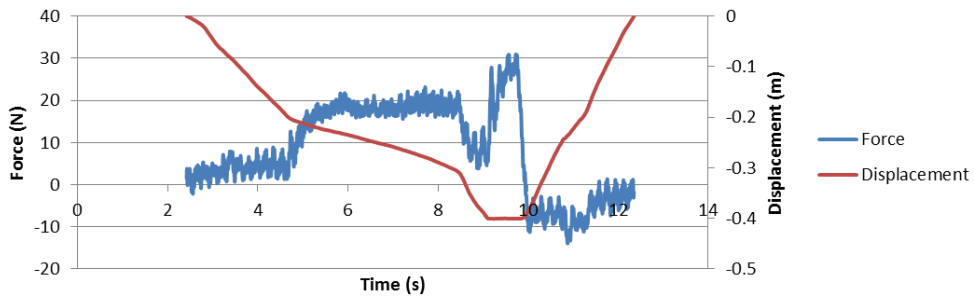


13.5MM

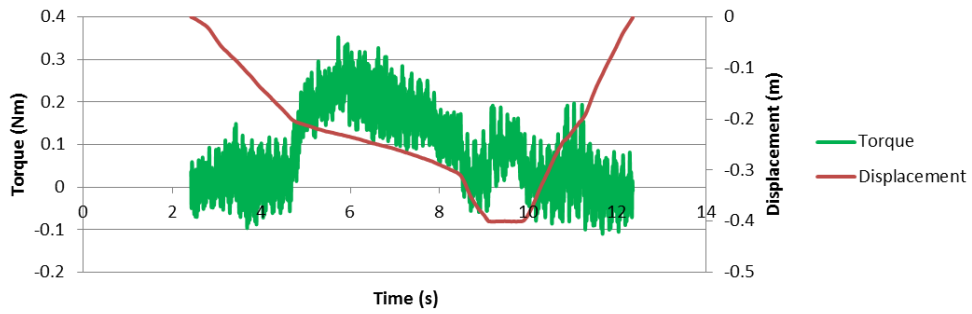
**SAMPLE NO. 5 - Right - Attending: 13.5mm**



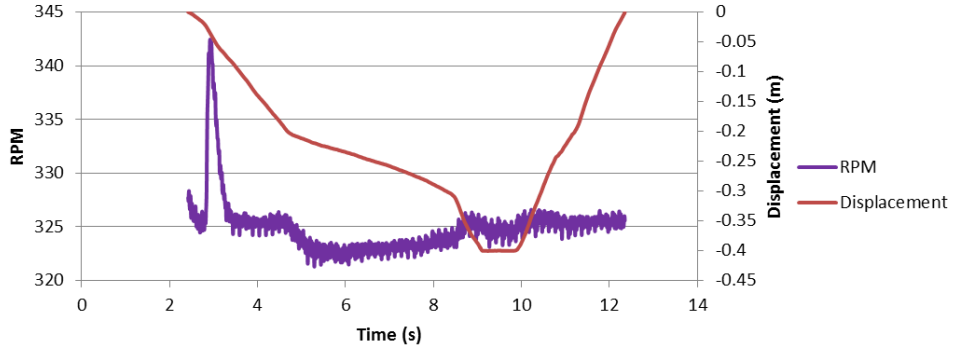
**SAMPLE NO. 5 - Right - Attending: 13.5mm**



**SAMPLE NO. 5 - Right - Attending: 13.5mm**

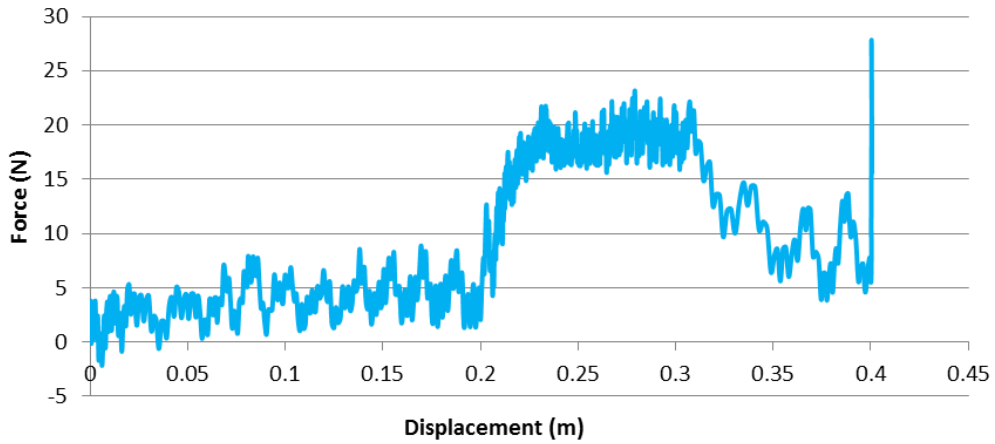


**SAMPLE NO. 5 - Right - Attending: 13.5mm**

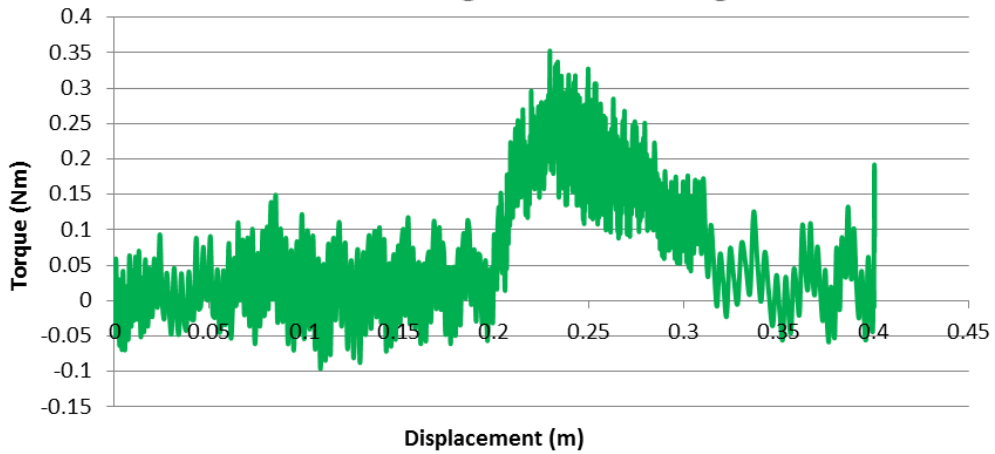




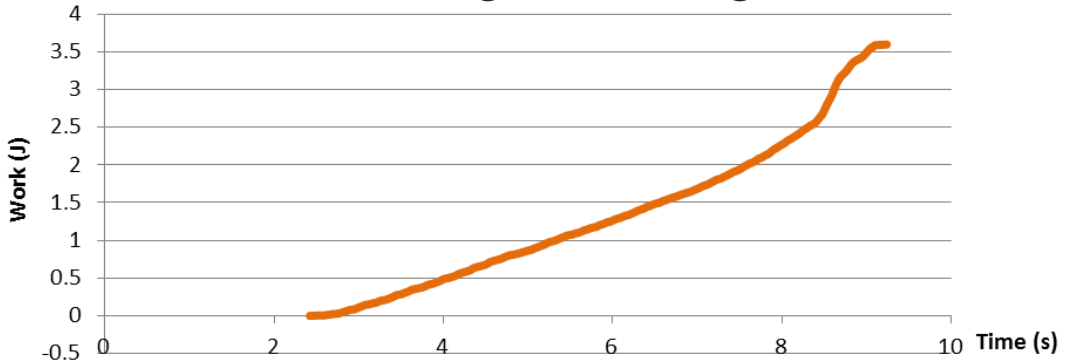
**SAMPLE NO. 5 - Right - Attending: 13.5mm**



**SAMPLE NO. 5 - Right - Attending: 13.5mm**

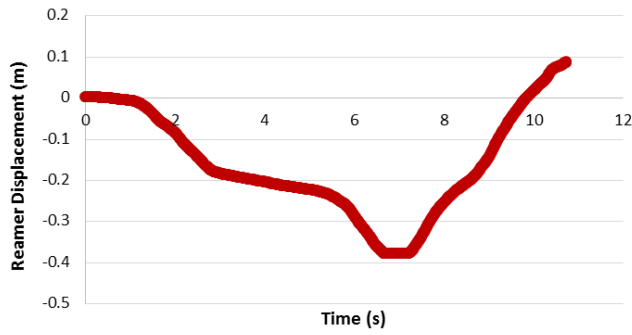


**SAMPLE NO. 5 - Right - Attending: 13.5mm**

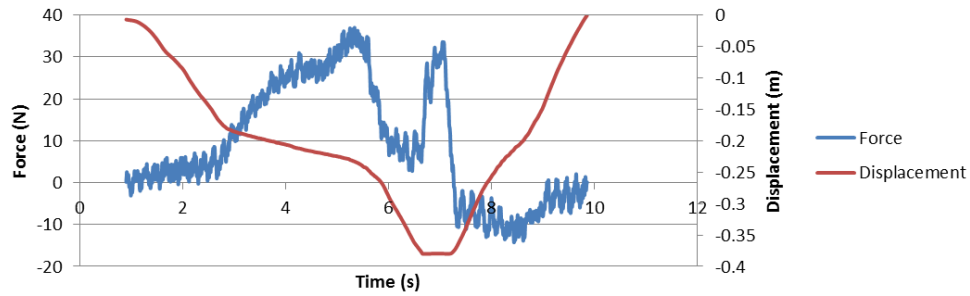


14MM

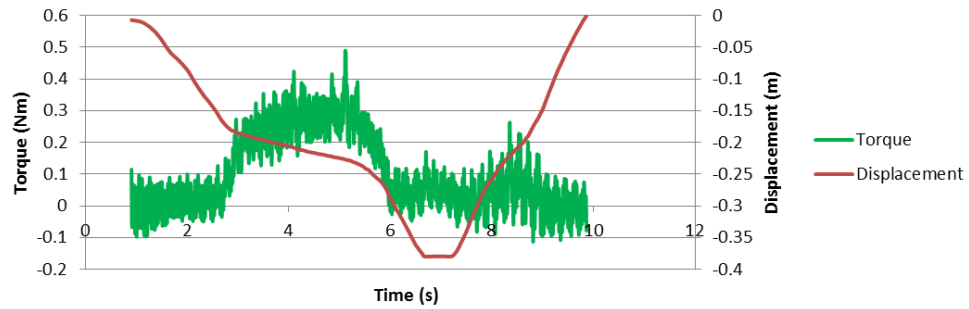
**SAMPLE NO. 5 - Right - Attending: 14mm**



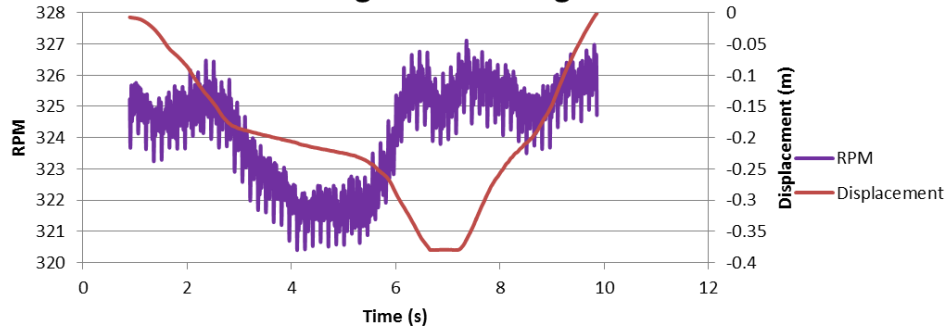
**SAMPLE NO. 5 - Right - Attending: 14mm**



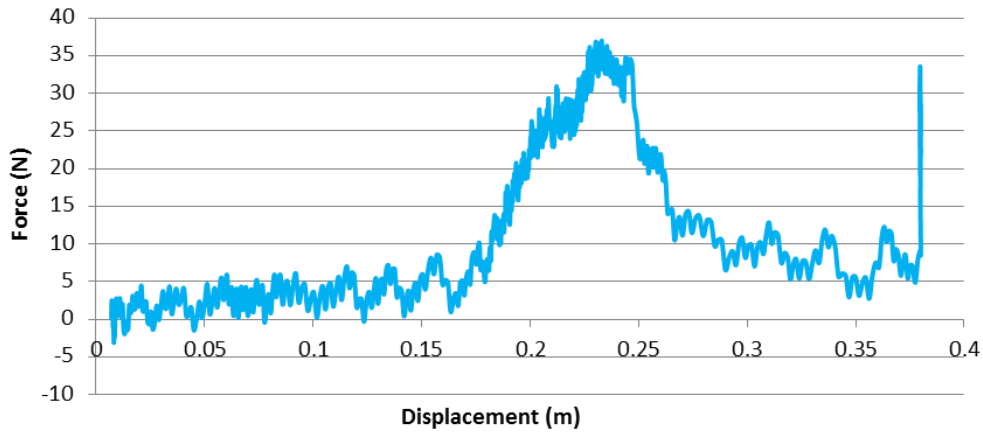
**SAMPLE NO. 5 - Right - Attending: 14mm**



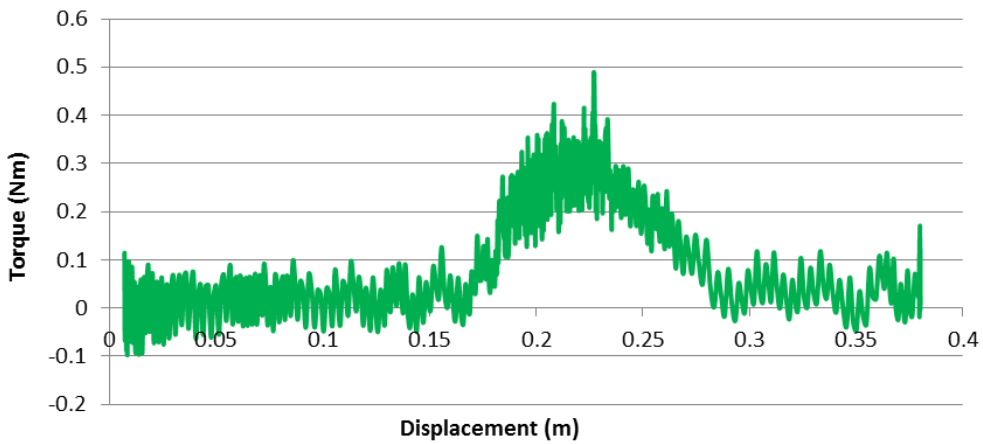
**SAMPLE NO. 5 - Right - Attending: 14mm**



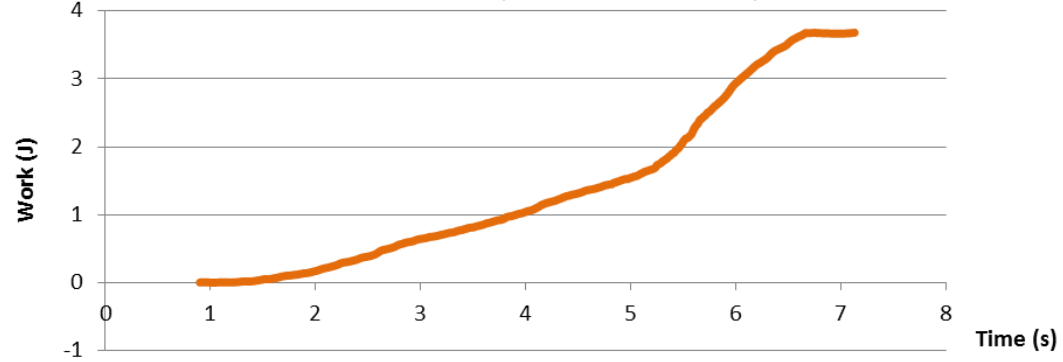
**SAMPLE NO. 5 - Right - Attending: 14mm**



**SAMPLE NO. 5 - Right - Attending: 14mm**



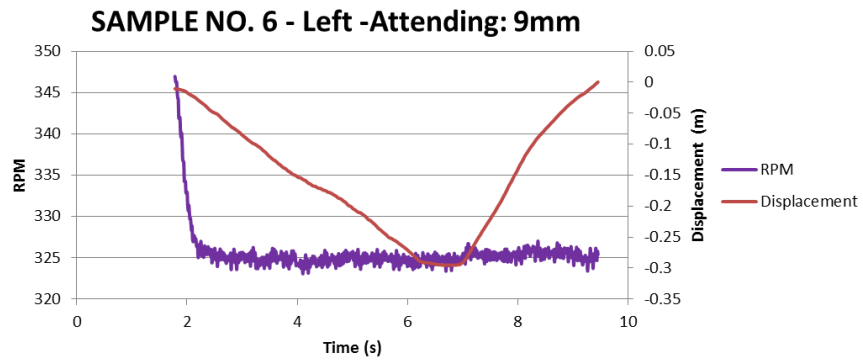
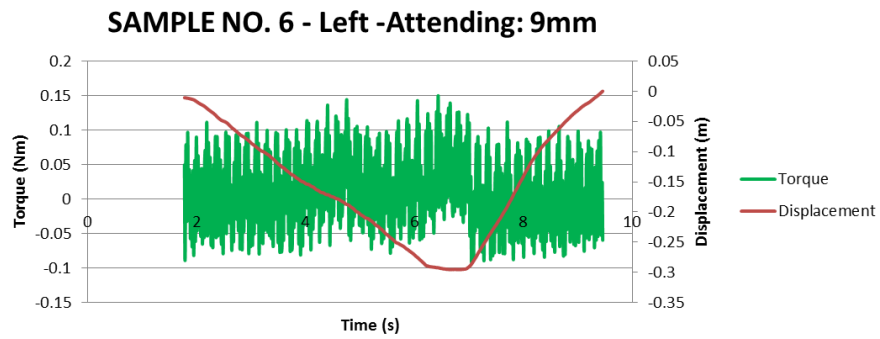
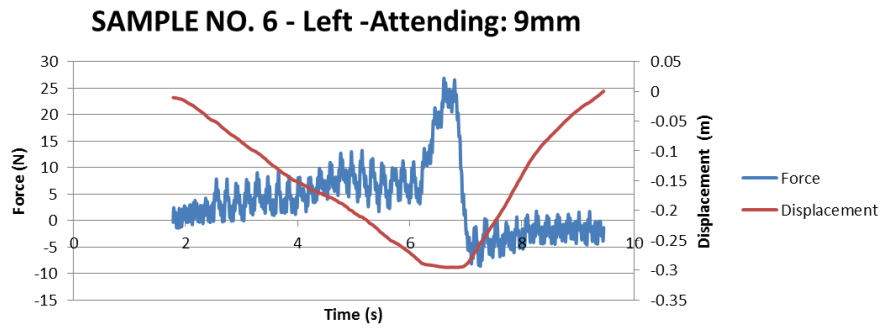
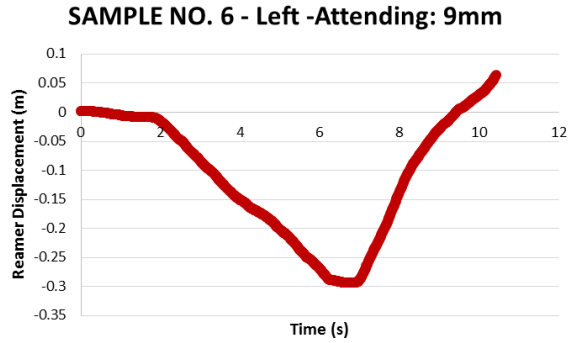
**SAMPLE NO. 5 - Right - Attending: 14mm**



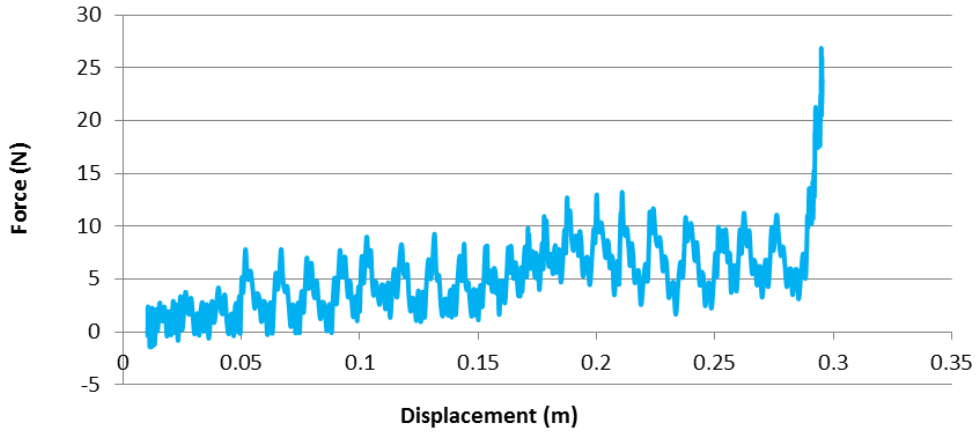
## 13.6 SAMPLE 6 RESULTS

LEFT: ATTENDING

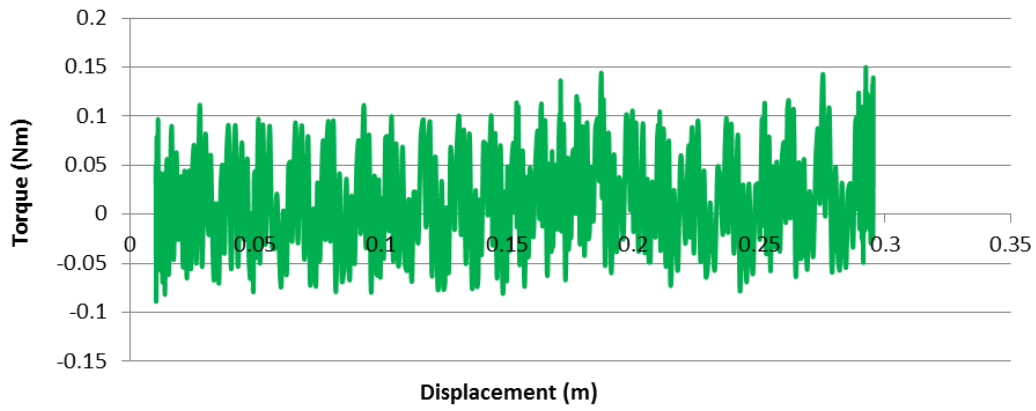
9MM



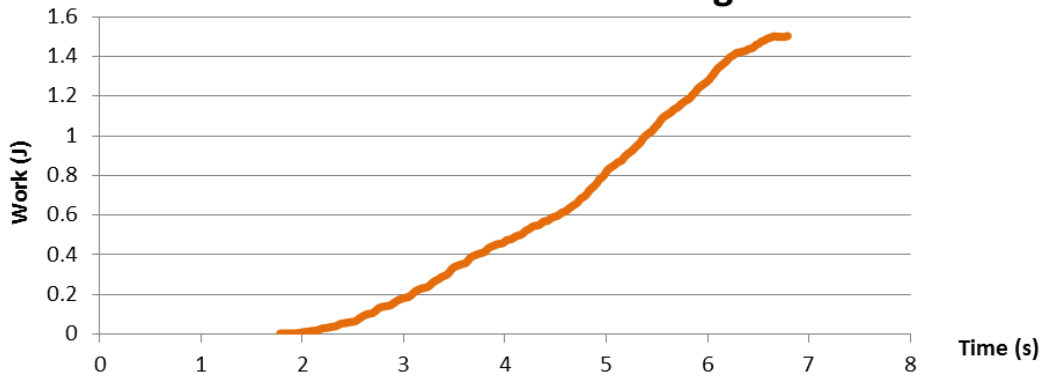
**SAMPLE NO. 6 - Left -Attending: 9mm**



**SAMPLE NO. 6 - Left -Attending: 9mm**

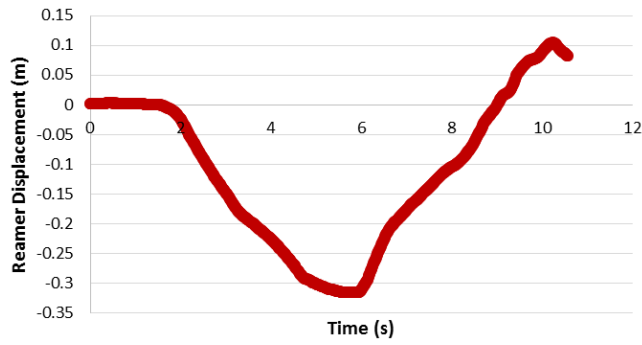


**SAMPLE NO. 6 - Left -Attending: 9mm**

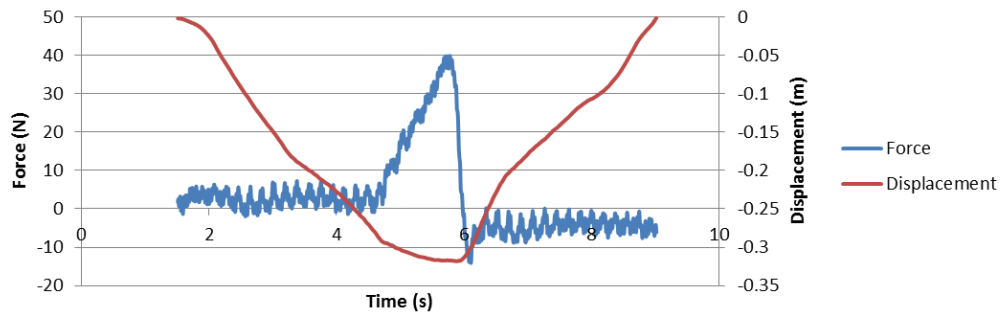


9.5MM

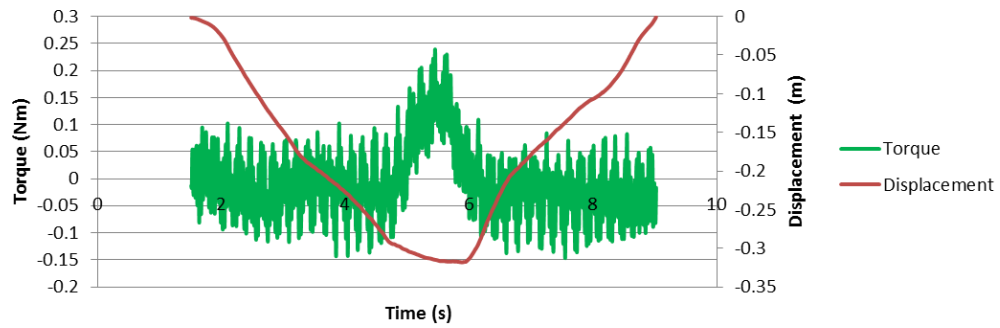
SAMPLE NO. 6 - Left -Attending: 9.5mm



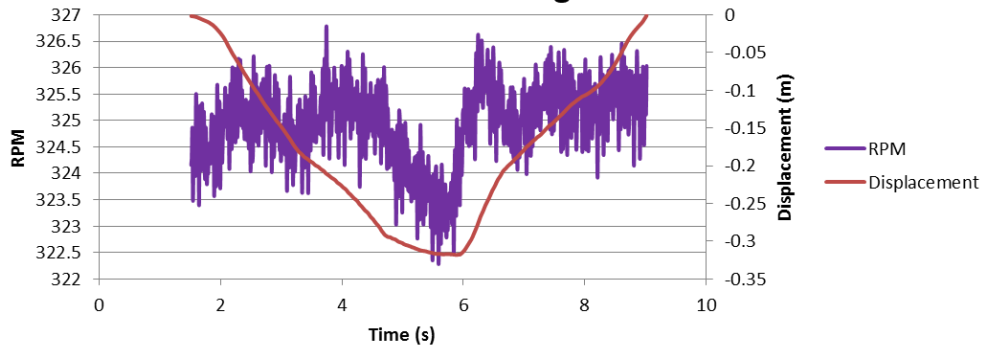
SAMPLE NO. 6 - Left -Attending: 9.5mm



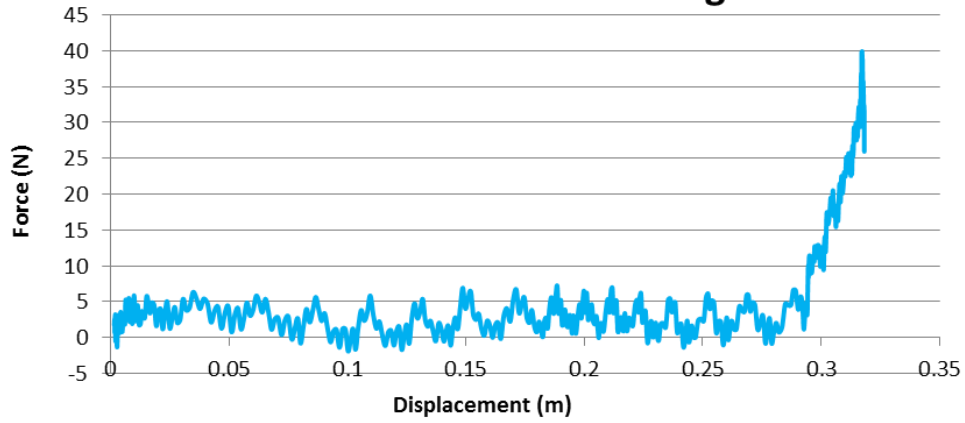
SAMPLE NO. 6 - Left -Attending: 9.5mm



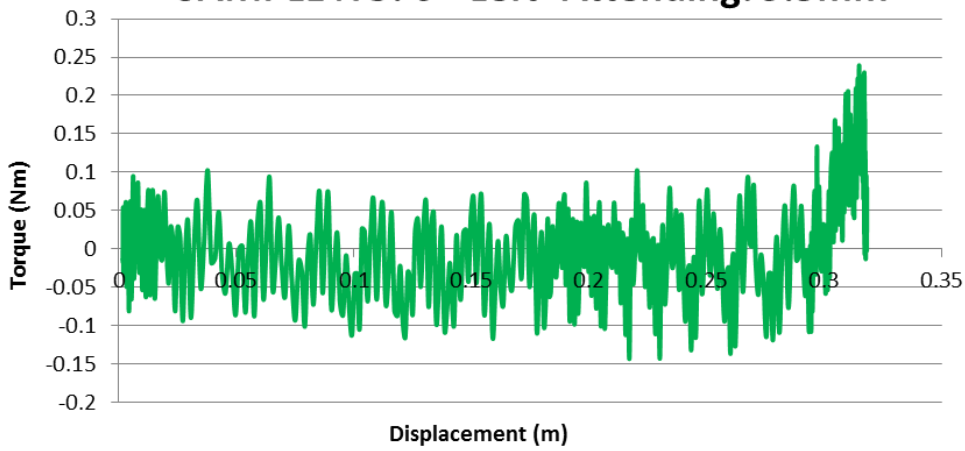
SAMPLE NO. 6 - Left -Attending: 9.5mm



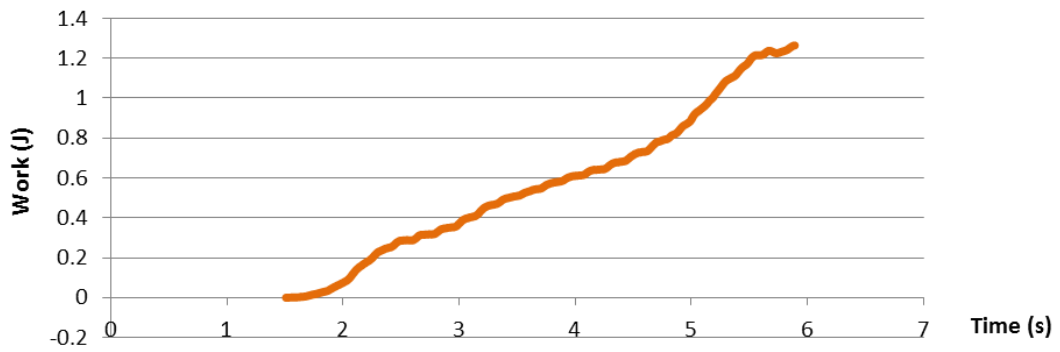
**SAMPLE NO. 6 - Left -Attending: 9.5mm**



**SAMPLE NO. 6 - Left -Attending: 9.5mm**

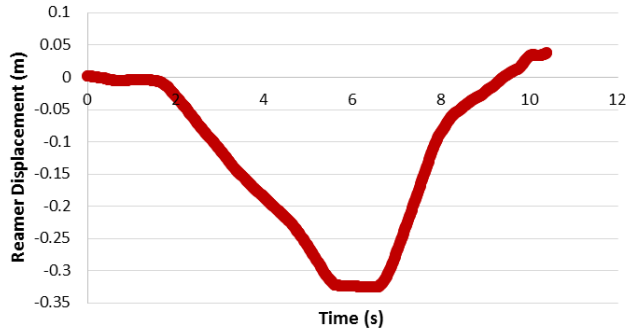


**SAMPLE NO. 6 - Left -Attending: 9.5mm**

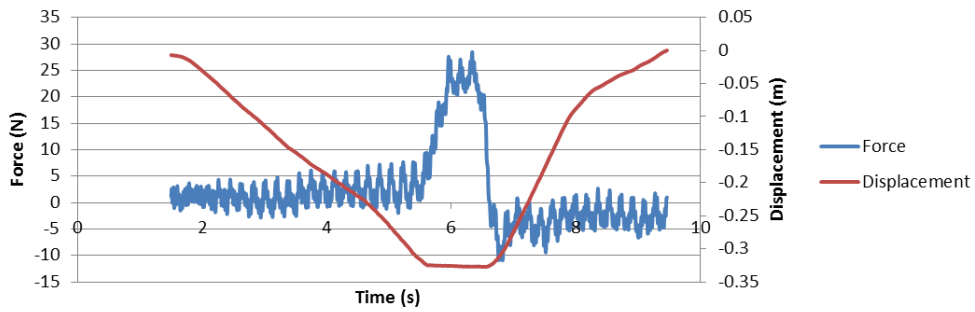


10MM

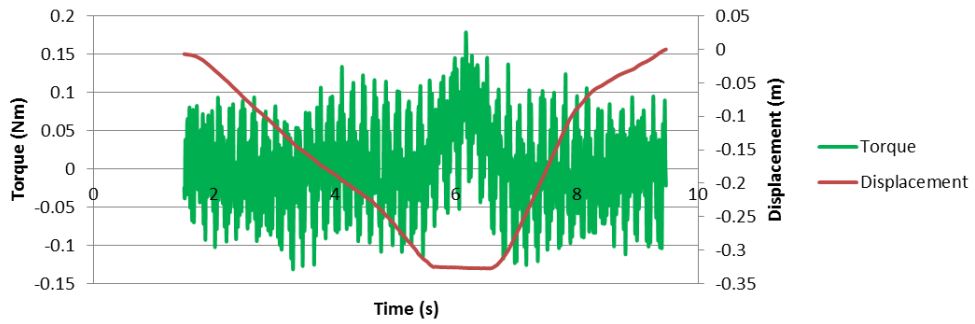
SAMPLE NO. 6 - Left -Attending: 10mm



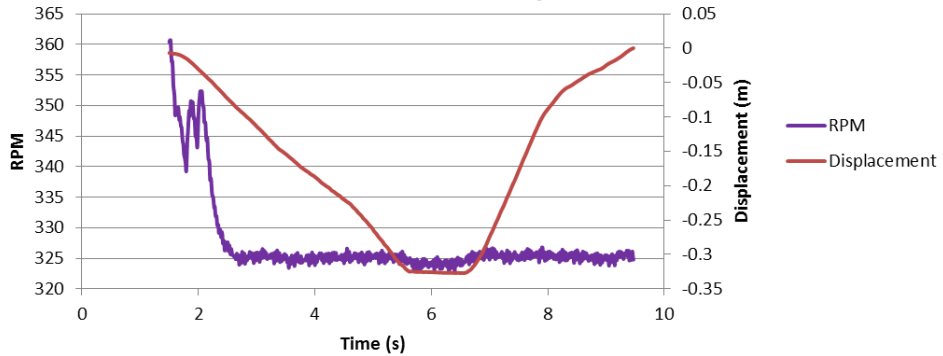
SAMPLE NO. 6 - Left -Attending: 10mm



SAMPLE NO. 6 - Left -Attending: 10mm

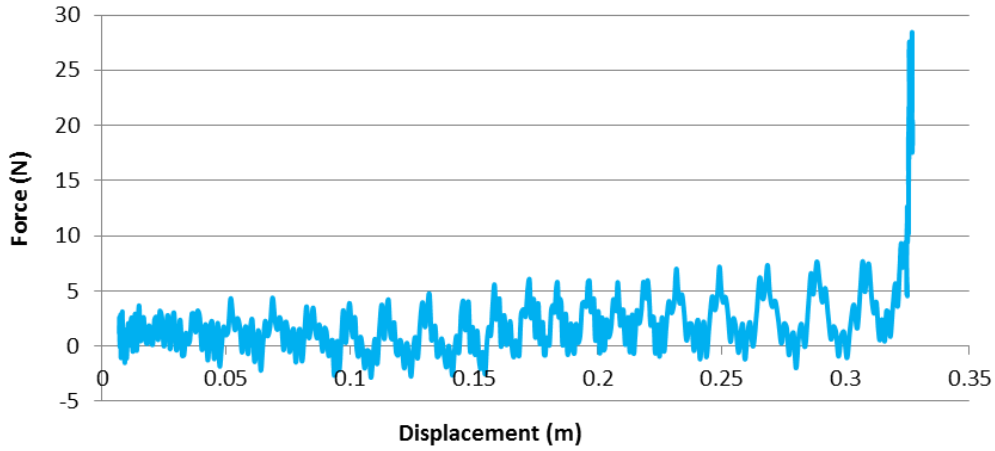


SAMPLE NO. 6 - Left -Attending: 10mm

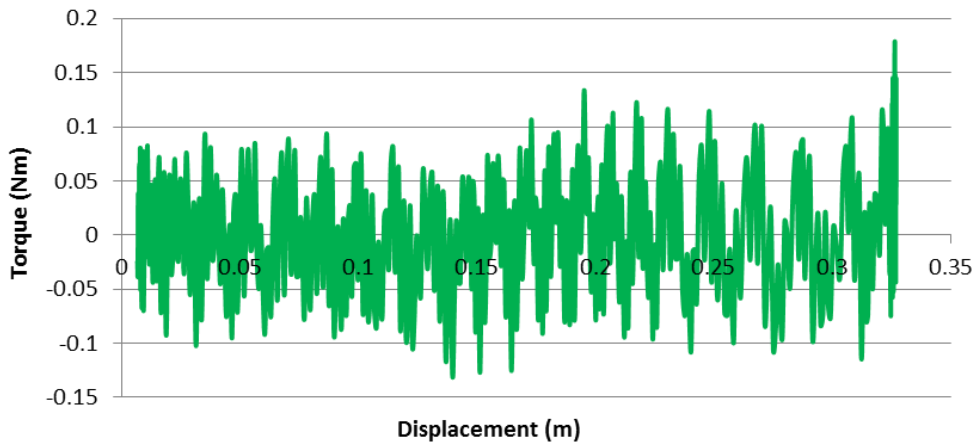




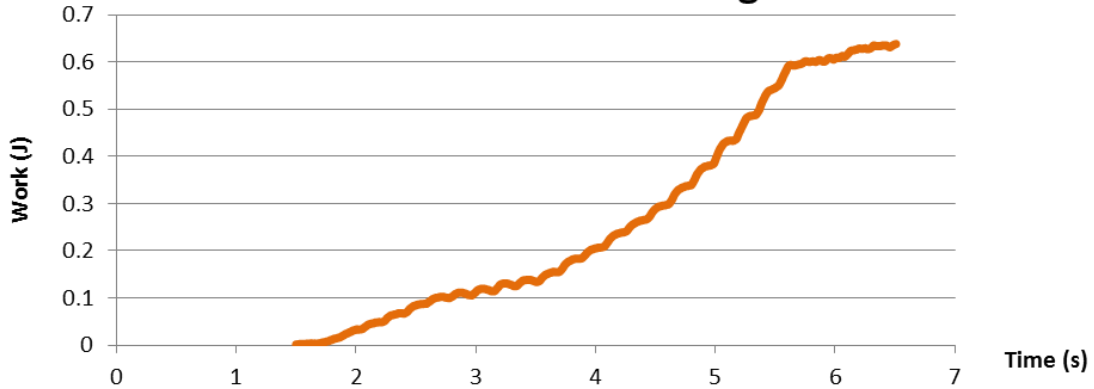
**SAMPLE NO. 6 - Left -Attending: 10mm**



**SAMPLE NO. 6 - Left -Attending: 10mm**

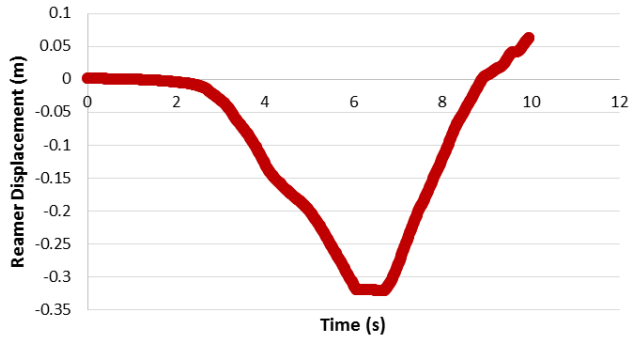


**SAMPLE NO. 6 - Left -Attending: 10mm**

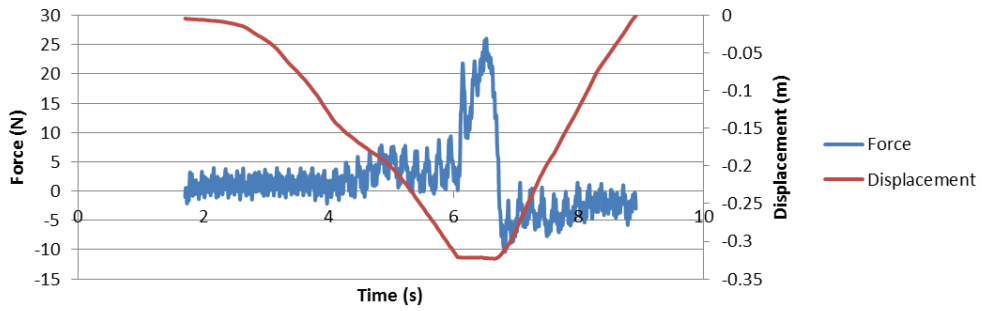


10.5MM

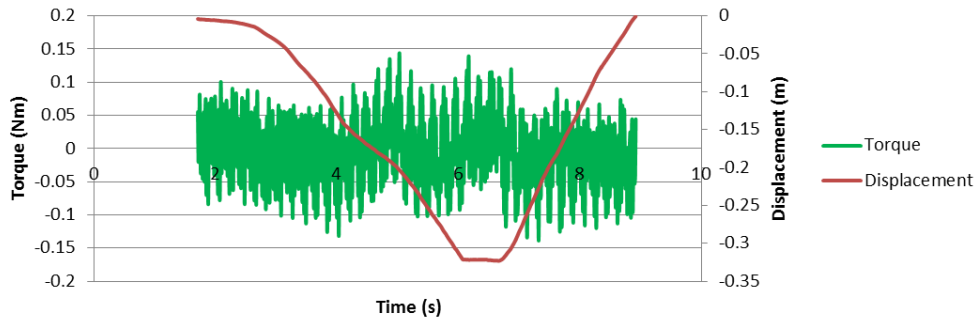
SAMPLE NO. 6 - Left -Attending: 10.5mm



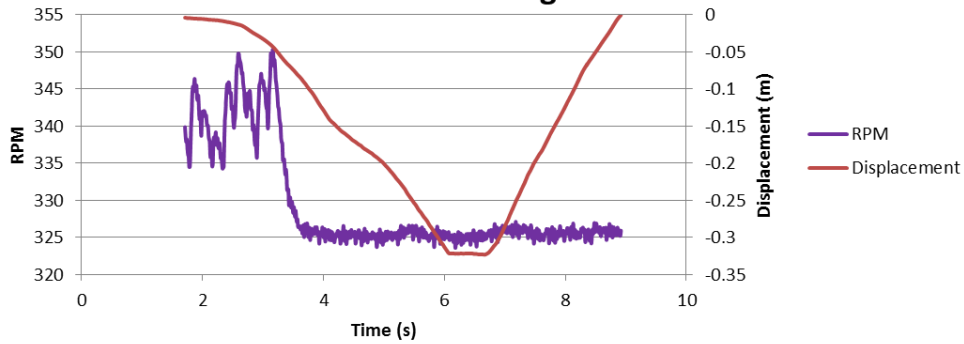
SAMPLE NO. 6 - Left -Attending: 10.5mm



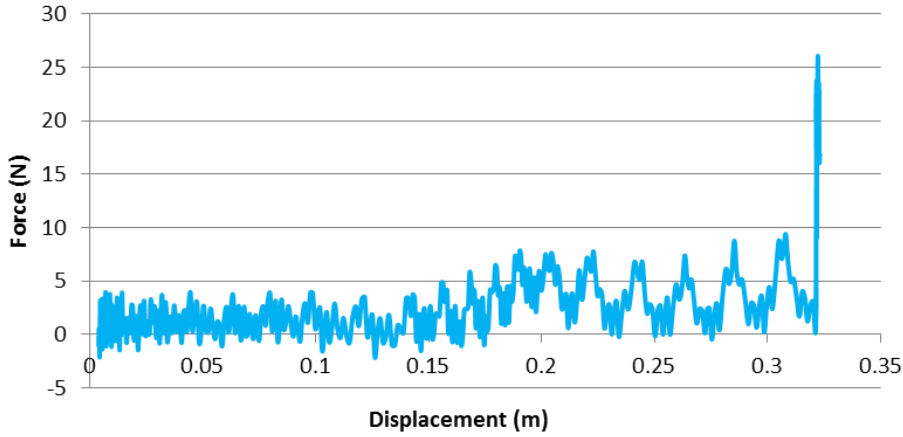
SAMPLE NO. 6 - Left -Attending: 10.5mm



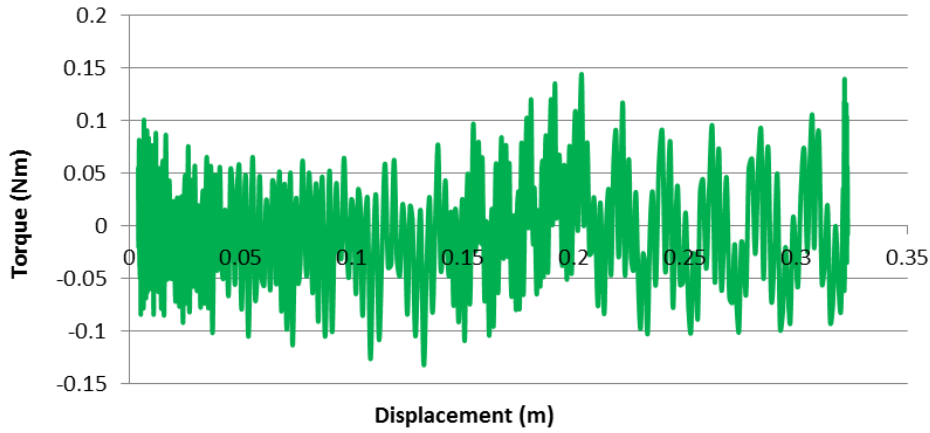
SAMPLE NO. 6 - Left -Attending: 10.5mm



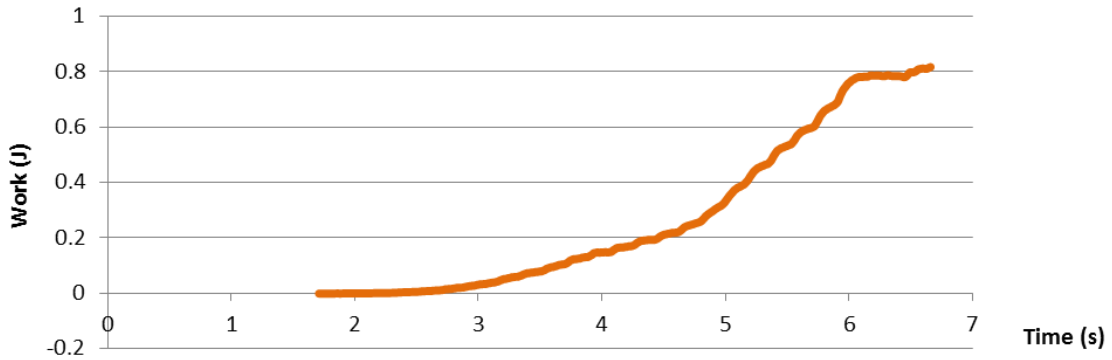
**SAMPLE NO. 6 - Left -Attending: 10.5mm**



**SAMPLE NO. 6 - Left -Attending: 10.5mm**

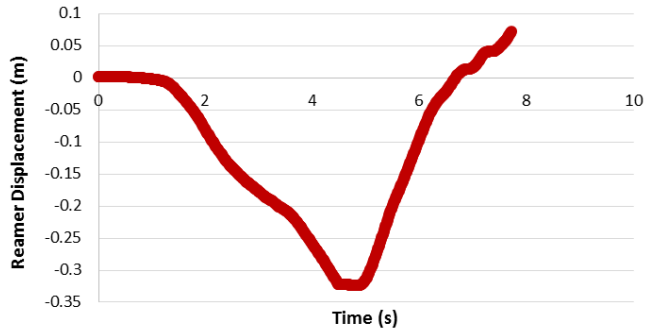


**SAMPLE NO. 6 - Left -Attending: 10.5mm**

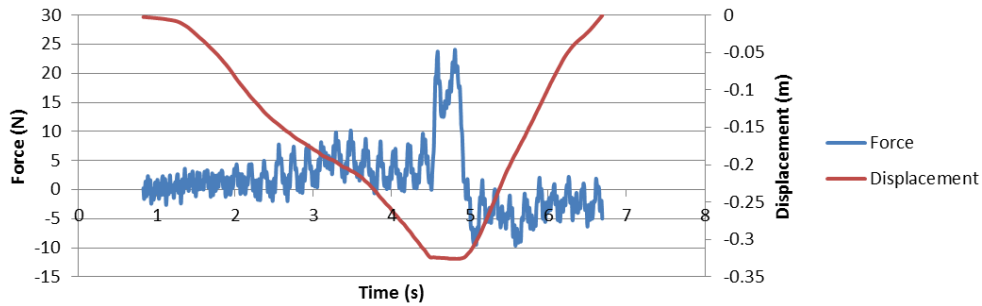


11MM

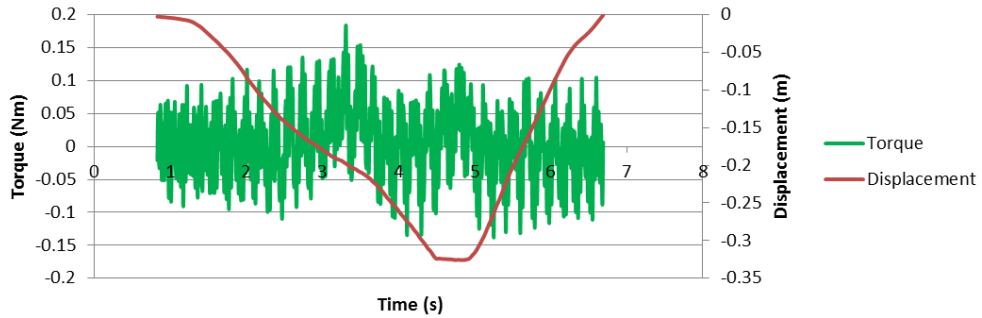
SAMPLE NO. 6 - Left -Attending: 11mm



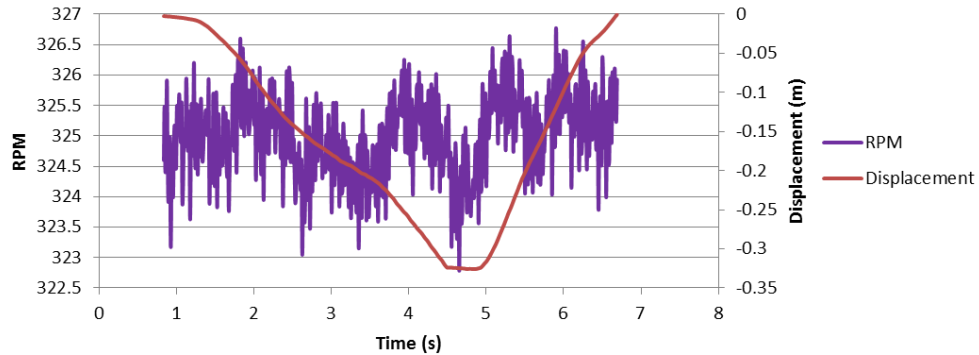
SAMPLE NO. 6 - Left -Attending: 11mm



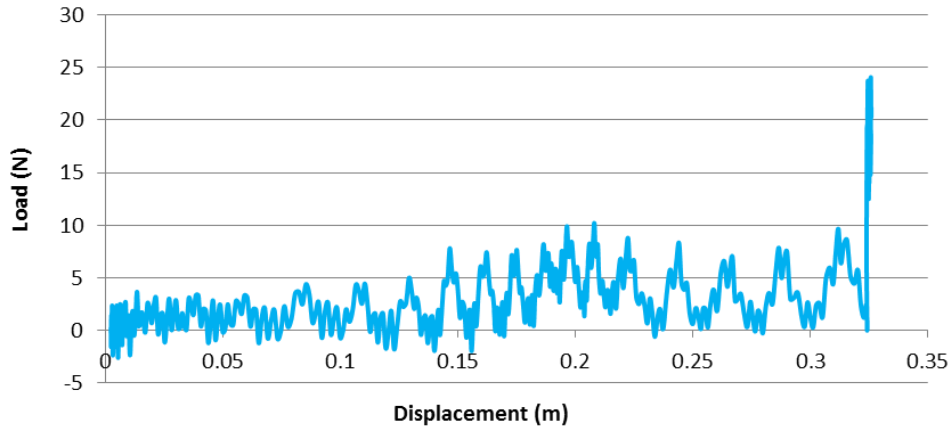
SAMPLE NO. 6 - Left -Attending: 11mm



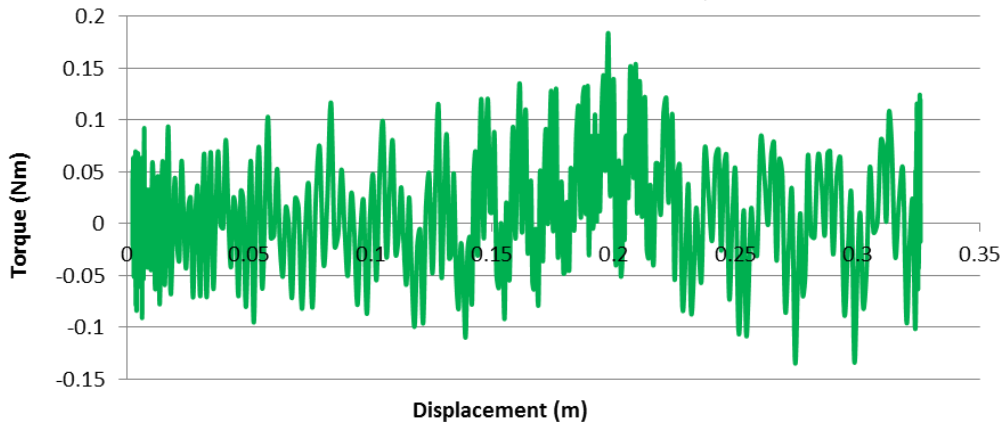
SAMPLE NO. 6 - Left -Attending: 11mm



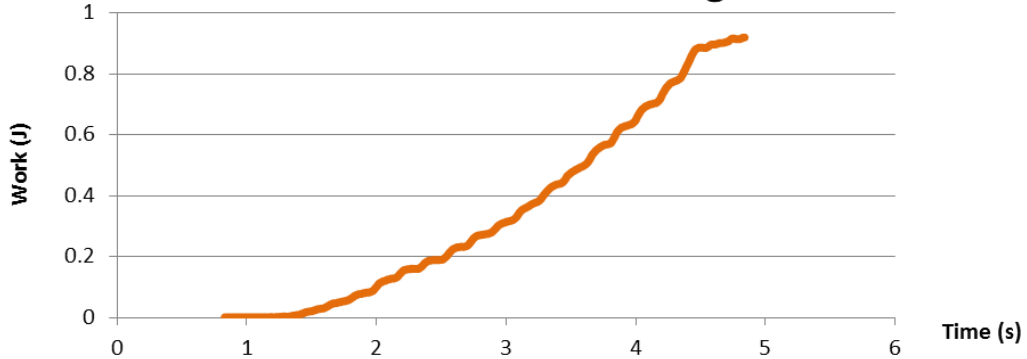
**SAMPLE NO. 6 - Left -Attending: 11mm**



**SAMPLE NO. 6 - Left -Attending: 11mm**

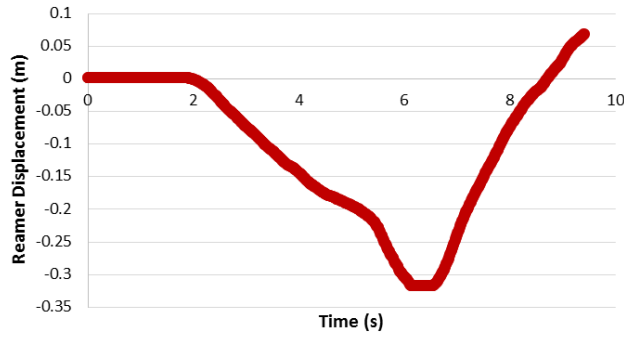


**SAMPLE NO. 6 - Left -Attending: 11mm**

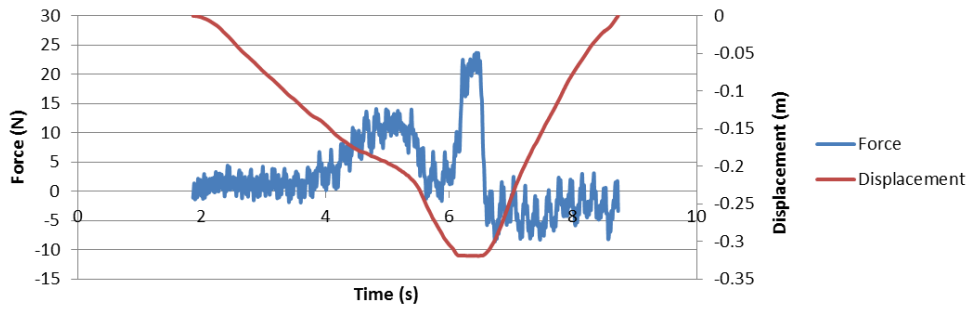


11.5MM

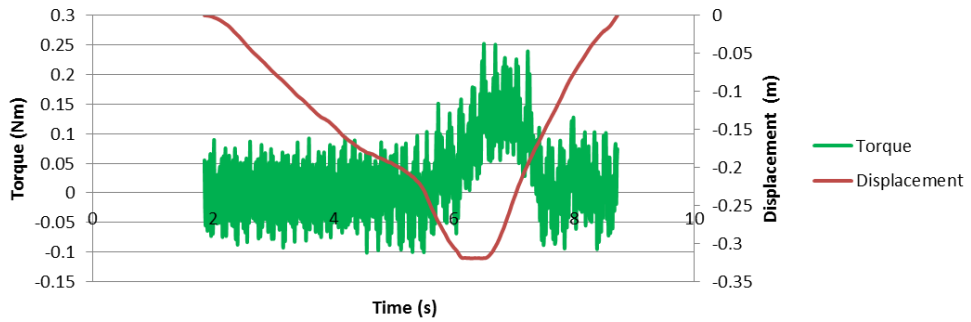
SAMPLE NO. 6 - Left -Attending: 11.5mm



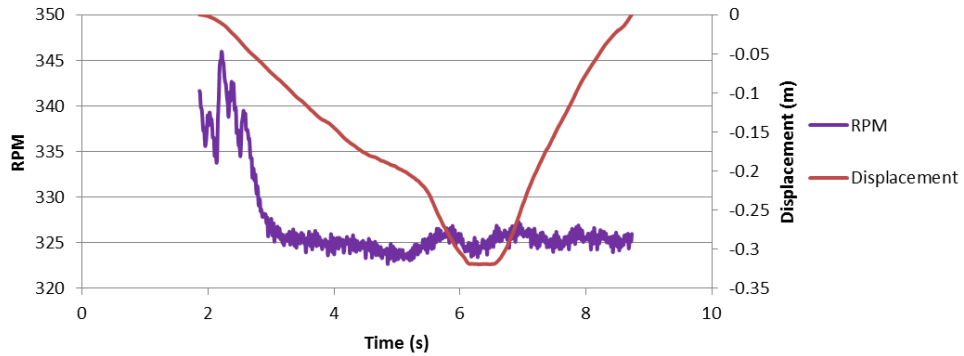
SAMPLE NO. 6 - Left -Attending: 11.5mm



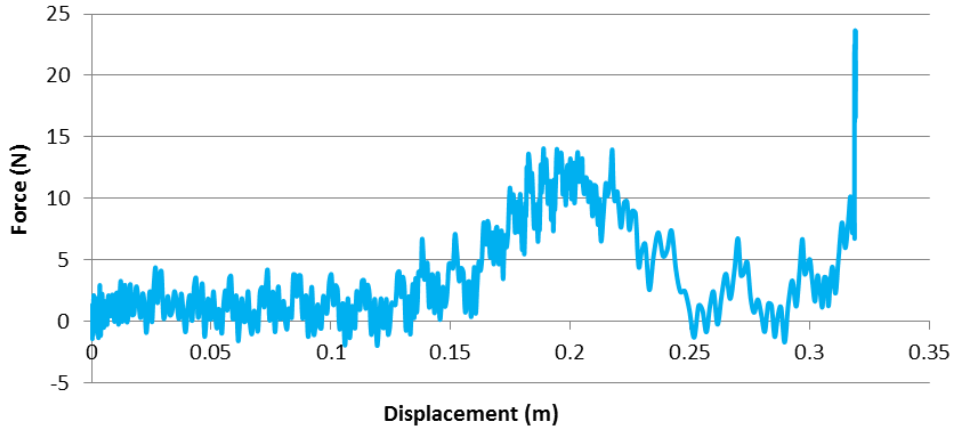
SAMPLE NO. 6 - Left -Attending: 11.5mm



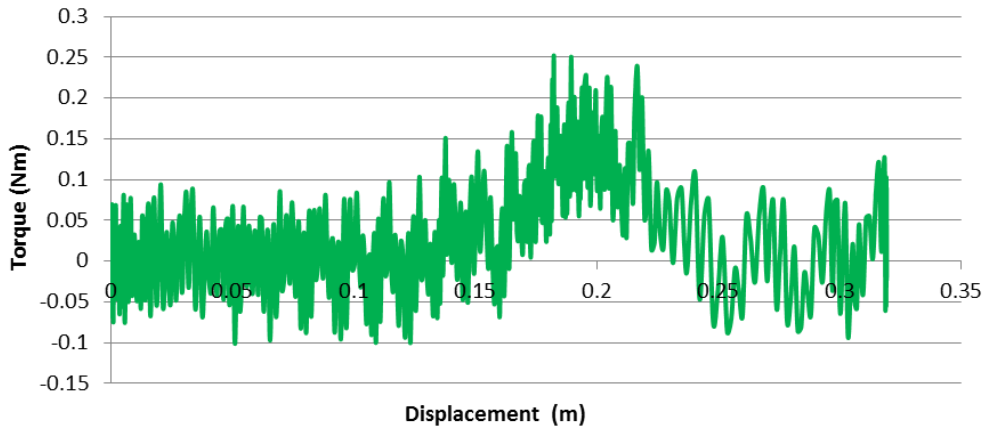
SAMPLE NO. 6 - Left -Attending: 11.5mm



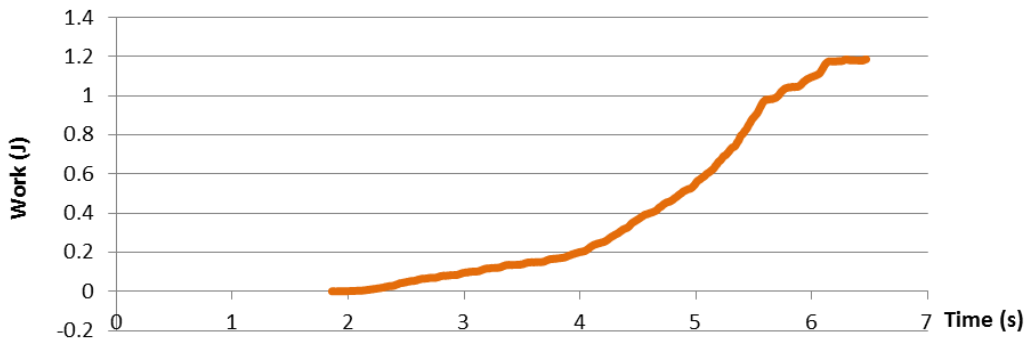
**SAMPLE NO. 6 - Left -Attending: 11.5mm**



**SAMPLE NO. 6 - Left -Attending: 11.5mm**

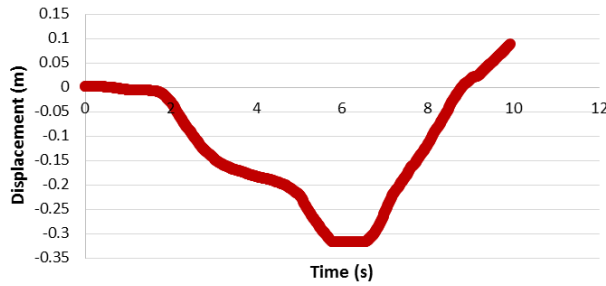


**SAMPLE NO. 6 - Left -Attending: 11.5mm**

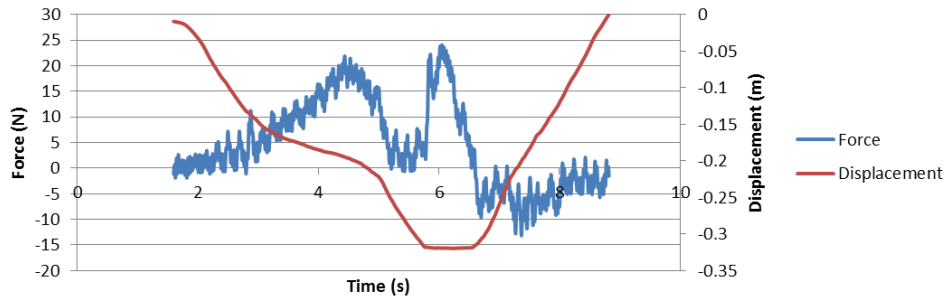


12MM

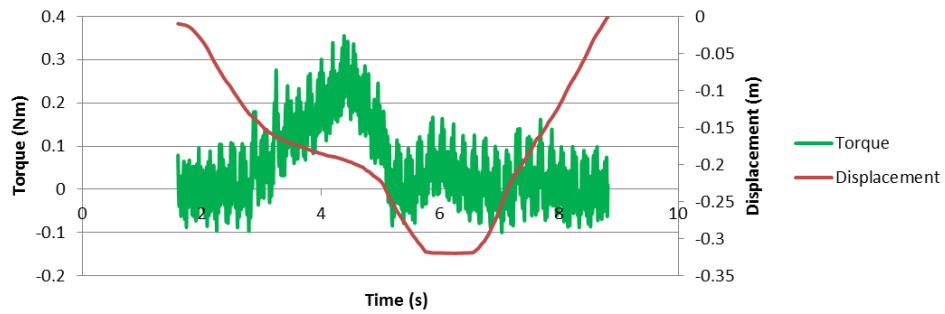
**SAMPLE NO. 6 - Left -Attending: 12mm CHATTER**



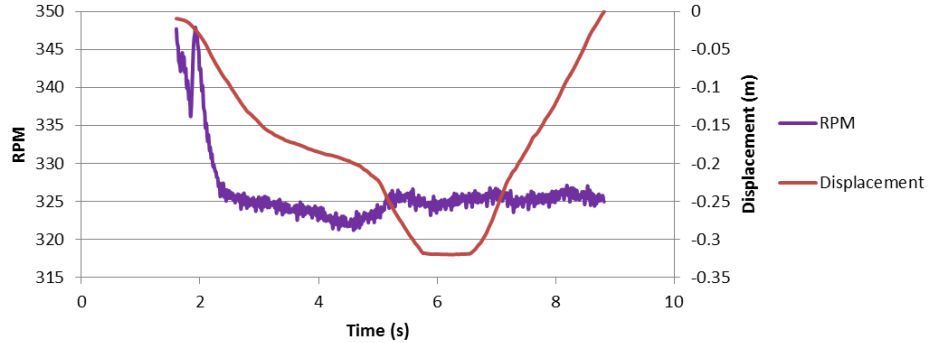
**SAMPLE NO. 6 - Left -Attending: 12mm CHATTER**



**SAMPLE NO. 6 - Left -Attending: 12mm CHATTER**

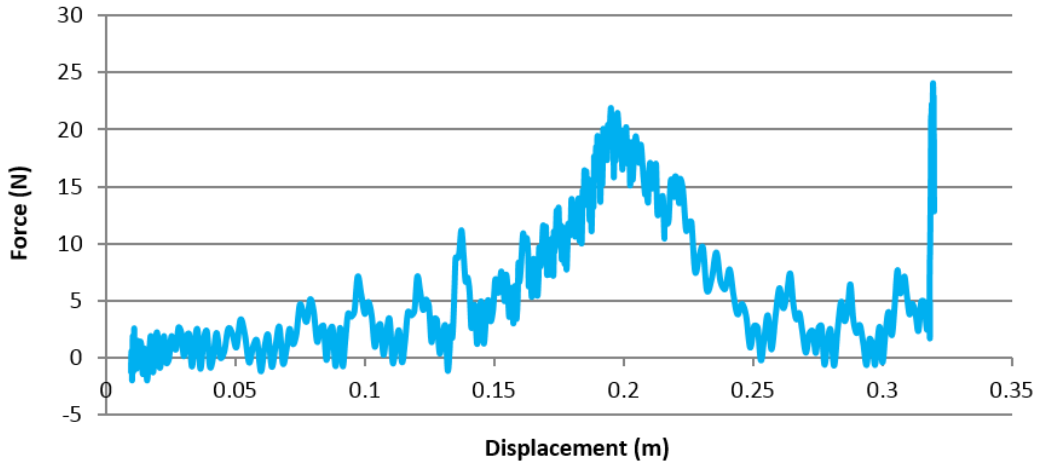


**SAMPLE NO. 6 - Left -Attending: 12mm CHATTER**

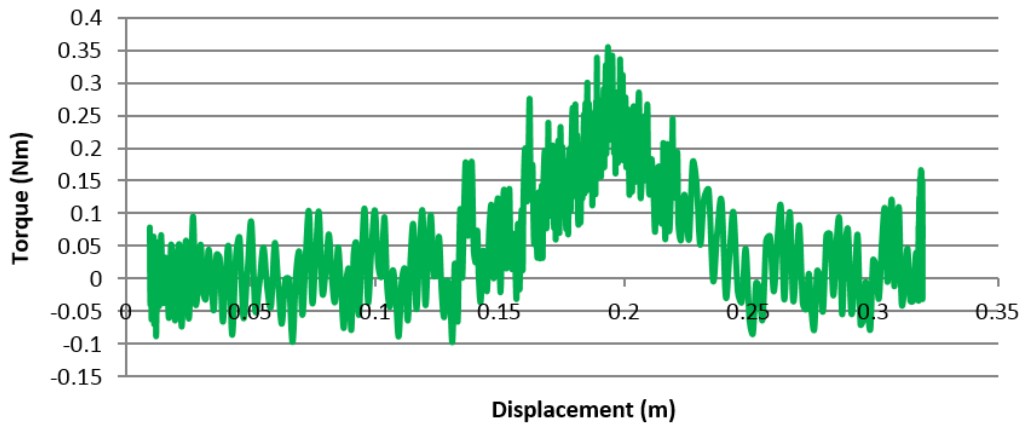




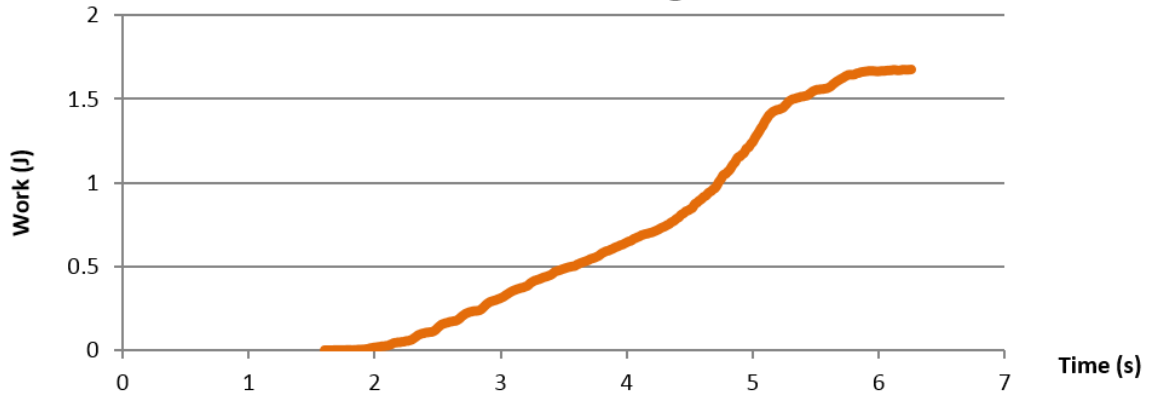
**SAMPLE NO. 6 - Left -Attending: 12mm CHATTER**



**SAMPLE NO. 6 - Left -Attending: 12mm CHATTER**

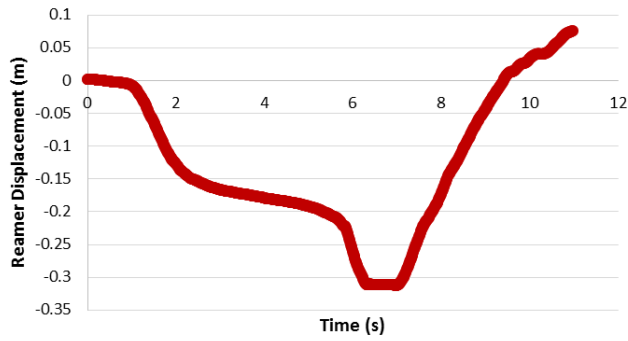


**SAMPLE NO. 6 - Left -Attending: 12mm CHATTER**

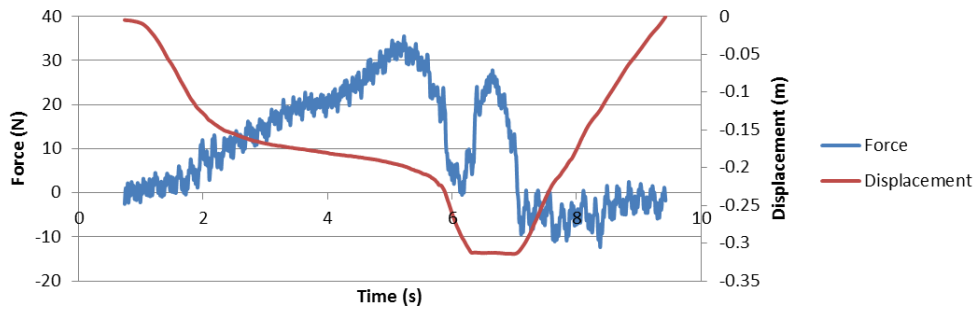


12.5MM

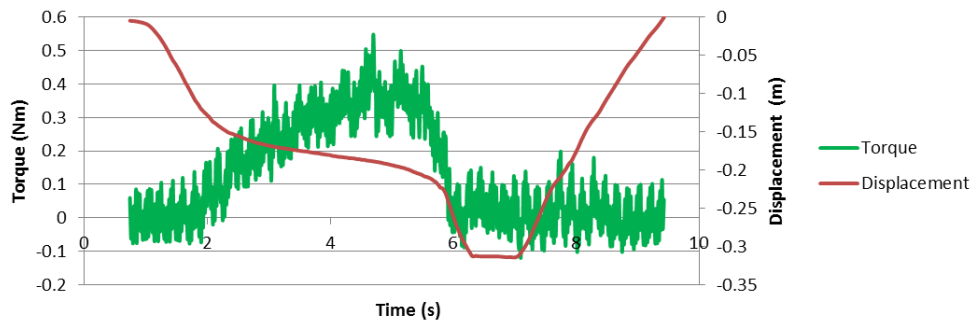
SAMPLE NO. 6 - Left -Attending: 12.5mm



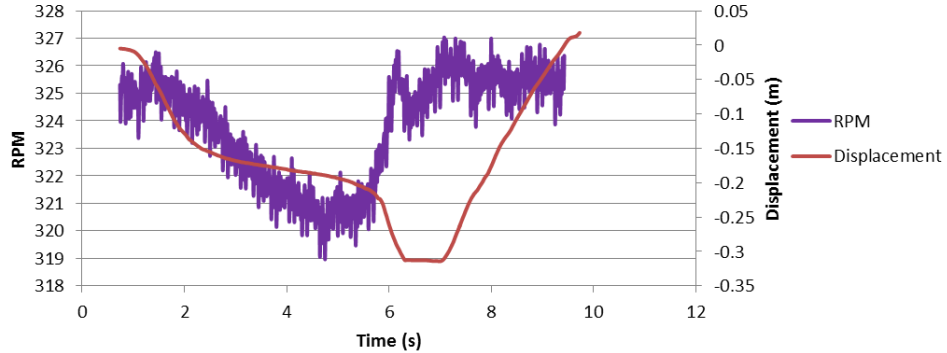
SAMPLE NO. 6 - Left -Attending: 12.5mm



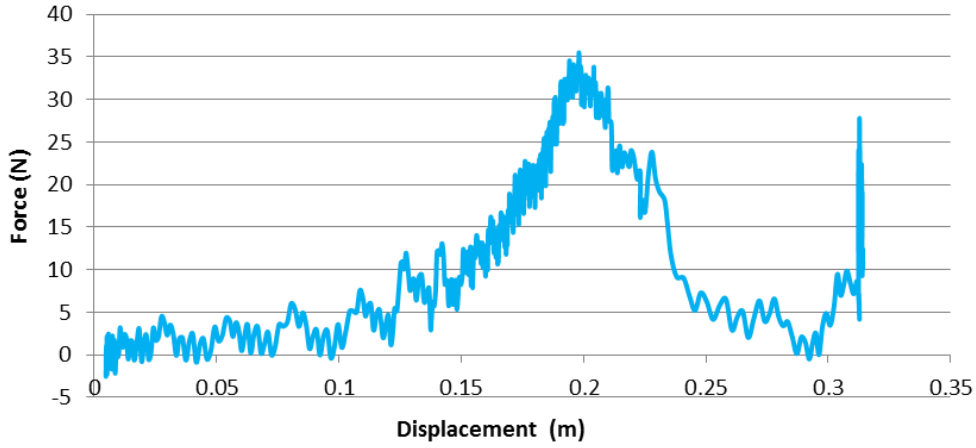
SAMPLE NO. 6 - Left -Attending: 12.5mm



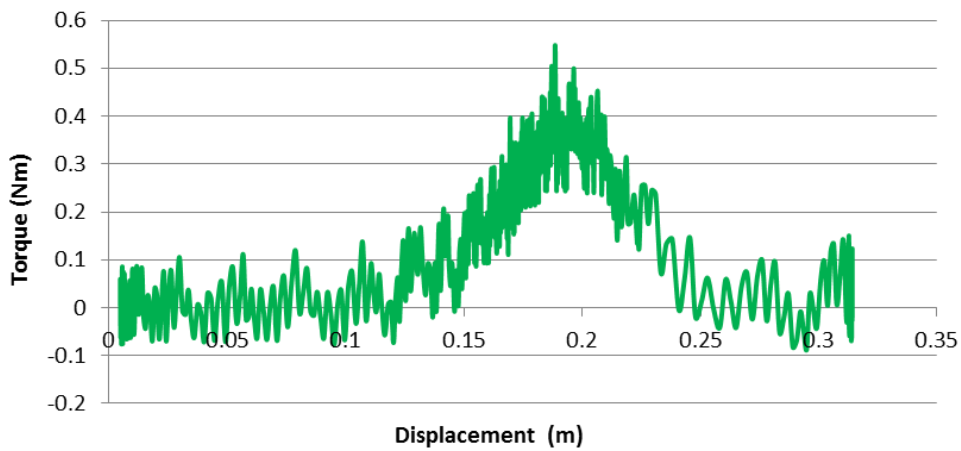
SAMPLE NO. 6 - Left -Attending: 12.5mm



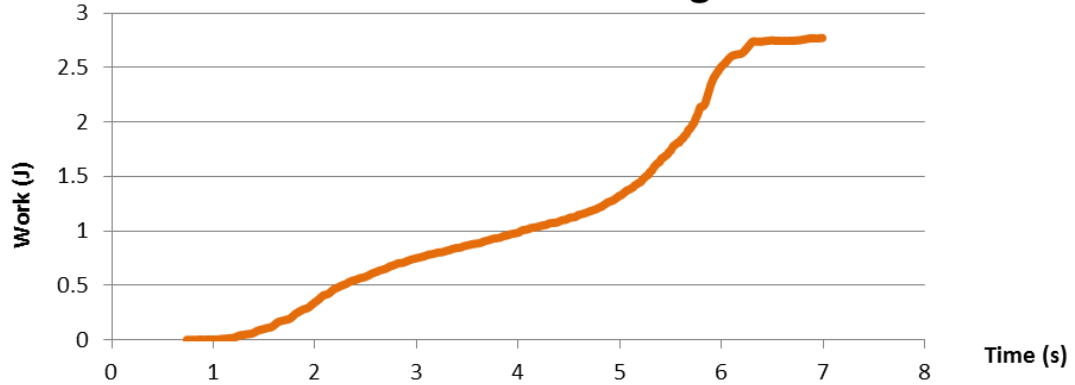
**SAMPLE NO. 6 - Left -Attending: 12.5mm**



**SAMPLE NO. 6 - Left -Attending: 12.5mm**

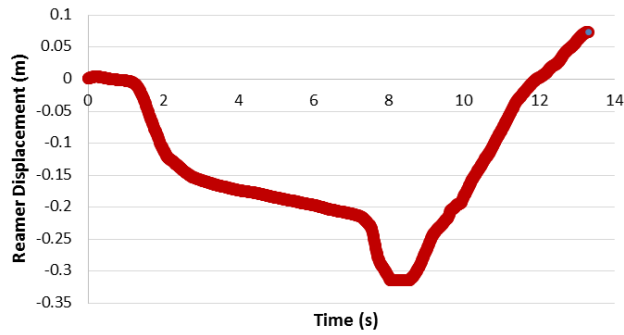


**SAMPLE NO. 6 - Left -Attending: 12.5mm**

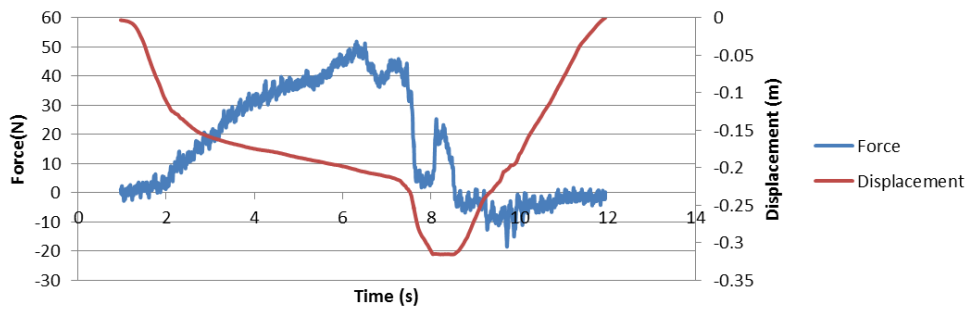


13MM

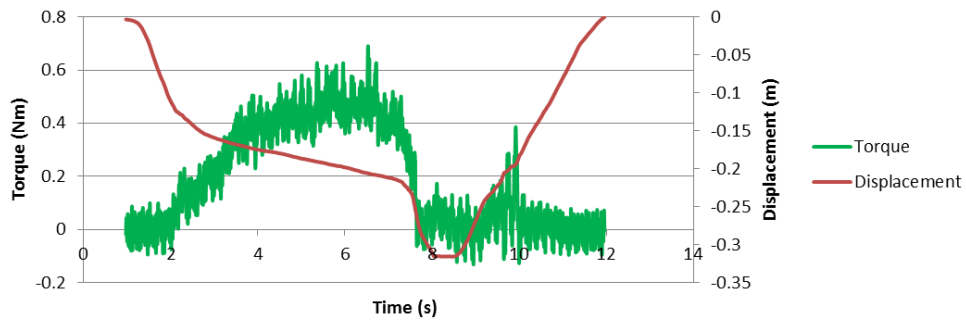
SAMPLE NO. 6 - Left -Attending: 13mm



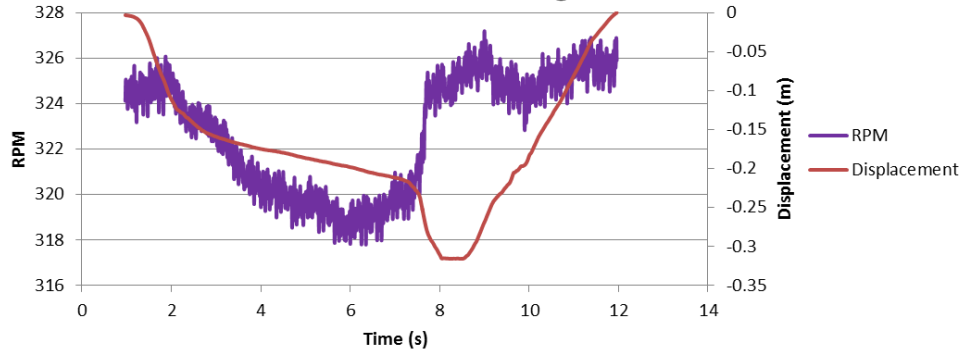
SAMPLE NO. 6 - Left -Attending: 13mm



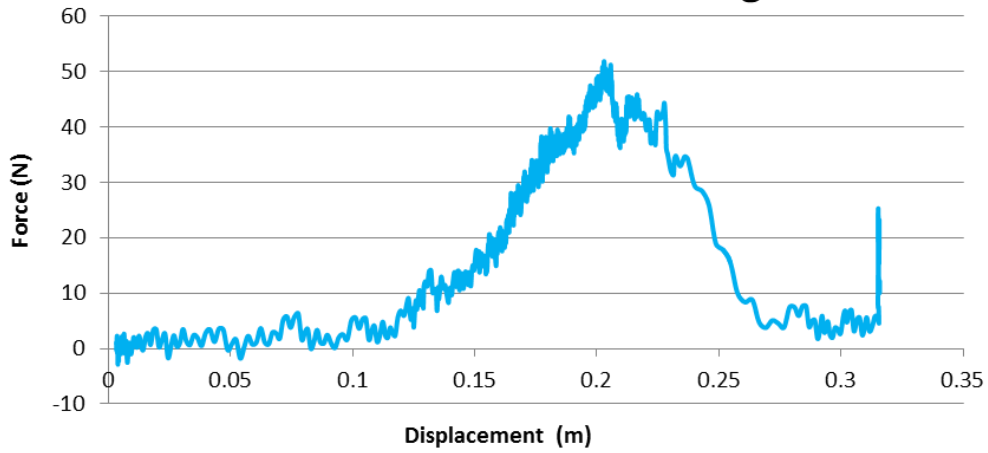
SAMPLE NO. 6 - Left -Attending: 13mm



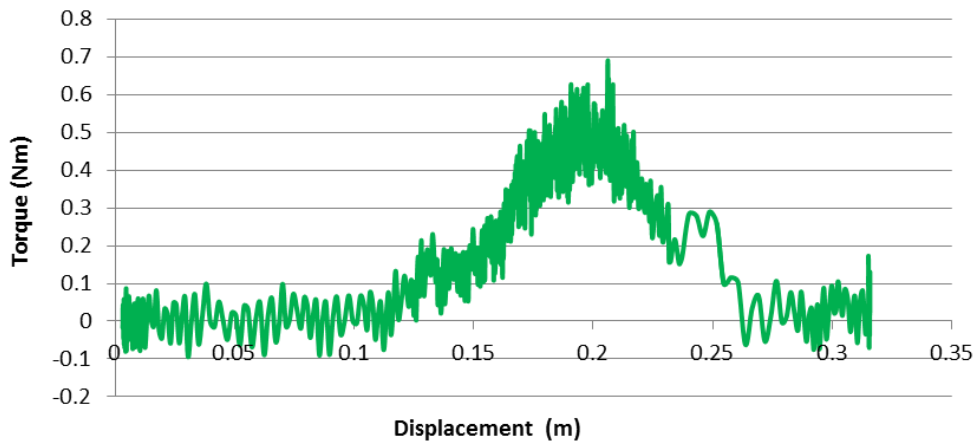
SAMPLE NO. 6 - Left -Attending: 13mm



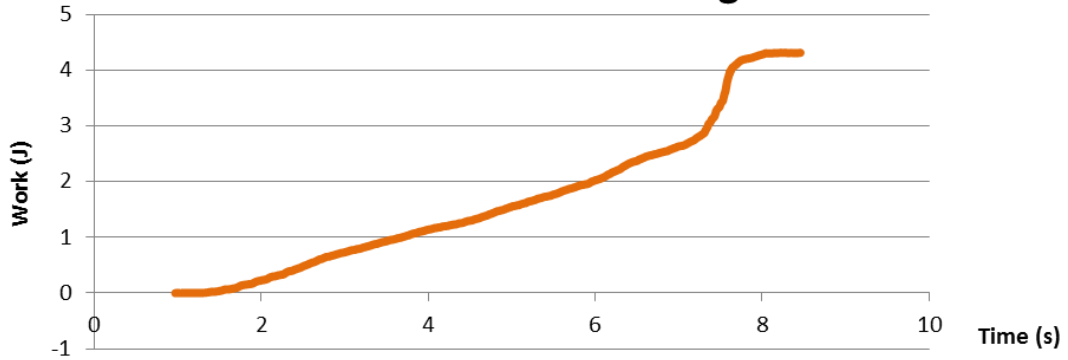
**SAMPLE NO. 6 - Left -Attending: 13mm**



**SAMPLE NO. 6 - Left -Attending: 13mm**

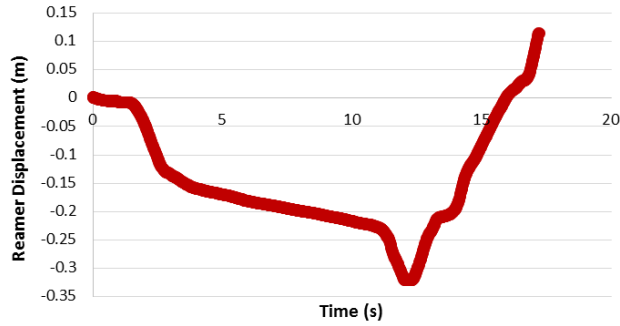


**SAMPLE NO. 6 - Left -Attending: 13mm**

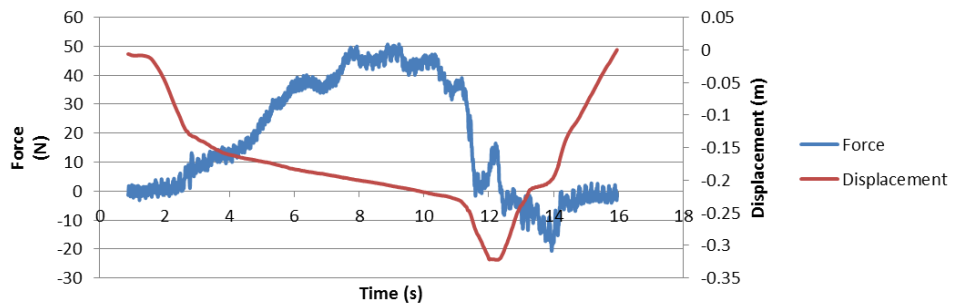


13.5MM

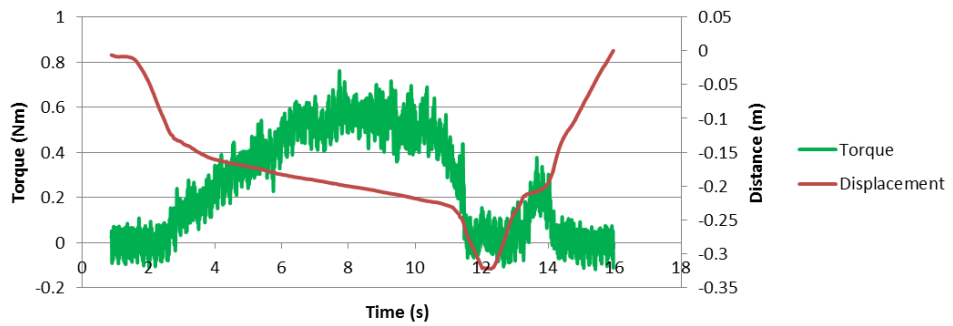
SAMPLE NO. 6 - Left -Attending: 13.5mm



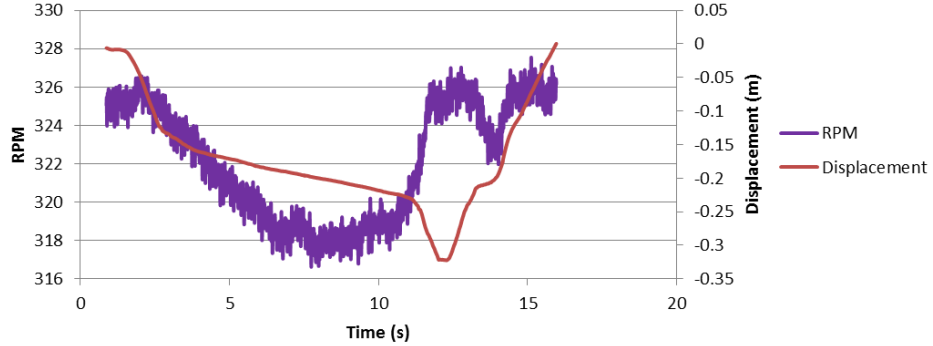
SAMPLE NO. 6 - Left -Attending: 13.5mm



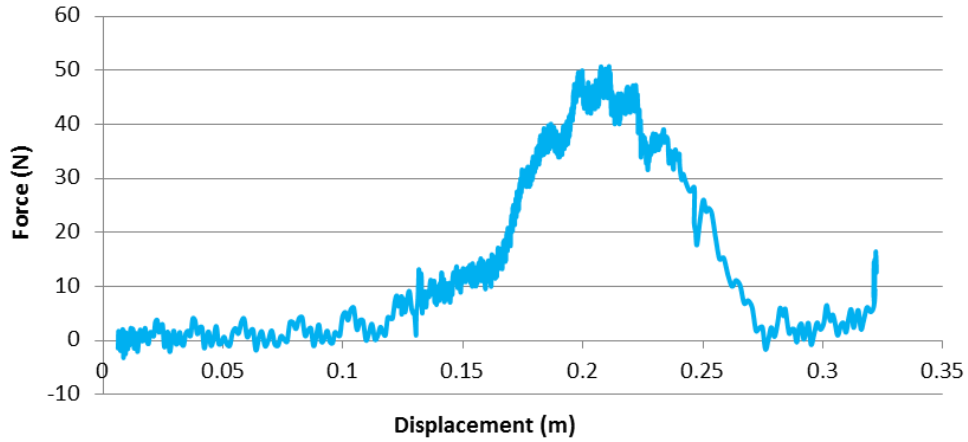
SAMPLE NO. 6 - Left -Attending: 13.5mm



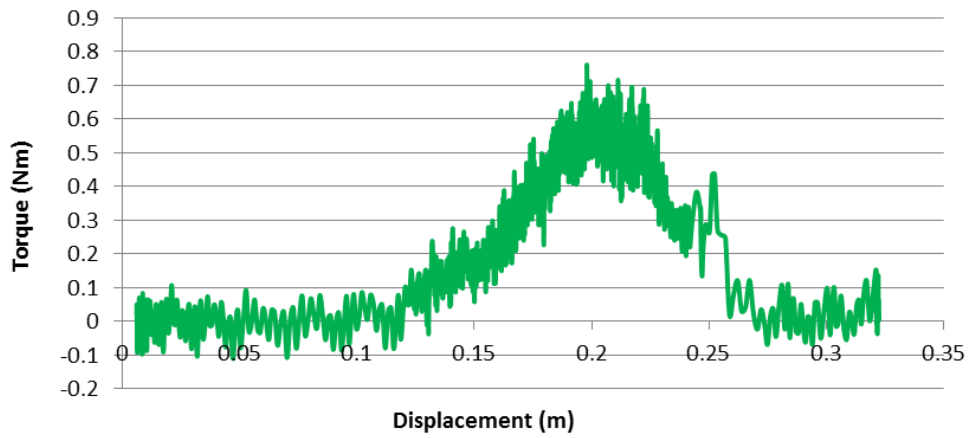
SAMPLE NO. 6 - Left -Attending: 13.5mm



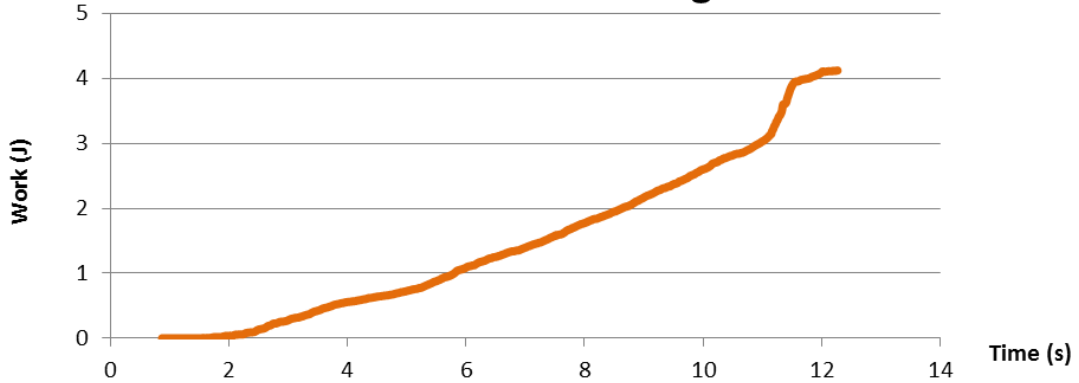
**SAMPLE NO. 6 - Left -Attending: 13.5mm**



**SAMPLE NO. 6 - Left -Attending: 13.5mm**



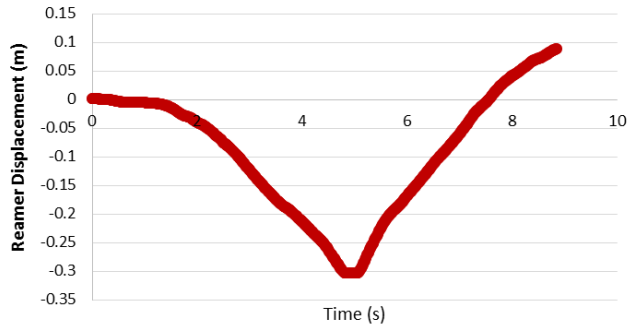
**SAMPLE NO. 6 - Left -Attending: 13.5mm**



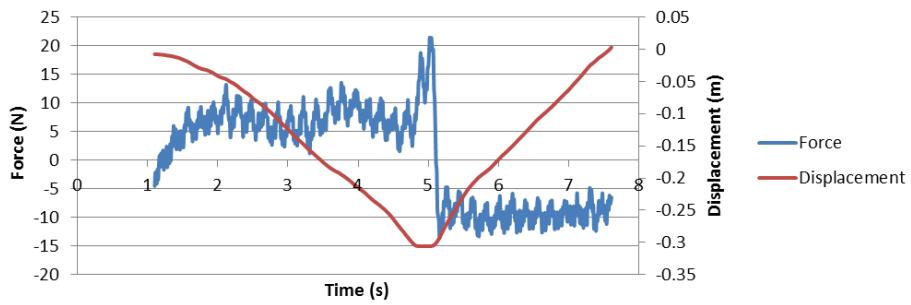
RIGHT: RESIDENT

9MM

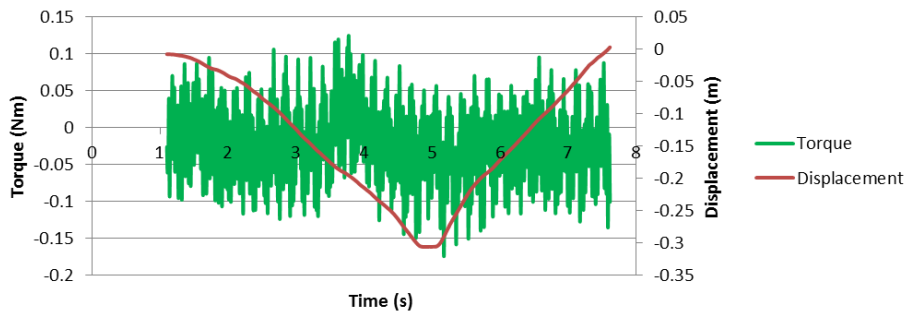
**SAMPLE NO. 6 - Right - Resident: 9mm**



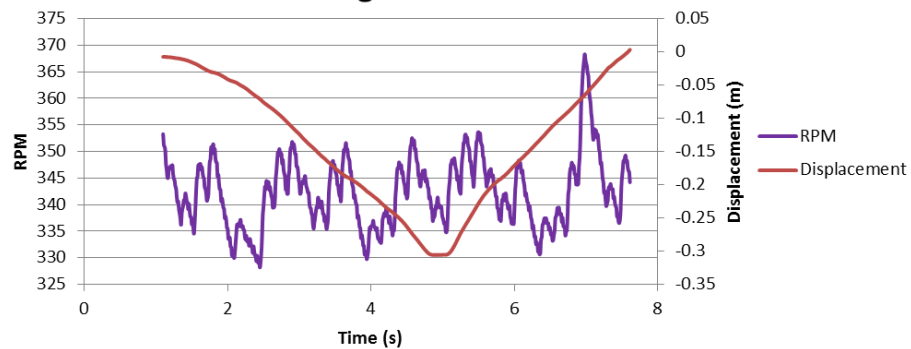
**SAMPLE NO. 6 - Right - Resident: 9mm**



**SAMPLE NO. 6 - Right - Resident: 9mm**

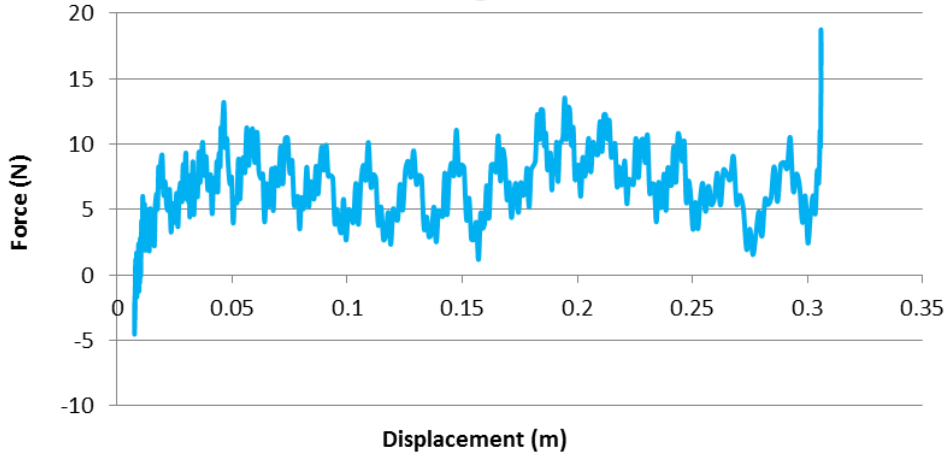


**SAMPLE NO. 6 - Right - Resident: 9mm**

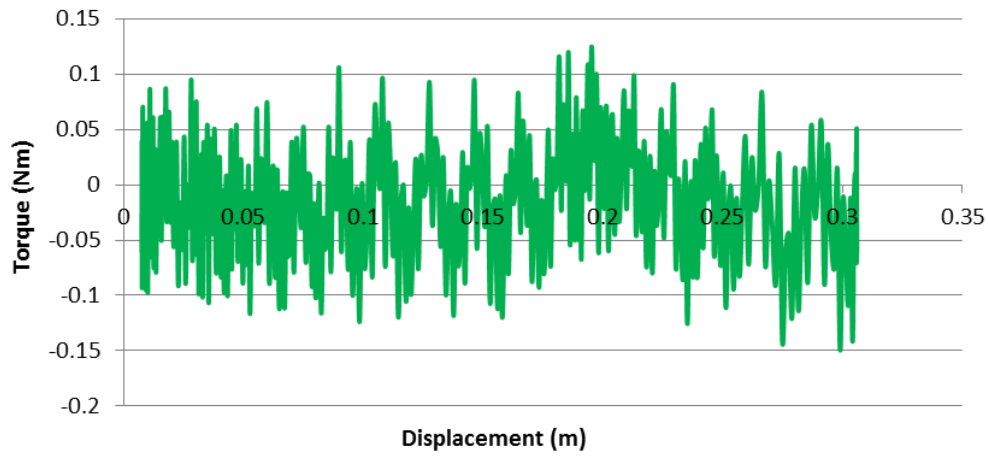




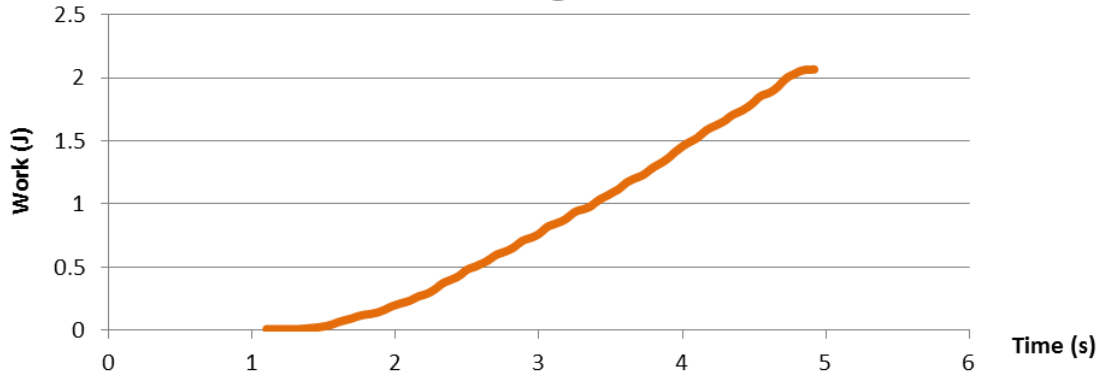
**SAMPLE NO. 6 - Right - Resident: 9mm**



**SAMPLE NO. 6 - Right - Resident: 9mm**

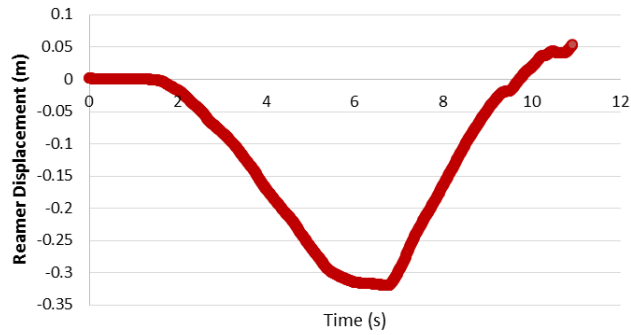


**SAMPLE NO. 6 - Right - Resident: 9mm**

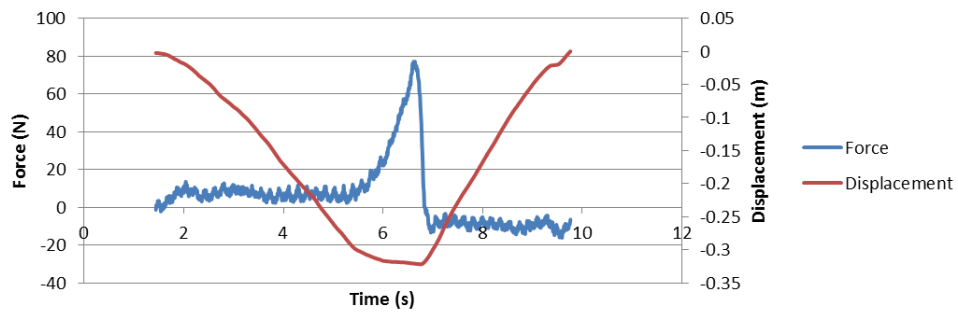


9.5MM

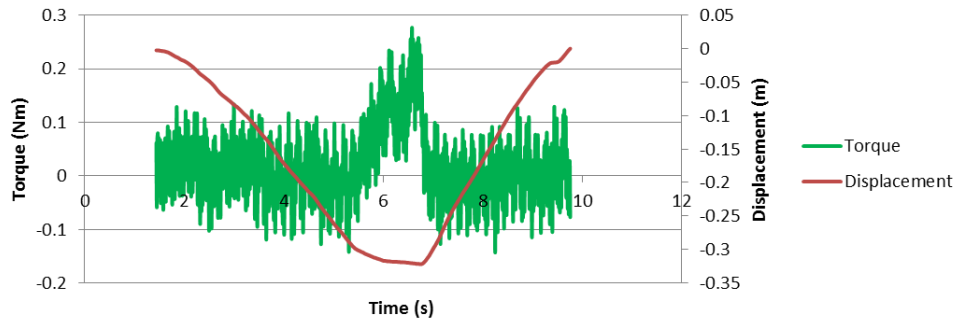
**SAMPLE NO. 6 - Right - Resident: 9.5mm**



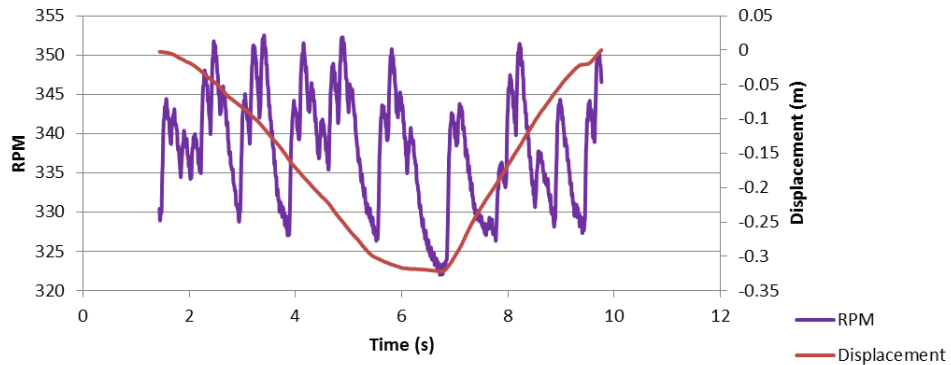
**SAMPLE NO. 6 - Right - Resident: 9.5mm**



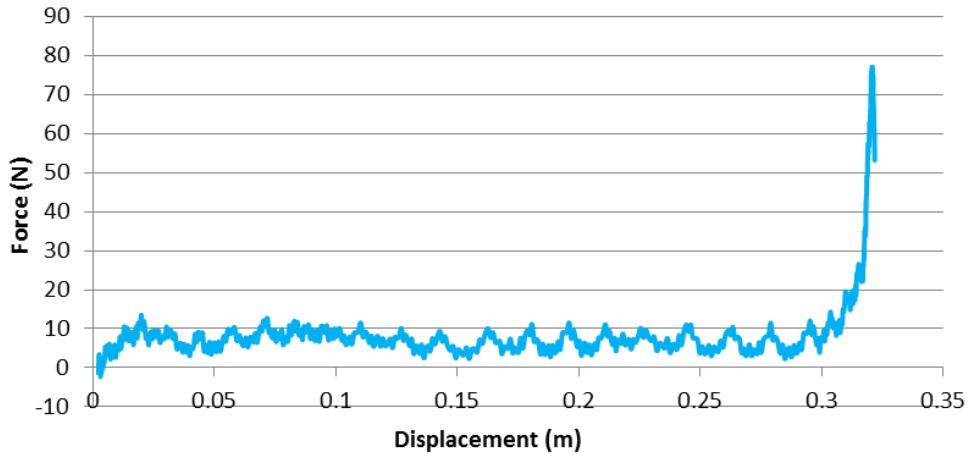
**SAMPLE NO. 6 - Right - Resident: 9.5mm**



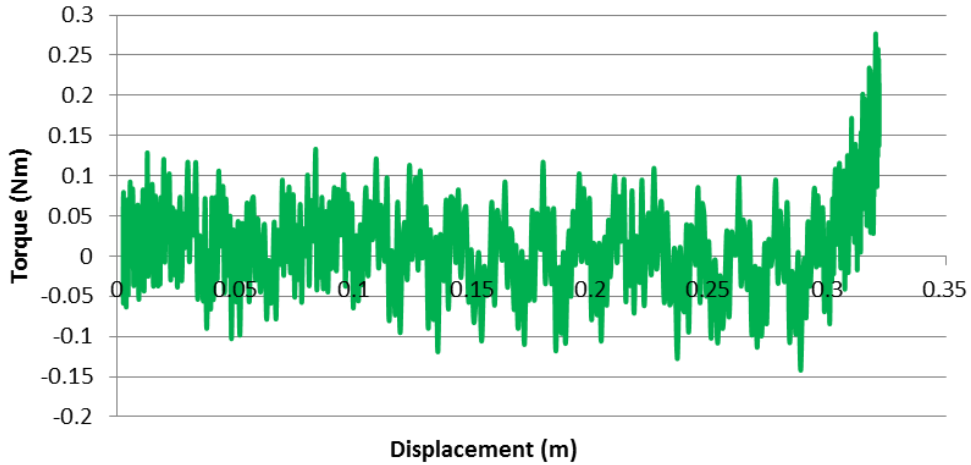
**SAMPLE NO. 6 - Right - Resident: 9.5mm**



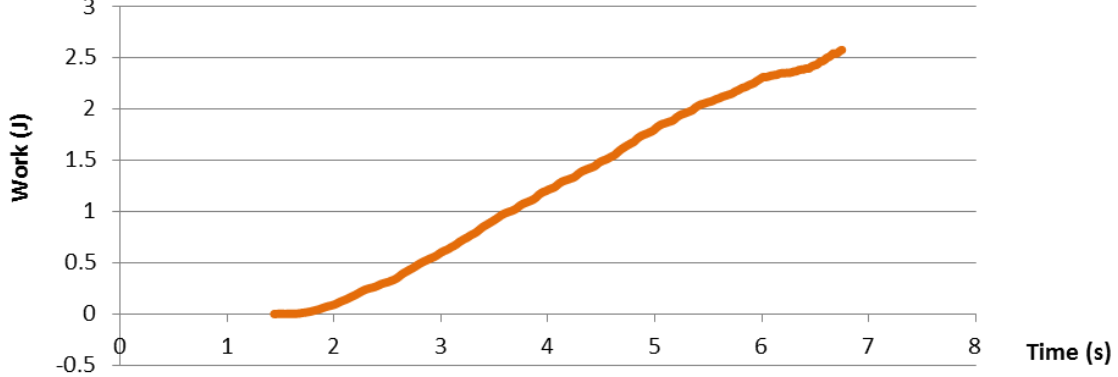
**SAMPLE NO. 6 - Right - Resident: 9.5mm**



**SAMPLE NO. 6 - Right - Resident: 9.5mm**

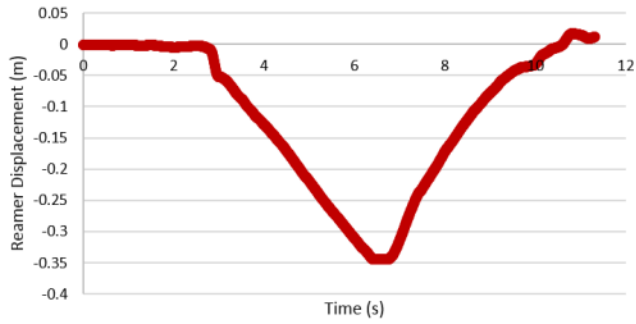


**SAMPLE NO. 6 - Right - Resident: 9.5mm**

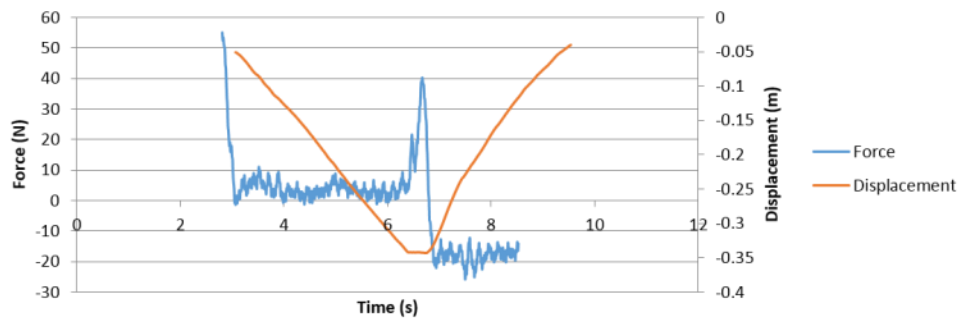


10MM

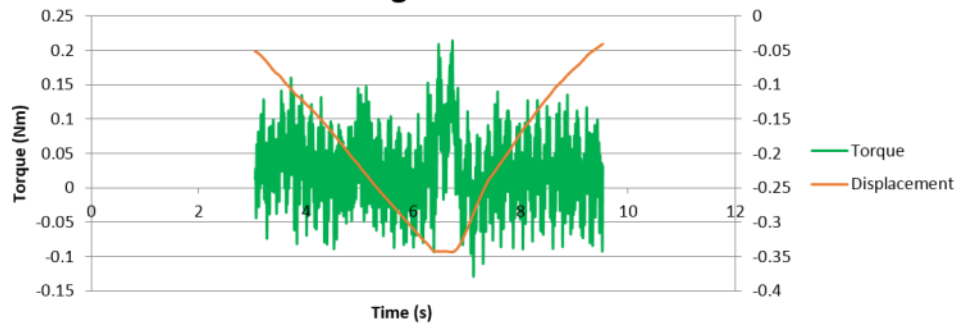
**SAMPLE NO. 6 - Right - Resident: 10mm**



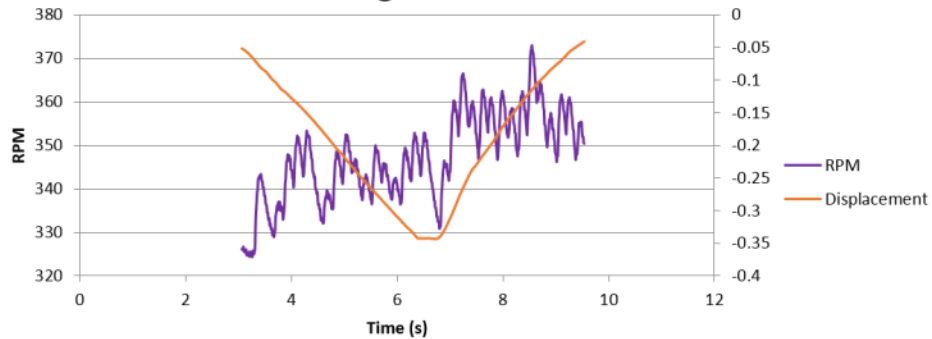
**SAMPLE NO. 6 - Right - Resident: 10mm**



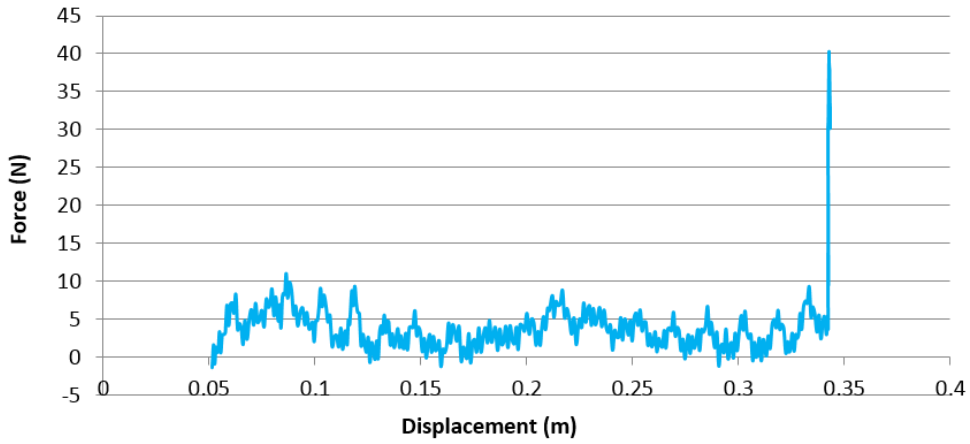
**SAMPLE NO. 6 - Right - Resident: 10mm**



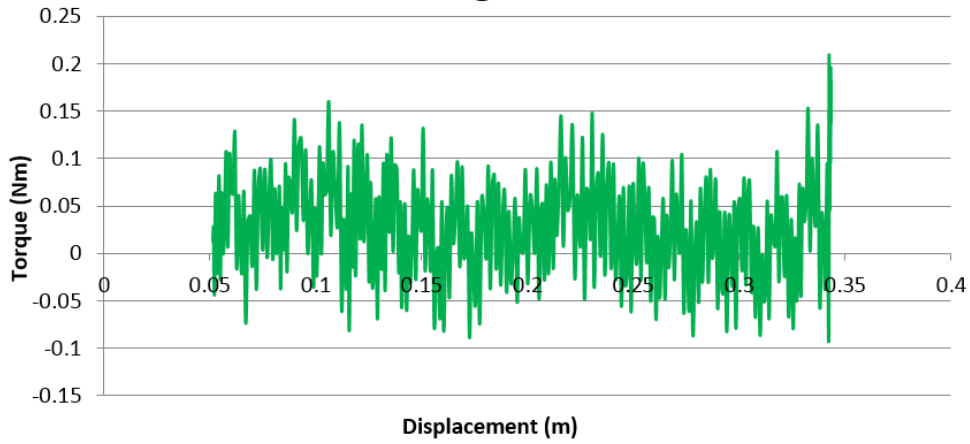
**SAMPLE NO. 6 - Right - Resident: 10mm**



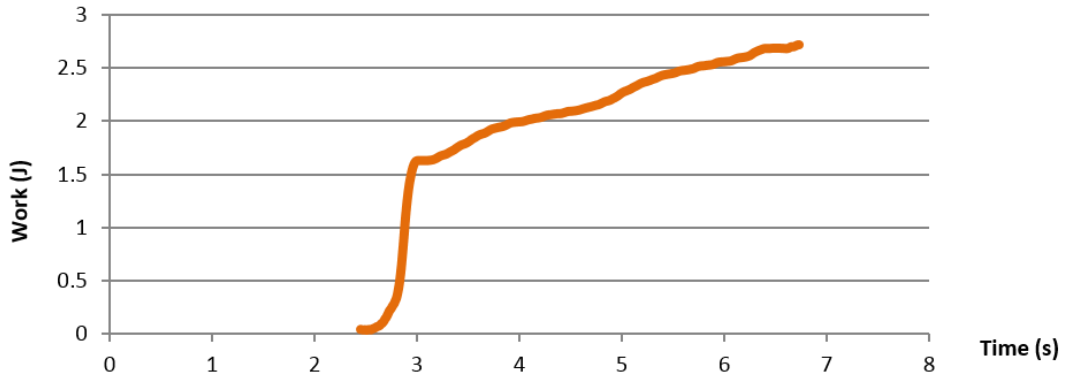
**SAMPLE NO. 6 - Right - Resident: 10mm**



**SAMPLE NO. 6 - Right - Resident: 10mm**

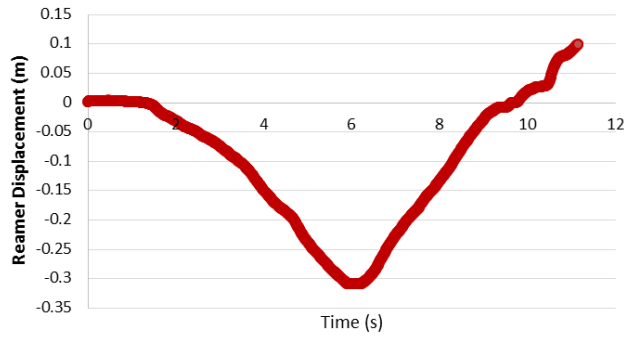


**SAMPLE NO. 6 - Right - Resident: 10mm**

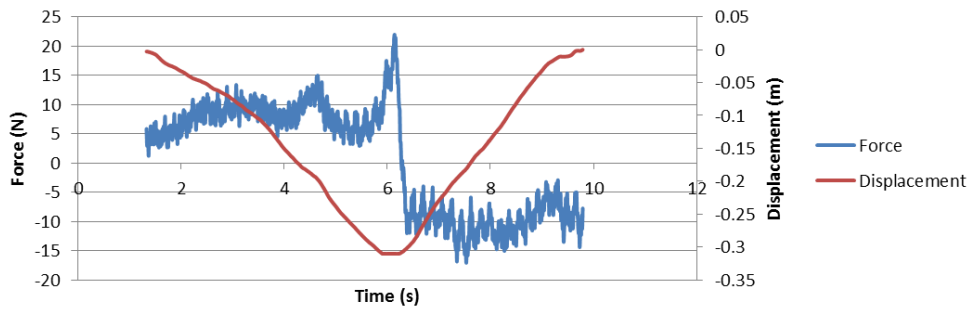


10.5MM

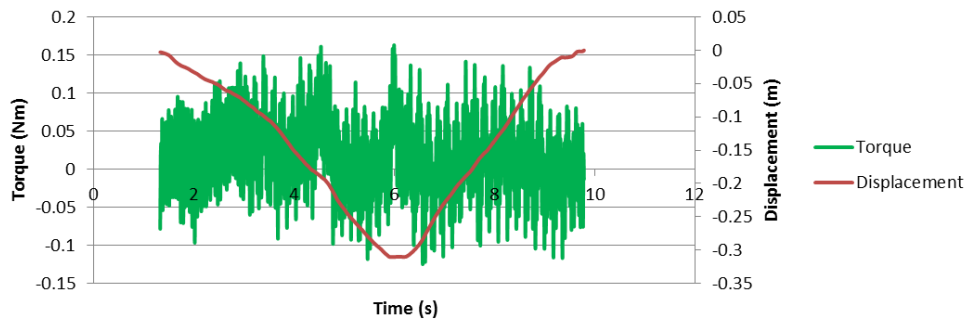
SAMPLE NO. 6 - Right - Resident: 10.5mm



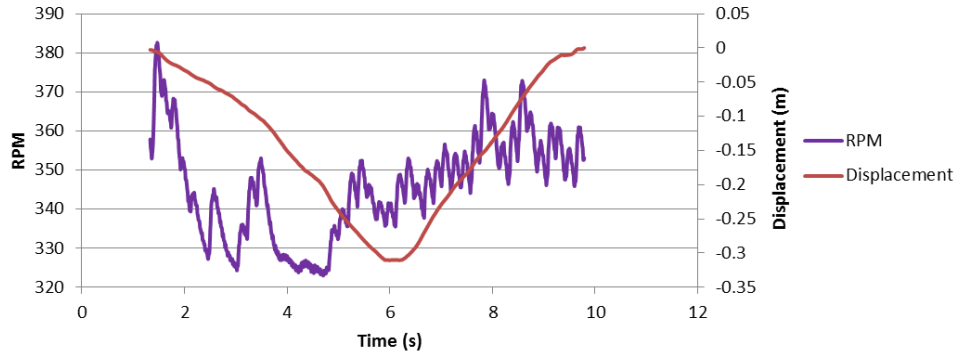
SAMPLE NO. 6 - Right - Resident: 10.5mm



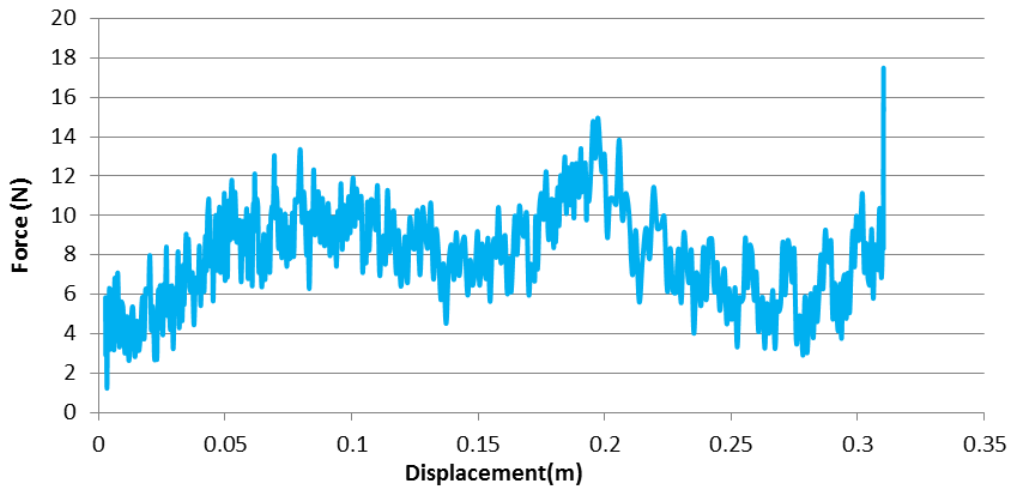
SAMPLE NO. 6 - Right - Resident: 10.5mm



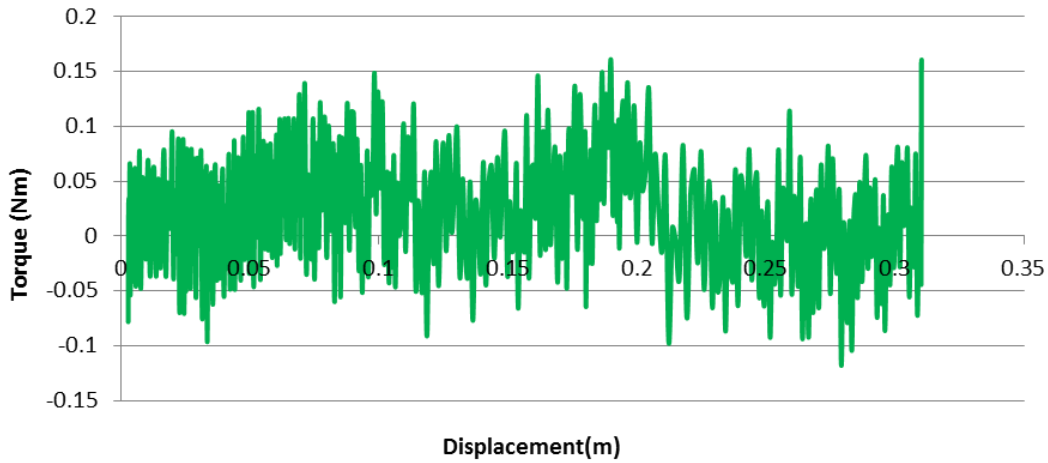
SAMPLE NO. 6 - Right - Resident: 10.5mm



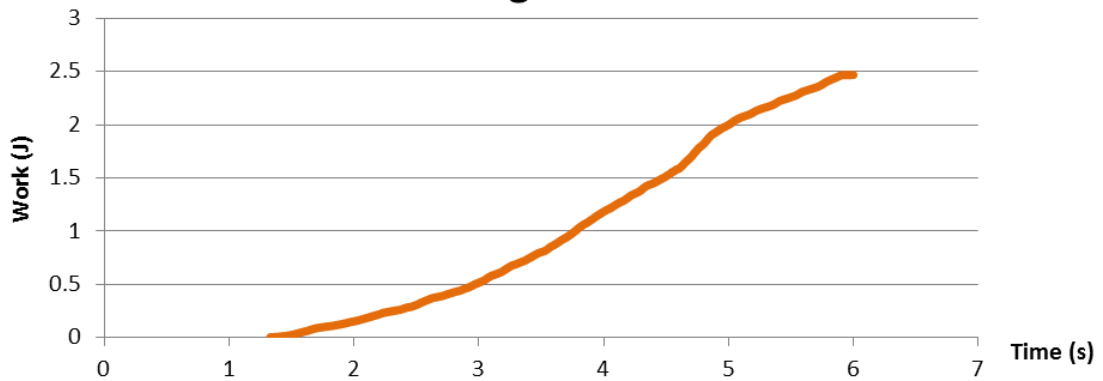
**SAMPLE NO. 6 - Right - Resident: 10.5mm**



**SAMPLE NO. 6 - Right - Resident: 10.5mm**

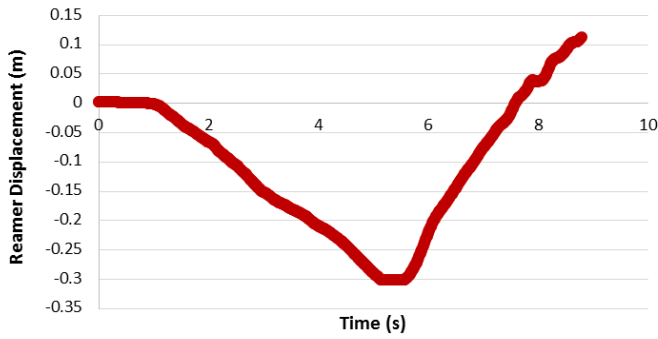


**SAMPLE NO. 6 - Right - Resident: 10.5mm**

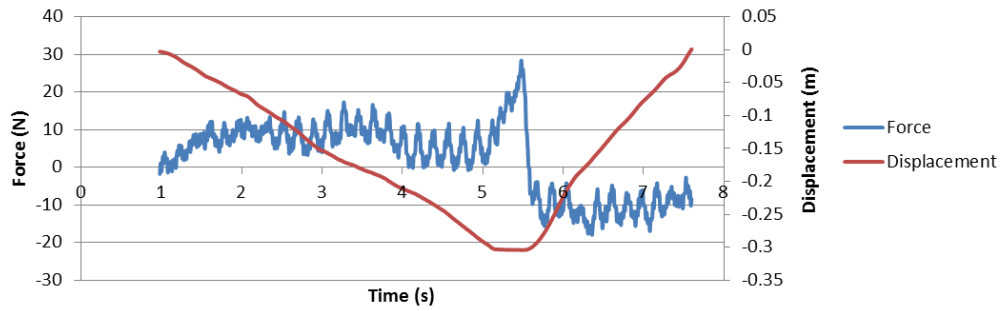


11MM

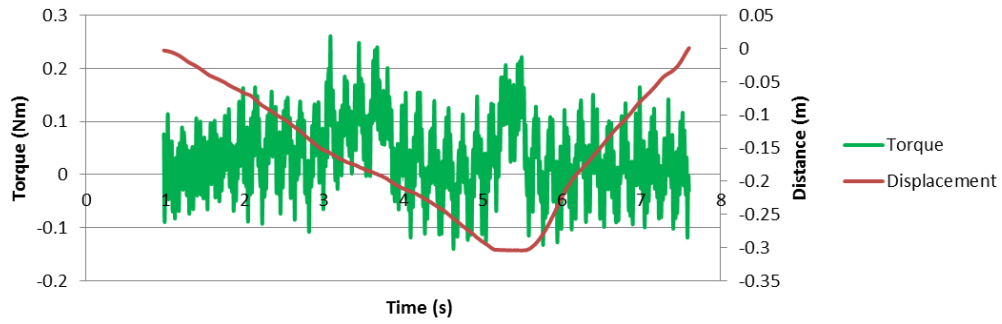
**SAMPLE NO. 6 - Right - Resident: 11mm**



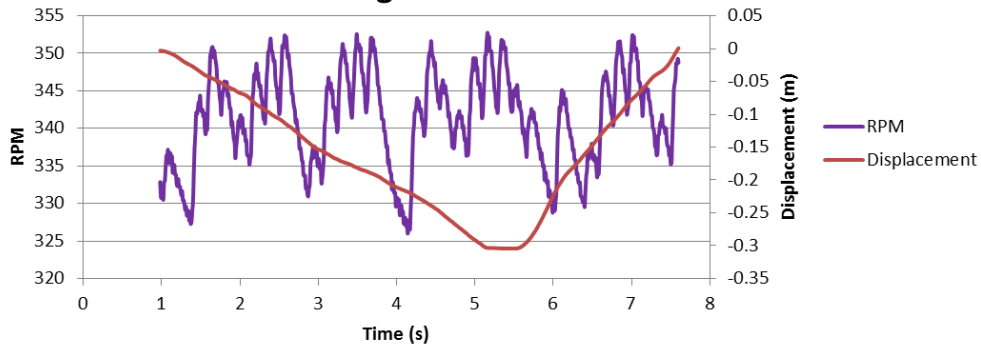
**SAMPLE NO. 6 - Right - Resident: 11mm**



**SAMPLE NO. 6 - Right - Resident: 11mm**

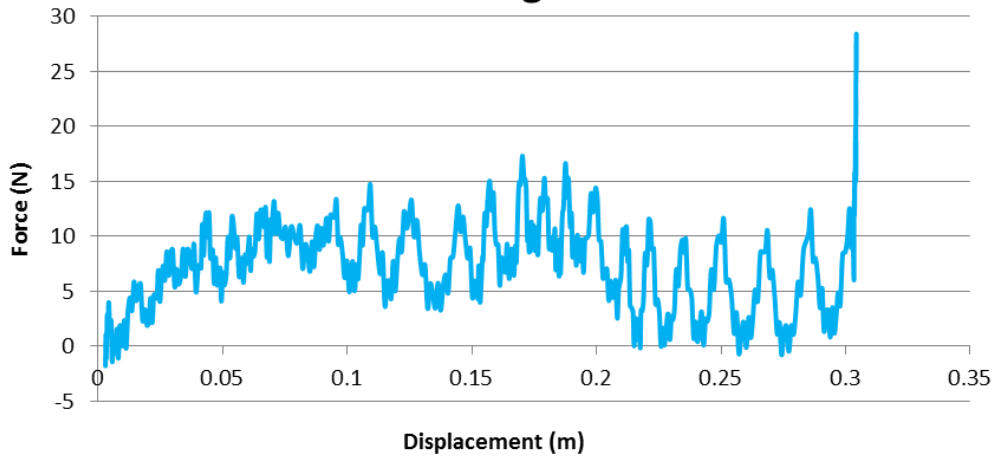


**SAMPLE NO. 6 - Right - Resident: 11mm**

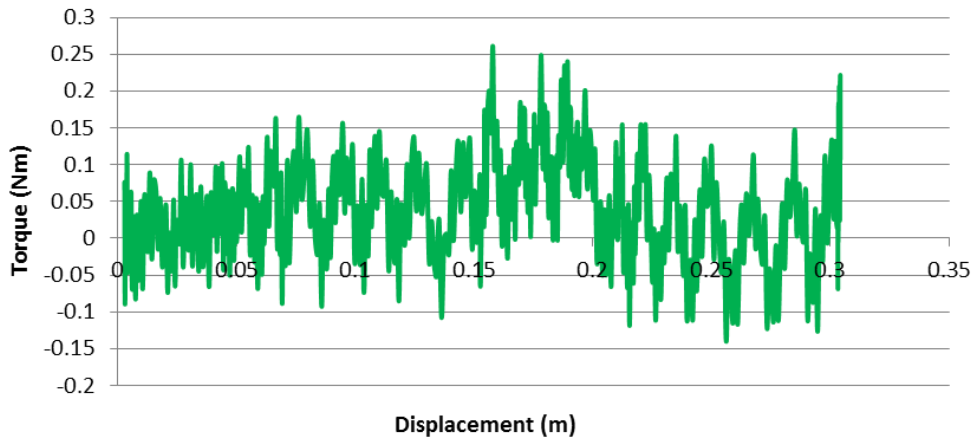




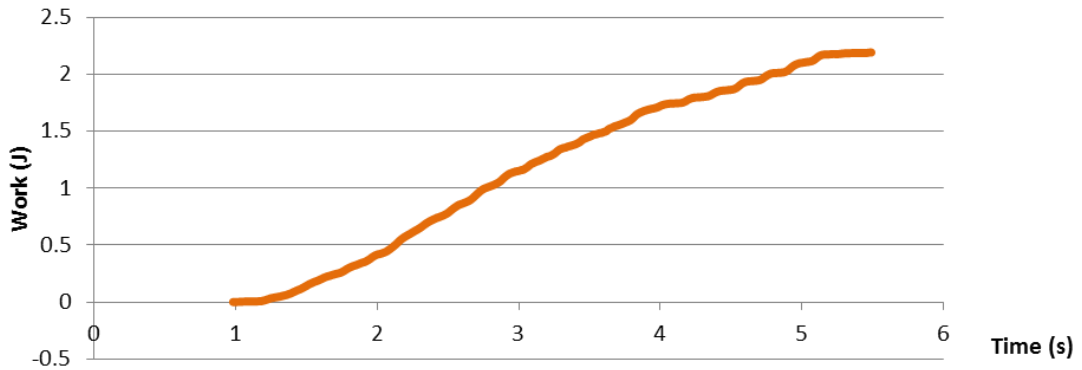
**SAMPLE NO. 6 - Right - Resident: 11mm**



**SAMPLE NO. 6 - Right - Resident: 11mm**

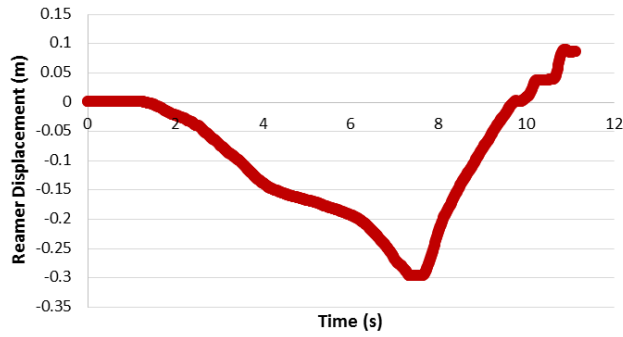


**SAMPLE NO. 6 - Right - Resident: 11mm**

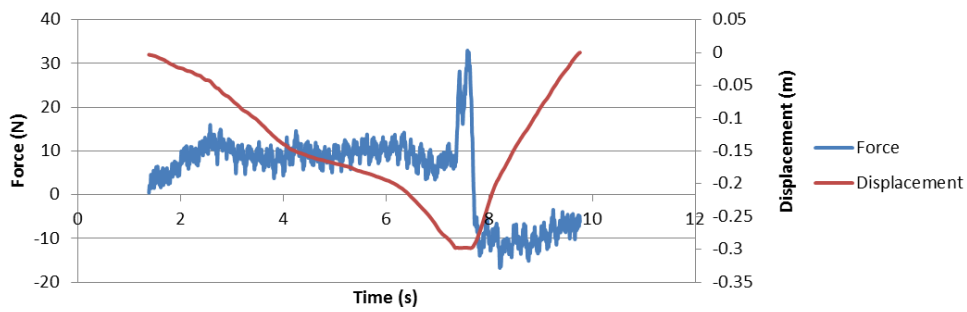


11.5MM

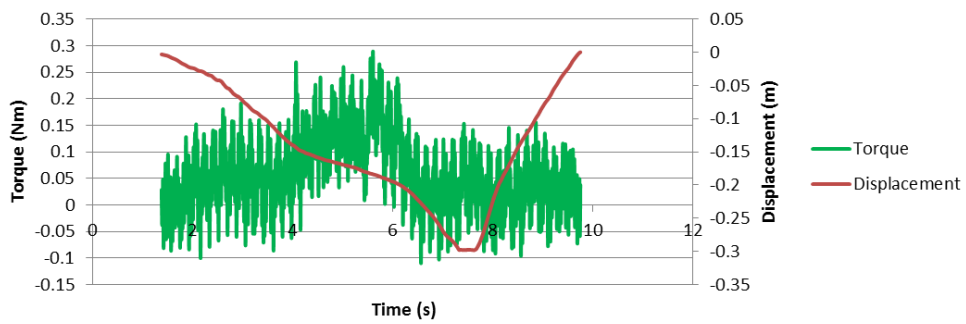
SAMPLE NO. 6 - Right - Resident: 11.5mm



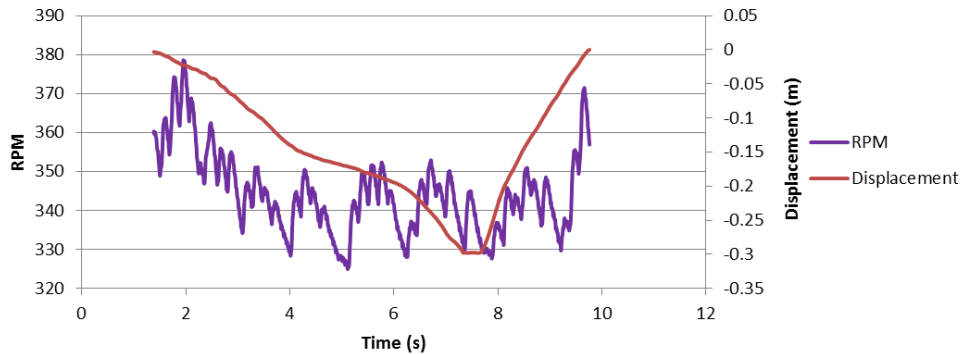
SAMPLE NO. 6 - Right - Resident: 11.5mm



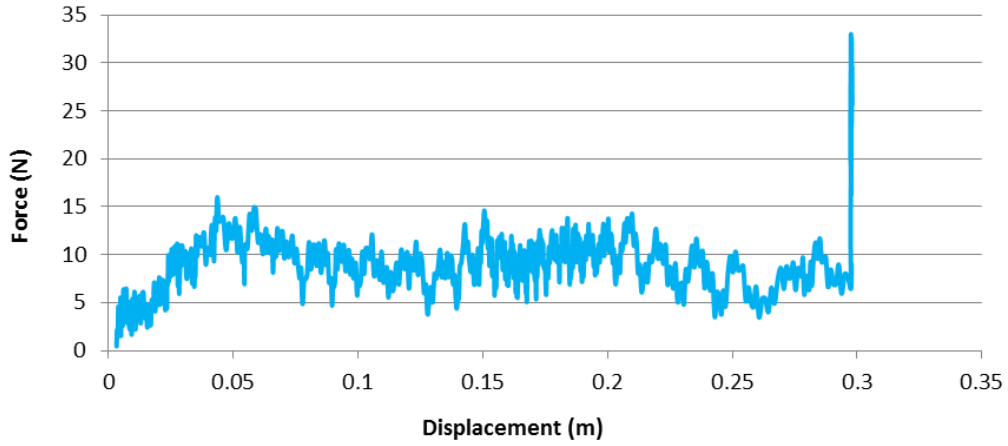
SAMPLE NO. 6 - Right - Resident: 11.5mm



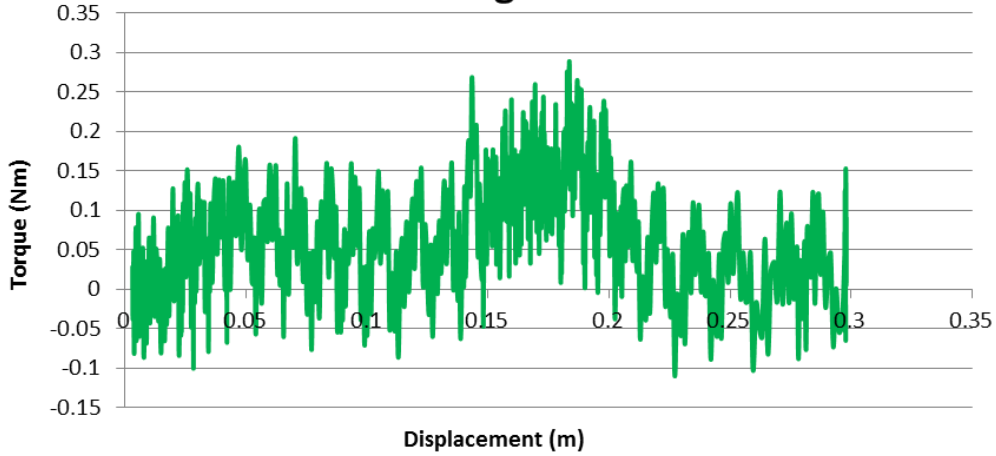
SAMPLE NO. 6 - Right - Resident: 11.5mm



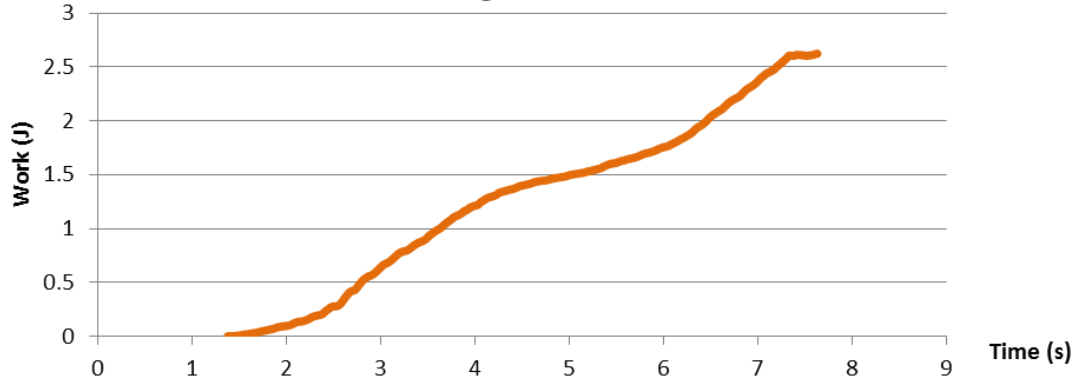
**SAMPLE NO. 6 - Right - Resident: 11.5mm**



**SAMPLE NO. 6 - Right - Resident: 11.5mm**

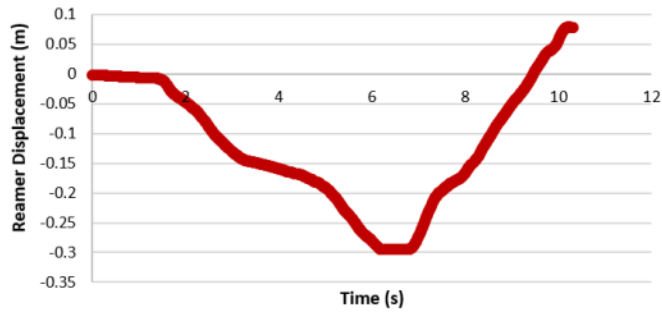


**SAMPLE NO. 6 - Right - Resident: 11.5mm**

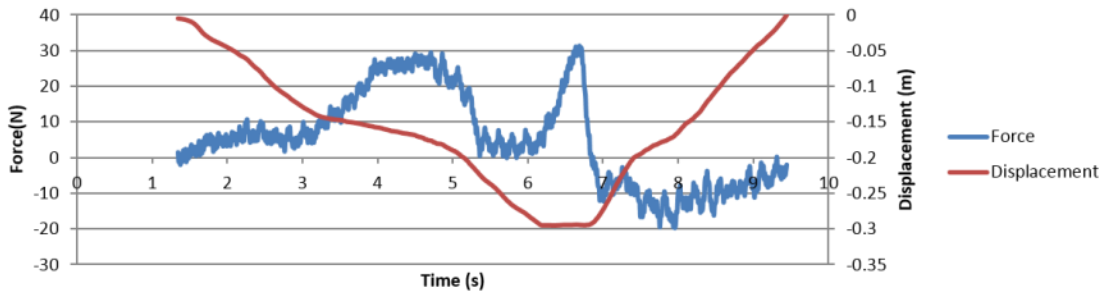


12MM

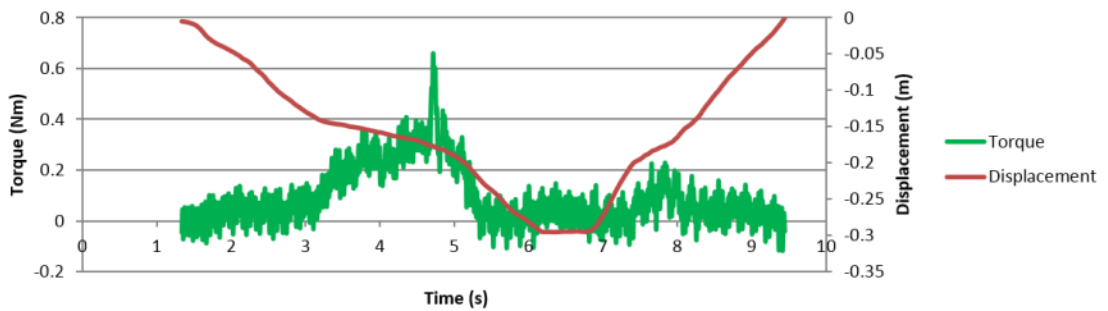
**SAMPLE NO. 6 - Right - Resident: 12mm  
CHATTER**



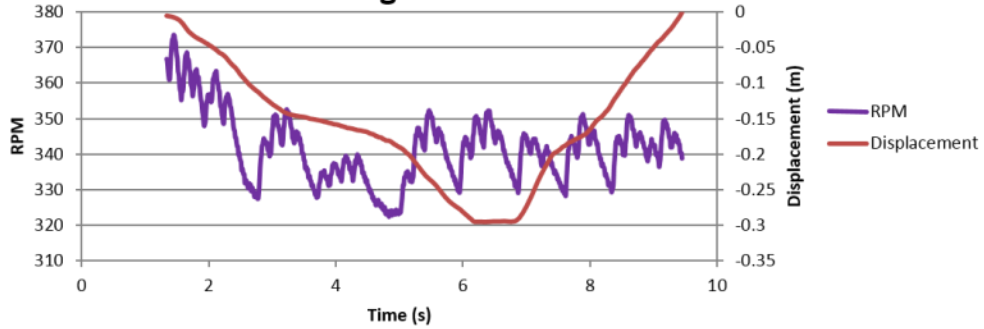
**SAMPLE NO. 6 - Right - Resident: 12mm CHATTER**



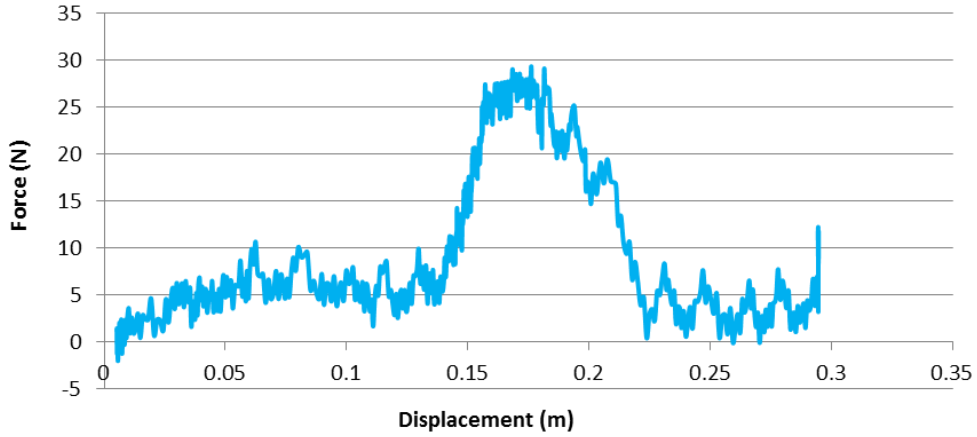
**SAMPLE NO. 6 - Right - Resident: 12mm CHATTER**



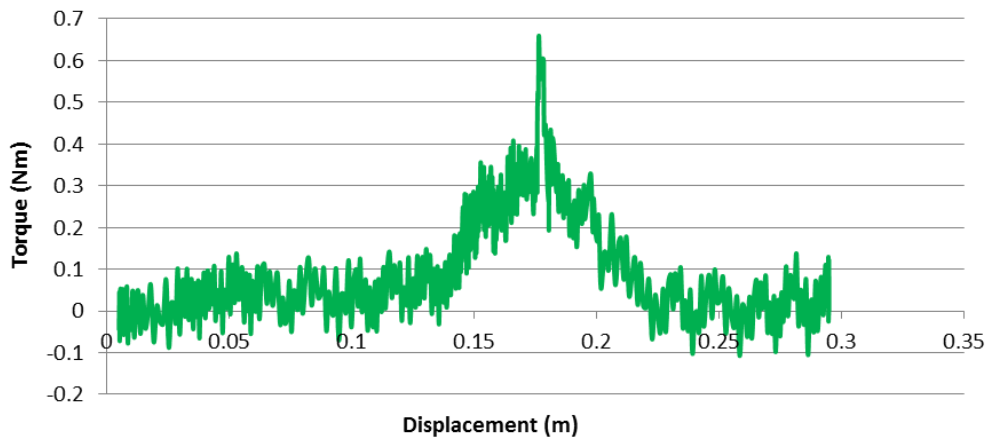
**SAMPLE NO. 6 - Right - Resident: 12mm CHATTER**



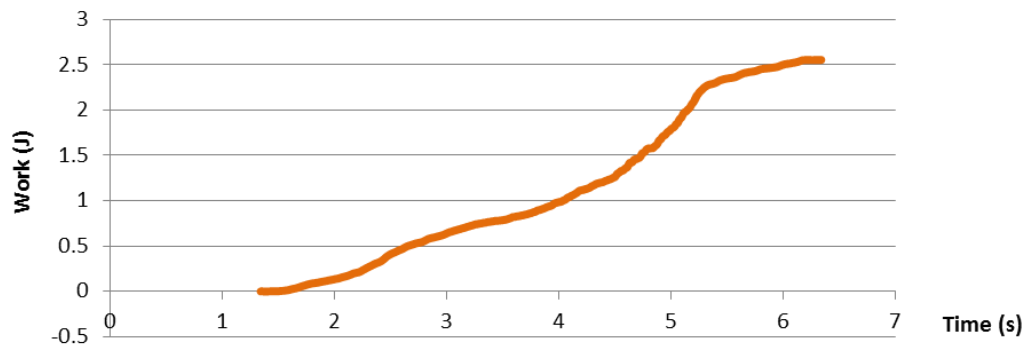
**SAMPLE NO. 6 - Right - Resident: 12mm CHATTER**



**SAMPLE NO. 6 - Right - Resident: 12mm CHATTER**

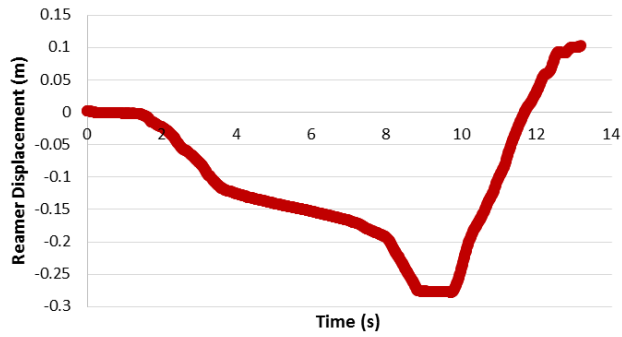


**SAMPLE NO. 6 - Right - Resident: 12mm CHATTER**

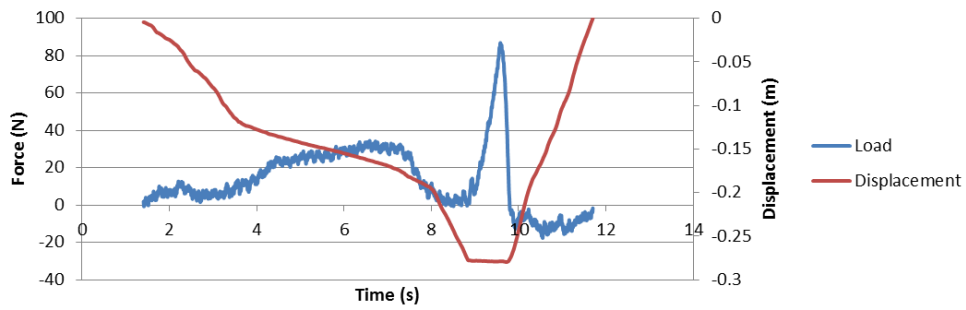


12.5MM

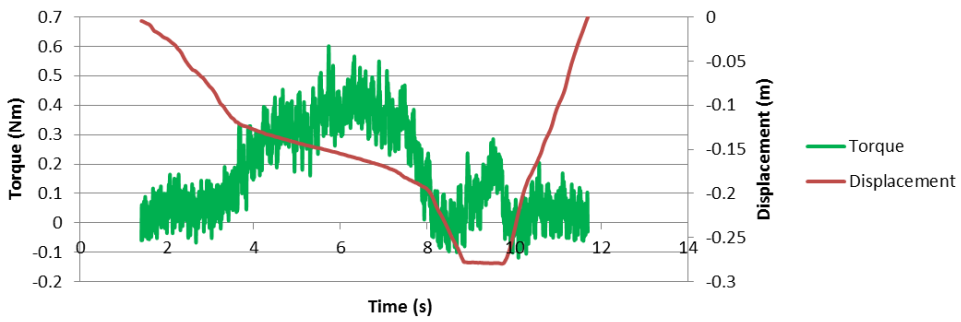
SAMPLE NO. 6 - Right - Resident: 12.5mm



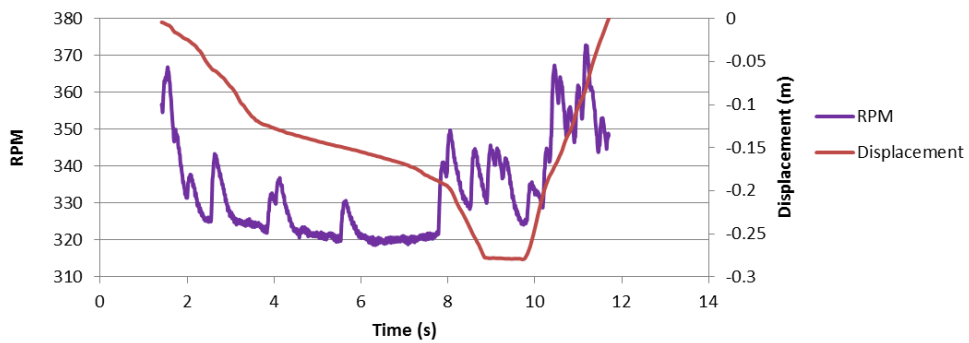
SAMPLE NO. 6 - Right - Resident: 12.5mm



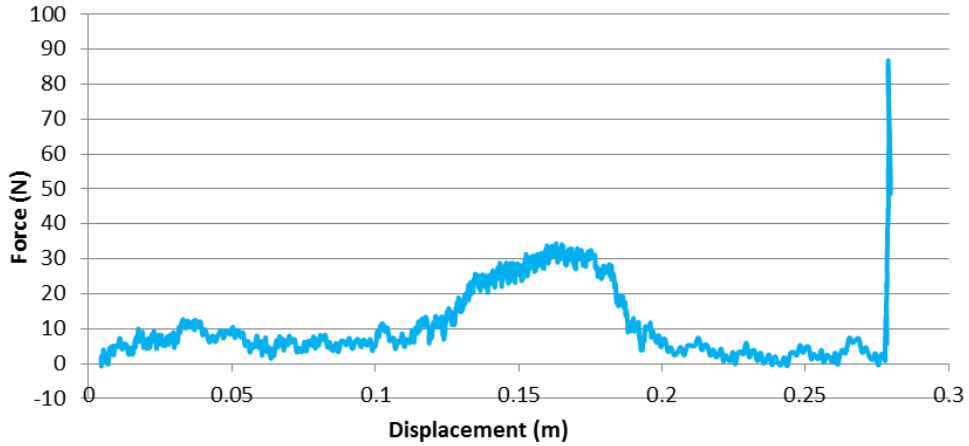
SAMPLE NO. 6 - Right - Resident: 12.5mm



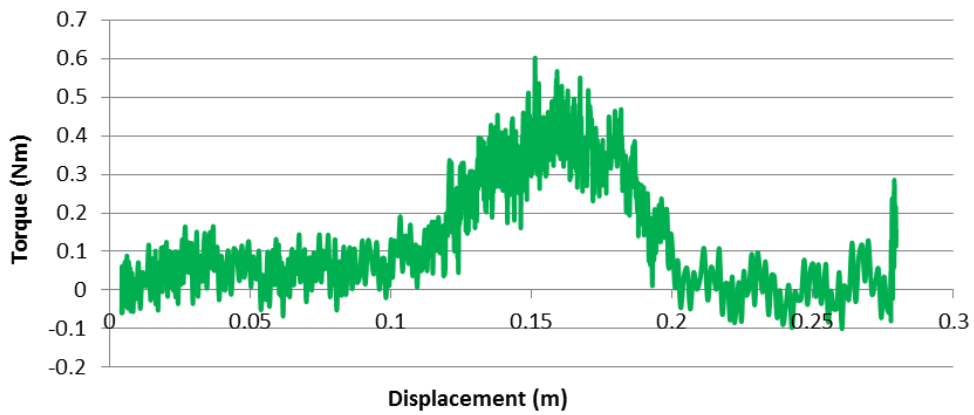
SAMPLE NO. 6 - Right - Resident: 12.5mm



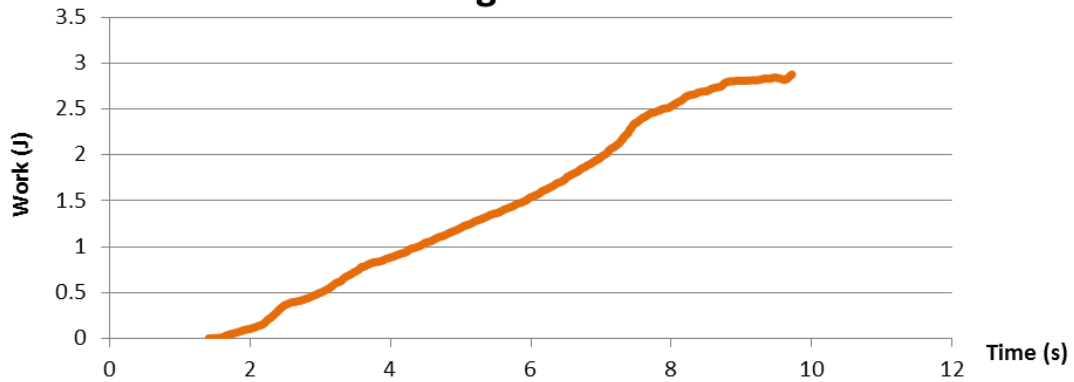
### SAMPLE NO. 6 - Right - Resident: 12.5mm



### SAMPLE NO. 6 - Right - Resident: 12.5mm

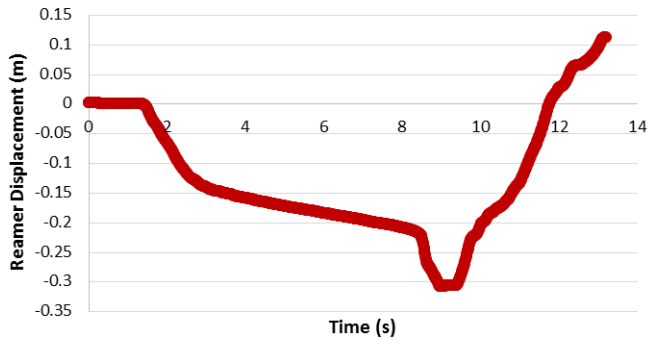


### SAMPLE NO. 6 - Right - Resident: 12.5mm

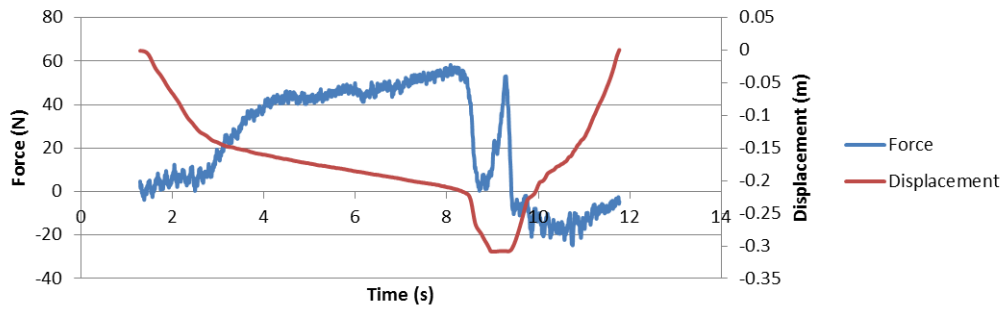


13MM

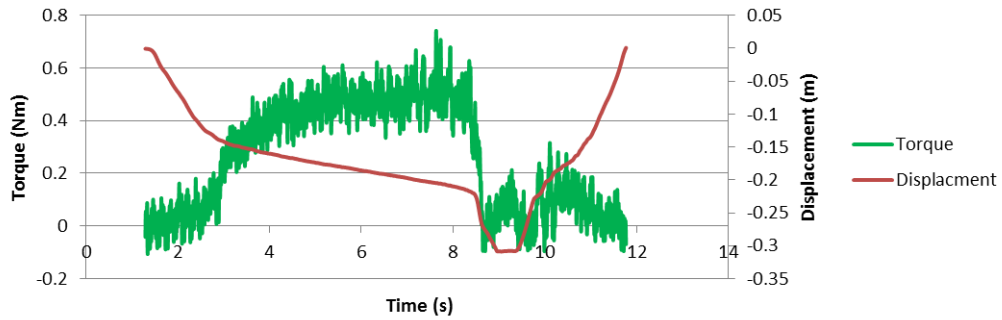
SAMPLE NO. 6 - Right - Resident: 13mm



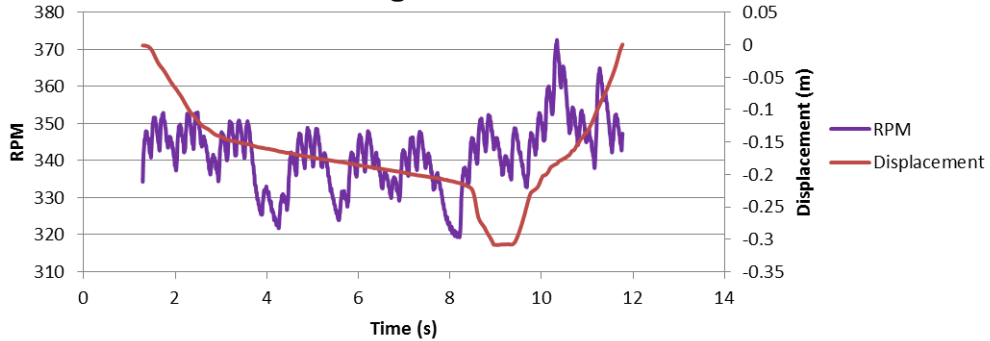
SAMPLE NO. 6 - Right - Resident: 13mm



SAMPLE NO. 6 - Right - Resident: 13mm

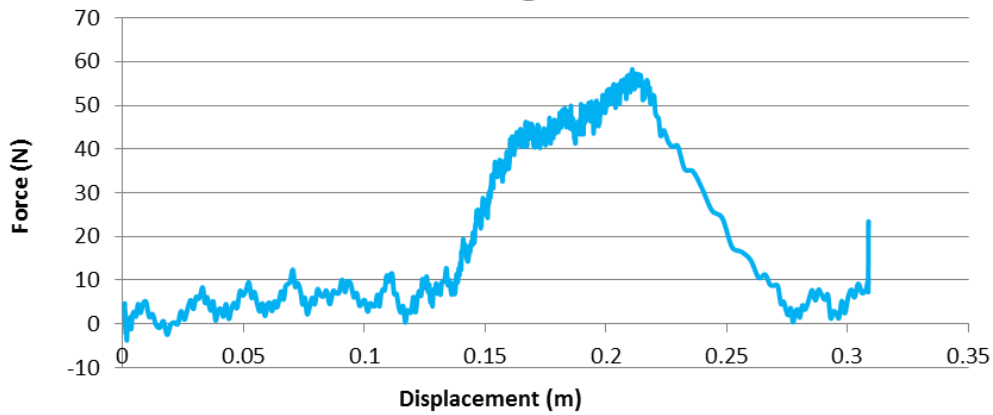


SAMPLE NO. 6 - Right - Resident: 13mm

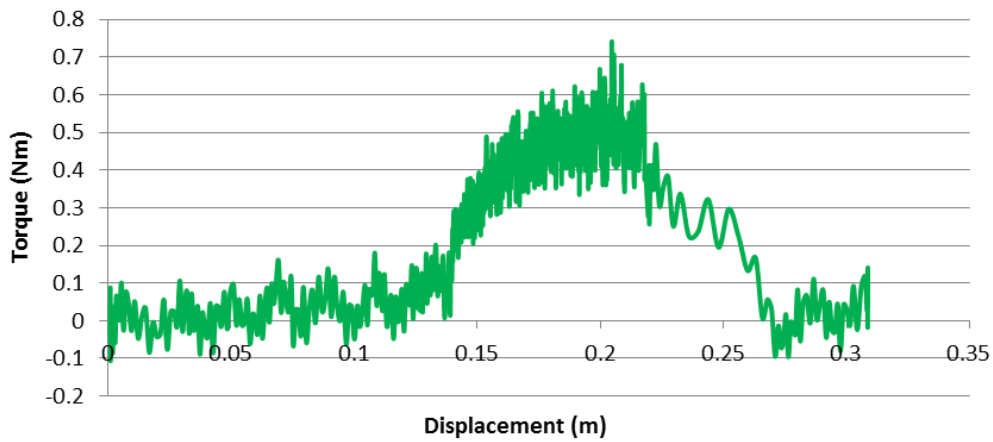




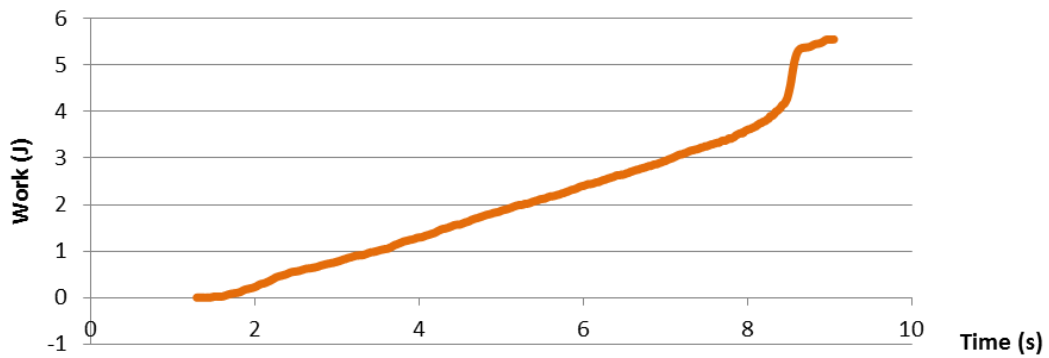
**SAMPLE NO. 6 - Right - Resident: 13mm**



**SAMPLE NO. 6 - Right - Resident: 13mm**

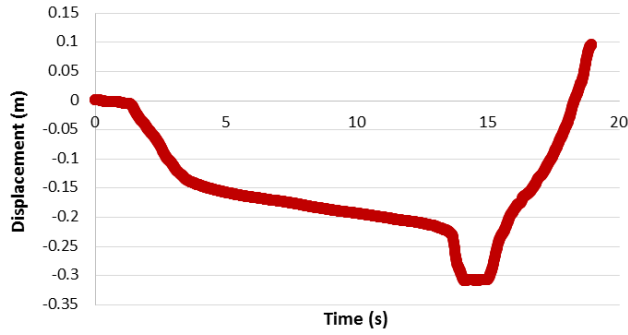


**SAMPLE NO. 6 - Right - Resident: 13mm**

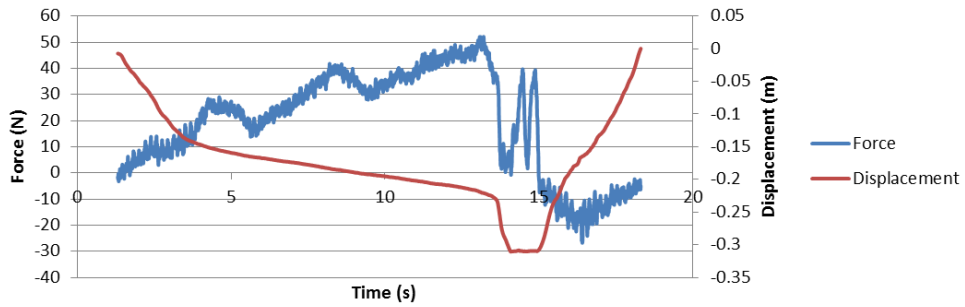


13.5MM

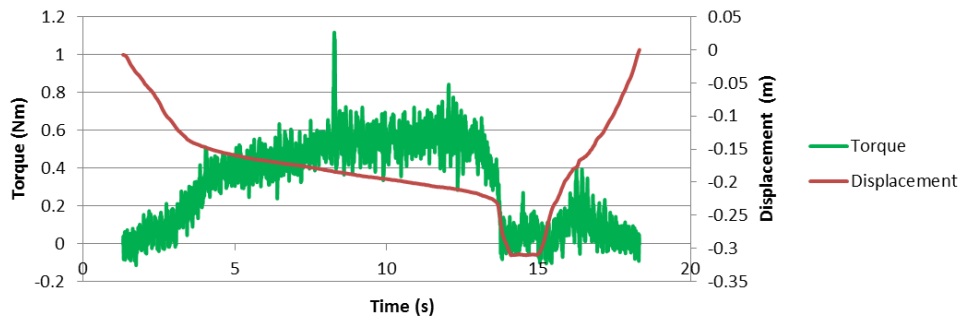
SAMPLE NO. 6 - Right - Resident: 13.5mm



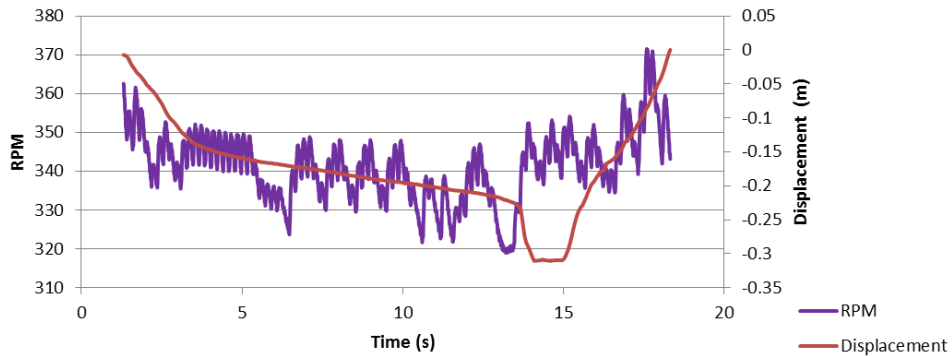
SAMPLE NO. 6 - Right - Resident: 13.5mm



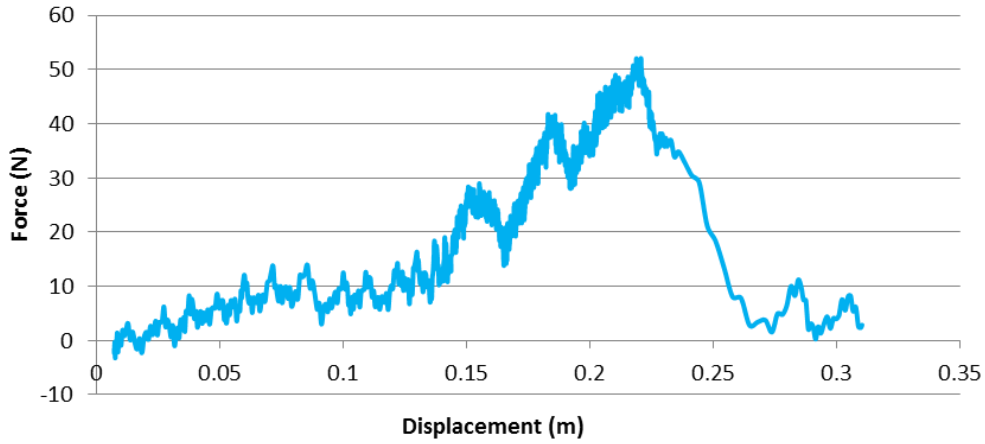
SAMPLE NO. 6 - Right - Resident: 13.5mm



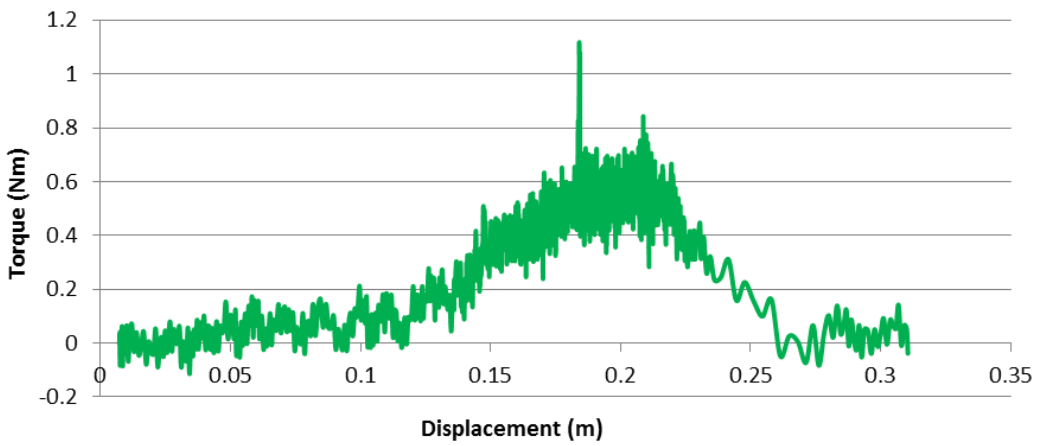
SAMPLE NO. 6 - Right - Resident: 13.5mm



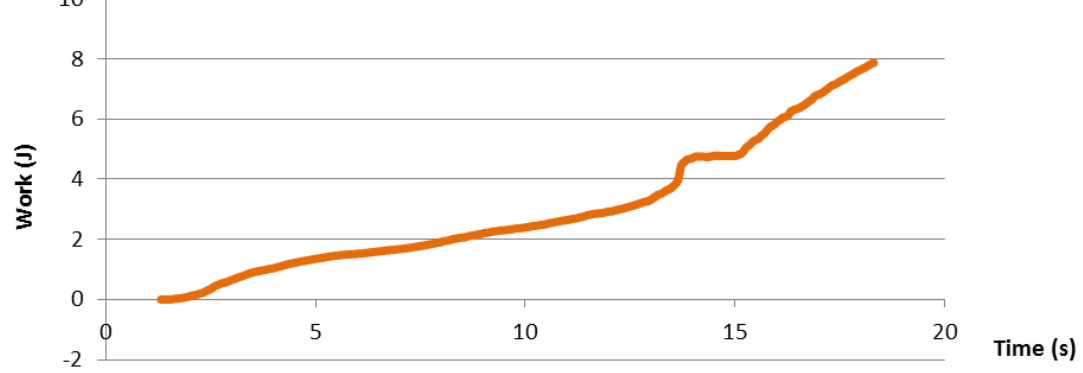
**SAMPLE NO. 6 - Right - Resident: 13.5mm**



**SAMPLE NO. 6 - Right - Resident: 13.5mm**



**SAMPLE NO. 6 - Right - Resident: 13.5mm**

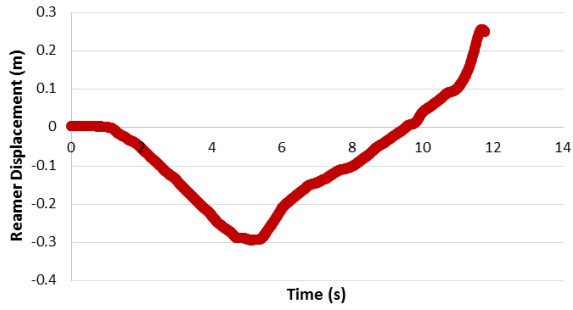


# 13.7 SAMPLE 7 RESULTS

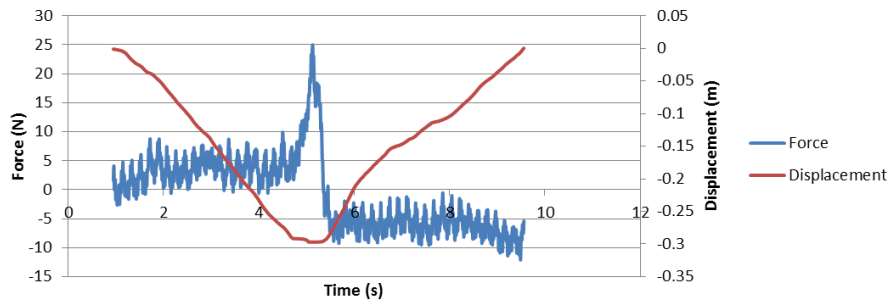
LEFT: RESIDENT

9MM

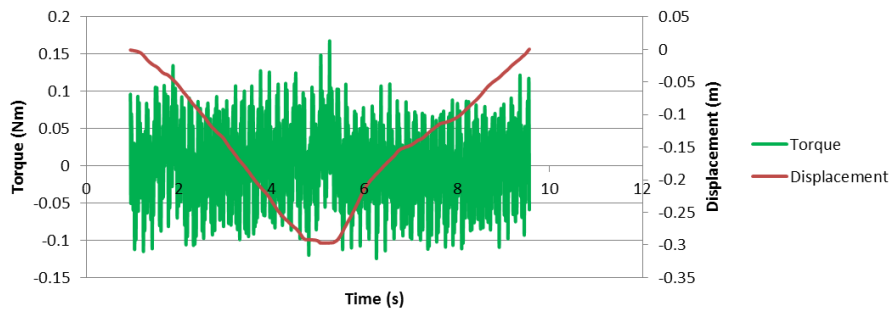
SAMPLE NO. 7 - Left - Resident: 9mm



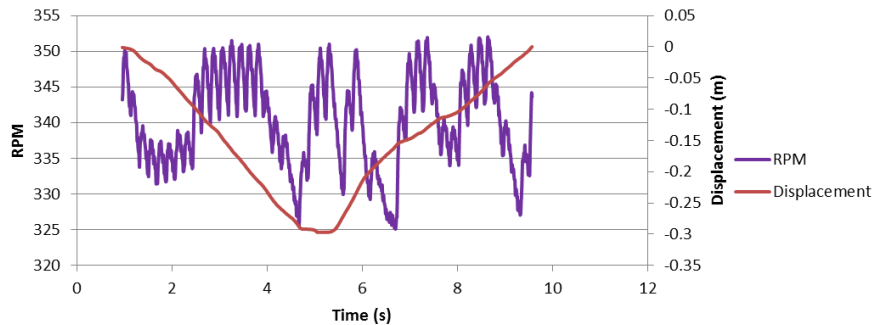
SAMPLE NO. 7 - Left - Resident: 9mm



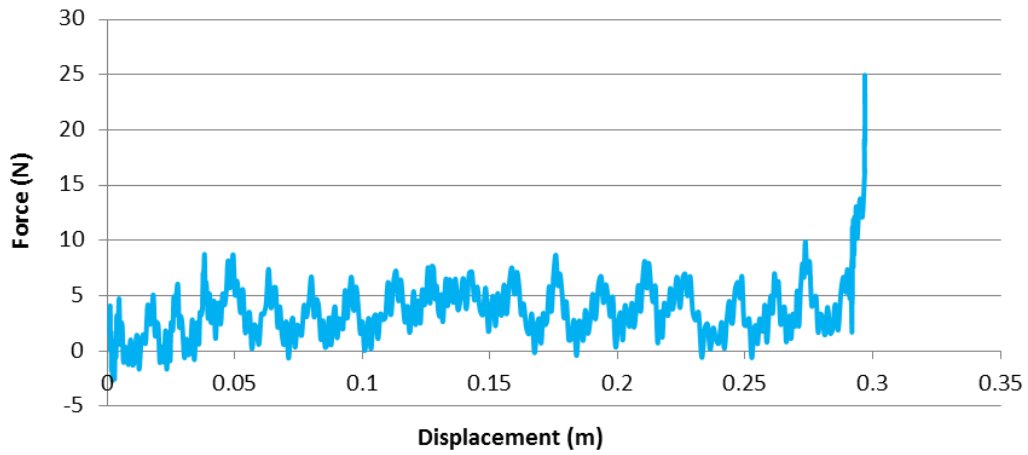
SAMPLE NO. 7 - Left - Resident: 9mm



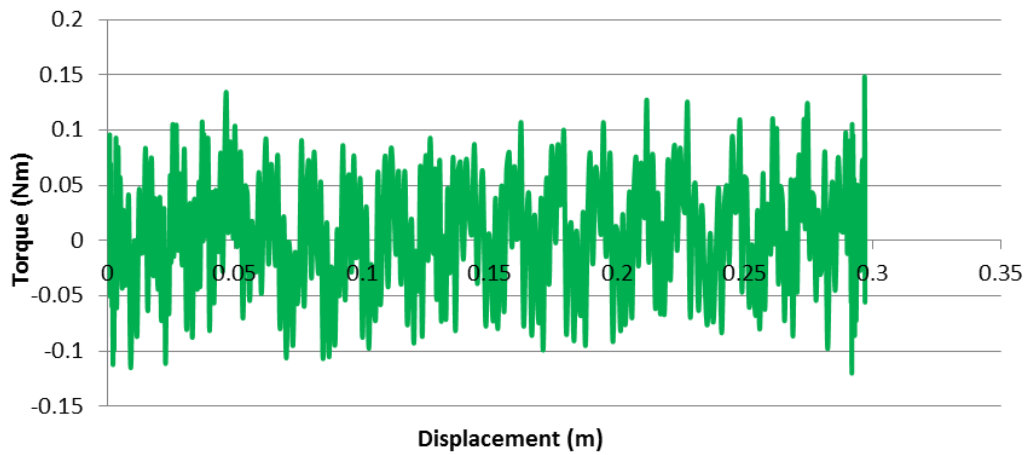
SAMPLE NO. 7 - Left - Resident: 9mm



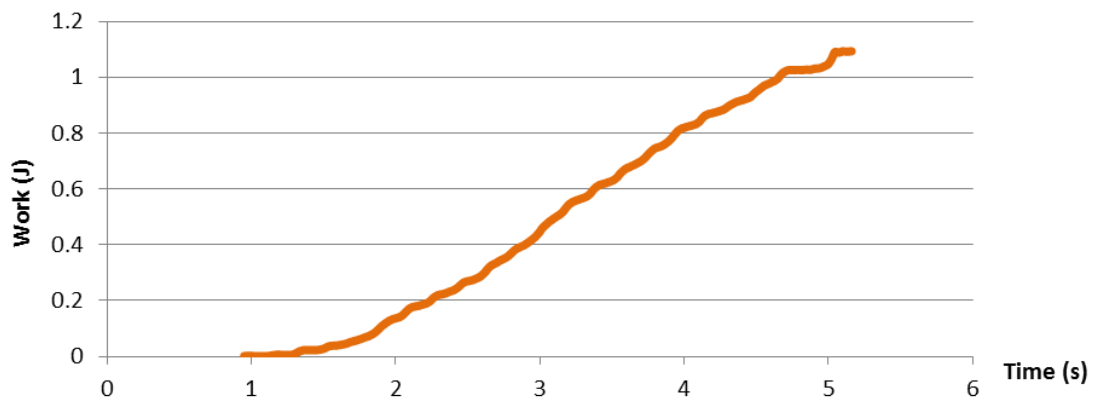
**SAMPLE NO. 7 - Left - Resident: 9mm**



**SAMPLE NO. 7 - Left - Resident: 9mm**

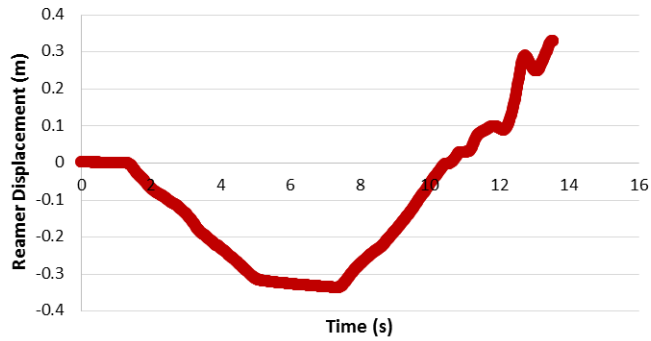


**SAMPLE NO. 7 - Left - Resident: 9mm**

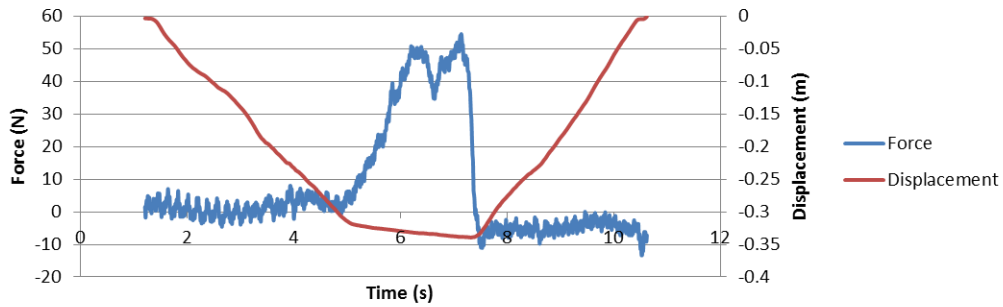


9.5MM

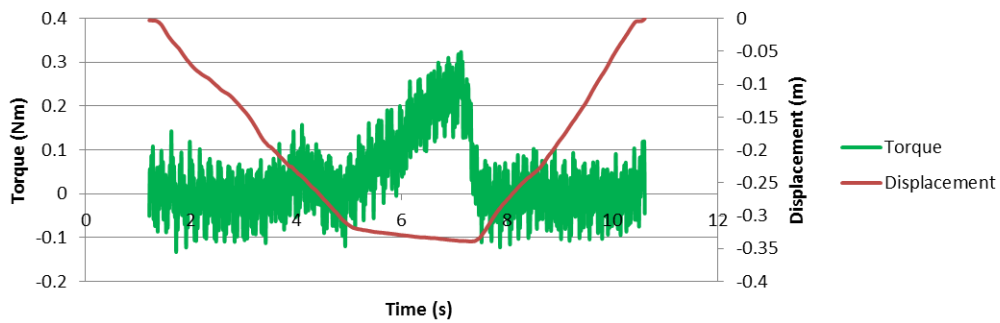
**SAMPLE NO. 7 - Left - Resident: 9.5mm**



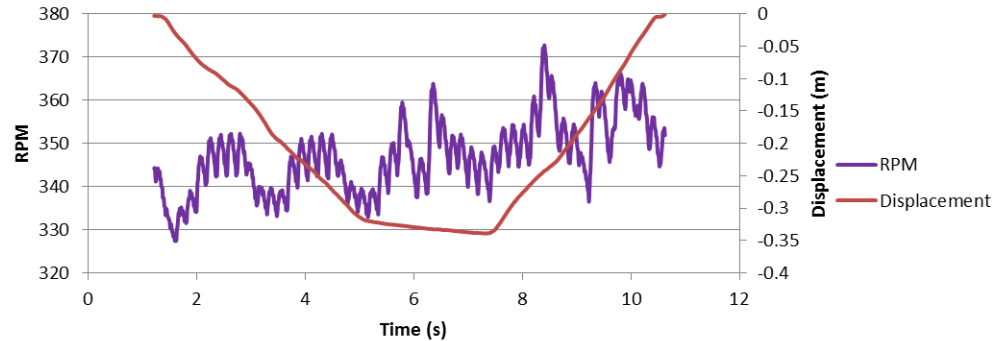
**SAMPLE NO. 7 - Left - Resident: 9.5mm**



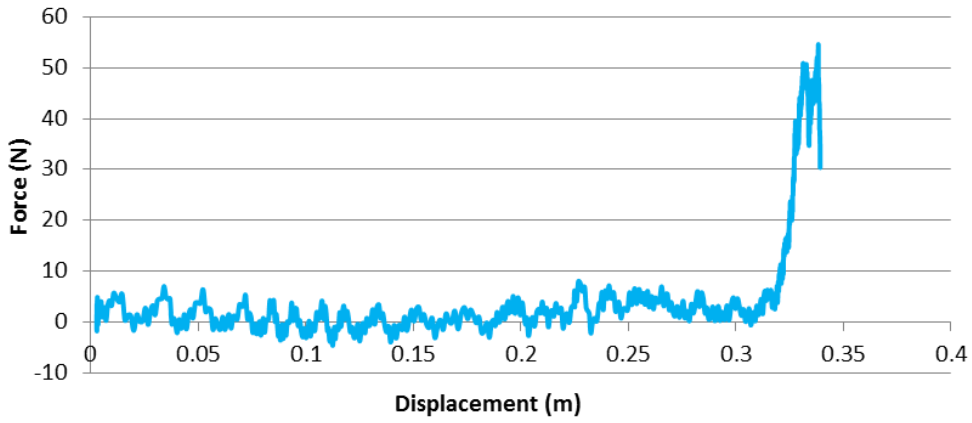
**SAMPLE NO. 7 - Left - Resident: 9.5mm**



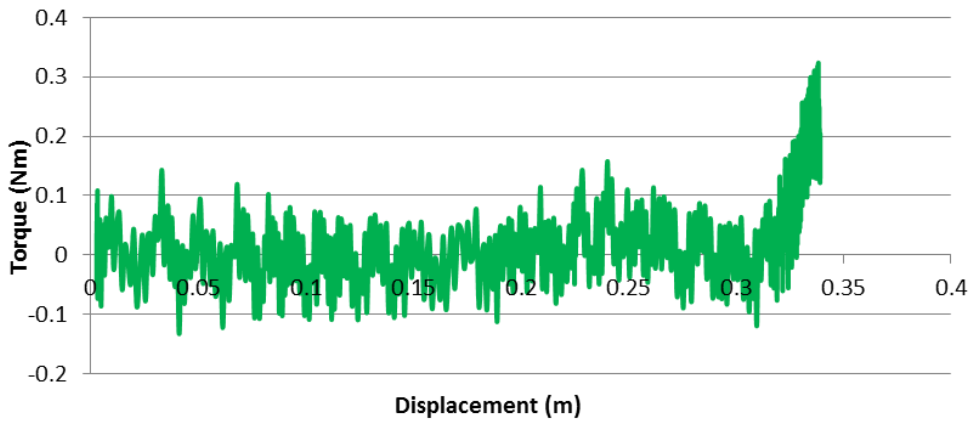
**SAMPLE NO. 7 - Left - Resident: 9.5mm**



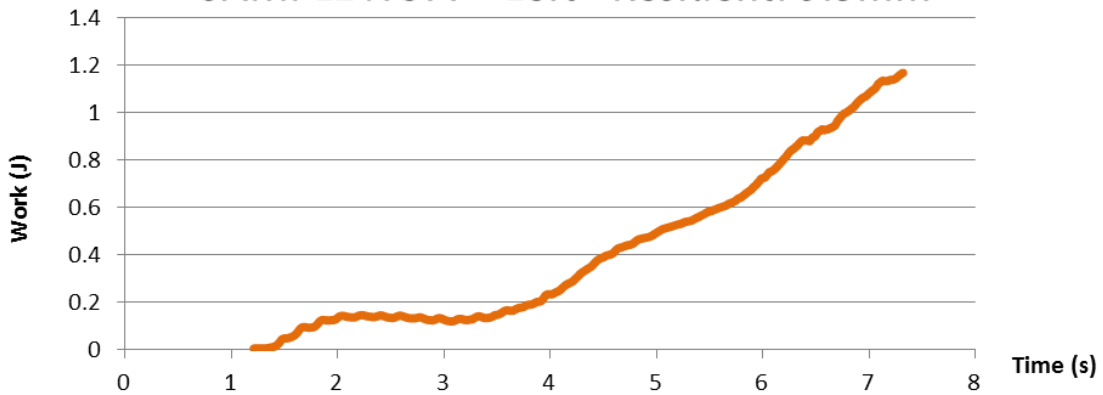
### SAMPLE NO. 7 - Left - Resident: 9.5mm



### SAMPLE NO. 7 - Left - Resident: 9.5mm

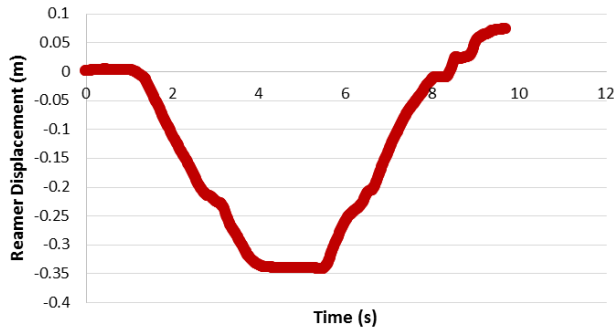


### SAMPLE NO. 7 - Left - Resident: 9.5mm

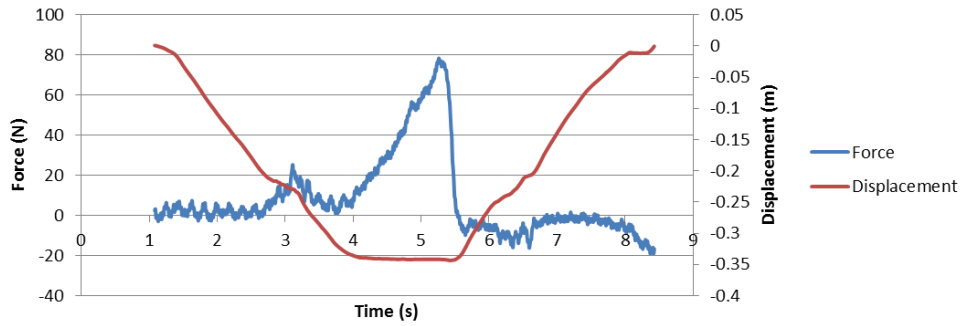


10MM

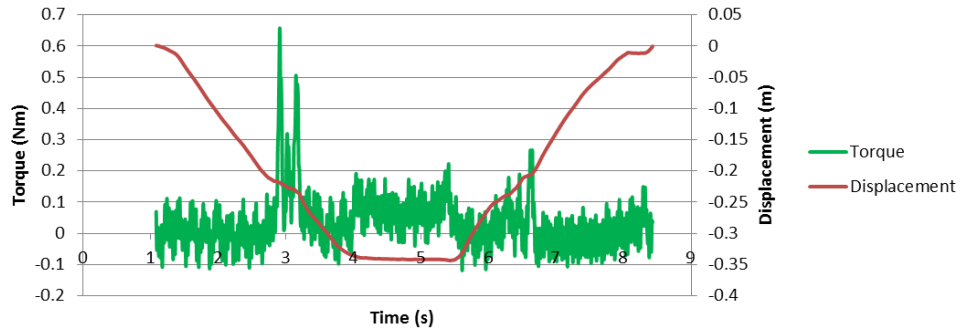
**SAMPLE NO. 7 - Left - Resident: 10mm**



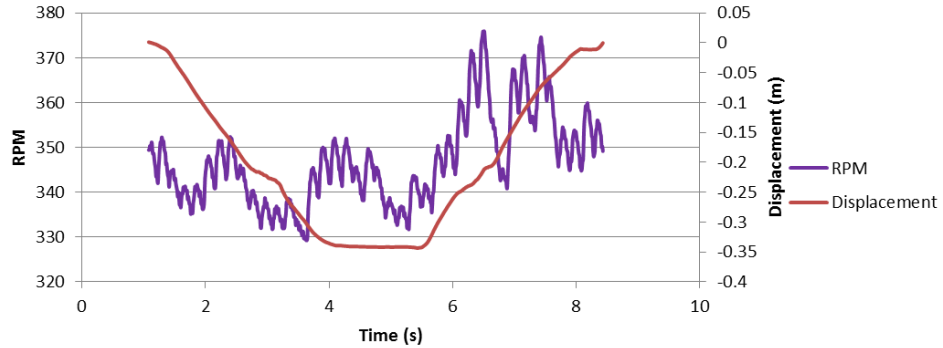
**SAMPLE NO. 7 - Left - Resident: 10mm**



**SAMPLE NO. 7 - Left - Resident: 10mm**

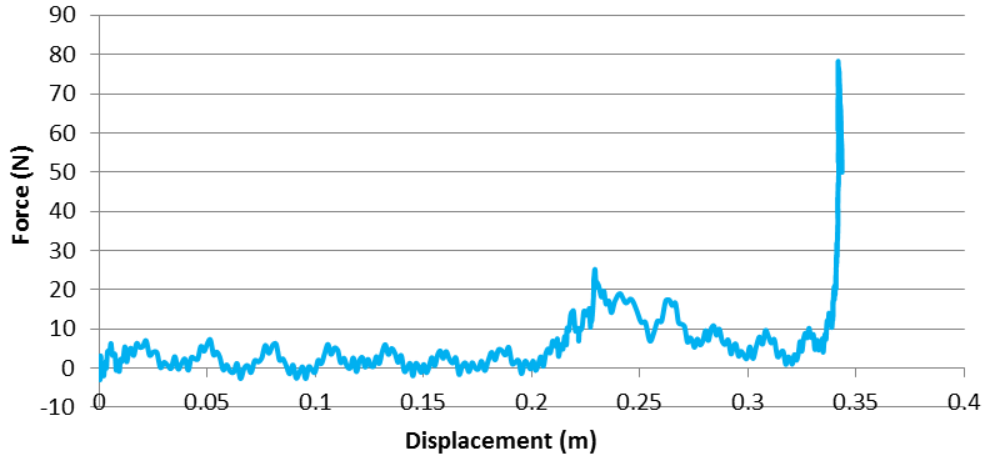


**SAMPLE NO. 7 - Left - Resident: 10mm**

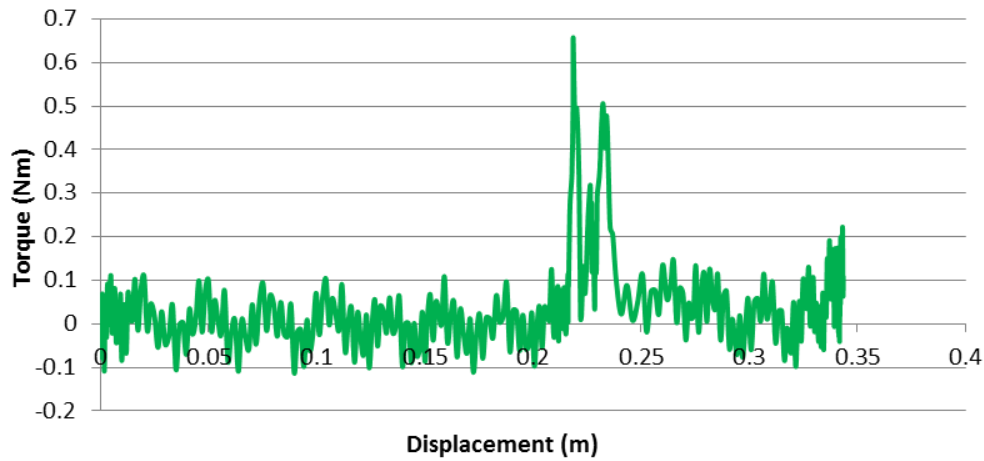




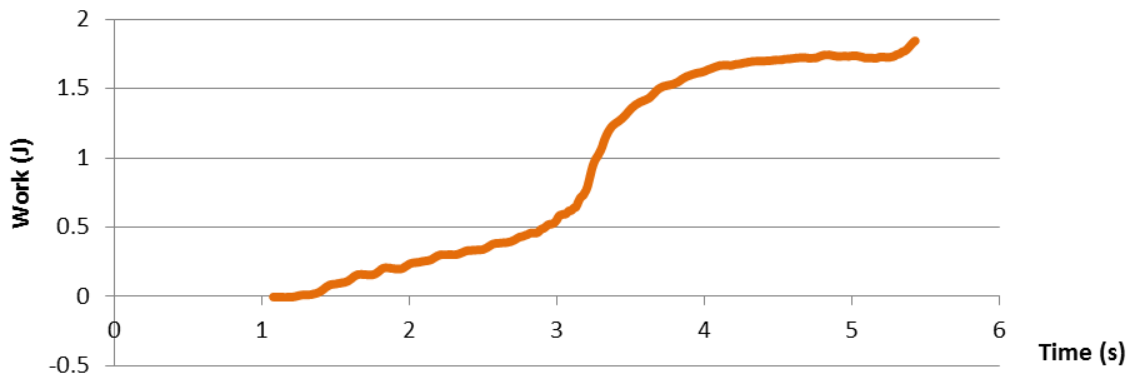
### SAMPLE NO. 7 - Left - Resident: 10mm



### SAMPLE NO. 7 - Left - Resident: 10mm

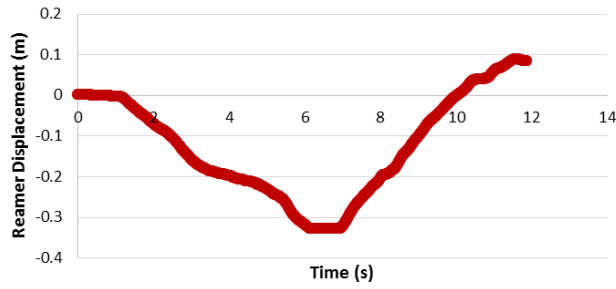


### SAMPLE NO. 7 - Left - Resident: 10mm

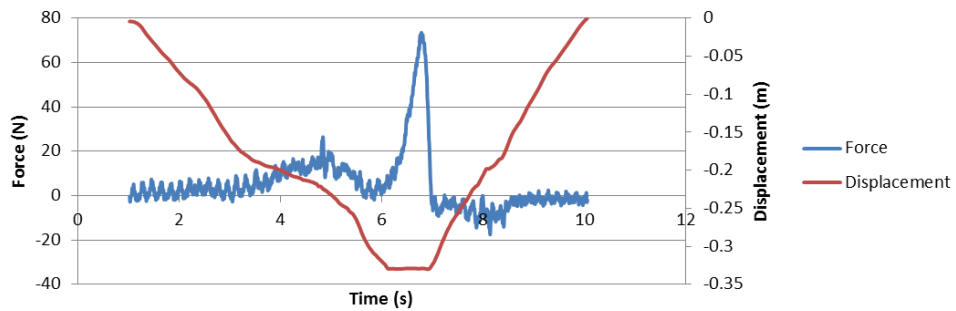


10.5MM

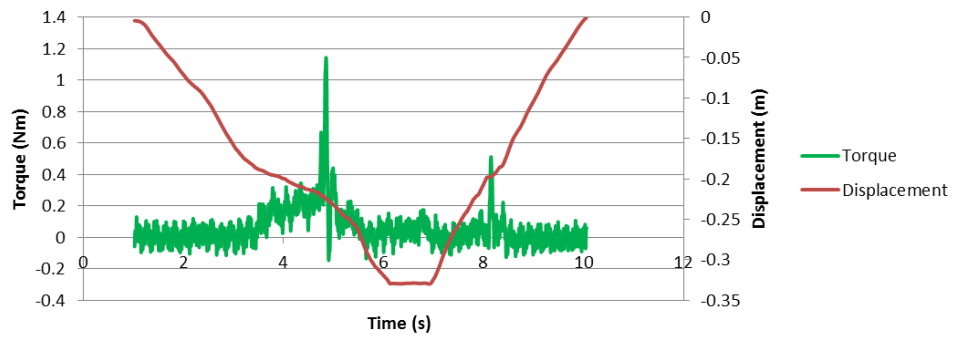
### SAMPLE NO. 7 - Left - Resident: 10.5mm CHATTER



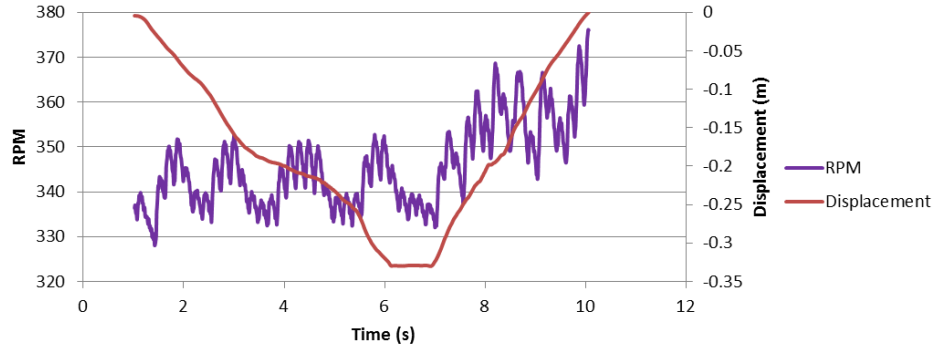
### SAMPLE NO. 7 - Left - Resident: 10.5mm CHATTER



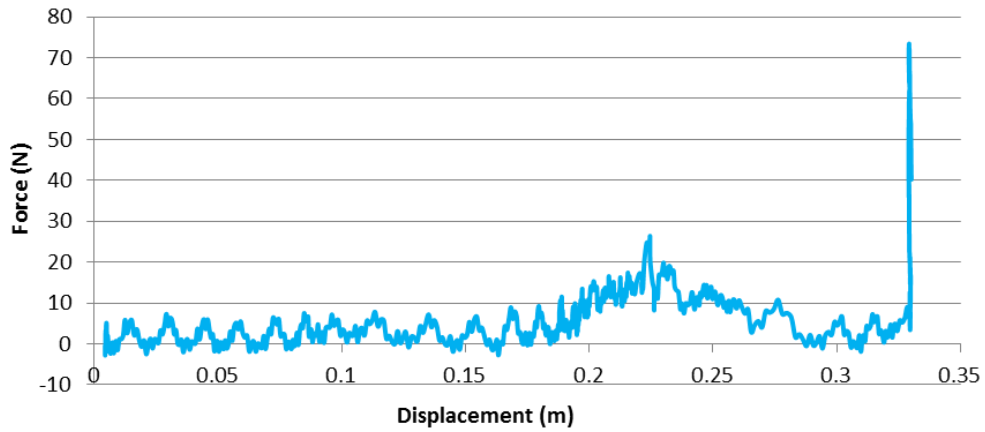
### SAMPLE NO. 7 - Left - Resident: 10.5mm CHATTER



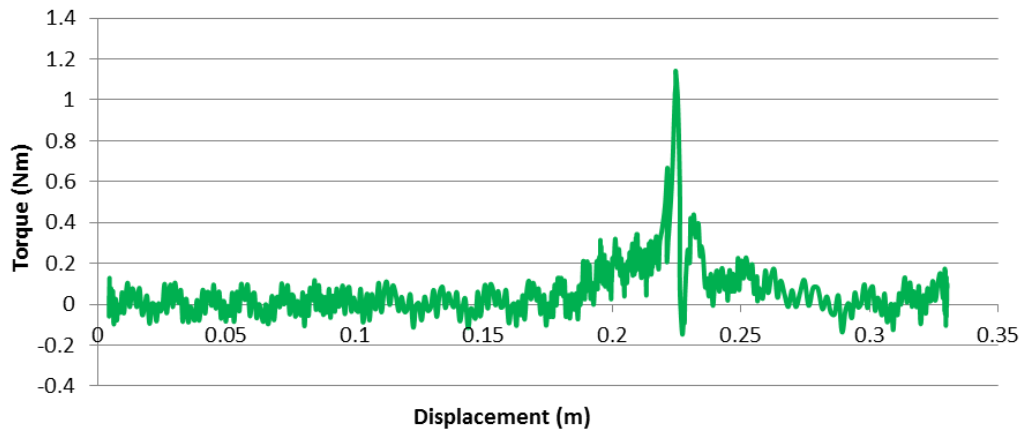
### SAMPLE NO. 7 - Left - Resident: 10.5mm CHATTER



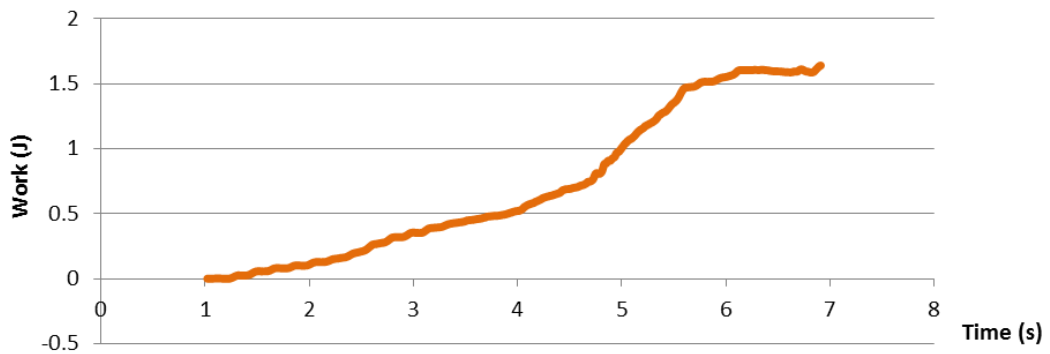
### SAMPLE NO. 7 - Left - Resident: 10.5mm CHATTER



### SAMPLE NO. 7 - Left - Resident: 10.5mm CHATTER

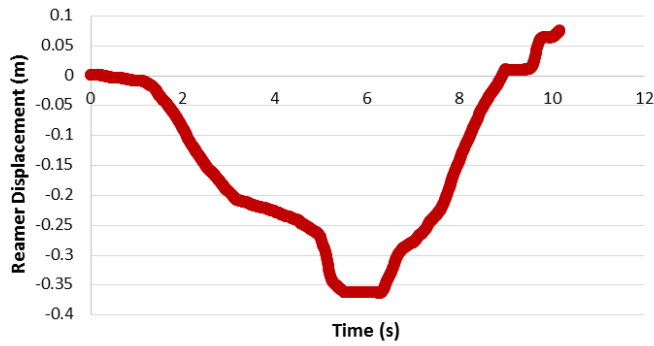


### SAMPLE NO. 7 - Left - Resident: 10.5mm CHATTER

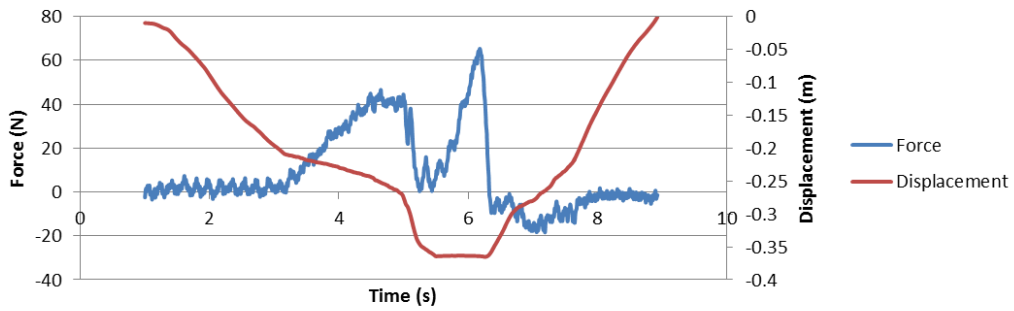


11MM

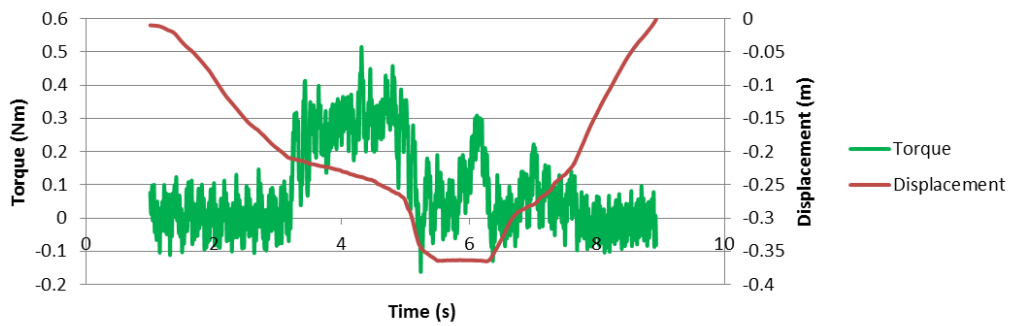
**SAMPLE NO. 7 - Left - Resident: 11mm**



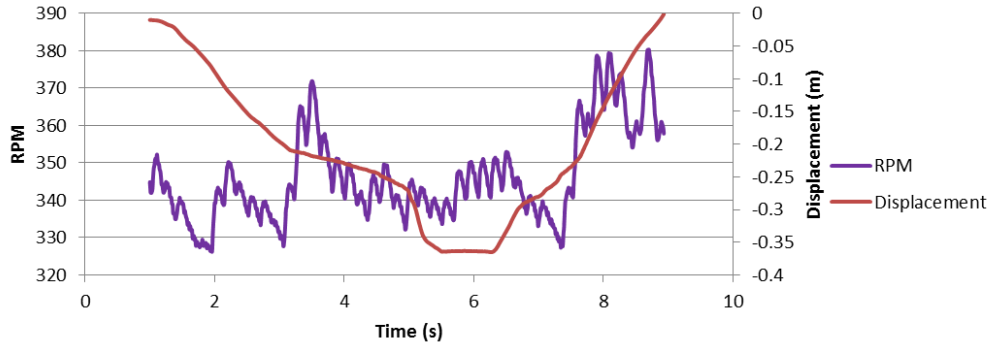
**SAMPLE NO. 7 - Left - Resident: 11mm**



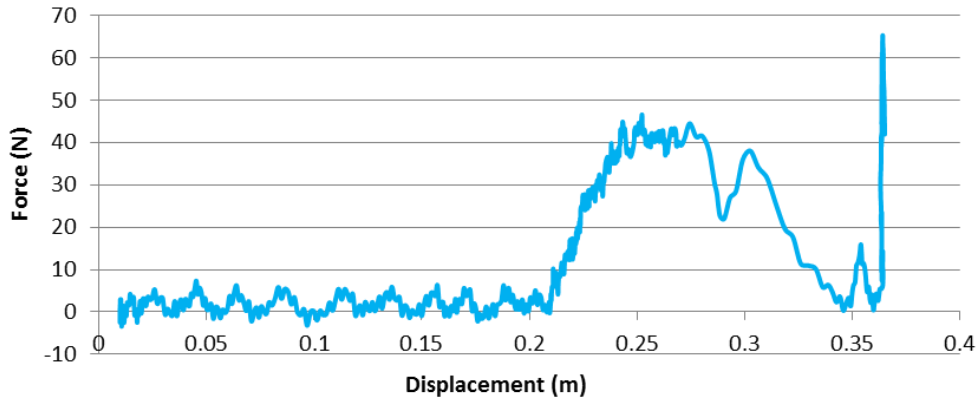
**SAMPLE NO. 7 - Left - Resident: 11mm**



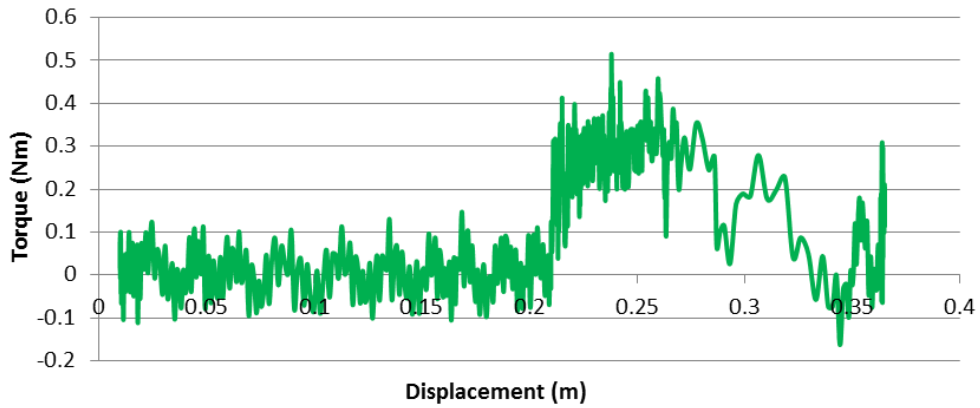
**SAMPLE NO. 7 - Left - Resident: 11mm**



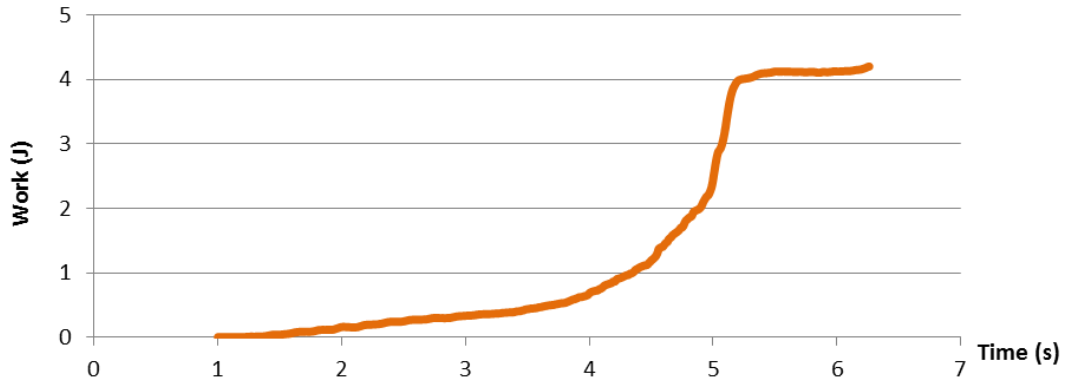
**SAMPLE NO. 7 - Left - Resident: 11mm**



**SAMPLE NO. 7 - Left - Resident: 11mm**

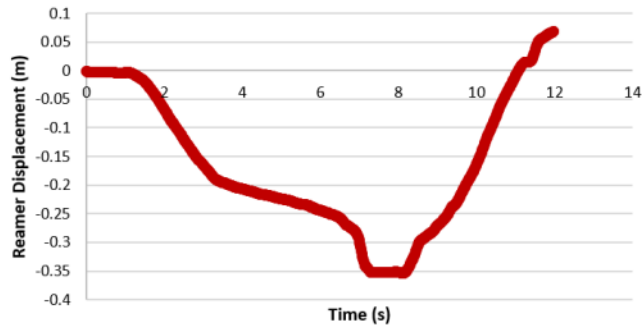


**SAMPLE NO. 7 - Left - Resident: 11mm**

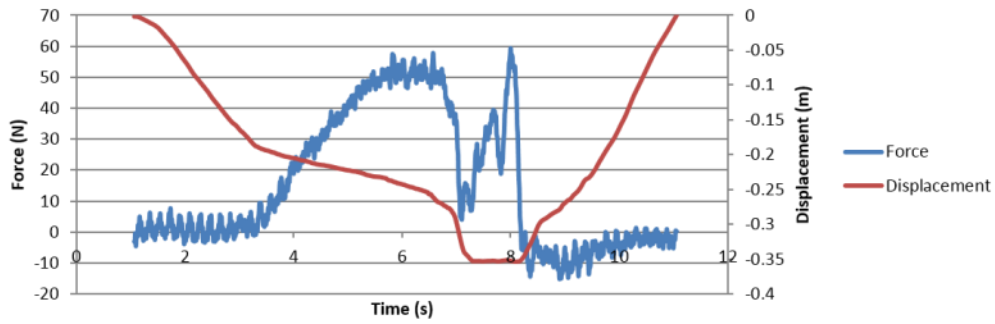


11.5MM

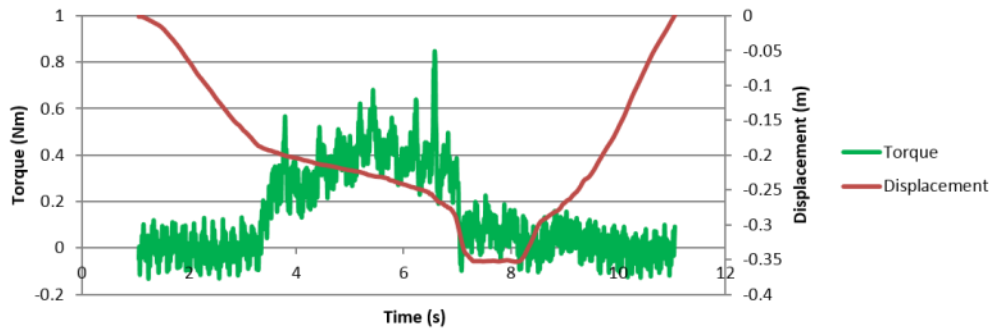
**SAMPLE NO. 7 - Left - Resident: 11.5mm**



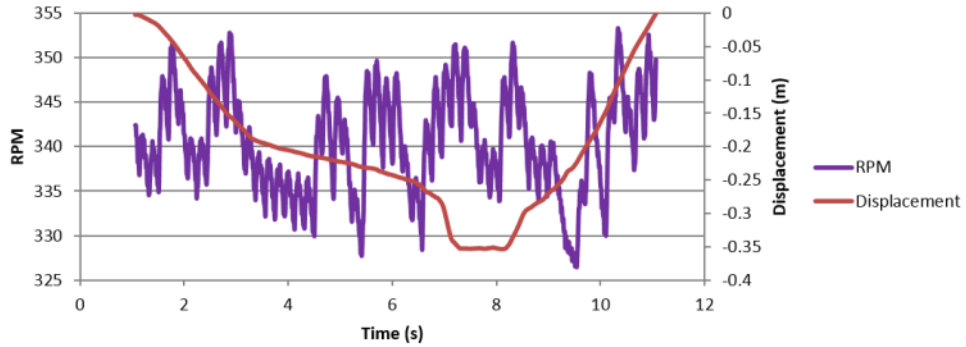
**SAMPLE NO. 7 - Left - Resident: 11.5mm**



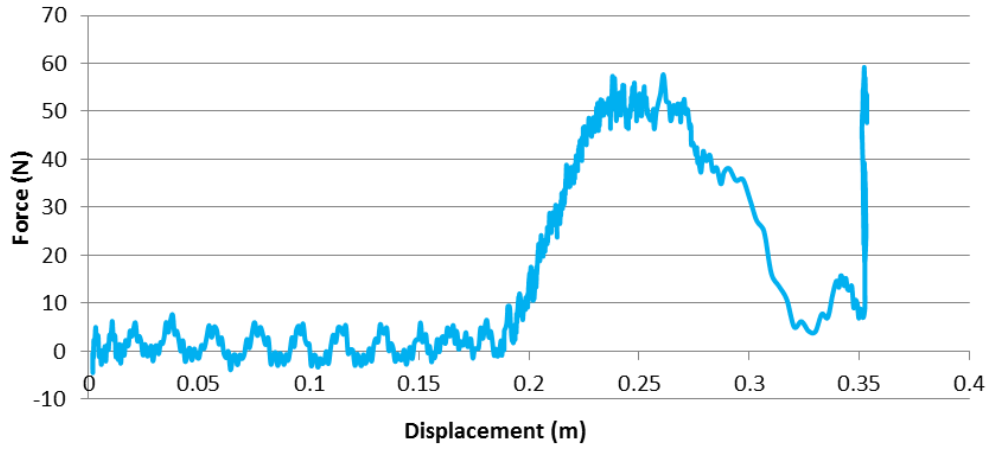
**SAMPLE NO. 7 - Left - Resident: 11.5mm**



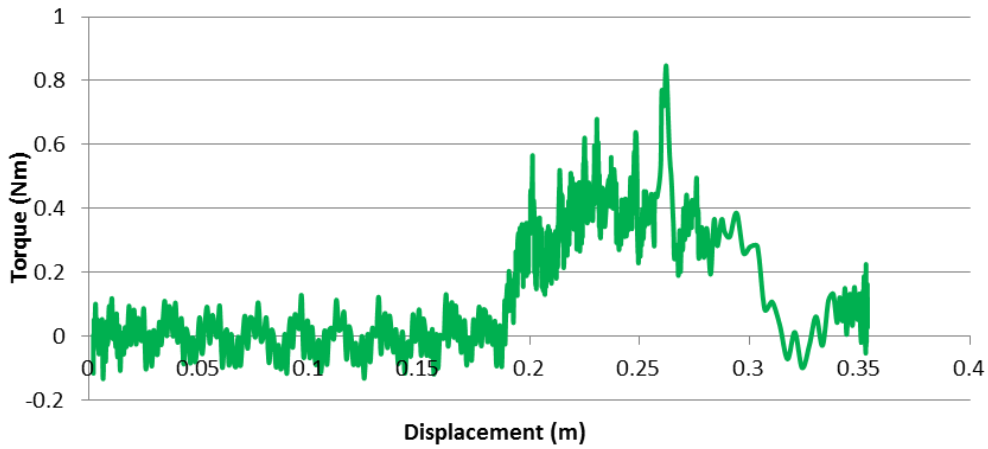
**SAMPLE NO. 7 - Left - Resident: 11.5mm**



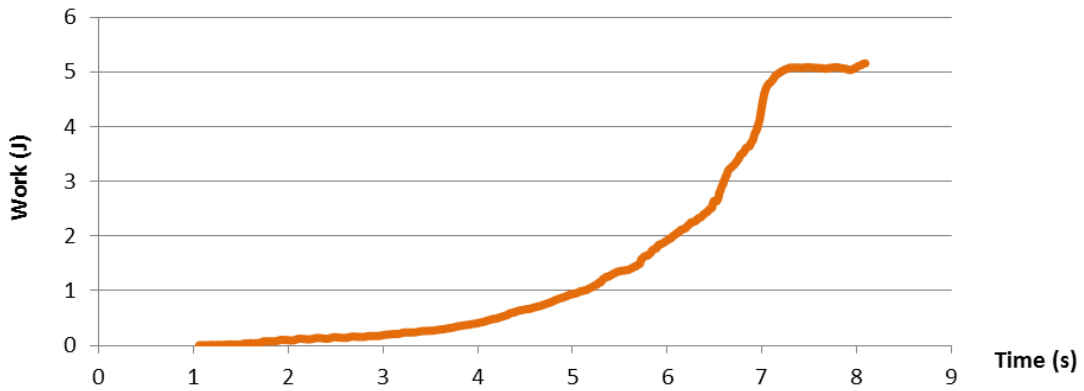
**SAMPLE NO. 7 - Left - Resident: 11.5mm**



**SAMPLE NO. 7 - Left - Resident: 11.5mm**

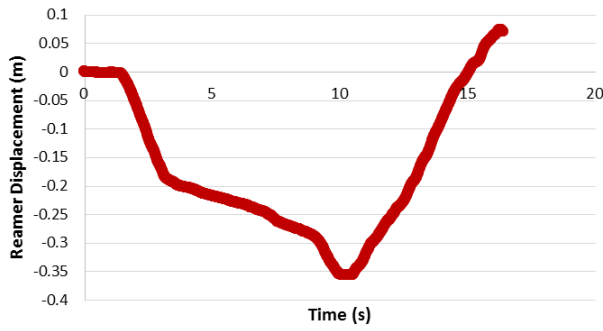


**SAMPLE NO. 7 - Left - Resident: 11.5mm**

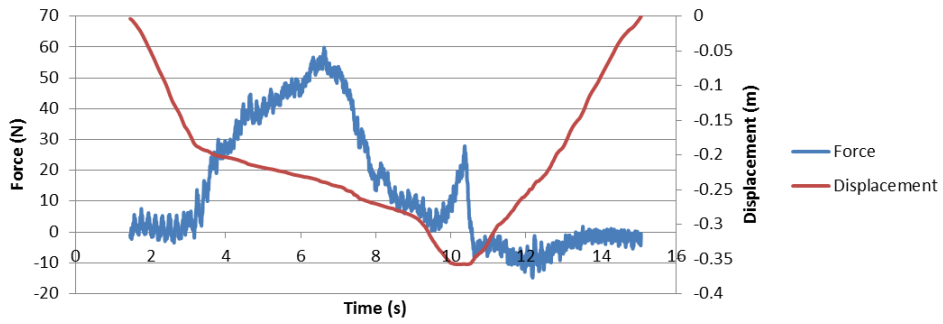


12MM

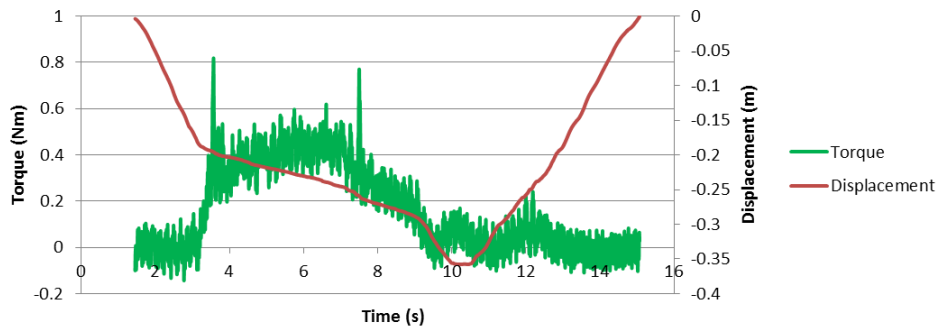
SAMPLE NO. 7 - Left - Resident: 12mm



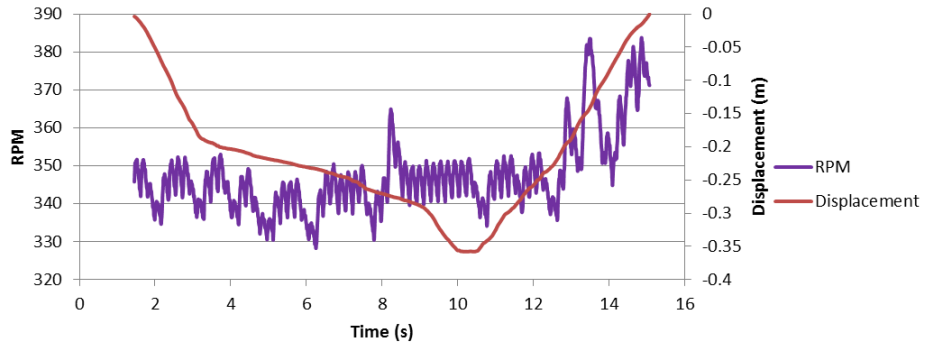
SAMPLE NO. 7 - Left - Resident: 12mm



SAMPLE NO. 7 - Left - Resident: 12mm

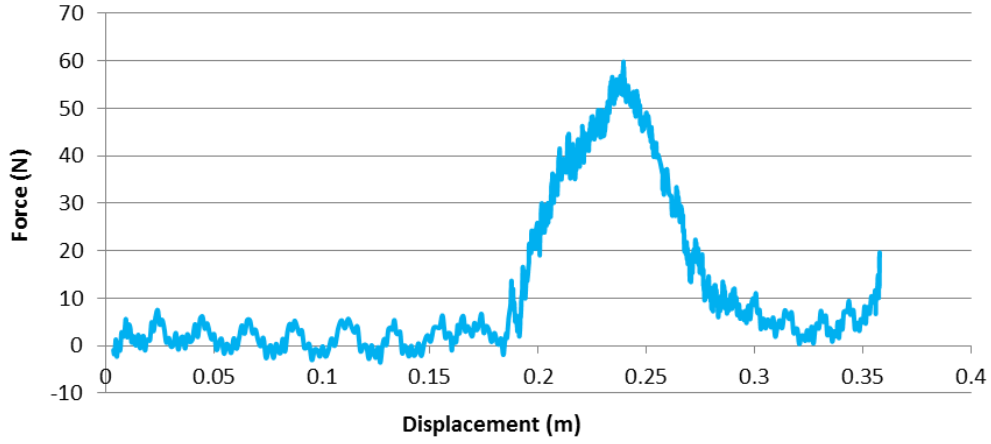


SAMPLE NO. 7 - Left - Resident: 12mm

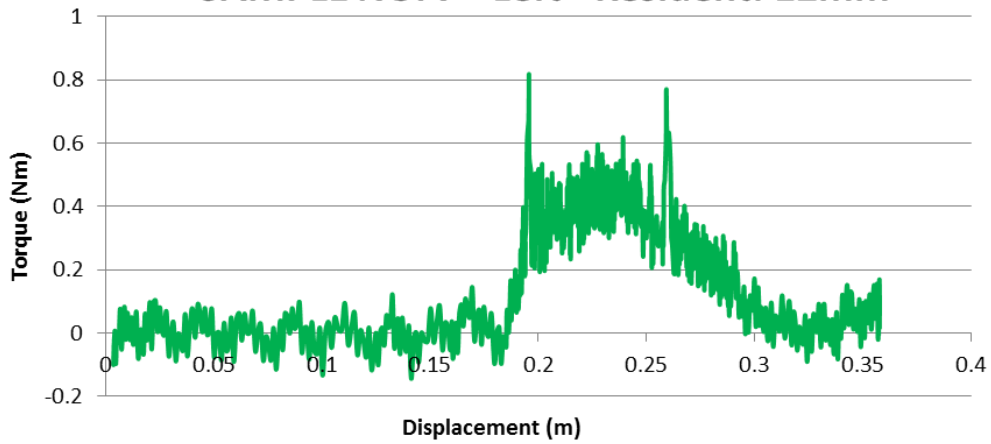




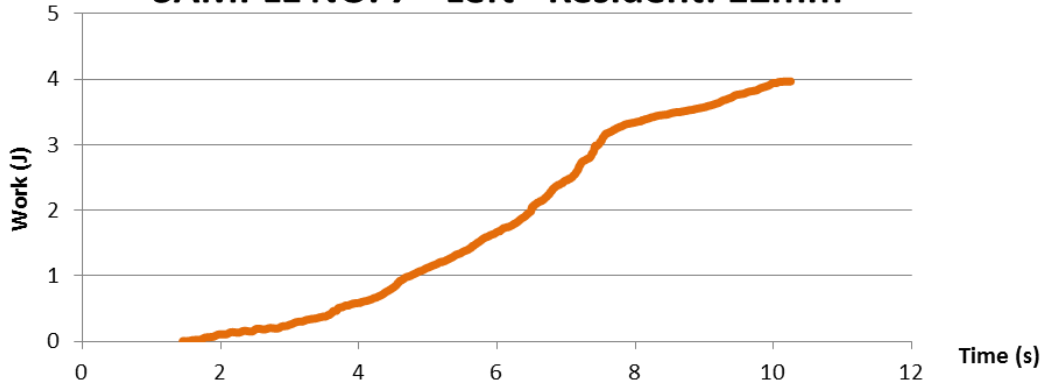
**SAMPLE NO. 7 - Left - Resident: 12mm**



**SAMPLE NO. 7 - Left - Resident: 12mm**



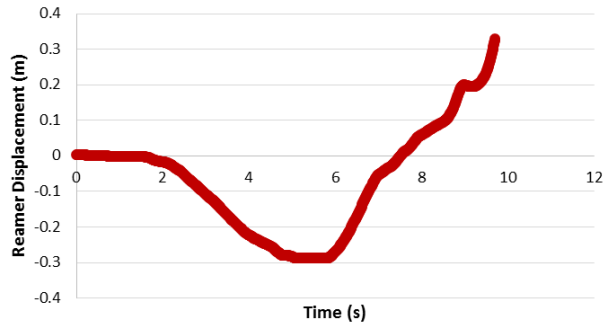
**SAMPLE NO. 7 - Left - Resident: 12mm**



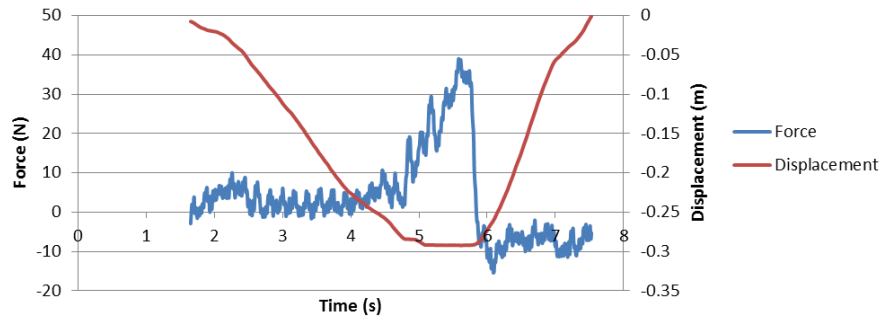
RIGHT: ATTENDING

9MM

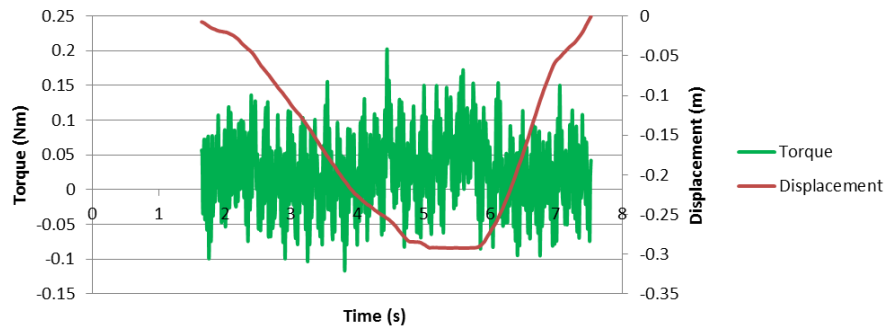
SAMPLE NO. 7 - Right - Attending: 9mm



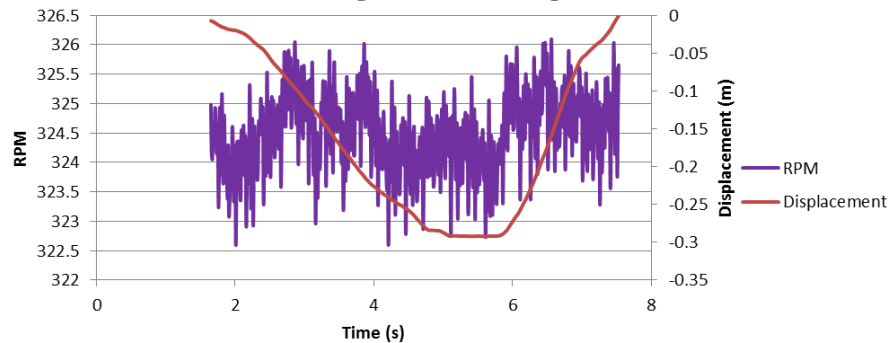
SAMPLE NO. 7 - Right - Attending: 9mm



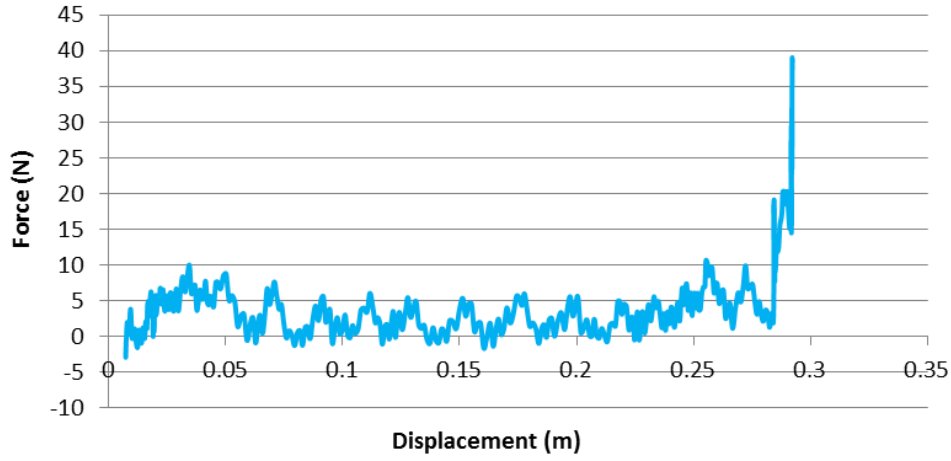
SAMPLE NO. 7 - Right - Attending: 9mm



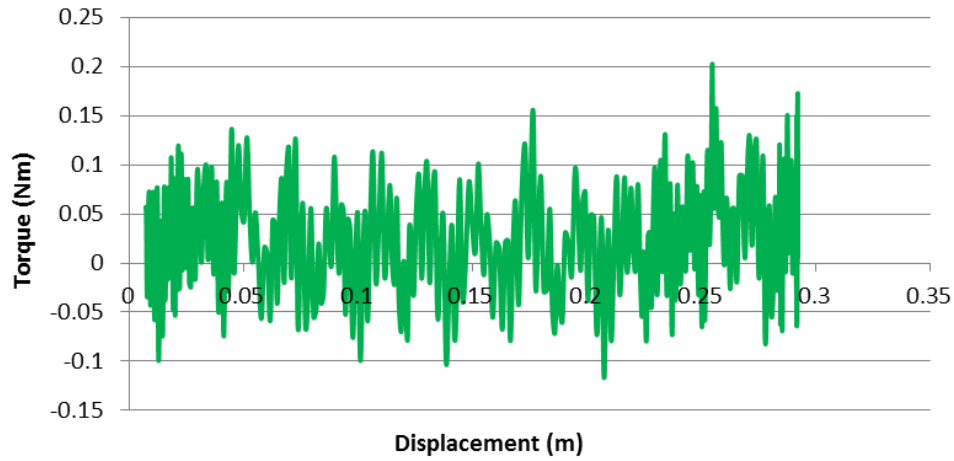
SAMPLE NO. 7 - Right - Attending: 9mm



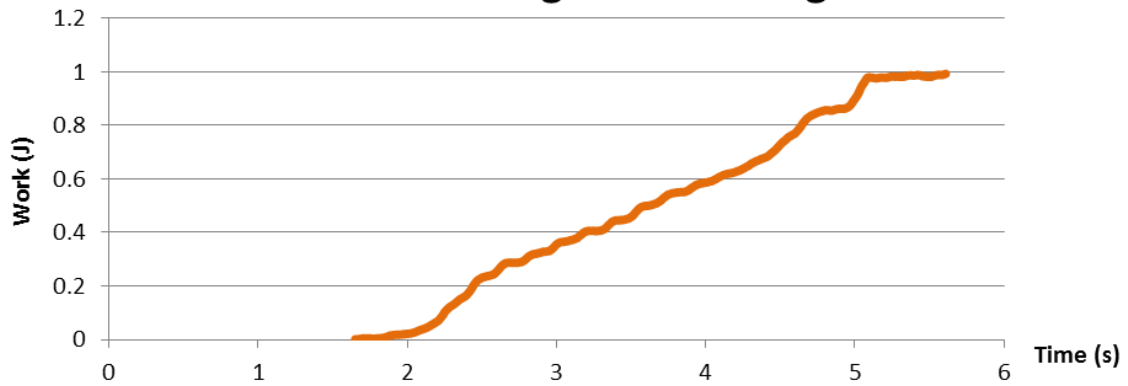
### SAMPLE NO. 7 - Right - Attending: 9mm



### SAMPLE NO. 7 - Right - Attending: 9mm

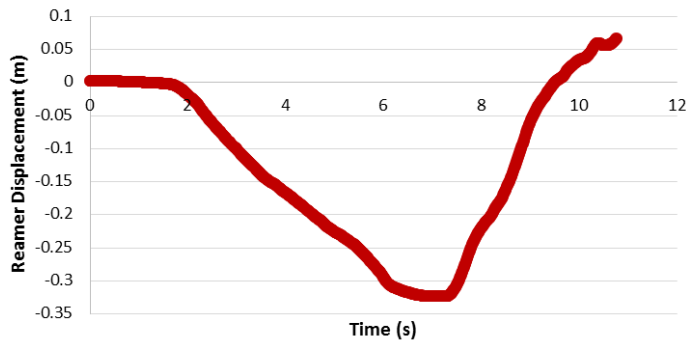


### SAMPLE NO. 7 - Right - Attending: 9mm

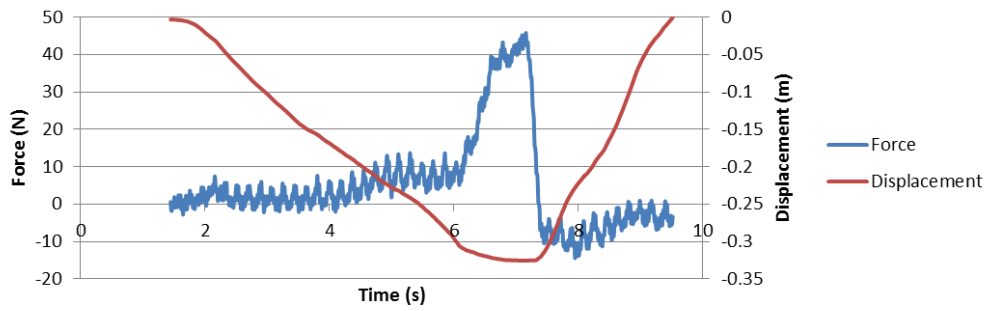


9.5MM

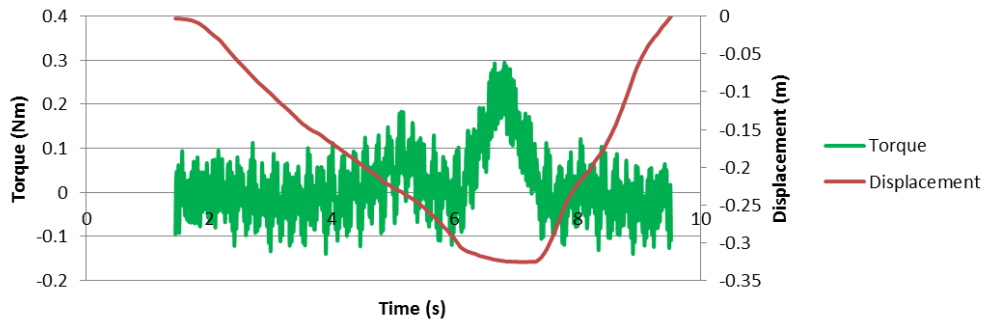
SAMPLE NO. 7 - Right - Attending: 9.5mm



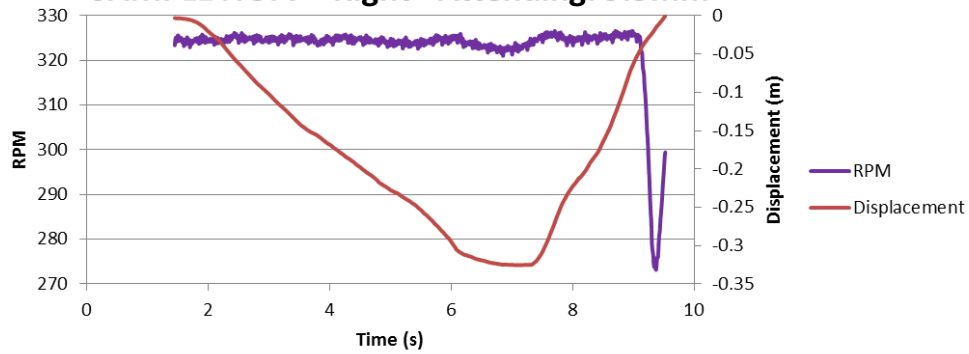
SAMPLE NO. 7 - Right - Attending: 9.5mm



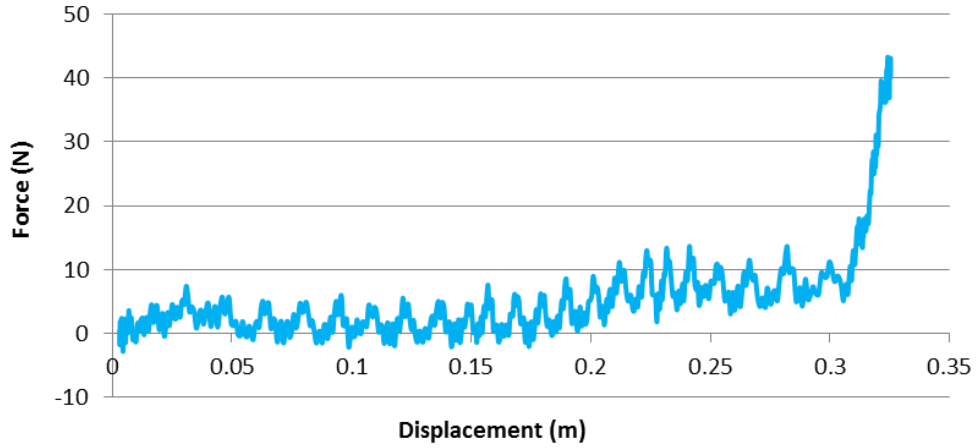
SAMPLE NO. 7 - Right - Attending: 9.5mm



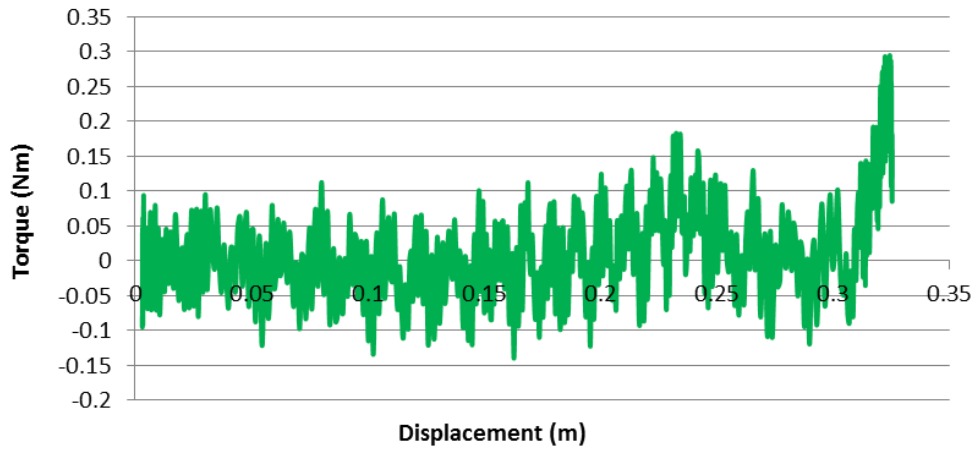
SAMPLE NO. 7 - Right - Attending: 9.5mm



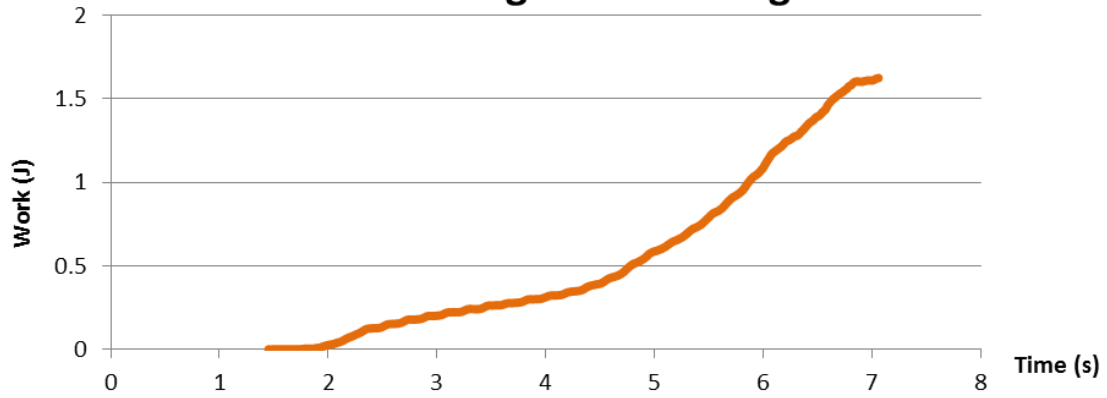
### SAMPLE NO. 7 - Right - Attending: 9.5mm



### SAMPLE NO. 7 - Right - Attending: 9.5mm

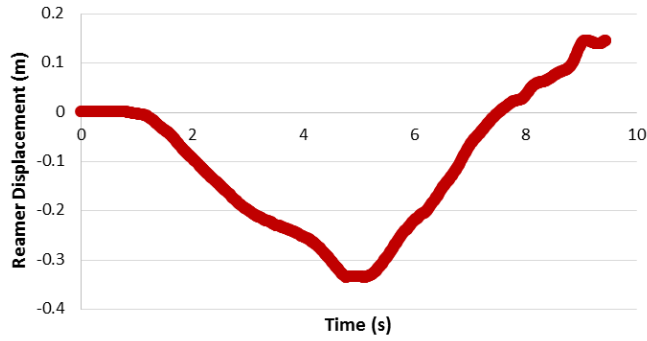


### SAMPLE NO. 7 - Right - Attending: 9.5mm

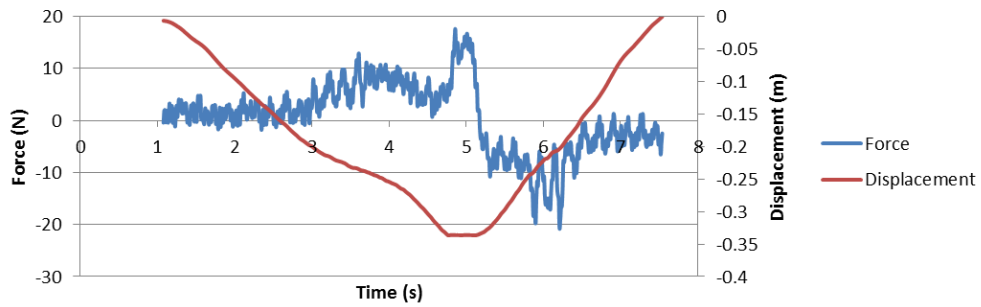


10MM

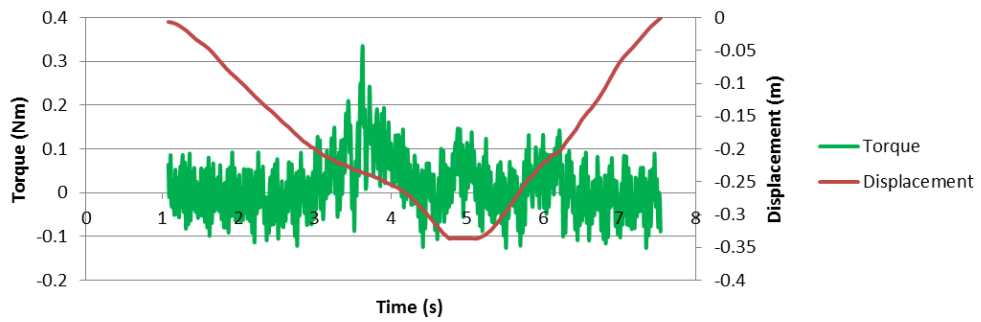
**SAMPLE NO. 7 - Right - Attending: 10mm**



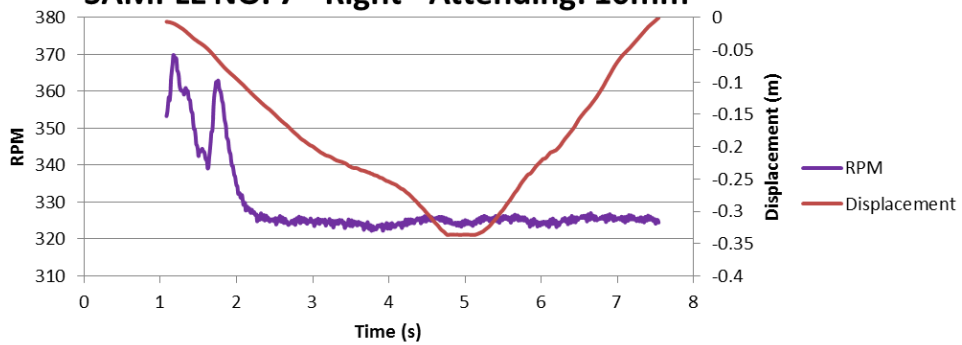
**SAMPLE NO. 7 - Right - Attending: 10mm**



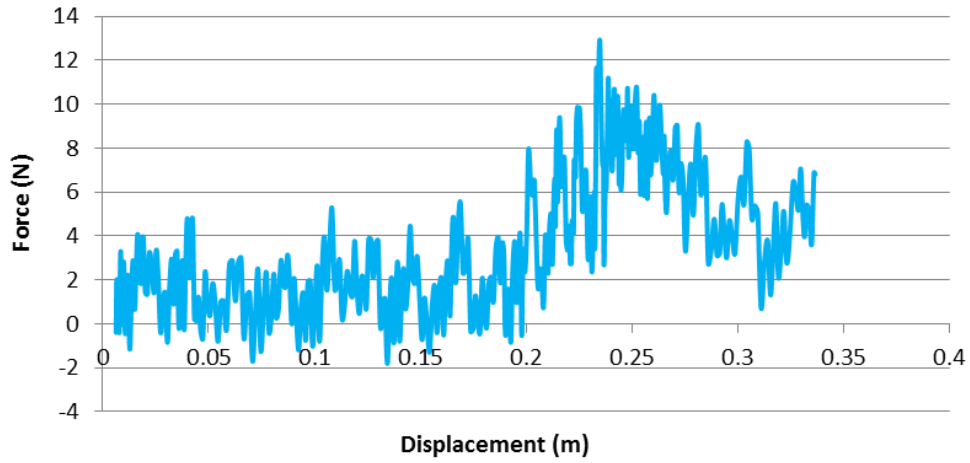
**SAMPLE NO. 7 - Right - Attending: 10mm**



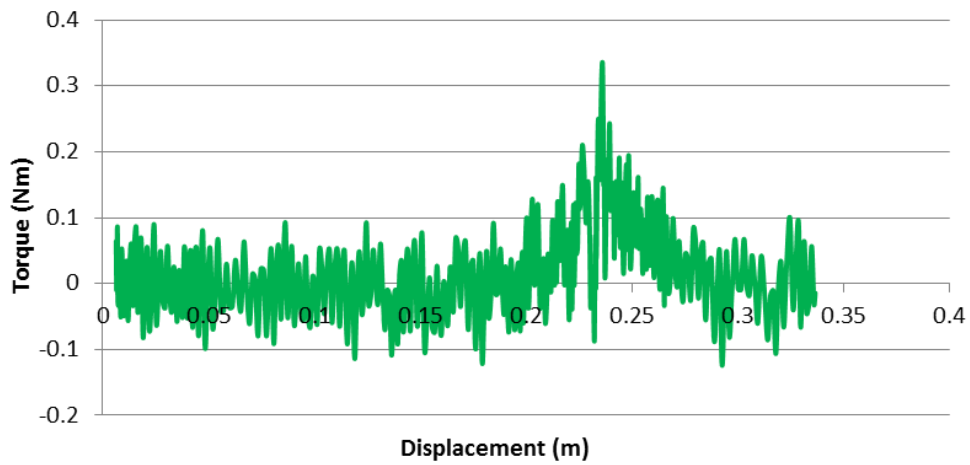
**SAMPLE NO. 7 - Right - Attending: 10mm**



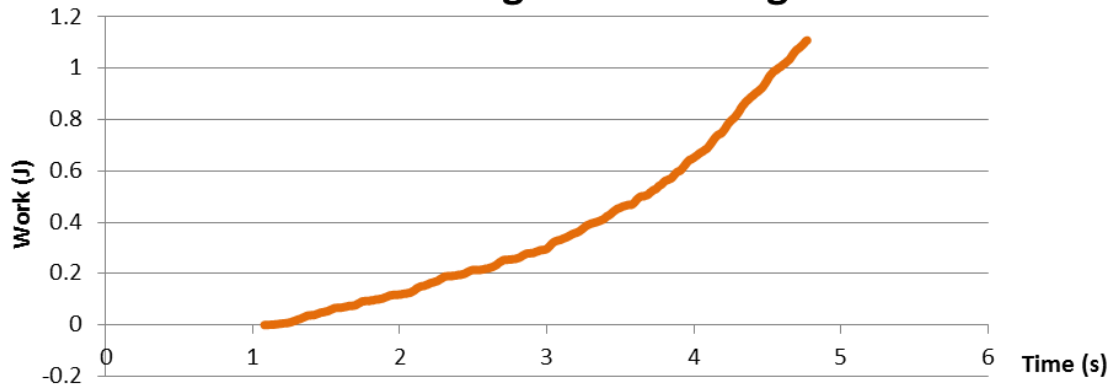
### SAMPLE NO. 7 - Right - Attending: 10mm



### SAMPLE NO. 7 - Right - Attending: 10mm

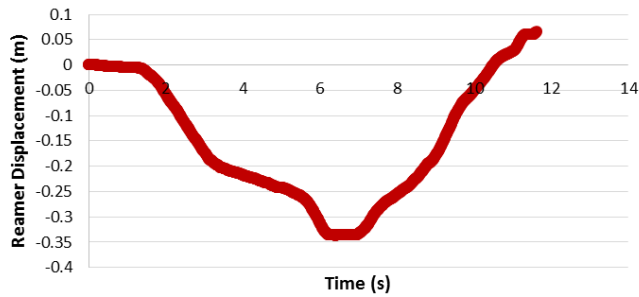


### SAMPLE NO. 7 - Right - Attending: 10mm

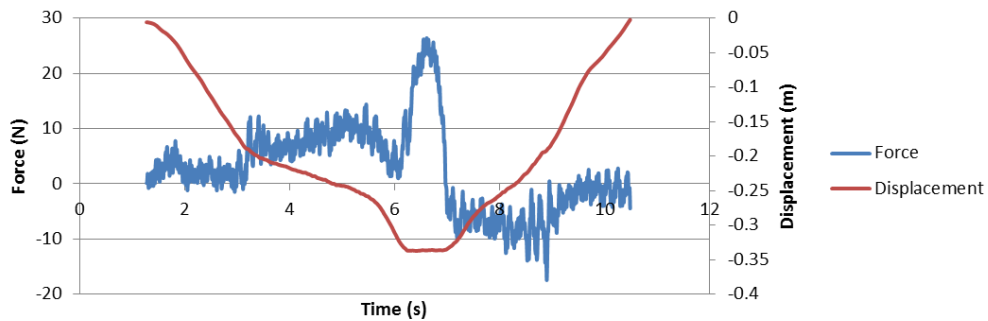


10.5MM

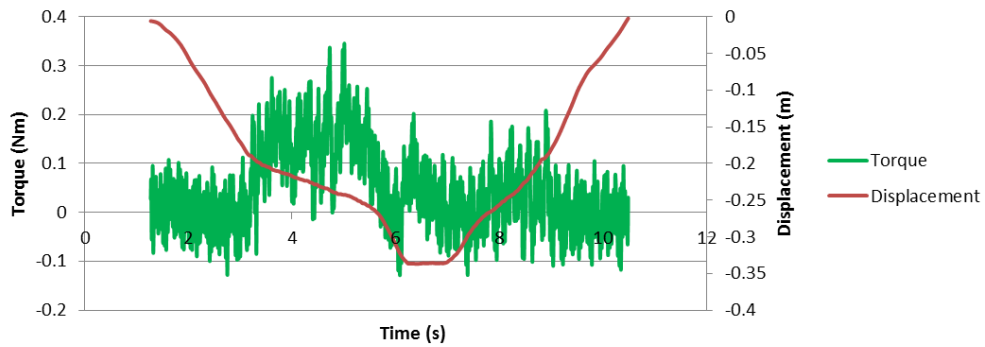
**SAMPLE NO. 7 - Right - Attending:  
10.5mm CHATTER**



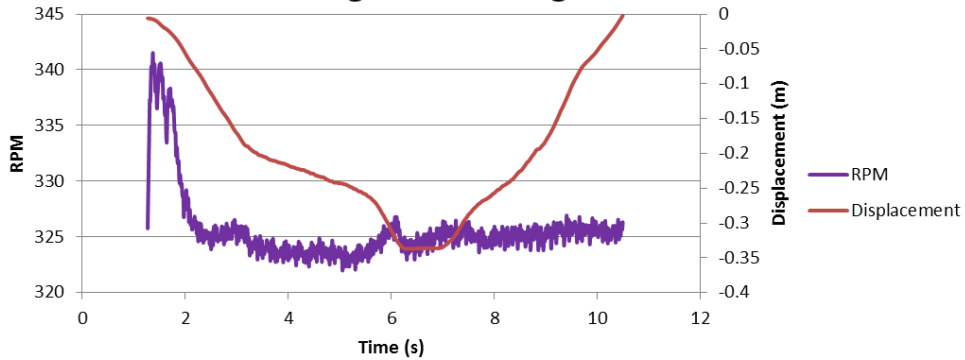
**SAMPLE NO. 7 - Right - Attending: 10.5mm CHATTER**



**SAMPLE NO. 7 - Right - Attending: 10.5mm CHATTER**

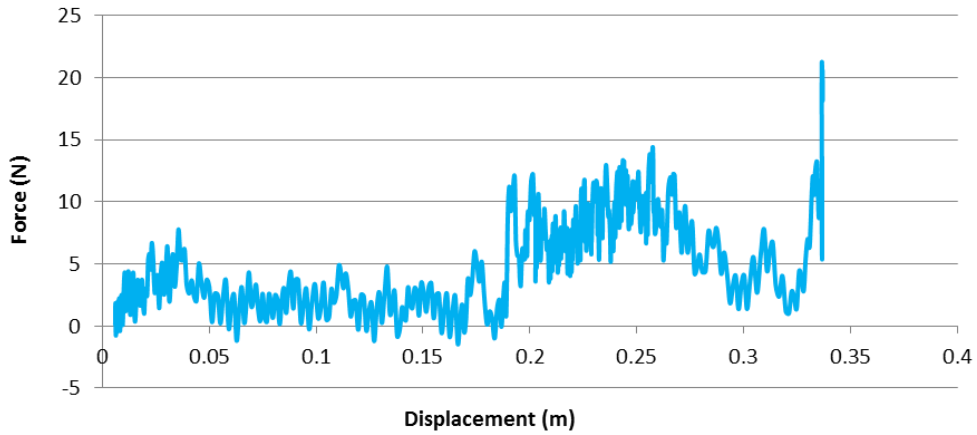


**SAMPLE NO. 7 - Right - Attending: 10.5mm CHATTER**

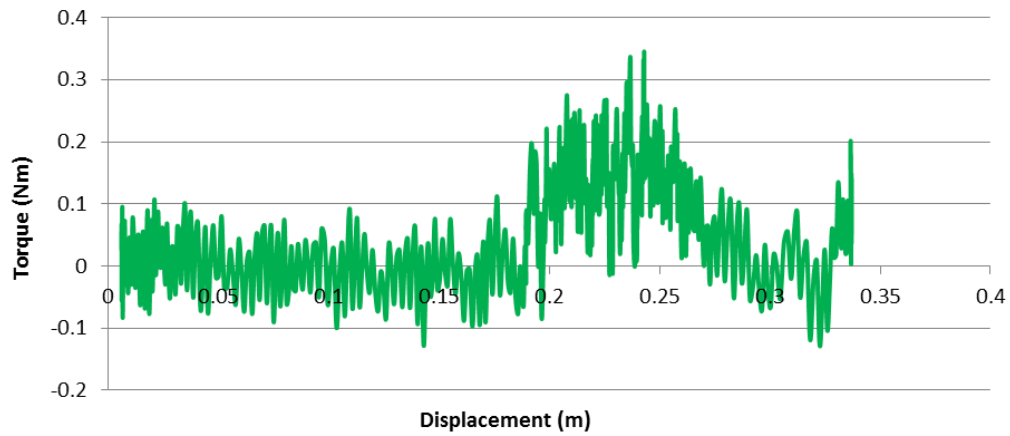




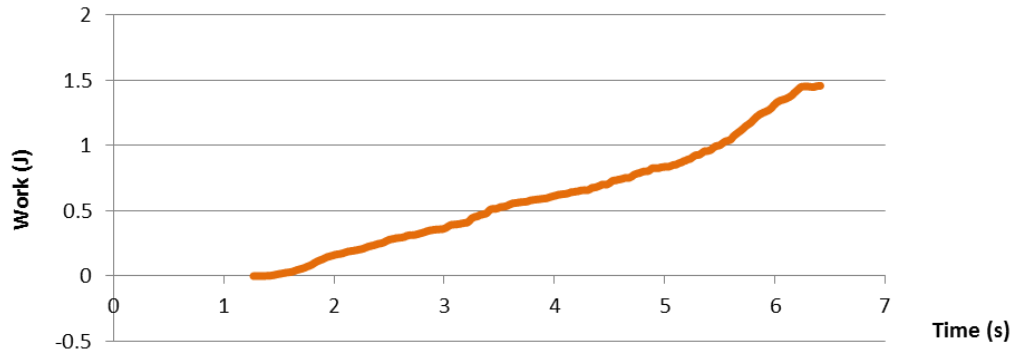
**SAMPLE NO. 7 - Right - Attending: 10.5mm CHATTER**



**SAMPLE NO. 7 - Right - Attending: 10.5mm CHATTER**

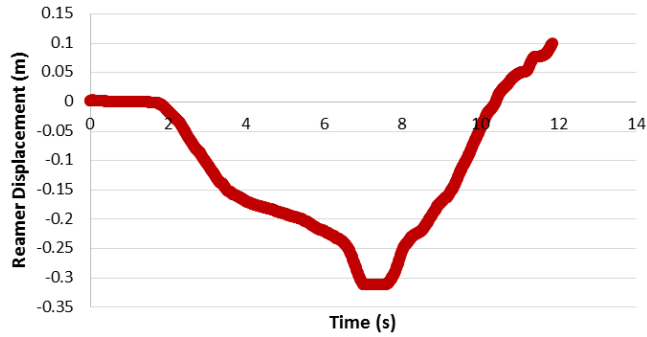


**SAMPLE NO. 7 - Right - Attending: 10.5mm CHATTER**

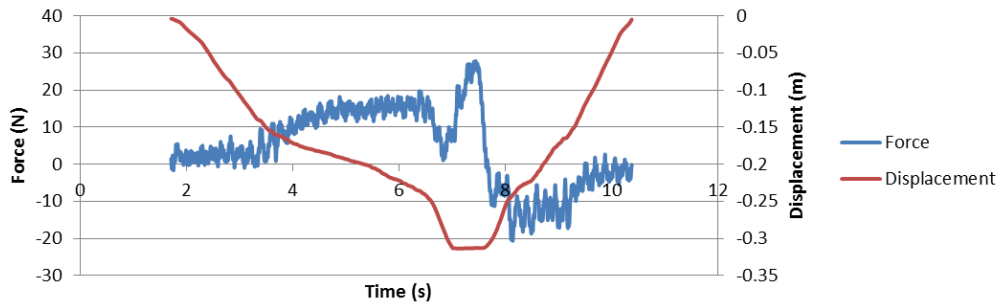


11MM

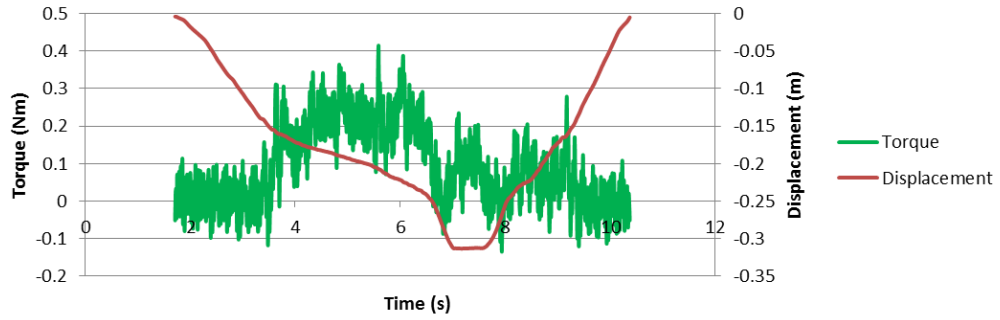
**SAMPLE NO. 7 - Right - Attending: 11mm**



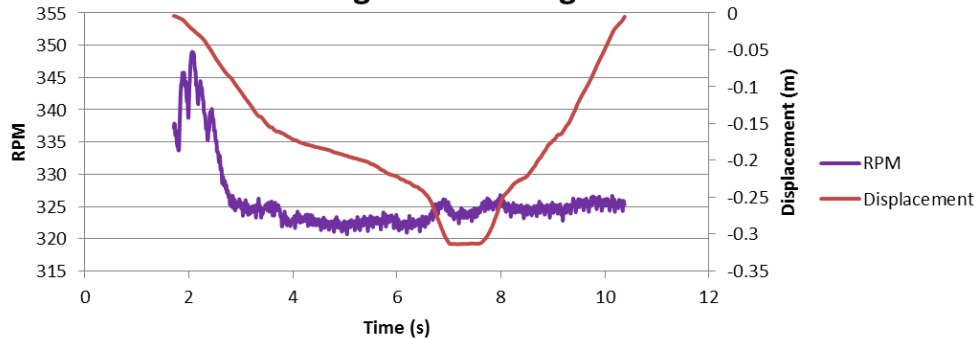
**SAMPLE NO. 7 - Right - Attending: 11mm**



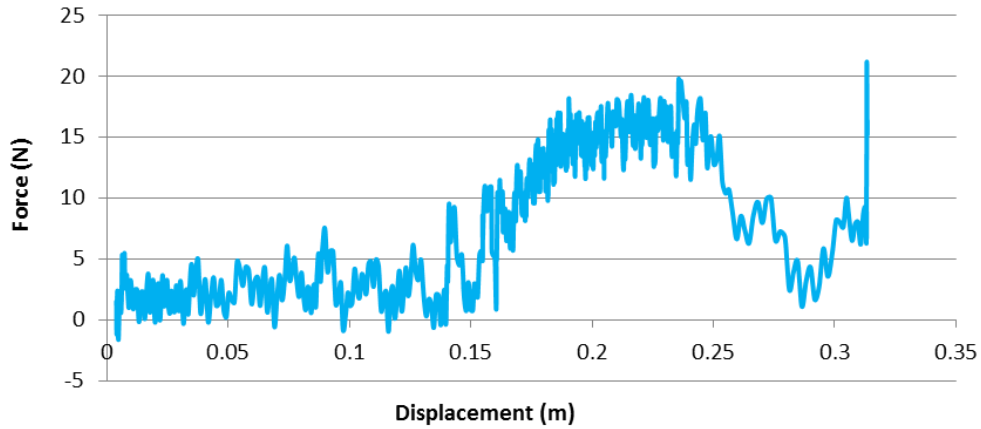
**SAMPLE NO. 7 - Right - Attending: 11mm**



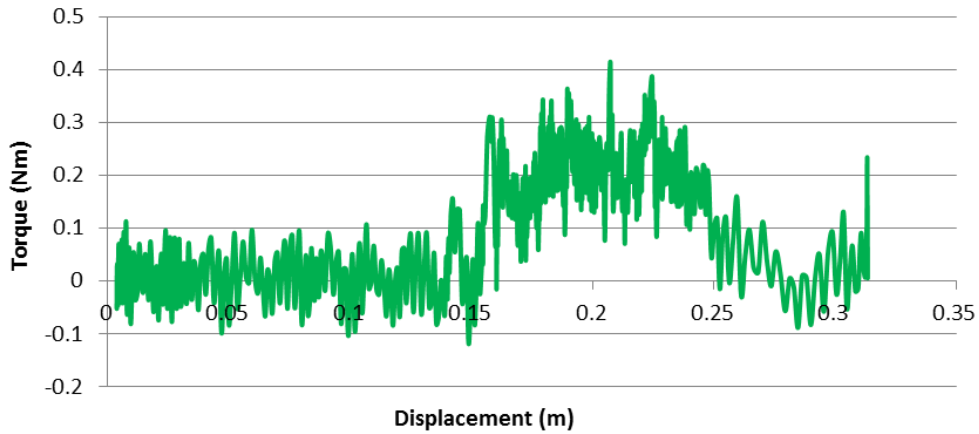
**SAMPLE NO. 7 - Right - Attending: 11mm**



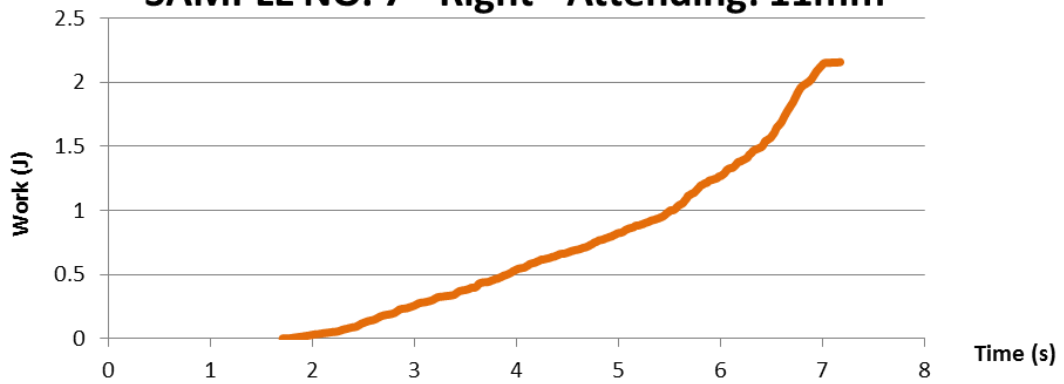
**SAMPLE NO. 7 - Right - Attending: 11mm**



**SAMPLE NO. 7 - Right - Attending: 11mm**

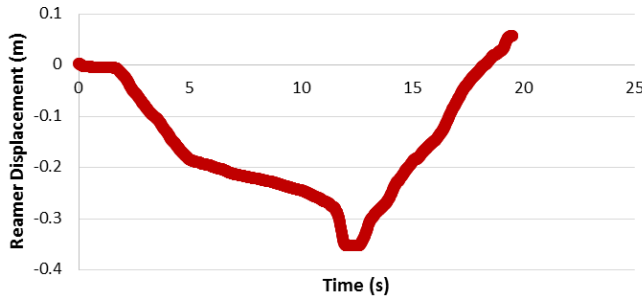


**SAMPLE NO. 7 - Right - Attending: 11mm**

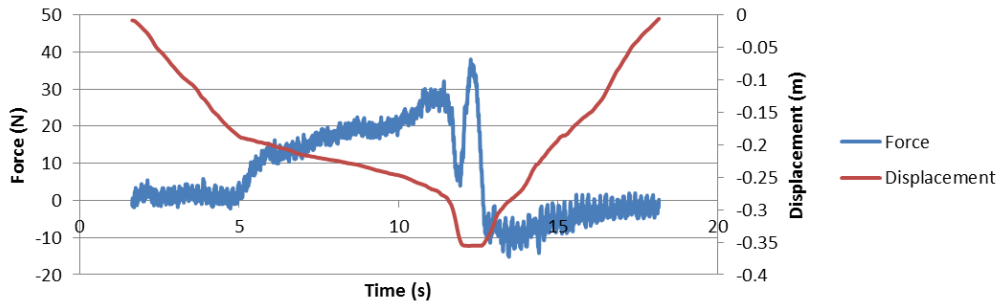


11.5MM

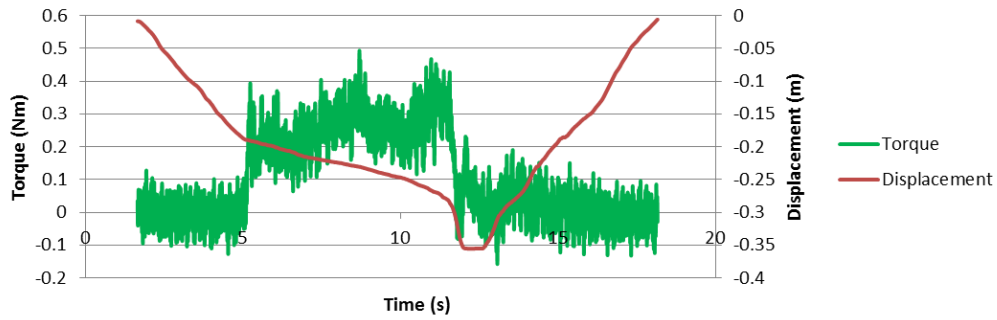
**SAMPLE NO. 7 - Right - Attending:  
11.5mm**



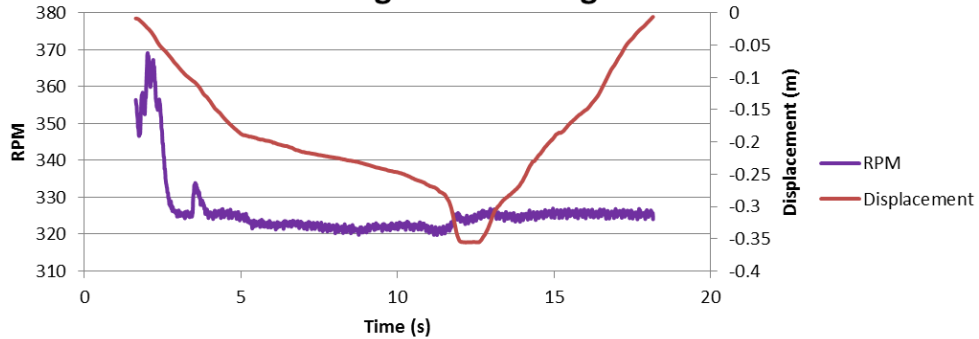
**SAMPLE NO. 7 - Right - Attending: 11.5mm**



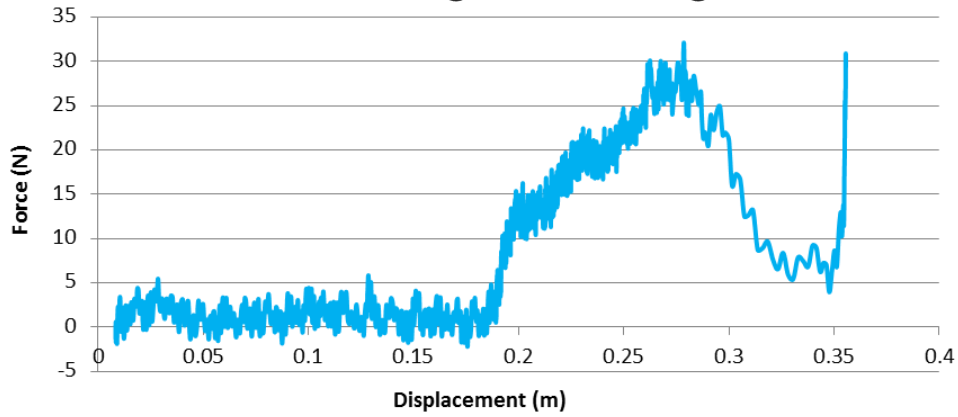
**SAMPLE NO. 7 - Right - Attending: 11.5mm**



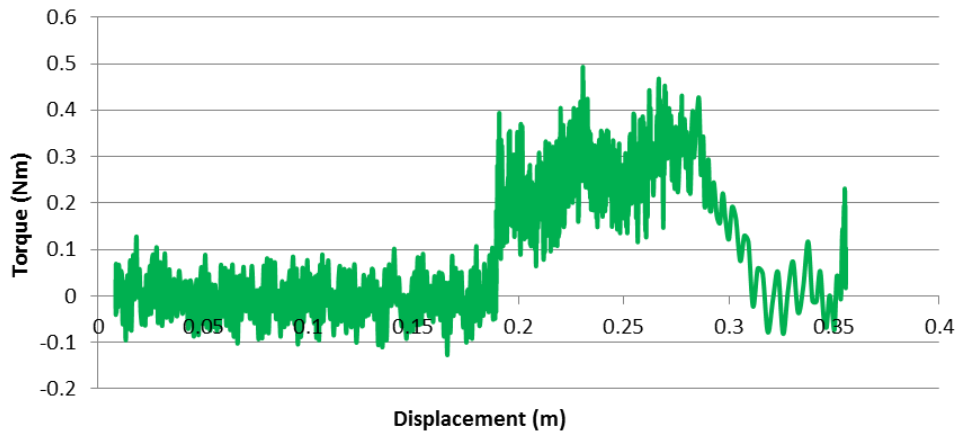
**SAMPLE NO. 7 - Right - Attending: 11.5mm**



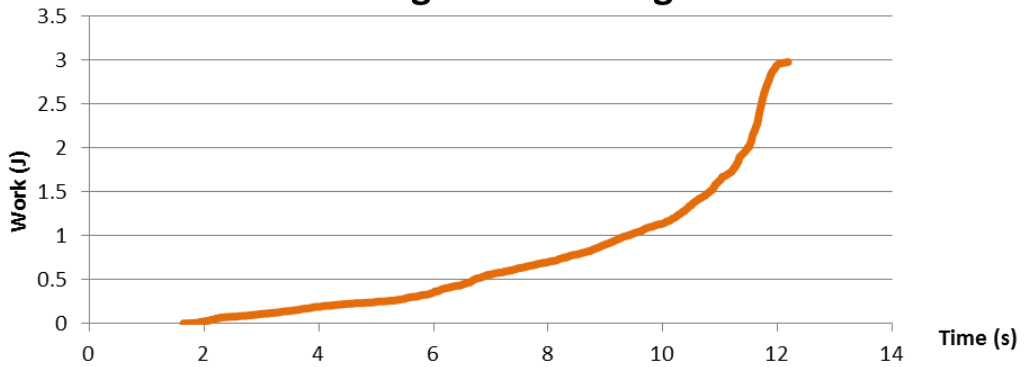
**SAMPLE NO. 7 - Right - Attending: 11.5mm**



**SAMPLE NO. 7 - Right - Attending: 11.5mm**

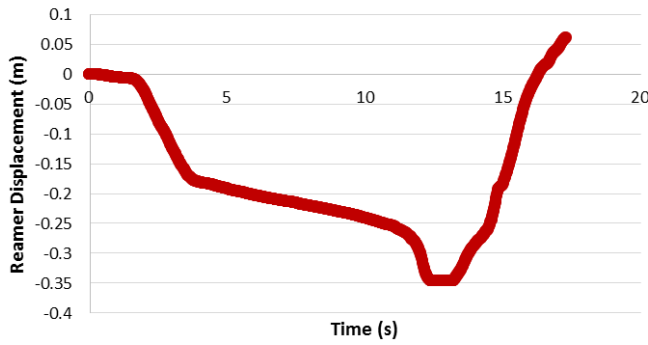


**SAMPLE NO. 7 - Right - Attending: 11.5mm**

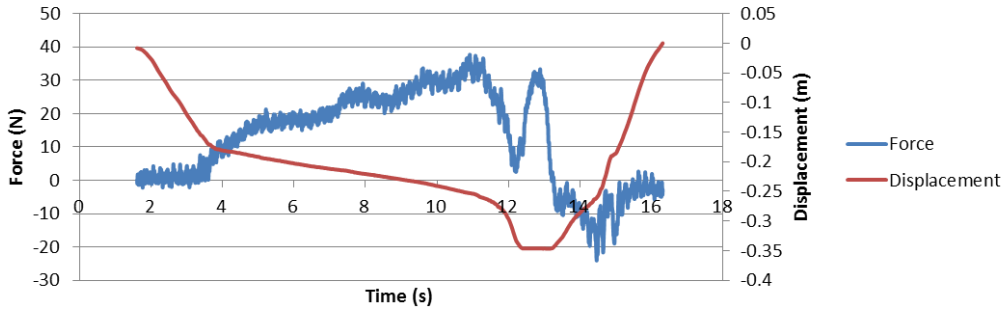


12MM

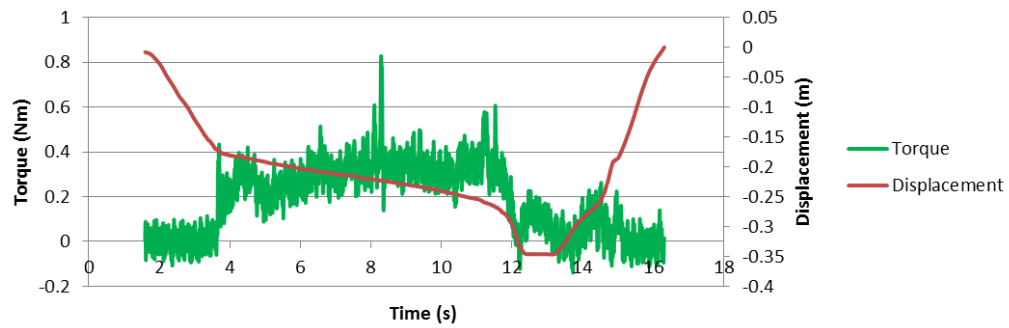
**SAMPLE NO. 7 - Right - Attending: 12mm**



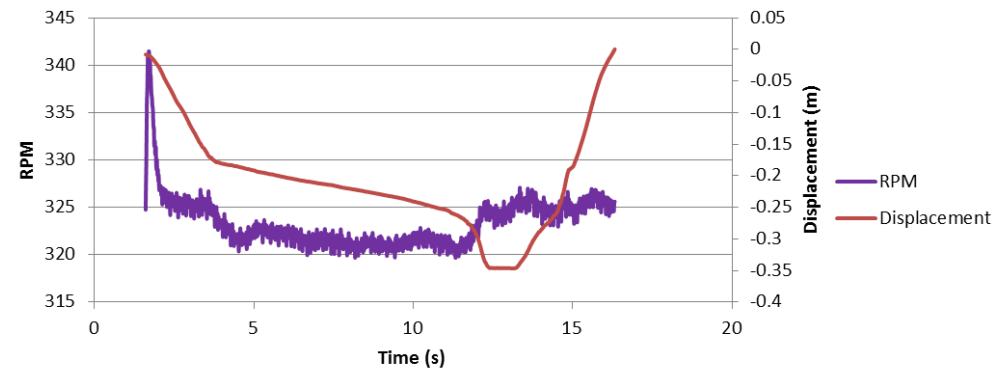
**SAMPLE NO. 7 - Right - Attending: 12mm**



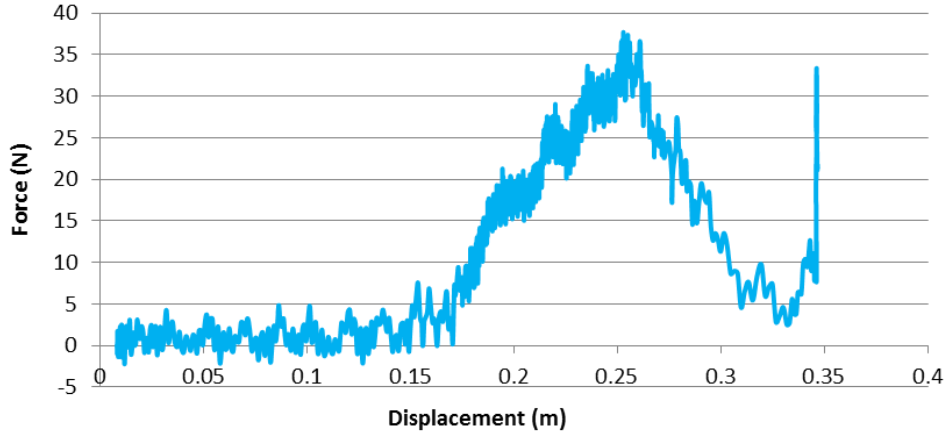
**SAMPLE NO. 7 - Right - Attending: 12mm**



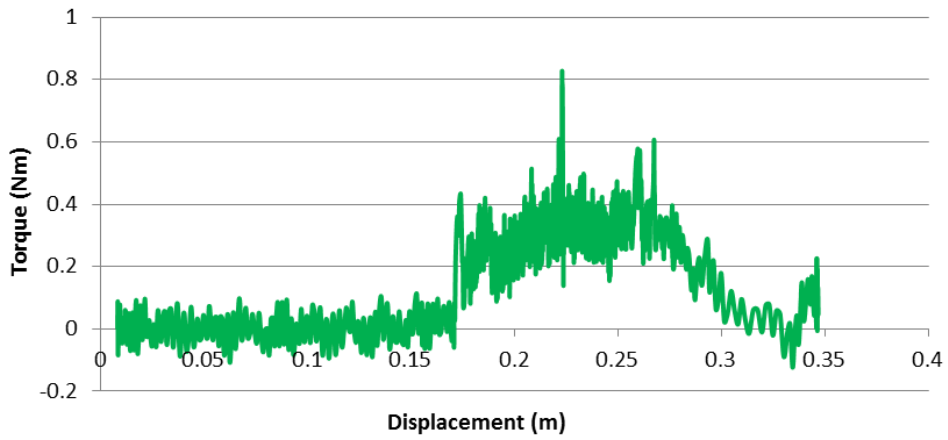
**SAMPLE NO. 7 - Right - Attending: 12mm**



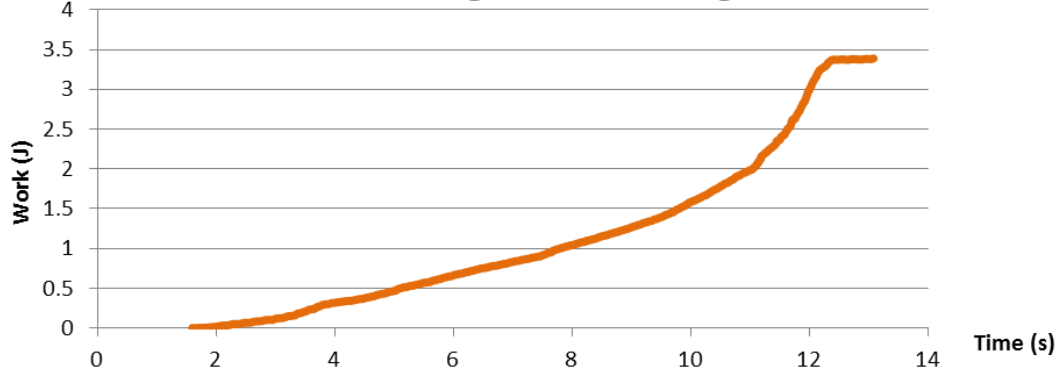
**SAMPLE NO. 7 - Right - Attending: 12mm**



**SAMPLE NO. 7 - Right - Attending: 12mm**



**SAMPLE NO. 7 - Right - Attending: 12mm**



## 14. REFERENCES

- [1] S. Standring, N. Borley, P. Collins, C. AR, M. Gatzoulis, J. Healy, *et al.*, "Leg," in *Gray's Anatomy*, 40 ed: Elsevier Limited, 2008, pp. 1411-1428.
- [2] F. Martini, "Osseous Tissue and Skeletal Structure," in *Fundamentals of Anatomy & Physiology*, 5 ed Upper Saddle River, New Jersey: Prentice Hall, 2001, pp. 168-181.
- [3] P. Kelly, "Anatomy, Physiology, and Pathology of the Blood Supply of Bones," *Journal of Bone and Joint Surgery, American*, vol. 50-A, pp. 766-783, 1968.
- [4] J. Trueta, "Blood supply and the rate of healing of tibial fractures," *Clinical Orthopaedics and Related Research*, vol. 105, pp. 11-26, 1974.
- [5] C. Boulton and R. O'Toole, "Tibia and Fibula Shaft Fractures," in *Rockwood & Green's Fractures in Adults*. vol. 2, 7 ed: Lippincott Williams & Wilkins, 2010, pp. 2415-2472.
- [6] P. Wolinsky, "Tibial Shaft Fractures," in *Orthopaedic Trauma Association 29th Annual Meeting*, Minneapolis, Minnesota, 2013.
- [7] S. Nork, "Fractures of the Shaft of the Femur," in *Rockwood & Green's Fractures in Adults*, J. Heckman, R. Bucholz, C. Court-Brown, and P. Tornetta, Eds., 7 ed: Lippincott Williams & Wilkins, 2010, pp. 1655-1714.
- [8] R. Pfeifer, R. Sellei, and H. Pape, "The biology of intramedullary reaming," *Injury*, vol. 41, pp. S4-S8, 2010.
- [9] H. Reid and C. Court-Brown, "(iii) Intramedullary nailing: the case for reaming," *Current Orthopaedics*, vol. 13, pp. 99-104, 1999.
- [10] I. Reichert, I. McCarthy, E. Draper, and S. Hughes, "An experimental study: Reamed versus unreamed nailing," *Journal of Orthopaedic Trauma*, vol. 13, pp. 304-305, 1999.
- [11] P. Tornetta and D. Tiburzi, "Reamed Versus Nonreamed Anterograde Femoral Nailing," *Journal of Orthopaedic Trauma*, vol. 14, pp. 15-19, 2000.
- [12] J. Frölke, H. Van de Krol, F. Bakker, P. Patka, and H. Haarman, "Destination of Debris During Intramedullary Reaming. An Experimental Study on Sheep Femurs," *Acta Orthopaedica Belgica*, vol. 66, pp. 337 - 340, 2000.
- [13] P. Brownson, P. Radford, and N. Smith, "Minimizing the risk of guide-wire displacement during intramedullary reaming," *Injury*, vol. 28, pp. 713-714, 1997.
- [14] Synthes. (March 3). *SynReam - The Synthes Reaming System*.
- [15] C. Müller, F. Baumgart, D. Wahl, P. SM, and U. Pfister, "Technical Innovations in Medullary Reaming: Reamer Design and Intramedullary Pressure Increase," *Trauma*, vol. 49, pp. 440-445, 2000.



- [16] R. Smith and P. Glannoudis, "Femoral Shaft Fractures," in *Skeletal Trauma: Basic Science, Management, and Reconstruction*. vol. I, B. Browner, J. Jupiter, A. Levine, P. Trafton, and C. Krettek, Eds., 4 ed Philadelphia, PA: Saunders, 2009, p. 2047.
- [17] J. Frölke, "Intramedullary Reaming of Long Bones," in *Practice of Intramedullary Locked Nails; New Developments in Techniques and Applications*. vol. III, K. Leung, G. Taglang, and R. Schnettler, Eds., ed: Springer, 2006, pp. 43-56.
- [18] C. Müller, J. Green, and N. Sudkamp, "Physical and technical aspects of intramedullary reaming," *Injury*, vol. 37S, pp. 39-49, 2006.
- [19] K. Stürmer, "Measurement of Intramedullary Pressure in Animal Experiments," *Injury*, vol. 24, 1993.
- [20] K. Wenda, M. Runkel, J. Degreif, and G. Ritter, "Pathogenesis and clinical relevance of bone marrow embolism in medullary nailing - demonstrated by intraoperative echocardiography," *Injury*, vol. 24, pp. S73-S81, 1993.
- [21] C. Müller, T. McIlff, B. Rahn, U. Pfister, S. Perren, and S. Weller, "Influence of the compression force on the intramedullary pressure development in reaming of the femoral medullary cavity," *Injury*, vol. 24, pp. 36-39, 1993.
- [22] C. Müller and B. Rahn, "Intramedullary Pressure Increase and Increase in Cortical Temperature During Reaming of the Femoral Medullary Cavity: The Effect of Draining the Medullary Contents before Reaming," *Trauma*, vol. 55, pp. 495-503, 2003.
- [23] C. Müller, B. Rahn, U. Pfister, and S. Weller, "Extent of bluntness and damage to reamers from hospitals," *Injury*, vol. 24, pp. S31-S35, 1993.
- [24] C. Müller, T. McIlff, B. Rahn, U. Pfister, and S. Weller, "Intramedullary pressure, strain on the diaphysis and increase in cortical temperature when reaming the femoral medullary cavity--a comparison of blunt and sharp reamers.," *Injury*, vol. 24, pp. S22-S30, 1993.
- [25] J. Lundskog, "Heat and bone tissue. An experimental investigation of the thermal properties of bone tissue and threshold levels for thermal injury," *Scandinavian Journal of Plastic and Reconstructive Surgery*, vol. 9, pp. 1-80, 1972.
- [26] A. T. Eriksson AR, "Temperature threshold levels for heat-induced bone tissue injury: A vital microscopic study in the rabbit," *Journal of Prosthetic Dentistry*, vol. 50, pp. 101-107, 1983.
- [27] F. Baumgart, G. Kohler, and P. Ochsner, "The physics of heat generation during reaming of the medullary cavity," *Injury*, vol. 29, pp. B11 - B25, 1998.
- [28] O. García, F. Mombiola, C. De La Fuente, M. Aránguez, D. Escribano, and J. Martín, "The influence of the size and condition of the reamers on bone temperature during intramedullary reaming.," *The Journal of Bone and Joint Surgery*, vol. 86, pp. 994-999, 2004.
- [29] M. Karunakar, E. Frankenburg, T. Le, and J. Hall, "The Thermal Effects of Intramedullary Reaming," *The Journal of Orthopaedic Trauma*, vol. 18, pp. 674-679, 2004.

- [30] J. Frölke, R. Peters, K. Boshuizen, P. Patka, F. Bakker, and H. Haarman, "The assessment of cortical heat during intramedullary reaming of long bones," *Injury*, vol. 32, pp. 683-688, 2001.
- [31] M. Klein, B. Rahn, R. Frigg, S. Kessler, and S. Perren, "Reaming versus non-reaming in medullary nailing: Interference with cortical circulation of the canine tibia," *Archives of Orthopaedic and Trauma Surgery*, vol. 109, pp. 314-316, 1990.
- [32] O. Grundnes, S. Utvag, and O. Reikeras, "Effects of graded reaming on fracture healing. Blood flow and healing studied in rat femurs," *Acta Orthopaedica Scandinavica*, vol. 65, pp. 32-36, 1994.
- [33] A. ElMaraghy, B. Humeniuk, G. Anderson, E. Schemitsch, and R. Richards, "Femoral Bone Blood Flow After Reaming and Intramedullary Canal Preparation. A Canine Study Using Laser Doppler Flowmetry," *The Journal of Arthroplasty*, vol. 14, pp. 220-226, 1999.
- [34] O. Grundnes, S. Utvag, and O. Reikeras, "Restoration of bone flow following fracture and reaming in rat femora," *Acta Orthopaedica Scandinavica*, vol. 65, pp. 185-190, 1994.
- [35] P. Giannoudis, S. Snowden, S. Matthews, S. Smye, and R. Smith, "Temperature rise during reamed tibial nailing," *Clinical Orthopaedics and Related Research*, vol. 395, pp. 255-261, 2002.
- [36] S. Henry, R. Adcock, J. Von Fraunhofer, and D. Seligson, "Heat of Intramedullary Reaming," *Southern Medical Journal*, vol. 80, pp. 173-176, 1987.
- [37] S. Sarasin and N. Vannet, "A Comparison of Pressures Created By Various Commonly Used Intramedullary Reamers," *The Internet Journal of Orthopaedic Surgery*, vol. 7, 2007.
- [38] E. Schemitsch, D. Turchin, G. Anderson, R. Byrick, J. Mullen, and R. Richards, "Pulmonary and Systemic Fat Embolization after Medullary Canal Pressurization: A Hemodynamic and Histologic Investigation in the Dog," *Trauma*, vol. 45, pp. 738-742, 1998.
- [39] P. Smith, A. Leditschke, D. McMahon, R. Sample, D. Perriman, A. Prins, *et al.*, "Monitoring and Controlling INtramedullary Pressure Increase in Long Bone Instrumentation: A Study on Sheep," *Journal of Orthopaedic Research*, vol. 26, pp. 1327-1333, 2008.
- [40] K. Wenda and M. Runkel, "Systemic complications of intramedullary reaming," *Orthopade*, vol. 25, pp. 292-299, 1996.
- [41] S. Olson and D. Hahn, "Surgical treatment of non-unions: A case for internal fixation," *Injury*, vol. 37, pp. 681-690, 2006.
- [42] H. Pape and P. Giannoudis, "The biological and physiological effects of intramedullary reaming," *The Journal of Bone and Joint Surgery (Br)*, vol. 89-B, pp. 1421-1426, 2007.

- [43] M. Rudloff and W. Smith, "Intramedullary Nailing of the Femur: Current Concepts Concerning Reaming," *The Journal of Orthopaedic Trauma*, vol. 23, pp. S12-S17, 2009.
- [44] R. Peindl, M. B. Harrow, DM, M. Bosse, and J. Kellam, "Comparison of Mechanical Loads Produced by Current Intramedullary Reamer Systems," *Journal of Orthopaedic Trauma*, vol. 12, pp. 531-539, 1998.
- [45] A. Ho, I. Elhajj, W. Li, N. Xi, and T. Mei, "A Bone Reaming System Using Micro Sensors For Internet Force-feedback Control," in *IEEE International Conference on Robotics & Automation*, Seoul, Korea, 2001, pp. 656-661.